Springer Series on Polymer and Composite Materials

Thomas Heinze
Omar A. El Seoud
Andreas Koschella

# Cellulose Derivatives

## Synthesis, Structure, and Properties

Springer

# Springer Series on Polymer and Composite Materials

**Series editor**

Susheel Kalia, Army Cadet College Wing, Indian Military Academy, Dehradun, India

More information about this series at http://www.springer.com/series/13173

Thomas Heinze · Omar A. El Seoud
Andreas Koschella

# Cellulose Derivatives

## Synthesis, Structure, and Properties

Springer

Thomas Heinze
Institut für Organische Chemie und Makromolekulare Chemie
Universität Jena
Jena
Germany

Andreas Koschella
Institut für Organische Chemie und Makromolekulare Chemie
Universität Jena
Jena
Germany

Omar A. El Seoud
Institute of Chemistry
University of São Paulo
São Paulo
Brazil

ISSN 2364-1878 ISSN 2364-1886 (electronic)
Springer Series on Polymer and Composite Materials
ISBN 978-3-319-73167-4 ISBN 978-3-319-73168-1 (eBook)
https://doi.org/10.1007/978-3-319-73168-1

Library of Congress Control Number: 2017962538



Printed on acid-free paper

This Springer imprint is published by the registered company Springer International Publishing AG part of Springer Nature
The registered company address is: Gewerbestrasse 11, 6330 Cham, Switzerland

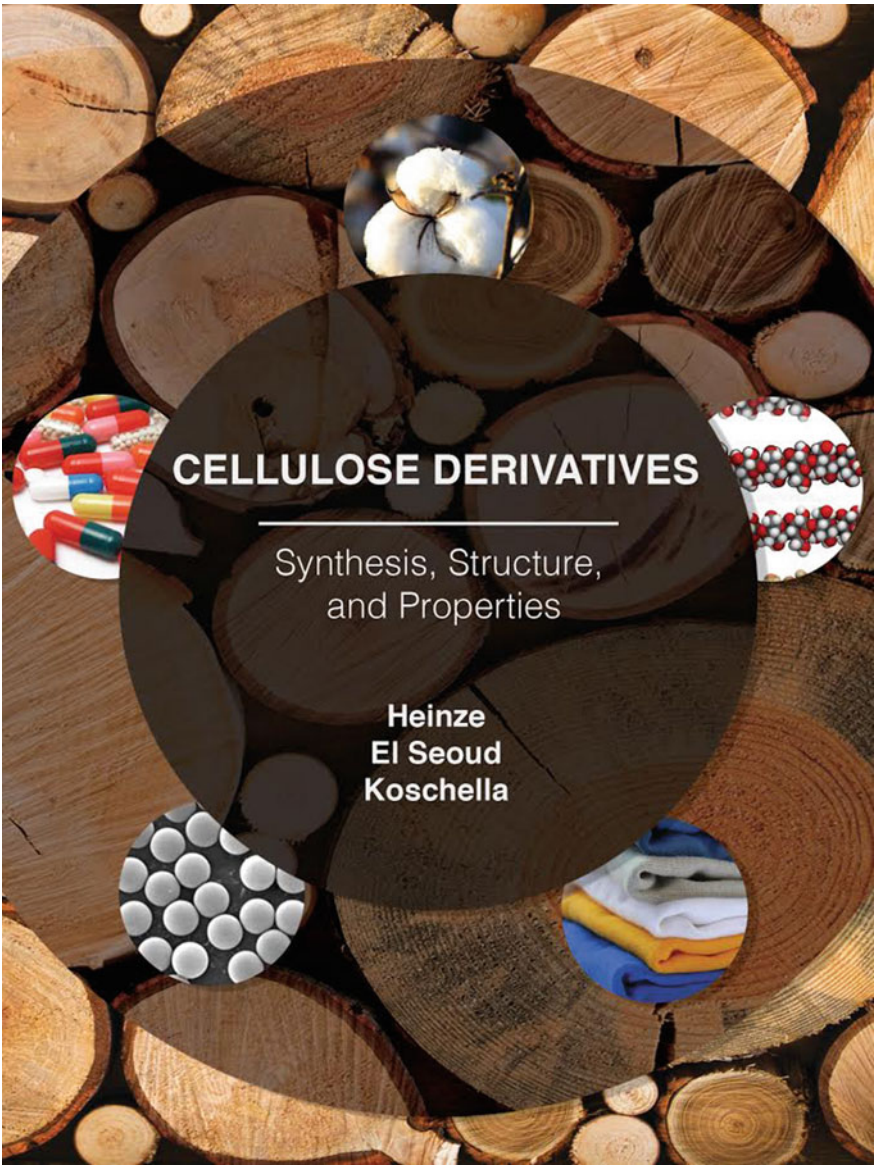
CELLULOSE DERIVATIVES
Synthesis, Structure, and Properties
Heinze
El Seoud
Koschella

*Es ist nicht genug, zu wissen, man muß auch anwenden; es ist nicht genug, zu wollen, man muß auch tun*
*"Knowing is not enough; we must apply. Willing is not enough; we must do"*

Johann Wolfgang von Goethe
(1749–1832)

*We dedicate this work to our families, who supported us enthusiastically all along the birth of this book*

# Preface

The last two decades witnessed an impressive progress in cellulose chemistry, in particular the use of efficient solvents and novel approaches to synthesize derivatives of controlled structures, hence properties and applications. The impetus for this progress is that sustainability became a major concern of the society. Therefore, the use of renewable raw materials, and the production of biodegradable products by atom-efficient, safe routes became major goals, as dictated by the principles of green chemistry. Cellulose is, by far, the most abundant renewable biopolymer. Its derivatives, in particular esters of organic and inorganic acids and ethers are employed on a large scale, because of their favorable chemical/mechanical properties and ready biodegradability.

The recent developments in cellulose chemistry include, *inter alia*: Unconventional methods to synthesize esters and ethers by heterogeneous reaction schemes (for example iodine/carboxylic acid anhydride; cellulose activation by induced phase separation); introduction of novel solvents (electrolytes/dipolar aprotic solvents; base/urea); introduction of ionic liquids; use of radiation energy (microwave and ultrasound) for cellulose dissolution and derivatization; novel approaches to regioselective derivatization of cellulose; preparation of nanoparticles and nanocomposites designed for specific applications, based on cellulose and its derivatives.

Although several review articles were published on some of the above-mentioned themes, there is a clear demand for a summarized, up-to-date and, more importantly, comprehensive discussion of the principles of the above-mentioned new developments. Understanding aspects such as the relationship between cellulose structure and its reactivity, and details of cellulose-solvent interactions is fundamental because achieving process economy dictates that we understand and quantify these aspects at the molecular level.

We wrote this book with these aspects in mind. It is aimed at those who are interested in the organic- and physical organic chemistry of cellulose and its derivatives as well as their applications, including graduate- and advanced undergraduate students. We hope that the latter categories find the material presented both interesting and comprehensive. This book fills an important gap in teaching,

because most organic chemistry textbooks concentrate on the relatively simple chemistry of mono- and disaccharides, with a scant discussion of native carbohydrate polymers and their derivatives, in particular those of cellulose and starch. The lecturer can use the material of this book, e.g., in order to introduce the strategies that are employed for regioselective synthesis of simple sugar derivatives, and to show how these are extended to more complex carbohydrates. Additionally, cellulose esters and ethers constitute an important class of compounds whose life cycle, from synthesis to biodegradation, conform to the principles of green chemistry.

To make reading this book simple, we included a separate part on "Organization of this book", in order to help the reader finding what he is looking for with minimum effort.

## Organization of This Book

We took into account that the background and specific interests of the readers of this book are diverse. Therefore, we divided the chapters in a way that permits the reader to go directly to the subject of his immediate interest. This approach is exemplified by Chap. 2; we have separated the theoretical background of each technique from the corresponding experimental aspects and applications to cellulose and its derivatives. The subject covered by this book is vast; keeping it relatively concise imposes limitation on the volume of the material presented. Where possible, we opted to discuss recent developments, from which the reader has access to older literature.

The first chapter on sources of cellulose is timely, because of the increased use of cellulose obtained from unconventional sources, e.g., bacterial cellulose and that extracted from agricultural residues. The former is finding important biomedical and pharmaceutical applications. We need to find better end-uses (instead of composting and burning) for the large amounts of solid waste that are generated from cotton (stems), rice and wheat (straw) and from the production of bio-fuels, in particular sugarcane bagasse. We give in Chap. 1 a brief introduction to this vast subject (specialized references are listed); we balanced its contents according the scale of production, and the stage of development of cellulose extraction from a particular natural source.

A book on cellulose derivatives is not complete without discussing the biopolymer structural features that control its accessibility, hence successful derivatization. The properties of cellulose depend on its source and methods of extraction from raw materials. Determination of these properties, e.g., average degree of polymerization and index of crystallinity constitutes a standard start to any research on cellulose. On the other hand, the properties, hence applications of cellulose derivatives depend on their molecular structure, in particular, their degree and pattern of substitution within the repeating unit (anhydroglucose), and along the biopolymer backbone. In Chap. 2, we address the determination of these molecular- and structural aspects using a variety

of techniques. For brevity, we restricted our discussion to the fundamental properties necessary to characterize cellulose (average molar mass and index of crystallinity) and its derivatives (average molar mass and substitution patterns). Our strategy to include the determination of the physico-chemical and structural properties of cellulose and its derivatives in a single chapter is coherent because the equipment, experimental procedures, and data manipulations are practically the same for the precursor biopolymer and its derivatives.

The main body of this book is contained in Chaps. 3–7. The former is devoted to "activation and dissolution of cellulose" because proper biopolymer activation is crucial to its derivatization under heterogeneous conditions. A similar activation pretreatment is also important for many cellulose derivatization reactions under homogeneous conditions. In the second part of the same chapter, we address cellulose dissolution, because this is a central step in analysis of cellulose and its derivatives, and for homogeneous derivatization of the biopolymer. Additionally, cellulose is regenerated from these solutions and the regenerated fibers (e.g., Lyocell fibers) are important commercial substitute for Rayon. Cellulose ester solutions, in particular cellulose acetate are regenerated as industrially important fibers and filter tow.

In Chap. 4 we address the basic concepts of cellulose derivatization under heterogeneous and homogeneous reaction conditions with emphasis on the use of protecting groups to achieve regioselective synthesis. We included overviews on the synthesis of cellulose ethers and esters.

The cellulose esters, which we discuss in Chap. 5, cover those commercialized on a large scale, namely esters and mixed esters of lower carboxylic acids (acetic to butyric acid), and cellulose nitrate. Other esters included are those used in regioselective synthesis of cellulose derivatives, e.g., the tosylates, and esters of inorganic acids, namely, borates, carbonates, nitrate, phosphates, sulfates, and carbamates. The latter ester is potentially important for obtaining cellulose fibers via the carbamate process. We discuss the synthesis and properties of industrially important ionic and nonionic ethers of cellulose in Chap. 6, including alkyl and hydroxyl alkyl ethers and carboxymethyl cellulose. We devoted Chap. 7 to miscellaneous cellulose derivatives including those obtained via Huisgen-, thiol-Michael/thiol-ene-, and Diels–Alder reaction. We also included important miscellaneous reactions, e.g., oxidation, dendronization, and grafting.

We hope that the material of this book covers wide and interesting aspects of the chemistry and applications of cellulose and its derivatives. It should increase our interest in using this, and other structurally related carbohydrates (starch, dextran, and other glucans as well as chitin) as a viable platform to a wide variety of new, environmentally friendly products, including fibers and material designed for specific applications, *inter alia*, catalysis, biomedical and separation.

Jena, Germany — Thomas Heinze
São Paulo, Brazil — Omar A. El Seoud
Jena, Germany — Andreas Koschella

# Acknowledgements

We express our gratitude to all persons who supported us in writing this book. In particular, we thank Dr. Tim Liebert and Dr. Martin Gericke for their substantial effort regarding making and evaluating literature reviews as well as for compiling a part of the chapters. We are very thankful to Dr. Martin Gericke for the preparation of Chap. 6 about Cellulose ethers. The members of the Heinze group (Dr. Jan-Markus Teuscher, Dr. Konrad Hotzel, Dipl.-Chem. Robert Hampe, Dipl.-Chem. Peter Schulze, Dipl.-Chem. Christian Achtel) and Dr. Kerstin Jedvert (postdoc) were very helpful in proofreading parts of the manuscript. We thank Gabriel (Gagá) El Seoud for the art work at page V.

We express our gratitude to Springer for agreeing to publish this book and Dr. Arda Alkan for his conscientious effort. O. A. El Seoud thanks FAPESP, CNPq and CAPES-DAAD for travel funds to Jena.

# Contents

# Abbreviations and Symbols

| | |
|---|---|
| %Sw | Percent swelling |
| θ | Scattering angel |
| $\overline{M}$ | Average molar mass, with specifying the type, e.g., number- or weight-average |
| $\overline{M}_n$ | Number-average molar mass |
| $\gamma^{\circ}$ | Shear rate |
| $\overline{M}_V$ | Viscosity-average molar mass |
| $\overline{M}_W$ | Weight-average molar mass |
| $\overline{M}_Z$ | Zeta-average molar mass, calculated from sedimentation in the ultracentrifuge |
| [η] | Intrinsic viscosity |
| 1D | One dimensional |
| 1-PrOH | 1-Propanol |
| 2D | Two dimensional |
| 3D | Three dimensional |
| $A_2$ | Second virial coefficient |
| Abs | Absorbance |
| Ac | Acetyl |
| ADA | Alkylene diamine |
| AE | Aminoethyl |
| AFM | Atomic force microscopy |
| AGU | Anhydroglucose unit |
| Al | Allyl |
| AlBuImCl | 1-(1-butyl)-3-methylimidazolium chloride |
| AlMeImX | 1-allyl-3-methylimidazolium; X is the counter ion, e.g., Cl or Ac |
| AN | Gutman's (electron) acceptor number by the solvent |
| Ara*f* | Arabinofuranose |
| ATR | Attenuated total reflectance |
| ATRP | Atom transfer radical polymerization |

| | |
|---|---|
| AX | Arabinoxylan |
| b.p. | Boiling point |
| BC | Bacterial cellulose |
| BET | Brunauer, Emmett, Teller surface adsorption equation employed for the determination of the surface area of solids |
| BJH | Barrett–Joyner–Halenda surface adsorption equation employed for the determination of the surface area of solids |
| BMAF-0.1 $H_2O$ | Dibenzyldimethylammonium fluoride with 0.1 mol of water of hydration |
| Bu | 1-Butyl |
| Bu-2,3-$Me_2$ImCl | 1-(1-Butyl)-2,3-dimethylimidazolium chloride) |
| BuMeIm$BF_4$ | 1-(1-Butyl)-3-methylimidazolium tertafluoroborate |
| BuMeImCl | 1-(1-butyl)-3-methylimidazolium chloride |
| BuPyAc | *N*-(1-Butyl)pyridinium acetate |
| c | Concentration |
| CA | Cellulose acetate |
| CAB | Cellulose acetate butyrate mixed ester |
| Cadoxen | Cadmium triethylenediamine dihydroxide |
| CAP | Cellulose acetate propionate mixed ester |
| CAPh | Cellulose acetate phthalate mixed ester |
| CC | Cellulose carbamate |
| CCOA | Carbazole-9-carboxylic acid [2-(2-aminooxyethoxy)ethoxy] amide |
| CD | Circular dichromism |
| CDA | Cellulose diacetate |
| CDI | Carbonyldiimidazole |
| CE | Capillary electrophoresis |
| CHPTMA | (3-Chloro-2-hydroxypropyl) trimethylammonium |
| CI | Chemical ionization |
| CID | Collision induced dissociation |
| CIS | Coordination-induced shift |
| Clb | Cellobioside |
| CM | Carboxymethyl group |
| CMA | Cellulose monoacetate |
| CMC | Carboxymethyl cellulose |
| CMG | Carboxymethyl glucose |
| CN | Cellulose nitrate |
| COSY | Correlation spectroscopy |
| CP/MAS | Cross-polarization magic angle spinning |
| CPhos | Cellulose phosphate |
| CS | Cellulose half-ester of sulfuric acid (commonly known as cellulose sulfate) |
| CSP | Chiral stationary phase |
| CT | Charge transfer, or Cellulose tosylate |
| CTA | Cellulose triacetate |

| | |
|---|---|
| CTC | Cellulose tricarbanilate |
| CTs | Cellulose tosylate (4-toluene sulfonate) |
| CuAAC | Copper(I)-catalyzed Azide-Alkyne Cycloaddition |
| Cuam | Cuprammonium hydroxide |
| Cuen | Cupriethylene diamine |
| D | Translational diffusion coefficient, |
| DA | Derivatizing agent |
| DAC | Dialdehyde cellulose |
| DADMAC | Diallyldimethylammonium chloride |
| DAS | Dipolar aprotic solvent |
| DBU | 1,8-Diazabicyclo[5.4.0]undec-7-ene |
| DCA | Dicyanamide $(CN)_2N^-$ |
| DCC | Dicyclohexylcarbodiimide, or dicarbonyl cellulose |
| DCE | 1,2-Dichloroethane |
| DCM | Dichloromethane |
| DEAE | Diethylaminoethyl |
| DEEPA | *N,N*-diethylepoxypropylamine |
| DEPT | Distortionless enhancement by polarization transfer |
| DGT | Diffusive gradients in thin films technique |
| DHB | 2,5-Dihydroxybenzoic acid |
| DMAc/LiCl | Solution of LiCl in *N,N*-Dimethylacetamide |
| DMAc | *N,N*-Dimethylacetamide |
| DMAP | 4-*N,N*-Dimethylaminopyridine |
| DMF | *N,N*-Dimethylformamide |
| DMI | 1,3-Dimethyl-2-imidazolidinone |
| DMPA | Dimethylpropylamine |
| DMSO | Dimethylsulfoxide |
| DN | Gutmann's donor number |
| DNA | Deoxyribonucleic acid |
| DOSY | Diffusion ordered spectroscopy |
| DP | Degree of polymerization |
| DPA | Days post-anthesis |
| $DP_w$ | Weight average degree of polymerization |
| DRIFTS | Diffuse Reflectance Infrared Fourier Transform Spectroscopy |
| DS | Average degree of substitution |
| $DS_{Ac}$ | Average degree of substitution of acetyl groups |
| $DS_{Acyl}$ | Average degree of substitution of acyl groups |
| DSC | Differential scanning calorimetry |
| $DS_{CM}$ | Average degree of substitution of carboxymethyl groups |
| $DS_{Me}$ | Average degree of substitution of methyl groups |
| DTA | Differential thermal analysis |
| DTGA | Differential thermal gravimetric analysis |
| EC | Ethyl cellulose |
| ECM | Extracellular matrix |

| | |
|---|---|
| EDA | Ethylene diamine |
| EDC | 1-Ethyl-3-(3-dimethylaminopropyl) carbodiimide |
| $E_{flow}$ | Activation energy for viscous flow |
| EHEC | Ethylhydroxyethyl cellulose |
| EHPC | Ethylhydroxypropyl cellulose |
| EI | Electron impact |
| EI-MS | Electron impact mass spectrometry |
| en | Ethylene diamine (complex ligand) |
| EPTMA | 2,3-(Epoxypropyl) trimethylammonium |
| ESI | Electrospray ionization |
| ESW | Excess surface work |
| $E_T$(probe) | Empirical solvent (overall) polarity scale, based on use of solvatochromic probes |
| Et | Ethyl |
| $Et_3OctNCl$ | Triethyloctylammonium chloride |
| EtMeImAc | Ethylmethylimidazolium acetate |
| $EtMeImBF_4$ | Ethylmethylimidazolium tetrafluoroborate |
| EWG | Electron withdrawing group |
| FAB-MS | Fast atom bombardment mass spectroscopy |
| FeTNa | Ferric tartaric acid sodium salt |
| FID | Flame ionization detector |
| FTIR | Fourier-transform infrared |
| $G(\tau)$ | Auto-correlation function |
| G | Shear modulus |
| GC | Gas chromatography |
| GC-FID | Gas chromatography with flame ionization detector |
| GC-MS | Gas chromatography mass spectrometry |
| GLC | Gas liquid chromatography |
| Glc | Glucose |
| GPC | Gel-permeation chromatography |
| GX | 4-*O*-Methylglucurono xylan |
| $H_0$ | Magnetic field, magnetic field strength |
| HCCA | α-Cyano-4-hydroxycinnamic acid |
| HE | Hydroxyethyl |
| HEC | Hydroxyethyl cellulose |
| HMBC | Heteronuclear multiple bond correlation |
| HMDS | 1,1,1,3,3,3-Hexamethyldisilazane |
| HMPA | Hexamethylphosphotriamide |
| HP | Hydroxypropyl |
| HPAEC/PAD | High-pH anion-exchange chromatography with pulsed detection |
| HPC | Hydroxypropyl cellulose |
| HPLC | High performance liquid chromatography |
| HPLC-MS | High performance liquid chromatography mass spectrometry |

| | |
|---|---|
| HPMC | Hydroxypropylmethyl cellulose |
| HPTMA | Hydroxypropyltrimethylammonium |
| HRS | Homogeneous reaction scheme |
| HSQC | Heteronuclear single quantum coherence |
| Hx | Hexyl |
| $HxMeImN(TFMS)_2$ | 1-(1-Hexyl)-3-methylimidazolium bis(trifluoromethane) sulfonimide |
| $I_c$ | Index of crystallinity |
| IL | Ionic liquid |
| Im | Imidazole |
| INADEQUATE | Incredible natural abundance double quantum transfer experiment |
| IR | Infrared |
| ISV | Iodine sorption value |
| $k_H$ | Huggins constant |
| $K_{SEC}$ | SEC, fraction of the stationary phase that is available to the solute |
| LALLS | Low-angle laser light scattering |
| LB | Langmuir-Blodgett |
| LCST | Lower critical solution temperature |
| LODP | Leveling-off degree of polymerization |
| LS | Light-scattering |
| LVDT | Linear variable differential transformer |
| Lyocell | Generic name for regenerated cellulose fibers from aqueous NMMO bath |
| $M_\infty$ | Sorbate mass at equilibrium |
| *M* | Molar mass of |
| MALDI | matrix assisted laser desorption ionization |
| MALS | Multi-angle light-scattering detector for light scattering |
| MAS | Magic angle spinning |
| MC | Methyl cellulose |
| MCC | Microcrystalline cellulose |
| M-Cellulose | Mercerized cellulose. Similarly, M-cotton, M-eucalyptus refer to the corresponding mercerized celluloses |
| Me | Methyl |
| $Me_2ImCl$ | 1,3-Dimethylimidazolium chloride |
| $Me_2PMBr_2$ | 2,6-Dibromo-4-(*E*)-2-1(1-methylpyridinium-4-yl)ethenyl] phenolate |
| MeCN | Acetonitrile |
| MeGa | 4-*O*-Methyl-α-D-glucopyranosyl uronic acid |
| MeOH | Methanol |
| Me-β-D-clb | Methyl-β-D-cellobioside |
| Me-α-D-Glc*p* | Methyl-α-D-glucopyranoside |
| MFC | Microfibrillated cellulose |
| MHEC | Methylhydroxyethyl cellulose |

| | |
|---|---|
| MHPC | Methylhydroxypropyl cellulose |
| $M_i$ | molecular weight of polymer repeating unit |
| MM | Molar mass of |
| $M_{mol}$ | Molar mass of sorbate |
| MNP | Magnetic nanoparticles |
| MS | Molar substitution, or mass spectrometry |
| $MS_{HE}$ | Molar substitution of hydroxyethyl groups |
| $MS_{HP}$ | Molar substitution of hydroxypropyl groups |
| MW | Microwave |
| $N(TFMS)_2$ | Bis(trifluoromethanesulfonyl)imide anion; $(F_3CSO_2)_2N^-$ |
| n | Refractive index |
| $n_{ads}$ | Number of adsorbed molecules |
| $N_{agg}$ | Average aggregation number |
| $N_{Av}$ | Avogadro's number |
| n-BuOEtOH | n-Butoxyethanol |
| Nc | Number of carbons of carboxylic acid anhydride, or number of carbon atoms in a derivative of cellulose. For esters, this number includes the acyl carbon |
| Nd-YAG | Neodym-Yttrium-Aluminium-garnet |
| NFC | Nanofibrillated cellulose |
| NHS | *N*-Hydroxysuccinimide |
| $n_i$ | Number of polymer repeating units |
| NIR | Near infrared |
| Ni-tren | Nickel tris(2aminomethyl)amine |
| NMMO | *N*-Methylmorpholine-*N*-oxide |
| NMP | *N*-Methyl-2-pyrrolidinone |
| NMR | Nuclear magnetic resonance |
| NOE | Nuclear Overhauser effect |
| NOESY | Nuclear Overhauser enhancement spectroscopy |
| NS | Not specified |
| $nS_w$ | Moles of solvent molecules per mole AGU |
| Oc | 1-Octyl group |
| $P_\theta$ | Zimm scattering function (scattering factor) |
| P; Pa s; mPa s | Poise, Pascal-second, milli Pascal-second, respectively, units of viscosity |
| PAMAM | Polyamidoamino |
| PBA | Phenylboronic acid |
| PCS | Photon correlation spectroscopy |
| PDA | 1,4-phenylenediamine |
| PEC | Polyelectrolyte complexes formed, usually, between polyelectrolytes of opposite charges, e.g., CS and polyDADMAC |
| PEI | poly(ethylene imine) |
| PET | Polyethylene terephthalate |
| PI | Polymer polydispersity index |

| | |
|---|---|
| $pK_a$ | - lg (acid dissociation constant) |
| Pr | 1-Propyl |
| pren | 1,3-Diamino propane (complex ligand) |
| PS/DVB | Porous, cross-linked polystyrene/divinylbenzene gel |
| PSS | Poly(styrene sulfonate) |
| PTFE | Poly(tetrafluoroethylene) |
| Py | Pyridine |
| PyCIMS | Pyrolysis ammonia chemical ionization mass spectroscopy |
| QELS | Quasi-elastic light scattering |
| $R_\theta$ | Rayleigh ratio |
| R | Universal gas constant |
| R10 | Insoluble in 10% aqueous NaOH |
| R18 | Insoluble in 18% aqueous NaOH |
| $R_4NF\text{-}xH_2O$ | General formula for the hydrate of a quaternary ammonium fluoride |
| RAFT | Reversible addition-fragmentation chain transfer |
| RFDR | Radio frequency driven dipolar recoupling |
| $R_g$ | Radius of gyration of a scattering particle |
| $R_h$ | Hydrodynamic radius of a scattering particle |
| RH | Relative humidity of the atmosphere above a cellulosic material |
| ROESY | Rotating frame Overhauser effect spectroscopy |
| ROP | Ring opening polymerization |
| RT | Room temperature |
| RTIL | Room temperature ionic liquid |
| RU | Repeating unit |
| SA | Lewis solvent acidity |
| SAM | Self-assembled monolayer |
| SANS | Small angle neutron scattering |
| SB | Lewis solvent basicity |
| $SC\text{-}CO_2$ | Super critical carbon dioxide |
| SD | Solvent dipolarity |
| SDO | Spectroscopic degree of order |
| SDS | Sodium dodecylsulfate |
| SE | Strong electrolyte |
| SEC | Size exclusion chromatography |
| SEM | Scanning electron microscopy |
| SLS | Static light scattering |
| $S_N$ | Nucleophilic substitution |
| SP | Solvent polarizability |
| T | Absolute temperature |
| t | Time |
| $T_1$ | NMR longitudinal relaxation time |
| $T_2$ | NMR transverse relaxation time |
| TA | Thermal analysis |

| | |
|---|---|
| TAAF-$H_2O$ | Tetraalkylammonium fluoride monohydrate |
| TBAFx3$H_2O$ | Tetra(n-butyl)ammonium fluoride. The crystalline electrolyte is, *nominally*, the trihydrate |
| TBD | 1,5,7-Triazabicyclo[4.4.0]dec-5-ene |
| TBDMS | Tertiarybutyldimethylsilyl, tert.-butyldimethylsilyl |
| TBP | Triphenylboroxole |
| t-BuOH | Tert.-Butanol |
| $T_{Decomp}$ | Decomposition temperature of a polymer in TA analysis |
| TDMS | Tertiaryhexyldimethylsilyl, thexyldimethylsilyl |
| TEA | Triethylamine |
| TEM | Transmission electron microscopy |
| TEMPO | 2,2,6,6-Tetramethylpiperidine-*N*-oxyl |
| TFA | Trifluoroacetic acid |
| TFAA | Trifluoroacetic acid anhydride |
| TFMSA | Trifluoromethanesulfonyl azide |
| $T_g$ | Glass transition temperature |
| TG | Thermogravimetry |
| TGA | Thermogravimetric analysis |
| THF | Tetrahydrofuran |
| $T_m$ | Melting point, including polymers |
| TMA | Thermomechanical analysis |
| TMAF | Tetramethylammonium fluoride |
| TMDP | 2-Chloro-4,4,5,5-tetramethyl-1,3,2-dioxaphospholane |
| TMS | Trimethylsilyl group |
| TMSC | Trimethylsilyl cellulose |
| TMSCl | Trimethylsilyl chloride |
| TOCSY | Total correlation spectroscopy |
| TOF | Time of flight |
| ToF-SIMS | Time-of-Flight Secondary Ion Mass Spectrometry |
| TPB | Triphenylboroxole |
| tren | tris(2-Aminoethyl)amine (complex ligand) |
| Trityl | Triphenylmethyl |
| TsCl | Tosyl chloride or 4-toluenesulfonyl chloride |
| UDP-glucose | Uridine diphosphoglucose |
| UV | Ultraviolet |
| UV-vis | Ultraviolet-Visible |
| $V_h$ | SEC; Hydrodynamic volume of the solute |
| $V_i$ | SEC; Solvent volume within the gel particles, |
| Vo | SEC; Void volume of the solvent between porous gel particles |
| $V_s$ | Molar volume |
| $W_{(crystalline)}$ | Absolute crystalline weight fraction |
| WAXD | Wide angle X-ray diffraction |
| WAXS | Wide angle X-ray scattering |
| $W_{B,\ freezing}$ | Bound, freezing water in cellulose |

| | |
|---|---|
| $W_{B,\ non\text{-}freezing}$ | Bound, non-freezing water in cellulose |
| $W_{F,\ freezing}$ | Free, freezing water in cellulose; also referred to as freezing water |
| $w_i$ | Weight of polymer repeating unit |
| WRV | Water retention value |
| $W_{Total}$ | Total amount of water present in a cellulosic material |
| $x_c$ | Degree of crystallinity |
| XPS | X-ray photoelectron spectroscopy |
| Xyl*p* | Xylopyranose |
| $2\theta$ | Diffraction angel |
| $\Delta G_{Dissolution}$ | Change of free dissolution energy |
| $\Delta H_{Dissolution}$ | Change of dissolution enthalpy |
| $\Delta S_{Dissolution}$ | Change of dissolution entropy |
| $\Delta\mu$ | Change of the chemical potential |
| $\alpha_S$ | Solvent Lewis acidity |
| $\beta_S$ | Solvent Lewis basicity |
| $\delta_D$ | van der Waals dispersion force |
| $\delta_H$ | Hydrogen-bonding |
| $\delta_{Hildebrand}$ | Hildebrand's solubility parameter |
| $\delta_P$ | Keesom's dipole interactions |
| $\eta$ | Dynamic viscosity of the solution |
| $\eta_0$ | Dynamic viscosity of the solvent |
| $\eta_{apparent}$ | Apparent viscosity |
| $\eta_p$ | Plastic viscosity, Bingham viscosity |
| $\eta_{red}$ | Reduced viscosity |
| $\lambda_{max}$ | Wavelength of maximum absorption |
| $\pi^*_S$ | Solvent dipolarity/polarizability |
| $\rho$ | Density |
| $\sigma_{12}$ | Stress in 1-2-direction |
| $\tau$ | Shear stress |

# Chapter 1
# Production and Characteristics of Cellulose from Different Sources

Cellulose constitutes the most abundant renewable polymer resource available world-wide. It has been estimated that by photosynthesis, $10^{11} - 10^{12}$ t are synthesized annually in a rather pure form, for example in the seed hairs of the cotton plant, but mostly cellulose is combined with lignin and other polysaccharides (hemicelluloses) in the cell wall of woody plants [1]. Although the primary occurrence of cellulose is the existing material in forests with wood as the most important source, cellulose-containing materials include agricultural residues, water plants, grasses, and other plant substances. Besides cellulose, they contain hemicelluloses, lignins, and comparable small amounts of extractives (Table 1.1) [2]. Commercial cellulose production concentrates on harvested sources such as wood or on naturally highly pure sources such as cotton.

Production of cellulose by several bacteria of the genera *Acetobacter, Agrobacterium, Sarcina, Rhizobium* gains some importance [9, 10]. The bacterial cellulose (BC) is generally very pure (contains no lignin and hemicelluloses), highly crystalline, and possesses high degree of polymerization (DP) values.

Algae (*Valonia ventricosa, Chaetamorpha melagonicum*) are another source of cellulose of very high crystallinity that was used to study the polymorphs of the biopolymer (see Chap. 2). Cellulose of the *Valonia* type is found also in fungal cell walls. In addition, there are several celluloses of animal origin, of which tunican, a cell wall component of ascidians, has been extensively studied.

The de novo synthesis of cellulose was realized by ring-opening polymerization of 3,6-di-*O*-benzyl-α-D-glucopyranose-1,2,4-orthopivalate and subsequent complete deprotection [11] and by stepwise reactions of selectively protected β-D-glucose as, e.g., 1-allyl-2,6-di-*O*-acetyl-3-benzyl-4-*O*-(*p*-methoxybenzyl)-β-D-glucopyranoside [12]. Although the cellulose samples obtained possess a rather low DP of max. 50, which depends on the protecting groups applied, the strategy has recently become important for the preparation of model compounds with controlled sequence and position of functionalization that are very helpful in analysis and the determination of structure-property-relationships [11]. This approach can be used to



T. Heinze et al., *Cellulose Derivatives*, Springer Series on Polymer and Composite Materials, https://doi.org/10.1007/978-3-319-73168-1_1

**Table 1.1** Chemical composition of some typical cellulose containing materials (adapted from [2])

| Source | Composition (%) | | | |
|---|---|---|---|---|
| | Cellulose | Hemicellulose | Lignin | Extract |
| Hardwood | 43–47 | 23–25 | 16–24 | 2–8 |
| North American hardwood [3] | 66–67 | 17–21 | 20–36 | 3–6 |
| Softwood | 40–44 | 25–29 | 25–32 | 1–5 |
| Bagasse | 40 | 30 | 20 | 10 |
| Corn cobs | 45 | 35 | 15 | 5 |
| Corn stalks | 35 | 25 | 35 | 5 |
| Corn stalks [4] | 35–45 | 25 | 17–21 | 4–7 |
| Cotton | 95 | 2 | 1 | 0.4 |
| Flax (retted) | 71 | 21 | 2 | 6 |
| Flax (unretted) | 63 | 12 | 3 | 13 |
| Hemp | 70 | 22 | 6 | 2 |
| Henequen | 78 | 4–8 | 13 | 4 |
| Jute | 71 | 14 | 13 | 2 |
| Kenaf | 36 | 21 | 18 | 2 |
| Ramie | 76 | 17 | 1 | 6 |
| Rice straw [5] | 43 | 33 | 20 | <1 |
| Sisal | 73 | 14 | 11 | 2 |
| Sisal fibers [7] | 73 | 13 | 11 | <2 |
| Sugarcane bagasse [6] | 45–55 | 20–25 | 18–24 | >1 |
| Wheat straw [8] | 58–73 | 25–31 | 16–23 | 3–5.8 |
| Wheat straw | 30 | 50 | 15 | 5 |

synthesize cellulose derivatives with a regioselective functionalization pattern [13] and even with block copolymer structures (see Chap. 4) [14].

The non-biosynthetic preparation of cellulose was carried out with β-D-cellobiosyl fluoride as the substrate for purified cellulose in a mixture of acetonitrile and acetate buffer at pH 5 [15, 16]. The DP of the samples is about 40. This approach is quite interesting from a scientific point of view, but will not open up novel sources for cellulose.

## 1.1 Plant Cellulose

### *1.1.1 Cellulose from Conventional Sources*

#### 1.1.1.1 Wood

The formation of wood by cell wall biogenesis proceeds in aqueous media even though the principle component of the cell wall, cellulose, is water insoluble. The

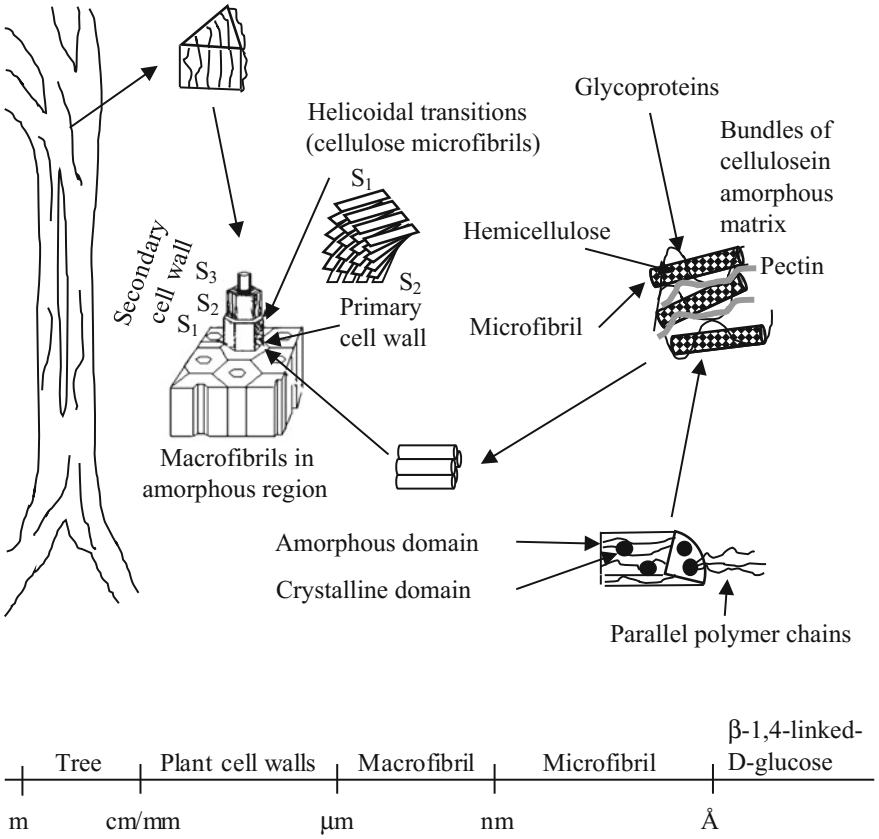


**Fig. 1.1** The hierarchical structure of wood (adapted from [17])

fundamental incompatibility between coil-like lignin and rod-like cellulose fibers is overcome through a hierarchical assembly (Fig. 1.1) whereby hemicelluloses assemble at the cellulose/lignin interface.

Hemicelluloses are known to occur in several structural varieties in terrestrial plants and algae and, even in different plant tissues, within one plant. Xylan-type polysaccharides are the most frequently occurring hemicelluloses (Fig. 1.2, [18]). Xylans of all higher plants possess ß-(1 → 4) linked xylopyranose (Xyl*p*) units as the backbone, usually substituted with sugar units and *O*-acetyl groups. In the wood of deciduous trees, only the 4-*O*-methyl-glucuronoxylan (GX) type (Fig. 1.2a) was found to be present, which contains single side chains of 2-linked 4-*O*-methyl-α-D-glucopyranosyl uronic acid (MeGA) units. The xylose to MeGA ratios of GX isolated from different hardwoods range from 4 to 16:1. Arabino(glucurono)xylan types, containing single side chains of 2-*O*-linked α-D-glucopyranosyl uronic acid units and/or its 4-*O*-methyl derivative and 3-linked α-L-arabinofuranosyl (Ara*f*) units (Fig. 1.2b), are typical of softwoods and the lignified tissues of grasses and

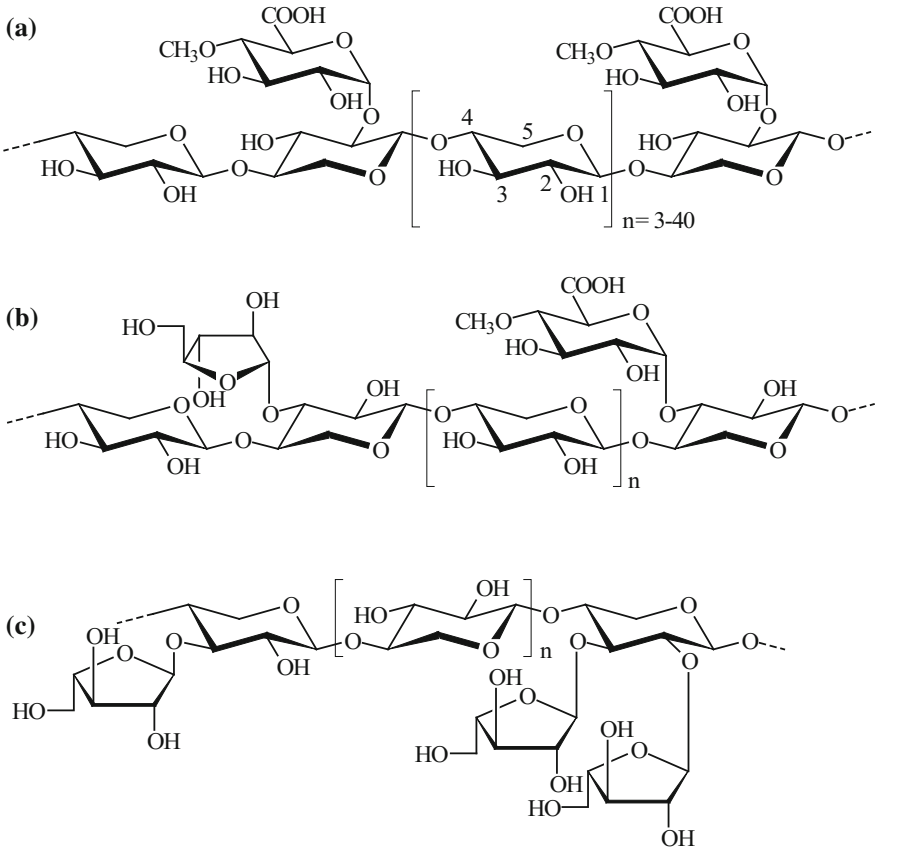


**Fig. 1.2** Structures of **a** 4-*O*-methylglucuronoxylan, **b** arabino-(glucurono)-xylan, and **c** arabinoxylan (Reprinted from [19] with permission of Springer)

annual plants. Highly branched water soluble arabinoxylans (AX, Fig. 1.2c) differing in frequency and distribution of mono- and disubstituted Xyl*p* residues, are present in the endospermic as well as pericarp tissues. The DP of xylans is in the range from 100 to 200. In coniferous trees mannans are predominant containing mannose, glucose, and galactose acetylated to a various extent. A typical glucomannan from softwood is depicted in Fig. 1.3.

Lignin is a complex three-dimensional network of aromatic building blocks with a variety of linkages. Besides covalent bonds between aromatic units, carbon-carbon single and double bonds are present as well as carbon-oxygen linkages. Depending on the type of wood, the structure is a phenylpropanoide formed from different amounts of paracoumaryl alcohol, coniferyl alcohol and sinapyl alcohol (Fig. 1.4). Thus, the major structural elements are benzene rings, propane chains, hydroxy- and alkoxy-moieties. Due to the extended network, the molecular weight of native lignin can be several million g/mol [20].

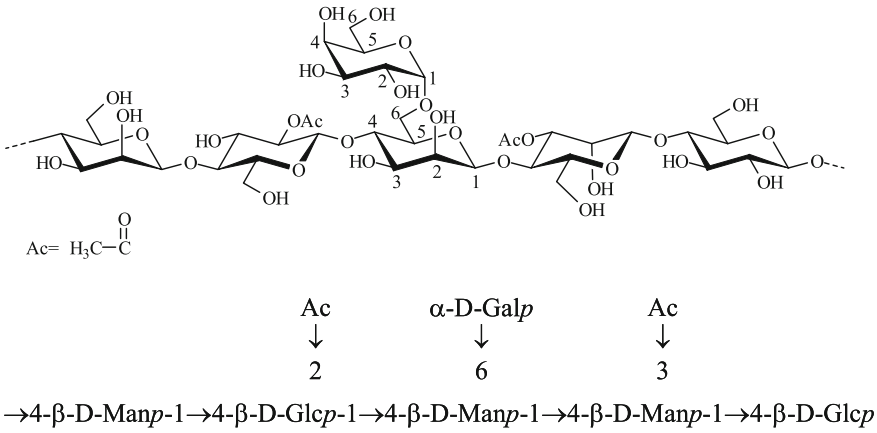


**Fig. 1.3** Molecular structure of a softwood glucomannan (reprinted from [19] with permission of Springer)

To liberate the cellulose fibers, either mechanical or chemical treatments, so-called pulping processes, must be applied. Mechanical pulping involves the treatment of wood with steam prior to separation into fibrous material by abrasive refining or grinding. Chemical pulping relies mainly on chemical reactants and heat to dissolve the lignin and other substances of the plant material, followed by mechanical refining to separate the fibers. Both processes are predominantly carried out to produce industrially the fiber material, paper grade pulp that is re-assembled as a structural network for the manufacture of paper (Table 1.2) [21]. The annual global pulp production reached a value of more than $4 \times 10^8$ t in 2010 [23].

For cellulose shaping and production of cellulose derivatives, pulp of high purity must be employed (Table 1.2). The dissolving grade pulp represents a specialty pulp that is chemically refined by bleaching and is composed of more than 90% of pure cellulose (α-cellulose, which is the material insoluble in 17.5% aqueous NaOH, see Chap. 3). The processes to produce dissolving pulp are the dominant sulfite process (content of α-cellulose about 90–92%) and prehydrolysis kraft pulp process (content of α-cellulose of up to 94–96%). Special alkaline treatment can even yield pulps of α-cellulose content of up to 98%; the alkali-soluble hemicelluloses are removed, i.e., alkali-soluble degraded cellulose and heteropolysaccharides like degraded xylans and mannans are removed. Wood-derived cellulose accounts for about 85–88% of dissolving pulp; the rest is cotton linters.

Briefly, in the sulfite process the wood chips are treated with hydrogen sulfite ($Ca^{2+}$, $Mg^{2+}$, $Na^+$, or $NH_4^+$ salt) and sulfur dioxide under pressure at elevated temperature (cooking process). The degree of delignification depends on the concentration of $[H^+] \times [HSO_3^-]$, while the $[H^+]$ concentration affects the rate of cellulose hydrolysis (i.e., decrease of DP). Depending on the progress of cooking, the composition both of bound $SO_2$ ($HSO_3^-$) and protons changes according to the equilibrium:

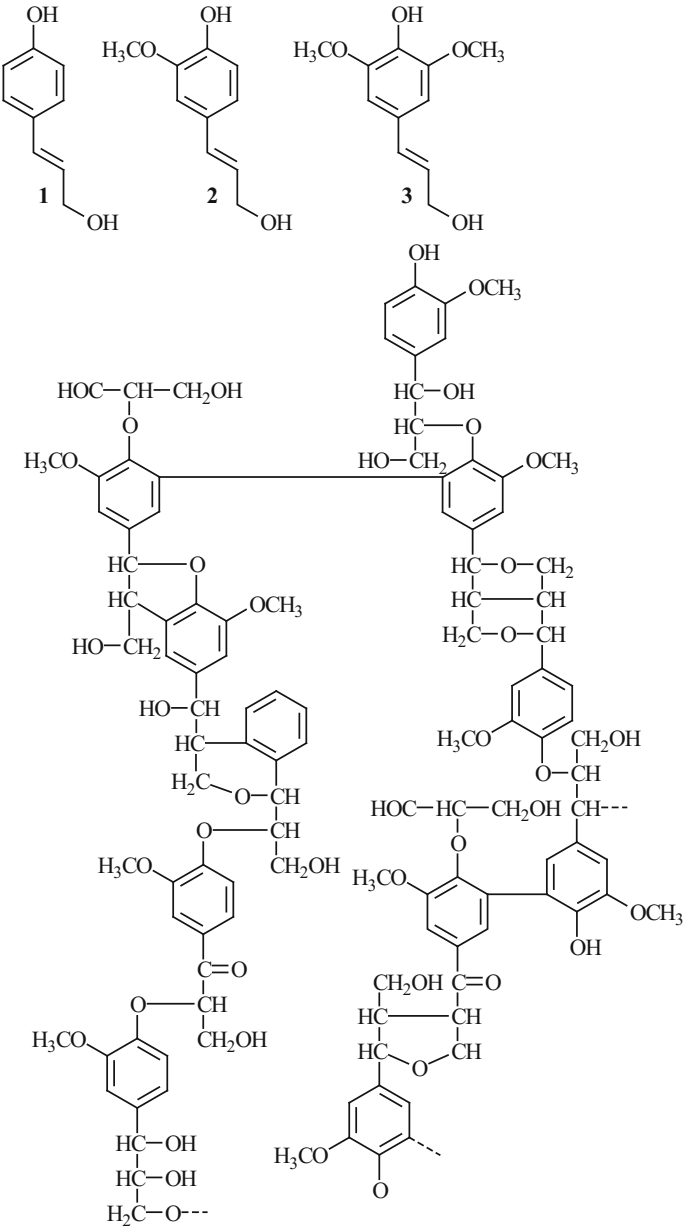


**Fig. 1.4** The basic building units of lignin paracoumaryl alcohol (**1**), coniferyl alcohol (**2**) and sinapyl alcohol (**3**) and a segment of a generalized lignin structure

**Table 1.2** Carbohydrate composition, α-cellulose content, average degree of polymerization (DP), and degree of crystallinity ($x_c$) of some cellulose samples

| Sample | Producer | Carbohydrate composition[a] (%) | | | α-Cellulose (%) | DP | $x_c^b$ (%) |
|---|---|---|---|---|---|---|---|
| | | Glucose | Mannose | Xylose | | | |
| Sulfate pulp V-60 | Buckeye[c] | 95.3 | 1.6 | 3.1 | – | 800 | 54 |
| Sulfate pulp A-60 | Buckeye[c] | 96.0 | 1.8 | 2.2 | – | 2000 | 52 |
| Sulfite pulp 5-V-5 | Borregaard[c] | 95.5 | 2.0 | 2.5 | – | 800 | 54 |
| MoDo | Mo och Domsjö | n.a. | – | – | 93.5[d] | 611 | n.a. |
| Sappi | Sappi | n.a. | – | – | 94.1[d] | 514 | n.a. |
| BaCell | Bahia Pulp S. A. | n.a. | – | – | 95.2[d] | 540 | n.a. |
| Alistaple | Western Pulp | n.a. | – | – | 94.9[d] | 1168 | n.a. |
| Cordenka | Cordenka | n.a. | – | -. | 98.2[d] | 859 | n.a. |
| Rosental Kraft | Mercer | n.a. | – | – | 89.5[d] | 881 | n.a. |
| BWL Hyosung | Hyosung | n.a. | – | – | 94.7[d] | 623 | |
| Ethenier F-HV | Rayonier | n.a. | – | – | 93.7[d] | 1246 | |

[a]Determined by acid hydrolysis and chromatography, data kindly provided by J. Puls, Bundesforschungsanstalt für Forst- und Holzwirtschaft, Hamburg, Germany (n.a. not available)
[b]Determined by X-ray analysis [22], data kindly provided by H.-P. Fink, Fraunhofer Institute of Applied Polymer Research, Teltow, Germany (-: n.a.)
[c]Buckeye Cellulose Corp., 1001 Tillman Street, Memphis/Tennessee 38108-0407, U.S.; Borregaard ChemCell, P.O. Box 162, N-1701 Sarpsborg, Norway; Sappi International Head Office, 154 Chaussée de la Hulpe, Brussels, B-1170, Belgium; Bahia Specialty Cellulose, Rua Alfa 1033, AIN-Complexo Industrial de Camacari, Camacari, 42810-290, Brazil; Western Pulp, Corporate Office, 5025 SW Hout St., Corvallis, OR 97333, U.S.; CORDENKA GmbH, Industrie Center Obernburg, D-63784 Obernburg, Germany, Mercer Pulp Sales GmbH, Charlottenstraße 59, D-10117 Berlin, Germany; Hyosung Corporation, Head Office, Hyosung Bldg. 450 Gongdeok-dong, Mapo-gu, Seoul (121–720), Korea
[d]Cellulose not soluble in 17.5% (w/v) NaOH in water

$$SO_2 + H_2O \rightleftharpoons H_2SO_3 \rightleftharpoons HSO_3^{\ominus} + H^{\oplus}$$

Depending on the detailed conditions, sulfonation of lignin (under acidic conditions) renders the biopolymer soluble in the cooking liquor. Moreover, hydrolysis of linkages between lignin and carbohydrates and also of inter-lignin bonds (see Fig. 1.4) takes place although somewhat slower than the sulfonation [24].

The prehydrolysis kraft pulping consists of treatment of the wood chips under acidic conditions that may be carried out with water, with dilute acid (0.3–0.5% aqueous sulfuric acid), or with rather concentrated aqueous hydrogen chloride (20–30%) at different temperatures (160–180, 120–140, and 40 °C, respectively).

Applying water, the cleavage of the acetic acid esters at the xylan occurs that leads to an autocatalytic hydrolysis process. The prehydrolysis prior to kraft pulping is solely carried out without the addition of mineral acids at present [25]. Subsequently, the material is treated with an aqueous solution of sodium hydroxide and sodium sulfide denoted as white liquor at elevated temperature until the desired delignification is reached. Details about the processes are comprehensively discussed as well as various alternatives to produce dissolving grade pulp are reviewed in the excellent book of Sixta et al. [25]. The content of residual lignin in dissolving pulps is generally very low. The kappa number is typically between 0.2 and 0.5 units meaning a lignin content of 0.05% [26]. More important are the remaining hemicelluloses (i.e., alkali-soluble cellulose of low DP and heteropolysaccharides) that may influence the reactivity and processability as well as the properties of the final product. The extent of extraction of this short-chain material by hot and cold caustic soda contributes to a considerable increase in production costs, mainly due to the high yield loss and high chemical charges. Consequently, the purification is adjusted to the demand, i.e., the dissolving pulp is characterized by R18- and R10 values (see Chap. 3.2) in the range from 93 to 98% and 88 to 98%, respectively.

Dissolving pulps possess $DP_W$ values of up to 4750 (for commercial ethers of ultra high solution viscosity), 1400–1800 (for Viscose production) and 2100 (for cellulose acetate manufacture). In 2003, about $3.65 \times 10^6$ t of dissolving pulp were commercially used to produce cellulose derivatives, for regeneration of cellulose to fibers, sponges, and films as well as for the production of microcrystalline cellulose (see Sect. 1.3.1). There are various other dissolving pulps on the market that represent typical cellulose properties and are very useful starting material for cellulose derivatization (see Table 1.2). Recent developments concerning the isolation of cellulose from plant material, such as the organosolv process or steam explosion will be discussed for cellulose from alternative sources (Sect. 1.1.2).

#### 1.1.1.2 Cotton Linters

The cotton plant—botanically *Gossypium*—is an annual shrub, which is grown in the subtropical and tropical regions of North and South of the equator. The cotton flowers seed capsules consist of 30–40 oil-containing seeds. As schematically shown in Fig. 1.5, each cotton seed is capable of producing about 5000 up to 20,000 single seed hairs, the cotton fibers [27]. Basically, it is distinguished between lint and linters. The lint (staple cotton) is the long-fiber population. The short and thick-walled fibers of the fuzz are known as cotton linters [28–30].

Although the main purpose for growing cotton was and still is to gain the staple cotton fiber (lint) for textile industry (global production for 2008/09 is about 2.4–$2.5 \times 10^7$ metric tons of staple cotton), cotton linters are an important by-product regarded as a valuable cellulose raw material for paper manufacture, for cellulose derivatization and for the production of regenerated fibers both in technical- and lab-scale processes.

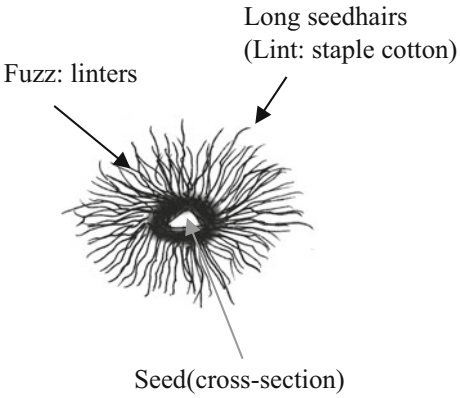


**Fig. 1.5** Cross-section of a cotton seed (adapted from [28])

The isolation of the cotton linters is included in the oil and cotton lint production. The cotton harvested in the form of cotton balls are ginned to isolate the staple fibers, which are further processed in the spinning- and the weaving mills. The remaining cotton seed with the linters fuzz is used to produce cottonseed oil, which is a valuable vegetable oil [31]. In this process, cotton linters (first-cut linters, second-cut linters, and mill-run linters), seed hulls, and seed cake (meat) are obtained. The terminology "first-cut", "second-cut", and "mill-run" refers to the oil mill process and to the number of delinting operations used. In the oil mill, a rotating saw is used to remove the linters before the oil is pressed. This machine is called "linter", resulting in the name cotton linters. The linters are generated typically in two successive stages (first and second-cut). Characteristics of cotton linters compared with those of staple cotton fibers are summarized in Table 1.3 [28].

**Table 1.3** Comparison of fibers from cotton linters and staple cotton

| Attribute | Cotton linters | | Staple cotton (Lint) |
|---|---|---|---|
| Fiber length | Short (2–6 mm) | | Long (20–45 mm) |
| Wall thickness | Thick (6–12 μm) | | Thin (2.5–6 μm) |
| Lumen shape | Roundish | | Flat, kidney-like, relatively large |
| Fiber diameter | Thick (17–27 μm) | | Thin (12–22 μm) |
| Fiber shape | Basically cylindrical, quite curly, tapers to a point | | Flat, twisted ribbon with a little curl |
| Cross-section |  | | |
| Relative chemical reactivity | Second-cut | First-cut/Mill-run | Staple cotton |
| | | ← decreasing ← | |

Cotton linters are short, thick-walled, quite curly and basically cylindrical whereas staple cotton fibers are long, thin-walled, and relatively straight and shaped like a flat twisted ribbon. The curl of a fiber is defined as the ratio of the true length ($L$) to the projected length ($L_p$) and is expressed in % according to Eq. 1.1.

$$\text{Curl} = \frac{L}{L_P - 1} \cdot 100\% \tag{1.1}$$

Cotton linters fibers possess a higher reactivity than cotton staple fibers due to their better accessibility for chemical reagents. In addition, the curly shape provides a three-dimensional character especially for the second-cut linters, which produces bulky and porous structures. Staple fibers have a two-dimensional character being the precondition for high strength. The photomicrographs shown in Fig. 1.6 visualize the difference in the cross-section of a second-cut cotton linters fiber and a cotton staple fiber. The cross-section of the linters fiber is more round, the cell wall is thicker [31].

Cotton linters comprise a certain amount of staple fibers because—after ginning—the fuzz remaining on the seed consists of cotton linters fibers and a varying quantity of staple fibers. A method for visually estimating the staple fiber content in linters is to comb out cotton linters samples and to generate linters bands where the over-lengths can be recognized by a fibrosampler classification [32].

Typically, cotton linters have a cellulose content of 80% on bone-dry basis [28, 29, 33]. By a bleaching process, the natural and non-natural contaminations are removed in order to get cotton linters cellulose of very high purity. The bleaching process is a collection of mechanical and chemical purification steps. The cleaning, after bale opening, is to remove physical impurities like field trash (via dry cleaning) and sand, stones, and seed hulls (via wet cleaning). A side effect of wet-cleaning is the reduction of natural contaminations like pectins, proteins, and fats. The digesting in caustic soda is a primary chemical purification stage. The fats and waxes are saponified, the degradation products as well as pectins and proteins

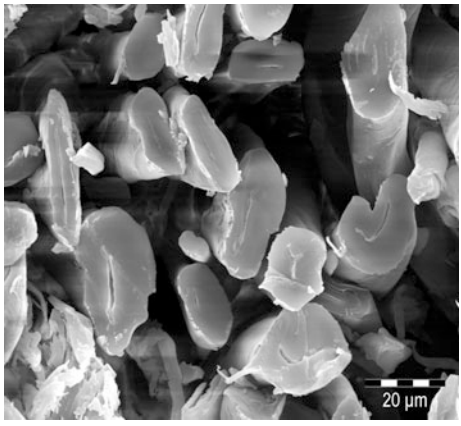


**Fig. 1.6** SEM of cross-section of second-cut cotton linters (samples sputtered with gold, accelerating voltage 20 kV)

**Table 1.4** Some commercial sources of cotton linters

| Producer | Carbohydrate composition (%) | | | DP |
|---|---|---|---|---|
| | Glucose | Mannose | Xylose | |
| **Buckeye**<br>Buckeye Cellulose Corp., 1001 Tillman Street, Memphis/Tennessee 38108-0407, USA | 100 | – | – | 1470 |
| | 100 | – | – | 2000 |
| **Anhui Snow Dragon Fibre Technology Co. Ltd.**<br>No.318 HuaiYuan South Road Suzhou City Anhui Province | Not known | – | – | 1100–1600 |
| | $\geq 98$ | | | 450–2250 |
| **Milouban**<br>Milouban M.C.P. Ltd., European Office, Am Markt 9, D-25348 Glückstadt, Germany | Not known | | | 700–3410 |

are dissolved in the alkaline medium. Finally, the proper DP is adjusted roughly by the conditions (temperature and caustic soda concentration). To promote mixing and uniformity, the linters are cooked in tumbling digesters or in continuous horizontal tube digesters. During digesting, the cuticle of the fibers is totally removed, the primary wall loses the parts that are soluble in caustic soda, and the secondary walls with their screw structure are chemically attacked. The design of the final section for finishing and drying depends on whether the cotton linters cellulose is to be marketed in flock form (flash-dried) or in sheeted form. Rolls and sheets require a wet grinding stage where the cellulose linters are shortened and fibrillated (beating, refining). The purity of the resulting cotton linters is typically $\geq 99\%$ (bleached) and $\geq 98\%$ (unbleached).

The purified cotton linters possess a high DP (compared to most wood pulps) and are characterized by a very high purity, a very high content of α-cellulose (see Chap. 2) of high crystallinity (Table 1.4). They are free of lignin and possess a low amount of carbonyl- and carboxyl groups. As a consequence, applying cotton linters in cellulose chemistry in general leads to high yields, products that are resistant against light, heat, ageing (for cellulose acetates) and the derivatives form clear, transparent, and colorless solutions of high viscosity. In case of fiber production a good filterability and spinnability of the dissolved biopolymer, e.g., applying the cuprammonium- and viscose process is observed.

### *1.1.2 Cellulose from Alternative Sources: Sisal and Agriculture Residues*

The impetus for the increased interest in cellulose extraction from agricultural lignocellulosic residues is clear: The demand for wood in the construction, furniture manufacturing, fiber, and pulp and paper industries is increasing by 1–2% per year [33, 34]. The demand can eventually outpace the offer of wood because of the slow

**Fig. 1.7** Banana plant residues, corn cobs, and rice straw as agricultural waste products (from left to right)

growth of trees. On the other hand, agriculture residues, e.g., straw from rice and wheat, corn cobs, and sugarcane bagasse are being produced in huge amounts because of two factors: The increasing use of bioethanol; the dry weight ratio of straw to grain for different crops is ca. 1 (Fig. 1.7) [35]. They represent either an environmental and health problem, e.g., when burned in the open, on a massive scale [36], or an economic asset, if they are transformed into material of higher economic value, e.g., fodder, cellulose, and biofuels. Conversion of the abundant lignocellulosic biomass into biofuels presents a viable option for improving energy security and reducing environmental impact, because they are renewable; burn cleaner than fossil fuels; their use generates very low net greenhouse emissions [37].

The production of cellulose from sources that are currently most employed (wood and cotton) has been addressed in Sect. 1.1.1. Here, cellulose extraction from 5 agricultural residues, corn cob and stalks; rice straw, sugar cane bagasse, and wheat straw, and from a relatively less employed source (sisal) is described. Figure 1.8 shows some possibilities for the applications of agricultural residues.

An approximate calculation shows the amount of sugar cane bagasse, produced worldwide. In 2009, the world production of sugar is put at 157.16 million tons [38]. The yield of sugar from sugarcane is 10 ± 2% [39], therefore the world production of sugarcane plant is ca. $1571.6 \times 10^6$ t. The processing of one ton of sugarcane produces ca. 300 kg of wet bagasse, containing typically 40–50% moisture [40]. Therefore, the world production of sugar cane bagasse, on dry basis, is ca. $235.7 \times 10^6$ t. This is just a fraction of the amount of agricultural residues available, considering the ca. $570 \times 10^6$ t of rice straw [41], and ca. $366.8 \times 10^6$ t of cereals straw [35]. Table 1.1 shows typical compositions of sisal and some agricultural residues, along with that of North American hardwood. The agricultural residues are somewhat lower grade, i.e., their cellulose contents are lower and ash contents are higher. This difference in composition represents a challenge because of the higher cost, in terms of energy and chemicals, required for cellulose recovery. In general, pulping of non-wood plants is less expensive than pulping wood. The reason is that their lignin content is somewhat lower; less chemicals are required for the delignification step. However, the cost advantage achieved in pulping and bleaching is offset in the subsequent steps of the process, due to:

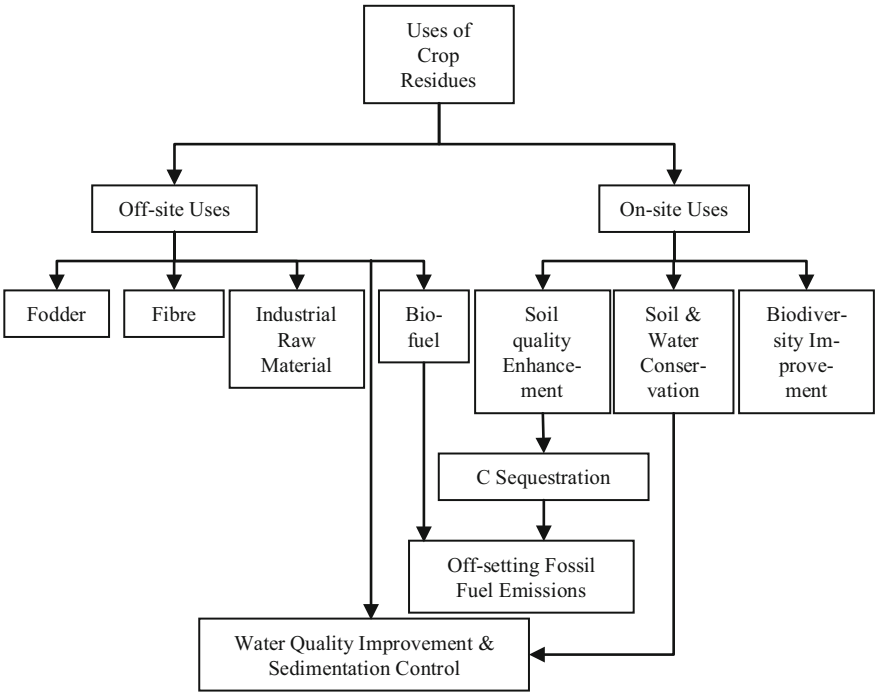


**Fig. 1.8** Some possibilities for the applications of agricultural residues. Redrawn from [35]

(i) Washing is more expensive because the resulting black liquor is highly viscous. This entails the use of larger washing equipment; a larger volume of water (required in order to reduce the solid content of the liquor), and more energy consumption in the evaporators;
(ii) Additional pretreatment is required before the material is used. During storage, most of the non-wood fibers tend to deteriorate and become colored. The resultant pulp, therefore, requires either an enzymatic pretreatment or relatively severe bleaching. This adds to the cost of production since the resultant pulp has a higher chemical/enzyme requirement [73].

Extraction of cellulose from agricultural residues entails reduction of their contents of hemicellulose, lignin, and ash. As shown in the representative examples of Table 1.8 (annex), these goals are usually achieved by a combination of pretreatment, pulping, and bleaching steps. The pretreatment results in enlargement of the inner surface area of substrate particles, due to the partial solubilization and/or degradation of hemicellulose and lignin. This leads to the fractionation of the three components, and opening of the cellulose structure. A combination of chemical and/or physico-chemical pretreatments are employed. These include the use of: dilute acids under moderate conditions, alkali treatment alone or under oxidizing

conditions, e.g., in the presence of $H_2O_2$; treatment with oxidizing agents, e.g., NaOCl; $NaClO_2$; Caro´s acid, or organic per-acids, see Table 1.8 (annex).

The possibilities of cost effective removal of hemicelluloses and lignin do not stop at the use of these conventional processes; several technically attractive alternatives have been tested [74]. The use of the organosolv process represents an important modification of both acid- or base treatment. In these, mixtures of water with an organic solvent, e.g., methanol, ethanol, 1-propanol, 1-butanol, propylene glycol, THF, are used at higher temperatures (170–250 °C) and pressures. Less acid or base is used in the organosolv process; the solubility of lignin is enhanced; the delignification selectivity is better controlled; the recovery of lignin by solvent evaporation consumes less energy than the aqueous process counterpart [75, 76]. The steam explosion process was proposed as an alternative to the thermo-mechanical treatment of wood; the aim is to obtain a reduced aggregate size, near that of the single fiber [44, 77]. The improvement in process technology, in particular the possibility of accurately controlling the decompression phase during the process, together with using organic solvent instead of water, has led to modulation of the shearing force that develops within the biomass, and hence to the predetermination of the morphological and supra-molecular structure of the treated materials. This has led to an increased application of agricultural residues. Under the drastic pressure and temperature conditions of steam explosion, the resultant steam ionization and acetic acid formation catalyze the degradation of hemicellulose and lignin, while only a partial degradation of cellulose occurs. Extraction treatments of the steam exploded biomass with water and organic solvents have made it possible to obtain fractions rich in oligomers of hemicelluloses and lignin, simple phenols, and a lignocellulosic fraction with better than 90% cellulose content. By increasing the severity of the steam explosion treatment, i.e., the residence time and temperature, a regular decrease in hemicellulose content is observed, while the lignin content reaches a minimum, corresponding to maximum delignification [78]. Other alternatives for delignification include the use of sonication [59, 62], enzymatic hydrolysis [78], and supercritical fluid technology [79]. More recently, ionic liquids have been successfully employed for dissolving cellulose under sonication [80], for dissolution and partial delignification of wood [81], and for delignification of rice straw [78]. It is expected that the use of ionic liquids will grow in view of their structural versatility, hence the concomitant variation of their physico-chemical properties and their abilities in dissolving the plant components.

## 1.2 Bacterial Cellulose

Various bacteria of the genera *Acetobacter*, *Acanthamoeba,* and *Achromobacter* spp. form cellulose that is, in principle, also an interesting approach to pure cellulose of high DP (Fig. 1.9). BC possesses an extraordinary ultra-fine network structure of high crystallinity and contains a high amount of water that is rather stable included in the structure.

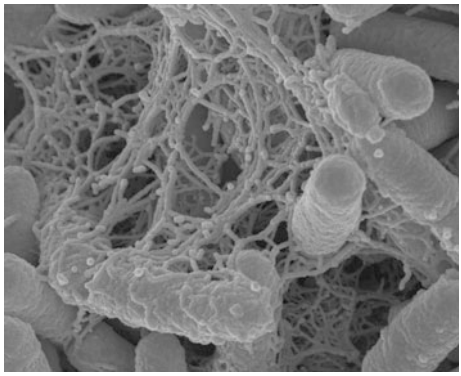

**Fig. 1.9** Microscopic picture of *Acetobacter xylinum*

The biosynthesis of cellulose by *Acetobacter xylinum* (today reclassified as *Gluconacetobacter xylinum*) occurs between the outer membrane and cytoplasma membrane by a cellulose-synthesizing complex, which is in association with pores at the surface of the bacterium. The cellulose synthase is considered to be the most important enzyme in this process. Uridine diphosphoglucose (UDP-glucose) obtained from glucose-1-phosphate trough the activity of UDP-glucose pyrophosphorylase is used in the β-1,4-glucan polymerization reaction (Fig. 1.10). When acetic acid bacteria including *Gluconacetobacter xylinum* are grown in a suitable statically incubated surface culture medium, cellulose is produced and forms a thick, leather-like pellicle at the air-liquid interface. During the growth and cellulose production, the bacterial cells become entrapped in the pellicle [82, 83].

For producing BC, cultivation is carried out under static or agitated (aerated) conditions at 27–30 °C by addition an aliquot of bacterial suspension from the exponential growth phase to the culture medium. The mostly used culture medium is the Schramm-Hestrin medium consisting of glucose (20.0 g/l), yeast extract (5.0 g/l), bactopeptone (5.0 g/l), disodium hydrogen phosphate (2.7 g/l), citric acid

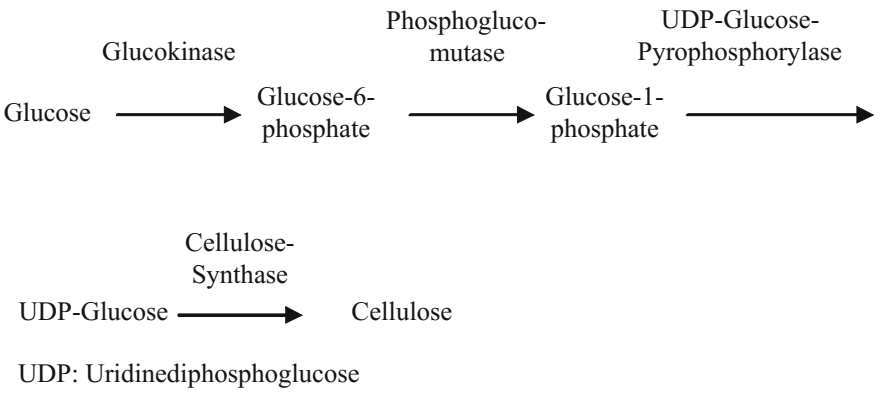


**Fig. 1.10** Proposed biochemical path for cellulose synthesis in *Acetobacter xylinum* [84]

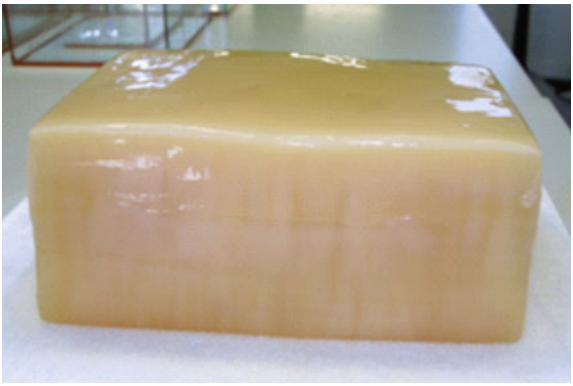

**Fig. 1.11** Bacterial cellulose produced by *Gluconacetobacter xylinum* before purification (photo courtesy of K. Schlufter, fzmb GmbH, Bad Langensalza, Germany)

monohydrate (1.15 g/l) according to [85]. In the initial stage, the bacteria increase their population by taking dissolved oxygen and produce a certain amount of cellulose in the entire liquid phase, as observed by the appearance of turbidity. After the consumption of the dissolved oxygen, bacteria existing only in the vicinity of the surface can maintain their activity and produce cellulose in the form of island-like cellulose fragments on the broth surface. The fragments close together and form a pellicle of cellulose. The thickness of the cellulose layer increases up to 40 mm within 4 weeks (Fig. 1.11). In order to get a pure product, the pellicles obtained are washed thoroughly in running water, and boiled 3 times in 0.1 N aqueous NaOH for 30 min. Subsequently, the pellicles are washed again in running water until the pH value of water becomes neutral. The bacterial cells and other ingredients of the nutrient solution are removed completely.

With respect to molecular structure, BC is identical to those made by plants. However, BC demonstrates unique properties including high mechanical strength, high crystallinity, high water holding capacity and high porosity, which make it a very useful biomaterial in many different applications. Moreover, BC is very pure; it is free of lignin, hemicelluloses and other biogenic by-products.

Regarding the supramolecular- and morphological structure, a three-dimensional fiber-network of cellulose is formed as a result of the biosynthetic polymerization of single glucose residues into β-1,4-glucan chains and the assembly and crystallization of the glucan chains into ribbons. The BC network comprises a random assembly of extreme fine fibrils with a diameter smaller than 130 nm, in comparison to fibers of wood- and cotton cellulose with diameters of about 10 μm [86, 87] (Fig. 1.12). By choosing different strains of *Gluconacetobacter xylinum,* use of additives and several carbon sources, the supramolecular structure and morphology of the BC may be controlled to a certain extent. As demonstrated by scanning electron micrographs from several fleeces obtained in static culture applying different *Acetobacter* strains, there are some differences in the structure of the network. Regarding the strain used, fleeces of variable thickness, texture and properties are formed [88] (Fig. 1.13).

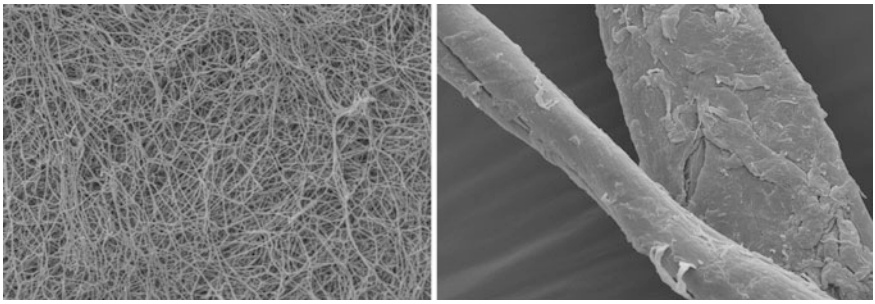

**Fig. 1.12** SEM of BC pellicle (left, dried with $scCO_2$, magnification 5000×), right of cotton linters (magnification 2000×)

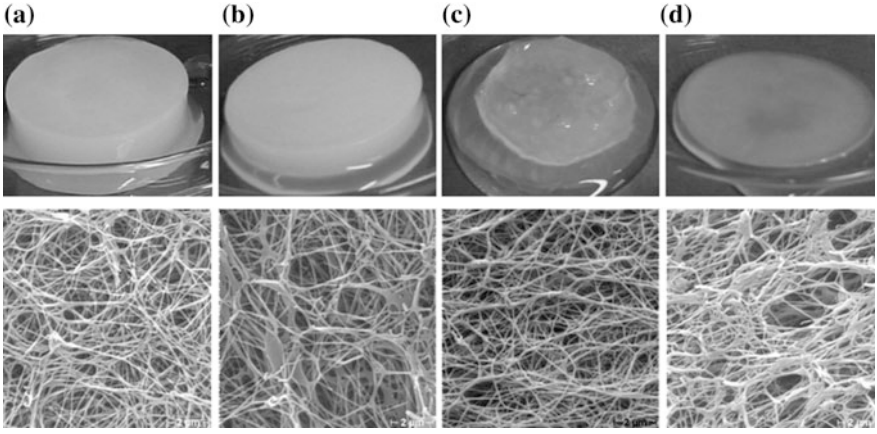


**Fig. 1.13** Pellicles and SEM of bacterial cellulose depending on the *Gluconacetobacter* strains, magnification 10,000×: **a**—DSM 14666; **b**—ATCC 53582; **c**—ATCC 23769; **d**—ATCC 10245 (photo courtesy of D. Klemm, Friedrich Schiller University of Jena, Germany)

The nanofibrillar structure of BC membranes creates an extensive surface area, which allows it to hold a huge amount of water (about 97% of its own weight). The hydrogen bonds between these fibrillar units stabilize the whole structure and are important for the mechanical strength. The DP value of BC is significantly higher than those of cellulose made from plants; DP values up to 10,000 are found [89]. BC from *Gluconacetobacter* bacteria belongs crystallographically to Cellulose I polymorph, common with plant cellulose, in which two cellobiose units are arranged parallel in the unit cell. However, the Cellulose $I_\alpha$ content is much higher in BC. VanderHart and Atalla estimated for BC a content of 65% (Cellulose $I_\alpha$) while cotton linters contain 25% Cellulose $I_\alpha$ only [90].

The macroscopic shape may be controlled using different methods of culture, namely static, submerged or agitated; it is possible to form fleeces, foils, spheres, or

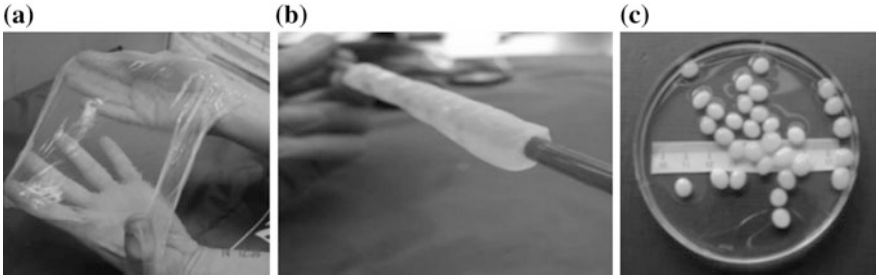


**Fig. 1.14** Bacterial cellulose shapes: **a**—foil (thickness 200 µm); **b**—tube; **c**—spheres (produced by shaking rate of 80–100 rpm, photo courtesy of D. Klemm, Friedrich Schiller University of Jena, Germany)

tubes (Fig. 1.14). There are various applications of pure BC; examples are summarized in Table 1.5.

Air drying or application of temperature leads irreversibly to a collapse of the original structure and the ability for re-swelling with water is drastically reduced. Freeze drying and critical point drying is proved to be a more appropriate drying method to retain the original three-dimensional pore structure at least to a high extent. It is also possible to remove the included water by solvent exchange with organic solvents, for example with methanol, ethanol, and acetone. Solvent exchange and freeze drying are also appropriate to remove the water prior to a chemical modification.

BC has found also some interest as starting material of chemical modification reactions although the reactivity is low compared to plant based cellulose. It is even difficult to dissolve BC in typical cellulose solvents. These differences may result from the very special supra- and morphological structure of BC.

**Table 1.5** Selected applications of bacterial cellulose

| Material | Application | References |
|---|---|---|
| Cubes in sugar syrup | Cholesterol free desert (Nata de Coco) | [91] |
| Wet pads | Therapy of chronic wounds, diabetic and venous ulcers | [92–94] |
| | Masks for cosmetic use | [95, 96] |
| Solvent or thermally modified material | Tissue repair material, human tissue substitute, implantable materials | [97–99] |
| Molded material | Artificial blood vessels, tubular structures | [100, 101] |
| Membranes | Regeneration of periodontal tissue (Gengiflex®) | [102, 103] |
| | Scaffold for tissue engineering | [104–106] |
| | High fidelity headphones, speaker membrane | [107, 108] |
| Pulverized material | Addition to food, dietary fiber | [109] |
| Fragments of fibrils | Medium for DNA-Separation | [110, 111] |

**Table 1.6** Manufacturer of BC

| Company | | Product |
|---|---|---|
| **fzmb GmbH**<br>Bad Langensalza, Germany | www.fzmb.de | NanoMasque® |
| **Lohmann & Rauscher GmbH und Co. KG**<br>Neuwied, Germany | www.lohmann-rauscher.de | SupraSorb® |
| **Monsanto Co.**<br>San Diego, CA, United States | www.lohmann-rauscher.de | Cellulon® |
| **Nutra Sweet Kelco Co.** (Monsanto)<br>Chicago, IL, United States | www.nutrasweet.com | PrimaCell® |
| **Xylos Co.**<br>Langhorne, PA, United States | www.xyloscorp.com | X-Cell® |

Bacteria of the genus *Gluconacetobacter* are also capable of synthesizing cellulose from other carbon sources than glucose. Products from beets (molasses, sugar syrup, and saccharose), corn (starch, hydrolyzed starch, glucose syrup) and other agricultural waste can be used for producing bacterial polysaccharide. Coconut- and pineapple juice are widely used for the traditional cultivation of bacterial cellulose in Southeast Asia. In principle, all carbohydrate- and protein-rich compositions are suitable as nutrient media for cellulose producing bacteria [112–115]. The utilization of inexpensive residues from agriculture or food processing is one interesting alternative to make the fermentation process of bacterial cellulose more economically. BC can be purchased from different producers (see Table 1.6).

## 1.3 Structurally Modified Cellulose

### *1.3.1 Microcrystalline Cellulose*

Heterogeneous treatment of cellulose with dilute mineral acids applying certain conditions including evaluated temperature leads to the degradation of the amorphous parts while the crystalline regions are comparably stable. After an initially fast decrease of the DP, the rate of degradation slows down and finally a nearly constant DP value is reached, the so-called levelling-off DP (LODP, [116]). Another result of the heterogeneous hydrolysis is a brittle cellulose fiber that can be easily disintegrated into cellulose powder, so-called microcrystalline cellulose (MCC). A usual procedure to obtain MCC is the acid-catalyzed depolymerization using HCl, $SO_2$ and $H_2SO_4$ at higher temperature (110 °C) for 15 min [117, 118]. The shape, size, and LODP of the products (commercial samples are, e.g., Avicel®, Heweten®, Microcel®, Nilyn®, Novagel®) may be controlled by the depolymerization conditions and especially by the starting material, i.e., by the supramolecular and morphological structure (Table 1.7; Fig. 1.15).

**Table 1.7** Level-off DP (LODP) of cellulose samples [119]

| Cellulose | LODP |
|---|---|
| Wood pulp, commercial | 100–300 |
| Beech sulfite dissolving pulp | 209 |
| Wood pulp, mercerized | 60–100 |
| Cotton linters, bleached and scoured | 140–180 |
| Viscose rayon (filament and staple) | 25–50 |

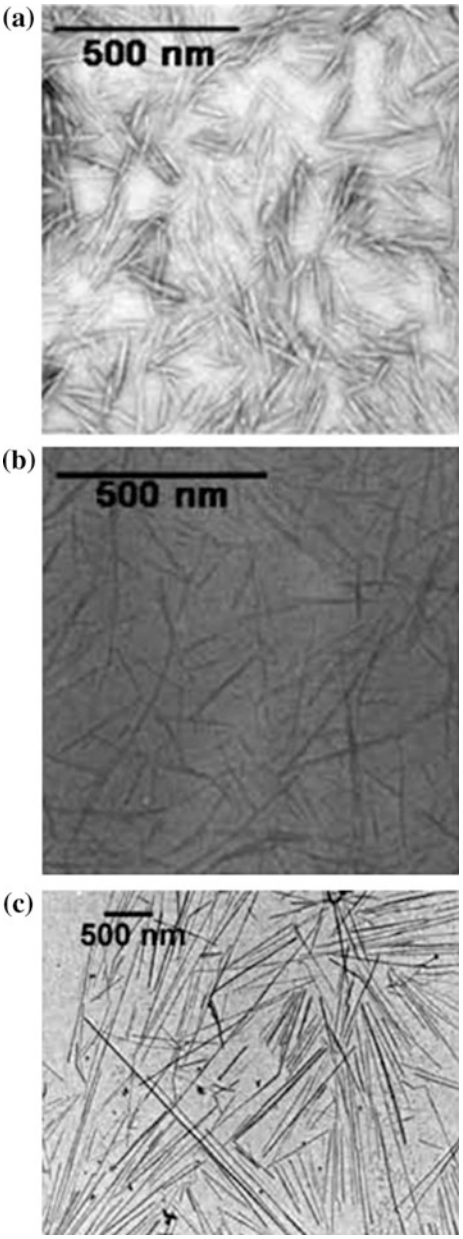


**Fig. 1.15** Transmission electron micrograph from a dilute suspension of hydrolyzed **a** cotton, **b** sugar-beet pulp and **c** tunicin (Reprinted from [150] Copyright (©2005) American Chemical Society)

MCC forms colloidal dispersions in water with interesting rheological properties [118]. There are commercial applications including non-caloric bulking agents, opacifiers, anti-cracking agents, and extrusion aids. Moreover, MCC greatly improves the mouth-feeling and impart or enhance desirable fat-like properties in food products. Another area of commercial use is the pharmaceutical industry (carriers and tablet media) and cosmetics (hair conditioners, dyes, shampoos, toothpastes [120]. MCC may form robust liquid crystalline phases [121].

From the chemist's point of view, it is important to note that MCC samples are convenient starting materials of very high purity for derivatization reactions on the laboratory scale. They still represent the polymer cellulose but show a sufficiently low viscosity in the dissolved state for convenient handling of homogeneous and quasi-homogeneous reaction systems. Moreover, the rather low DP of the products is an important prerequisite to acquire well resolved liquid state NMR spectra. It should be mentioned that in this regard a number of degradation steps were established to prepare low molecular weight cellulose of adjustable DP, so called cellodextrines [122]. Even model compounds with a blocked reducing end group were synthesized [123].

### *1.3.2 Cellulose Whiskers*

The hydrolysis or high energy milling of cellulose of different origin may result in various products denoted as "nano structural material" using terms like whiskers, nano-crystals, nano-fiber, nano-rods, nano-wires, etc. [124]. MCC is a cellulose powder with dimensions of the particles above 1 μm in contrast to whiskers with dimensions of about 8–20 nm in thickness and lengths that may even exceed 1 μm.

Cellulose nanocrystals (whiskers) are highly crystalline, nanometer-sized, rod-like fragments of cellulose microfibrils (Fig. 1.16), which can be obtained by

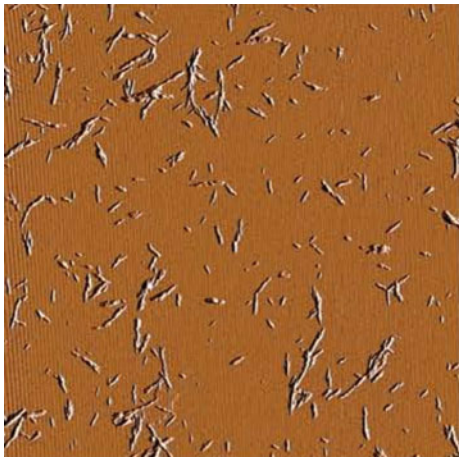

**Fig. 1.16** AFM images of cellulose nanocrystals (Reprinted from [125] Copyright (©2007) American Chemical Society)

intense hydrolysis of microcrystalline cellulose. By subsequent treatment with ultrasound, the cellulose crystallites assemble into rigid rod-like cellulose particles, namely cellulose whiskers [126]. Cellulose whiskers could also be prepared by mechanical treatments whereby the amorphous parts are cleaved by mechanical disintegration of a cellulose suspension. This highly energy consuming process could be optimized by an enzymatically produced precursor resulting in a more efficient two-step process yielding longer and highly entangled nanoscale fibrils with a drastically enhanced strength of the resulting gel network (see Sect. 1.3.3). [127]. The stability of the cellulose whiskers also strongly depends on the dimensions of the particles, the size polydispersity and their surface charge. Suspensions prepared in $H_2SO_4$ possess a negative surface charge due to generated sulfate groups on the surface [128]. On the contrary, the hydrolysis with HCl results in neutral particles, which are less stable because of the absence of electrostatic repulsion and, thus, exhibit less interesting properties than the $H_2SO_4$-treated cellulose microfibrils.

The nanocrystals obtained by such procedures occur as small but long crystals resemble a cat's whiskers in terms of straightness and the length to width ratio. The cellulose whiskers show no chain folding and contain only a small number of defects. Therefore, it is not surprising that the whiskers have a large modulus of elasticity ($\sim$150 GPa), strength ($\sim$7 GPa) and a very low coefficient for thermal expansion ($\sim 10^{-7}$ $K^{-1}$) [129, 130]. The dimensions, which could be determined by microscopy and scattering techniques, depend on the amount of amorphous regions, and thus on the origin of the substrate, the hydrolysis conditions, and the ionic strength. The particles can be separated, e.g., in isotropic suspensions. With increasing concentration, the smaller particles are located in the isotropic phase (top) whereas the larger particles are in the anisotropic phase [131]. The anisotropic nanoparticles may spontaneously self-assemble into helicoidal superstructures with very unusual properties [121].

Due to the rigid rod-like character of the cellulose whiskers, a macroscopic birefringence can be directly observed through crossed polarizers [132]. At low concentrations, the particles are randomly oriented and appear as spherical or oval droplets [133]. As mentioned, with increasing concentration, the whiskers self-align along a vector director resulting in a typical cholesteric liquid crystalline state. The chiral nematic orders can even be retained after evaporation of the solvents resulting in iridescent films of cellulose I. The color of the films can easily be tuned by varying the ionic strength of the suspension [134]. Figure 1.17 shows differently colored domains suggesting an ordered phase of the cellulose rods (a) and the well defined cholesteric phase (b) [135].

Small angle neutron scattering experiments further point out that the cholesteric axis of the chiral nematic phase aligns along an applied magnetic field [136]. The distance between the cellulose particles is shorter along the cholesteric axis than perpendicular to it, which evidences the suggestion that cellulose whiskers are helically twisted.

The hydrodynamic properties of cellulose whiskers are directly correlated to their size and their length distribution as well as their orientation in suspensions

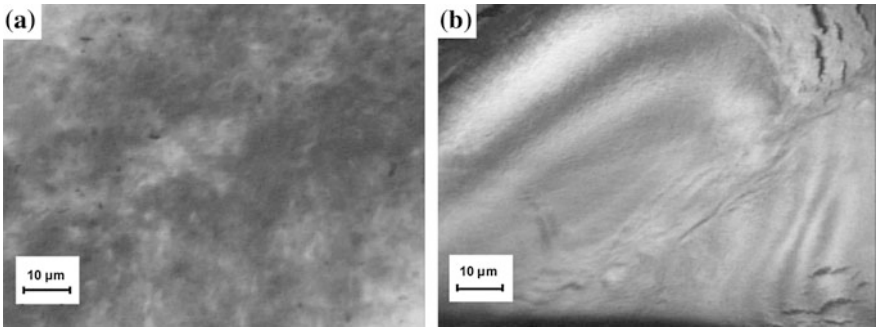


**Fig. 1.17** Crosspolarised optical microscopy images of tunicate whiskers **a** at initial ordered phase and **b** at cholesteric phase (reproduced from [135] with permission of John Wiley and Sons)

[137]. The typical rheological behavior of the cellulose suspensions shows three distinct regions [138, 139]. The first region was observed at low shear rates corresponding to the shear thinning, which indicates the initial alignment of the domains formed by the particles. With increasing shear rate, the domains are broken up, which results in a plateau in the flow curve. At even higher shear rates, the viscosity shows a constant decrease due to the alignment of individual rods, which is characteristic of liquid crystals. The rheological behavior of the cellulose suspensions also depends on the particle charge. The $H_2SO_4$-treated suspensions show no time dependence in viscosity, whereas the HCl-treated suspensions are thixotropic at higher [>0.5% (w/w)] and antithixotropic at lower concentrations [>0.3% (w/w)] [140, 141].

Cellulose whiskers can also be dispersed in dipolar aprotic solvents like DMF and DMSO, e.g., for the preparation of birefringent cellulose films [142]. Moreover, dichloromethane can be used as dispersing medium which allows film casting with poly(ε-caprolactone) [143]. Such materials possess an increased glass transition-, crystallization-, and melting temperature compared to the pure poly(ε-caprolactone) matrix. Latex (styrene butadiene rubber) [144], poly(β-hydroxyalkanoate) [145, 146], starch [147], cellulose acetate butyrate [148], poly(vinyl chloride) [149], poly (vinyl alcohol) [135], and several other natural and synthetic polymers can be blended with cellulose whiskers resulting in an enhanced reinforcement of the material [124, 150]. Attempts were made to disperse the whiskers in non-polar solvents by coating with surfactants [151] or after a chemical modification for example by grafting with poly(ethylene glycol) and silylation [152, 153]. The large amount of surfactant that is required to coat the high surface area of the particles (150 $m^2/g$) limits the use of this technique for composite applications [151, 154].

A related application is the use of whiskers for low-thickness polymer electrolytes for lithium batteries [155, 156]. A cellulosic nanocomposite was produced with poly(ethylene oxide) and a lithium imide salt for conducting ions. Cellulose whiskers incorporated in a mixture for sol-gel mineralization can be incinerated

during annealing to produce the ceramic [157]. The resulting mesoporous silicas have unique narrow and uniform pores.

Cellulose is biocompatible and, thus, does not cause an inflammatory response in body tissue. Therefore, application in the biomedical field seems reasonable. Thus, functionalization of cellulose whiskers on the surfaces with fluorescein gives labeled cellulosic nanocrystals that can be used to study the interaction with biological systems such as cells [158, 159].

### *1.3.3 Microfibrillated Cellulose*

Cellulose nano fibers (nano- or microfibrillated cellulose, NFC or MFC, Fig. 1.18), with a diameter below 100 nm, are a subject of much attention because of their unique characteristics such as a very large surface-to-volume ratio compared with common pulp fibers. The fibrillation of plant fibers has mainly employed

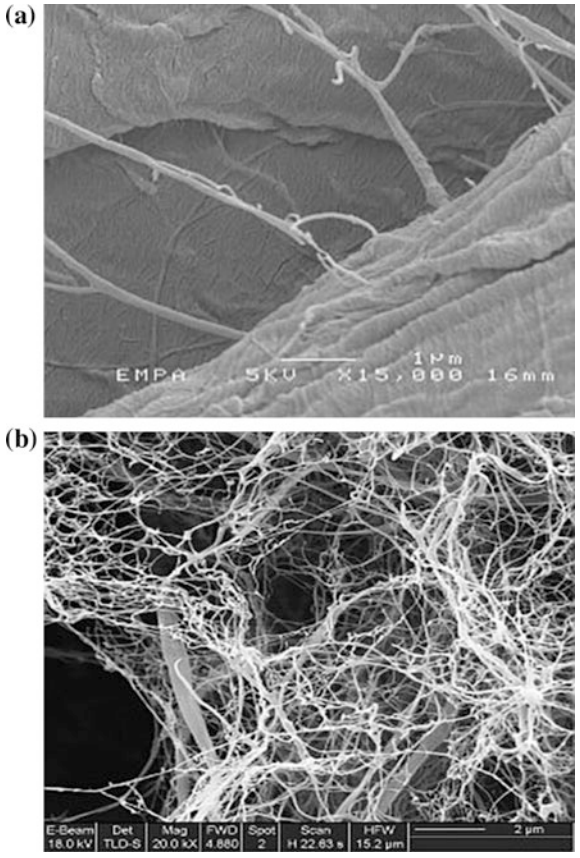


**Fig. 1.18** Electron micrographs of **a** wood cell wall with single fibrils (photo courtesy of T. Zimmermann, Empa—Materials Science & Technology, Dübendorf, Switzerland) and **b** reproduced from [160] with permission of John Wiley and Sons

mechanical treatments using a high-pressure homogenizer [161], a grinder [162, 163], cryocrushing [164, 165], ultrasonic treatment [166], and enzymatic methods in combination with mechanical shearing and high-pressure homogenization [127].

The fibrils and fibril aggregates are highly entangled, inherently connected, and form mechanically strong networks and gels [127]. A less energy consuming procedure for the manufacture of microfibrillated cellulose is the dissolution of carboxymethylated pulp under a very high shear stress [167]. Subsequent ultrasound treatment results in smaller, highly charged and more heterogeneously microfibrillated cellulose. The combination of high-pressure shear forces and mild enzymatic hydrolysis constitutes an additional method to prepare microfibrillated cellulose with a well-controlled diameter in the nanoscale range and, thus, a tunable storage modulus useful for multicomponent mixtures.

By applying lithographic methods, patterned surfaces of microfibrillar cellulose can be prepared [168]. The geometric features can be patterned either by microcontact printing of oppositely charged poly(ethylene imine) (PEI) on a PEI/poly (styrene sulfonate) (PSS) surface with subsequent treatment with microfibrillated cellulose (Fig. 1.19a) or by using a PEI-coated poly(dimethyl siloxane) stamp to remove homogeneously deposited cellulose (Fig. 1.19b). The surfaces modified could possibly be used to create filters or membranes, where both the pore openings and open areas can be controlled by varying the pattern of the microstamp.

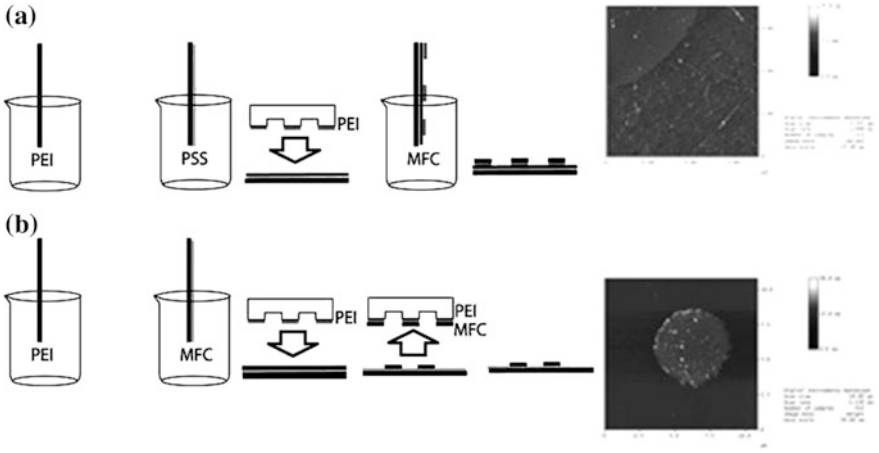


**Fig. 1.19** Schematic illustration of the preparation and a representative AFM image of **a** the selective adhesion technique using poly(ethylene imine) (PEI) and poly(styrene sulfate) (PSS) to pattern microfibrillated cellulose (MFC) and **b** the lift-off technique, where MFC is partially removed by a PEI-modified stamp (reproduced from [168] with permission of the Royal Society of Chemistry)

The addition of microfibrillated cellulose to a variety of suspensions in food, cosmetic, pharmaceutical formulations, and colors, e.g., improves their homogeneity and stability significantly [169]. Oil-in-water emulsions can be stabilized by addition of only 1% (w/w) MFC as completely biocompatible component. The stability can be further improved in combination with hydrophilic polymers like cellulose ethers or starch. Microfibrillated cellulose cannot be dispersed in dichloromethane, probably due to residual hemicelluloses at the surface [170]. This limitation can be overcome by chemical modification of the surface, e.g., with *N*-octadecyl isocyanate, leading to materials that are applicable for film casting processes in combination with synthetic polymers [143]. Moreover, polymer brushes, vinyl groups, and charge can be introduced at the surface of the microfibrils by using glycidyl methacrylate, succinic anhydride, and maleic anhydride, respectively [171]. Acetylation [172], silanization [153], and carboxymethylation [173] was used for surface functionalization as well as corona or plasma treatment [174] leading to cellulose based materials possessing defined characteristics. For example, a layer-by-layer self-assembly of polycations such as poly(ethyleneimine) and anionic poly(thiophene) were used to construct the multilayer nanofilms on wood microfibers to develop papers for monitoring electrical and optical signals [175].

## Annex

See Table 1.8.

**Table 1.8** Typical treatments of agricultural residues and sisal and characteristics of the pulps obtained[a,b,c,d]

| Raw material | Treatment | Final values of cellulose physical properties or final value and % changes of its property due to the treatment | | | | | References |
|---|---|---|---|---|---|---|---|
| | | Yield, % | DP | $I_c$ | Lignin | Ash | |
| CC | Steam explosion, 220 °C, 2 min → extraction by water at 80 °C → extraction with 20% NaOH at 80 °C, 1 h → bleaching with alkaline $H_2O_2$, 65 °C, 2 h → treatment with 1–2.5 M $H_2SO_4$, 90 °C, 1 h | | 189 | 0.5 | | | [42] |
| CC | Treatment with 88% $HCO_2H$ plus 0.2% HCl, 60 °C, 8 h | | 433, +26% | 0.44; +83% | 4.41; −70% | | [43] |
| CS | Steam explosion, 180–220 °C, 5 min; → extraction with 20% NaOH, 80 °C, 1 h → NaOCl, 40 °C, 2 h | 40.8 | 167 | 0.70 | 40.5%; +47.3% | 4.3%; +253% | [44] |
| RS | NaOH (1.5–5%), 80 °C, 2 h → wash → 2 mol/L HCl, 105 °C, 15 min | | 80–150 | 0.8 | | | [45] |
| RS pulp | $H_2O_2$ (4%) → NaOH (0.5%) + sodium silicate plus $MgS0_4$, 80 °C → repeat treatment in the second stage. All aqueous solutions. | | 310; +24% | | 2.5%; −53% | 1.82%; −75% | [46] |
| RS pulp | $H_2O_2$ (4%) → NaOH (0.5%) + sodium; silicate plus $MgS0_4$, 80 °C → repeat treatment in the second stage. In aqueous solutions containing 10, 30 and 50 v% solvent: methanol, ethanol, acetone, dioxane. Results reported here are for 30% ethanol. | | 130 | | 4.3% | 2.01 | [46] |
| SB-pulp | $H_2O_2$ (4%) → NaOH (0.5%) + sodium; silicate plus $MgS0_4$, 80 °C → repeat treatment in the second stage. All aqueous solutions | | 210; + 10.5% | | 1%; −83.8% | 0.8%; −27.8% | [46] |
| SB-pulp | $H_2O_2$ (4%) → NaOH (0.5%) + sodium; silicate plus $MgS0_4$, 80 °C → repeat treatment in the second stage. In aqueous solutions containing 10, 30 and 50 v% organic solvent; methanol, ethanol, acetone, dioxane. Results reported here are for 30% ethanol. | | 300 | | 0.52 | 0.39 | [46] |
| RS | Steam explosion after 5 or 10 min heating at 6 MPa and 275 °C; | | | | Decrease | | [47] |
| RS | NaOH (20%) 6–42 h; RT | 50 | | Increase | 1.2%; −92.4% | 1.9; −86.6 | [48] |
| RS | Dewax by toluene-ethanol extraction → bleach by 2% alkaline $H_2O_2$, 45 °C, 16 h → acid wash 80% acetic acid, 120 °C, 15 min | 23.4 | 173 | Little change | 3.6 | | [49] |

(continued)

**Table 1.8** (continued)

| Raw material | Treatment | Final values of cellulose physical properties or final value and % changes of its property due to the treatment | | | | | References |
|---|---|---|---|---|---|---|---|
| | | Yield, % | DP | $I_c$ | Lignin | Ash | |
| RS | Pretreatment with 1% $H_2SO_4$, 121 °C, pressure, 1 h → wash with 10 M NaOH, then with water. Product converted to cellulose acetate (13.5% yield) by $H_2SO_4$-catalyzed acetylation by acetic anhydride in $CH_2Cl_2$; DS = 2.8 | | | | | | [50] |
| RS-B-pulp | Acid treatment with 2 M HCl, reflux for 45 min | | 237 | 0.78 | 1.32 | 13.8 | [51] |
| SB-B-pulp | Acid treatment with 2 M HCl, reflux for 45 min | | 317 | 0.76 | 0.87 | 1.3 | [51] |
| RS | Treatment with 6% NaOH, 20 °C, 3 weeks → anaerobic digestion by activated sludge | 29.9 | | | 5.7%; −23% | 20.8% + 62% | [52] |
| RS | Treatment under pressure with 3–4.5% Caro´s acid in dioxane-water → treatment with 2% NaOH, pressure, 130 °C, 2 h | 25 | | | | | [53] |
| R hulls | Treatment with 0.5 to 5% $H_2SO_4$ or HCl, 80–120 °C, 30–120 min | 28.6–37.5; −55 to −41 | | | 17–28%; +5 to +70% | 18–23+6% to +39% | [54, 55] |
| SB | Treatment with 0.7 M NaOH, 60–150 °C, 15 min, or 160 °C, 2 h | | | | 5.6%; −75% | | [56] |
| SB | Boil with 1 M NaOH, 2 h → acetylated with acetic anhydride/$HClO_4$ catalyst to cellulose acetate; DS = 2.82 | | | | | | [57] |
| SB | Hydrothermal treatment at 200–280 °C | 24.5 | | Increase | 6.44%; −60% | | [58] |
| SB | Extraction with toluene-ethanol, 6 h → Extraction with water, with or without sonication, 55 °C, 40 min to 2 h → treatment with 0.5 to 3% $H_2O_2$ in 0.5 M NaOH, 55 °C, 2 h | 44.7–45.9% | 1185 | | 3.35; −81.4% | | [59] |
| SB | Dewaxing with toluene-ethanol, 6 h → Treatment with acidified 1.3% $NaClO_2$, 75 °C, 2 h → 10% NaOH | 44.2–44.7 | 1396 | | 1.45; −92% | | [59] |

(continued)

**Table 1.8** (continued)

| Raw material | Treatment | Final values of cellulose physical properties or final value and % changes of its property due to the treatment | | | | | References |
|---|---|---|---|---|---|---|---|
| | | Yield, % | DP | $I_c$ | Lignin | Ash | |
| SB | Extraction with 80% acetic acid-70% nitric acid (10:1, v/v), 110–120 °C, 20 min | 43–43.6 | 822 | | 0.18; −99% | | [59] |
| SB | Two-stage treatment with 3% NaOH, 50 °C, 1 h, followed by treatment with 1.5 to 6% Caro's acid, 30–40 °C, 3 h | 33.8–40.2 | | | 5.8–6.5% −71 to −67.5% | | [60] |
| SB | Three-stage treatment with 3% NaOH, 50 °C, 1 h; treatment with 1.5 to 6% Caro´s acid, 30–40 °C, 3 h; treatment with 3% NaOH, 70 °C, 1 h | 31.7–38.1 | | | 2.3–5.5% −88.5 to −72.3% | | [60] |
| SB | Acid prehydrolysis, 1.5% $H_2SO_4$, 90 min at 120 °C; 5% NaOH pulping, 165 °C, 120 min; in the presence of 0.05% anthraquinone catalyst; four-stage conventional bleaching ($Cl_2$; NaOCl; $NaClO_2$, NaOH) | 30.8–31.6 | 780–830 | | 1–2% −90 to −95% | 0.14-0.21% | [61] |
| SB | Dewaxing with chloroform-ethanol, 6 h → sonication, 100 W in water, 60 °C, 30 min; delignification with 6% NaOCl, 75 °C, 2 h; extraction with alkali (NaOH or KOH), 8 to 18%, RT, 2 to 12 h | 21.2–24.1 | 1913–2040 | | 1.5; −91.7% | | [62] |
| SB | Delignification by acidified $NaClO_2$, 75 °C, 1 h; pulping, 10% KOH, 25 °C, 10 h | 52.4 | 162 | | | | [63] |
| SB | Organosolv pulping by etanol-water (1:1), pressure, 5% NaOH, 185 °C, 3 h; bleaching with 3% $NaClO_2$, at 75 °C, 1 h | | | | 6.6%; −76.5% | | [64] |
| SB | Treatment with 30–60% peracetic acid | 11.2–36 | | 0.62 | 0.93–1.85; −95 to −90% | | [65] |
| WS | Reflux with 0.25–1.25 M $H_2SO_4$, 10–60 min; delignification with 1 M $H_2SO_4$ in aqueous ethanol, 81 °C, 90 min; followed by a second-stage acid-delignification | 37; 93 | | | | | [66] |
| WS | Extraction with toluene-ethanol, 6 h → Treatment with 0.5 M NaOH aqueous methanol, 60 °C, 2.5 h with sonication → 2% | 17.9–19.4 | | | 2.7–2.9; −92 | | [67] |

(continued)

**Table 1.8** (continued)

| Raw material | Treatment | Final values of cellulose physical properties or final value and % changes of its property due to the treatment | | | | | References |
|---|---|---|---|---|---|---|---|
| | | Yield, % | DP | $I_c$ | Lignin | Ash | |
| | $H_2O_2$ plus base, 48 °C, 12 h → 80% acetic acid-70% nitric acid (10:1, v/v), 110–120 °C, 15 min | | | | | | |
| Sisal | Kraft or soda pulping at 170 °C | 73.5; 68 | | | 1.83; 1.22 | | [68] |
| Sisal | Kraft pulping, 75 min to reach 170 °C, then cooking for 120 min at 170 °C; or soda pulping 85 min to reach 170 °C, then cooking for 120 min at 170 °C | 55.4; 45.9 | | | 4.87 | | [69, 70] |
| Sisal | Dewaxing by toluene/ethanol, 6 h; pre-treatment, 3 h, 0.1 M NaOH in 50% ethanol, 45 °C; $H_2O_2$, 1–3%, pH = 11.5, 45 °C; 10% w/v NaOH plus 1% w/v $Na_2B_4O_7$, 28 °C, 15 h, agitation; 70% $HNO_3$ plus 80% HAc (1/10 v/v) at 120 °C, 15 min; or Dewaxing by toluene/ethanol, 6 h; 0.7 w/v.% $NaClO_2$, pH = 4, boiling for 2 h; 5% w/v $NaHSO_4$; 17.5 w/v % NaOH solution | | | 0.75 | | | [71] |
| Sisal | Stirring, three times, each with 4 wt% NaOH, 80 °C, 2 h; Bleaching, 4 times, each with 1.7 wt% $NaClO_2$ in acetate buffer, 80 °C, 4 h | | | 0.93 | | | [72] |

[a]Abbreviations: *CC* Corn cob; *CS* Corn stalks; *RS* Rice Straw; *SB* Sugarcane bagasse. RS-pulp and SB-pulp are commercial unbleached pulps; RS-B-pulp and SB-B-pulp are commercial bleached pulps; *WS* wheat straw; *RT* room temperature

[b]After *each* procedure (pretreatment; delignification, etc.), the pulps produced are usually washed free of the reagent, and then dried

[c]The reader should consult the original literature in order to know how the reagent concentrations have been calculated. In most cases, they are based on dry pulp weight. The same observation applies to the liquor ratio employed, i.e., volume of solution to dry pulp weight

[d]The yields and physicochemical properties of the cellulose samples produced are reported in the columns yield, %; degree of polymerization, DP, index of crystallinity, $I_c$; lignin%, and ash%, respectively. Where available, the final property is listed, along with the effect of treatment on this property. For example, the second entry of the table reports DP = 433; +26%, $I_c$ = 0.44, +83%, and lignin content = 4.41 and −70%. These results mean that the DP, $I_c$, and lignin content of the final product are 433, 0.44, and 4.41%, respectively; the treatment has resulted in 26% increase in DP; 83% increase in $I_c$, and 70% decrease in the lignin content

## References


1. Krässig HA (1993) Cellulose: structure, accessibility and reactivity. Gordon and Breach, Yverdon
2. Hon DNS (1996) Chemical modification of lignocellulosic materials. Marcel Dekker Inc, New York, Basel, Hong Kong
3. Pettersen RC (1984) The chemical composition of wood. Adv Chem Ser 207:57–126
4. Qu T, Guo W, Shen L, Xiao J, Zhao K (2011) Experimental study of biomass pyrolysis based on three major components: hemicellulose, cellulose, and lignin. Ind Eng Chem Res 50:10424–10433
5. Chen X, Yu J, Zhang Z, Lu C (2011) Study on structure and thermal stability properties of cellulose fibers from rice straw. Carbohydr Polym 85:245–250
6. http://en.wikipedia.org/wiki/Bagasse
7. Mwaikambo LY, Ansell MP (2002) Chemical modification of hemp, sisal, jute, and kapok fibers by alkalization. J Appl Polym Sci 84:2222–2234
8. The Clean Washington Center (1997) Wheat straw as a paper fiber source, Washington. http://www.cwc.org/paper/pa971rpt.pdf
9. Jonas R, Farah LF (1998) Production and application of microbial cellulose. Polym Degrad Stab 59:101–106
10. Tarchevsky JA, Marchenko GN (1991) Cellulose: biosynthesis and structure. Springer, Heidelberg
11. Nakatsubo F, Kamitakahara H, Hori M (1996) Cationic ring-opening polymerization of 3,6-di-O-benzyl-alpha-D-glucose 1,2,4-orthopivalate and the first chemical synthesis of cellulose. J Am Chem Soc 118:1677–1681
12. Nishimura T, Takano T, Nakatsubo F, Murakami K (1993) Synthetic studies of cellulose. 10. Selection of suitable starting materials for the convergent synthesis of cello-oligosaccharides. Mokuzai Gakkaishi 39:40–47
13. Kamitakahara H, Koschella A, Mikawa Y, Nakatsubo F, Heinze T, Klemm D (2008) Synthesis and characterization of 2,6-di-O-methyl celluloses both from natural and synthetic celluloses. Macromol Biosci 8:690–700
14. Kamitakahara H, Nakatsubo F, Klemm D (2006) Block co-oligomers of tri-O-methylated and unmodified cello-oligosaccharides as model compounds for methylcellulose and its dissolution/gelation behaviour. Cellulose 13:375–392
15. Kobayashi S, Kashiwa K, Kawasaki T, Shoda S (1991) Novel method for polysaccharide synthesis using an enzyme: the first in vitro synthesis of cellulose via a nonbiosynthetic path utilizing cellulase as catalyst. J Am Chem Soc 113:3079–3084
16. Kobayashi S, Shoda S, Lee J, Okuda K, Brown RM Jr, Kuga S (1994) Direct visualization of synthetic cellulose formation via enzymatic polymerization using transmission electron-microscopy. Macromol Chem Phys 195:1319–1326
17. Committee on Synthetic Hierarchical Structures, National Materials Advisory Board, Commission on Engineering and Technical Issues, National Research Council (1994) Hierarchical structures in biology as a guide for new materials technology. National Academy Press, Washington, DC
18. Ebringerová A, Heinze T (2000) Xylan and xylan derivatives—biopolymers with valuable properties. 1. Naturally occurring xylans structures, isolation procedures and properties. Macromol Rapid Commun 21:542–556
19. Heinze T, Liebert T, Koschella A (2006) Esterification of polysaccharides, structure of polysaccharides. Springer, Berlin
20. Sjöström E (1993) Wood chemistry: fundamentals and applications. Academic Press, Cambridge. ISBN 012647480X
21. Sixta H (2006) Introduction. In: Sixta H (ed) Handbook of pulp, vol 1. Wiley-VCH, Weinheim, pp 3–19

22. Fink H-P, Walenta E (1994) X-ray diffraction investigations of cellulose supramolecular structure at processing. Papier (Bingen, Germany) 48:739–742
23. Toland J, Galasso L, Lees D, Rodden G (2002) Pulp Paper International, Paperloop, p 5
24. Sixta H (2006) Sulfite chemical pulping. In: Sixta H (ed) Handbook of pulp, vol 1. Wiley-VCH, Weinheim, pp 392–510
25. Sixta H (2006) Handbook of pulp, vol 1. Wiley-VCH, Weinheim, p 325
26. Berzings V, Tasmanm JE (1957) The relationship of the kappa number of the lignin content of pulp materials. Pulp Pap Can 9:154–158
27. Bremer Baumwollbörse (2008) "Cotton School", Produktinformationen zur Baumwolle
28. Temming H, Grunert H, Huckfeldt H (1973) Temming linters—Technical information on cotton cellulose. English translation of the 2nd revised German edition (1972), Peter Temming AG, Glückstadt; Bremer Baumwollbörse, "Cotton School", Produktinformationen zur Baumwolle, 2008
29. Rafiq Chaudhry M, Guitchounts A (2003) International Cotton Advisory Committee, Cotton Facts, Technical Paper No. 25, ISBN 0-9704918-3-2
30. Bremer Baumwollbörse, Bremen Cotton Report No. 33/34, August 29, 2008, pp 8–9
31. Sczostak A (2009) Cotton linters: an alternative cellulosic raw material. Macromol Symp 280:45–53
32. Carpenter F (1967) Evaluation of the fibrosampler and the digital fibrograph for sampling cotton fibers and measuring length characteristics (Marketing research report). Agricultural Research Service, U.S. Department of Agriculture, ASIN: B0006RFSGI
33. Chandra M (1998) Use of non-wood plant fibers for pulp and paper industry in Asia: potential in China. Master's degree thesis, Virginia Polytechnic Institute and State University, Blacksburg, Virginia, USA
34. McNutt JA, Rennel J (1997) The future of fiber in tomorrow's world. Pulp Pap Int 39:34–36
35. Lal R (2005) World crop residues production and implications of its use as a biofuel. Environ Int 31:575–584
36. http://www.environment.gov.au/atmosphere/airquality/publications/biomass.html
37. Wyman CE (1999) Biomass ethanol: technical progress, opportunities, and commercial challenges. Annu Rev Energy Environ 24:189–226
38. http://www.xmarks.com/site/www.indiansugar.com/briefings/wsm.htm
39. http://ipmworld.umn.edu/chapters/meagher.htm
40. Sun JX, Sun XF, Sun RC, Su YQ (2004) Fractional extraction and structural characterization of sugarcane bagasse hemicelluloses. Carbohydr Polym 56:195–204
41. Van Nguu N (2000) Issues and opportunities of wide adoption of hybrid rice outside china, with emphasis on south and southeast Asia. FAO Rice Information, Vol. 2, Chapter I
42. Agblevor FA, Ibrahim MM, El-Zawawy WK (2007) Coupled acid and enzyme mediated production of microcrystalline cellulose from corn cob and cotton gin waste. Cellulose 14:247–256
43. Zhang M, Qi W, Liu R, Su R, Wu S, He Z (2010) Fractionating lignocellulose by formic acid: characterization of major components. Biomass Bioenergy 34:525–532
44. Ibrahim M, Agblevor FA, El-Zawawy WK (2010) Isolation and characterization of cellulose and lignin from steam-exploded lignocellulosic biomass. BioResources 5:397–418
45. Chen J, Yan S, Ruan J (1996) A study on the preparation, structure and properties of microcrystalline cellulose. J Macromol Sci Part A Pure Appl Chem A33:1851–1862
46. Selim IZ, Mansour OY, Mohamed SA (1996) Physical characterization of pulps. II. Rice straw and bagasse pulps bleached by nonconventional two-stage hydrogen peroxide method and paper sheet making. Polym-Plast Technol Eng 35:649–667
47. Moniruzzama M (1996) Effect of steam explosion on the physicochemical properties and enzymic saccharification of rice straw. Appl Biochem Biotechnol 59:283–297
48. Lim SK, Son T-W, Lee D-W, Park BK, Cho KM (2001) Novel regenerated cellulose fibers from rice straw. J Appl Polym Sci 82:1705–1708
49. Sun JX, Xu F, Geng ZC, Sun XF, Sun RC (2005) Comparative study of cellulose isolated by totally chlorine-free method from wood and cereal straw. J Appl Polym Sci 97:322–335

50. Biswas A, Saha BC, Lawton JW, Shogren RL, Willett JL (2006) Process for obtaining cellulose acetate from agricultural by-products. Carbohydr Polym 64:134–137
51. El-Sakhawy M, Hassan ML (2007) Physical and mechanical properties of microcrystalline cellulose prepared from agricultural residues. Carbohydr Polym 67:1–10
52. He Y, Pang Y, Liu Y, Li X, Wang K (2008) Physicochemical characterization of rice straw pretreated with sodium hydroxide in the solid state for enhancing biogas production. Energy Fuels 22:2775–2781
53. Abdel-Mohdy FA, Abdel-Halim ES, Abu-Ayana YM, El-Sawy SM (2009) Rice straw as a new resource for some beneficial uses. Carbohydr Polym 75:44–51
54. Adel AM, Abd El-Wahab ZH, Ibrahim AA, Al-Shemy MT (2010) Characterization of microcrystalline cellulose prepared from lignocellulosic materials. Part I. Acid catalyzed hydrolysis. Bioresour Technol 101:4446–4455
55. Adel AM, Abd El-Wahab ZH, Ibrahim AA, Al-Shemy MT (2011) Characterization of microcrystalline cellulose prepared from lignocellulosic materials Part II: Physicochemical properties. Carbohydr Polym 83:676–687
56. Chen HT, Funaoka M, Lai YZ (1998) Characteristics of bagasse in situ and in alkaline delignification. Holzforschung 52:635–639
57. Rajini R, Venkateswarlu U, Rose C, Sastry TP (2001) Studies on the composites of cellulose triacetate (prepared from sugar cane pulp) and gelatin. J Appl Polym Sci 82:847–853
58. Sasaki M, Adschiri T, Arai K (2003) Fractionation of sugarcane bagasse by hydrothermal treatment. Bioresour Technol 86:301–304
59. Sun JX, Sun XF, Zhao H, Sun RC (2004) Isolation and characterization of cellulose from sugarcane bagasse. Polym Degrad Stab 84:331–339
60. Abou-Yousef H, El-Sakhawy M, Kamel S (2005) Multi-stage bagasse pulping by using alkali/Caro's acid treatment. Ind Crops Prod 21:337–341
61. Ibrahim AA, Nada AMA, Hagemann U, El Seoud OA (1996) Preparation of dissolving pulp from sugarcane bagasse, and its acetylation under homogeneous solution condition. Holzforschung 50:221–225
62. Liu C-F, Ren J-L, Xu F, Liu J-J, Sun J-X, Sun R-C (2006) Isolation and characterization of cellulose obtained from ultrasonic irradiated sugarcane bagasse. J Agric Food Chem 54:5742–5748
63. Liu CF, Sun RC, Zhang AP, Ren JL (2007) Preparation of sugarcane bagasse cellulosic phthalate using an ionic liquid as reaction medium. Carbohydr Polym 68:17–25
64. Ruzene DS, Silva DP, Vicente AA, Teixeira JA, de Amorim MTP, Gonçalves AR (2009) Cellulosic films obtained from the treatment of sugarcane bagasse fibers with *N*-methylmorpholine-*N*-oxide (NMMO). Appl Biochem Biotechnol 154:217–226
65. Zhao X-B, Wang L, Liu D-H (2008) Peracetic acid pretreatment of sugarcane bagasse for enzymatic hydrolysis: a continued work. J Chem Technol Biotechnol 83:950–956
66. Papatheofanous MG, Billa E, Koullas DP, Monties B, Kuokios EG (1995) Two-stage acid-catalyzed fractionation of lignocellulosic biomass in aqueous ethanol systems at low temperatures. Bioresour Technol 54:305–310
67. Sun X-F, Sun R-C, Su Y, Sun J-X (2004) Comparative study of crude and purified cellulose from wheat straw. J Agric Food Chem 52:839–847
68. Coutts RSP, Warden PG (1992) Sisal pulp reinforced cement mortar. Cem Concr Composites 14:17–21
69. Savastano H Jr, Warden PG, Coutts RSP (2000) Brazilian waste fibers as reinforcement for cement-based composites. Cem Concr Composites 22:379–384
70. Savastano H Jr, Warden PG, Coutts RSP (2004) Evaluation of pulps from natural fibrous material for use as reinforcement in cement product. Mater Manuf Processes 19:963–978
71. Morán JI, Alvarez VA, Cyras VP, Vásquez A (2008) Extraction of cellulose and preparation of nanocellulose from sisal fibers. Cellulose 15:149–159
72. Siqueira G, Bras J, Dufresne A (2010) New process of chemical grafting of cellulose nanoparticles with a long chain isocyanate. Langmuir 26:402–411

73. Hammett AL, Youngs RL, Sun X, Chandra M (2001) Non-wood fiber as an alternative to wood fiber in china's pulp and paper industry. Holzforschung 55:219–224
74. Kumar P, Barrett DM, Delwiche MJ, Stroeve P (2009) Methods for pretreatment of lignocellulosic biomass for efficient hydrolysis and biofuel production. Ind Eng Chem Res 48:3713–3729
75. Johansson A, Aaltonen O, Ylinen P (1987) Organosolv pulping: methods and pulp properties. Biomass 13:45–65
76. Sixta H, Harms H, Dapia S, Parajo JC, Puls J, Saake B, Fink H-P, Roeder T (2004) Evaluation of new organosolv dissolving pulps. Part I: preparation, analytical characterization and viscose processability. Cellulose 11:73–83
77. Focher B, Marzetti A, Crescenzi V (eds) (1991) Steam explosion techniques fundamentals and applications. Gordon and Breach Publishers, Philadelphia
78. Fu D, Mazza G, Tamaki Y (2010) Lignin extraction from straw by ionic liquids and enzymatic hydrolysis of the cellulosic residues. J Agric Food Chem 58:2915–2922
79. Schacht C, Zetzl C, Brunner G (2008) From plant materials to ethanol by means of supercritical fluid technology. J Supercrit Fluids 46:299–321
80. Mikkola J-P, Kirilin A, Tuuf J-C, Pranovich A, Holmbom B, Kustov LM, Murzin DY, Salmi T (2007) Ultrasound enhancement of cellulose processing in ionic liquids: from dissolution towards functionalization. Green Chem 9:1229–1237
81. Sun N, Rahman M, Qin Y, Maxim ML, Rodríguez H, Rogers RD (2009) Complete dissolution and partial delignification of wood in the ionic liquid 1-ethyl-3-methylimidazolium acetate. Green Chem 11:646–655
82. Iguchi M, Yamanaka S, Budhiono A (2000) Bacterial cellulose—a masterpiece of nature's arts. J Mater Sci 35:261–270
83. Brown RM Jr, Saxena IM (2000) Cellulose biosynthesis: a model for understanding the assembly of biopolymers. Plant Physiol Biochem 38:57–67
84. Cannon RE, Anderson SM (1991) Biogenesis of Bacterial Cellulose. Crit Rev Microbiol 17:435–447
85. Hestrin S, Schramm M (1954) Synthesis of cellulose by acetobacter xylinum 2. Preparation of freeze-dried cells capable of polymerizing glucose to cellulose. Biochem J 58:345–352
86. Brown RM, Willison ZH, Richardson CL (1976) Cellulose biosynthesis in Acetobacter xylinum: visualization of the site of synthesis and direct measurement of the in vivo process. Proc Natl Acad Sci 73:4565–4569
87. Zaar K (1977) Biogenesis of cellulose by Acetobacter xylinum. Cytobiologie 16:1–15
88. Klemm D, Schumann D, Kramer F, Heßler N, Koth D, Sultanova B (2009) Nanocellulose materials—Different cellulose, different functionality. Macromol Symp 280:60–71
89. Yoshinaga F, Tonouchi N, Watanabe K (1997) Research progress in production of bacterial cellulose by aeration and agitation culture and its application as a new industrial material. Biosci Biotech Biochem 61:219–224
90. VanderHart DL, Atalla RH (1984) Studies of microstructure in native celluloses using solid-state C-13 NMR. Macromolecules 17:1465–1472
91. Budhiono A, Rosidi B, Taher H, Iguchi M (1999) Kinetic aspects of bacterial cellulose formation in nata-de-coco culture system. Carbohydr Polym 40:137–143
92. Czaja W, Krystynowicz A, Bielecki S, Brown RM (2006) Microbial cellulose—the natural power to heal wounds. Biomaterials 27:145–151
93. Ring DF, Nashed W, Dow T (1984) Liquid loaded pad for medical applications. GB 2131701 A CAN 101:149803
94. Serafica C, Mormino R, Oster GA, Lentz KE, Koehler P (2006) Mikrobieller Cellulose-Wundverband zur Behandlung chronischer Wunden. DE 60203264
95. Frankenfeld K, Hornung M, Lindner B, Ludwig M, Mülverstedt A, Schmauder H-P (2001) Procedure for the production of specific molded shapes or layers from bacterial cellulose. DE 10022751 A1 CAN 135:256211

96. Klemm D, Schumann D, Kramer F, Hessler N, Hornung M, Schmauder HP, Marsch S (2006) Nanocelluloses as innovative polymers in research and application. Adv Polym Sci 205:49–96
97. Oster G, Lentz K, Koehler K, Hoon R, Serafica G, Mormino R (2002) Solvent dehydrated microbially-derived cellulose for in vivo implantation. US 2002107223 A1 CAN 137:145652
98. Damien CJ, Oster GA, Beam HA (2005) Thermally modified microbial-derived cellulose for in vivo implantation. US 2005042250 A1 CAN 142:246277
99. Beam H, Serafica G, Damien C, Wright FS (2007) Implantable microbial cellulose materials for various medical applications. WO 2007064772 A2 CAN 147:39244
100. Yamanaka S, Ono E, Watanabe K, Kusakabe M, Suzuki Y (1990) Production of hollow cellulose produced by microorganisms for artificial blood vessels. EP 0396344, CAN 114:235093
101. Klemm D, Schumann D, Udhardt U, Marsch S (2001) Bacterial synthesized cellulose—artificial blood vessels for microsurgery. Prog Polym Sci 26:1561–1603
102. Dos Anjos B, Novaes AB Jr, Meffert R, Barboza EP (1998) Clinical comparison of cellulose and expanded polytetrafluoroethylene membranes in the treatment of class II furcations in mandibular molars with 6-month re-entry. J Periodontol 69:454–459
103. Macedo NL, Matuda FS, Macedo LGS, Monteiro ASF, Valera MC, Carvalho YR (2004) Evaluation of two membranes in guided bone tissue regeneration: histological study in rabbits. Braz J Oral Sci 3:395–400
104. Helenius G, Bäckdahl H, Bodin A, Nannmark U, Gatenholm P, Risberg B (2006) In vivo biocompatibility of bacterial cellulose. J Biomed Mater Res 76A:431–438
105. Svensson A, Nicklasson E, Harrah T, Panilaitis B, Kaplan DL, Brittberg M, Gatenholm P (2005) Bacterial cellulose as a potential scaffold for tissue engineering of cartilage. Biomaterials 26:419–431
106. Watanabe K, Eto Y, Takano S, Nakamori S, Shibai H, Yamanaka S (1993) A new bacterial cellulose substrate for mammalian cell culture. Cytotechnology 13:107–114
107. Uryu M, Kurihara N (1993) Acoustic diaphragm and method producing same. US 5274199
108. Hwang JU, Park SH, Pyun YR, Yang YG (1999) Speaker vibration plate containing microbial cellulose al principal ingredient KO 100246726 B1
109. Stephens RS, Westland JA, Neogi AN (1990) Production of cholesterol-absorbing bacterial cellulose for use as dietary fiber. US 4960763 A, CAN 114:60730
110. Tabuchi M, Baba Y (2005) Design for DNA separation medium using bacterial cellulose fibrils. Anal Chem 77:7090–7093
111. Tabuchi M, Kobayashi K, Fujimoto M, Baba Y (2005) Bio-sensing on a chip with compact discs and nanofibers. Lab Chip 5:1412–1415
112. Kongruang S (2008) Bacterial cellulose production by Acetobacter xylinum strains from agricultural waste products. Appl Biochem Biotechnol 148:245–256
113. Goelzer FDE, Faria-Tischer PCS, Vitorino JC, Sierakowski M-R, Tischer CA (2009) Production and characterization of nanospheres of bacterial cellulose from Acetobacter xylinum from processed rice bark. Mater Sci Eng C 29:546–551
114. Keshk S, Sameshima K (2006) The utilization of sugar cane molasses with/without the presence of lignosulfonate for the production of bacterial cellulose. Appl Microbiol Biotechnol 72:291–296
115. Thompson DN, Hamilton MA (2001) Production of bacterial cellulose from alternate feedstocks. Appl Biochem Biotechnol 91–93:503–513
116. Battista OA, Coppick S, Howsmon JA, Morehead FF, Sisson WA (1956) Level-off degree of polymerization—relation to polyphase structure of cellulose. Ind Eng Chem 48:333–335
117. Battista OA (1985) Cellulose, microcrystalline. In: Kroschwitz JI (ed) Encycl Polym Sci Eng 3:86–90
118. Battista OA, Smith PA (1962) Microcrystalline cellulose—oldest polymer finds new industrial uses. Ind Eng Chem 54:20–29

119. Steege HH, Philipp B (1974) Characterization and use of microcrystalline cellulose. Zellst Pap 23:68–73
120. Engelhardt J (1995) General introduction on cellulose: sources, industrial derivatives and commercial application of cellulose. Carbohydr Eur 12:5–14
121. Fleming K, Gray D, Prasannan S, Matthews S (2000) Cellulose crystallites: a new and robust liquid crystalline medium for the measurement of residual dipolar couplings. J Am Chem Soc 122:5224–5225
122. Meiland M, Liebert T, Heinze T (2011) Tailoring the degree of polymerization of low molecular weight cellulose. Macromol Mater Eng 296:802–809
123. Meiland M, Liebert T, Baumgaertel A, Schubert US, Heinze T (2011) Alkyl β-D-cellulosides: non-reducing cellulose mimics. Cellulose 18:1585–1598
124. Hubbe MA, Rojas OJ, Lucia LA, Sain M (2008) Cellulosic nanocomposites: a review. BioResources 3:929–980
125. Dong S, Roman M (2007) Fluorescently labeled cellulose nanocrystals for bioimaging applications. J Am Chem Soc 129:13810–13811
126. Dufresne A (2008) Polysaccharide nano crystal reinforced nanocomposites. Can J Chem 86:484–494
127. Pääkkö M, Ankerfors M, Kosonen H, Nykänen A, Ahola S, Österberg M, Ruokolainen J, Laine J, Larsson PT, Ikkala O, Lindström T (2007) Enzymatic hydrolysis combined with mechanical shearing and high-pressure homogenization for nanoscale cellulose fibrils and strong gels. Biomacromol 8:1934–1941
128. Angellier H, Putaux J-L, Molina-Boisseau S, Dupeyre D, Dufresne A (2005) Starch nanocrystal fillers in an acrylic polymer matrix. Macromol Symp 221:95–104
129. Kroon-Batenburg LMJ, Kroon J, Northolt MG (1986) Chain modulus and intramolecular hydrogen bonding in native and regenerated cellulose fibers. Polym Commun 27:290–292
130. Nishino T, Matsuda I, Hirao K (2004) All-cellulose composite. Macromolecules 37:7683–7687
131. Odijk T, Lekkerkerker HNW (1985) Theory of the isotropic-liquid crystal phase separation for a solution of bidisperse rodlike macromolecules. J Phys Chem 89:2090–2096
132. Marchessault RH, Morehead FF, Walter NM (1959) Liquid crystal systems from fibrillar polysaccharides. Nature 184:632–633
133. Revol JF, Godbout L, Dong XM, Gray DG, Chanzy H, Maret G (1994) Chiral nematic suspensions of cellulose crystallites; phase separation and magnetic field orientation. Liq Cryst 16:127–134
134. Revol JF, Godbout L, Gray DGJ (1998) Solid self-assembled films of cellulose with chiral nematic order and optically variable properties. J Pulp Pap Sci 24:146–149
135. De Souza Lima MM, Borsali R (2004) Rodlike cellulose microcrystals: structure, properties, and applications. Macromol Rapid Commun 25:771–787
136. Orts WJ, Godbout L, Marchessault RH, Revol J-F (1998) Enhanced ordering of liquid crystalline suspensions of cellulose microfibrils: a small-angle neutron scattering study. Macromolecules 31:5717–5725
137. Marchessault RH, Morehead FF, Koch MJ (1961) Hydrodynamic properties of neutral suspensions of cellulose crystallites as related to size and shape. J Colloid Sci 16:327–344
138. Onogi S, Asada T (1980) Rheology and rheo-optics of polymer liquid crystals. In: Astarita G, Marrucci G, Nicolais L (eds) Rheology. Plenum, New York
139. Orts WJ, Godbout L, Marchessault RH, Revol JF (1995) Shear-induced alignment of liquid-crystalline suspensions of cellulose microfibrils. ACS Symp Ser 597:335–348
140. Araki J, Wada M, Kuga S, Okano T (1999) Influence of surface charge on viscosity behavior of cellulose microcrystal suspension. J Wood Sci 45:258–261
141. Araki J, Wada M, Kuga S, Okano T (1998) Flow properties of microcrystalline cellulose suspension prepared by acid treatment of native cellulose. Colloids Surf A 142:75–82
142. Viet D, Beck-Candanedo S, Gray DG (2007) Dispersion of cellulose nanocrystals in polar organic solvents. Cellulose 14:109–113

143. Siqueira G, Bras J, Dufresne A (2009) Cellulose whiskers versus microfibrils: Influence of the nature of the nanoparticle and its surface functionalization on the thermal and mechanical properties of nanocomposites. Biomacromolecules 10:425–432
144. Favier V, Chanzy H, Cavaille JY (1995) Polymer nanocomposites reinforced by cellulose whiskers. Macromolecules 28:6365–6367
145. Dubief D, Samain E, Dufresne A (1999) Polysaccharide microcrystals reinforced amorphous poly(β-hydroxyoctanoate) nanocomposite materials. Macromolecules 32:5765–5771
146. Dufresne A, Kellerhals MB, Witholt B (1999) Transcrystallization in Mcl-PHAs/cellulose whiskers composites. Macromolecules 32:7396–7401
147. Anglès MN, Dufresne A (2000) Plasticized starch/tunicin whiskers nanocomposites 1. Structural analysis. Macromolecules 33:8344–8353
148. Grunert M, Winter WT (2002) Nanocomposites of cellulose acetate butyrate reinforced with cellulose nanocrystals. J Polym Environ 10:27–30
149. Chazeau L, Cavaillé JY, Perez J (2000) Plasticized PVC reinforced with cellulose whiskers. II. Plastic behaviour. J Polym Sci Part B: Polym Phys 38:383–392
150. Azizi Samir AS, Alloin F, Dufresne A (2005) Review of recent research into cellulosic whiskers, their properties and their application in nanocomposite field. Biomacromolecules 6:612–626
151. Heux L, Chauve G, Bonini C (2000) Nonflocculating and chiral-nematic self-ordering of cellulose microcrystals suspensions in nonpolar solvents. Langmuir 16:8210–8212
152. Araki J, Wada M, Kuga S (2001) Steric stabilization of a cellulose microcrystal suspension by poly(ethylene glycol) grafting. Langmuir 17:21–27
153. Goussé C, Chanzy H, Excoffier G, Soubeyrand L, Fleury E (2002) Stable suspensions of partially silylated cellulose whiskers dispersed in organic solvents. Polymer 43:2645–2651
154. Terech P, Chazeau L, Cavaille JY (1999) A small-angle scattering study of cellulose whiskers in aqueous suspensions. Macromolecules 32:1872–1875
155. Samir MASA, Alloin F, Gorecki W, Sanchez J-Y, Dufresne A (2004) Nanocomposite polymer electrolytes based on poly (oxyethylene) and cellulose nanocrystals. J Phys Chem B 108:10845–10852
156. Schroers M, Kokil A, Weder C (2004) Solid polymer electrolytes based on nanocomposites of ethylene oxide-epichlorohydrin copolymers and cellulose whiskers. J Appl Polym Sci 93:2883–2888
157. Dujardin E, Blaseby M, Mann S (2003) Synthesis of mesoporous silica by sol-gel mineralization of cellulose nanorod nematic suspensions. J Mater Chem 13:696–699
158. Dong S, Roman M (2007) Fluorescently labeled cellulose nanocrystals for bioimaging applications. J Am Chem Soc 129:13810–13811
159. Roman M, Dong S, Hirani A, Lee YW (2009) Cellulose nanocrystals for drug delivery. In: Edgar KJ, Heinze T, Buchanan CM (eds) Polysaccharide materials: performance by design. ACS Symposium Series. American Chemical Society, Washington DC, pp 81–91
160. Zimmermann T, Pöhler E, Geiger T (2004) Cellulose fibrils for polymer reinforcement. Adv Eng Mater 6:754–761
161. Turbak AF, Synder FW, Sandberg KR (1983) Microfibrillated cellulose, a new cellulose product: properties, uses, and commercial potential. J Appl Polym Sci Appl Polym Symp 37:815–827
162. Taniguchi T, Okamura K (1998) New films produced from microfibrillated natural fibres. Polym Int 47:291–294
163. Iwamoto S, Nakagaito AN, Yano H, Nogi M (2005) Optically transparent composites reinforced with plant fiber-based nanofibers. Appl Phys A 81:1109–1112
164. Chakraborty A, Sain M, Kortschot M (2005) Cellulose microfibrils: a novel method of preparation using high shear refining and cryocrushing. Holzforschung 59:102–107
165. Bhatnagar A, Sain M (2005) Processing of cellulose nanofiber-reinforced composites. J Reinf Plast Compos 24:1259–1268
166. Zhao H-P, Feng X-Q, Gao H (2007) Ultrasonic technique for extracting nanofibers from nature materials. Appl Phys Lett 90:073112/1-073112/2

167. Wagberg L, Decher G, Norgren M, Lindström T, Ankerfors M, Axnäs K (2008) The build-up of polyelectrolyte multilayers of microfibrillated cellulose and cationic polyelectrolytes. Langmuir 24:784–795
168. Werner O, Persson L, Nolte M, Fery A, Wagberg L (2008) Patterning of surfaces with nanosized cellulosic fibrils using microcontact printing and a lift-off technique. Soft Matter 4:1158–1160
169. Turbak AF, Snyder FW, Sandberg KR (1982) Suspensions containing microfibrillated cellulose EP19810108847
170. Dinand E, Vignon MR (2001) Isolation and NMR characterization of a (4-O-methyl-D-glucurono)-D-xylan from sugar beet pulp. Carbohydr Res 330:285–288
171. Stenstad P, Andresen M, Tanem BS, Stenius P (2008) Chemical surface modifications of microfibrillated cellulose. Cellulose 15:35–45
172. Cavaille J-Y, Chanzy H, Fleury E, Sassi J-F (1997) Surface-modified cellulose microfibrils, method for making same, and use thereof as a filler in composite materials. US6117545
173. Cash MJ, Chan AN, Conner HT, Cowan PJ, Gelman RA, Lusvardi KM, Thompson SA, Tise FP (2000) Derivatized microfibrillar polysaccharides, their formation and use in dispersions. US6602994
174. Dong S, Sapieha S, Schreiber HP (1993) Mechanical properties of corona-modified cellulose/polyethylene composites. Polym Eng Sci 33:343–346
175. Agarwal M, Lvov Y, Varahramyan K (2006) Conductive wood microfibres for smart paper through layer-by-layer nanocoating. Nanotechnology 17:5319–5325

# Chapter 2
# Structure and Properties of Cellulose and Its Derivatives

## 2.1 Molecular and Supramolecular Structure of Cellulose

The first systematic clarification of the cellulose structure began in 1837 with investigations of the French agricultural chemist Anselme Payen and finally the French Academy named the carbohydrate "Cellulose" [1, 2]. The cellulose molecule consists of β-(1→4)-glycosidically linked glucose units. The anhydroglucose unit (AGU) exists as D-glucopyranose ring in $^4C_1$-chair configuration, which exhibits the lowest energy conformation [3]. The β-linkage results in a turning around of the cellulose chain axis by 180° of each second AGU. Consequently, the repeating unit of cellulose is cellobiose with a length of 1.3 nm [4]. From the chemist's point of view, it is useful to consider the AGU as repeating unit because it possesses three reactive hydroxyl groups, one primary (position 6) and two secondary ones (positions 2 and 3), which undergo typical reactions of hydroxyl groups (Fig. 2.1). The hydroxyl groups are positioned in the plane of the ring. The chain ends of the cellulose molecule are chemically different [5], i.e., one end has the anomeric carbon atom involved in the glycosidic linkage, whereas the other consists of the D-glucopyranose unit in the hemiacetal form, in equilibrium with the aldehyde function that is the reducing end of the chain. However, these end groups do not influence the overall properties of cellulose and their derivatives. Although the reducing end groups may be used for selective modification, e.g., by reductive amination, e.g., the main work of cellulose chemistry is focused on the hydroxyl groups or, after transforming the hydroxyl groups to a good leaving group (e.g., by tosylation) on the C atoms that undergo nucleophilic displacement ($S_N$) reactions (see Sect. 5.2).

Deviations from the ideal structure of D-anhydroglucopyranose units linked together by β-(1→4)-glycosidic linkages are usually observed in technical cellulose samples due to the presence of carbonyl and carboxyl groups. Carboxyl groups may cover a range from 2 to 40 mmol/kg in cotton linters and pulp. They are quantified by alkalimetric titration after converting the carboxylate function to the free acid.



T. Heinze et al., *Cellulose Derivatives*, Springer Series on Polymer and Composite Materials, https://doi.org/10.1007/978-3-319-73168-1_2

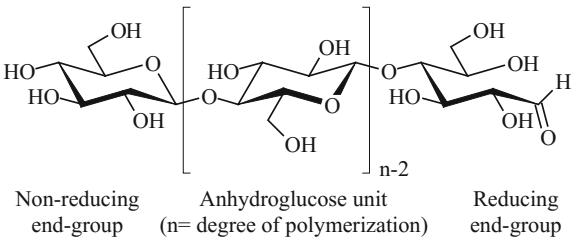


**Fig. 2.1** Schematic representation of the chemical structure of cellulose

A fast method is based on the binding of the methylene blue cation by the COOH moieties and subsequent determination of the dye concentration [6].

A conventional method to determine the carbonyl groups is their reaction with hydroxylamine to form the corresponding hydroxamic acid and the determination of the nitrogen content by elemental analysis [7]. More recently, fluorescence labeling with carbazole-9-carboxylic acid [2-(2-aminooxyethoxy)ethoxyl]amide was shown to be an accurate method for the determination of carbonyls in cellulose. The labeling could be carried out heterogeneously or homogeneously (by employing DMAc/LiCl as solvent). This procedure is suitable to determine the distribution profile relative to the molecular weight of the samples by applying SEC/MALS [8]. Fluorescence labeling by 9*H*-fluoren-2-yl-diazomethane has been also employed for determining carboxylic groups. SEC/MALS measurements with an additional fluorescence detector give information about the carboxyl content versus the molecular weight of the sample. It turned out that the carboxyl groups are concentrated in the low molecular weight fraction of the pulp samples [9].

### Hydrogen Bonding in Cellulose

The formation of hydrogen bonds in cellulose is considered to have a strong influence on the properties. The limited solubility in usual solvents, the reactivity of the hydroxyl groups, and the crystallinity of cellulose are originated from the strongly hydrogen-bonded system. The three hydroxyl groups of the AGU and the oxygens of both the ring and the glycosidic linkage interact with each other within the chain or with another cellulose chain by forming secondary valence bonds, namely intramolecular and intermolecular hydrogen bonds. The versatile possibilities for the formation of the hydrogen bonds give rise to various three-dimensional structures. Solid-state $^{13}C$ NMR measurements [10] and IR spectroscopy [11, 12] reveal intramolecular bonds between the OH of C3 and the adjacent ether oxygen of the AGU as well as a second one between the hydroxyl oxygen at C6 and the adjacent OH at the position C2 (Fig. 2.2). The intramolecular hydrogen bonds are responsible for the relative stiffness and rigidity of the cellulose molecules in combination with the β-glycosidic linkage [4]. The chain stiffness results in highly viscous solutions (in comparison to α-glycosidically linked polysaccharides like starch or dextran), a high tendency to crystallize, and the formation of fibrillar assemblies (see Sect. 2.3.1).

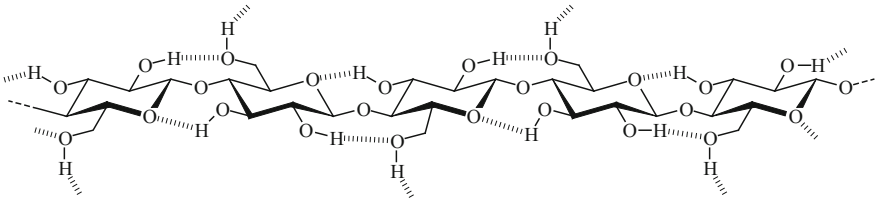

**Fig. 2.2** Hydrogen-bonding system of cellulose I (according to [13])

In the crystal lattice, the cellulose molecules are bonded by intermolecular hydrogen bonds, in particular, between the OH of C6 and the oxygen of C3 of an adjacent chain along the (002) plane of cellulose I (Fig. 2.2) [14]. Consequently, the cellulose molecules are linked together in a layer, but the layers are only held together by hydrophobic interactions and weak C–H–O bonds, which could be confirmed by synchrotron X-ray and neutron diffraction data [15]. Detailed discussion of these methods and the structures determined by these measurements are found in Sects. 2.3.1 and 2.3.3.

## 2.2 Molar Mass and Its Distribution

The determination of the molar mass is important to any research on cellulose and its derivatives because it is a fundamental physicochemical property. The results obtained bear on dissolution, regeneration, and accessibility/reactivity of the biopolymer. Examples are the detection of oxidative degradation that may accompany mercerization under relatively strong alkaline conditions, e.g., by using 12–20% NaOH solution [16], evaluation of the effect of cellulose dissolution in solvents on its DP [17–19], and the determination of the effects of functionalization of cellulose into derivatives on the chain length of the biopolymer [20].

Most polymeric materials are composed of mixtures of molecules of various sizes. Consequently, the molar mass of a polymer is described by an average molar mass, $\overline{M}$. A complete description of the molar mass distribution of a homopolymer is necessary in order to understand the physical, rheological, and mechanical properties, hence evaluate its performance and predict possible applications.

If the chains are counted by number, it is the number average molar mass $\overline{M}_n$, whereas if they are counted by weight, it is the weight average molar mass, $\overline{M}_W$. For homopolymers like cellulose, these averages are defined in terms of the molar mass ($M_i$), the number ($n_i$) or the weight ($w_i$) of the repeating unit, i.e., AGU. Table 2.1 shows the definitions of the different $\overline{M}$ employed, where the exponent ($a$) of $\overline{M}_V$ is that of the Mark–Houwink–Sakurada equation. Inspection of the formulas listed in Table 2.1 shows that $\overline{M}_n = \overline{M}_W = \overline{M}_Z$ for monodisperse population of molecules. A simple calculation shows that this is not the case for polydisperse mixtures; there

**Table 2.1** Different types of average molar masses and the corresponding definitions

| Name | Definition |
|---|---|
| Number average molar mass | $\overline{M}_n = \frac{\sum n_i \cdot M_i}{\sum n_i} = \frac{\sum w_i}{\sum \frac{w_i}{M_i}}$ |
| Weight average molar mass | $\overline{M}_w = \frac{\sum n_i \cdot M_i^2}{\sum n_i \cdot M_i} = \frac{\sum w_i \cdot M_i}{\sum w_i}$ |
| z-Average molar mass | $\overline{M}_z = \frac{\sum n_i \cdot M_i^3}{\sum n_i \cdot M_i^2} = \frac{\sum w_i \cdot M_i^2}{\sum w_i \cdot M_i}$ |
| Viscosity average molar mass | $\overline{M}_v = \left(\frac{\sum n_i \cdot M_i^{1+a}}{\sum n_i \cdot M_i}\right)^{\frac{1}{a}} = \left(\frac{\sum w_i \cdot M_i^a}{\sum w_i}\right)^{\frac{1}{a}}$ |

is "bias" of each $\overline{M}$ scale to the presence of the monomer. Consider the chemical or enzymatic hydrolysis of cellulose to give a mixture composed of 10 molecules of glucose ($\overline{M}_W$ = 180.16 g/mol) and 90 molecules of cellulose, whose DP is 150. The $\overline{M}_W$ of the latter molecule is 24,321 g/mol, based on $\overline{M}_W$ of 162.14 g/mol for the AGU, considering that the terminal groups are also AGU. Based on the same assumption, the values of $\overline{M}_n$, $\overline{M}_W$, and $\overline{M}_Z$ are 21,907, 24,301, and 24,321 g/mol, respectively. That is, the presence of a few monomer molecules has a marked influence on $\overline{M}_n$, whereas $\overline{M}_Z$ is dominated by the presence of the polymer. Therefore, for a polydisperse population of molecules $\overline{M}_n < \overline{M}_W < \overline{M}_Z$; one should always specify the type of $\overline{M}$ that has been discussed.

The parameter $\frac{\overline{M}_w}{\overline{M}_n}$, the polydispersity index (PI), is characteristic of the biopolymer, or the method of obtaining synthetic polymers. For example, ionic and coordination polymerization produces material with $\frac{\overline{M}_w}{\overline{M}_n}$ approaching 1.05; between 1.5 and 4.5, and 5 and 20 for synthetic polymers obtained by radical reactions, and by using the Ziegler–Natta catalyst, respectively.

A discussion of the different experimental techniques employed for the determination of $\overline{M}$ is beyond the scope of the present chapter. The reader is referred to specialized literature on polymer analysis/characterization techniques [21–29]. It is worthwhile, however, to list some of the techniques employed for these determinations. The method is absolute (or primary), if no calibration is required or relative (or secondary), if calibration against an absolute method is required. Ebullioscopy, cryoscopy, and vapor pressure osmometry are absolute methods that are usually employed for the calculation of $\overline{M}_n$. Light scattering, LS, sedimentation equilibrium (ultracentrifugation), and X-ray small-angle scattering are also absolute methods that are employed to calculate $\overline{M}_W$. Viscometry and size exclusion chromatography, SEC, are relative methods that are usually calibrated against LS. The techniques, which we will discuss, are viscometry, SEC, and LS. In addition to the determination of $\overline{M}$, these measurements give insight into several important characteristics of interactions within the biopolymer solution, including the average conformations of the polymer chain, polymer/solvent, and polymer/polymer interactions. For each

technique, the theoretical bases and the relevant information, which can be obtained from the experiment are briefly discussed. Comments on the experiments and representative examples of applications to cellulose and its derivatives are given.

## 2.2.1 Rheology and Viscometry

### 2.2.1.1 Theoretical Background

Rheology (Greek: *rheos* = current or stream) is concerned with the relationship between forces and deformations. A body responds to stress by deformation. Figure 2.3 shows the nine possible deformations of a body (for simplicity shown as a cube) with three types of surfaces areas (1, 2, and 3). The stresses $\sigma_{11}$, $\sigma_{22}$, and $\sigma_{33}$ are called normal stresses, they are perpendicular to the areas. The differences ($\sigma_{11} - \sigma_{22}$) and ($\sigma_{22} - \sigma_{33}$) are called the first and the second normal stress, respectively.

Viscometry (or viscosimetry) characterizes the flow of fluids by their viscosity. Shear viscosities [shear rate = $f$(shear stress)] are important for the molecular characterization of polymers via intrinsic viscosities of their dilute solutions. Shear viscosities are most commonly investigated, hence are simply designated as "viscosities", on one hand. On the other, extensional or elongation viscosities [extensional rate = $f$(tensile stress)] are relevant to the extrusion of polymer melts and solutions into fibers and films. The reason is that shear flow causes the coiled (polymer) molecules to undergo rotation in addition to Brownian motion, whereas tensile flow stretches the coiled molecules.

By definition, the body shown in Fig. 2.3 is sheared in the 2-1 direction. This shear requires a (shearing) stress $\tau = \sigma_{21}$. The ratio of the first normal stress difference to the shear stress is the elastic shear deformation (Eq. 2.1) and the ratio of shear stress to elastic shear deformation is the shear modulus, $G$ (Eq. 2.2):

$$\gamma = \frac{\sigma_{11} - \sigma_{22}}{\sigma_{21}} \tag{2.1}$$

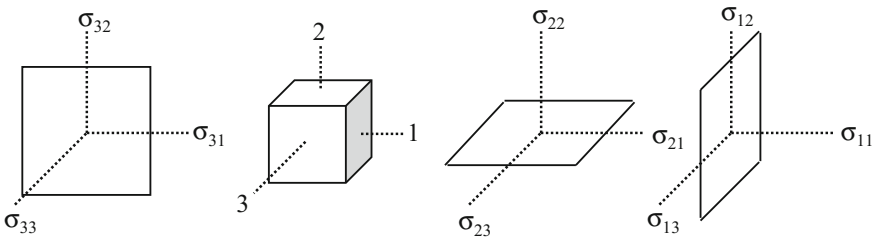


**Fig. 2.3** Possible deformations of a (cube) body

**Table 2.2** Common and IUPAC names; symbols, and common units of forms mostly employed to present viscosity

| Common name | IUPAC name | Functional form | Symbol | Common units |
|---|---|---|---|---|
| Viscosity | – | – | $\eta$ | Pa s; mPa s |
| Relative viscosity | Viscosity ratio | $\frac{\eta}{\eta_0}$ | $\eta_r$ | None |
| Specific viscosity | – | $\frac{\eta}{\eta_0} - 1$ | $\eta_{sp}$ | None |
| Reduced viscosity | Viscosity number | $\frac{\frac{\eta}{\eta_0}-1}{c}$ | $\eta_{red}$ | dL/g |
| Inherent viscosity | Logarithmic viscosity number | $c^{-1} \cdot \ln\left(\frac{\eta}{\eta_0}\right)$ | $\eta_{inh}$ | dL/g |
| Intrinsic viscosity | Limiting viscosity number | $\lim_{c\to 0} \eta_{red}$ or $\lim_{c\to 0} \eta_{inh}$ | $[\eta]$ | dL/g |

$$G = \frac{\tau}{\gamma} = \frac{\sigma_{21}}{\gamma} = \frac{\sigma_{21}^2}{\sigma_{11} - \sigma_{22}} \tag{2.2}$$

The dynamic viscosity, $\eta$, is the ratio between shear stress to shear rate, $\overset{\circ}{\gamma}$, and is thus equal to the product of ($G$) and the time ($t$), Eq. 2.3:

$$\eta = \frac{\tau}{\overset{\circ}{\gamma}} = \frac{\sigma_{21}}{\overset{\circ}{\gamma}} = \frac{G \cdot \gamma}{\overset{\circ}{\gamma}} = G \cdot \tau \tag{2.3}$$

The unit of viscosity is Pascal-second or milliPascal-second (Pa s or mPa s), which is related to the Poise, P, by: 1 Pa s = 10 P. Materials vary widely in viscosities, e.g., $\eta = 10^{-5}$; $10^{-3}$; $10^{-2}$; $10^{-1}$, 10 Pa s, for air, water, light mineral oil, olive oil, and glycerol [21]. The different viscosity scales are listed in Table 2.2, where $c$ is the concentration, $\eta$ and $\eta_0$ refer to the viscosities of solution and solvent, respectively.

**Response of Solutions to Shear: Newtonian and Non-Newtonian Flow Models**

Several flow models have been proposed for describing flow patterns of fluids [30]. Although they are not likely to describe the rheological behavior over an extended shear rate range, they are useful for summarizing most of the experimental data. According to Eq. (2.2), $\sigma_{12}$ is a linear function of $\overset{\circ}{\gamma}$, whereas $\eta$ is independent of the shear rate. A fluid that shows these characteristics is called Newtonian fluid. Water, DMAc/LiCl, many ILs, and solutions of cellulose and its derivatives in these solvents, in particular at low temperature under low shear, belong to this category [31–35].

The Newtonian viscosity is also called zero shear or stationary viscosity (Eq. 2.4). Both $\eta_0$ and $G_0$ (shear modulus at rest) are material constants.

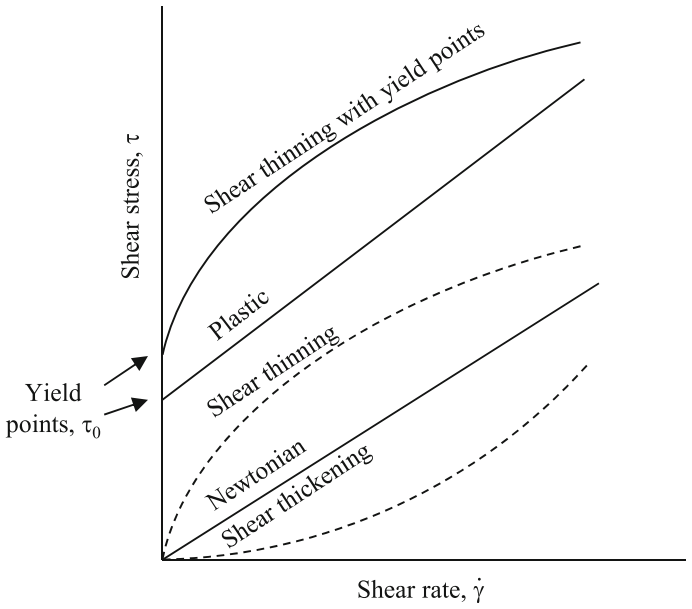


**Fig. 2.4** Flow curves (shear stress vs. shear rate) for the different types of flow behavior

$$\eta_0 = G_0 \cdot \left(\frac{\gamma}{\overset{\circ}{\gamma}}\right) \tag{2.4}$$

As shown in Fig. 2.4, fluids may not conform to Newton's law (Eq. 2.5),

$$\tau = \eta \cdot \overset{\circ}{\gamma} \tag{2.5}$$

i.e., under shear, their viscosities are nonlinear functions of shear rate. This (nonlinear) behavior can be time independent or time dependent. The plastic or Bingham body model predicts constant plastic viscosity above a yield stress. This model describes the behavior of some dispersions and pigment pastes. Yield stress, $\tau_0$, and plastic (Bingham) viscosity (Eq. 2.6),

$$\eta_P = (\tau - \tau_0) \cdot \overset{\circ}{\gamma} \tag{2.6}$$

are obtained from the intercept and slope beyond the intercept of the shear stress versus shear rate plot. Many technically important fluids, e.g., polymer melts, lattices, pigment slurries, solutions of cellulose in ILs show other shear-dependent behaviors [36, 37]. At high shear rates, most of these fluids show Newtonian behavior. At low shear, they tend either to a yield point or to a low shear Newtonian limiting viscosity. At intermediate shear rates, the power law (Eq. 2.7),

$$\tau = k \cdot \left(\overset{\circ}{\gamma}\right)^n \tag{2.7}$$

$k$ is a constant, holds for many fluids and describes Newtonian, shear-thinning, and shear-thickening behaviors, depending on the value of $n = 1$, <1, or >1, respectively. Although the viscosity response to shear rate is expected to be attained "immediately", some fluids show time-dependent change in viscosity at a constant shear rate. These include thixotropic fluids whose viscosities decrease with time (Greek: *thixis* = movement; *tropos* = change) and anti-thixotropic ones that show the opposite behavior.

#### 2.2.1.2 Practical Aspects

**Measurement of Viscosity and Information from the Experimental Data**

The use of viscometry to study polymer solutions is attractive because the measurements are simple and the accuracy is high due to the availability of computer-controlled, low-cost viscometers, of which the capillary and cone-and-plate types will be briefly discussed (Fig. 2.5).

Most capillary viscometers are designed with relatively large bulbs at both ends of the capillary. A constant volume in the upper bulb (part A) is marked with etched lines. The experiment involves measuring the time ($t$) required for the fluid to flow through this bulb, i.e., between the two lines. The only pressure difference across the liquid is its weight. Under these conditions, the appropriate (Poiseuille) equations are given by Eqs. 2.8 (for one liquid) and 2.9 (for two liquids):

$$\eta = A \cdot \rho \cdot t \tag{2.8}$$

$$\eta_2 = \frac{\rho_2 \cdot t_2}{\rho_1 \cdot t_2} \cdot \eta_1 \tag{2.9}$$

The constant $A$ incorporates all the parameters that characterize the viscometer, and can be eliminated by comparing two liquids, 1 and 2, as shown in Eq. 2.9. The unknown viscosity $\eta_2$ is calculated from the flow times and densities of the two liquids and the known viscosity of one of them $\eta_1$.

In the cone-and-plate viscometer, Fig. 2.5b, the fluid is placed between a stationary plate and a cone that touches the plate at its apex; cones with different dimensions permit measuring a wide range of viscosities. To determine the viscosity of the fluid, the torque $T$ necessary to turn the cone at an angular velocity $\omega$ is measured. It depends on the viscosity of the fluid. This equipment can be operated at different angular velocities, thus $\eta$ can be determined at different rates of shear.

Capillary viscometers are useful for studying liquids of low molar mass and dilute solutions in such solvents. The reason is that they generally display Newtonian behavior, i.e., there is no advantage in being able to vary the shear rate.

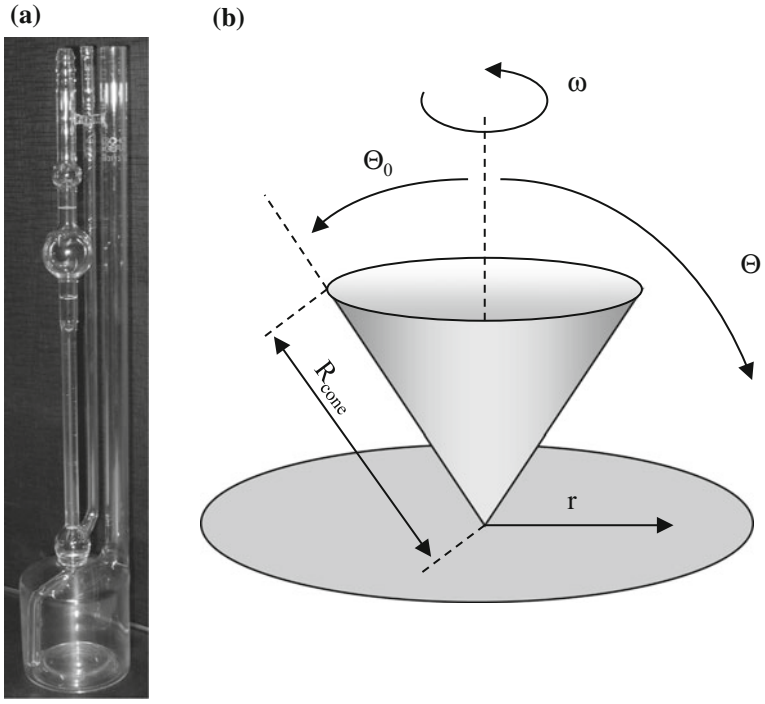


**Fig. 2.5** Schematic representations of a capillary with a dilution reservoir (**a**), and cone-and-plate viscometers (**b**)

The shear dilution viscometer shown in Fig. 2.5a is very convenient because only one (concentrated) polymer solution is required. Solutions of other concentration are obtained by dilution with the solvent inside the viscometer, e.g., by use of a computer-controlled peristaltic pump. This mode of operation eliminates the labor involved in preparing various polymer solutions (of increasing concentration). Dilution is automatic, which eliminates volume-based errors. For cellulose solution in Cuen, it minimizes the oxidative degradation of the biopolymer. The cone-and-plate viscometers and the similar concentric cylinder viscometer (not discussed) are appropriate to study fluids, including Newtonian ones, where the viscosity is very high, e.g., polysaccharide solutions in ILs. They are the equipments of choice to study non-Newtonian fluids like shear-thinning solutions of cellulose in ILs [34, 36–38].

For a solution of cellulose in aqueous Cuen [39] or of cellulose acetate (with high DS) in DMAc [40], $\overline{M}_V$ can be obtained as follows by applying the empirical Huggins equation for solutions of nonelectrolytes:

$$\eta_{\text{red}} = [\eta] + k_{\text{H}} \cdot [\eta]^2 \cdot c, \tag{2.10}$$

where $k_{\text{H}}$ is Huggins constant whose values are between 0.33 and 0.8. The value of $[\eta]$ is obtained by extrapolation of the plot of $\eta_{\text{red}}$ versus $c$ to infinite dilution ($c \rightarrow 0$). The logarithmic form of the Mark–Houwink–Sakurada equation is

$$\ln[\eta] = \ln K + a \ln \overline{M}_V, \tag{2.11}$$

where $K$ and $a$ are system-specific constants that depend on the polymer, the solvent, and the temperature. The value of ($a$) depends on the shape and segment distribution of the molecule. Theory predicts values of 0 for spheres; 0.5 for unperturbed coils (in theta solvents); 0.764 for perturbed coils (in good solvents), and 2 for infinitely thin, rigid rods.

Viscometry is a relative method, i.e., calibration against a absolute method is required for the determination of $\overline{M}_V$. For solution of a given polymer in a specific solvent, values of $K$ and $a$ are determined by measuring $[\eta]$ for samples of different molar mass; the latter quantity is determined by a primary method, e.g., end group analysis or LS; values of $K$ and $a$ of Eq. 2.11 are calculated, then employed in the calculation of $\overline{M}_V$ of other samples.

#### 2.2.1.3 Applications of Viscometry in Cellulose Chemistry

The most extensive application of viscometry is the determination of DP of cellulose and its derivatives. Cellulose may be dissolved in various solvents including cuprammonium hydroxide (Cuam) [41–43], cupriethylene diamine (Cuen) [44], and quaternary organic bases [45]. The intrinsic viscosities of a cellulose sample dissolved in Cuen and cadmium ethylenediamine (Cadoxen) were found to be linearly correlated, enabling the conversion of viscosities in one solvent to that in the other [46]. Since all these solutions are alkaline, biopolymer chain degradation may occur [47, 48].

An alternative path is the transformation of the cellulose into an easily soluble derivative, e.g., its nitrate, which is soluble in acetone or ethyl acetate [49] or triphenyl carbamate (solutions in acetone or dioxane) for the determination of $\overline{M}_V$. The cellulose triphenylcarbamate is prepared under mild conditions compared with cellulose nitrate. The biopolymer is essentially fully substituted. This is an important requirement because the DS has a marked effect on the state of solution, hence its viscosity [50–52]. Generally, dilute solutions, 1–5 g/L, are employed for viscosity measurements, the value of $\eta_{\text{r}}$ should be $\leq 2.5$, since the dependence of viscosity on composition may not be linear at higher polymer concentrations.

The following examples show further applications of viscometry in cellulose chemistry. A point that may bear on the accessibility, hence reactivity of cellulose in non-derivatizing solvents is its degree of association, especially at (desirable) high cellulose contents. This question can be readily answered by comparing the

DP values calculated for dilute cellulose solutions in aqueous Cuen or Cadoxen (molecularly dispersed) [53]. This comparison has shown that cellulose solutions in DMAc/LiCl or ILs form aggregates [54–56], whose size is correlated with DS [57].

Values of $\eta_r$ showed solution aging as a function of time, whereas values of $[\eta]$ increased as a function of increasing concentration LiCl from 3 to 7%, reaching a plateau at higher electrolyte concentrations [58]. This (aggregation) problem can be solved by derivatization of the biopolymer, followed by measuring the viscosity of its (non-aggregated) derivative in an appropriate solvent. Several cellulose samples (MCC, cotton linters, regenerated cellulose, DP range from 173 to 2505) were transformed into cellulose tricarbanilates (CTC). Their DP values, as measured by LS and SEC in THF, were in good agreement, showing that these derivatives do not aggregate [59]. For solutions of several cellulose samples in DMAc/LiCl, the concentration dependence of viscosity on solution composition increases rapidly above a critical weight fraction of the biopolymer, where the chains begin to overlap. The formation of such aggregates is not restricted to the solvent DMAc/LiCl. Depending on the solvent and cellulose concentration, the biopolymer chains build up a loose network with gel particles (Viscose), or an entanglement network with high swollen aggregates (Lyocell) [60]. Finally, the Mark–Houwink–Sakurada equation applies to 1–3% cellulose solutions in 8% DMAc/LiCl, the corresponding value of the parameter ($a$) was found to be 0.85 [31].

Viscosity measurements can be also employed in order to detect the transition isotropic → anisotropic of dissolved cellulose in, e.g., aqueous NMMO. Plots of $\log \eta_{\text{apparent}}$ (at $\overset{\circ}{\gamma} = 50\ s^{-1}$) versus cellulose concentration showed abrupt increase at [cellulose] = 20% (w/w), at 85 or 90 °C, but not at 100 or 110 °C. The viscosity data were treated according to an Arrhenius-type equation, where $E_{\text{flow}}$ is the corresponding activation energy for viscous flow

$$\log \eta = \frac{\log A + E_{\text{flow}}}{2.303 \cdot R \cdot T} \tag{2.12}$$

Plots ($\overset{\circ}{\gamma} = 50\ s^{-1}$) of $\log \eta_{\text{apparent}}$ versus $\frac{1}{T}$ were linear at 15 and 18% (w/w) cellulose and showed two distinct lines for 20, 23, and 25% (w/w) cellulose. This behavior (two lines) was also observed for solutions of 25% (w/w) cellulose in the solvent at different shear rates, $\overset{\circ}{\gamma}$ from 30 to 300 $s^{-1}$. These abrupt changes in viscosity have been attributed to the isotropic → anisotropic change of the cellulose/NMMO solution [61]. The rapid increase in viscosity of cellulose solutions in DMAc/LiCl, above 12% (w/w) cellulose, has been also attributed to isotropic → anisotropic transition [58].

## 2.2.2 Size Exclusion Chromatography, SEC

### 2.2.2.1 Theoretical Background

The term chromatography is derived from the Greek words *chroma* (color) and *graphein* (to write). Column, gas, and size exclusion chromatographic techniques have been developed thanks to the pioneering work of Tswett [62], Martin and Golay [63, 64], and Lathe, Ruthven, and Porath, respectively [65, 66]. SEC is now established as one of the most convenient methods for polymer fractionation, and determination of molar mass and its distribution. Reliable and reproducible chromatograms are obtained in relatively short times (elution <1 h); permitting routine characterization and convenient application in quality control. Initial work on GPC focused on the conversion of a chromatogram into molar mass distribution. Several detectors (index of refraction, UV, LS) were introduced; the advantages of using rigid, small gel particles (diameter $\sim$ 10 μm) were demonstrated, resulting in the use of much shorter columns (30 cm) and thus in the reduction of the elution time. Online molar mass determination was made feasible by the introduction of multi-angle LS detectors and differential viscometers.

SEC is a special type of chromatography, where the species present in solution are separated according to their size, not their affinity toward the (porous) stationary phase. The technique introduced by Porath and Flodin has been designated as gel permeation because separation of water-soluble polymers was performed on cross-linked, highly swollen dextran gels. The description of gel permeation chromatography (GPC) by Moore [67], the introduction of an efficient stationary phase (porous, cross-linked polystyrene/divinylbenzene (PS/DVB) gel), the direct coupling of an online refractometer, and the subsequent availability of commercial instruments attracted wide spread interest in this technique.

The chromatographic resolution of a complex mixture depends on two mechanisms: The separation process in which the stationary phase controls the differential migration of the molecules and, in case of SEC, all the mechanisms that determine the permeation of the molecules in the column packing, and the dispersion process, which controls the band width of each component. An important part of data interpretation in SEC is the establishment of the relationship between the molar mass and the retention volume of the substrate.

In SEC and GPC, a dilute polymer solution is placed on top of a column filled with a solvent-soaked porous material, e.g., PS/DVB, and the column is then eluted with the solvent. The resultant elution curve is between material concentration and elution time or volume; detectors, vide supra, are used to determine the polymer concentration in the eluent.

Separation by SEC is based on the assumption that the column packing is "inert". That is, solute–stationary phase interactions are negligible; separation of the components present depends on pore volume distribution within gel particles and on solute size. There are few stationary phase pores available to accommodate large polymer molecules. Consequently, their time of residence in the column is shorter

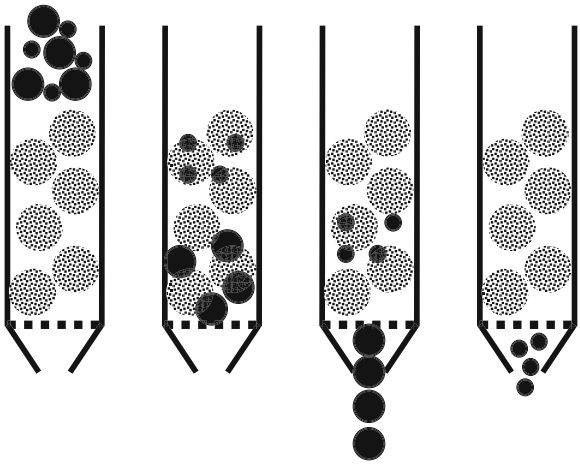

**Fig. 2.6** Schematic representation of the separation of two components in SEC, according to their molar volumes

than that of smaller molecules; hence large molecules are eluted first (Fig. 2.6). In principle, elution curves of uniform polymers should consist of sharp signals, each corresponding to a fraction (or size) of the polymer present. In practice, these curves have finite widths due to diffusion.

Benoit et al. have shown that solute size can be expressed as its hydrodynamic volume, $V_h$, defined by Einstein's equation 2.13

$$V_h = 40 \cdot \frac{\eta \cdot M}{N_{Av}}, \tag{2.13}$$

where $N_{Av}$ is Avogadro's number. Therefore, a plot of log $\eta_M$ versus the retention volume, $V_R$, should be a universal calibration curve for all polymers [68] as verified experimentally [69]. A corollary of this "universal calibration" principle is that two polymers having equal $V_h$ elute with the same $V_R$; therefore, $\overline{M}_W$ of one polymer may be determined from the calibration curve of a reference samples, e.g., polystyrene (with narrow molar mass distribution) by employing the equation

$$\log \overline{M}_W(\text{sample}) - \log \overline{M}_W(\text{reference}) = \log \frac{[\eta]_{\text{sample}}}{[\eta]_{\text{reference}}} \tag{2.14}$$

#### 2.2.2.2 Practical Aspects

One obvious application of SEC is to determine the distribution of $M$ of cellulose and its derivatives. This determination is not simple for cellulose because of its limited solubility in common solvents. In principle, this problem can be solved by transforming cellulose into derivatives (e.g., cellulose trinitrate or CTC) soluble in organic solvents, e.g., THF and DMSO. The problems associated with this

approach include the extra labor and may be problematic due to nonuniformity of derivatization and, sometimes, reduced solubility in the solvent employed [70]. The use of special solvents for cellulose, e.g., Cadoxen, NMMO, DMAc/LiCl, NMP/LiCl, and ILs is, in principle, superior and less laborious than its derivatization, thus it has gained some popularity in SEC analysis of celluloses [71, 72]. Cadoxen is an interesting solvent because of its favorable UV–Vis absorption (<220 nm), so that determination of the concentrations of dissolved species, e.g., CTC and benzyl ethers of cellulose by using UV–Vis is feasible [73].

In addition to the labor involved in the preparation of Cadoxen, this solvent is very aggressive and may destroy the column packing. This problem is minimized by diluting the solvent with water [74].

At present, ILs cannot be employed in SEC analysis because of the high viscosity of the pure solvents and still higher viscosities of cellulose solutions therein. Provided that the IL does not attack the column packing, the preceding assessment will change as very low viscosity ILs, which dissolve cellulose, are being introduced. The most popular solvent for cellulose is DMAc/LiCl. This eluent has been applied to investigate the effects of pulping, bleaching, enzymatic treatments, and the viscose process on $\overline{M}_W$ of celluloses [48, 75–77]. SEC column calibration has been carried out by using different reference polymers, including commercial polystyrene [78, 79] and pullulan [80–82] by using the Mark–Houwink constants for cellulose, pullulan, dextran, and amylose in 0.5% LiCl, at 80 °C [83]. It has been shown, however, that cellulose and pullulan have different hydrodynamic volume, i.e., the latter may not be an appropriate reference for the determination of $\overline{M}_W$ of celluloses in DMAc/LiCl [84]. This conclusion has been corroborated by analysis of the Mark–Houwink constants of celluloses and reference polymers in different solvents. This analysis has shown that the order of backbone rigidity is: Cellulose $\gg$ dextran $\geq$ pullulan $\geq$ amylose $\gg$ polystyrene. That is, at the same $\overline{M}_W$, cellulose will elute earlier than any of these polymers. Thus, their use as references is open to question [71].

Because of their solubility in common solvents, cellulose derivatives can be readily analyzed by SEC as shown by the following representative examples for the determination of $\overline{M}_W$: Propionate–, butyrate–, pentanoate–, hexanoate–, heptanoate–, and propionate/pentanoate of cellulose were analyzed using THF as eluent [85]. Cellulose trinitrate was dissolved in THF and analyzed over a Styragel column [86]. The values of $\overline{M}_W$ of water-soluble derivatives such as MC, CMC, MHPC, EHPC, and HPC have been calculated from SEC analysis by employing water/sodium nitrate eluent and a porous polycarbonate stationary phase [87]. Cellulose acetates and benzyl ethers of cellulose were dissolved in NMP and analyzed on a PS/DVB column [88]. CMC was analyzed using water containing several salts, including $NaNO_3$ [89], NaCl [90], acetate buffer [91], and $NH_4NO_3$ [92].

### 2.2.3 Light Scattering (LS)

#### 2.2.3.1 Theoretical Background

For colloids and polymers, light scattering (LS) is usually referred to as static light scattering (SLS, elastic) or dynamic light scattering (QELS, quasi-elastic) measurements. SLS is an absolute analytical method to measure the time average scattering intensity. QELS measures scattering intensity fluctuation; this is where the term dynamic comes from. In the discussion that follows, any scattering object, e.g., a macromolecule will be designated as "particle". In LS, the visibility of the scattering particles depends on the refractive index difference (dn) between the scattering particle and the medium (solvent or dispersion medium).

**Static Light Scattering, SLS**

At low solute concentration, $c$, small scattering angles, and large particles, the basic scattering equation takes the form (Eq. 2.15).

$$\frac{K_\theta \cdot c}{R_\theta} = \frac{1}{\overline{M}_W \cdot P_\theta} + 2 \cdot A_2 \cdot c + \cdots, \tag{2.15}$$

where $K_\theta$ is the optical constant, $\theta$ is the scattering angle, $R_\theta$ is the Rayleigh ratio, $\overline{M}_W$ is the weight-averaged molar mass, $P_\theta$ is the Zimm scattering function (or simply the scattering factor), and $A_2$ is the second virial coefficient. In the Zimm plot, $\frac{K_\theta \cdot c}{R_\theta}$ is plotted against $[\sin^2(\theta/2) + kc]$, and extrapolated to $c \to 0$ and $\theta \to 0$ (the scattering is concentration and angle dependent), as shown in Fig. 2.7, where kc on the $X$-axis is an adjustable parameter whose sole purpose is to result in an acceptable $X$–$Y$ spread of the grid-shaped Zimm plot.

The Zimm plot method may be relatively difficult to use for the calculation of $\overline{M}_W$ of cellulose of high molar mass. The reason is that the intercept will be very small compared with $Y$-values of the experimental data. Hence, small errors in the intercept induce relatively large errors in $\overline{M}_W$ [94]. Instead, Berry's method can be employed, where the intercept is $\sqrt{\overline{M}_W}$ [95], i.e., will be larger relative to the experimental $Y$-values, hence subject to less relative error [96].

**Dynamic or Quasi-elastic Light Scattering, QELS**

The scattering intensities discussed in the preceding section are time averaged. However, the intensity accessible in a scattering experiment also depends on time, $t$, because the particles are in a constant random (Brownian) motion. QELS is concerned with this dynamic aspect of scattering. Because of the Doppler effect, the frequency of scattering by a particle depends on whether it is moving toward or away from the detector. The frequency distribution of the scattered light is, therefore, slightly broader, by $\Delta f$ than that of the incident light. This frequency broadening is recorded in the time domain via a correlation function, so that QELS

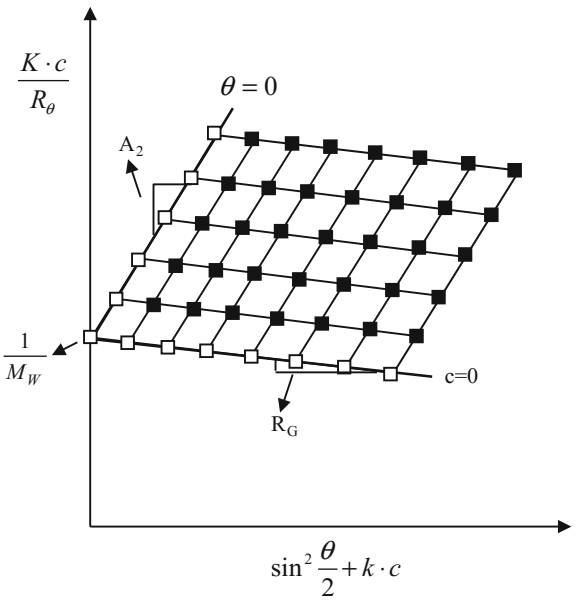


**Fig. 2.7** A typical representation of a Zimm plot. The scattering intensity at different concentrations ($c$) of the polymer and at different angles ($\theta$) are plotted. Extrapolation of $c \rightarrow 0$ and $\theta \rightarrow 0$ gives $\frac{1}{M_W}$ as the intercept. Values of $A_2$ and $R_g$ are determined from the slope of the line at $\theta = 0$, and $c = 0$, respectively (reprinted from [93], copyright (© 2000) with permission from Elsevier)

is sometimes called Photon Correlation Spectroscopy (PCS). The variation of the scattering intensity with time, therefore, contains information about the random motion of the particles; this information is used to calculate the diffusion coefficients of the particles, hence their size distribution.

Briefly, in a typical experiment, a detector measures the intensity of scattered laser light at 90°, over a period of time in discrete steps. The difference between two successive measurements, $\tau$, is usually a few microseconds. The autocorrelation function, $G(\tau)$ is given by Eq. 2.16.

$$G(\tau) = \langle i(t) \cdot i(t+\tau) \rangle \tag{2.16}$$

The translational diffusion coefficient, $D$, is related to $G(\tau)$ by Eq. 2.17.

$$G(\tau) = A \cdot \left(1 + B \cdot e^{-2 \cdot q2 \cdot D \cdot \tau}\right) \tag{2.17}$$

where $q$ is the scattering vector and $B$ is an instrument-related empirical term. The value of the hydrodynamic radius, $R_h$, is then calculated from the Stokes–Einstein expression (Eq. 2.18).

$$R_h = \frac{k \cdot T}{6 \cdot \pi \cdot \eta \cdot D} \tag{2.18}$$

where $k$, $T$, and $\eta$ refer to the Boltzmann constant, the absolute temperature, and the shear viscosity of the solvent, respectively [97].

#### 2.2.3.2 Practical Aspects

**Applications of LS to Cellulose and Its Derivatives**

The fact that the scattering intensity is proportional to $\frac{1}{\lambda^4}$, where $\lambda$ is the wavelength of the incident light shows the advantage of using a laser light of shorter wavelength, e.g., argon ion, $\lambda$ = 498 or 514.5 nm, instead of He/Ne laser, $\lambda$ = 632.8 nm. The frequency-doubled Nd-YAG laser (532 nm) is an attractive choice because it is less expensive, more stable, and more coherent than gas lasers. The glass cells employed for SLS are cylindrical and are placed inside a cell holder filled with a liquid, e.g., xylene whose refractive index matches that of glass ($\sim$1.5). Since QELS measurements are usually carried out at 90°, rectangular cells, e.g., those used for fluorescence measurements, are preferred. The only limitations with respect to sample solution are that it does not absorb the incident light and that it is free of (strongly scattering) dust particles. Filtration through inert membranes (ceramic or PTFE) and centrifugation are routinely employed in order to remove dust [98]. The value of $R_\theta$ depends on $\left(\frac{dn}{dc}\right)^2$, where $n$ is the refractive index of the solution. Therefore, an $x$ error in $\frac{dn}{dc}$ leads to an error of $2x\%$ in $\overline{M}_W$. Since $\frac{dn}{dc}$ depends on $\lambda$, the wavelength used in the scattering experiment and in determination of $\frac{dn}{dc}$ should be the same. This can be achieved by employing (expensive) differential refractometers, or by determining the refractive index of the polymer solution as a function of its concentration; this correlation is surprisingly linear over a large concentration range, i.e., concentrated solutions can be employed, leading to more precise $\frac{dn}{dc}$. Another source of error is when the value of $\frac{dn}{dc}$ is small, e.g., $\frac{dn}{dc}$ = 0.061 for cellulose in 8.33% (w/w) DMAc/LiCl compared with 0.324 for pure DMAc/LiCl solution [99]. This leads to a relatively large uncertainty in the dn/dc value itself and to weak scattering. A solution to this problem is to transform cellulose into a derivative with larger $\frac{dn}{dc}$, e.g., CTC [100].

LS measurements have been employed in order to detect the state of aggregation of cellulose in electrolyte/dipolar aprotic solvents, in particular, DMAc/LiCl and ILs. This information is relevant to cellulose functionalization. The reason is that the formation of a macroscopically clear and isotropic cellulose solution does not necessarily mean a molecularly dispersed biopolymer solution, similar to that present in Cuen, Cuoxam, and Ni-tren [98, 101]. Thus, relatively diluted cellulose solutions in aqueous NMMO (0.2–3% at 80 °C) showed a large $R_g$ > 160 nm indicating the presence of aggregates that may contain up to 1000 cellulose molecules [102, 103]. SLS, DLS, and SANS data have shown that cellulose auto-aggregates even in ILs that are known to be efficient solvents, e.g., BuMeImCl and EtMeImAc. In EtMeImAc, cellulose (DP = 494) forms 21-mer [56, 104]. The state of aggregation of hardwood kraft pulps, dissolved in DMAc/LiCl, was not affected by addition of urea (a hydrogen-bond breaking additive), by increasing the

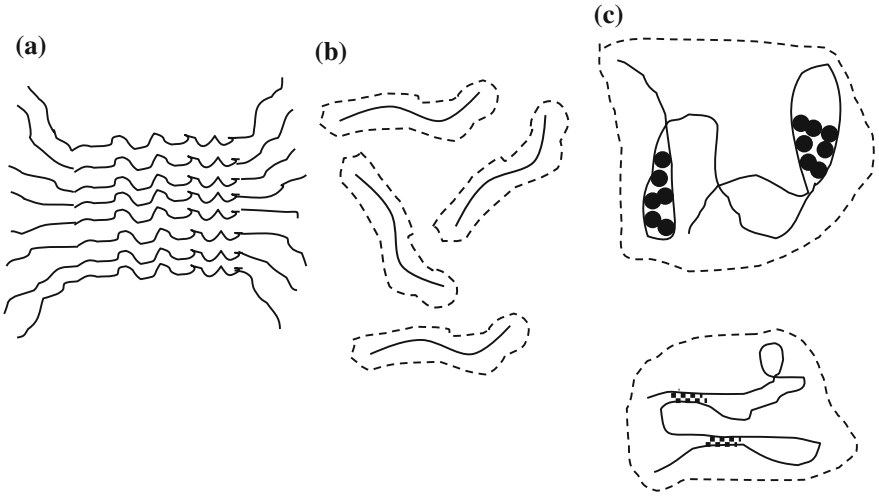


**Fig. 2.8** Schematic representation of cellulose structures in solution: Part **a** shows the "fringed" micellar structure. Parts **b** and **c** show possible chain conformations of celluloses of different DP. For high molecular weight cellulose (**c**), intramolecular hydrogen bonding is possible (adapted from [105])

dissolution temperature, or the concentration of LiCl (from 6 to 10%) but is affected by the length of time of mechanical treatment during dissolution [81]. The structure of these aggregates has been described in terms of a "fringed" micellar structure. Figure 2.8 shows a schematic representation of such aggregate, composed of laterally aligned chains, forming a rather compact and probably geometrically anisotropic core, immiscible with the solvent. The "coronas" at both ends of the particle consist of solvated amorphous cellulose chains. Formation of a fringed micellar structure is backed by experimental evidence. For example, increasing cellulose concentration results in a pronounced increase in molar mass of the particle, although its dimensions increase only slightly. The geometric anisotropy of the central part of the micelle is expected to be associated with optical anisotropy. Additionally, it may be visualized by an appropriate experimental technique. Both expectations have been confirmed by use of shear-induced birefringence and electron microscopy [106]. The number of chain molecules forming the aggregate and the thickness of the coronas increase as a function of both cellulose concentration and the interfacial tension between the particle core and the solvent system [107]. Parts (b) and (c) of Fig. 2.8 refer to monodisperse solutions of small DP (b) and large DP (c) cellulose molecules. The former part shows that the length of the short cellulosic chain is practically equal to its persistent length, i.e., there is neither coiling, nor interactions between the chains. In part (c), the flexibility of the long-chain polymer permits the formation of strong intramolecular hydrogen bonds, provided that the OH groups reside for some time within a "critical distance" from each other, sufficient for the van der Waals interactions to operate [108].

Consequently, the properties of cellulose, in particular its DP, $I_c$, and concentration affect its state of solution, hence its derivatization. For the same cellulose, the accessibility of the hydroxyl groups increases as a function of decreasing the biopolymer concentration. For different celluloses, at the same concentration, only the outer surface of the fringed micellar core is accessible, the area of this part decreases as a function of increasing DP and $I_c$.

QELS has indicated that cellulose diacetate occurs as single chains in equilibrium with aggregates in DMAc/LiCl at temperatures from 10 to 60 °C [109]. SLS measurements have shown that solutions of unactivated cellulose or water- and ammonia-activated cellulose in NMMO, cellulose xanthate (Viscose) in 1 M NaOH, cellulose acetate (DS = 2.5) in acetone, MHEC, MHPC, and CMC (in water) form aggregates, with an aggregation number that depends on the DP, on one hand. On the other, CTC in dioxane forms a molecularly dispersed solution [110]. The effects of solvent composition (10 and 50% methanol) and ionic strength on the aggregation state of three samples of MHPC were studies by LS. The solvent effect on $\overline{M}_W$ and $R_g$ was found to be pronounced. For example, $\overline{M}_W$ of one sample doubled (310,000–650,000 g/mol) when the solvent was changed from 50% aqueous methanol to 1 mM aqueous NaCl solution. This was accompanied by an increase of 12% in $R_g$ [93].

### 2.2.4 *Use of Integrated Analytical Techniques*

The most important recent development in investigation of cellulose and its derivatives has been the physical integration of the techniques discussed in Sects. 2.2.1–2.2.3 into a single equipment, in particular, where the fractions separated by SEC are analyzed by several types of detectors. Figure 2.9 shows a schematic representation of an integrated chromatographic/LS setup.

Universal calibration involves the use of a single detector (concentration), if the Mark–Houwink constants of the reference samples are known, or dual detectors (concentration and viscosity), if these constants are unknown. Absolute molecular weight determination involves the use of a molecular weight-sensitive detector (LS), so that $\overline{M}_W$ of each fraction eluted is directly measured and no calibration standards are needed. This experiment has been made expedient due to the introduction of (fixed) multi-angle light scattering detectors, MALS.

Nonionic cellulose ether samples, e.g., EHEC, HEC, differing in DS dissolved in aqueous methanol were investigated by SEC/LALS, SLS, QELS, and viscosity. The results showed that sufficient information on these ethers, relevant to their applications, can be only obtained by a combination of chemical information (DS, ratio of alkyl/hydroxyalkyl moieties, structure of substituents), thermodynamic properties (cloud point, second virial coefficient), hydrodynamic properties ($[\eta]$, $k_H$), geometric size parameters from the scattering experiments $R_g$, as well as molar mass and its distribution [111].

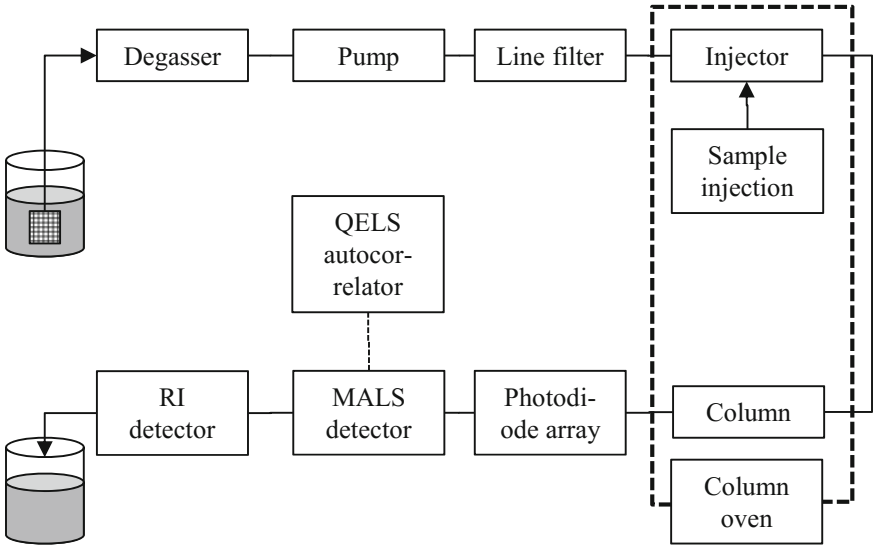


**Fig. 2.9** Schematic representation of a SEC-MALS-QELS integrated system (according to [100])

A comparison between LALS and MALS detectors for SEC has been carried out by examining HPC samples from different suppliers, having relatively close $\overline{M}_W$ (111,600, 116,800, and 95,300 g/mol). Two of the samples showed compact components, presumably aggregated HPC and the third sample did not show aggregation. Both SEC-MALS and SEC-LALS were shown to be efficient techniques for characterization of complex mixtures, e.g., HPC, containing mixtures of solvated polymer chains, as well as micelle-like aggregates [112].

The interactions between nonionic cellulose ethers and the surfactant sodium dodecyl sulfate (SDS) in aqueous solutions containing a fixed concentration of NaCl have been studied by SEC, equipped with refractive index and MALS detectors. This arrangement allowed reliable calculation of the molar masses of the ether-SDS complexes and some of its properties, e.g., $\frac{dn}{dc}$. Because of the separation efficiency of SEC, the free cellulose ether, and ether-SDS complexes were eluted separately avoiding the necessity of laborious dialysis. There is a significant association at low SDS concentrations. Adsorption of higher concentrations of the surfactant prevents intermolecular interactions, so that the ether-SDS complexes begin to be formed from single-polymer coils carrying micellar clusters [113].

Filter paper cellulose has been examined as received and after being aged by heat. The samples were additionally converted into CTC. Solutions of these cellulose samples in DMAc/LiCl and of CTC in acetone have been examined by SEC/MALS. Moreover, solution of the biopolymer in Cadoxen has been examined by viscosity. The values of the average molar masses obtained using the different techniques were quite different for both samples of cellulose. These discrepancies were discussed in terms of possible degradation during the synthesis of CTC, and

overestimation of $\overline{M}_W$ of cellulose in DMAc/LiCl due to biopolymer aggregation [114]. Thus, care should be exercised when cellulose is transformed into derivatives for subsequent determination of molar mass. Sample examination by a combination of techniques is worth the effort because it underlines the presence of problems that may not be detected when a single technique is employed.

Other similar applications of SEC with several detectors, including LS, are made with HPMC acetate succinate [115], HPC [116], hydroxyethylsulfoethyl cellulose, sulfoethyl cellulose, carboxymethyl sulfoethyl cellulose, carboxymethyl amylose [117], and a large series of water-soluble cellulose ethers [118].

## 2.3 Structural Information

### *2.3.1 X-ray Diffraction*

#### 2.3.1.1 Theoretical Aspects

The semicrystalline nature of cellulose fibers bears on their useful mechanical properties and is crucial to their accessibility, hence reactivity in any intended application, dyeing, derivatization, etc. In fact, the basic objective of different fiber "activation" is also to decrease cellulose crystallinity, hence enhance its accessibility. This ensures reproducible product properties. The degree of crystallinity of cellulose depends, inter alia, on its origin, processing, DP, and inter- and intramolecular hydrogen bonding within and between the chains of the bio-polymer. X-ray diffraction can probe some details of cellulose structure (hydrogen bonding and dimensions of the crystalline regions), and can be used to determine $I_c$ (X-ray).

X-ray is produced when thermal electrons released from a heated filament under reduced pressure are accelerated toward, then hit, a metal anode kept under high electric potential. If a bombarding electron ejects an electron, say from the K shell of an atom, the resulting vacancy will be filled by an electron falling from a higher energy shell (L, M, etc.); the energy difference being radiated as X-ray. For a given target material, the various shells have fixed energies, hence the emitted radiation has fixed values of $\lambda$, e.g., 2.289, 1.936, 1.789, 1.540 Å, for the $K_{\alpha 1}$ line of Cr, Fe, Co, Cu target metal, respectively. Synchrotron radiation is obtained from an electron synchrotron (electron storage ring) by accelerating the electron to several GeV, versus ca. 5–9 kV for the excitation voltage of the above-mentioned metals. It is now employed as a more powerful, high-intensity X-ray source. The use is limited by the access time to the synchrotron equipment.

### 2.3.1.2 Probing the Structure and Hydrogen Bonding in Cellulose

Three-dimensional lattices are composed of smaller units, unit cells, whose repetition generates the crystal. As shown in Fig. 2.10, primary unit cells contain only lattice sites from corner sites. Centered unit cells comprise also lattice sites that are not corner sites. The three-dimensional lattices of crystal diffract coherent X-ray from two-dimensional lattice planes. This is depicted in Fig. 2.11 for a two adjacent lattice planes, $G_1$ and $G_2$, located at a distance $d$. An approaching wave L hits the lattice site A of the $G_1$ plan at an angle $\theta$ (Bragg's angle), a parallel wave $L_1$ hits the lattice plane $G_2$ at $A_2$, etc. The phases of the waves are shifted by Eq. 2.19.

$$PA_2 + A_2Q = 2 \cdot d \cdot \sin\theta \tag{2.19}$$

Under certain geometric conditions, first specified by Laue and Bragg, they interfere constructively if they arrive simultaneously at the plane $N$–$N_2$. This requires the plane shift to be equal to, or a multiple of $n$ of $\lambda$ of the incident radiation, according to Bragg's equation (Eq. 2.20).

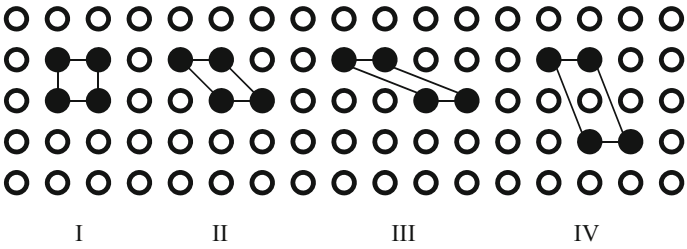


**Fig. 2.10** Schematic representation of three primary unit cells, I to III, and one centered unit cell IV. In the three-dimensional lattices, centered unit cells may be body centered (lattice point at the intersection of body diagonal) or face-centered (lattice point at the intersection of face diagonal) (according to [119])

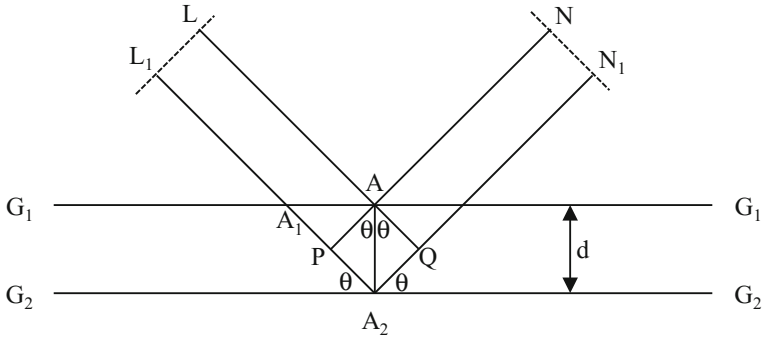


**Fig. 2.11** Schematic representation of Bragg's law, showing the diffraction of two parallel waves (L and $L_1$) with two adjacent planes ($G_1$ and $G_2$) of a lattice (according to [119])

$$n \cdot \lambda = 2 \cdot d \cdot \sin\theta \tag{2.20}$$

When a crystalline substance is placed into a monochromatic X-ray beam, a large number of interferences will be obtained whose diffraction angles are determined by $\lambda$, the nature of the crystal, and the experimental setup. From the diffraction angle $2\theta$ of the various reflections, the lattice plane distance can be calculated from Bragg's law leading to the conclusions about the size and symmetry of the crystal unit cell and the crystalline perfection of the sample. When the intensities of the various diffraction bands are considered, it is possible to describe the exact location of the atoms in the unit cell, an information that bears, e.g., on hydrogen bonding in cellulose.

**Determination of the Dimensions of Crystalline Regions**

Knowledge of the dimensions of the crystallites is important because it bears on cellulose accessibility and reactivity. The dimension of the crystallite is usually extracted by applying Scherrer's equation (Eq. 2.21) to wide-angle X-ray diffraction (WAXD) data [120].

$$\beta_{0.5} = \frac{K \cdot \lambda \cdot 57.3}{\mathrm{Dim} \cdot \cos\theta} \tag{2.21}$$

where $\beta_{0.5}$ refers to the diffraction peak width at half-height, $K$ is the crystal "form factor", its value varies between 0.89 and 1.39, but may be safely taken as unity. The symbols $\lambda$, Dim, and $\theta$ refer to the wavelength of the X-ray radiation, the average dimension of the perfectly crystallized area, measured perpendicularly to the corresponding reflection lattice plane (101, 002, and 040) [121–123] and Bragg's diffraction angle of X-rays from the plane under consideration. The use of the conversion factor 57.3 is necessary when $\theta$ is measured in angular degrees. The average width and length of the crystallite are obtained from the line width of the equatorial and meridianal X-ray diffraction after applying corrections for stray radiations, sample, and beam dimensions. The method is based on the (simplifying) assumption that line broadening is caused, more or less solely, by crystallite dimensions [124]. However, broadening associated with lateral disorganization of cellulose chains probably leads to underestimation of $\beta_{0.5}$ by about 10% for celluloses from most sources [26, 125]. Suggestions for corrections have been published [126, 127].

Alternatively, $\beta_{0.5}$ can be calculated from the experimental data after subtraction of the "amorphous" background scattering. An evaluation of the different approaches to calculate the crystallite dimensions has been published [128]. The calculated crystallite dimensions have narrow ranges, as shown by the following representative examples (cellulose studied; width, $\perp$ 101 plane, Å; length, $\perp$ 040 plane, Å,

respectively): Untreated cotton, 47–49, 125; high-wet modulus rayon, 45–81, 110–156; polynosic-type rayon, 43, 174–190 [129].

### Calculation of the Index of Crystallinity, $I_c$ (X-ray)

There are two approaches for the calculation of the degree or index of crystallinity, an absolute and (much more employed) a relative one. In the absolute method, the assumption is made that a three-dimensional order exists in crystalline regions and that the order is not strongly anisotropic. The method requires either a completely amorphous sample or a properly oriented one. Obtaining both samples is experimentally feasible. The absolute crystalline weight fraction, $W_{(\text{crystalline})}$, is calculated by comparing the diffraction intensity concentrated in the sharp diffraction spots, $I_{(\text{crystalline})}$ due to the crystalline region, with the total intensity of coherently diffracted X-ray, $I_{(\text{total})}$, as given in Eq. 2.22 [130, 131].

$$W_{(\text{crystalline})} = \frac{\int s^2 \cdot I_{(\text{crystalline})} \cdot \mathrm{d}s \cdot \int s^2 \cdot f^2 \cdot \mathrm{d}s}{\int s^2 \cdot I_{(\text{total})} \cdot \mathrm{d}s \cdot \int s^2 \cdot f^2 \cdot D \cdot \mathrm{d}S} \tag{2.22}$$

where $s = (2/\lambda)\sin\theta$, $D$ is a disorder function, and $f^2$ represents the mean square of the atomic scattering factors.

On the basis of the two-phase fringe micellar structure of cellulose and assuming that the intensities of scattering from the amorphous and crystalline regions are proportional to their concentration in the fiber, one can calculate a relative crystallinity index, $I_c$ (X-ray), from the intensities or areas of scattered X-ray peaks assigned to the above-mentioned regions. For example, for cellulose I, the value of $I_c$ (X-ray) has been calculated from ratios between the crystalline scatter of the 002 reflection plane at $2\theta = 22.5°$ and $2\theta = 18.5°$. The corresponding values for cellulose II (101 reflection plane) are 19.8° and 15°, respectively (Eq. 2.23) [132–134].

$$I_c = 1 - \frac{I_{(\text{amorphous})}}{I_{(\text{crystalline})}} \tag{2.23}$$

### Practical Aspects

The "powder diffraction" and "single crystal" are the two principal experimental methods to study X-ray diffraction of cellulose and its derivatives. With regard to the first technique, consider the interaction of a monochromatic X-ray beam with a crystalline powder [135]. Because the lattice planes of particles are disordered with respect to the incident radiation, the latter will be diffracted from all planes that fulfill the condition of Bragg's law, in the form of concentric diffraction cones, as shown in part (a) of Fig. 2.12. Parts (b) and (c) of the same figure show the two commonly employed techniques for recording the diffracted radiation. In the Debye–Scherrer method (b), a film strip is placed in a circle around the sample;

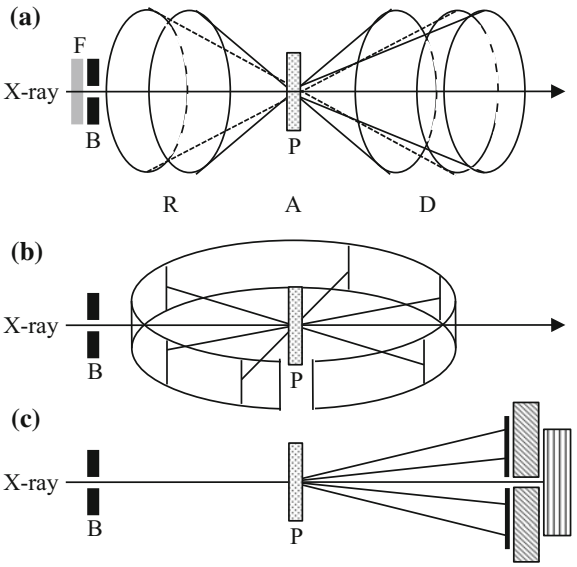


**Fig. 2.12** Schematic representations of the diffraction of monochromatic X-ray radiation from a crystalline substance (**a**), and methods of recording the diffracted radiation by the Debye–Scherrer (**b**), and flat-film camera method (**c**)

sectors of the diffraction circles are recorded. Alternatively, a flat film can be employed as shown in part (c); a vertical cut through the diffraction cone is recorded. The powder diffraction technique is employed whenever our interest lies in probing the nature of the crystal lattice (its polymorphic form), or calculation of the amount of crystalline material $I_c$ (X-ray)and the crystallite size, the latter by use of Scherrer's equation [136].The use of densimeters to determine the intensities of scattered radiation recorded on photographic films has been surpassed by use of X-ray detectors including scintillation counters, solid-state detectors, proportional and position sensitive proportional counters [137].

The single-crystal diffraction technique is employed when information on the exact crystallographic nature of the unit cell is required. A single crystal is mounted with one of its optical axis in the X-ray beam; the resulting spot reflections of the various crystal lattice planes are recorded, generally on a flat film. When the sample is mounted with the length of its axis (*b*-axis) vertical to the incident X-ray beam, all reflections from the lattice planes that are parallel to the length of the axis will appear on the "equator", equatorial reflections. Reflection from planes that are perpendicular to the *b*-axis will be registered on the "meridian". The angle between the crystal and the incident X-ray beam can be controlled and varied by use of a goniometer head. Figure 2.13 is a schematic representation of the distribution of crystallites and the resulting X-ray diffraction diagrams.

X-ray diffraction has been extensively employed in order to determine the crystal structure of cellulose fibers with the aim of calculating the crystallite length and width dimensions; and probing inter- and intramolecular hydrogen bonds in native and activated cellulose (in particular by activating treatment with a base). Another

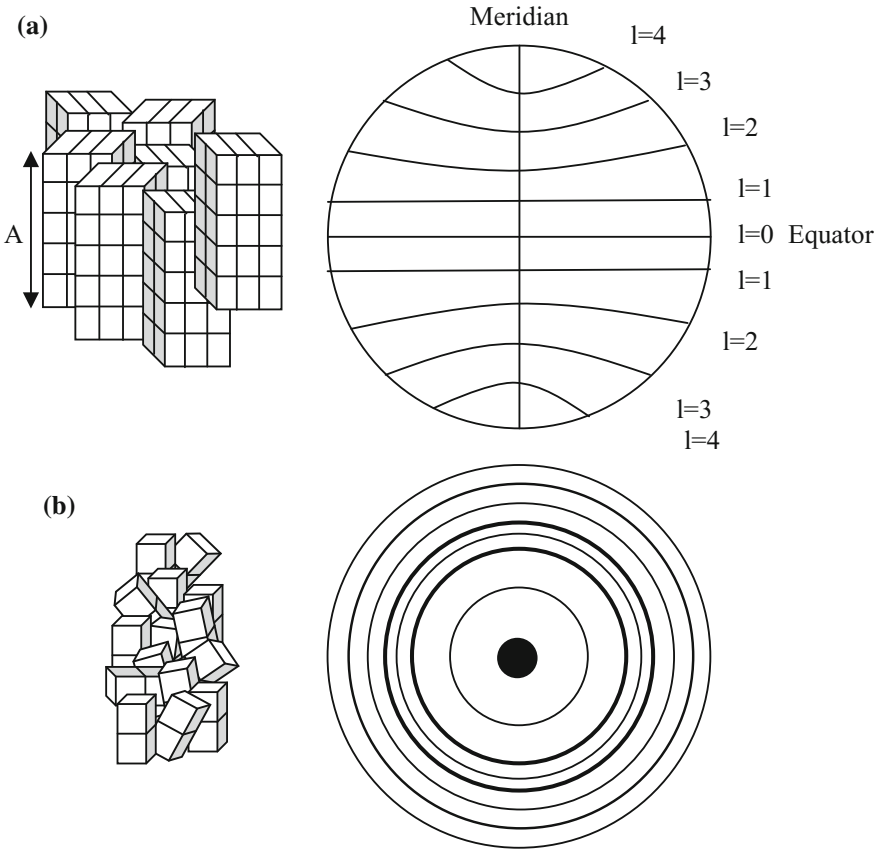


**Fig. 2.13** Schematic representation of the distribution of crystallites and the corresponding X-ray diffraction diagram. In **a**, the uniaxially distributed crystallites around the axis A results in a fiber pattern. In **b**, the crystallites are isotropically distributed crystallites produce a Debye–Scherrer pattern of concentric rings (redrawn from [138])

important use is to determine index of crystallinity, e.g., as shown by Eq. 2.20; representative examples of these applications are discussed below.

The first question addressed is that of cellulose polymorphism. Highly crystalline cellulose, e.g., that of *Valonia*, exists in two crystalline allomorphs, namely cellulose $I_\alpha$ and cellulose $I_\beta$ [139, 140]. On the other hand, only the $I_\beta$ allomorph is present in tunicin, another highly crystalline cellulose from animal origin [141]. By using special purification procedures, it was possible to determine the crystal structure and hydrogen bonding of cellulose $I_\alpha$, extracted from culture of *Glaucocystis nostochinearum*, [142] and $I_\beta$, extracted from tunicate (*Halocynthia roretzi*) [15]. The results obtained showed that cellulose $I_\alpha$ has a one-chain triclinic unit cell with all the glucosyl linkages and the hydroxymethyl groups identical. However, adjacent sugar rings alternate in conformation, giving the chain a cellobiosyl repeating unit.

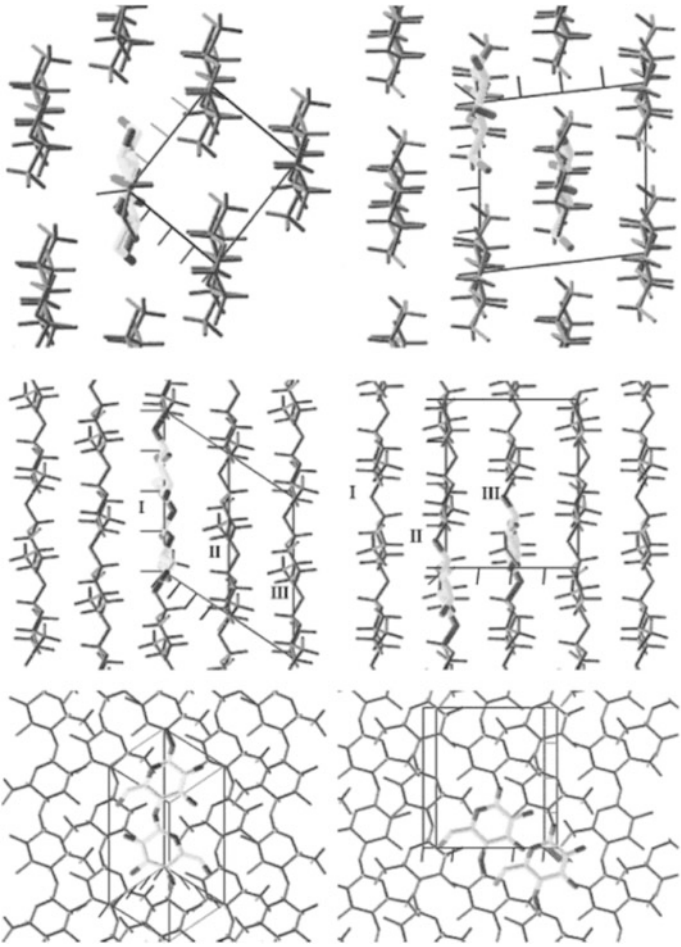


**Fig. 2.14** Projections of the crystalline structures of cellulose $I_\alpha$ (left) and $I_\beta$ (right) down the chain axis (top), perpendicular to the chain axis and in the plane of the hydrogen-bonded sheets (middle), and perpendicular to the hydrogen-bonded sheets. The asymmetric unit of each structure is represented in thicker line with carbons in gray; the unit cell of each structure is shown (reprinted with permission from [142], copyright (© 2003) American Chemical Society)

The chains organize in sheets packed in a "parallel-up" fashion. The structure of $I_\beta$ differs from that of $I_\alpha$ in having two unique sheets containing conformationally distinct chains with different hydrogen bonding, see Fig. 2.14.

Based on X-ray diffraction, two models, (A) and (B′), have been suggested for cellulose II. Both models have two antiparallel chains organized in a $P2_1$ space group, with unit cell parameters: $a = 8.01$ Å, $b = 9.04$ Å, $c = 10.36$ Å, and $\gamma = 117.1°$. Model (A) has equivalent backbone conformations for both chains but different conformations for the hydroxymethyl moieties (*gt*) for the original chain and (*tg*) for the center chain. In model (B′), the conformations of the two chains are

different, but those of the hydroxymethyl moieties are nearly equivalent [143, 144]. The presence of two types of conformation has been challenged because C6 of the AGU of cellulose II shows a single $^{13}C$ NMR peak at 64 ppm [145, 146]. Additionally, studies on the crystalline structure of cellodextrins that have crystalline packing almost equivalent to that of cellulose II (β-cellotetraose hemihydrates, and methyl β-cellotrioside monohydrate) showed that all hydroxymethyl groups are in the same (*gt*) conformation [147, 148]. The crystalline structure of cellulose II has been examined by neutron diffraction, making use of the fact that it is possible to exchange the hydrogens of the AGU by deuterium (treatment with $NaOD/D_2O$) without any loss of crystalline perfection. The H/D exchange is advantageous because the scattering of OD group is large ($1.245 \times 10^{-12}$ cm) compared with that of the OH group ($0.206 \times 10^{-12}$ cm). The results obtained

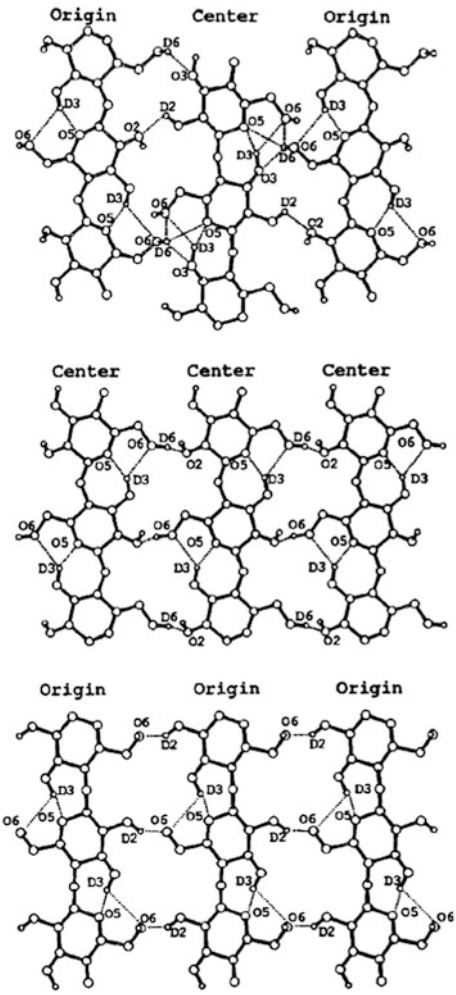


**Fig. 2.15** A schematic representation of hydrogen bonds (dashed lines) in deuterated cellulose II (reprinted with permission from [149], copyright (© 1999) American Chemical Society)

confirmed that a 3D network of hydrogen bonds exists in cellulose II. The conformation of the chains is similar to that found in the crystal structure of β-D-cellotetraose, i.e., they eliminate model (A) in favor of (B′), see Fig. 2.15 [149].

The crystal structure of cellulose $III_I$ has been examined by X-ray diffraction, $^{13}C$ CP/MAS NMR spectroscopy, SEM, and FTIR spectroscopy. A sample of improved crystallographic properties (because of its high crystallinity) was obtained by treatment of cellulose extracted from *Cladophora* by ammonia under supercritical conditions (140 °C, critical temperature of ammonia = 132.5 °C). The results indicated that the structure of cellulose $III_I$ can be fully described by one-chain unit cell and a $P2_1$ space group, with the cellulose chain axis on one of the $2_1$ screw axis of the cell. The latter has the following parameters: $a$ = 4.48 Å, $b$ = 7.85 Å, $c$ (chain axis) = 10.31 Å, and $\gamma$ = 105.1°. The C6 atom showed a single NMR peak at 62.3 ppm, indicating that the hydroxymethyl moiety is in the (*gt*) conformation. The single chain of cellulose $III_I$ may have some conformational similarities with one of the two chains existing in the crystal of cellulose II [150].

An example of polymorphism of a cellulose derivative is CTA. It exists as three polymorphs producing different Debye–Scherrer diagrams or fiber patterns. CTA-I is obtained by the heterogeneous acetylation of native cellulose I. Its chains are packed in parallel structure. CTA-II is obtained by acetylation of regenerated or mercerized cellulose-containing chains packed in antiparallel structure. The transformation of CTA-I into CTA-II can be achieved by several methods, e.g., by treatment with superheated steam [151] or by annealing the third polymorph, CTA-N (obtained by placing CTA-I in nitromethane saturated atmosphere) at high temperature [152]. Figures 2.16 and 2.17 show the parallel and antiparallel structures of CTA-I; CTA-II and CTA-N.

Another extensively employed application of X-ray diffraction is the calculation of $I_c$ and crystallite dimensions of celluloses. For instance, the response to different "activation" methods can be determined. The impetus for these studies is practical because the AGU of cellulose samples of lower $I_c$ is more accessible, hence is expected to swell more and react faster with the reagent. Thus, mercerization of cotton and eucalyptus fibers under controlled conditions has resulted in decrease of ca. 2.7% in DP and ca. 5% in $I_c$ accompanied, presumably, with cellulose I → cellulose II transformation and a change in crystallite dimensions. This has led to an increase in fiber swelling (% (w/w); 20 protic solvents) by factors from 2.4 to 11.8 and from 1.7 to 6.3 for cotton and eucalyptus [154]. The correlation of $I_c$ with solvent sorption and reactivity is discussed in detail in Sects. 3.1.2–3.1.4. Table 2.3 lists some representative data on the use of X-ray diffraction to probe the changes in $I_c$ and crystallite size of cellulose produced by different treatments.

It is obvious that X-ray diffraction is perhaps the technique that has contributed most to the elucidation of the structure of cellulose and the changes produced therein by different treatments [164–170]. Values of $I_c$ can be determined by various techniques in addition to X-ray diffraction, namely from water sorption, iodine adsorption, NMR-, IR-, and Raman spectroscopy. The scales obtained by use of different techniques agree qualitatively and, in many cases, correlate linearly. The technique of choice appears to be a matter of convenience and personal preference.

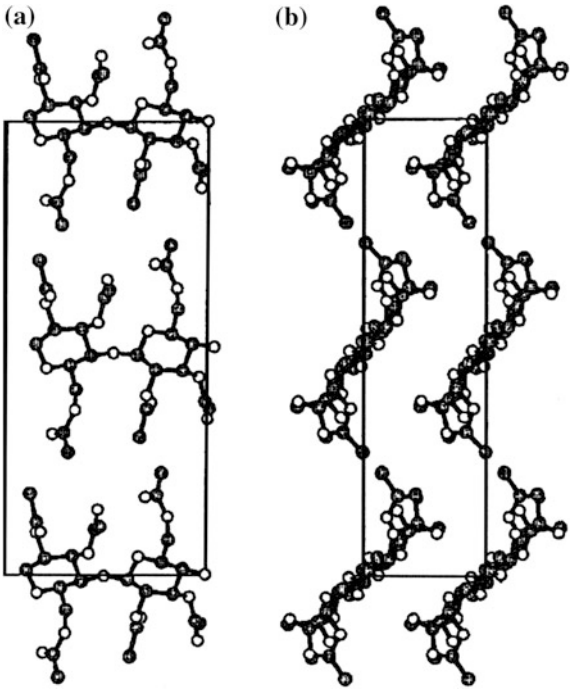


**Fig. 2.16** Representation of the structure of CTA-I in two projections: **a** perpendicular to the *a*-plane; **b** down the helix (*c*-axis). For simplicity, the hydrogen atoms are not shown (according to [153])

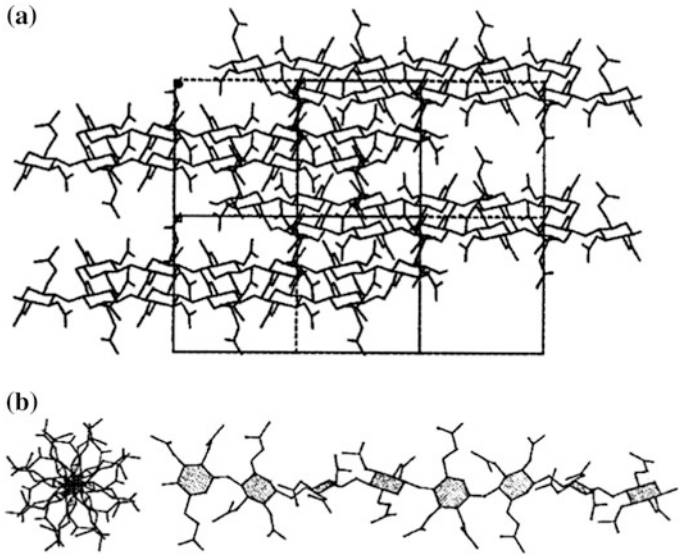


**Fig. 2.17** Representations of the structures of CTA-II in the *b* and *c* planes (**a**) and of CTA-N along the chain axis, and down the same axis (**b**) (according to [153])

**Table 2.3** Typical results of the application of X-ray diffraction for determination of the index of crystallinity $I_c$ (X-ray) and crystallite dimensions of untreated and treated celluloses

| Entry | Cellulose | Treatment; effect of treatment on $I_c$ | | Crystallite size, Å | References |
|---|---|---|---|---|---|
| **1** | | Treatment with 0.2 M HCl, 100 °C; liquor ratio 1:50 | | | [155] |
| | Cotton | Untreated | 0.842 | | |
| | | 0.5 h | 0.880 | | |
| | | 2 h | 0.927 | | |
| | | 10 h | 0.963 | | |
| | | 20 h | 0.97 | | |
| | Viscose | Untreated | 0.392 | | |
| | | 0.5 h | 0.582 | | |
| | | 2.5 h | 0.679 | | |
| | | 12 h | 0.791 | | |
| | | 20 h | 0.813 | | |
| **2** | | Mercerization, 18% (w/w) NaOH, r.t., 1 h | | ⊥ 020 | [156] |
| | Valonia | 0.95 → 0.66 | | 154 → 36 | |
| | Ramie | 0.83 → 0.65 | | 58 → 40 | |
| | Kraf | 0.67 → 0.66 | | 40 → 37 | |
| | Celery | 0.41 → 0.50 | | 30 → 34 | |
| | Swiss chard | 0.43 → 0.60 | | 29 → 44 | |
| **3** | Wheat straw | Original; 0.79 | | 31 | [157] |
| | | Drying 105 °C, 24 h, 0.71 | | 29 | |
| | | Ball milling 2 h, 0.72 | | 30 | |
| | | Ball milling 6 h, 0.57 | | 16 | |
| | | Ball milling 14 h, 0.33 | | 16 | |
| | | Ball milling 24 h, 0 | | – | |
| | | 72% (w/w) $H_2SO_4$, 30 °C | | | |
| | | 2 min, 0 °C | | | |
| | | 5 min, 0 °C | | | |

(continued)

**Table 2.3** (continued)

| Entry | Cellulose | Treatment; effect of treatment on $I_c$ | | Crystallite size, Å | References |
|---|---|---|---|---|---|
| **4** | Cotton | Mercerization; NaOH 20% (w/w), 0 °C, 1 h, followed by different washings, with water; water then pyridine; ethanol then pyridine; 0.94; 0.85; 0.86, respectively | | | [134] |
| **5** | | Treatment with 2.5 M HCl, 105 °C, 15 min | | ⊥ 101 | [158] |
| | Viscose | 0.54 → 0.64 | | 40 → 68 | |
| | Bagasse | 0.65 → 0.72 | | 40 → 49 | |
| | Cotton | 0.80 → 0.84 | | 57 → 55 | |
| | Ramie | 0.83 → 0.86 | | 49 → 49 | |
| **6** | Cotton | Treatment with aqueous acetone; no acid catalysis; 150 °C; 2 h | | ⊥ 002 | [159] |
| | | Original | 0.744 | 40.2 | |
| | | 50 vol. % acetone | 0.744 | 37.8 | |
| | | 60 vol. % acetone | 0.743 | 37.4 | |
| | | 70 vol. % acetone | 0.746 | 37.6 | |
| | | 80 vol. % acetone | 0.747 | 37.2 | |
| | | 90 vol. % acetone | 0.754 | 37.2 | |
| | | Treatment with HCl in 90 vol.% aqueous acetone; 150 °C; 2 h | | | |
| | | 0.16 mol/L acid | 0.745 | 36.2 | |
| | | 0.8 mol/L acid | 0.718 | 34.4 | |
| | | Treatment with $F_3CCO_2H$ in 90 vol.% aqueous acetone; 150 °C; 2 h | | | |
| | | 0.75 mol/L acid | 0.749 | 39.6 | |
| | | 1.50 mol/L acid | 0.752 | 36.3 | |
| | | 3.00 mol/L acid | 0.715 | 35.0 | |
| | | Treatment with 1.5 mol/L $F_3CCO_2H$ in 90 vol.% aqueous acetone; 2 h | | | |
| | | $T$ = 130 °C | 0.745 | 37.1 | |
| | | $T$ = 150 °C | 0.750 | 36.7 | |

(continued)

**Table 2.3** (continued)

| Entry | Cellulose | Treatment; effect of treatment on $I_c$ | Crystallite size, Å | References |
|---|---|---|---|---|
| | | $T$ = 180 °C | 36.3 | |
| **7** | Bacterial cellulose I and II | Enzyme hydrolysis by cellulases; $I_c$ (X-ray) = 976.791-32.076 (digestion, % (w/w)) + 0.266 (digestion, % (w/w))$^2$; $r^2$ = 0.9962; $n$ = 4 | | [160] |
| **8** | Bamboo cellulose | Mercerization by NaOH, 20 °C, 20 min. Little change in $I_c$ for [NaOH] 1–10% (w/w); decreases sharply between 10 and 16% (w/w); little change from [NaOH] 16 to 24% (w/w), 0.75 | | [161] |
| **9** | Cotton | Samples subjected to 7 T magnetic field; $I_c$ increases as a function of exposure time (90–180 min) to the field | | [162] |
| **10** | MCC; cotton, 9 commercial celluloses | Good agreement between $I_c$ by X-ray diffraction and by CP/MAS $^{13}$C NMR for 12 cellulose samples | | [163] |

## 2.3.2 *Infrared and Raman Spectroscopy*

### 2.3.2.1 Theoretical Background

The theory of IR and Raman spectroscopy is taught in any science course, therefore its discussion in this book is redundant. The essential details will be touched upon and the reader is referred to specialized textbooks [171, 172]. Infrared refers to that part of the electromagnetic spectrum between the visible and microwave regions. The total energy of a molecule is a combination of its electronic (UV–Vis), vibrational, and rotational energy (IR and Raman). A molecule absorbs IR radiation if this absorption leads to a change in its dipole moment. The interaction of radiation with material also leads to scattering. In the inelastic or Raman scattering, the frequency of the scattered radiation (usually a laser light) is different from that of the incident one. Raman scattering involves changes in the molecule's polarizability.

The power of IR and Raman spectroscopy lies in structure determination, which is based on the fact that each bond or functional group has one or more stretching and deformation modes, associated with characteristic vibration frequencies. These group frequencies are sensitively dependent, inter alia, on the molecular structure of the compound, its physical state (solid or liquid), and substance–solvent interactions. Thus, it is relatively easy to discern an aliphatic from aromatic carbonyl or acyl group. As shown below, the applications of these two techniques go much beyond functional group determination.

### 2.3.2.2 Practical Aspects

IR and Raman spectroscopy have been employed in order to gain information on the structure of cellulose, and the presence, introduction, or transformation of functional groups (both qualitative and quantitative). These aspects will be treated in the same sequence, after briefly discussing the question of the sample physical state. Being solids, cellulose and its derivatives are usually analyzed in pure form, as solutions in solvents, or as solid/solid mixtures, mostly in potassium bromide. Because of the difficulty of dissolving cellulose, the solution techniques have been limited to analysis of its (soluble) derivatives [173–176]. It is expected, however, that this situation will change because ILs readily dissolve celluloses of different DP [177]. Most work on cellulose and its derivatives has been done on solid samples, either pure [178, 179] or as their (solid/solid) mixtures in potassium halides [180–188]. A major problem of using pellets to study polymers is that the IR light is scattered by the polymeric material that may result in spectra with sloping baselines that complicates quantitative analysis. Grinding of the substance plus KBr into a fine powder, e.g., to pass through a 250 mesh screen results in spectra that may be free of excessive scattering. This grinding, however, may also change $I_c$, an important property that is obtained from IR [180]. These problems can be

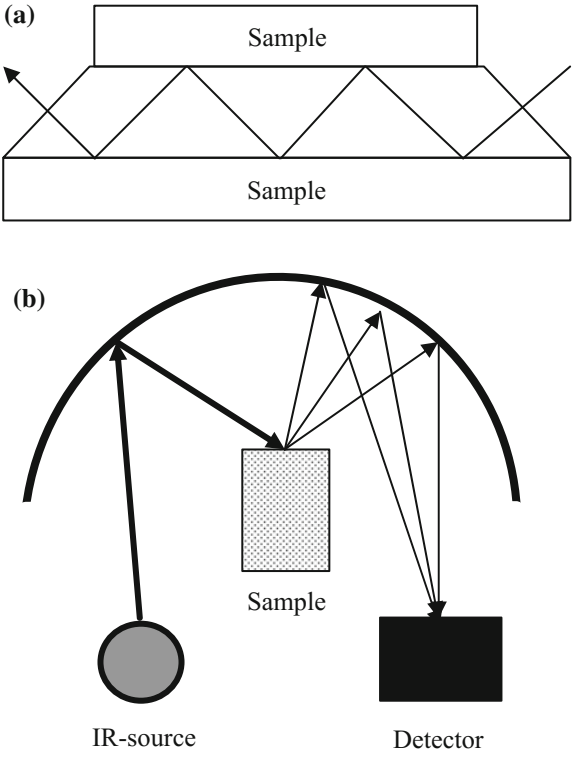


**Fig. 2.18** Schematic representations of the ATR (**a**) and DRIFTS IR cells (**b**)

minimized/avoided by using reflectance techniques, because fine grinding (substance plus potassium halide) is not required applying *A*ttenuated *T*otal *R*eflectance, ATR, and *D*iffuse *R*eflectance *I*nfrared *F*ourier *T*ransform *S*pectroscopy, DRIFTS [189]. In the first technique, the sample is examined between two crystals of high refractive index material (ZnSe, Ge, thallium bromide–thallium iodide). This difference in the refractive index (between the sample and the crystal) causes the incident IR beam to be reflected on the sample surface several times before it exits to the IR detector, Fig. 2.18a.

In DRIFTS, one compares the scattered radiation from the sample in a non-absorbing solid matrix (KBr or KCl) to that of a background spectrum of the inorganic halide, Fig. 2.18b. The reflectance spectrum is then converted into absorbance. For quantitative treatment of the resulting spectra, the Kubelka–Munk theory is applied in a way similar to transmittance spectra [190]. These techniques have been employed for the study of cellulose [178, 191, 192] and its derivatives [193–198]. The reflectance techniques are attractive because of their simplicity, although the transmittance method (KBr pellet) is more useful if a low amount of functional group or water is investigated.

These applications are based on assignment of the frequencies observed to the proper vibrations, and using them for molecular structure determination and/or

**Table 2.4** General assignments of the most important IR absorption frequencies for cellulose and its derivatives

| Wave number ($cm^{-1}$) | Assignment |
|---|---|
| 3450–3570 | OH stretch, intramolecular H-bridge between the OH groups |
| 3200–3400 | OH stretch, intermolecular H-bridge between the OH groups |
| 2933–2981 | $CH_2$ antisymmetric stretch |
| 2850–2904 | $CH_2$ symmetric stretch |
| 2247 | CN |
| 1725–1730 | C=O stretch from acetyl or COOH groups |
| 1635 | Adsorption of water |
| 1591 | $COO^-$ in CMC |
| 1455–1470 | $CH_2$ symmetric ring stretch at pyrane ring; OH in-plane deformation |
| 1416–1430 | $CH_2$ scissors vibration |
| 1374–1375 | CH deformation |
| 1335–1336 | OH in-plane deformation |
| 1315–1317 | $CH_2$ tip vibration |
| 1370, 1176–1162 | O–$SO_2$–R (tosylates, mesylates) |
| 1277–1282 | CH deformation |
| 1225–1235 | OH in-plane deformation, also in COOH groups |
| 1200–1205 | OH in-plane deformation |
| 1125–1162 | C–O–C antisymmetric stretch |
| 1107–1110 | Ring antisymmetric stretch |
| 1015–1060 | C–O stretch |
| 985–996 | C–O stretch |
| 925–930 | Pyran ring stretch |
| 892–895 | C-anomeric groups stretch, C1–H– deformation; ring stretch |
| 826–800 | C–O–S (tosylates, mesylates) |
| 800 | Pyran ring stretch |

Adapted from [181]

quantitative analysis. In Table 2.4, the general assignments of the most important frequencies for cellulose and its derivatives are listed. More data are found in the following references: acyl [199], cyano, imino, chloro-deoxy [200] carboxymethyl [201], phosphate [202], propargyl [203], and sulfonate [178].

An illustrative example of the use of IR spectroscopy is shown by the conversion of cellulose into derivatives. Figure 2.19 shows the reaction schemes and the molecular structures of cationic ethers. Figure 2.20 shows the peaks of the starting biopolymer and the additional peaks due to product formation. Other examples have been published, including the transformation of CMC into trifunctional aminoamide derivatives [205] and the transformation of cellulose into its trimethylsilyl derivatives [206].

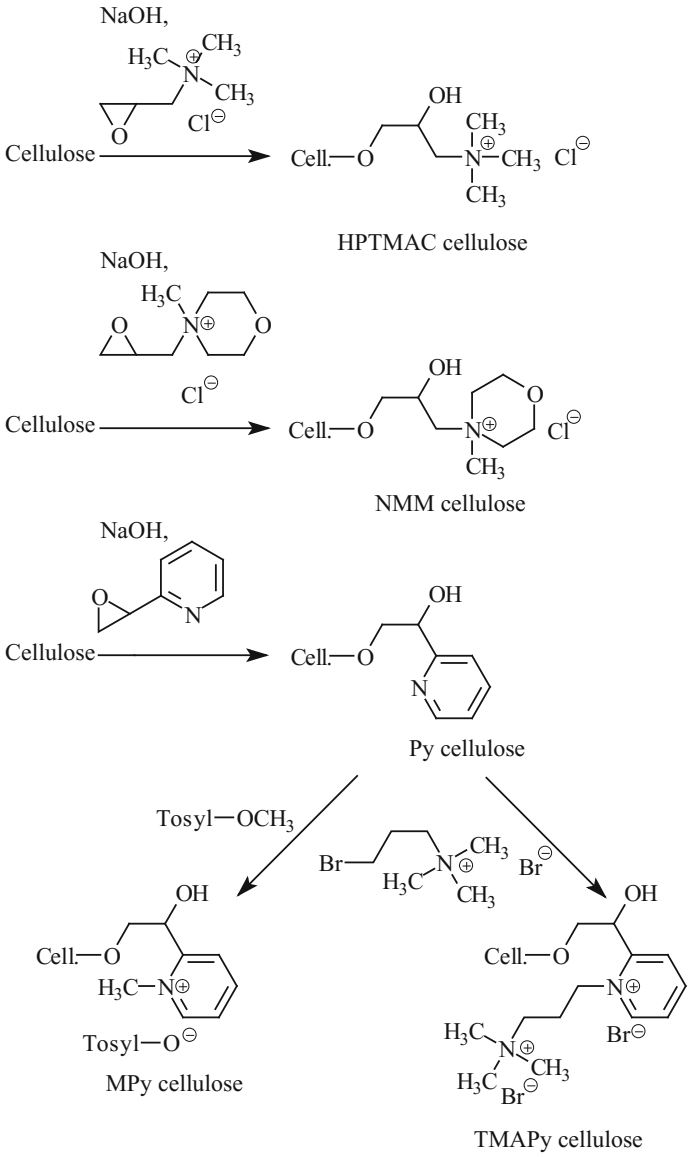


**Fig. 2.19** Reaction schemes for the synthesis of ionic ethers ([204])

IR and Raman spectroscopy have been employed in order to investigate hydrogen bonding in cellulose. For cellulose I, the intramolecular hydrogen bonds of 2-OH…*O*-6 and 3-OH…*O*-5, and the intermolecular hydrogen bonds of 6-OH…O-3′ appear at 3455–3410, 3375–3340, and 3310–3230 $cm^{-1}$, respectively, along

with the valence vibrations of hydrogen-bonded OH groups at 3570–3450 $cm^{-1}$ [207, 208]. This frequency attribution is similar to that suggested for the OH groups of the structurally related β-cyclodextrin [209]. Consequently, the broad OH absorption band can be dissected into the peaks of contributing individual groups, as shown in Fig. 2.21 for celluloses I and II.

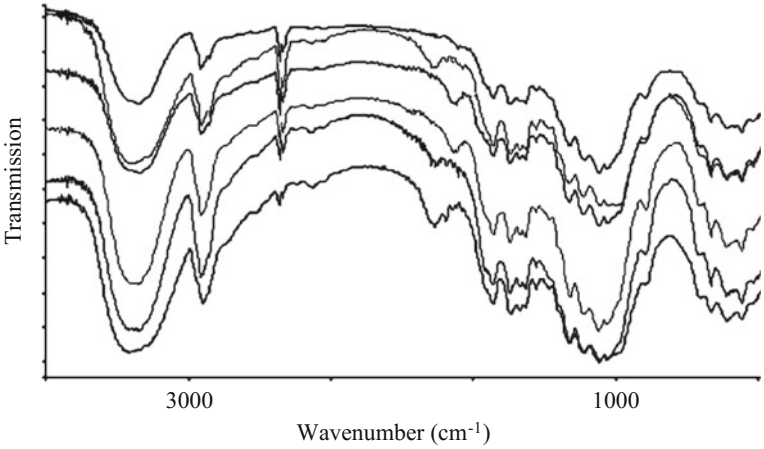


**Fig. 2.20** IR spectra of the starting cellulose (cotton linters) and the cationic ether products (from top: cellulose, Py cellulose, HPTMAC cellulose, NMM, MPy cellulose, TZMAPy cellulose; see structures in Fig. 2.19; adapted from [204])

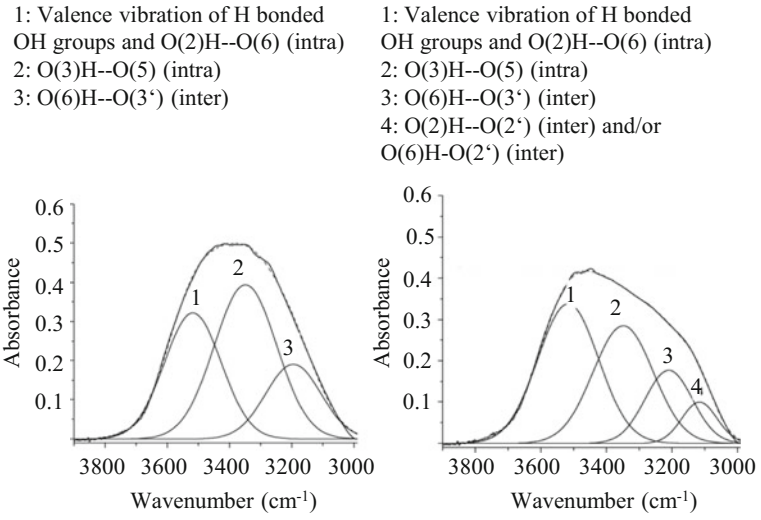


**Fig. 2.21** Deconvolution of the OH band into contributions from the different OH groups in Cellulose I (part a) and cellulose II (part b) (reprinted from [188], copyright (© 2005) with permission from Elsevier)

Provided that the deleterious effect of grinding on the crystal structure of cellulose is avoided/minimized, IR is an attractive experimental technique for the determination of $I_c$ because IR spectrophotometers are available in most research laboratories. Low-cost, powerful, and user-friendly software is commercially available for the required curve deconvolution. As in X-ray diffraction (Sect. 2.3.1), the determination of $I_c$ by IR spectroscopy relies on attributing the absorbances of pairs of signals or their areas to the amorphous and crystalline domains of cellulose. Table 2.5 shows some results along with relevant comments.

Several pairs of IR peaks have been employed for the determination of $I_c$. The correlations between $I_c$ (IR) and $I_c$ (X-ray) are excellent. The slopes differ for each pair of IR frequencies because different modes of vibration are associated with different molar absorptivities.

For a cellulose derivative, the determination of the total DS and the distribution of the substituent among the positions 2, 3, and 6 of the AGU are relevant to the properties, hence applications of the derivative include solubility, permeability to gases and liquids [215], water vapor sorption [216], and compatibility with the blood [74]. These aspects can be readily appreciated from Fig. 2.22 that shows the haemocompatibility of benzylcellulose. The dependence of water solubility of cellulose acetates on the acetate content is a further example (Table 2.6). The sample may be insoluble, partially soluble, or water-soluble, depending on its DS.

Complementary structural information on cellulose derivatives with DS < 3 can be gained, in principle, by examining the OH region (the remaining hydroxyl groups) and the region of the functional group introduced. This type of analysis has been carried out for samples of CA, cellulose acetomaleates, and acetophthalates in different solvents ($CH_2Cl_2$, 9% (v/v) ethanol in $CH_2Cl_2$, $CHCl_3$, $CH_3NO_2$). By using curve deconvolution, the 3700–3300 $cm^{-1}$ region was separated into contributions from the AGU primary OH group (free 3600 $cm^{-1}$; hydrogen bonded 3580 $cm^{-1}$), and the two secondary OH groups (3520 and 3460 $cm^{-1}$), as shown in Fig. 2.23 [173, 176].

Likewise, the peaks in the 1770–1730 $cm^{-1}$ region (CA in $CH_2Cl_2$) can be divided into contributions from the acetyl moiety at C2 and C3, and C6 at 1752 and 1740 $cm^{-1}$ (Fig. 2.24) [176]. Figure 2.24 is in particular interesting because the IR-based procedure is a much simpler and faster approach than $^{13}C$ NMR spectroscopy for the determination of the regioselectivity in the AGU. The reason is that integration of $^{13}C$ NMR peak, e.g., by using the inverse-gated decoupling program [220], is very time consuming [221]. Note, however, that the IR method does not distinguish between substitution at the C2 and C3 positions. This may not be readily accepted in some cases.

An obvious application of IR and Raman spectroscopy is to determine the total DS of cellulose derivatives and the compositions of cellulose-containing blends. This technique is based on the construction of Beer's law plot. However, the synthesis of cellulose samples whose DS covers the range is a major problem.

**Table 2.5** Published data on the determination of $I_c$ by IR spectroscopy, $I_c$ (IR), and comparison with $I_c$ (X-ray)

| Entry | Cellulose | Frequencies ($cm^{-1}$)[a] | Results; comments[b] | References |
|---|---|---|---|---|
| **1** | Birch, cotton, spruce | 1435/894 | Dependence of $I_c$ (IR) on % (w/w) cellulose II content analyzed; $n = 9$<br>$I_c$ (IR) = 2.608% (w/w) cell II (birch) − 0.019; $r = 0.971$<br>$I_c$ (IR) = 5.029% (w/w) cell II (cotton) − 0.044; $r = 0.989$<br>$I_c$ (IR) = 3.002% (w/w) cell II (spruce) − 0.022; $r = 0.995$ | [210] |
| **2** | Cotton, rayon | 1372/2900 | Linear correlations of $I_c$ (IR) with $I_c$ (X-ray) and with accessibility from moisture sorption | [211] |
| **3** | Cotton, filter paper, MCC | 1108/1091; 1430/1403; 1459/1403 | Linear correlations of $I_c$ (IR) using the three ratios of the frequencies and $I_c$ (X-ray); linear correlation of $I_c$ (IR) with $T_{Decomp}$ | [191] |
| **4** | Cotton, bagasse, Rayon grade | 1435/900 | $I_c$ (X-ray) = 0.400 $I_c$ (IR) − 0.198; $r = 0.997$; $n = 4$ | [212] |
| **5** | Cotton, pine | 1370/670 | Complex (decrease then increase) correlation of $I_c$ (IR) with concentration of NaOH used for mercerization (5–50% (w/w)) | [184] |
| **6** | Cotton, HCl-hydrolyzed cotton | 1429/893 | For 12 samples (3 [HCl] × 3 T) $I_c$ (IR) and $I_c$ (X-ray) change in a similar manner; plots of $I_c$ versus reaction conditions are not linear | [213] |
| **7** | MCC, cellulose powders | 1280/1200 | $I_c$ (X-ray) = 1.06 $I_c$ (IR) + 0.19, for $0.26 < I_c$ (X-ray) $< 0.75$; $n = 7$ | [192] |
| **8** | Cotton, MCC, sugar cane bagasse, pine, cellulose powders | 1432/896; 1459/1403; 1108/1091 | $I_c$ (X-ray) = 0.333 $I_c$ (IR) − 0.03; $r = 0.996$; $n = 22$ | [185] |
| **9** | Rayon grade | 1430/894; 1278, 1282/1263; 1372/894; | Linear correlations between the different $I_c$ (IR) and $I_c$ (X-Ray) | [188] |
| **10** | Bamboo | 1430/898 | $I_c$ (X-ray) = 0. 322 $I_c$ (IR) + 0.247; $r = 0.992$; $n = 3$ | [214] |

[a]Peak frequencies whose absorbance, or area ratios have been employed in the calculation of $I_c$ (IR)

[b]The symbols $r$, $n$, and $T$ stand for the correlation coefficient of the linear correlation, the number of cellulose samples that have been employed in the study, and the temperature, respectively

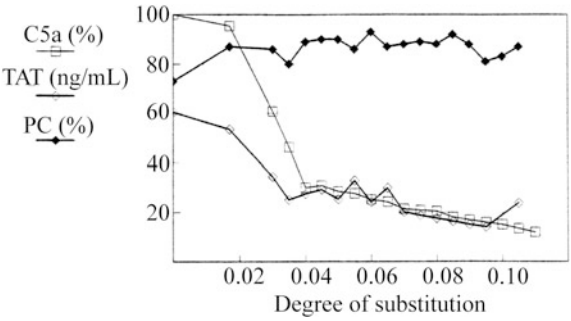


**Fig. 2.22** Dependence of haemocompatibility of benzylcellulose on its DS (adapted from [73])

**Table 2.6** Dependence of water solubility of cellulose acetates on the DS of the ester

| Method[a] | Total DS[b] | Degree of acetylation at position[b] | | | Water-soluble fraction [%, w/w] |
|---|---|---|---|---|---|
| | | 2 | 3 | 6 | |
| **1** | 0.49 | 0.16 | 0.13 | 0.20 | 29 |
| **1** | 0.66 | 0.23 | 0.20 | 0.23 | 99 |
| **1** | 0.90 | 0.31 | 0.29 | 0.30 | 93 |
| **2** | 0.73 | 0.18 | 0.19 | 0.36 | 30 |
| **3** | 1.10 | 0.33 | 0.25 | 0.52 | 5 |

Adapted from [217]

[a]Methods applied: (**1**) deacetylation of cellulose triacetate with aqueous acetic acid, (**2**) reaction of cellulose triacetate with hydrazine, and (**3**) acetylation of cellulose with acetic anhydride in DMAc/LiCl

[b]Determined by $^{13}C$ NMR spectroscopy

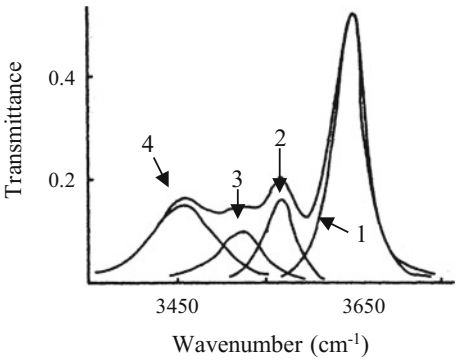


**Fig. 2.23** IR spectrum (0.15–3.0% solution in methylene chloride, measured in a KBr cell) of cellulose acetates (OH group region, 1, primary OH, 2, hydrogen bond of primary OH group, 3 and 4, secondary OH functions). Adapted from [218]

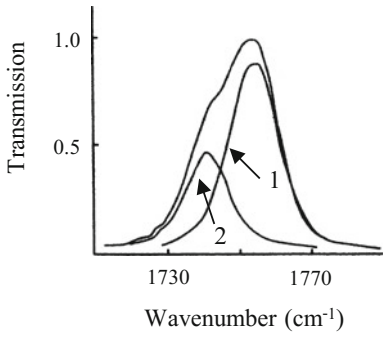


**Fig. 2.24** Representative deconvolutions of the acyl stretching region into individual contributions from the C2, C3, and C6 positions of the AGU (adapted from [219])

This has been solved by mixing cellulose derivative with the highest DS, e.g., cellulose acetate with DS ≈ 3 with cellulose, in order to obtain "equivalent" intermediate DS [177, 198]. Illustrative examples of DS determination are listed in Table 2.7. Both the KBr pellet/absorbance and the ATR and DRIFTS techniques have been successfully employed.

As the examples of Table 2.7 show there are good correlations between DS for several cellulose derivatives as determined by IR and Raman spectroscopy and by other methods. A similar result has been observed for starch derivatives [195]. This favorable result is a consequence of the fact that peak area calculation is rendered relatively easy because most of the functional groups of interest, e.g., acyl, cyano, and sulfonyl have strong, symmetric absorption bands that can be easily handled as pure Lorentzian or a Lorentzian peak with a Gaussian component.

Finally, a complete analysis of the IR absorption (4000–450 $cm^{-1}$) of cotton, rayon, bacterial cellulose, ramie, linen, and sisal cellulose has been given [181, 183]. Values of $I_c$ of cyanoethylated cellulose (1430/900 and 1370/2900 $cm^{-1}$) showed complex dependence on DS [186]. The peak areas of the C=O groups of several esters of cellulose (undecanoate, stearate, undecylenate, oleate) were examined by DRIFT and CP/MAS $^{13}C$ NMR. The values of $\nu_{C=O}$ were found to be practically independent of the structure of the acyl moiety, 1743–1751 $cm^{-1}$; the peak areas of the C=O group (NMR, 173.5–180.8 ppm) correlated with DS, determined by gravimetric analysis [196]. It is also important to mention that solvatochromic probes have successfully been employed in order to determine the DS of cellulose acetates, butyrates, hexanoates, and CMC. In this technique, the values of $\lambda_{max}$ of a solvatochromic dye correlate linearly with DS [198, 224].

**Table 2.7** Illustrative examples of the use of IR and Raman spectroscopy to determine DS of different cellulose derivatives or the compositions of cellulose-containing blends

| Entry | Derivative; functional group, $\nu$ ($cm^{-1}$) | Technique[a] | Results, comments[b] | References |
|---|---|---|---|---|
| **1** | Cyanoethylated, CN, 2247 | Abs, KBr | Linear correlation of Abs with % N | [180] |
| **2** | Cellulose–polyester blends –C=O, 1725 | Abs, KBr | $Abs_{C=O}$ = 0.1048 + 0.0061 (% (w/w) polyester); $r$ = 0.9843; $n$ = 6 ($Abs_{C=O} \times \Delta\nu_{0.5}$) = 0.6267 + 0.263 (% (w/w) polyester); $r$ = 0.9986; $n$ = 6 | [222] |
| **3** | Cotton–wool blends, $\nu_{(O)C-N}$, amide II band, 1520 (wool), –C–O, 1160 (cotton) | Abs, KBr | Combined use of peaks from both components gives reliable compositions ± 3% (w/w) | [223] |
| **4** | Acetate, –C=O, 1760 | Abs; KBr | Linear correlation of Abs with % acetyl | [180] |
| **5** | Tosylate, C=C aromatic, 1600, C–O–S, 810 | Abs; KBr | Linear correlations of both peaks with % S | [180] |
| **6** | Several esters of poly-carboxylic acids, C=O, 1780–1864 | DRIFTS | Correlations, ascending, between $Abs_{C=O}$ and temperature of curing of the ester. | [193] |
| **7** | Benzyl cellulose; cellulose tosylate, C=C aromatic, 1605 | UV–Vis; NIR; Raman | For ether, linear correlations of NIR with DS (UV-Vis); for tosylate, cubic dependence of peak area on DS | [73] |
| **8** | CA, –C=O, 1740 | ATR | Solvent IL-DMSO, almost linear correlation between DS and peak area | [177] |
| **9** | CA, C=O, 1860–1691 | Abs, KBr, DRIFTS | With and without an internal standard (1,4-dicyanobenzene, DCB); Linear correlations between DS and $\nu_{C=O}$ peak area, or ratio of areas ($\nu_{C=O}/\nu_{C\equiv N}$) | [198] |

[a]Except for entry **7**, IR was employed. Abs; KBr denote measurement of the IR absorbance of the sample in KBr disc; DRIFTS and ATR denote reflectance measurements, see text for explanation. The techniques employed in entry **7** for benzyl cellulose are UV–Vis (258 nm), NIR (1050–1100 and 1600–1800 nm); and for cellulose tosylate, Raman (1560–1640 $cm^{-1}$)

[b]The symbols ($r$), ($n$), and $\Delta\nu_{0.5}$ denote correlation coefficient of the linear correlation, the number of cellulose samples that have been employed in the study, and the peak width (in $cm^{-1}$) at half-height, respectively

### 2.3.3 NMR Spectroscopy

Nuclear magnetic resonance (NMR) is among the most powerful methods for the determination of molecular structures and the investigation of the supramolecular behavior of chemical compounds. It is based on a physical phenomenon in which nuclei in a magnetic field absorb electromagnetic radiation. This energy is at a specific resonance frequency, which depends on the strength of the magnetic field and the magnetic properties of the nuclei under investigation. All isotopes that contain an odd number of protons and/or of neutrons have an intrinsic magnetic moment and angular momentum and can be studied with this technique. In case of cellulose and its derivatives, suitable nuclei are, e.g., $^{1}H$, $^{13}C$, $^{11}B$, $^{15}N$, $^{19}F$, $^{31}P$, or $^{35/37}Cl$. The principle of NMR usually involves two sequential steps:

- The alignment (polarization) of the magnetic nuclear spins in an applied, external magnetic field $H_0$.
- The perturbation of this alignment of the nuclear spins by employing an electromagnetic, usually radio frequency (RF) pulse. The required perturbing frequency is dependent upon $H_0$ and the nuclei under observation.

The two fields are usually chosen to be perpendicular to each other. The resulting response by the total magnetization (M) of the nuclear spins is the phenomenon that is exploited in NMR spectroscopy. Depending on the electronic shielding of the atom of interest, a shift of the resonance signal can be observed. These comparably small shifts are given in the spectra in units of parts per million (ppm). Tetramethylsilane has become the reference compound of choice for $^{1}H$ and $^{13}C$ NMR measurements, i.e., in the spectra its chemical shift, $\delta$, has been assigned 0 ppm. The chemical shift is an important indicator for the chemical environment of the atom studied and is, thus, the basic information obtained from NMR experiments concerning the molecular structure.

The second information one can gain is the coupling constant and the splitting pattern. If an atom under examination is perturbed or influenced by a nearby nuclear spin (or set of spins), the observed nucleus responds to such influences, and its response is manifested in its resonance signal. This spin coupling is transmitted through the connecting bonds and it functions in both directions. Thus, when the perturbing nucleus becomes the observed nucleus, it also exhibits signal splitting with the same coupling constant *J*. For spin coupling to be observed, the sets of interacting nuclei must be bonded in relatively close proximity (e.g., vicinal and geminal locations for $^{1}H$) or be oriented in certain optimal and rigid configurations. In case of NMR of cellulose and its derivatives, these splitting patterns are very complex (see below) and hard to assign. In the $^{13}C$ NMR experiments, the splitting between the $^{13}C$ and $^{1}H$ nuclei is usually suppressed by irradiating the $^{1}H$ (decoupling) while observing $^{13}C$ signals. All $^{13}C$ signals will appear as singlets, because the possibility of finding two adjacent $^{13}C$ nuclei is very small; this simplifies greatly the spectrum. For more details on the theoretical background and the principle of NMR spectroscopy, see the following references [225–228].

Although NMR studies on cellulose and its derivatives were more or less exotic about 40 years ago, they are suitable today for the investigation of the crystallinity of cellulose in solid state or the behavior of cellulose in solution. In addition, NMR spectroscopy is the method of choice for the determination of the molecular structure of cellulose derivatives. This is due to the development of NMR equipment with powerful magnets for measurements in liquid state, the use of solid-state measurements, and the application of two-dimensional techniques. Without dwelling too much on theory, the basic NMR experiments used in cellulose chemistry are discussed below.

#### 2.3.3.1 Solid-State NMR of Cellulose

Cellulose molecules generally pack together in a nonuniform manner, with ordered (crystalline) and disordered (amorphous) regions (see Sect. 2.3.1). Crystalline domains occur by structural orientation of the polymer chains in a uniform three-dimensional matrix. Thus, an increased crystallinity is, e.g., associated with an increase in rigidity and tensile strength. Amorphous parts are less rigid, weaker, and more easily deformed. This means that polymer crystals are stiffer and stronger than amorphous regions, whereas the chain-like constitution of repeating units must be the basis of both long- and short-range order in cellulose. Due to differences in the mechanical characteristics of crystalline and amorphous polymers, an understanding of the cellulose crystallinity and an accurate determination of its degree, influenced by chain length and interchain bonding, are most important.

As described in Sect. 2.3.1, the X-ray diffraction patterns of the two phases are very different because the amorphous phase contains no long-range order, meaning that there are no regular crystalline planes to diffract X-rays. To get detailed information about the supramolecular structures of cellulose, techniques other than X-ray scattering are important tools. In particular, solid-state NMR spectroscopy has been widely used.

A typical solid-state proton-decoupled $^{13}C$ NMR spectrum including resonance assignment of bacterial cellulose from *Gluconacetobacter xylinus* with a crystallinity $I_c$ of about 66% (measured by X-ray—see Sect. 2.3.1) is shown in Fig. 2.25. Solid-state NMR measurements on cellulose are usually carried out at cross-polarized/magic angle spinning (CP/MAS) $^{13}C\{^1H\}$ NMR experiments. The spectrum shows the typical line splitting of a cellulose modification I. Signals for each carbon atom of the anhydroglucose unit C-1-C-6 can be detected: at 106–104 ppm (C-1), and at 78–70 ppm (C-2, 3, 5). The $^{13}C$ NMR signal of C-4 is split into a sharp peak at 92–88 ppm for the crystalline part ($C\text{-}4_{cr}$) and a broader peak near 84 ppm for the amorphous regions ($C\text{-}4_a$ region) due to the different electronic environments of this carbon. A similar line splitting is observed in the C-6 region ($C\text{-}6_{cr}$: 66–64 ppm, $C\text{-}6_a$: 64–60 ppm), while the signal of C-1 is not split (crystalline and amorphous parts).

Caused by the differences between crystalline and amorphous regions of cellulose, a distinction between cellulose in the solid state and in solution is possible by

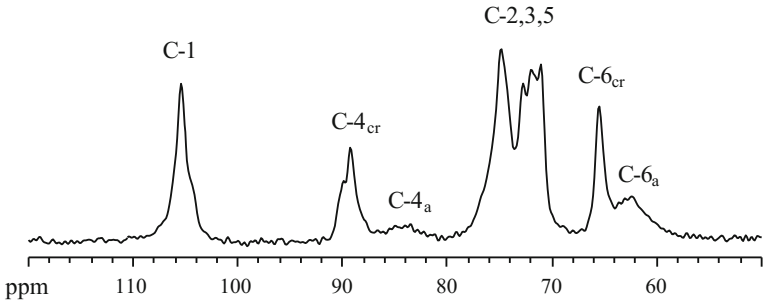


**Fig. 2.25** CP/MAS $^{13}C\{^{1}H\}$ NMR spectrum of bacterial cellulose of *Gluconacetobacter xylinus* ATCC 53582 (cr means crystalline, a amorphous)

verifying the position of the C-4 signal in $^{13}C$ NMR spectra. Changes in bond lengths and angles, especially the bond shortening of the O–C-4 bond from 1.43 to 1.36 Å, determined by the NMR force field, are responsible for a large shift decrease of C-4 of about 10 ppm that appeared after decrystallization of cellulose. As the intrachain hydrogen bonds are responsible for the special geometry of the glycosidic linkage, the characteristic chemical shift of C-4 resonances near 90 ppm is only visible in crystalline cellulose polymorphs [229, 230].

An NMR spectroscopic degree of order (SDO) of solid cellulose samples can be derived from the evaluation of the carbon resonances, which is, however, not proportional to the crystallinity $I_c$ obtained by X-ray studies [231]. It is emphasized that $I_c$ comprises a region of long-range order while the crystallinity degree, derived from NMR spectral analysis of the C4 signal, e.g., is sensitive to the short-range order of cellulose [232]. Compared with the $I_c$ value obtained by X-ray, the NMR degree of order of the bacterial cellulose sample shown in Fig. 2.26 is higher (71%).

However, different kinds of cellulose (algae, plant, or animal cellulose) exhibit variability in their crystalline characteristics. Table 2.8 gives a general survey of such values. Furthermore, the decrease of crystallinity in relation to the method of sample treatment can be illustrated quite easily in the case of bacterial cellulose. Crystallinity data of differently dried pellicles of the same strain of *Gluconacetobacter xylinus* (Table 2.8) correspond to the CP/MAS $^{13}C\{^{1}H\}$ NMR spectra in Fig. 2.26. The examples depict varieties in the crystalline arrangement of polymer chains. It is known that in the wet state of cellulose pellicles, sharpness, and resolution of the multicomponent lines of the $^{13}C$ NMR spectra are remarkable. Structure parameters like crystallinity and the NMR SDO are thus strongly influenced by the water content and drying method of the sample [233].

It should be noted that the line splitting and spectral features of the NMR spectra of cellulose I vary and that the number of the resonance lines is much more than that of carbons of the AGU composing cellulose chains. A correlation between the chemical shifts and the dihedral angles defined by the bonds associated with these particular carbons is recognized [239]. For example, there is a correlation between the chemical shift of the C-6 resonance and the value of the dihedral angle $\phi$

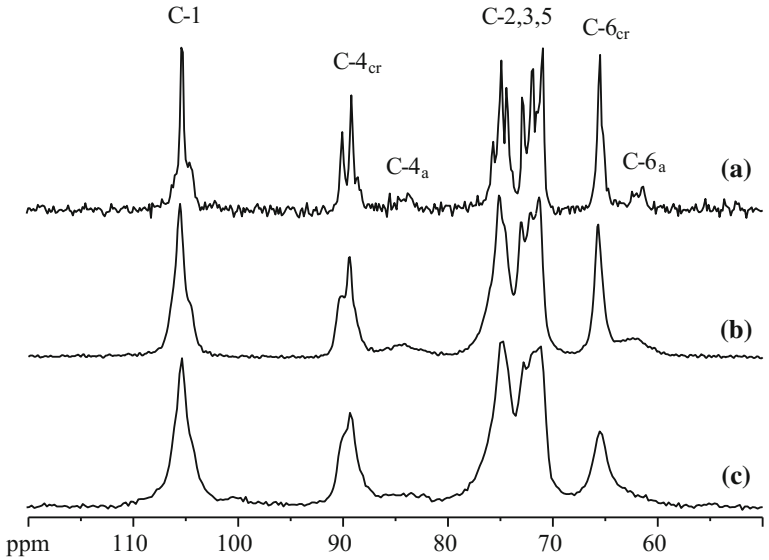


**Fig. 2.26** CP/MAS $^{13}C\{^{1}H\}$ NMR spectra of bacterial cellulose of *Gluconacetobacter xylinus* DSM 14666 (cr means crystalline, a amorphous); **a** never dried, **b** air-dried, **c** freeze-dried [233]

**Table 2.8** Typical values of the NMR spectroscopic degree of order (SDO) and $I_\alpha/I_\beta$ ratio of different cellulose samples [233–238]

| Cellulose | | NMR SDO (%) | $I_\alpha/I_\beta$ |
|---|---|---|---|
| Powder | | 24 | |
| Algal (*Valonia*) | | 60 | 1.8:1 |
| Bacterial (*G. xylinus*) | Freeze-dried | 68 | 2.6:1 |
| | Air-dried | 72 | 2.7:1 |
| | Never-dried | 80 | 2.9:1 |
| Tunicate (*Halocynthia*) | | 85 | 1:10 |

defining the orientation of the OH group at C-6 relative to the C-4–C-5 bond in the glucopyranose ring. This correlation is of value in interpretation of the solid-state $^{13}C$ NMR spectra with respect to splitting of the C-6 resonances. Moreover, $\delta$ of C-1 and C-4 are correlated with the dihedral angles between the bonds in the glycosidic linkage [239].

Furthermore, the line shape of C-4 and of C-1 signals permits the discrimination between crystalline sub-modifications. Using CP/MAS $^{13}C\{^{1}H\}$ NMR on highly crystalline native cellulose I, the presence of two distinct crystalline phases, the presence of allomorphs $I_\alpha$ and $I_\beta$, was proven [140]. This $I_\alpha/I_\beta$ ratio in native cellulose differs greatly from species to species. Cellulose $I_\alpha$ is the dominant form in algae and bacterial celluloses, while $I_\beta$ is mainly found in higher plants and animal celluloses [234, 235, 239, 240].

A successful assignment of all $^{13}C$ NMR signals in the cellobiose repeating unit (the two AGUs that compose cellobiose give different NMR signals) was achieved by a solid-state experiment incredible natural abundance double quantum transfer experiment (INADEQUATE) of specifically prepared allomorphs $I_\alpha$ (purified *Cladophora*) and $I_\beta$ (purified *Halocynthia* = tunicate cellulose), cf. [241]. Both allomorphs contain two magnetically different D-glucose residues in the unit cells. Radio-frequency-driven dipolar recoupling (RFDR) experiments on uniformly $^{13}C$-labeled bacterial cellulose samples have shown the sequence of D-glucose residues: A1 and A2 in $I_\alpha$, and B and B′ in $I_\beta$. According to [242], the chains in cellulose $I_\alpha$ consist of –A1–A2– repeating units, whereas cellulose $I_\beta$ is composed of two independent –B–B– and –B′–B′– chains. This interpretation fully supports the crystallographic results on cellulose $I_\alpha$ and $I_\beta$ of synchrotron X-ray and neutron diffraction experiments [15, 142].

Line shape analysis

An exact determination of the $^{13}C$ NMR spectrum of cellulose is possible by line shape analysis. It allows an assignment of all $^{13}C$ chemical shifts as well as the determination of the $I_\alpha/I_\beta$ ratio and the value of crystallinity [235, 243–245]. The analysis is based on deconvolution of the spectral features into combinations of line functions centered at the assigned shifts for the particular resonances. It should be noted that the use of line functions, in particular Lorentzian and Gaussian, does not have a solid justification in terms of understanding line widths in the CP/MAS $^{13}C$ $\{^1H\}$ NMR spectra of organic materials like cellulose. That is, the values thus obtained should not be taken literally [246]; however, it is a useful tool for approximating the amounts of various constituents and for generating a relative ranking of composition [245].

Figure 2.27 shows spectral line fitting of the C-1 position of cellulose in the $^{13}C$ NMR spectrum consistent with the crystal-composite model. The line shape used for analysis should reproduce the form of the resonance peak investigated. Accordingly, lines can be resolved into three constituent lines according to the analysis for the $I_\alpha/I_\beta$ composite crystal mode [247], whereas an additional broad Lorentzian line should be introduced for amorphous regions. Another possibility for line shape analysis is the use of both Gaussian and Lorentzian line shape

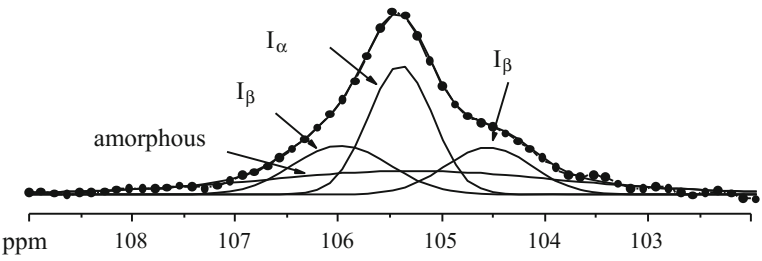


**Fig. 2.27** Line shape analysis of the C1 position of native cellulose I, especially bacterial cellulose of *Gluconacetobacter xylinus*, by Gaussian lines

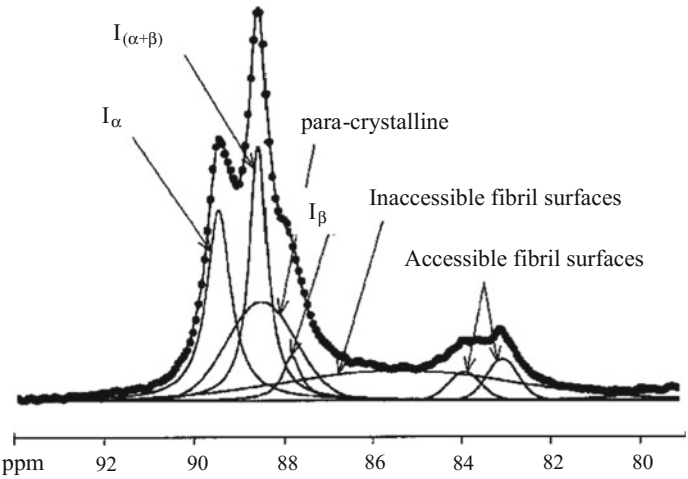


**Fig. 2.28** Spectral fitting analysis for the C4 region of native cellulose I

components—altogether eight lines, each with variable width, amplitude, and central frequency [237], or using Gaussian peaks only according to Fig. 2.27. In adjustment to the C-1 resonance, three Gaussian peaks of small widths are taken into account for the crystalline regions of the two allomorphs, $I_\alpha$ and $I_\beta$, and a broad Gaussian peak characterizes the amorphous parts of the C-1 position of cellulose.

In case of bacterial cellulose, however, a further line component has to be considered, which is interpreted as an extra structural part in the never-dried sample [248]. This part arises from interactions between noncrystalline cellulose chains and chains on the surface of crystallites with the surrounding water. The splitting into several line components can be very well observed in case of the C-4 position in the $^{13}C$ NMR spectrum of BC because the signals from ordered and less ordered regions are well separated [238, 249]. For analysis, three Lorentzian peaks for the signals from cellulose $I_\alpha$, $I_{(\alpha+\beta)}$, and $I_\beta$, as well as four Gaussian peaks for the signals from paracrystalline cellulose, two accessible fibril surfaces, and inaccessible fibril surfaces are assigned, as indicated in Fig. 2.28. Including Gaussian peaks for this analysis is empirical; however, this can be considered an ad hoc extension to compensate for the shortcomings of a Lorentzian-only model [250]. The extraction of the $I_\alpha/I_\beta$ ratio is not nearly straightforward, especially in the case of the higher plant celluloses where the spectral resolution of the multiplet components is poor [251].

### $^{13}C$-labeling of bacterial cellulose

Isotope enrichment is very useful to enhance the sensitivity of nuclei with a low natural abundance and a small gyromagnetic rate such as $^{13}C$ ($\sim 1.1\%$). To increase $^{13}C$ content, isotopically exchanged samples are widely used in NMR spectroscopy to study the structure of cellulose from different sources [230, 242, 252, 253].

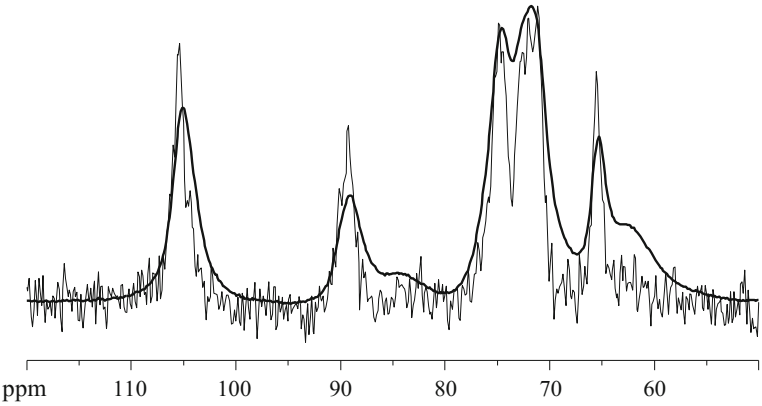


**Fig. 2.29** CP/MAS $^{13}C\{^{1}H\}$ NMR spectra of air-dried bacterial celluloses of the strain *Gluconacetobacter xylinus* DSM 14666 recorded at identical experimental conditions; thick line —$^{13}C$-labeled sample; thin line—BC with $^{13}C$ natural abundance

Due to the fact that formation and structure of bacterial cellulose can be controlled by varying the components of nutrient medium and cultivation conditions, bacterial cellulose can be easily labeled using an appropriate carbon source for biosynthesis. The impact of the $^{13}C$ labeling on spectral resolution can be seen in Fig. 2.29. It shows that the $^{13}C$ NMR spectra of $^{13}C$-labeled (thick line) cellulose of the same strain of *Gluconacetobacter xylinus*, recorded under the same experimental conditions have a much better signal/noise ratio.

Compared to NMR spectra of non-enriched material, the line shape characteristics and resolution of the CP/MAS $^{13}C\{^{1}H\}$ NMR spectra of fully $^{13}C$-labeled pellicles are rather limited because of the strong homonuclear dipolar carbon–carbon couplings. The $^{13}C$ chemical shifts of $^{13}C$-labeled bacterial celluloses of different *Gluconacetobacter xylinus* strains, however, can be readily assigned by line shape analysis described above, taking into account data from the literature, e.g., [241].

Non-enriched and $^{13}C$-labeled BC samples do not show significant varieties in their supramolecular arrangement. However, it should be mentioned that β-D-glucose-$^{13}C6$ ($^{13}C$, 99%) enhances the cellulose production of *Gluconacetobacter xylinus* depending on the cell type [254, 255]. ATCC 53582 cells, for instance, produce a larger quantity of averaged smaller fibers in the presence of the $^{13}C$-isotope, meaning that β-D-Glucose-U-$^{13}C6$ ($^{13}C$, 99%) stimulates the cell division. The crystallite sizes of bacterial cellulose pellicles average out to be 5–12 nm independent of the $^{13}C$ enrichment of the samples. Bacterial cellulose samples possess about 70% crystalline regions and ratios of cellulose modifications of $I_\alpha$:$I_\beta \approx 2.6$:1 [255].

In summary, the increasing number of publications in the field of solid-state NMR spectroscopy during the recent years attests to the importance of NMR techniques in the conformational analysis of cellulose. Investigations on different cellulose modifications (I, II, $III_I$, $III_{II}$, $IV_I$, and $IV_{II}$) as well as cellulose derivatives delivered insight into the fibrous structure and the reversibility of the hydrogen-bonding system during conformational changes [241, 245, 252, 256–259].

### 2.3.3.2 Application of Liquid Phase NMR

Cellulose

A major limitation of liquid NMR spectroscopy of cellulose is certainly the insolubility of the polymer in common NMR solvents. Thus, for solution $^{13}C$ NMR investigation of cellulose specific solvents must be applied. Cellulose can be measured in solvents, such as DMAc/LiCl and DMSO/TBAF [260], ionic liquids [261], or salt melts [262]. A $^{13}C$ spectrum of cellulose dissolved in DMSO/TBAF-$d_6$ is shown in Fig. 2.30.

In this well-resolved spectrum, every carbon atom of the cellulose backbone shows a separate signal. The chemical shifts of the AGU carbon signals depend, to a certain amount, on the solvent used as shown in Table 2.9 [263]. It should be

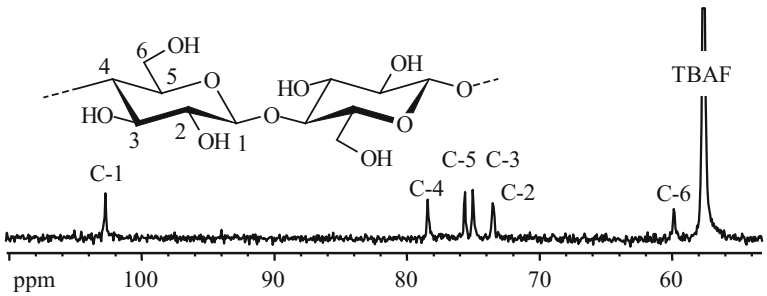


**Fig. 2.30** $^{13}C$ NMR spectrum of cellulose dissolved in DMSO/TBAF-$d_6$

**Table 2.9** Chemical shifts in $^{13}C$ NMR spectra of cellulose depending on the solvent [263, 264]

| Solvent | Chemical shift (ppm) | | | | | |
|---|---|---|---|---|---|---|
| | C-1 | C-2 | C-3 | C-4 | C-5 | C-6 |
| NaOH/$D_2O$[a] | 104.5 | 74.7 | 76.3 | 79.8 | 76.2 | 61.5 |
| Cadoxen | 103.8 | 74.9 | 76.6 | 78.9 | 76.4 | 61.8 |
| Triton B | 104.7 | 74.9 | 76.7 | 80.1 | 76.4 | 61.8 |
| DMAc/LiCl | 103.9 | 74.9 | 76.6 | 79.8 | 76.6 | 60.6 |
| NMMO/DMSO | 102.5 | 73.3 | 75.4 | 79.2 | 74.7 | 60.2 |
| TFA/DMSO | 102.7 | 72.9 | 74.7 | 80.2 | 74.7 | 60.2 |
| LiCl/DMI[a] | 103.0 | 74.1 | 75.8[c] | 78.7 | 75.8[c] | 59.6 |
| DMSO/TBAF[b] | 102.8 | 73.5 | 75.1 | 78.6 | 75.8 | 60.0 |
| DMSO | 102.7 | 72.9 | 74.7 | 80.2 | 74.7 | 60.2 |

[a]*DMI* 1,3-dimethyl-2-imidazolidinone [265]
[b][160]
[c]not fully resolved

mentioned that for solutions of cellulose in non-deuterated solvents, e.g., cellulose in BuMeImCl, $^{13}C$ NMR spectroscopy needs to be carried out using a NMR coaxial tube with an interior tube filled with a deuterated liquid, in order to serve as a deuterium "lock" for the spectrometer.

$^{13}C$ NMR spectroscopy on cellulose in solution is a suitable tool for the determination of impurities and for the investigation of cellulose–solvent interactions. Thus, the formation of ester functions at the cellulose backbone during dissolution of cellulose in trifluoroacetic acid (TFA), or formic acid was revealed by $^{13}C$ NMR spectroscopy [264, 266]. In case of cellulose dissolved in TFA, two sets of peaks were observed, at 159.6 and 115.9 ppm for free TFA and 156.6 and 114.5 ppm for the TFA ester of cellulose formed by dissolution. Moreover, a peak at 67.3 ppm indicates trifluoroacetylation at position C6 of the AGU. In esterification of cellulose with formic acid, the formation of a formate was also observed by $^{13}C$ NMR spectroscopy. As Fig. 2.31 shows, a signal at 63.1 ppm is present, revealing the formylation [267]. On the basis of NMR measurements on cellulose models, the end group functionalization of cellulose by ionic liquids was determined by NMR technique, as discussed in Sect. 3.2.1. In addition to $^{13}C$ NMR chemical shifts, the DEPT 135 NMR is employed in order to determine the number of protons linked to carbons (CH, $CH_2$ or $CH_3$).

Hydrolytically unstable six and seven-membered rings with cellulose are formed in the presence of boric and boronic acids (see Fig. 2.32). In Fig. 2.33, the shifts of the signals for carbons 4, 5, and 6 of the AGU show the formation of the six-membered ring in position 4/6 (Fig. 2.32 structure 2). The separate peak at 78.7 ppm indicates conversion of the trans-1,2-diol unit in position 2/3 (Fig. 2.32 structure 3a). Moreover cross-linking was found for this reaction (Fig. 2.32 structure 3b). Besides $^{13}C$ NMR spectroscopy, most of the structural information were gained and verified by coordination-induced shift (CIS) calculations, two-dimensional techniques and $^{11}B$ NMR spectroscopy. This example is suitable

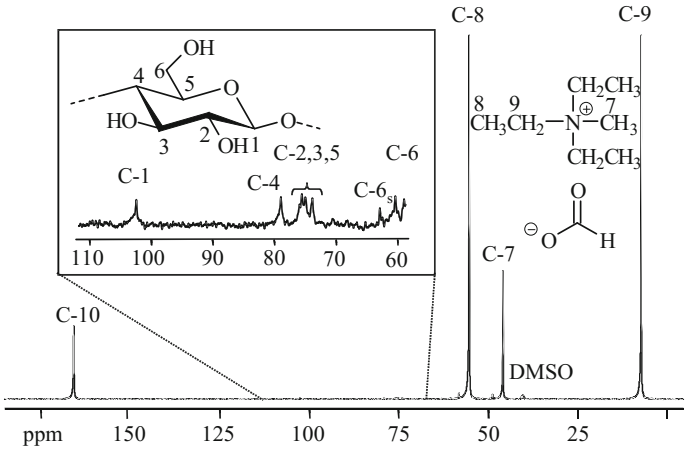


**Fig. 2.31** $^{13}C$ NMR spectrum of cellulose dissolved in triethylmethylammonium formate in deuterated dimethyl sulfoxide; R means formate group or H according to the DS

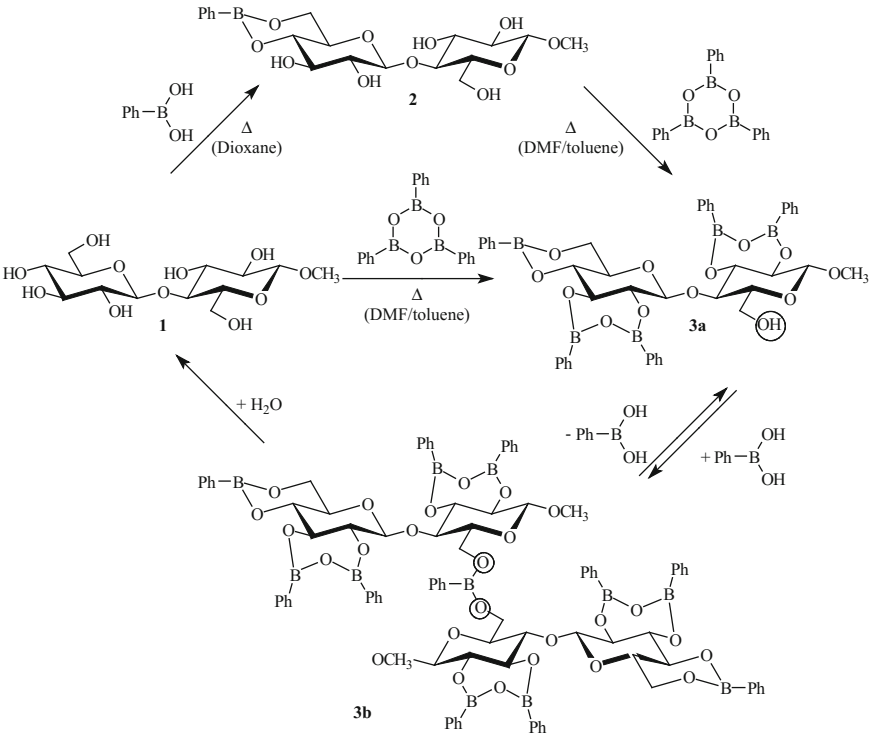


**Fig. 2.32** Summary of structures formed during the interaction of methyl-β-D-cellobioside (**1**) with phenylboronic acid and the anhydride of phenylboronic acid. $^{13}C$ NMR spectra reveal the existence of six (**2**) and seven-membered (**3a**) rings and cross-linking (**3b**) reactions

to illustrate the potential combination of NMR methods has for a comprehensive structure elucidation and will be discussed in detail in this Chapter (see below). Here, only the results of 1D (one dimensional) $^{11}B$ NMR experiment on methyl-D-glucopyranoside/phenylboronic acids mixtures are discussed. In comparison with $^{11}B$ NMR spectra of other five-, six-, and seven-membered ring systems, this spectroscopy gives a first evidence for the occurrence of a seven-membered ring (peak at about 20 ppm) formed on a trans-diol moiety of a carbohydrate as can be seen in Fig. 2.34 [268, 269].

Structure analysis by $^{1}H$ NMR spectroscopy is limited because of the structural diversity of the different protons along the chain and their coupling patterns resulting in complex, strongly coupled spectra. This is displayed for a chain prolongation of cellulose oligomers and the assignment of the corresponding proton signals [270]. The complete spectroscopic data for a methyl-β-D-cellohexaose are listed in Table 2.10 illustrating the large number of different signals contributing to broad lines in case of a polymer. Two separate signals are observed for H-6 due to the neighboring chiral carbon atom of position 5.

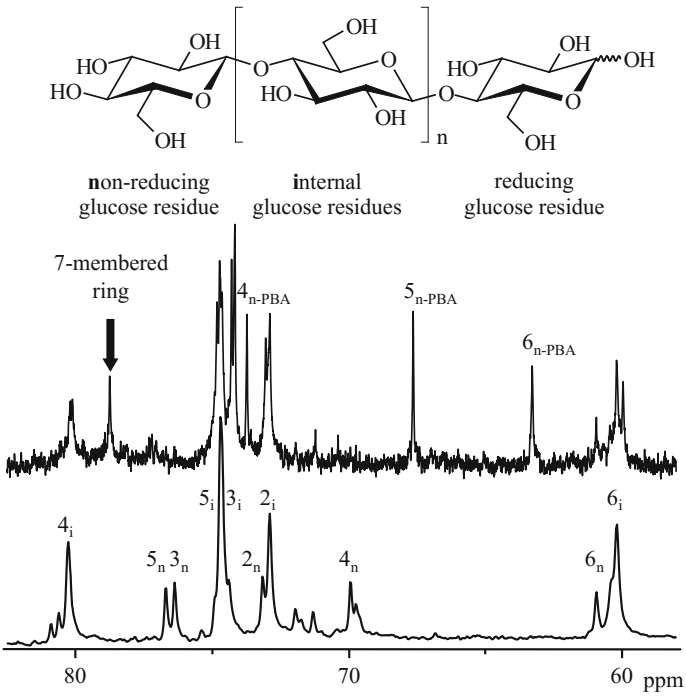


**Fig. 2.33** $^{13}C$ NMR spectrum (range 57–83 ppm) of cellodextrin (DP 12; bottom); and cellodextrin after reaction with phenylboronic acid anhydride in DMSO-$d_6$ (top)

Nevertheless, $^{1}H$ NMR spectroscopy is a very helpful tool for certain tasks including the determination of impurities or characterization of the interaction with other molecules. Advantages of $^{1}H$ NMR spectroscopy are that it is a fast method and the signal intensities can be used for quantification in contrast to standard $^{13}C$ NMR spectroscopy. In addition, solutions with about 1% (w/w) polymer are sufficient for acquiring a spectrum. Therefore, $^{1}H$ NMR spectroscopy is the method of choice for the determination of "natural impurities" such as lignin. Thus, a rapid and efficient process for the measurement of lignin content in the plant cell walls was developed. The method includes direct dissolution and $^{1}H$ NMR analysis of biomass exploiting perdeuterated pyridinium chloride/DMSO-$d_6$ as solvent [271]. It gives very accurate data for the lignin content (Fig. 2.35).

Detailed assignment of complex $^{1}H$ and $^{13}C$ NMR measurements may be carried out by spectra simulation of an oligomer using standard software (e.g., ChemDraw Ultra Version 5.0). Nevertheless, more suitable are state-of-the-art NMR techniques such as decoupling experiments, dynamic spectroscopy, relaxation measurements or two- (2D) and three-dimensional (3D) techniques. For a detailed discussion on the practical aspects of NMR, see [220]. Cellulose/solvent interactions were investigated with such methods. $^{13}C$ and $^{35/37}Cl$ NMR relaxation studies of cellulose (again cellooligomers as model) for elucidation of the dissolution mechanism

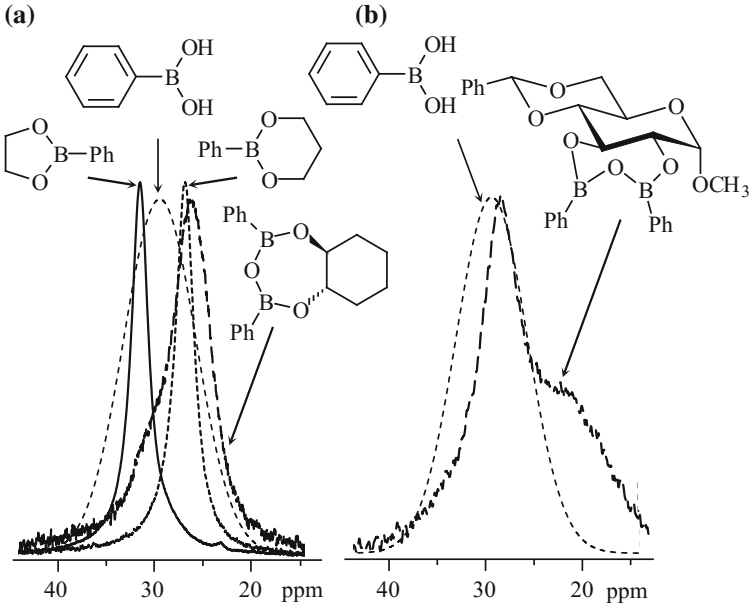


**Fig. 2.34** $^{11}$B NMR spectra of **a** model compounds with five (solid line), six (dotted line) and seven-membered rings (long dashed line); **b** phenylboronate of methyl-D-glucopyranoside (long dashed line) in comparison with PBA (short dashed line) in DMSO-$d_6$

of cellulose in BuMeImCl showing the crucial role of the "free" chloride anion for the solubilization of cellulose [272].

2D NMR spectra are obtained by performing a series of 1D NMR measurements with introduction of a time increment (mixing time or mixing period). This is an additional approach to the two basic sequential steps mentioned in the introduction part. In the mixing period, one or several radio frequency pulses create an observable transversal magnetization recorded in the detection period $t_2$ (see Fig. 2.36).

The data recorded give information about the interaction of atoms in a molecule. Atoms interacting by bonding system (scalar coupling) or through space cause cross-peaks in the 2D spectra depending on the experiment. One divides between homonuclear 2D experiments such as 2D correlated spectroscopy (COSY) and 2D total correlation spectroscopy (TOCSY), where usually proton–proton coupling is detectable, and heteronuclear experiments such as heteronuclear single quantum coherence (HSQC) and heteronuclear multiple bond correlation (HMBC), which are most common $^{1}$H-$^{13}$C coupling experiment. In HSQC spectra, only the coupling of atoms in direct neighborhood is observed. Consequently, the spectra are simple. In HMBC experiments, long-range coupling can be observed making the spectra more complicated. Additional techniques are nuclear Overhauser enhancement spectroscopy (NOESY), which detects correlation via the nuclear Overhauser effect

**Table 2.10** Signal assignment of $^1$H NMR spectra of methyl β-D-cellohexaose

| Ring | $^1$H (ppm) | Multiplicity | Ring | $^1$H (ppm) | Multiplicity |
|---|---|---|---|---|---|
| A | | | D | | |
| H-1 | 4.405 | d | H-1 | 4.533 | d |
| H-2 | 3.304 | dd | H-2 | 3.358 | t |
| H-3 | 3.64 | m | H-3 | 3.65 | m |
| H-4 | 3.63 | m | H-4 | 3.69 | m |
| H-5 | 3.59 | m | H-5 | 3.62 | m |
| H-6 | 3.819 | dd | H-6 | 3.828 | dd |
| H-6′ | 3.991 | dd | H-6′ | 3.976 | d |
| B | | | E | | |
| H-1 | 4.533 | d | H-1 | 4.533 | d |
| H-2 | 3.358 | t | H-2 | 3.358 | t |
| H-3 | 3.65 | m | H-3 | 3.65 | m |
| H-4 | 3.69 | m | H-4 | 3.69 | m |
| H-5 | 3.62 | m | H-5 | 3.62 | m |
| H-6 | 3.828 | dd | H-6 | 3.828 | dd |
| H-6′ | 3.976 | d | H-6′ | 3.976 | d |
| C | | | F | | |
| H-1 | 4.533 | d | H-1 | 4.509 | d |
| H-2 | 3.358 | t | H-2 | 3.313 | dd |
| H-3 | 3.65 | m | H-3 | 3.506 | t |
| H-4 | 3.69 | m | H-4 | 3.416 | t |
| H-5 | 3.62 | m | H-5 | 3.486 | ddd |
| H-6 | 3.828 | dd | H-6 | 3.736 | dd |
| H-6′ | 3.976 | d | H-6′ | 3.915 | dd |

*d* doublet, *dd* doublet of doublets, *m* multiplet, *t* triplet

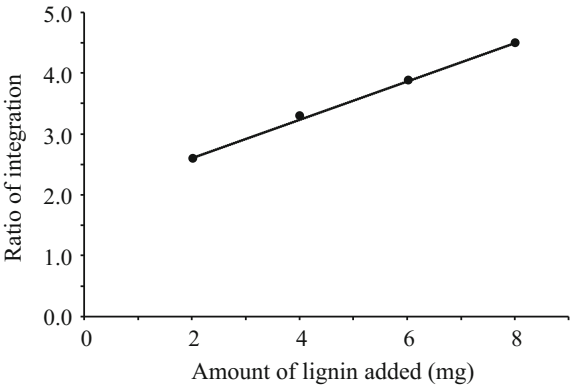


**Fig. 2.35** Calibration curve for the determination of the lignin content in lignocelluloses obtained by $^1$H NMR experiments in the solvent perdeuterated pyridinium chloride/DMSO-$d_6$ (according to [271])

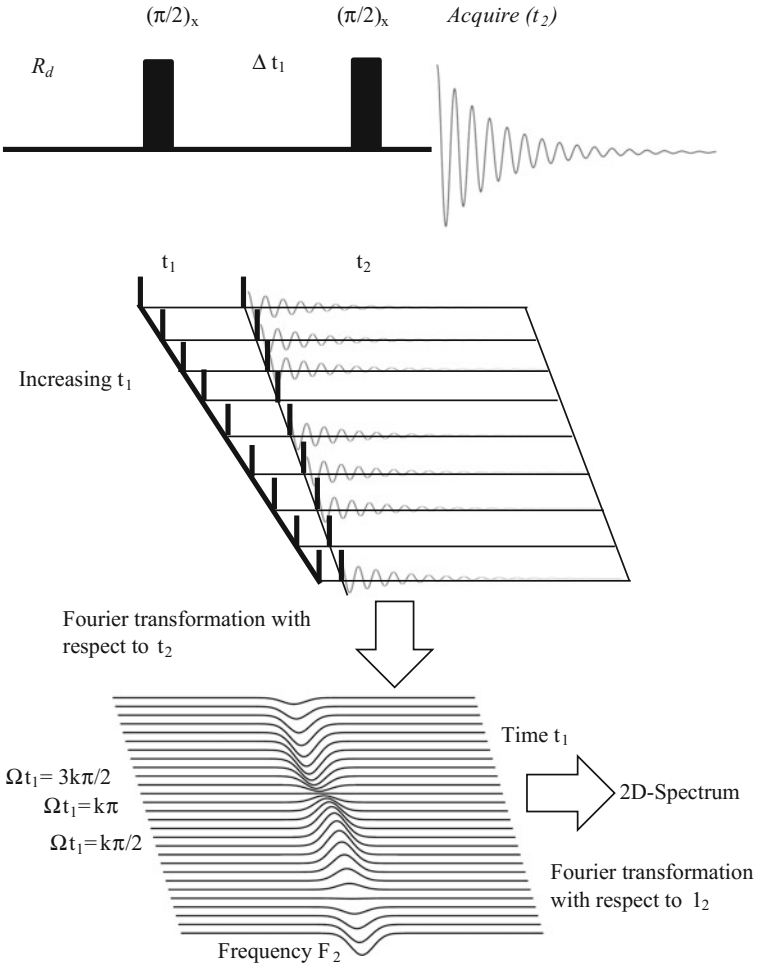


**Fig. 2.36** General approach for the acquisition of a 2D NMR spectrum (according to [273])

instead of a scalar coupling along a bond. Therefore, this approach is suitable for a determination of interactions through space. A method, which is especially useful for the investigation of polymer solutions, is diffusion ordered spectroscopy (DOSY). This NMR technique is combined with a field gradient. It is suitable for the observation of, e.g., the diffusion behavior of molecules and can thereby give information on the molecular weight.

A number of such 2D experiments were applied to study the structures formed in boric and boronic acid containing activating agents for cellulose that is a nice example for illustrating the usefulness and the strategy of the NMR spectroscopy for structure determination.

Thus, analysis of structures formed during the conversion of cellulose models such as methyl-D-glucopyranoside, methyl-β-D-cellobioside (Me-β-D-cellobiose) and cellodextrins with phenylboronic acids by means of NMR spectroscopy will be discussed in detail. Comparable methods are carried out for cellulose derivatives as discussed in the following chapters.

The structures formed during the reaction of phenylboronic acid (PBA) or its anhydride with Me-β-D-cellobiose are shown in Fig. 2.32. These structures can be obtained by a stepwise conversion of Me-β-D-cellobiose with increasing amounts of PBA. In the $^{1}$H NMR spectrum of the phenylboronate sample **2**, five instead of seven signals for unmodified OH moieties between 5.5 and 4.0 ppm were found. Consequently, esterification of two hydroxyl groups with PBA occurred. Figure 2.37 displays the 2D HMBC NMR spectrum of sample **2**. With this method, complete assignment both of the $^{1}$H and $^{13}$C NMR spectra is possible.

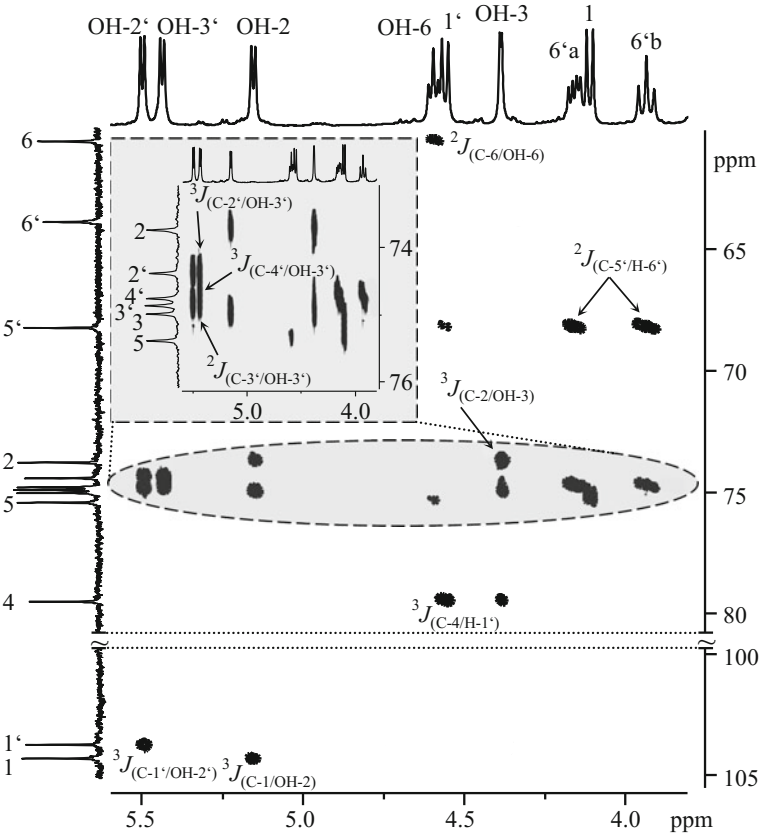


**Fig. 2.37** 2D [$^{1}$H, $^{13}$C] HMBC NMR spectrum of Me-4,6(PhB)-β-D-cellobiose (**2**) in DMSO-$d_6$ (reprinted from [268], copyright (© 2010) with permission from Elsevier)

The two signals for H-6′a/b (′means bearing a substituent at this position), which are shifted downfield (0.5 ppm) in comparison to signals of unmodified Me-β-D-cellobiose, have cross-peaks with an upfield-shifted (9.1 ppm) carbon atom in position 5′. The proton of the unmodified primary hydroxyl moiety in position 6 of the methylated reducing end group (4.59 ppm) couples via two bonds with the carbon in position 6. Along the glycosidic bond, there is a 3 J-coupling of H-1′ and C-4 of the methylated reducing glucose residue. The secondary hydroxyl protons of OH-2 and OH-2′ reveal the corresponding cross-peaks with the anomeric carbons C-1 and C-1′. OH-3′ as well as OH-3 show heteronuclear J-coupling with directly linked carbons in position 3 via two bonds and with adjacent carbons in position 2 and 4 respectively via three bonds (see inset of Fig. 2.37). These results illustrate that despite the high number of signals, especially in the region 73–76 ppm, complete assignment of the spectrum is possible. The full assignment of proton and carbon shifts of structure 2 using the experiment discussed in combination with other 2D NMR techniques (correlation spectroscopy like COSY and HSQC-DEPT) revealed that the two missing hydroxyl protons in $^{1}$H NMR spectra of esterification product of Me-β-D-cellobiose with PBA using a molar ratio of 1:1.1 of PBA are the esterified OH functions in position 4 and 6. The trend of signal movement (CIS) in the $^{13}$C NMR spectrum of that methyl-4′,6′-*O*-phenylboronate-β-D-cellobioside (**2**) resulting from the formation of a six-membered boronate ring correlates with data obtained for Me-D-Glc*p*. Thus, binding site carbons are shifted downfield (C-4′ and C-6′ 2–4 ppm), whereas for adjacent carbon atoms upfield shift (C-5′ 9 ppm) is observed.

In the case of esterification of Me-β-D-cellobiose with PBA using a molar ratio of 1:3 and higher, a product with a six-membered ring at OH-4′ and OH-6′ and an additional seven-membered pyroboronate ring at one of the trans-1,2-diol groups of the disaccharide is expected. This expectation is based on MS studies [268], $^{11}$B NMR studies on Me-D-Glc*p* (see Fig. 2.34) and 2D [$^{1}$H, $^{1}$H] NOESY NMR spectroscopy on Me-D-Glc*p* which clearly showed the coupling of the proton in ortho-position of the phenylboronate moiety ($\delta$(O-H) = 7.8 ppm) with protons of the carbohydrate backbone.

If the esterification of Me-β-D-cellobiose with a molar ratio 1:5.5 of PBA is carried out, the formation of two phenylboronate structures (**3a** and **3b**) is concluded from the occurrence of two singlets for methyl protons (**3a**: 3.60 ppm and **3b**: 3.54 ppm) of the anomeric methoxyl group (OMe) in the $^{1}$H NMR spectra, which can be confirmed by means of 1D NOESY NMR experiments.

A series of 2D [$^{1}$H, $^{1}$H] TOCSY NMR experiments with different mixing times (12, 40, and 90 ms) allow the identification of the resonance signals for the remaining protons of the cellobioside. The position of the shifts for H-2 and H-3, and H-2′ and H-3′, respectively, can be detected by comparing the TOCSY spectra of 12 and 40 ms. Using the total correlation spectroscopy NMR experiment with the longest mixing time (90 ms), the signals for H-4 and H-5 and H-4′ and H-5′ can be determined (Figs. 2.38 and 2.39).

Assignment of protons H-6 and H-6′ was carried out by HSQC-DEPT NMR spectroscopy. The cross-peaks with opposite sign show the position of these protons (Fig. 2.40).

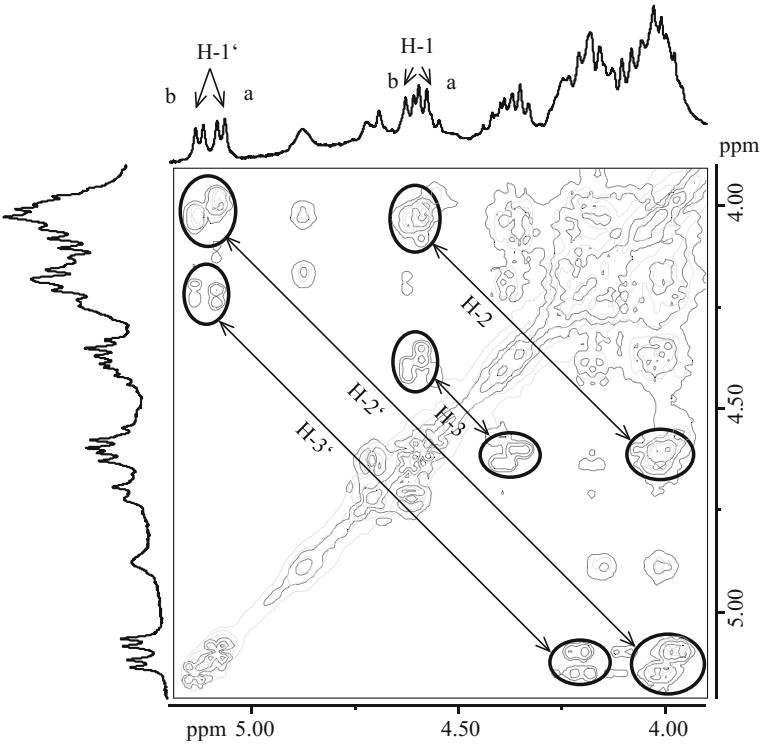


**Fig. 2.38** Overlay of 2D [$^1$H, $^1$H] TOCSY NMR spectra of phenylboronate sample **3** in DMSO-$d_6$ (mixing time: light gray 40 ms; black 12 ms, courtesy of M. Meiland, University of Jena, Germany)

The determination of the neighboring protons at C-5 and C-5′ can be managed by the combination of 2D NMR experiments mentioned above and 2D [$^1$H, $^1$H] ROESY NMR spectroscopy (rotating frame Overhauser effect spectroscopy) as additional proof. Thus, the only resonance signal for hydroxyl protons at 4.87 ppm can be identified as OH-6(**3a**) because of two cross-peaks in 2D [$^1$H, $^1$H] TOCSY spectrum (mixing time 40 ms) with H-6(**3a**).

In contrast, structure **3b** has no unmodified primary hydroxyl group. The esterification of this OH moiety can be supported by the two downfield shifted proton signals for H-6(**3b**) by about 0.5–0.6 ppm in comparison to the H-6(**3a**) for a structure with unmodified primary hydroxyl group in position 6. Therefore, it is concluded that in both compounds all secondary hydroxyl groups are esterified, meaning that besides one six-membered ring (OH-4′ and OH-6′) two seven-membered diphenylpyroboronate rings at the trans-1,2-diol systems of neighboring glucose units are present. The absence of a primary hydroxyl group for structure **3b** can only be explained by a dimerization of two molecules of **3a** via a PBA-bridge (Fig. 2.32). This assumption was confirmed by a DOSY NMR

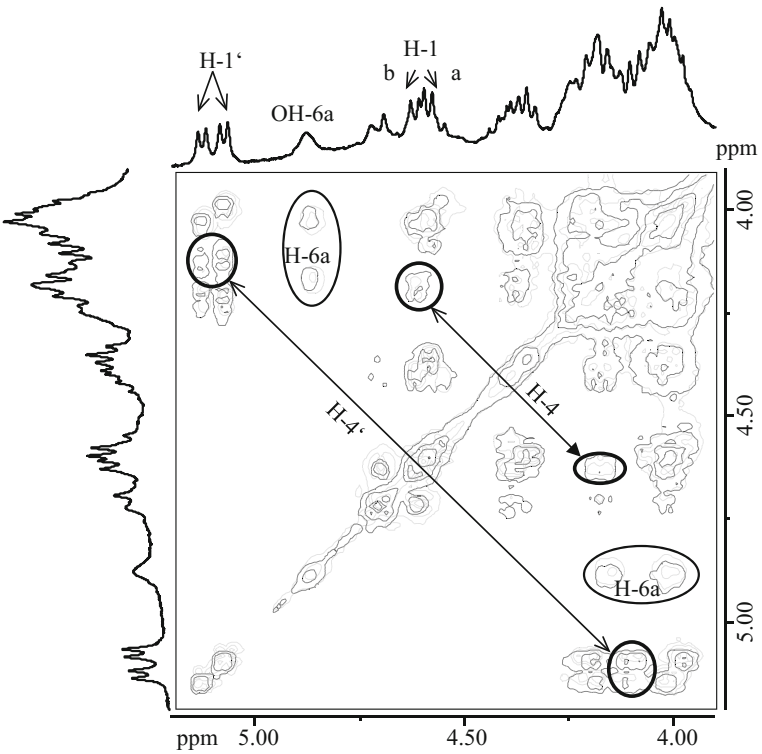


**Fig. 2.39** Overlay of 2D [$^{1}$H, $^{1}$H] TOCSY NMR spectra of phenylboronate sample **3** in DMSO-$d_6$ (mixing time: dark gray 90 ms; light gray 40 ms, cortesy M. Meiland, University of Jena, Germany)

experiment, because DOSY yields signals of individual components in a mixture, separated by diffusion in different rows of a 2D data matrix. The DOSY spectrum shows that the two compounds in the sample are slightly different in the gradient dimension F1. The difference in molecular weight of structure **3a/b** is rather small indicating that only dimerization occurs and cross-linking of several phenylboronates with PBA units to a polymeric structure can be excluded.

These extended NMR studies give a fairly complete picture of the structures that may appear. On the basis of the 2D NMR assignment, the trend of signal movement in $^{13}$C NMR spectra was established. Based on these results, esterification of cellodextrins and cellulose can be investigated by $^{13}$C NMR spectroscopy. Besides the formation of a 4,6-phenylboronate at the nonreducing glucose residue of the oligomer, functionalization at the trans-1,2-diol system with a six-membered boronate structure is confirmed by a sharp signal at 78.7 ppm in $^{13}$C NMR spectra (see Fig. 2.40).

Another interesting example of a 2D NMR experiment, which gives insight in cellulose–solvent interactions, is the application of $^{7}$Li/$^{1}$H NMR spectroscopy.

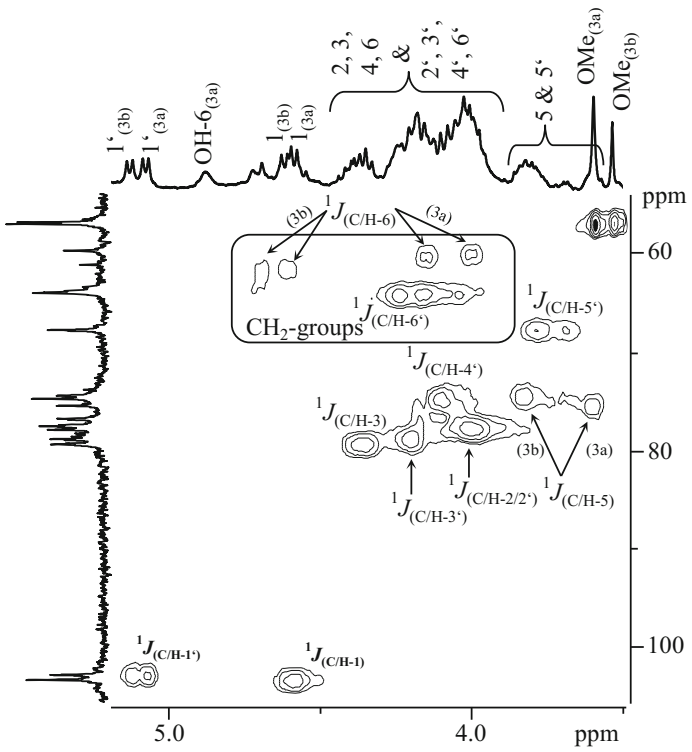


**Fig. 2.40** [$^{1}$H, $^{13}$C] HSQC-DEPT NMR spectrum of phenylboronate sample **3** consisting of Me-2,3(PhB)2-2′,3′(PhB)2-4′,6′(PhB)-β-D-cellobiose (**3a**) and the dimer **3b** in DMSO-$d_6$ (reprinted from [268], copyright (© 2010) with permission from Elsevier)

This revealed the interaction of the Li cations with the OH functions of the cellulose (Fig. 2.41) in salt melts such as LiCl*5 $H_2O$ [262]. More examples on the study of cellulose–solvent interactions are discussed in Sect. 3.2.1.

NMR spectroscopy of cellulose derivatives

NMR spectroscopy is one of the best methods in order to obtain comprehensive information about the molecular structure of a cellulose derivative. The analysis goes far beyond the simple evidence for obtaining a desired structure, as in case of low molecular weight chemistry. The chemical structure of the function introduced, the DS, the distribution of the functions on both the AGUs, and along the polymer backbone (Fig. 2.42) can influence the properties drastically and need to be determined comprehensively.

Additionally, the chemical functionalization may be connected with side reactions that cause slight modification of the polymer backbone structure. These “structural impurities” introduced have to be detected because they are not removable from the polymer chain. All of these tasks can be fulfilled by NMR

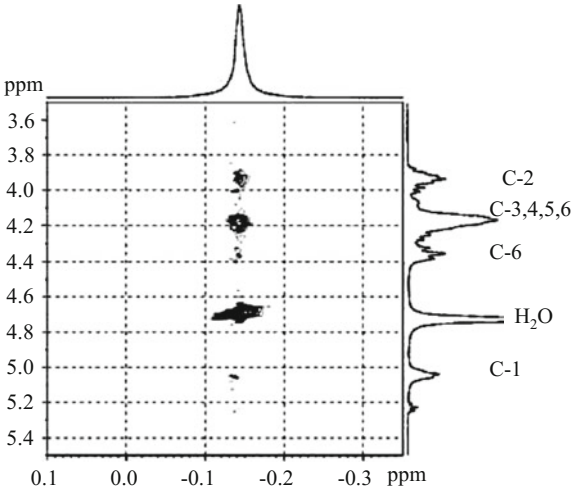


**Fig. 2.41** $^{7}$Li-$^{1}$H HOESY NMR spectrum of 5% cellulose dissolved in LiCl*5$H_2O$ (reproduced from [274] with permission of Springer)

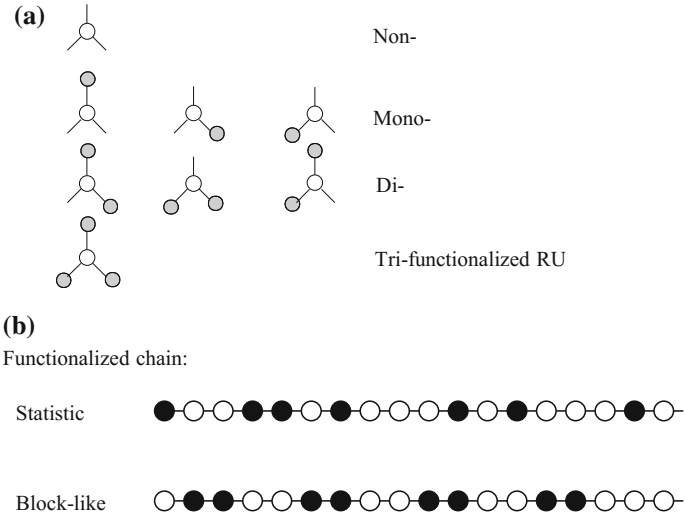


**Fig. 2.42** Schematic plot of the possible patterns of functionalization regarding the repeating units (**a**) and regarding the distribution along the polymer chain (**b**) of polysaccharides with three reactive sites (reprinted from [275, p. 143] with permission of Springer)

spectroscopy. Thus from the synthesis point of view, this technique is reliable, powerful, and efficient for detailed structure elucidation on the molecular level.

The application of NMR techniques was among the first attempts for the structure analysis of cellulose derivatives that exceeds the simple DS determination.

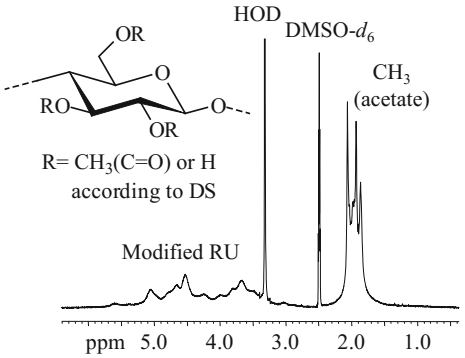


**Fig. 2.43** $^1$H NMR spectrum of a cellulose acetate (DS 2.37) (reprinted from [275, p. 153] with permission of Springer)

The pioneering works of both Goodlett et al. [276] using $^1$H NMR spectroscopy and Kamide and Okajima [277] applying $^{13}$C NMR measurements were done on cellulose acetates. General remarks concerning sample preparation and typical signals of the polymer backbones are given in Chapter "Practical aspects of liquid state NMR".

Although fast and useable for quantitative evaluation of structural features, $^1$H NMR spectroscopy on partially functionalized cellulose derivatives is limited because of the complexity of the spectra resulting from the un-, mono-, di-, and trisubstituted AGUs with different combinations of the functionalized sites as illustrated for partially acetylated cellulose (Fig. 2.43).

Consequently, solution state $^1$H NMR spectroscopy gives only limited information concerning obtaining the targeted derivative because most of the spectra are badly resolved and contain a large number of overlapping signals. Most complicated are spectra for partially functionalized derivatives where the variety of differently functionalized AGUs occurs with a specific substitution pattern; proper assignment is almost impossible.

Nevertheless, cellulose acetates were studied with phase-sensitive COSY and relayed COSY NMR spectroscopy. Comparing both of the spectra with simulated ones (nine different sub-spectra) and model compounds, e.g., cellotetrose peracetate, nine different types of spin networks were found. They are four types of 2,3,6-triacetyl glucose residues flanked by different acetyl glucose units, two different types of 2,3-diacetyl glucose residues, a 2,6-diacetyl glucose residue, and a 6-monoacetyl glucose residue [278].

Although solution state $^{13}$C NMR spectroscopy on cellulose ethers, deoxy cellulose, and different ionic cellulose derivative has been described, the technique has been most widely applied to cellulose esters [263]. In general, esterification or etherification of the primary OH group results in a down field shift ca. 2–8 ppm of the signal for the carbon atom of position 6. In contrast, the signal of a glycosidic C-atom in neighborhood to a carbon adjacent to an esterified or etherified OH moiety shifts upfield by 1–4 ppm. In case of deoxy units, the signals for the adjacent C atoms appear up to 15 ppm lower than the unmodified carbon atom. The signal splitting and the corresponding shifts of the other carbon atoms of the

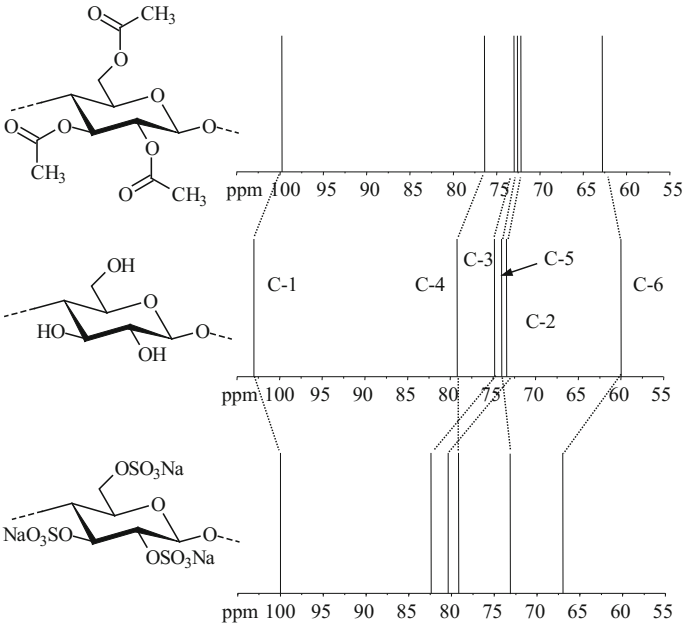


**Fig. 2.44** Schematic $^{13}C$ NMR spectra of cellulose (spectrum in the middle) and completely sulfated (lower picture) as well as fully acetylated cellulose (upper picture) and the characteristic shifts caused by the esterification (reprinted from [275, p. 150] with permission of Springer)

polysaccharide strongly depend on the electronic structure of the moiety bound. This is illustrated for cellulose sulfuric acid half ester and cellulose acetate in Fig. 2.44. A general assignment is not feasible. The specific assignment needs to be carried out with two-dimensional NMR techniques.

In spectra of partially functionalized derivatives, a blend of the sub-spectra is observed (Fig. 2.43). In combination with the line broadening caused by different patterns of substitution, the spectra obtained are very complex. Nevertheless, the signal splitting and the intensities of the carbon atoms of the glycosidic linkage give an insight in the amount of functionalization at the neighboring positions.

The structure elucidation can be nicely explained with cellulose acetates, however, the techniques can be applied for other cellulose derivatives in a similar manner. Table 2.11 shows representative $^{13}C$ NMR spectroscopic data of cellulose triacetate.

The assignment of the signals is based on the chemical shift of model compounds like peracetylated cellobiose, cellotetraose, and cellopentaose as well as cellulose [280–282]. $^{13}C$ NMR spectra of cellulose acetates are used not only as proof for the molecular structure but also for determination of both total DS and distribution of acetyl functions within the AGU concerning position 2, 3, and 6 in partially functionalized polymers [221, 283]. The exact distribution of substituents over a wide range of DS is not readily estimated by simple comparison of the relevant peak intensities. A major problem is the overlapping of signals at around 70–85 ppm

**Table 2.11** Chemical shifts of the $^{13}C$ NMR signals for cellulose triacetate

| 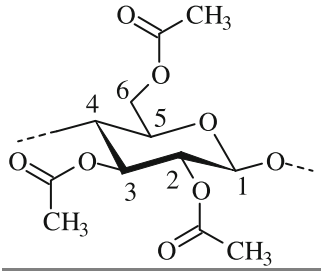 | $\delta$ (ppm)[a] | |
|---|---|---|
| | DMSO-$d_6$ 90 °C | $CDCl_3$ 25 °C |
| C-1 | 99.8 | 100.4 |
| C-2 | 72.2 | 71.7 |
| C-3 | 72.9 | 72.5 |
| C-4 | 76.4 | 76.0[b] |
| C-5 | 72.5 | 72.7 |
| C-6 | 62.8 | 61.9 |

Assignment according to [279], reprinted from [275, p. 151] with permission of Springer
[a]Relative to $CDCl_3$ at 77.0 ppm or DMSO-$d_6$ at 35.9 ppm
[b]The coupled resonance overlaps with the solvent resonance

resulting from the unmodified C-2–C-5 and the corresponding acylated position 2 and 3 as well as the influence of an acylated position 3 on the chemical shift of C-4. In addition, line broadening of the signals due to the ring carbons is frequently observed in the quantitative mode of $^{13}C$ NMR measurements. The fairly long pulse acquisition time and large number of scans applied causes $T_2$ relaxation of the relevant signals.

Several attempts were made to assign the signals of the C=O of the acetyl moieties [284]. Acetyl methyl and C=O signals appear as overlapped multi-peaks reflecting the detailed substitution pattern with regard to the eight different AGUs as well as the hydrogen-bond system of cellulose acetate with DS < 3. A reasonable assignment of the C=O signals of cellulose acetate is achieved by applying a low power selective decoupling method to the methyl carbon atoms of the acetyl groups [285] and can be carried out via C-H COSY spectra of cellulose triacetate [286]. An elegant analysis concerning the structure elucidation of cellulose acetates enriched with $^{13}C$ at position 1 prepared in different ways with a wide range of DS values is described by Buchanan et al. [287]. A total of 16 carbonyl carbon resonances can be identified using a variety of NMR techniques including Insensitive Nuclei Enhanced by Polarization Transfer spectroscopy.

The assignment of $^{13}C$ NMR spectra of cellulose ethers is shown for two important examples namely CMC and the hydroxyalkyl ethers. Spectra of partially substituted carboxymethyl ethers of cellulose are again very complex as can be seen in Fig. 2.45. Nevertheless, a fairly good assignment was achieved by comparison with model compounds, i.e., glucose and all types of carboxymethylated glucoses

(Fig. 2.45; Table 2.12) [288, 289]. In Table 2.12 the influence of the substitution at one of the reactive positions on the shifts of the carbons in the AGU and the carbons in the substituent is listed [290].

This assignment was obtained by a combination of 2D experiments such as TOCSY, and reverse detected $^{1}H$-$^{13}C$ hetero-correlated spectroscopy HMQC with gradient selection. From the gated decoupled $^{13}C$ spectrum (an experiment that allows integration of the $^{13}C$ NMR spectrum), it is then possible to determine the DS and the amount of etherification in each position.

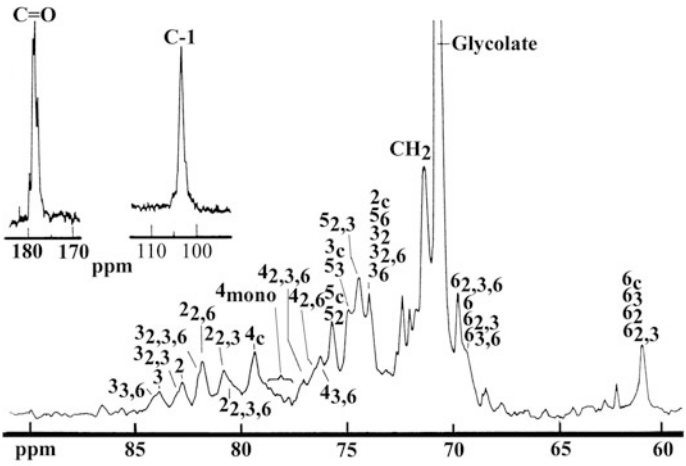


**Fig. 2.45** Detailed assignment of a $^{13}C$ NMR spectrum of a carboxymethyl cellulose (DS 1.5) in $D_2O$

**Table 2.12** $^{1}H$ and $^{13}C$ NMR shifts of sodium carboxymethyl cellulose

| C1, H1 | C2, H2 | C3, H3 | C4, H4 | C5, H5 | C6, H6,6′ | C7, H7,7′ |
|---|---|---|---|---|---|---|
| 105.3, 5.37 | 78.65, 4.53 | 76.78, 4.21 | 82.32, 4.48 | 77.95, 4.49 | 63.96, 4.64–4.80 | |
| | | | | 80.0, 4.63 | 72.75, 4.72–4.65 | 74.27, ≈4.78 |
| | | C3* | | | | |
| 105.8, 5.42 | ≈77.0, 4.60 | 85.85, 4.05 | 81.51, 4.57 | ≈77.5, 4.43 | | 75.06, 5.05–4.91 |
| | C2* | | | | | |
| 105.6, 5.40 | 87.29, 4.36 | ≈83.9, 4.26 | | | | 74.82, 5.10–5.05 |

Influence of the substitution on C* on the NMR peaks at different positions; the methylene carbon atoms of the substituent are labeled as 7; the carbonyl group, in the range from 180.0 to 181.5 ppm is not assigned

In case of hydroxyalkylated derivatives, especially hydroxyethyl and hydroxypropyl cellulose, the number of signals is even increased due to the occurrence of tandem reactions at the newly formed OH moiety of the substituent. Consequently, one can determine up to 64 repeating units in hydroxyalkylated cellulose. Nevertheless, DEPT-$^{13}$C NMR spectra are suitable to assign the basic structural elements as can be seen in Fig. 2.46.

As demonstrated, standard $^{13}$C NMR spectroscopy on cellulose derivatives yields information on the structure of the derivative, the purity and hints toward the substitution pattern. However, quantification of structural features such as the partial DS in the different positions is complicated. In principle, it can be done by inverse-gated decoupled measurements and line shape analysis, but this is time consuming. A more efficient approach is the subsequent functionalization of the ether, vide infra, or the degradation of the derivatives and $^{1}$H or $^{13}$C NMR spectroscopic investigation.

NMR spectroscopy on cellulose derivatives after subsequent functionalization

Complete subsequent functionalization of remaining OH moieties in partially functionalized cellulose derivatives results in a simplification of the $^{1}$H and $^{13}$C NMR spectra. Among the first experiments in this regard was the perpropionylation of the hydroxyl groups in cellulose acetates and $^{13}$C NMR spectroscopy of the mixed ester. The C=O carbons of the ester moieties are exploited as sensitive probe [291]. The range of C=O carbons in $^{13}$C NMR spectra of a perpropionylated cellulose acetate is shown in Fig. 2.47. The signals appear clearly resolved corresponding to position 2, 3, and 6 within the repeating unit. The triplet of the acetyl and the triplet of the propionyl moieties are distinctly separated from each other.

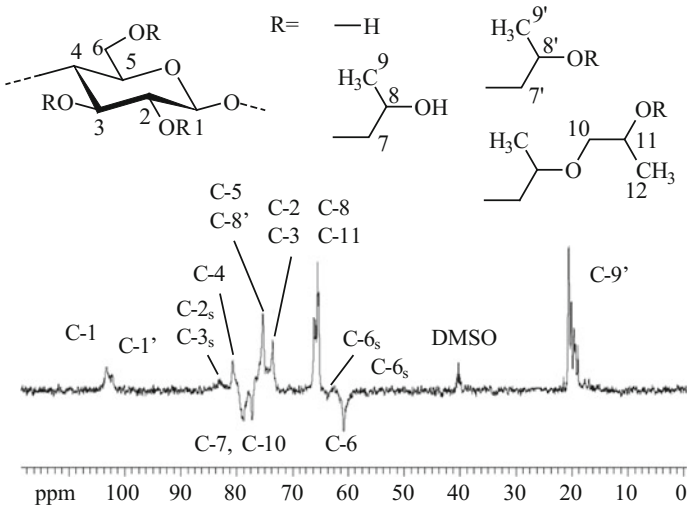


**Fig. 2.46** $^{13}$C DEPT 135 NMR spectrum of HPC (MS 0.85) in DMSO-$d_6$ at 70 °C

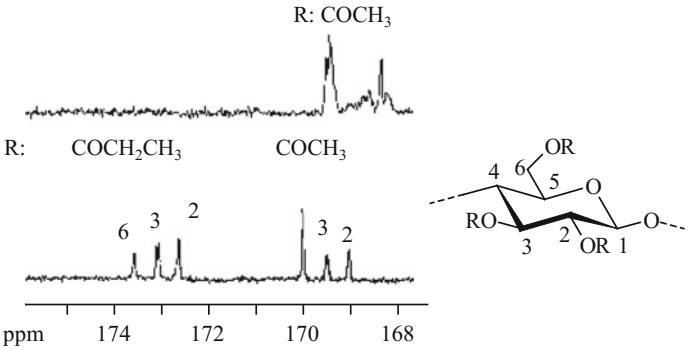


**Fig. 2.47** $^{13}$C NMR spectra of the carbonyl region of cellulose acetate (DS 1.43, top) and its perpropionylated product (bottom) (reprinted from [275, p. 156] with permission of Springer)

The expanded spectra of the C=O region of a perpropionylated cellulose acetate (DS 1.43) compared to the starting cellulose acetate reflect quite well the functionalization pattern.

Quantitative mode $^{13}$C NMR measurements of perpropionylated samples give the partial DS at position 2, 3, and 6. Typical $^{13}$C NMR spectra of perpropionylated cellulose acetate samples with DS ranging from 1.0 to 2.4 are shown in Fig. 2.48. The quantitative mode $^{13}$C NMR spectroscopy (inverse-gated decoupled experiments) is an expensive and time-consuming technique. Up to 20,000 scans and a relatively long pulse delay are necessary for sufficient resolution.

In contrast to $^{1}$H NMR spectra of partially substituted cellulose derivatives, completely substituted polymers yield assignable spectra as shown for cellulose triacetate in Fig. 2.49; Table 2.13.

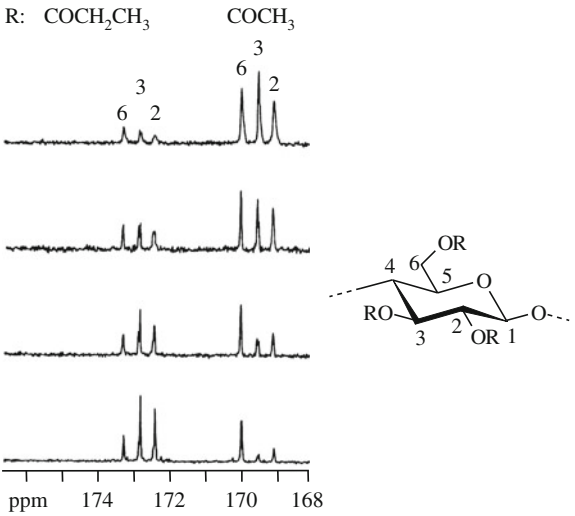


**Fig. 2.48** Typical $^{13}$C NMR spectra of perpropionylated cellulose acetate with DS 0.98, 1.43, 1.90, 2.42 (from bottom to top) (reprinted from [275, p. 157] with permission of Springer)

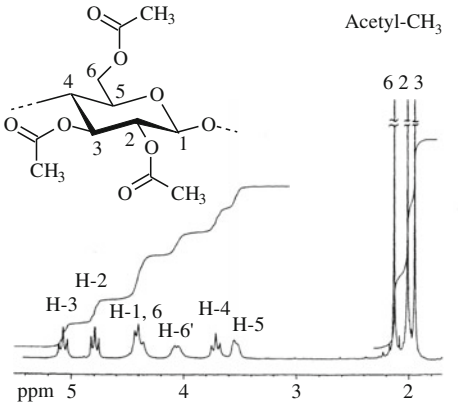


**Fig. 2.49** $^{1}$H NMR spectrum of a cellulose triacetate (reprinted from [275, p. 154] with permission of Springer)

**Table 2.13** Chemical shifts of $^{1}$H NMR signals for cellulose triacetate

| Signal | $\delta$ (ppm) of cellulose triacetate | | |
|---|---|---|---|
| | DMSO-$d_6$ 25 °C | DMSO-$d_6$ 80 °C | $CDCl_3$ 25 °C |
| H-1 | 4.65 | 4.65 | 4.42 |
| H-2 | 4.52 | 4.55 | 4.79 |
| H-3 | 5.06 | 5.04 | 5.07 |
| H-4 | 3.65 | 3.68 | 3.66 |
| H-5 | 3.81 | 3.77 | 3.47 |
| H-6′ | 4.22 | 4.26 | –[a] |
| H-6 | 3.98 | 4.04 | 4.06 |

Reprinted from [275, p. 154] with permission of Springer
[a]H-6′ results from the signal splitting due to the neighboring chiral C-5 and overlaps with H-1

Consequently, complete subsequent functionalization of partially functionalized cellulose derivatives is usually applied to obtain well-resolved $^{1}$H NMR spectra as well. This is an indispensable prerequisite for proper spectral resolution leading to NMR data for quantitative evaluation.

As shown in Fig. 2.50 for a deuteroacetylated cellulose acetate, the complete modification results in an enormous simplification of the spectra. $^{1}$H NMR spectroscopy after deuteroacetylation with acetyl-$d_3$-chloride or acetic anhydride-$d_6$ was, and still is a common technique [276, 292]. The disadvantage is the rather expensive deuteroacetylation, which is connected with a remarkable error if the acetyl-$d_3$-chloride is contaminated with acetyl chloride. Nevertheless, it is a useful technique to determine partial DS values at position 2, 3, and 6 in cellulose acetate, which can be readily calculated from the ratio of the spectral integrals of the protons of the AGU and the methyl protons of the acetyl moiety.

Alternatively, trimethylsilylation of cellulose esters with a wide range of DS values is carried out with *N,O*-bis(trimethylsilyl)acetamide and 1-methylimidazole

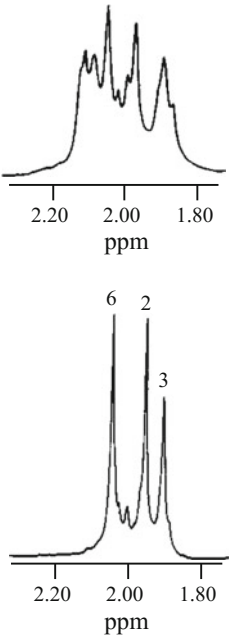


**Fig. 2.50** $^{1}$H NMR spectra (region of acetyl group) of a cellulose acetate before (top) and after (bottom) deuteroacetylation

**Table 2.14** Comparison of the DS for cellulose acetate obtained by silylation and NMR spectroscopy with values given by the suppliers

| Sample[a] | DS | | |
|---|---|---|---|
| | Reported | Method 1 | Method 2 |
| A | 0.80 | 0.81 | 0.76 |
| B | 2.10 | 1.97 | 2.05 |
| C | 2.50 | 2.28 | 2.50 |
| D | 3.00 | 2.77 | 3.00 |
| E | 2.45 | 1.86 | 2.43 |

The DS values were calculated from the integrals of the ring hydrogen and *O*-acetyl resonances (method 1) or from the integrals of the *O*-trimethylsilyl and *O*-acetyl resonances (method 2) in the $^{1}$H NMR spectra of the fully *O*-trimethylsilylated polymers (reprinted from [275, p. 158] with permission of Springer)

[a]Samples A–D are Eastman products, E is an Aldrich product

in DMF at room temperature. Analysis of the samples by IR spectroscopy shows complete absence of hydroxyl groups. As evident in Table 2.14, the DS values obtained by integration of the *O*-acetyl and *O*-trimethylsilyl resonances are in excellent agreement with values provided by the suppliers and vide infra, with those found by chemical analysis [293]. Nevertheless, partial DS values are not accessible.

Although perdeuteroacetylation and trimethylsilylation give good results concerning the functionalization of partially derivatized celluloses, perpropionylation is often the method of choice because it is less expensive and can be applied for a

broad variety of cellulose derivatives. Complete propionylation is achieved by reaction of the cellulose derivative, such as cellulose acetate or hydroxyalkyl cellulose [294] with propionic anhydride in pyridine using DMAP as catalyst. The complete conversion of the hydroxyl groups is confirmed by $^1$H NMR and IR spectroscopic studies (no signal for OH appears). In case of cellulose esters, ester exchange reactions can be excluded by constant total acyl content at different reaction conditions and by propionylation experiments with polysaccharide triesters. Standard $^1$H NMR spectra are usable for precise quantification, see below in "Practical aspects of liquid state NMR".

Perpropionylation is also helpful for analysis of aromatic and unsaturated cellulose derivatives with $^1$H NMR signals of the substituents in the region higher than 5.1 ppm. Cellulose furoates with additional peaks at 7.56, 7.20, and 6.50 ppm and the 3-(2-furyl)-acrylic acid esters with additional peaks at 7.82, 7.50, 6.87, 6.57, and 6.23 ppm and alicyclic esters of cellulose, e.g., the ester of the adamantane carboxylic acid were analyzed [295–297]. A representative $^1$H,$^1$H COSY NMR spectrum of a perpropionylated cellulose adamantane carboxylic acid ester is shown in Fig. 2.51. The signals for the protons of the two substituents are well resolved and can be used for the calculation of the DS.

As can be seen for these examples perpropionylation works very well but in case of cellulose derivatives with long aliphatic moieties (signals in range from 0.8 to 3.2 ppm), e.g., fatty acid esters, the $^1$H NMR spectra of the perpropionylated derivatives could not be assigned because of signal overlapping of the protons corresponding to the different moieties. Deuteroacetylation and alternatively per-4-nitrobenzoylation should be exploited. Nitrobenzoylation applying 4-nitrobenzoyl chloride in pyridine introduces signals in the aromatic region, at ca. 7.5–9.0 ppm in the $^1$H NMR spectra [298].

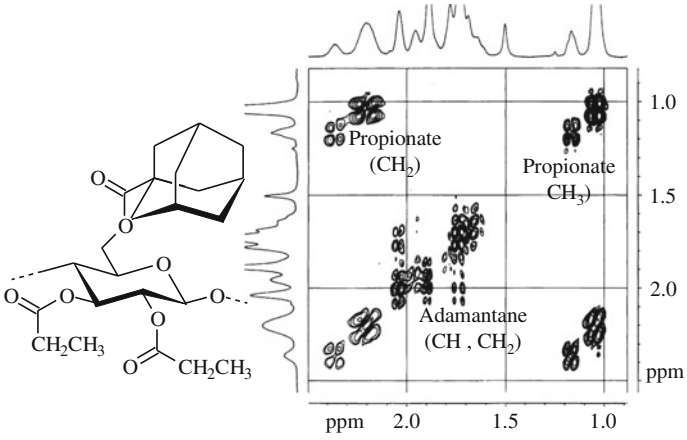


**Fig. 2.51** $^1$H,$^1$H COSY NMR spectrum of a perpropionylated cellulose adamantane carboxylic acid ester. The area of the protons of the substituents ($CH_3$, $CH_2$ of the propionate and $CH_2$ and CH of the adamantate) is displayed ($CDCl_3$, number of scans 32) (reprinted from [275, p. 161] with permission of Springer)

Propionylation and acetylation are suitable for the analysis of hydroxyalkyl ethers of cellulose such as hydroxyethyl cellulose as well. Due to the occurrence of tandem reactions (reaction on the newly formed OH group of the substituent) during the conversion of cellulose with epoxides, up to 64 differently functionalized repeating units in hydroxyalkylated celluloses are observed. Thus, even the NMR spectra of peracetylated hydroxyalkyl celluloses are very complex [294]. Nevertheless, basic assignment of the $^{1}$H NMR spectra of such mixed ester-ethers is possible by using regioselectively functionalized derivatives. In these fairly well-resolved spectra (Fig. 2.51), signals for all the relevant protons can be assigned by applying 2D NMR experiments such as HSQC-DEPT NMR spectroscopy as shown in Fig. 2.52.

Although the $^{1}$H NMR spectrum of peracetylated 2,3-*O*-hydroxyethyl cellulose can be completely understood, it is not resolved good enough to calculate partial DS values (see below). Nevertheless, calculation of the molar substitution (MS) can be carried out on the basis of the corresponding $^{1}$H NMR spectra (Fig. 2.53) by correlation of the integrals of signals for the AGU protons and the integrals of signals of the acetate moieties (see also Chapter "Practical aspects of liquid state NMR").

For ionic cellulose ethers such as CMC, subsequent peracylation is complicated because of the low reactivity of ionic cellulose derivatives, the solubility mostly limited to aqueous systems and a variety of side reactions during the esterification,

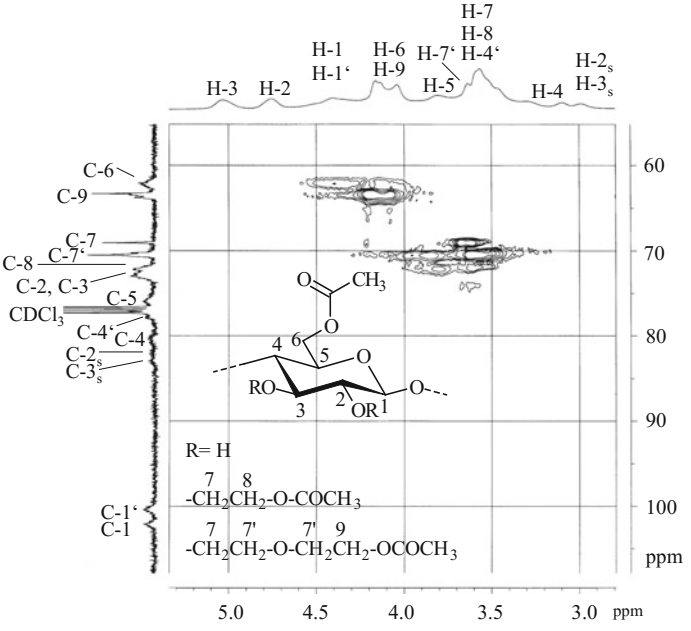


**Fig. 2.52** HSQC-DEPT NMR spectrum of peracetylated 2,3-*O*-hydroxyethyl cellulose (MS 1.13) in $CDCl_3$ at 40 °C, only $CH_2$ resonances are shown

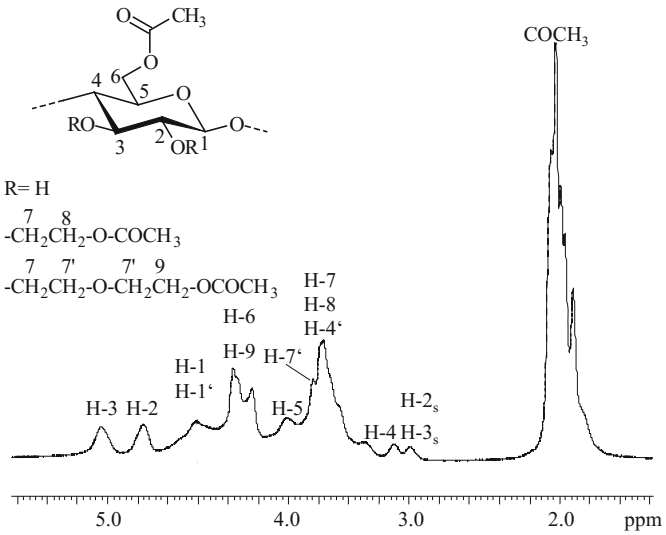


**Fig. 2.53** $^{1}$H NMR spectrum of peracetylated 2,3-*O*-hydroxyethyl cellulose (MS 1.13) in $CDCl_3$ at 40 °C

which result in an incomplete substitution, on one hand. On the other, analysis after depolymerization may be suitable due to the possibility to split the glycosidic bond without splitting the ether bond of the functional group (see below).

It should be mentioned that complete acetylation is also used to determine the structure of cell wall material in wood. 2D $^{13}$C-$^{1}$H HSQC NMR spectroscopy (see Fig. 2.54) of acetylated cell walls in solution gives a detailed fingerprint that can be used to assess the chemical composition of the complete wall without extensive degradation [299, 300].

Structure analysis by means of NMR spectroscopy after depolymerization

Another approach to increase the resolution of NMR spectra of partially functionalized cellulose derivatives is partial or complete depolymerization (degradation). Further advantage of this approach is that cellulose ethers give highly viscose solutions and the degradation decreases the viscosity. Consequently, higher concentrations can be employed, leading to better spectral resolution. Degradation is usually applied for cellulose ethers such as CMC because the side chains will not be split off during the hydrolysis, as occurring in case of cellulose esters. Therefore, the basic information concerning the substitution pattern is preserved. Complete degradation of partially functionalized CMC samples and comparison with model compounds were used for detailed assignment of NMR spectra (see above), but were also exploited for the determination of structural features of the derivatives [289]. Thus, $^{13}$C NMR studies on completely degraded samples fit perfectly with calculated spectra. On the basis of $^{13}$C NMR measurements, it was possible to

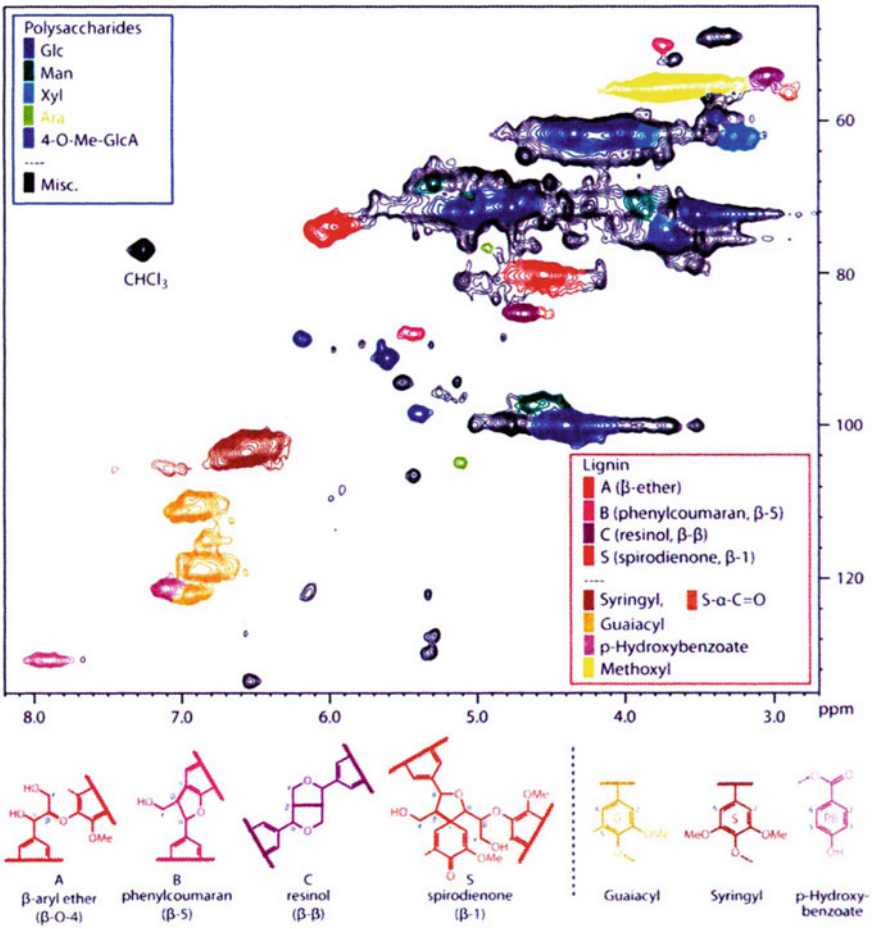


**Fig. 2.54** Typical 2D $^{13}C$-$^{1}H$ HSQC spectrum of dissolved acetylated cell wall from Populus. The polysaccharide abbreviations refer to the following residues in their respective polymers: *Glc* Glucosyl; *Man* Mannosyl; *Xyl* Xylosyl; *Ara* Arabinosyl; *4-O-Me-GlcA* 4-*O*-methyl glucuronic acid (reprinted from [299], copyright (© 2009), with permission from Elsevier)

determine the monomer composition (mole fractions of the differently substituted glucoses) of the original substitution pattern. This was done by statistical calculation of the monomer composition and comparison with the data obtained from the $^{13}C$ NMR spectra of the completely degraded polymer. The NMR data were also exploited to determine rate constants of the carboxymethylation in the different positions of the AGU. Consequently, NMR studies on degraded cellulose derivatives give a deep insight into the structures obtained during etherification especially carboxymethylation of cellulose but also the carboxymethylation process itself can be investigated in detail with such studies.

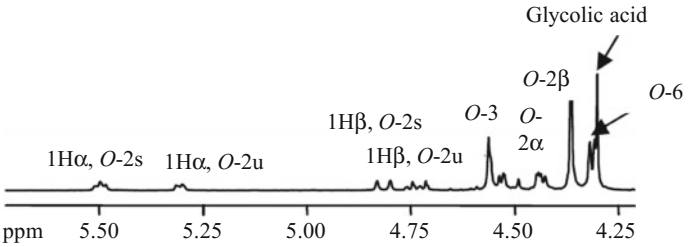


**Fig. 2.55** $^{1}$H NMR Spectrum of CMC after depolymerization in 25% $D_2SO_4/D_2O$

$^{1}$H NMR measurements can be applied in the same manner to obtain details of the partial degree of substitution. Usually partial degradation is sufficient. Both ultrasonic degradation and hydrolysis with sulfuric acid were used before investigation by means of $^{1}$H NMR spectroscopy. Well-resolved spectra are obtained (Fig. 2.55).

A comparison of the results for different methods of investigation is summarized in Table 2.15. The partial degrees of substitution determined by acid hydrolysis and by ultrasonic degradation are in good agreement. Therefore, both methods can be used for NMR spectroscopic investigations. The former, however, has the advantage that the polymer is not degraded down to the monomer and that the CMC can be investigated in the same form as used industrially. The polymer is not contaminated with monomers, since they cannot occur if cleavage occurs in the center of the main chain.

Other NMR techniques

A complex problem that is still not satisfactorily solved is the determination of the distribution of the functional groups along the polymer chain and the supramolecular structure of derivatized cellulose resulting from the functionalization pattern both in the AGU and along the chains. One possible approach is the application of NMR spectroscopy on samples with $^{13}$C-labeled acetyl groups [287]. In addition, formation of domains can be investigated, which may give information on the pattern of substitution [302, 303]. NMR spectroscopy after enzymatic treatments of the cellulose esters leads to information about the composition of the polymer with regard to the eight different AGUs [304].

In addition to the discussed $^{1}$H and $^{13}$C NMR techniques, there have been attempts to determine structural features of cellulose derivatives with NMR methods on other nuclei including $^{19}$F and $^{31}$P NMR spectroscopy for cellulose compounds where the remaining OH groups have been converted into trifluoroacetates [298] or phosphites [305]. Subsequent functionalization of partially substituted cellulose derivatives is carried out with 2-chloro-4,4,5,5-tetramethyl-1,3,2-dioxaphospholane. These phosphites can be quantitatively integrated against an internal standard, allowing for calculation of the DS of the functionalized cellulose starting material. The usefulness and accuracy of the method were investigated on a palmitoylated

**Table 2.15** A comparison of the results for different methods for the determination of the partial degrees of substitution determined by $^{13}C$ and $^{1}H$ NMR measurements after acid hydrolysis and by ultrasonic degradation

| | | Method | | | |
|---|---|---|---|---|---|
| Sample | | Titration[a] | $^{13}C$ NMR/HY[b] | $^{13}C$ NMR/US[b] | $^{1}H$ NMR/US/HY[b] |
| 1 | DS[c] | 0.77 | 0.79 | 0.89 | 0.86 |
| | $x_2$ | – | 0.38 | 0.49 | 0.35 |
| | $x_3$ | – | 0.12 | 0.09 | 0.19 |
| | $x_6$ | – | 0.29 | 0.31 | 0.32 |
| 2 | DS[c] | 0.96 | 0.93 | 0.94 | 0.99 |
| | $x_2$ | – | 0.43 | 0.46 | 0.43 |
| | $x_3$ | – | 0.19 | 0.17 | 0.22 |
| | $x_6$ | – | 0.31 | 0.31 | 0.34 |
| 3 | DS[c] | 1.19 | 1.25 | 1.30 | 1.31 |
| | $x_2$ | – | 0.59 | 0.56 | 0.56 |
| | $x_3$ | – | 0.22 | 0.30 | 0.31 |
| | $x_6$ | – | 0.43 | 0.44 | 0.44 |
| 4 | DS[c] | 1.67[a]/1.94[e] | 2.26 | 2.44 | 2.29 |
| | $x_2$ | – | 0.93 | 0.97 | 0.87 |
| | $x_3$ | – | 0.50 | 0.67 | 0.63 |
| | $x_6$ | – | 0.83 | 0.80 | 0.79 |
| 5 | DS[c] | 2.12[a]/2.30[e] | 3.00 | 2.96 | 2.96 |
| | $x_2$ | – | 1.00 | 0.92 | 1.00 |
| | $x_3$ | – | 1.00 | 1.02 | 0.92 |
| | $x_6$ | – | 1.00 | 1.02 | 1.05 |

Adapted from [301]
[a]Polyelectrolyte titration
[b]*HY* Acid hydrolysis; *US* Ultrasonic degradation
[c]*DS* Degree of substitution; 3 decimal places were taken into account in the summation operation to avoid errors based on rounding off
[d]*x* Partial degree of substitution
[e]ASTM titration

cellulose sample. The $^{31}P$ NMR spectrum of the subsequently functionalized cellulose palmitate is shown in Fig. 2.56.

Practical aspects of liquid state NMR

For $^{13}C$ NMR spectroscopy on cellulose or cellulose derivatives, solutions containing 8–10% (w/w) polymer should be used if the viscosity of the solutions permits this high concentration. In order to circumvent problems due to high viscosity, polymer degradation by means of acidic hydrolysis (Table 2.15) and ultrasonic degradation may be employed as pretreatment [301, 306]. The measurements should be carried out at elevated temperature usually in the range of

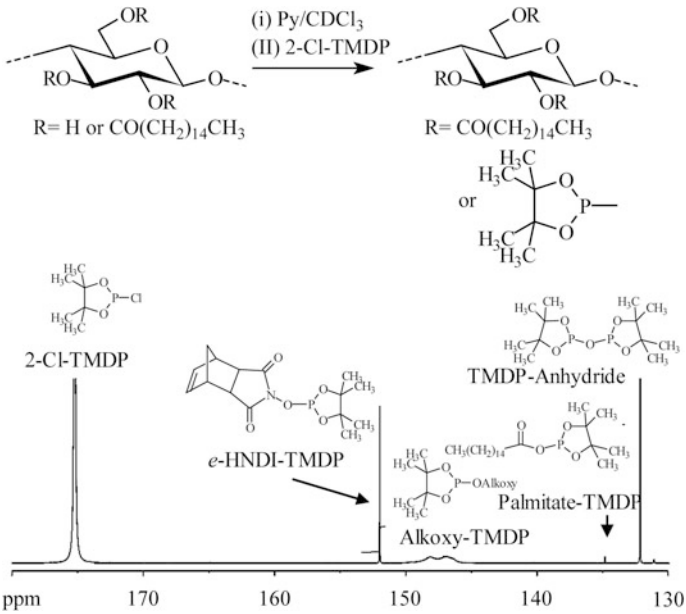


**Fig. 2.56** Derivatization mixture and $^{31}P$ NMR analysis of TMDP-phosphitylated palmitoyl cellulose (adapted from [305] with permission of The Royal Society of Chemistry)

60–80 °C depending on the solvent. In case of $^{1}H$ NMR, much lower amounts are needed. Usually, solutions with 1% are sufficient to obtain well-resolved spectra.

Although larger amounts of sample are needed compared to other methods, e.g., mass spectroscopy, NMR is non-destructive. Therefore, samples can be isolated from the solvent after the measurement and may be reused. With modern instruments, sufficient data may even be obtained with a sample amount of less than one milligram.

The solubility of the derivatives strongly depends on the DS and the type of polymer. Thus, a selection of NMR solvents used for the spectroscopy of cellulose derivatives is listed in Table 2.16. The preferred solvent for the investigation of partially substituted derivatives is DMSO-$d_6$, which dissolves the polymers within a wide range of DS values and is comparably inexpensive.

As discussed above, NMR in general and especially $^{13}C$ NMR measurements on unmodified cellulose derivatives (without subsequent functionalization or degradation) are used both for the qualitative structure determination and for quantification. Due to different relaxation times of various structural nuclei (different NOE), quantification is possible only for chemically equivalent subunits, or by using the inverse-gated-decoupling experiments. Thus, the investigation of cellulose acetate samples with DS of 1.7, 2.4, and 2.9 reveals that one and the same NOE for C-1–C-6 appears and thereby a valid basis for the quantitative assessment of partial DS values at position 2, 3, and 6 from the $^{13}C$ NMR spectrum is established. The

**Table 2.16** Selection of solvents used for NMR spectroscopic investigations

| Name | H shift (multiplicity) | H shift of water | C shift (multiplicity) | Boiling point (° C) |
|---|---|---|---|---|
| Acetone-$d_6$ | 2.04 (5) | 2.7 | 29.8 (7)<br>260.0 (1) | 57 |
| Acetonitrile-$d_3$ | 1.93 (5) | 2.1 | 1.3 (7)<br>118.2 (1) | 82 |
| $CDCl_3$ | 7.24 (1) | 1.5 | 77.0 (3) | 62 |
| $D_2O$ | 4.65 (1) | | | 101.4 |
| DMF-$d_7$ | 2.74 (5)<br>2.91 (5)<br>8.01 (1) | 3.4 | 30.1 (7)<br>35.2 (7)<br>162.7 (3) | 153 |
| DMSO-$d_6$ | 2.49 (5) | 3.4 | 39.5 (7) | 189 |
| $CD_2Cl_2$ | 5.32 (3) | 1.4 | 53.8 (5) | 40 |
| Py-$d_5$ | 7.19 (1)<br>7.55 (1)<br>8.71 (1) | 4.9 | 123.5 (5)<br>135.5 (3)<br>149.9 (3) | 116 |
| THF-$d_8$ | 1.73 (1)<br>3.58 (1) | 2.4 | 25.3 (1)<br>67.4 (5) | 66 |
| Toluene-$d_8$ | 2.09 (5)<br>6.98 (m)<br>7.00 (1)<br>7.09 (m) | – | 20.4 (7)<br>125.2 (3)<br>128.0 (3)<br>128.9 (3)<br>137.5 (1) | 111 |
| TFA-$d_1$ | 11.5 (1) | – | 116.6 (4)<br>164.2 (4) | 72 |

signals at 59.0 ppm (C-6 unsubstituted), 62.0 ppm (C-6 substituted), 79.6 ppm (C-4, no substitution at C-3), 75.4 ppm (C-4 adjacent to position 3), 101.9 ppm (C-1, no substitution at C-2), and 98.9 ppm (C-1 adjacent to position 2) are used for the calculation [221, 283].

More suitable for quantification are measurements after peresterification. The determination of both the DS and partial DS can be achieved with the signals of the subsequently introduced ester moiety both in $^1H$ and $^{13}C$ NMR spectra making the method very reliable. This is shown exemplarily for a commercial cellulose diacetate. Complete derivatization of the OH groups is carried out by treatment with excess of propionic anhydride in pyridine for 16 h at 70 °C. Completeness of the reaction is confirmed by the disappearance of the OH band in the FTIR spectra (apply KBr technique for sensitivity reasons). The mixed ester obtained is well soluble in $CDCl_3$ and the standard $^1H$ NMR spectrum (Fig. 2.57) shows the peaks for propionate functions at 1.03–1.07 ppm ($CH_3$ position 2 and 3), 1.21 ppm ($CH_3$ position 6), and at 2.21–2.37 ppm for the $CH_2$ moiety. Three separate peaks can be observed for $CH_3$ groups of acetyl moieties at 1.92 ppm (position 3), at 1.97 ppm (position 2), and 2.08 ppm (position 6). The signals for protons of the AGU are found in the range from 3.51 to 5.05 ppm. This conforms with results for

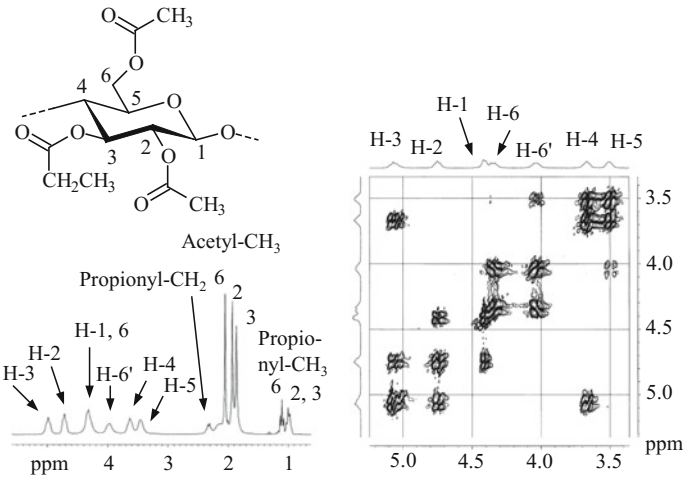


**Fig. 2.57** $^{1}$H NMR spectrum (left) and $^{1}$H,$^{1}$H COSY NMR spectrum (right, the area of the protons of the AGU is displayed) of cellulose acetate propionate prepared by complete propionylation of a commercial cellulose diacetate ($CDCl_3$, number of scans 32) (reprinted from [275, p. 159] with permission of Springer)

regioselectively functionalized cellulose esters where full assignment of NMR signals is carried out by high-sensitivity HMBC technique together with the conventional 2D NMR techniques [307].

The AGU signals can be completely assigned showing only one peak per proton (5.00, H-3, 4.73, H-2, 4.33, H-1,6, 3.99, H-6′, 3.64, H-4, 3.48 ppm, H-5), i.e., the existence of acetyl and propionyl moieties in the molecule does not induce a signal splitting of these protons. A $^{1}$H,$^{1}$H COSY NMR spectrum of this region is displayed in Fig. 2.57 confirming the assignment. Consequently, the spectral integrals of the protons of the AGU and the methyl protons of the propionyl moiety can be applied to calculate both the partial and the overall DS values of the acetate applying Eqs. 2.24 and 2.25.

$$\mathrm{DS_{Acyl}} = 3 - \frac{7 \cdot I_{\mathrm{H,Propionyl}}}{3 \cdot \mathrm{H_{H,AGU}}} \tag{2.24}$$

$$\mathrm{DS_{Acyl}}(n) = 1 - \frac{7 \cdot I_{\mathrm{H,Propionyl}}(n)}{3 \cdot I_{\mathrm{H,AGU}}} \tag{2.25}$$

$I$ = Integral

$n$ = Position 2, 3, or 6

Propionylation experiments of cellulose diacetate at temperatures between 60 and 120 °C show no significant changes in the DS and the distribution of the substituents. The results summarized in Table 2.17 confirm the accuracy of the method and yield a standard deviation of $s^2 = 1.32 \times 10^{-4}$. It has to be mentioned

**Table 2.17** DS values calculated from $^1$H NMR spectra of perpropionylated cellulose diacetate

| DS series 1 | DS series 2 |
|---|---|
| 2.35 | 2.37 |
| 2.35 | 2.37 |
| 2.32 | 2.38 |
| 2.32 | 2.38 |

The cellulose diacetate is propionylated twice (series 1 and series 2) and measured four times by $^1$H NMR spectroscopy (reprinted from [275, p. 160] with permission of Springer)

**Table 2.18** DS values of cellulose acetate with a broad variety of functionalization determined via $^1$H NMR spectroscopy after perpropionylation

| No. | Molar ratio | | | $DS_{Acetyl}$ at position | | | $DS_{Propionyl}$ | Over all DS |
|---|---|---|---|---|---|---|---|---|
| | AGU | Acetyl chloride | Base | 6 | 2, 3 | Σ | | |
| A1 | 1 | 1.0 | 1.2 | 0.35 | 0.13 | 0.48 | 2.49 | 2.97 |
| A2 | 1 | 2.0 | 2.4 | 0.82 | 0.51 | 1.33 | 1.66 | 2.99 |
| A3 | 1 | 3.0 | 3.6 | 0.91 | 0.65 | 1.56 | 1.41 | 2.97 |
| A4 | 1 | 4.5 | 4.5 | 1.0 | 1.24 | 2.24 | 0.77 | 3.01 |
| A5 | 1 | 5.0 | 6.0 | 1.0 | 1.62 | 2.62 | 0.37 | 2.99 |

Reprinted from [275, p. 160] with permission of Springer

that a prerequisite to this reliability of the method is complete removal of all impurities, i.e., drying at 60 °C under reduced pressure. If water or free acetic acid is present a much higher deviation is observed.

The $DS_{Acetyl}$ and $DS_{Propionyl}$ and the overall DS, which are obtained from $^1$H NMR spectra, are summarized in Table 2.18. Overall DS values in the range 2.97–3.01 are found, which is in the frame of the standard deviation of the method. Analysis of the partial $DS_{Acetyl}$ is possible by evaluation of the propionate signal intensities as described above or from the three separate signals for $CH_3$ groups of the acetyl moieties at 1.92 ppm (position 3), at 1.97 ppm (position 2) and 2.08 ppm (position 6).

As an alternative to the peracetylation, nitrobenzoylation can be used. This technique is suitable for derivatives in which perpropionylation would lead to signal overlap in the NMR spectra. Reactions of cellulose diacetate exploited as a model with 4-nitrobenzoyl chloride in DMF for 24 h at 60 °C confirm complete functionalization of the free OH groups. The product is well soluble in $CDCl_3$. A standard $^1$H NMR spectrum is shown in Fig. 2.58. Three separate peaks can be observed for the $CH_3$ group of the acetyl function at 1.88 ppm (position 3), at 2.02 ppm (position 2), and 2.14 ppm (position 6). The signals for protons of the AGU between 3.46 and 5.09 ppm are equally well resolved as in case of perpropionylated samples. No signal splitting of the AGU protons is induced by the

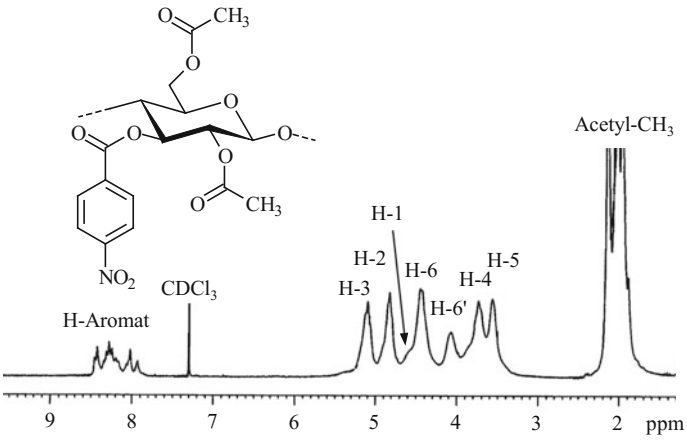


**Fig. 2.58** $^{1}$H NMR spectrum of a per-4-nitrobenzoylated cellulose acetate ($CDCl_3$, number of scans 32) (reprinted from [275, p. 162] with permission of Springer)

existence of acetyl and 4-nitrobenzoyl moieties in the polymer. The $DS_{Acetyl}$ can be determined from the ratio of the spectral integrals of the AGU protons and the methyl protons of the acetyl moiety. This approach is useful, e.g., for the DS determination of long-chain functions via the spectral integrals of the aromatic protons of the of 4-nitrobenzoyl moieties. The content of acylation is calculated according to $DS_{Acyl} = 3 - DS_{Nitrobenzoyl}$.

Peracetylation or perpropionylation is frequently applied for the structure determination of hydroxyalkylethers of cellulose as discussed above. The subsequent functionalization is also carried out with the corresponding anhydride in pyridine. In derivatives with a more random derivatization the MS can be calculated. This approach works for statistically modified HEC. The calculation is carried out by the Eq. 2.26:

$$MS_{HE} = \frac{1}{4} \cdot \frac{9 \int a}{\int b - 7} \tag{2.26}$$

$a$ = signals of AGU protons (5.1–2.9 ppm)

$b$ = signals of acetate ester groups (2.1–1.9 ppm).

Basically, the same technique can be applied for the determination of the MS in case of HPC. After complete acetylation of HPC, which is evidenced by the absence of the OH vibration at 3450 $cm^{-1}$ and the characteristic signal of the C=O vibration of the acetate group at 1740 $cm^{-1}$ in the corresponding IR spectrum, the $^{1}$H NMR spectrum allows calculation of the MS using one of Eqs. 2.27 and 2.28:

$$\mathrm{MS_{HP}} = \frac{1}{3} \cdot \frac{9 \int a}{\int b - 7} \tag{2.27}$$

$$\mathrm{MS_{HP}} = 3 \cdot \frac{\int c}{\int b} \tag{2.28}$$

$a$ = signals in the range from 5.1 to 2.9 ppm
$b$ = signals of the acetate groups (2.1–1.8 ppm)
$c$ = signals of the hydroxypropyl substituents (1.3–0.9 ppm) from the $^1$H NMR spectra of the peracetylated samples.

Due to the rather low spectral resolution of these peracylated hydroxyalkyl celluloses, determination of the partial DS values is usually not possible. In contrast, NMR spectroscopy can be used for the determination of the partial DS values in case of carboxymethylated celluloses. A prerequisite is degradation of the polysaccharide. For this purpose, the CMC samples were hydrolyzed in a mixture of 25% (v/v) $D_2SO_4/D_2O$ (50 mg/mL) 5 h at 90 °C. The partial $\mathrm{DS_{CM}}$ ($x_\mathrm{i}$) values are determined according to Eqs. 2.29–2.31:

$$x_\mathrm{i} = \frac{\frac{1}{2}\mathrm{A(CH_2(O-i)}}{\begin{aligned}&\mathrm{A(H-1\alpha,\ O-2s)+A(H-1\alpha,\ O-2u)}\\ +\ &\mathrm{A(H-1\beta,\ O-2s)+A(H-2\beta, O-2u)}\end{aligned}} \tag{2.29}$$

$$\mathrm{DS} = \sum_\mathrm{i} x_\mathrm{i} \tag{2.30}$$

$$x_\mathrm{i} = \frac{\mathrm{A(H-1\alpha,\ O-2s)+A(H-1\beta,\ O-2)}}{\begin{aligned}&\mathrm{A(H-1\alpha,\ O-2s)+A(H-1\alpha,\ O-2u)}\\ +\ &\mathrm{A(H-1\beta,\ O-2s)+A(H-2\beta,\ O-2u)}\end{aligned}} \tag{2.31}$$

A are the integral areas in the corresponding NMR spectra.

### 2.3.4 Chromatographic Analysis

As already discussed for SEC measurements (Sect. 2.2.2), modern chromatographic analyses use columns of different shape and filling to separate the compounds from a mixture and thereby determine with the aid of a detector system the presence and concentration of a substance in the mixture. SEC measurements exploit a gel-like porous packing in the column to separate molecules according to the molecular weight. On the contrary, Gas Chromatography (GC) or GLC and High-Performance Liquid Chromatography (HPLC), the methods most widely applied for structure analysis of polysaccharide derivatives, use specific physical and chemical

interactions of an analyte in a complex mixture with the column wall or the packing in the column to separate according to the chemical nature of molecules. In any case, subsequent treatment of the polysaccharide derivatives is necessary prior the chromatographic measurements are carried out. This may include complete degradation or a subsequent derivatization to preserve a functionalization pattern combined with degradation of the polymer and sometimes a second derivatization to make the glucose derivatives suitable for the method of choice. This is one of the major drawbacks of chromatographic approaches because one has to guarantee that all the steps occur quantitatively and that the recovery yield is 100%, which is hard to achieve.

For GC studies, the analyte has to be vaporized without degradation. It is then transported with an inert carrier gas (usually nitrogen or helium) through a long narrow capillary-like column that could be 10–200 m long. For more details on the basics of GC, see [308]. This column is made of metal or more commonly of quartz and can have a coating on the inside, e.g., a polyorganosiloxane layer, which is called the stationary phase. The whole column sits in an oven to be kept at a specified temperature during the measurement. The molecules are separated according to their mobility and the interactions with the stationary phase as they are transported through the column. For the determination of the separated compounds at the end of the column, a large number of detectors were developed which are as follows:

- Flame photometric detector (FPD),
- Infrared detector (IRD),
- Discharge ionization detector (DID),
- Photoionization detector (PID),
- Pulsed discharge ionization detector (PDD),
- Thermionic ionization detector (TID), and
- Mass spectrometer (MS).

The combination with MS, designated as GC–MS, is applied frequently for the analysis of cellulose derivatives as will be discussed in this chapter. To fulfill the prerequisite of a vaporizable analyte, a variety of subsequent functionalization steps were developed, e.g., silylation, acetylation, or methylation of the derivatives or more precisely the degraded derivatives.

HPLC is a highly effective and sensitive technique, even when only very small amount of sample is available. In case of HPLC, one employs columns packed with small sorbent particles (stationary phase). The particle size is in the range of about 5 μm. A dense packing provides better separation on columns of short length but it is also the reason for the required high pressure (historically, HPLC has been called high pressure liquid chromatography). Pressure may be as high as 40 MPa. In "Ultra-High Performance Liquid Chromatography" systems, pressure of up to 100 MPa is possible. Common mobile phases (eluent) include aqueous solutions or any miscible combination of water with various organic solvents, e.g., acetonitrile or methanol, which carry the analyte through the column. For detection, one may

use differences in the refraction index (between solute and solvent; RI detector), the UV absorbance (UV detector), the chirality (chiral detector), or also a combination with mass spectroscopy (HPLC-MS). The right combination of packing material, eluent and detection system for the separation of degradation products of cellulose derivatives is always the result of extensive optimization of a skilled analyst and it is hard to give general guidelines for such a setup. It has to be mentioned that retention times, i.e., the time a molecule needs to move from the injection to the detector, can only be compared for measurements with the same setup. A number of good reference books have been published on the basics and practical applications of HPLC [309–312].

Due to their relevance for the analysis of cellulose derivatives two closely related specific methods have to be mentioned; high-pH anion-exchange chromatography with pulsed detection (HPAEC/PAD) and capillary electrophoresis (CE). HPAEC/PAD is a common technique in carbohydrate analysis because at the applied pH values (12–13, NaOH solutions as eluent), the carbohydrate molecules can undergo deprotonation and thereby very specific interactions occur with the stationary phase leading to a good separation. The carbohydrates are easily oxidized in this state which is exploited for the detection, i.e., no additional labeling of the carbohydrates is necessary.

In CE, a capillary system is employed for the separation in combination with two electrodes at the end and a high-voltage power supply. It can be used to separate ionic species by their charge, frictional forces, and hydrodynamic radius. In case of neutral carbohydrates, an efficient approach for the introduction of the necessary charge is the conversion of the samples into the corresponding borates usually by applying a borate buffer. Additionally, a chromophore or a fluorophore is introduced for detection. This can be done by reductive amination as shown in Fig. 2.59.

#### 2.3.4.1 HPLC Analysis of Cellulose After Degradation

HPLC is a fast and reliable method for the determination of the purity of a cellulose sample. To apply HPLC to cellulose, a controlled depolymerization is necessary. A simple procedure is the degradation of the polysaccharide with sulfuric acid or perchloric acid (70% w/w, see experimental section) and separation of the sugars by means of HPLC (cationic exchange resin, e.g., BioRad Aminex HPX or Rezex ROA columns) using dilute sulfuric acid as eluent at elevated temperatures (65–80 °C). A summary of the retention time of different sugars commonly found in cellulose pulps is given in Table 2.19 for this analytical system. In most cases, the application of a RI detector is sufficient. The response factors of the sugars should be known or need to be determined. Alternatively, pulsed amperometric detection or UV detection can be used. If UV detection is applied, derivatization of the sugars is recommended (see above).

Thus, the hydrolysis in combination with HPLC is well suited for the determination and quantification of structural features and impurities, e.g., the presence of hemicelluloses in spruce sulfite pulp as shown in Fig. 2.60.

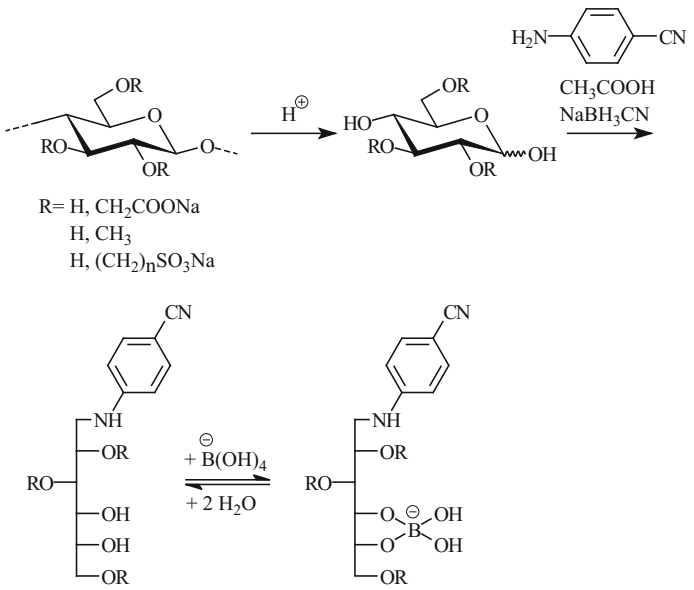


**Fig. 2.59** Principle work up strategy for the capillary electrophoresis (CE) analysis of a cellulose ether (in this example a carboxymethyl, methyl or sulfoalkyl ether) including depolymerization, reductive amination (labeling) and conversion into a charged borate (according to [313])

**Table 2.19** Summary of retention times found by HPLC for different sugars and uronic acids commonly found in polysaccharides with a combination of a BioRad Aminex HPX and a Rezex ROA column using 0.005 M sulfuric acid as eluent at 65 °C

| Sugar | Retention time (min) |
|---|---|
| Arabinose | 25.2–25.3 |
| Fructose | 23.5 |
| Glucose | 21.8–22.0 |
| Glucuronic acid | 19.5–19.7 |
| Mannose | 23.1–23.3 |
| Rhamnose | 24.6–24.7 |
| Ribose | 26.0–26.2 |
| Xylose | 23.3–23.5 |

### 2.3.4.2 Analysis of Cellulose Derivatives After Degradation

A very useful tool for structure analysis of cellulose derivatives is the complete or partial degradation of the polymer and subsequent analysis of the fragments obtained by chromatography [313]. Aqueous acid hydrolysis, methanolysis, and reductive depolymerization with Lewis acids and triethylsilane according to Gray

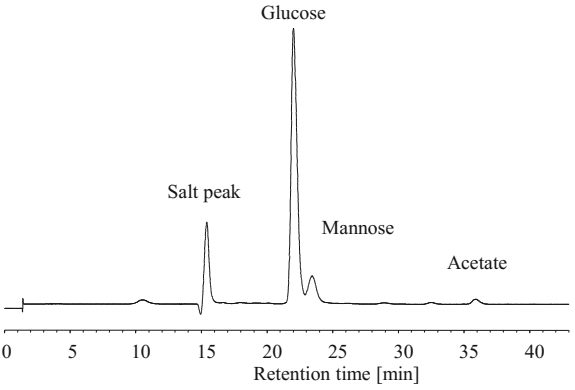


**Fig. 2.60** HPLC-elugramm of hydrolyzed spruce sulfite pulp showing the presence of mannose from hemicelluloses

are commonly applied for the degradation [314]. Without additional derivatization of the cellulose derivative, this technique can only be applied for cellulose ethers. The reason is that other derivatives such as esters will be hydrolyzed both in the main chain and at the side groups meaning that the structural information is lost. In contrast, during the gentle and complete depolymerization, the ether substituents remain at the glucose units and preserve the substitution pattern, at least at the level of the repeating unit.

Most commonly, the obtained mixture of differently substituted glucoses is reduced into the corresponding alditols (Fig. 2.61), which leads to a better resolution during the analysis. In addition, subsequent acetylation or trimethylsilylation make them suitable for GC measurements. This additional step is not necessary in case of HPLC analysis but this technique does not give a complete resolution of all substitution patterns as is possible with GC (Fig. 2.62). Following this route, MC with DS 1.7 was investigated by means of GC–MS after complete degradation with trifluoroacetic acid [315]. The partially methylated monosaccharides obtained by complete hydrolysis were converted into alditols by reduction. They were identified as their acetates and trimethylsilyl ethers by GC–MS and quantified by GC analysis (see Fig. 2.62). The main glucose methyl ethers obtained were in decreasing order 2,6-, 2,3,6-, 2-, 6-, and 2,3-. The 2- and 6-positions were occupied by methyl groups in 70.0 and 61.5%, respectively, while the 3-position contained only 37.4%. The GC–MS method gave a more accurate determination of the distribution of methyl groups in methylcellulose compared to NMR spectroscopy. It should be mentioned that a comparable method was established using HPLC and extending this path on the permethylation of esters or silylated cellulosics and analysis of the resulting pattern of distribution of methyl ether groups [316–318].

A rapid method has been developed for CMC analysis using hydrolysis with perchloric acid and analysis of the mixture of carboxymethylated glucose residues and glucose by HPAEC/PAD. The peaks of the chromatogram were identified by combined GC–MS measurements after pertrimethylsilylation. Molar response factors for each of the constituent monomers were established by $^{1}$H NMR

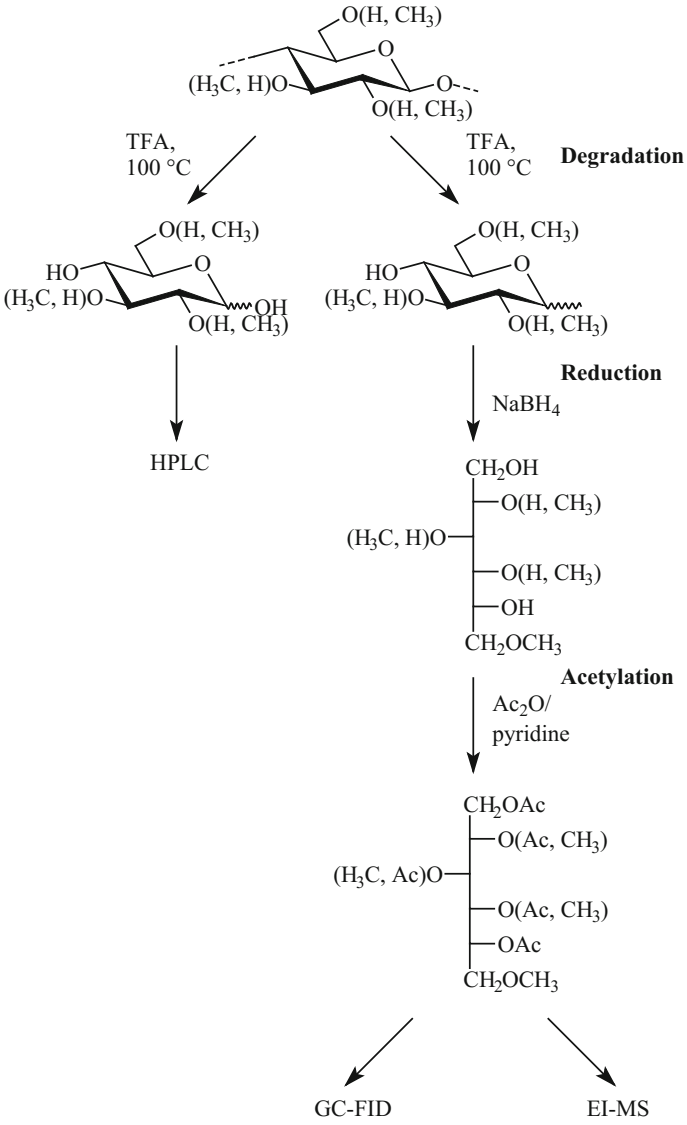


**Fig. 2.61** Two paths for the chromatographic analysis of methyl cellulose after degradation and subsequent modification (substituents in brackets indicate possible derivatization at these positions)

spectroscopy. The DS for three CMC were determined by the proposed method and by a standard titration procedure; the results of both were in excellent agreement [319]. This technique is also well suitable for the characterization of sulfoethyl cellulose [320].

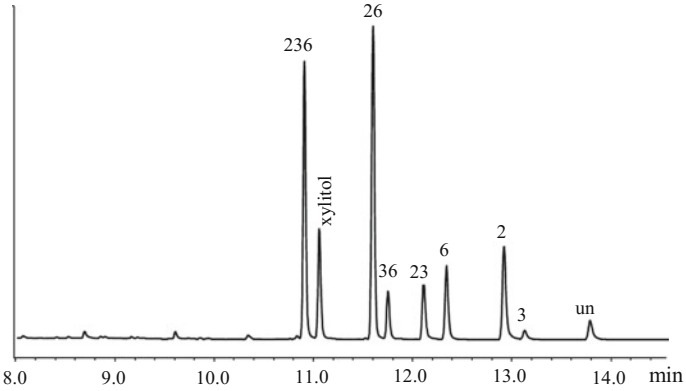


**Fig. 2.62** Result of a GC (FID) measurement of a methyl cellulose after hydrolysis, reduction and acetylation, (xylitol is the standard) (the numbers refer to the substitution pattern, i.e., the place of the substituent at AGU, un is unsubstituted glucose)

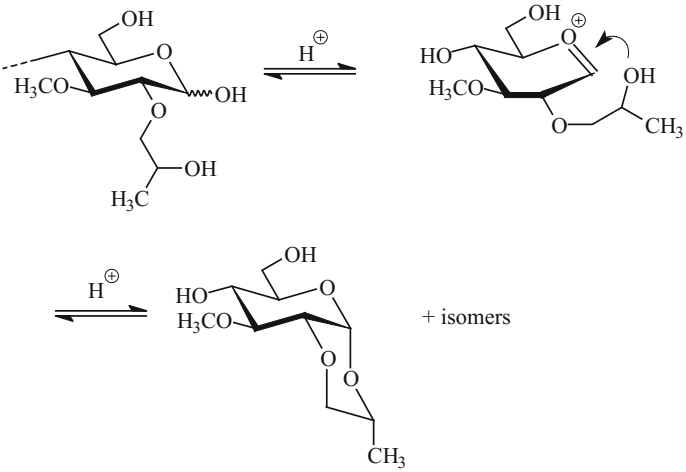


**Fig. 2.63** Possible intramolecular side reaction of 2-*O*-hydroxyalkyl cellulose during aqueous hydrolysis [321]

Hydroxyalkyl celluloses can be analyzed after degradation by means of GC and FAB-MS. In case of such cellulose ethers, utilization of aqueous hydrolysis is limited by the hydrophobicity of substituents, causing a severe underrating of more highly substituted glucose residues, and by intramolecular reactions of reactive groups in appropriate positions of the AGU leading to, e.g., the formation of six-membered rings. Examples for the latter are 2-(2-hydroxy)alkyl (Fig. 2.63) or 2-allyl ethers, forming intramolecular acetals and addition products, or derivatives

with strongly nucleophilic functions at C-6, such as 6-amino-6-deoxy derivatives, which are even more prone to 1,6-anhydroglucose formation than glucose itself.

In such cases, methanolysis with HCl/dry methanol is preferred, as this inhibits most of the intramolecular side reactions mentioned and enables better dissolution and accessibility of less polar samples [321]. The methyl glucosides obtained are less sensitive to side reactions, but cannot be further reduced to alditols or labeled by reaction of their carbonyl function.

Results of the discussed analytical approaches, giving information on the distribution of substituents on the basis of the AGU, can be compared with statistic calculations and yield information about the distribution of the ether groups along the chain [322]. Investigation of the distribution of CM groups along the chain for a number of carboxymethylated polysaccharides after depolymerization with perchloric acid and separation of the repeating units was carried out by means of HPLC measurements [323–325].

A highly specific interaction of the polymer used for analytical purposes is the enzymatic degradation of cellulose ethers with cellulases. In earlier studies, the degradation was followed by viscosity and reducing sugar measurements. Because of the selective depolymerization of low substituted parts of the cellulose ether, it was concluded that the enzyme cuts out the higher substituted regions. Therefore, this analysis yields information about the length of these regions, i.e., about the distribution of functional groups along the polymer chains [326, 327]. Fragments of HEC obtained by enzymatic degradation were analyzed by means of $^{13}C$ NMR spectroscopy [328]. On the basis of an enzymatic treatment of CMC, an efficient method was developed for its structure determination. This route includes an endoglucanase-catalyzed fragmentation of the polysaccharide followed by preparative SEC. The samples of each SEC fraction are subsequently converted into monosaccharide units by acid hydrolysis, followed by quantitative HPLC. This type of analysis was applied for a number of CMC samples with different patterns of substitution both within the AGU and along the polymer chain [90, 329–331]. Noteworthy is a review dealing with the analysis of substituents in cellulose ethers by Urbanski [332].

#### 2.3.4.3 Chromatographic Techniques Applied After Degradation and Subsequent Derivatization

In case of hydrolytically unstable cellulose derivatives, especially organic and inorganic esters and silyl ethers direct degradation of the polymer backbone is usually combined with partial or complete loss of the substituents. Exploitation of chromatographic techniques is still possible after subsequent derivatization and depolymerization illustrated schematically for a methylation step in Fig. 2.64. The inverse substitution pattern (methyl pattern) of the hydrolytically instable polysaccharide ester is then analyzed by means of chromatography. As shown in this scheme, an alternative to the acidic depolymerization is the reductive cleavage.

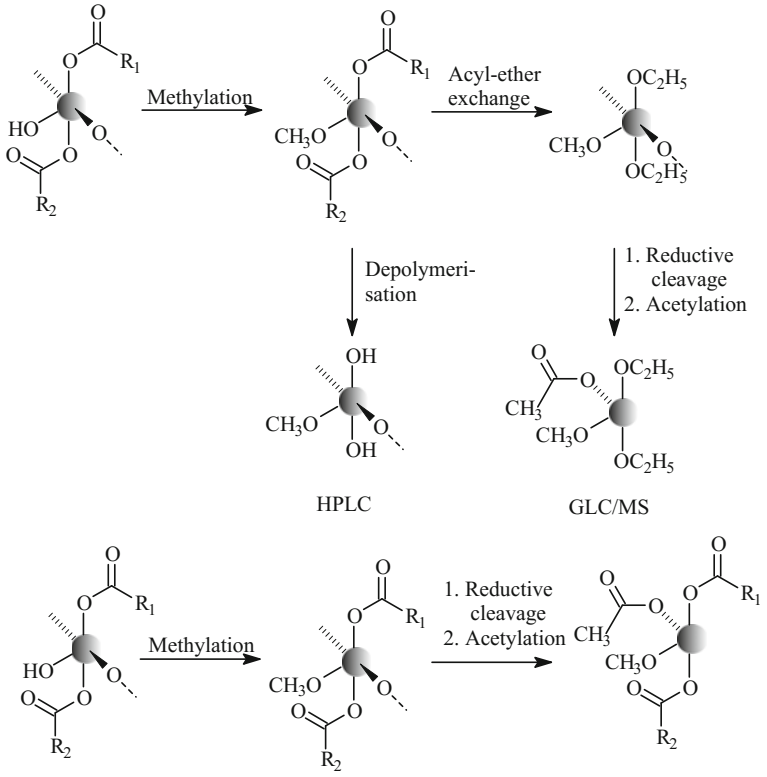


**Fig. 2.64** Analysis of polysaccharide esters with chromatographic methods after subsequent derivatization (reprinted from [275, p. 163] with permission of Springer)

For that purpose, an acetyl-ether exchange is recommended in order to obtain correct information on the ester distribution.

The chromatographic technique applied most frequently for the analysis of the building blocks is GC–MS. The advantage is that peaks can be unambiguously assigned without the synthesis of standard compounds. This topic is nicely reviewed by Mischnick et al. [333]. A few attempts of HPLC as chromatographic tool are known. The subsequent derivatization is easier because volatility of the derivatives is not necessary. Nevertheless, GC still provides better resolution.

Subsequent derivatization of polysaccharide esters may be carried out by etherification [334, 335] and by carbamoylation [336]. It is essential that the subsequent step does not involve conversion in the presence of water and a strong base otherwise ester hydrolysis or transesterification will occur leading to wrong results. Among the first attempts in this regard is a method developed by Björndal et al. [337]. The derivatization of cellulose acetate is performed by reaction with methyl vinyl ether in DMF in the presence of TsOH acid as catalyst. The anhydroalditol acetates are separated by means of GC [338]. Comparison of the results with data

**Table 2.20** Evaluation of the distribution of ester moieties in cellulose monoacetates (CMA) and cellulose diacetates (CDA) [221] with chemical analysis using saponification and titration (Titration), with $^{13}C$ NMR spectroscopy

| Sample | Method | DS of *O*-acetyl groups at position | | | Total DS |
|---|---|---|---|---|---|
| | | 2 | 3 | 6 | |
| CMA | Titration | – | – | – | 1.75 |
| | $^{13}C$ COM[a] | 0.60 | 0.55 | 0.58 | 1.73 |
| | $^{13}C$ NME[b] | 0.59 | 0.56 | 0.59 | 1.74 |
| | $^{1}H$ NMR | 0.59 | 0.56 | 0.59 | 1.74 |
| | GC | 0.60 | 0.60 | 0.59 | 1.79 |
| CDA | Titration | – | – | – | 2.41 |
| | $^{13}C$ COM | 0.84 | 0.83 | 0.72 | 2.39 |
| | $^{13}C$ NME | 0.84 | 0.84 | 0.73 | 2.41 |
| | $^{1}H$ NMR | 0.86 | 0.82 | 0.73 | 2.41 |
| | GC | 0.83 | 0.83 | 0.71 | 2.37 |

Reprinted from [275, p. 164] with permission of Springer
[a]Proton-decoupled mode with NOE
[b]Proton-decoupled mode without NOE, $^{1}H$ NMR spectroscopy and GC after methylation and degradation

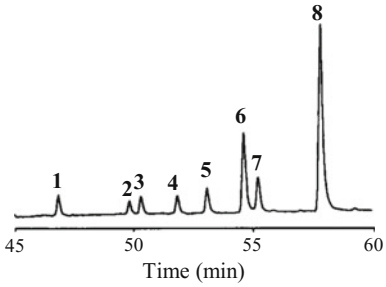


**Fig. 2.65** GLC of anhydroalditol acetates derived from cellulose acetate with DS 2.50 (reprinted from [275, p. 165] with permission of Springer)

obtained by $^{13}C$ and $^{1}H$ NMR spectroscopy showed good agreement in case of commercial cellulose monoacetate and cellulose diacetate (Table 2.20, [221]).

More reliable and efficient is methylation under neutral conditions with trifluoromethanesulfonic acid methylester (methyl triflate)/2,6-tert-butylpyridine in trimethyl phosphate [339] or treatment with trimethyloxonium tetrafluoroborate in dichloromethane [340]. These methylation procedures are used for derivatives with DS > 2. At lower DS, migration and chain degradation need to be considered. The methylated products can be subjected to acyl-ethyl exchange and reductive cleavage [293]. The molar ratios of the eight differently substituted RU are determined by GC (Fig. 2.65; Table 2.21) for pure cellulose acetates.

**Table 2.21** Assignment of the 8 differently substituted RU of anhydroalditol acetates derived from cellulose acetate with DS 2.50

| 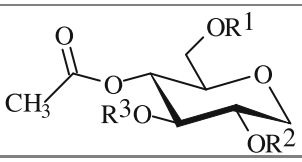 | $R^1$ | $R^2$ | $R^3$ |
|---|---|---|---|
| 1 (see Fig. 2.65) | $CH_3$ | $CH_3$ | $CH_3$ |
| 2 | $CH_3$ | $C_2H_5$ | $CH_3$ |
| 3 | $CH_3$ | $CH_3$ | $C_2H_5$ |
| 4 | $C_2H_5$ | $CH_3$ | $CH_3$ |
| 5 | $CH_3$ | $C_2H_5$ | $C_2H_5$ |
| 6 | $C_2H_5$ | $C_2H_5$ | $CH_3$ |
| 7 | $C_2H_5$ | $CH_3$ | $C_2H_5$ |
| 8 | $C_2H_5$ | $C_2H_5$ | $C_2H_5$ |

Reprinted from [275, p. 165] with permission of Springer

In contrast to the pure cellulose acetates, the method is not capable of establishing the partial DS of each ester in mixed cellulose esters, e.g., cellulose acetate butyrates. For analysis of mixed esters, reductive treatment of the methylated samples with an excess of a Lewis acid in combination with triethylsilane is exploited. In detail, the methylated mixed cellulose esters are subjected to reductive cleavage at room temperature for 7 days in the presence of $(C_2H_5)_3SiH$ (35 mol/mol AGU), $CH_3SO_3Si(CH_3)_3$ (70 mol/mol AGU), and $BF_3{*}O(C_2H_5)_2$ (17 mol/mol AGU). The procedure leads to a complete reduction of acyl residues to the corresponding alkyl ethers. GC combined with CI-MS and EI-MS is carried out after acetylation of the samples with acetic anhydride/1-methylimidazole. Assignment of the 27 separate signals obtained on a Restek RTx-200 column is summarized in Table 2.22. It is a fast and convenient one-pot analysis applied for a variety of derivatives [341–343].

Structure analysis of polysaccharide sulfuric acid half-esters is achieved via methylation under alkaline conditions. For trans-1,2-diol, however, structures as present in (1→4) linked glucans intramolecular nucleophilic displacement of the sulfate moieties under formation of an oxirane structure as intermediate needs to be avoided by optimized reaction conditions [316]. Due to the strongly enhanced acid lability of glycosyl linkages in 2-sulfates reductive hydrolysis is applied to stabilize early liberated glucose residues by direct reduction to glucitols [344, 345]. After complete hydrolysis, reduction, and acetylation partially methylated glucitol acetates are obtained, which can be analyzed by GC.

Methylation of cellulose esters, controlled depolymerization and HPLC are applied alternatively to study their structure. The advantage is that aqueous solutions of the derivatized sugar units can be investigated making the subsequent functionalization rather easy. Permethylation with methyl triflate and subsequent hydrolytic depolymerization with TFA can be used. This path can even be used for very instable cellulose derivatives such as cellulose trifluoroacetates [346]. For

**Table 2.22** Peak assignment (in the order of increasing retention times) of gas–liquid chromatograms of anhydroalditol acetates derived from cellulose acetate propionates by sequential permethylation, reductive cleavage, and acetylation

| 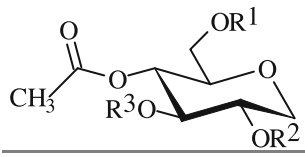 | $R^2$ | $R^3$ | $R^6$ | Molecular mass (g $mol^{-1}$) |
|---|---|---|---|---|
| | $CH_3$ | $CH_3$ | $CH_3$ | 248 |
| | $CH_3$ | $C_2H_5$ | $CH_3$ | 262 |
| | $CH_3$ | $CH_3$ | $C_2H_5$ | 262 |
| | $C_2H_5$ | $CH_3$ | $CH_3$ | 262 |
| | $CH_3$ | $C_2H_5$ | $C_2H_5$ | 276 |
| | $C_2H_5$ | $C_2H_5$ | $CH_3$ | 276 |
| | $C_2H_5$ | $CH_3$ | $C_2H_5$ | 276 |
| | $C_2H_5$ | $C_2H_5$ | $C_2H_5$ | 290 |
| | $CH_3$ | $C_3H_7$ | $CH_3$ | 276 |
| | $CH_3$ | $CH_3$ | $C_3H_7$ | 276 |
| | $C_3H_7$ | $CH_3$ | $CH_3$ | 276 |
| | $CH_3$ | $C_3H_7$ | $C_2H_5$ | 290 |
| | $CH_3$ | $C_2H_5$ | $C_3H_7$ | 290 |
| | $C_2H_5$ | $C_3H_7$ | $CH_3$ | 290 |
| | $C_3H_7$ | $C_2H_5$ | $CH_3$ | 290 |
| | $C_3H_7$ | $CH_3$ | $C_2H_5$ | 290 |
| | $C_2H_5$ | $CH_3$ | $C_3H_7$ | 290 |
| | $C_2H_5$ | $C_3H_7$ | $C_2H_5$ | 304 |
| | $C_2H_5$ | $C_2H_5$ | $C_3H_7$ | 304 |
| | $C_3H_7$ | $C_2H_5$ | $C_2H_5$ | 304 |
| | $CH_3$ | $C_3H_7$ | $C_3H_7$ | 304 |
| | $C_3H_7$ | $C_3H_7$ | $CH_3$ | 304 |
| | $C_3H_7$ | $CH_3$ | $C_3H_7$ | 304 |
| | $CH_3$ | $C_3H_7$ | $C_3H_7$ | 318 |
| | $C_3H_7$ | $C_3H_7$ | $C_2H_5$ | 318 |
| | $C_3H_7$ | $C_2H_5$ | $C_3H_7$ | 318 |
| | $C_3H_7$ | $C_3H_7$ | $C_3H_7$ | 332 |

Reprinted from [275, p. 166] with permission of Springer

separation of the methyl glucoses with inverse substitution patterns to the starting ester, a RP-18 column is employed. Assignment of the HPLC signals to the different patterns of substitution is feasible but quantification of the chromatograms is limited because of the comparably bad resolution. Nevertheless, the method can be

used to determine the amount of different groups of substitution (un-, mono-, di-, and trisubstituted glucoses) [316]. Besides cellulose esters such as acetates [340] and sulfates, other hydrolytically instable cellulose derivatives like benzyl [347] and silyl ethers [348] can be analyzed applying methylation as derivatization.

### 2.3.5 *Mass Spectroscopy (MS)*

Mass spectroscopy (MS) was already introduced as a method that can be combined with chromatographic techniques. In general, MS involves evaporation of a sample and ionization of the components, e.g., by bombarding them with an electron beam, which results in the formation of ions [349]. These are then separated according to their mass-to-charge ratio (m/z or m/Q) in an analyzer by electromagnetic field. Finally, a detector records either the charge induced or the current produced when an ion passes by or hits a surface. The ion signal is processed into mass spectra. In a scanning instrument, the signal produced in the detector during the course of the scan will produce a mass spectrum, a record of the intensity (or relative abundance) ions as a function of m/z.

The methods most employed in order to cause ionization of the gases and vapors include electron impact (EI) ionization and chemical ionization (CI). In the latter technique, ionization is achieved by collision of the analyte with ions of a reagent gas such as methane or ammonia. Due to the fact that the compounds in the analyte have to be evaporated, subsequent functionalization and degradation of the cellulose derivatives are indispensable for this type of analysis. More suitable for biological material and macromolecules are therefore modern techniques such as electrospray ionization (ESI), fast atom bombardment (FAB), and matrix-assisted laser desorption/ionization (MALDI) methods. These methods are comparably soft ionization tools and one can work with a solid or a liquid. FAB-MS and MALDI are closely related. Here, the analyte is embedded into a matrix such as glycerol, thioglycerol or 3-nitrobenzyl alcohol (3-NBA) which can be easily evaporated and carries the compounds in the analyte along. In case of FAB-MS, the analyte/matrix mixture is bombarded under vacuum with a high energy beam of atoms whereas MALDI exploits usually a UV laser beam. During the impact of the laser, the molecules of the analyte are also ionized in a relatively low energy manner. These ionization methods are mostly combined with a time of flight (TOF) detector system. The setup is commonly known as MALDI-TOF.

MS measurements are well suitable for the structure analysis of cellulose derivatives and for the basic understanding of interactions of cellulose with other molecules, e.g., solvents, in model experiments. Such an approach was already discussed for NMR studies on cellooligomers treated with boronic acids (see Sect. 2.3.3.2) to gain some insight into the industrially important activation of cellulose with boric acid. Investigation of this system with MS is an illustrative of the potential of such an approach and the basic strategies of MS analysis. Therefore, it will be discussed in detail.

Again the model compounds used are mostly methyl glycosides (Me-α-D-Glc*p*), methyl cellobiosides (Me-β-D-clb) or cellooligomers. The conversion of Me-α-D-Glc*p* with phenylboronic acid and its anhydride triphenylboroxole (TPB) is discussed in reference [268]. The MS (EI) of the compound obtained shows significant fragment ions at m/z 160 (**I**) and at m/z 250 (**II**) in addition to a peak for the molecular ion at m/z 470 (see Fig. 2.66 structure **1** and **2**). The fission patterns explaining the first two signals are shown as dotted lines in the formulas. The spectra reveal the existence of a seven- and a six-membered boronate ring. This was confirmed by conversion of a protected Me-α-D-Glc*p* into methyl-4,6-*O*-benzylidene-2,3-*O*-(diphenylpyroboronate)-α-D-glucopyranoside (**3**) where the same fragment for the seven-membered ring moiety m/z 250 (**II**) was found.

Structures predicted on the basis of these measurements, which can be formed during the treatment of Me-β-D-clb with TPB in aprotic organic solvents or water, are shown in Fig. 2.66; Table 2.23. MS measurements are simply carried out by introduction of the reaction mixture consisting of Me-β-D-clb and TPB into the mass spectrometer; (EI) ionization has been employed. All samples with molar ratio Me-β-D-clb:TPB higher than 1:1 showed again the typical fragment ions at m/z 250,

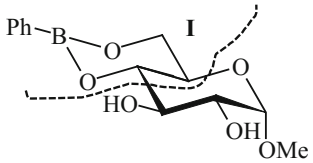


Me-$^{4,6}$(PhB)-α-D-Glc*p* **1**

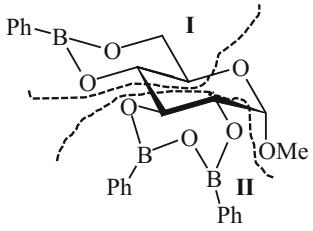


Me-$^{2,3}$(PhB)$_2$-$^{4,6}$(PhB)-α-D-Glc*p* **2**

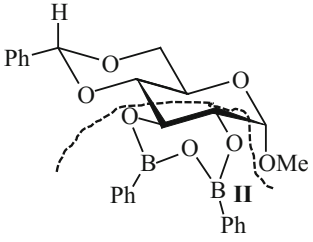


Me-$^{4,6}$-(Bz)-$^{2,3}$(PhB)$_2$-α-D-Glc*p* **3**

Benzyl (Bz)
Glucopyranoside (Glc *p*)
Methyl (Me)
Phenyl (Ph)

**Fig. 2.66** Fission processes of boronate structures obtained by conversion of Me-α-D-Glc*p* and a protected Me-α-D-Glc*p* (**3**) with phenylboronic acid (adapted from [269])

**Table 2.23** Phenylboronate structures of methyl-β-D-cellobioside and the detectability with different spectroscopic methods

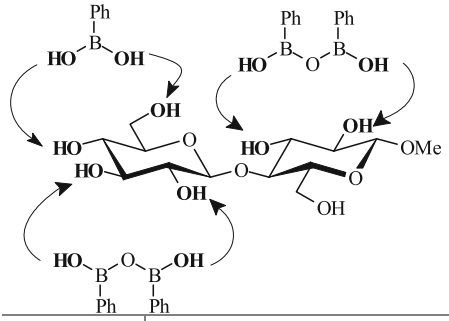


| Entry | Structure abbreviation | Mass | Detectability |
|---|---|---|---|
| **1** | Me-$^{4',6'}$(PhB)-β-D-clb | 442 | ESI, MALDI-TOF |
| **2** | Me-$^{2,3}$(PhB)$_2$-β-D-clb or Me-$^{2',3'}$(PhB)$_2$-β-D-clb | 546 | ESI, FAB, MALDI-TOF |
| **3** | Me-$^{2,3}$(PhB)$_2$-$^{4',6'}$(PhB)-β-D-clb or Me-$^{2',3'}$(PhB)$_2$-$^{4',6'}$(PhB)-β-D-clb | 632 | FAB, CI, MALDI-TOF |
| **4** | Me-$^{2,3}$(PhB)$_2$-$^{2',3'}$(PhB)$_2$-β-D-clb | 736 | MALDI-TOF |

Adapted from [268]

which is a hint for the existence of a seven-membered diboronate ring at trans-1,2-diol moieties at C-2 and C-3 [268]. It was confirmed by MS experiments using chemical ionization (CI) with water as reagent gas. In the spectrum, a peak for a molecular ion at m/z 632 was identified. This peak was assigned to a derivatized Me-β-D-clb with boronation in position 4′ and 6′ (six-membered boronate) and boronation at one trans-1,2-diol moiety at C-2 and C-3 or C-2′ and C-3′ (a seven-membered diboronate structure, see Table 2.23, entry **3**). An additional indication is the isotope pattern of the peak at m/z 632 revealing the existence of three boron atoms in the detected phenylboronate structure. The isotope pattern of mass peaks is significant for boron-containing compounds because of the unique isotope distribution of boron ($^{10}$B:$^{11}$B = 1:4.2).

Less destructive FAB-MS experiments confirmed the peak at m/z 632 and additionally one signal at m/z 546 (Table 2.23, entry **2**), which corresponds to one diphenylpyroboronate structure at trans-1,2-diol moiety. Occurrence of one seven-membered diboronate structure (m/z 546) and a six-membered boronate ring (m/z 442, cp. Table 2.23, entry **1**) was determined by nanoelectrospray ionization mass spectroscopy (ESI-MS), but none of these techniques gave a hint for conversion of the two trans-1,2-diol moieties at neighboring glucose units in one step. Therefore, MALDI-TOF MS was carried out. A multiple-layer spotting technique with three layers was found to be an appropriate sample preparation for

saccharide boronates. It can be performed as follows: first 2,5-dihydroxybenzoic acid (DHB) solution in THF was spotted on the MALDI target, as the second layer sodium iodide solution in acetone was applied, and after evaporation of organic solvents, the aqueous sample solution (mixture of Me-β-D-clb and TPB with concentration between 5 and 10 g/L) was added on top as the third and final layer. The removal of water and consequently the esterification of hydroxyl groups with PBA units were accelerated by drying. Figure 2.67 shows a MALDI-TOF MS spectrum (reflector mode) of an evaporated aqueous solution of Me-β-D-clb and TPB (molar ratio 1:0.6) on DHB and the peak assignment.

Remarkable are the recurring mass differences (Δm/z 86 and Δm/z 104), which may originate from an additional PBA unit. Thus, the molecular ions $[M+Na]^+$ at m/z 465, m/z 569, m/z 655, and m/z 759 correlate with boronate structures with different numbers of boronic acid units (Table 2.25, entries **1**–**4**). The detected molar masses confirm the transformation of secondary OH groups in position 2 and 3 in addition to the expected six-membered ring at C-4′ and C-6′. Moreover, there is the molecular ion at m/z 759, which is consistent with an esterification product with two seven-membered pyroboronate rings at neighboring glucose units. So, a multi-functionalization with diboronate moieties along an oligomer or polymer

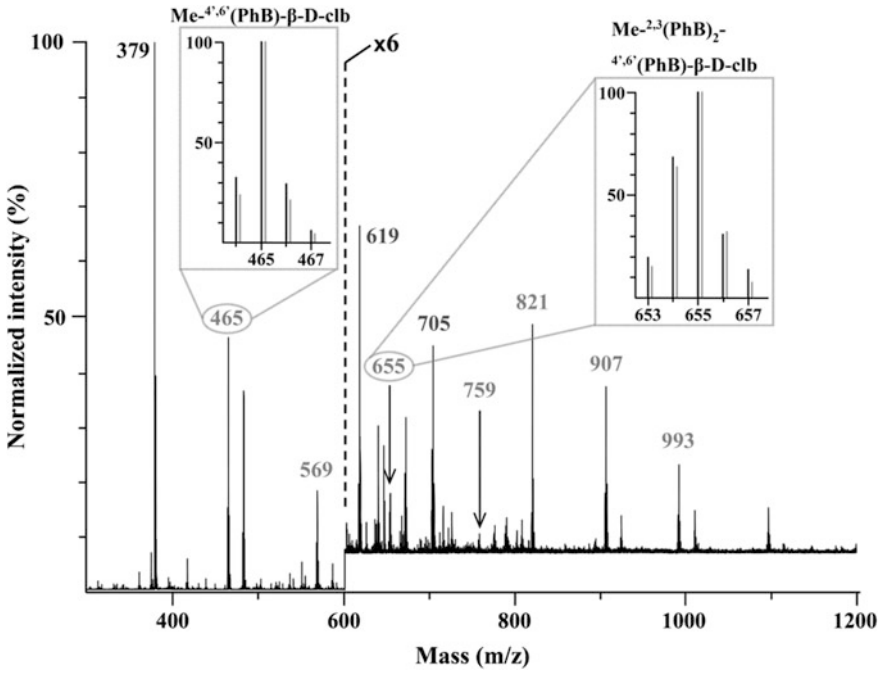


**Fig. 2.67** MALDI-TOF MS spectrum of an aqueous solution of Me-β-D-clb and TPB (molar ratio 1:0.6; matrix: DHB in THF; salt: NaI in acetone). The insets show the comparison of calculated isotope pattern (gray) with molecular ions of Me-$^{4',6'}$(PhB)-β-D-clb and Me-$^{2,3}$(PhB)$_2$-$^{4',6'}$(PhB)-β-D-clb (reprinted from [268], copyright (© 2010) with permission from Elsevier)

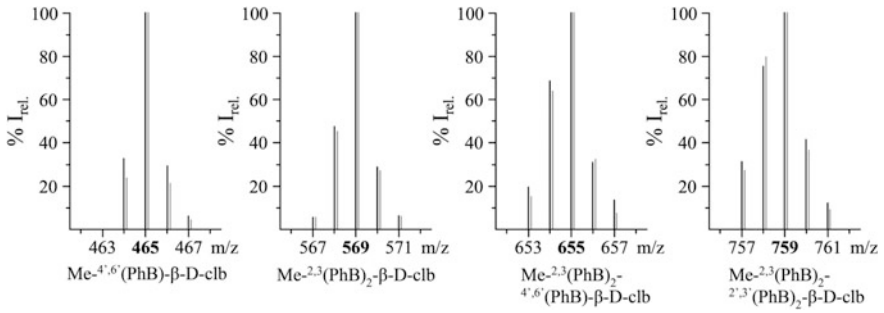


**Fig. 2.68** Comparison of calculated isotope pattern (gray) with molecular ions of phenylboronates of Me-β-D-clb (reprinted from [269], copyright (© 2009) with permission of Elsevier)

chain was found. Samples with other molar ratio of Me-β-D-clb:TPB and with α-cyano-4-hydroxy cinnamic acid as the matrix resulted in comparable spectra, confirming the existence of two seven-membered rings at one Me-β-D-clb molecule. Further evidence is gained from the comparison of patterns and intensities of mass peaks with calculated isotope patterns. On the basis of the isotope distribution of carbon and boron, the patterns for the main molecular ions were simulated (insets of Figs. 2.67 and 2.68).

A perfect fit of the predicted pattern with the peaks for molecular ions $[M+Na]^+$ was found. Besides the boronate ring formation at Me-β-D-clb, MALDI-TOF MS spectra show the formation of larger adducts when higher concentrations of TPB are applied. Dimerization of two molecules Me-β-D-clb with boronic acid moieties was concluded from the peaks at m/z 821, m/z 907, and m/z 993. The molecular ions at m/z 619 and m/z 705 in the spectrum are most likely caused by the formation of Me-β-D-clb DHB adducts bridged by one or two PBA units. These MS experiments gave a deep insight into the possible interactions of cellulose with boronic and boric acid which were confirmed by NMR measurements (Sect. 2.3.3.2).

MALDI-TOF MS may also be applied for the determination of the purity of cellooligomers and, in principal, for the determination of the molecular weight. A typical MALDI-TOF-MS of a cellooligomer mixture obtained by degradation of cellulose with phosphoric acid is shown in Fig. 2.69. It can be seen that the main peaks have a difference of m/z 162, which is an evidence for the pure cellodextrine structure consisting of glucoses only. The mass spectra support the results of the GPC measurements of this oligomer sample, i.e., most of the oligomers have 4–10 glucose units [350]. As in most spectra of pure cellooligomers or derivatized oligomers the absolute values of the molecular weight is higher than expected because adducts with cations are formed leading to a difference of m/z 41 in case of, e.g., sodium. The basicity, number, and orientation of coordinating sites influence the competition for cations to form quasimolecular ion adducts ($[M+Na]^+$, $[M+H]^+$). The molar signal intensity usually decreases in ESI-MS but increases in MALDI-MS over a certain range of molecular weight (or DP) of homooligosaccharides.

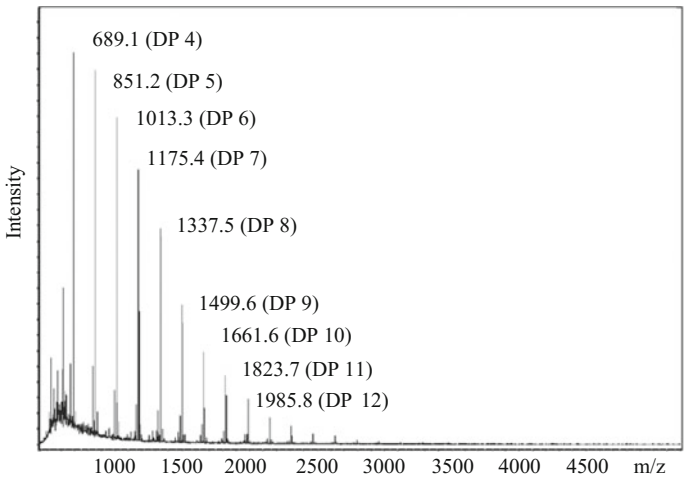


**Fig. 2.69** MALDI-TOF MS (ionization $N_2$ laser) of a cellooligomer mixture obtained by degradation of cellulose with phosphoric acid. The corresponding $DP_w$ (calculated from m/z vs. molar mass AGU) are assigned on the peaks (reproduced from [350] with permission from John Wiley and Sons)

**Fig. 2.70** Complexation of a cation by a disaccharide, according to Hofmeister [351]

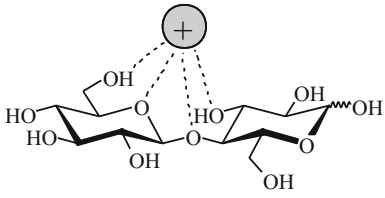


For instance, disaccharides are detected at a much higher sensitivity than monosaccharides, since the additional coordination sites and the conformational flexibility of the glycosidic linkage favor the formation of quasimolecular ions (Fig. 2.70 [351]). This is a further reason for biases in quantitative experiments.

Nevertheless, MS techniques are suitable tools for the detailed analysis of cellulose derivatives. The advantage here is that a complete degradation to the basic building blocks is not necessary. In case of, e.g., ESI or MALDI techniques, the amount of subsequent functionalization is limited compared to GC and older MS methods because it is not essential to have a vaporizable derivative. Thus, the possible bias is limited as well. MS, however, is not inherently a quantitative method. The relation of signal intensities to concentration of compounds is determined by ion yields in the ESI and MALDI processes, by the ion stability and transfer into the mass analyzer; these steps can cause biases. The possible influence of a cation adduct formation is discussed above. But for comparable structures and known ionization and fragmentation patterns, MS is a reliable method.

Another illustrative example is the use of MS for the structure elucidation of methyl celluloses. As mentioned, total depolymerization is not required here [352]. For structural uniformity, the partially substituted methyl cellulose has to be perdeuteromethylated in this approach. This guarantees comparable ionization and fission in the MS process and introduces a mass difference suitable for the determination of the substitution pattern. Deuteromethylation is possible with Me-$d_3$-I comparable to GC measurements [353]. After partial hydrolysis, the oligomeric mixture can be examined by ESI-MS. The pattern for the disaccharide fraction gives signals with m/z of the analytes, $[M+Na]^+$, between 449 and 467 depending on the number of methyl residues originally present and the number of deuteromethyl groups introduced for isotopic labeling of free OH groups (see Fig. 2.74).

The reliability of the method was evaluated by investigation of the fragmentation pattern of 2,3,6-*O*-methylated maltooligosaccharides in ESI-MS/collision-induced dissociation (CID) with positionally deuteromethyl-labeled compounds. A reproducible fragment ion pattern was found, following a defined mechanism of cross-ring cleavages [354]. Detailed analysis of the substitution pattern is possible by tandem MS, denoted $MS^2$ and $MS^3$ in Fig. 2.71. From the reproducible relative ion intensities of mother, daughter, and "granddaughter" spectra ($n$ = 1–3), the complete monomer composition could be calculated. Data are in good agreement with GC measurements.

As mentioned for NMR spectroscopic studies, the determination of the functionalization patterns of cellulose derivatives along the polymer chain is a more complex problem. The substituent distribution in trimers obtained from methyl cellulose after partial random hydrolysis and deuteromethylation were determined

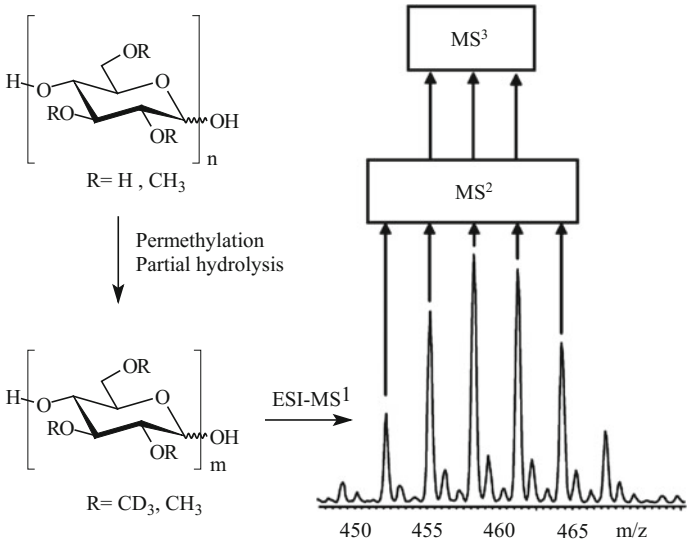


**Fig. 2.71** Monomer analysis by ESI-MS/CID of methylated cellulose after perdeuteriomethylation and partial hydrolysis (adapted from [352])

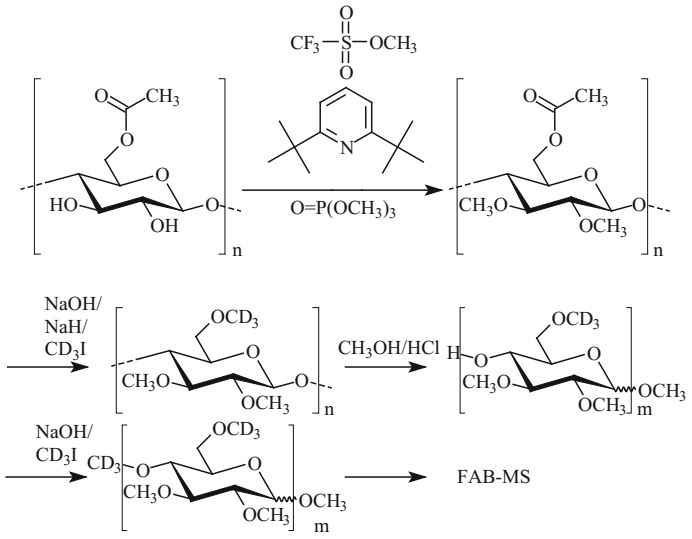


**Fig. 2.72** Analytical path for the structure determination of cellulose acetate by FAB-MS after permethylation, perdeuteromethylation, and random cleavage (reprinted from [275, p. 167] with permission of Springer)

by FAB-MS [322, 355]. This pattern was compared to a theoretical distribution, which can be calculated assuming that the state of neighboring repeating units is independent. Deviation from the model gives information on the distribution of the substituents (see below). Methylation is usable for the analysis of silyl ethers [333], cellulose sulfates [317, 318], and acetates [356] as well. For the structure determination of such derivatives, multistep subsequent functionalization is carried out consisting of (I) permethylation, (II) combined hydrolysis and perdeuteromethylation with methyl iodide-$d_3$ (III) methanolysis, (IV) deuteromethylation of the nonreducing functions, followed by FAB-MS analysis (Fig. 2.72). The first methylation is usually carried out with methyltriflate [339]. This is necessary because a methylation under alkaline conditions would cleave the primary substituent. In case of silyl ethers, a substituent migration has to be considered [348]. Nevertheless, this path gives a fairly complete picture of the substituent distribution in the mentioned cellulose derivatives because it yields information on the distribution on the basis of the AGU and along the polymer chain. Analysis of the substituent pattern on the basis of the AGU is more or less identical to the described method used for the methyl derivatives.

The approach is also suitable for the determination of the substitution pattern along the polymer chain. Comparison of the experimental data with those calculated for a random distribution of functional groups gives information about the homogeneity of functionalization. As can be seen in Fig. 2.73, the following patterns can be divided: homogeneous (i.e., as to be expected under independence of the reactivity of neighboring repeating units), more heterogeneous, more regular and

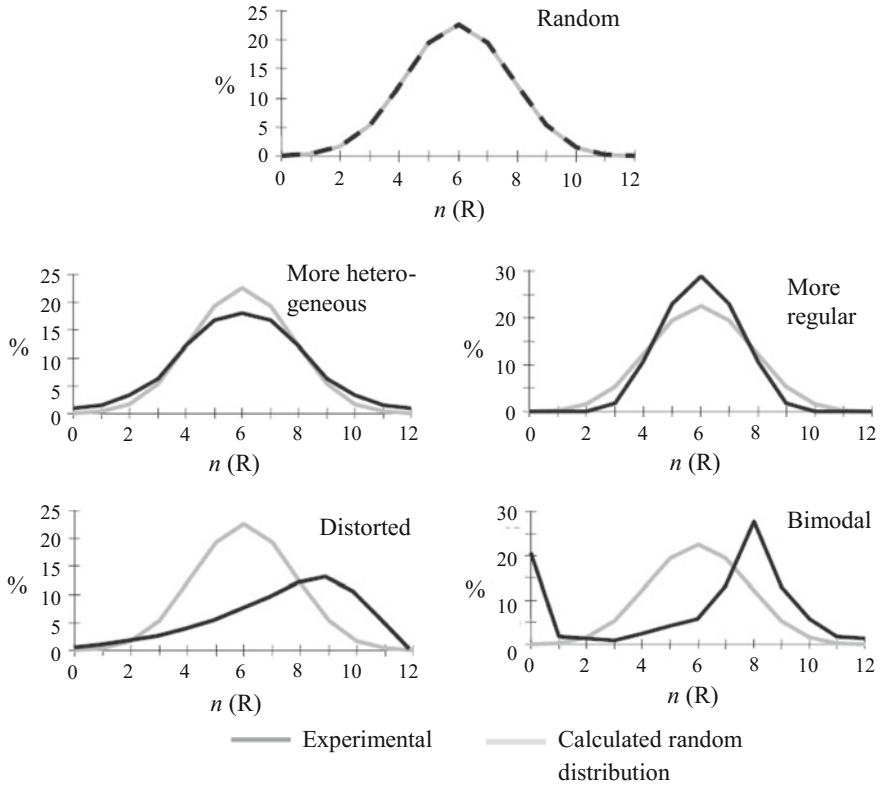


**Fig. 2.73** Patterns (random, more heterogeneous, more regular, distorted, and bimodal). DP4 for a sample with DS 1.5 is shown; *n*(R) is the number of substituents R. Amounts are given in mol% AGU (reprinted from [313], copyright (© 2010) with permission from Elsevier)

bimodal, depending on the reaction conditions. Although Arisz et al. [322, 355] calculated the standardized total deviation from the model and introduced it as a heterogeneity parameter $H_n$ ($n$ denoting the number of monomers in the oligomer fraction considered), the interpretation follows a more qualitative course. Therefore, a new mathematical model taking into account the influence of substitution of a glucosyl residue on the probability of substitution at the neighbored monomer units was established by Mischnick et al. Problems of the analysis path may be both undermethylation and migration or cleavage of the primary functional groups during the methylation yielding incorrect results [313].

An interesting path for the analysis of nonionic cellulose ethers, e.g., MC, HEC, HPC, or HEPC is the pyrolysis ammonia chemical ionization mass spectroscopy (PyCIMS, [355]). The peaks in the PyCI mass spectra of these cellulose ethers could be assigned to the ions of pyrolytic dissociation products. Structural information about the residual amount of nonderivatized cellulose, the relative chain length distributions of the substituents in hydroxyalkyl celluloses, and the

end-capping of hydroxyalkyl substituents by alkyl groups in the mixed cellulose ethers is obtained. Interference of secondary pyrolysis products in the PyCI mass spectra is found to be of minor importance, especially in the lower mass regions. Nevertheless, quantification of the substitution is not possible via this path. ESI-MS of hydrolysates, e.g., of HPMC was applied which gives well-resolved spectra (Fig. 2.74) which seemed suitable for quantification. But the obtained data are not in agreement with other measurements such as GC-FID. An explanation is the different tendency of the substituted glucoses and oligomers to form sodium complexes [357].

Again subsequent functionalization is necessary. If the cellulose ethers are labeled after the hydrolysis with a quaternary ammonium function (see Fig. 2.75) and the measurements are carried out with a MALDI-TOF equipment reliable data can be acquired. This was shown for a number of HECs with a high MS. The derivatives were analyzed with respect to their substituent distribution, tandem reaction in the glucosyl unit and along the polymer chain by MALDI-TOF MS after this multistep sample preparation. For comparison of the experimental data with a random pattern, an extended Bernoulli plot was applied to calculate a random distribution for the composition of un-, mono-, di-, tri-, and up to heptasubstituted glucosyl units [358].

For a more detailed discussion on MS techniques used for the structure determination of cellulose derivatives, see reference [313].

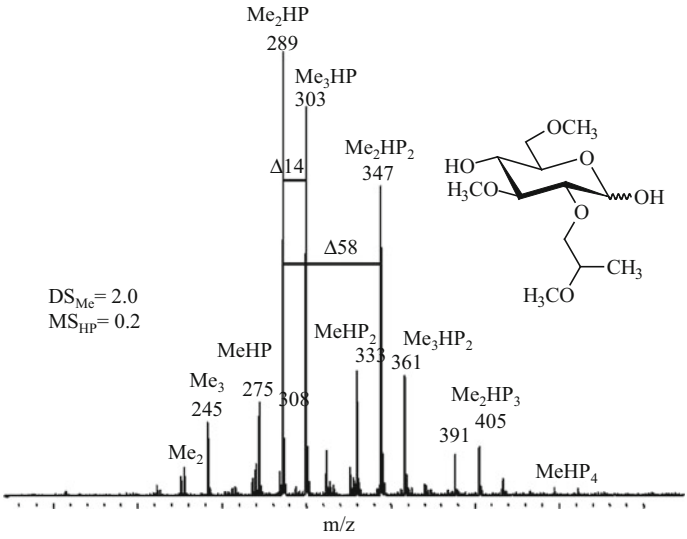


**Fig. 2.74** ESI-MS of completely hydrolyzed HPMC; signals are assigned according to the number of Me and HP residues (reprinted from [357])

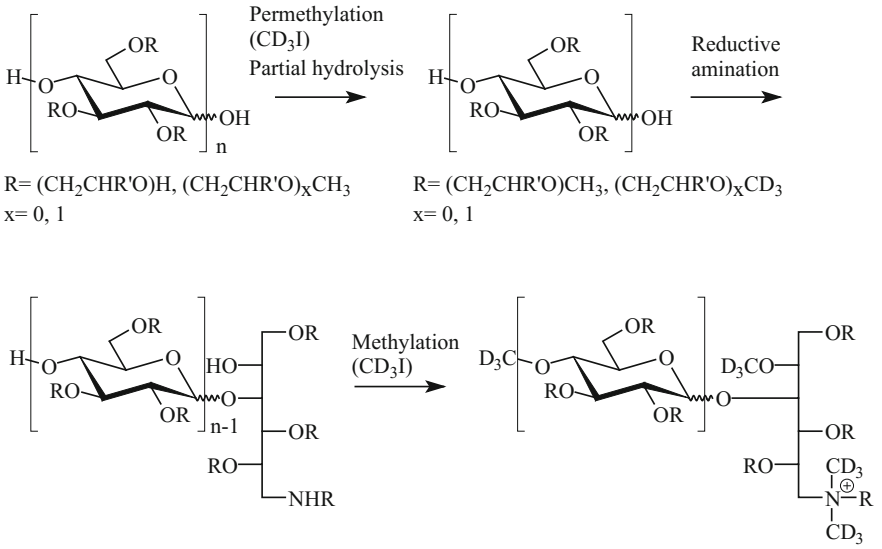


**Fig. 2.75** HEC sample preparation for MALDI-ToF-MS analysis

## *2.3.6 Thermal Analysis*

### 2.3.6.1 Theoretical Background

Unlike many synthetic polymers, cellulose cannot be processed by extrusion from the melt because of its thermal instability. Thus, heating cellulose in the temperature range of 190–390 °C, even in an inert atmosphere, results in a complex series of parallel and consecutive reactions, leading to the formation of aliphatic, aromatic, carbonyl compounds, furans, and carboxylic acids [359]. On the contrary, cellulose derivatives, in particular its simple and mixed carboxylic esters, can be processed by extrusion, e.g., into fibers, rods, and slabs [360]. The values of $T_m$ of these esters decrease as a function of increasing the length of the acyl moiety and, for the same acyl group, as a function of increasing the DS [361–365]. Therefore, the study of the effect of heating of cellulose and its derivative bears on the important questions of their thermal stability and potential applications.

The thermal analysis, TA, techniques that will be discussed here are those most extensively employed with cellulose and its derivatives, including thermogravimetric, TGA (or the synonymous TG, for thermogravimetry), differential thermal analysis (DTA), differential scanning calorimetry (DSC), and thermomechanical analysis (TMA). The extent of theory that is present is required to understand the applications. An elaborate discussion of these and other TA methods are given in specialized texts, e.g., [366–368].

According to the International Confederation of Thermal Analysis and Calorimetry, TA methods are defined as "a group of techniques in which a property

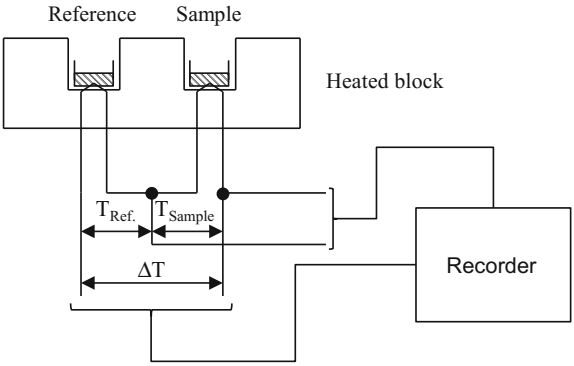


**Fig. 2.76** Schematic representation of a DTA equipment (adapted from [367])

of a sample is monitored against time or temperature while the temperature of the sample, in a specified atmosphere, is programmed" [369]. In practice, the temperature of the oven that contains the sample is programmed while the sample is measured continuously, in order to monitor any endothermic or exothermic event, due to loss of volatiles, decomposition, or phase transitions.

### DTA Analysis

The basic features of a DTA apparatus are shown in Fig. 2.76. The substance investigated is placed in a sample cell, or "pan", usually made of aluminum, whereas a reference sample is placed in an identical cell that is located close to the former. The latter sample may have a precise transition in the region of interest, e.g., naphthalene, m.p. 80.5 °C, or have a constant heat capacity, e.g., aluminum disc or powder (897 J/kg K). Both cells are heated in a uniform thermal block, under the same conditions. The objective of the reference is to provide a direct comparator for temperature measurement for the sample, thus minimizing inaccuracies due to, e.g., thermal lag in the equipment. One measures $\Delta T = (T_{\text{Sample}} - T_{\text{Reference}})$, this indicates whether the sample is undergoing an endothermic, or exothermic event as a function of increasing $T$, for negative, and positive values of $\Delta T$, respectively.

### DSC Analysis

In DSC, the sample and reference have independent micro-heaters; background heating of the thermal block is provided independently, so that the micro-heaters are sensitive to the requirements of the sample, and reference cell at the programmed temperature, $T_{\text{Prog}}(t)$, where $t$ is time, see Fig. 2.77. The temperature of each cell is measured continuously, and compared with the instantaneous $T_{\text{prog}}(t)$. Electric power is delivered to either cell so that both reach the same $T$. The power requirement of each cell is a function of the departure from $T_{\text{Prog}}$; i.e., $W_{\text{Sample}}(T_{\text{Sample}} - T_{\text{Prog}})$, and $W_{\text{Reference}}(T_{\text{Reference}} - T_{\text{Prog}})$. The differential power requirement is: $\Delta W = \{[W_{\text{Sample}}\ (T_{\text{Sample}} - T_{\text{Prog}})] - [W_{\text{Reference}}(T_{\text{Reference}} - T_{\text{Prog}})]\}$; $\Delta W$ is plotted as a function of $T_{\text{Sample}}$; $T_{\text{Reference}}$, or $T_{\text{Prog}}$, respectively.

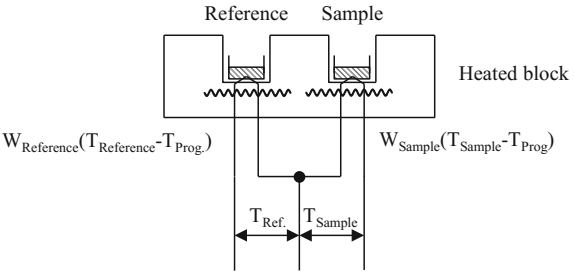


**Fig. 2.77** Schematic representation of a DSC equipment (adapted from [367])

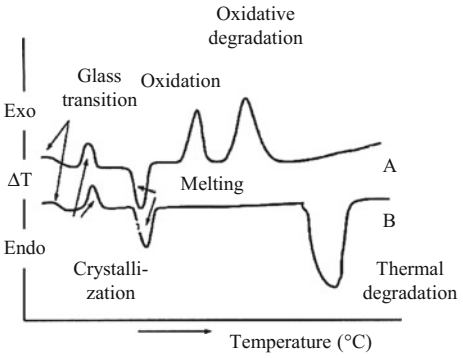


**Fig. 2.78** Schematic representation of typical transitions and reactions of a polymer as a function of increasing $T$, under oxidative (A) and inert (B) atmosphere

One important application of DSC is to determine $T_g$. The shape of the curve in the glass transition region depends on the rate of heating. Therefore, rather than using this part of the curve to calculate $T_g$, the data before (i.e., in the glass state) and after (i.e., in the rubber state) are manipulated (by extrapolation) in order to calculate $T_g$ [367].

Figure 2.78 shows a schematic representation of series of transitions, or events, in a DSC run of a typical polymer as a function of increasing $T$ under oxidative (curve A) and inert (curve B) conditions. The temperature for each event depends on the polymer being investigated, e.g., $T_g$ for elastomers is $\ll 0$ °C, whereas it is typically $\geq$ room temperature for thermoplastic polymers. Starting from the lowest $T$, the first change in the base line is observed at $T_g$; its magnitude is related to the amorphous material content of the polymer. At higher $T$, cold crystallization may be observed; this event can be eliminated by annealing the sample at a fixed temperature below $T_m$, so as to complete the crystallization process. The next peak is that due to crystalline melting, the area of which (after annealing) is directly related to the crystalline polymer content of the sample. These physical transitions are reversible, i.e., they are not accompanied by mass change and cannot, therefore, be followed by TGA. At higher $T$, the polymer may undergo a series of reactions, depending on the conditions of the analysis. It may undergo degradation, resulting in main chain scission, cross-linking, cyclization, and loss of volatiles. Under inert atmosphere, the degradation maybe endothermic, exothermic or both; under

oxidative conditions, the decomposition (oxidation and eventually combustion) is always exothermic. As expected, degradation occurs at much lower T in an oxidative atmosphere [370, 371].

### TGA Analysis

In TGA, the sample is kept under a constant atmosphere, inert or oxidative, and its mass is recorded continuously while the temperature is increased at a constant rate. As a function of increasing *T*, the volatiles adsorbed by the polymer (e.g., water) are driven off; further weight loss occurs at higher *T* is due to sample thermal decomposition and oxidation. Figure 2.79 shows a typical arrangement for the components of a TGA instrument [372]. There are three possibilities to link the sample to the balance, from above, below, or beside. The first is most common, the last is best because it minimizes the heat effects of the furnace, and is less affected by the flow patterns of the gases within the furnace and the chamber. Figure 2.80 is a schematic representation of the Cahn electrobalance of a TGA equipment.

Because of the well-resolved steps of the thermal decomposition of calcium oxalate monohydrate ($CaC_2O_4{\cdot}H_2O$), this compound is often used as a reference for the calibration of mass loss in thermogravimetry, Fig. 2.81. The three steps shown correspond to loss of water to form the anhydrous salt, loss of $CO_2$ to form calcium carbonate and, finally, loss of $CO_2$ to produce CaO. The graph shows these thermal events, plotted as weight loss, TGA trace, and its derivative, DTGA, respectively. The amount of information from TGA has increased massively due to coupling of the latter with techniques that are used to determine the chemical composition of the gases evolved during the run, in particular, FTIR, MS, and GC–MS.

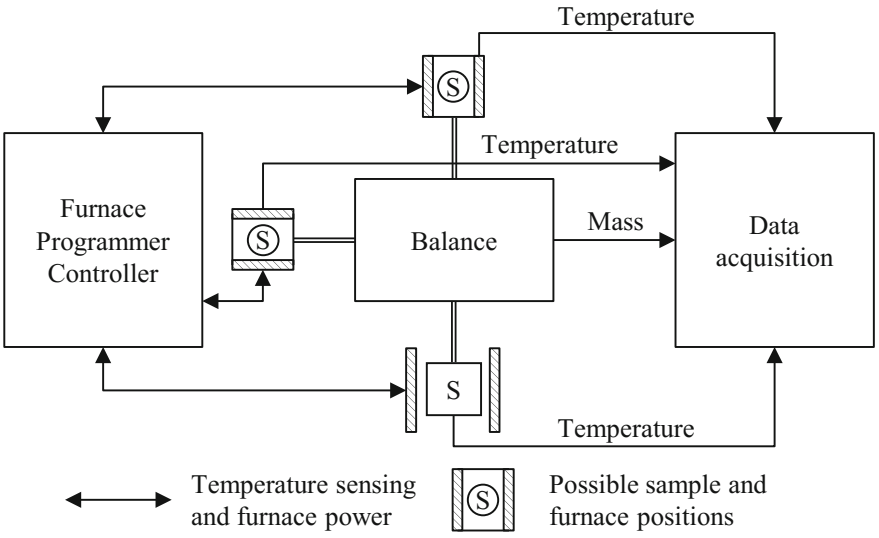


**Fig. 2.79** Typical arrangement for the components of a TGA equipment (adapted from [368, 372])

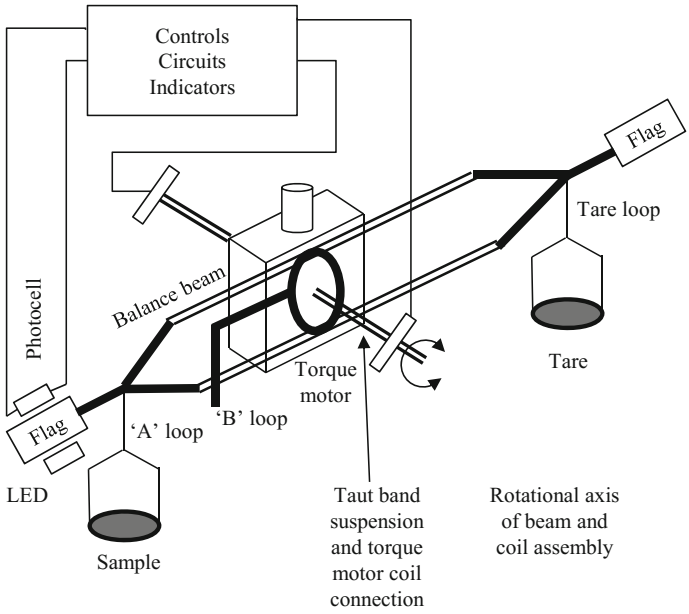


**Fig. 2.80** Schematic representation of the Cahn electrobalance of a TGA equipment (adapted from [373])

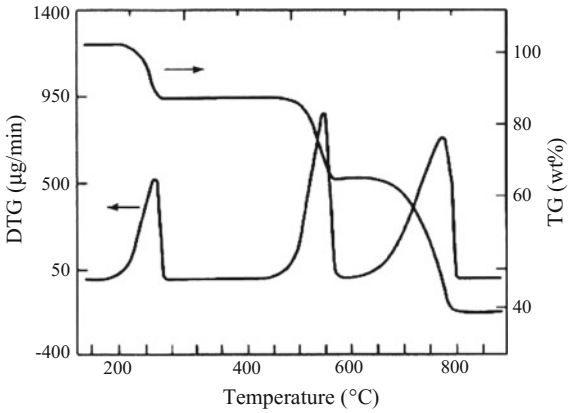


**Fig. 2.81** TGA and DTGA curves for the thermal decomposition of calcium oxalate in argon atmosphere, at 20 °C/min

## Thermomechanical Analysis, TMA

TMA measures the thermal expansion coefficient of a sample in contact with a mechanical probe, as a function of temperature, or time at a constant temperature. Sometimes it is employed for the determination of $T_g$. Figure 2.82 shows typical scheme for TMA apparatus. The probe (P) is made of quartz; its bottom end is flat and rests on the sample, located on the platform at the bottom of the sample holder,

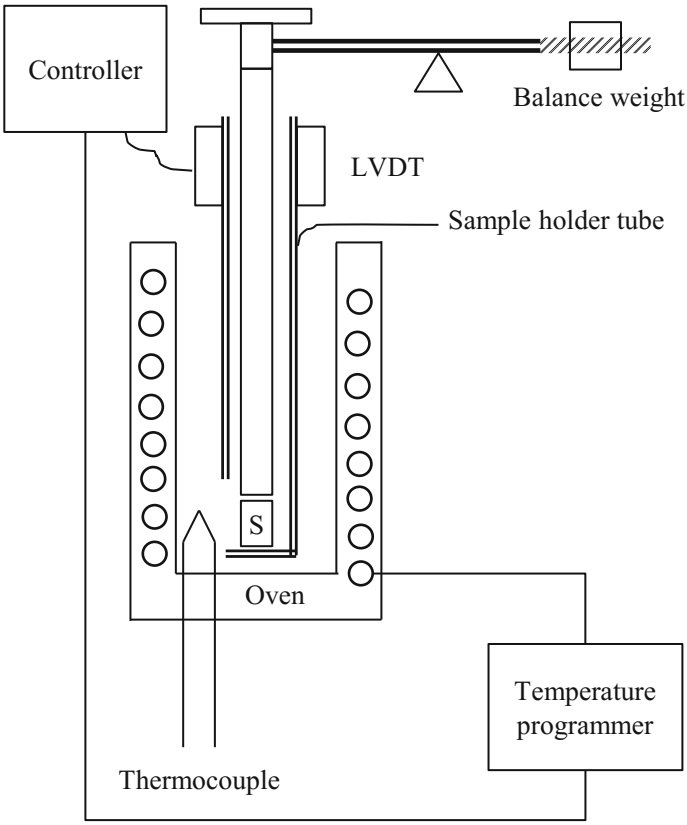


**Fig. 2.82** Schematic representation of a TMA apparatus (adapted from [367])

also made from quartz. The upper end of the probe is attached to a linear variable differential transformer (LVDT), which accurately monitors the variation in the sample (expansion or contraction), and transmits a signal to a display. Usually, the weight of the probe is counterbalanced so that (P) just floats above the surface of the sample. A weight is then added on the top of (P), so that it remains in contact with the sample; the weight is small enough, e.g., 0.5 or 1 g, so that the elastic compression can be neglected. The sample is present in a thermostated enclosure whose temperature can be varied from −100 to +200 °C, by use of liquid nitrogen and heaters. The sample is heated at a constant rate, 1–10 °C/min, and the LVDT signal is plotted against $T$. For $T_g$ measurements, the flat bottom of (P) is replaced by a tip that concentrates on the load applied to the sample. When the temperature passes through $T_g$, the probe starts to penetrate the softened surface, this change is detected on the TMA trace, as depicted in Fig. 2.83.

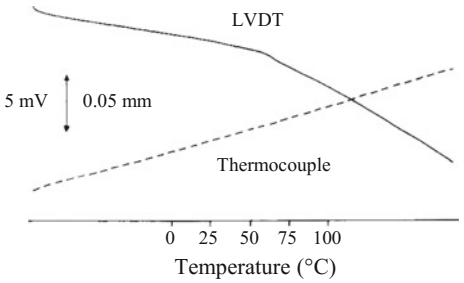


**Fig. 2.83** TMA results for a glass-fiber-filled polyamide cut from an injection molding and measured in the thickness direction. LVDT (solid line) shows the probe displacement; sensitivity 0.05 mm. The broken line shows the thermocouple output; sensitivity 5 mV

### 2.3.6.2 Practical Aspects—Applications of TA to Cellulose and Its Derivatives

As indicated above, the study of the effects of heat on cellulose and its derivatives bears on several important aspects. For example, the interaction between cellulosic fibers and water has a significant impact on the papermaking process in terms of drainage rate, press solids, and drying energy; this interaction is linked to the final strength of the paper products. Heating cellulose affects its total pore volume and pore volume distribution, both factors are crucial to its accessibility [374–376]. Finally, the effects of the substituent on values of $T_g$, $T_m$, $T_{Decomp}$ of dry cellulose derivatives and of the medium and additives on the thermal stability of cellulose solutions in solvents of industrial importance, e.g., NMMO (production of the Lyocell fiber) and ILs, are relevant to several end uses, especially in the textile industry [377–379].

The effects of increasing $T$ on water desorption from cellulose before the threshold of thermal decomposition will be discussed. The properties of water present in cellulose depend on its interaction with the biopolymer. For weak interactions, the melting/crystallization temperature and the corresponding enthalpies of water are not significantly different from those of bulk water. This type of water is defined as free, freezing water, $W_{F,freezing}$. The water molecules that interact strongly with cellulose are classified into bound, freezing; bound, nonfreezing, $W_{B,freezing}$, and $W_{B,nonfreezing}$, respectively. The former type of water exhibits melting/crystallization peaks, and shows considerable supercooling; the peak areas on the heating and cooling cycles are significantly smaller than those of bulk water. For water that interacts very strongly with cellulose, $W_{B,nonfreezing}$, it is frequently impossible to observe the crystallization exotherms, or the melting endotherms. Some literature has referred to $W_{F,freezing}$, $W_{B,freezing}$, and $W_{B,nonfreezing}$, as freezing water, freezing bound water, and nonfreezing water, respectively [380].

These different types of water have been detected for celluloses of distinct types/origins, including MCC [381–383], cotton [384, 385], sisal [386], Viscose rayon [387, 388], and various cellulose powders [202, 389–391]. Figure 2.84 shows an

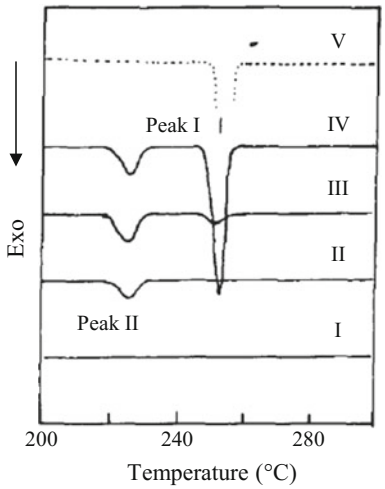


**Fig. 2.84** Schematic DSC cooling curves of sorbed water by a hydrophilic polymer like cellulose as a function of increasing the amount of water present. DSC traces I, and II refer to $W_{B,nonfreezing}$, and $W_{B,freezing}$, respectively. Traces III and IV show both $W_{B,freezing}$, and $W_{F,freezing}$, whereas V is that of bulk water (reprinted from [380], copyright (© 1998), with permission from Elsevier)

example of the detection, and analysis of the types of water present in a hydrophilic polymer like cellulose. The heat evolved is plotted against the total amount of water present in the polymer. At a low water content, curve I, all water present is of the $W_{B,nonfreezing}$ type, accordingly, the first-order transition is not observed. Absorption of more water leads to the formation of $W_{B,freezing}$, whose m.p. is below 0 °C, curve II. Another peak, due to $W_{F,freezing}$ is observed at still higher content of sorbed water, curves III and IV, the m.p. of this water is very similar to that of bulk water, curve V. The relative concentration of each type of water can be calculated from TGA, based on the total amount of water and the ratios of the peak areas, attributed to each type [392–394].

Figure 2.85a shows the dependence of $W_{B,nonfreezing}$ and $W_{B,freezing}$ on $I_c$ (X-ray) of cellulose, whereas Fig. 2.85b shows the number of water molecules of each type/AGU. The fact that $W_{B,freezing}$ decreases as a function of increasing $I_c$ indicates that this type of water interacts mainly with the amorphous region of cellulose. From curve II of part (b), the number of $W_{B,freezing}$ is shown to be practically constant at ca. 3.4 molecules, i.e., one water/each OH group of the AGU.

Other examples of the use of TA analysis in order to determine the distribution of the different types of water present in cellulosic materials include: cellulose, its esters and ethers [381], cellulose sulfonate, CMC [392], cellulose acetophthalate, acetosuccinate, CMC, and several ethers [390, 396], never-dried cotton fibers [393], and regenerated cellulose membrane [397]. From some of these results, we have calculated the correlations shown in Table 2.24.

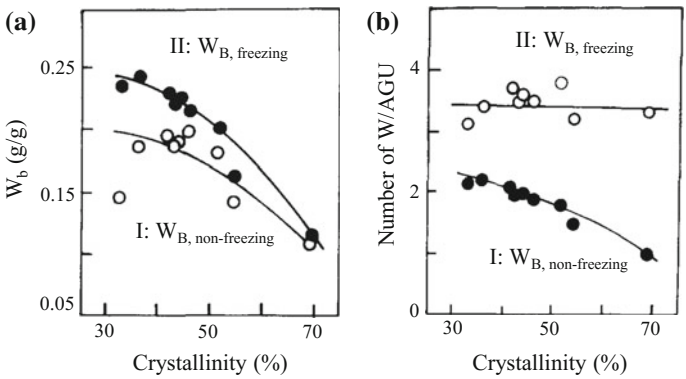


**Fig. 2.85** **a** The dependence of $W_{B,nonfreezing}$ and $W_{B,freezing}$ on $I_c$ of cellulose and **b** the dependence of number of $W_{B,nonfreezing}$/AGU, and $W_{B,freezing}$/AGU on $I_c$ of cellulose (redrawn from [395])

**Table 2.24** TA-based correlations of the types/properties of water present in cellulosic materials

| Material | Water type/property | Correlation | References |
|---|---|---|---|
| Cellulose | $W_{B,nonfreezing}$ | $W_{B,nonfreezing} = 0.355 + 0.005\ e^{(RH\%/18.274)}$ | [392] |
| CMC-acid form | $W_{B,nonfreezing}$ | $W_{B,nonfreezing} = 0.451 + 0.002\ e^{(RH\%/14.997)}$ | [392] |
| Na CMC salt | $W_{B,nonfreezing}$ | $W_{B,nonfreezing} = 0.883 + 0.210\ e^{(RH\%/29.064)}$ | [392] |
| Cellulose sulfonate-Na salt | $W_{B,nonfreezing}$ | $W_{B,nonfreezing} = 0.003 + 0.032$ (RH%) | [392] |
| Cotton, never dried | $W_{Total}$ | $W_{Total} = 120.529 - 1.832$ DPA | [393] |
| Cotton, never dried | $W_{B,nonfreezing}$ | $W_{B,nonfreezing} = 115.256 - 1.761$ DPA | [393] |
| Cellulose, kraft pulp | $T_m$ of $W_{B,freezing}$ | $T_m = 39.519\ e^{(pore\ diameter/3.218)}$ | [398] |

Table 2.24 shows some interesting results. For example, the interactions of $W_{B,nonfreezing}$ with ionic cellulosic materials are markedly dependent on the ions present, including the cation ($H^+$ vs. $Na^+$ for CMC) and the anion (carboxylate vs. sulfonate). The concentrations of all types of water in never-dried cotton (data for $W_{B,freezing}$ not shown) decrease linearly as a function of increasing DPA. The dependence on the ionic substituents in cellulose (e.g., $COO^-$ or $Na^+$) may be related to the hydration of these ions, as depicted in Fig. 2.86.

The last entry of Table 2.23 can be explained as follows: When water is evaporated from the pores of cellulose, they collapse due to the capillary forces with the high surface tension of water. Which pores collapse depends on their size and the ability of pore wall to resist collapse. The latter factor seems to be more

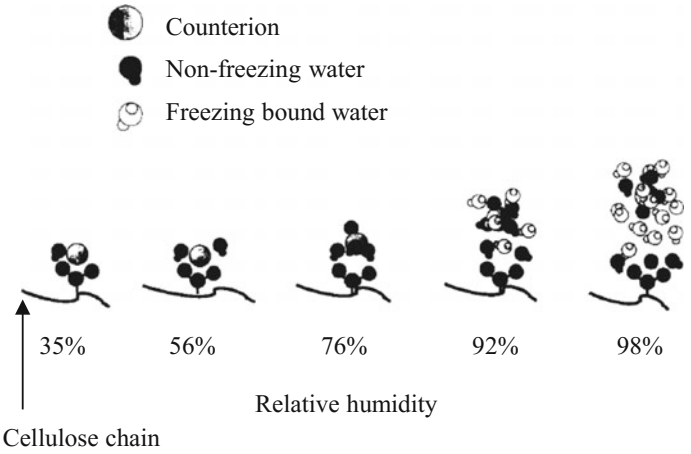


**Fig. 2.86** A schematic representation of the hydration of CMC as a function of RH%. The initial water reacts strongly with CMC, presumably by forming hydrogen bonds between the two head ions; leading to the formation of $W_{B,nonfreezing}$. The formation of $W_{B,freezing}$ is associated with the hydration of the cation (reprinted from [392], copyright (© 1996) with permission from Elsevier)

important, hence larger pores collapse first [398]. The same conclusion has been corroborated by X-ray scattering measurements on Tencel fibers, as shown schematically in Fig. 2.87 [375]. Part (a) depicts the microstructure of a water-swollen Tencel fiber, parallel to the fiber axis, whereas part (b) shows the pore collapse that accompanies fiber drying.

The second piece of information, which is usually obtained from TA analysis, is the value of $T_g$, $T_m$, and $T_{Decomp}$ and their correlation with the molecular structure of cellulose derivatives, in particular the number of carbon atoms in the substituent, Nc, and the activation energies for decomposition. Based on published data, the correlations shown in Table 2.25 have been calculated.

These correlations bear on the applications of cellulose derivatives because $T_g$, $T_m$ decrease, and $T_{Decomp}$ increase as a function of DS (for derivatives with a single substituent) and Nc for a homologous series of substituents [361, 403]. An interesting result is the $T_m$ of mixed esters. In principle, two $T_m$ should be observed related to the acyl moieties present. This may not always be the case. Extensive thermal annealing may be required in order to observe two $T_m$. Whereas $T_m$ of 159 and 254 °C, and 160 and 259 °C were observed for acetate/propionate (total DS = 2.8; $DS_{Ac}$ = 1.5) and acetate/butyrate (total DS = 2.4 $DS_{acetate}$ = 1.4), respectively, single $T_m$ values were observed for acetate/pentanoate and acetate/hexanoate esters, 158 and 143 °C, respectively [34]. The observation of two $T_m$ may suggest the existence of two crystalline morphologies, a consequence of chemically distinct polymer segments, i.e., blocks. The precise source and nature of morphologies giving rise to dual $T_m$ remains unexplored. Likewise, the values of

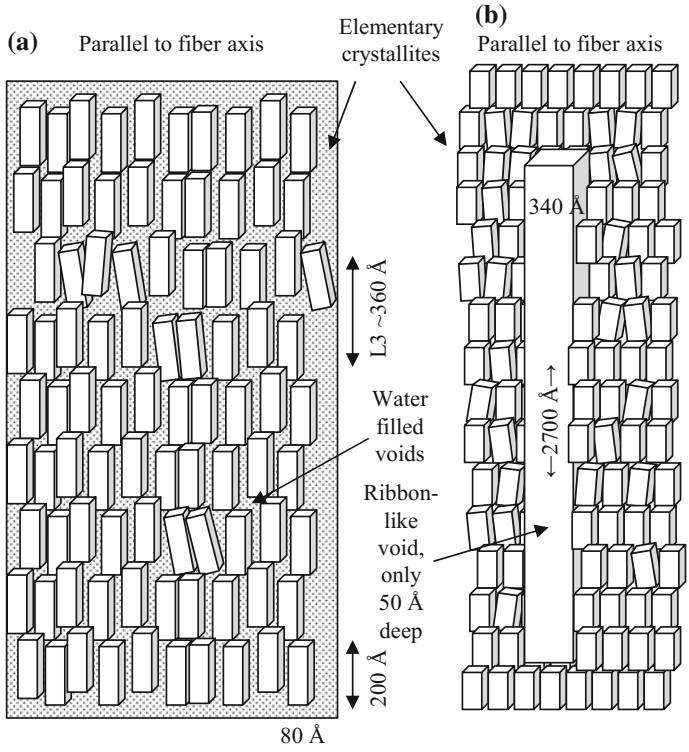


**Fig. 2.87** Schematic representation of the effect of heating on the microstructure of a Tencel Fiber. Parts **a** and **b** refer to water-swollen and dried fibers, respectively (adapted from [375])

**Table 2.25** TA-based correlations between the properties and structure of cellulose derivatives

| Derivative | Property correlated | Correlation | References |
|---|---|---|---|
| Triesters | $T_g$ | $T_g = 86.084 + 536.442\ e^{(-Nc/2.2679)}$ | [363, 399] |
| Triesters | $T_m$ | $T_m = 195.554 + 1565.128\ e^{(-Nc/0.728)}$ | [34] |
| Acetates, different DS | $T_g$ | $T_g = 523 - 20.3$ DS | [400, 401] |
| Acetates, different DS | $T_g$ | $T_g = 230.5 - 19.0$ DS<br>$r^2 = 0.9939$ | [365] |
| Acetates, different DS | $T_m$ | $T_m = 600.9 - 358.0 \times DS + 85.53 \times DS^2$<br>$r^2 = 0.9839$ | [365] |
| Triesters | $T_{Decomp}$ | $T_{Decomp} = 192.75 + 1.25$ Nc | [364] |
| Acetates, different DS | $T_{Decomp}$ | $T_{Decomp} = 353.7 - 364.9\ e^{(-DS/0.831)}$<br>$r^2 = 0.9950$ | [365] |
| Tosylates | $T_{Decomp}$ | $T_{Decomp} = 137.550 + 23.004$ DS | [384] |
| Ethers | $T_g$ | $T_g = 79.615 + 75.659\ e^{(-DS/0.476)}$ | [402] |

(partial) DS that dictate the formation of single, as opposed to dual crystalline morphology is still unknown [345, 404].

In addition to the onset of degradation of cellulose samples at temperatures >300 °C, TA analysis has been employed in order to determine rate constants, hence the energy of activation of these decomposition reactions, both in the solid state and in solvents of industrial importance, e.g., NMMO and ILs [378, 379]. This use has received attention and criticism, because the values obtained depend on the experimental conditions including, for solids, sample mass and shape, gas flow rate, and the heating rate [405, 406]. The several equations that are employed in order to calculate the activation energy of decomposition of polymers has been listed along with some results of cellulose derivatives/starch blends [386, 407]. Examples of the calculations of the activation energies of celluloses and its derivatives have been published [202, 384, 387, 389, 391].

## References

1. Payen ACR (1838) Mémoir sur la composition du tissue propre des plantes et du ligneux. Hebd Seances Acad Sci 7:1052
2. Payen ACR (1838) Hebd Seances Acad Sci 7:1125
3. Rao VSR, Sundararajan PR, Ramakrishnan C, Ramachandran GN (1957) In: Ramachandran GN (ed) Conformation of biopolymers, vol 1. Academic Press, New York, p 721
4. Krässig HA (1993) Cellulose: structure, accessibility and reactivity. Gordon and Breach, Yverdon
5. Pérez S, Mazeau K (2005) In: Dumitriu S (ed) Polysaccharides: structural diversity and functional versatility, vol 1. Marcel Dekker, New York, p 41
6. Fardim P, Holmbom B (2003) Fast determination of anionic groups in different pulp fibers by methylene blue sorption. Tappi J 2:28–32
7. Klemm D, Philipp B, Heinze T et al (1998) Comprehensive cellulose chemistry, vol I. Wiley–VCH, Weinheim, p 236
8. Roehrling J, Potthast A, Rosenau T, Lange T, Ebner G, Sixta H, Kosma P (2002) A novel method for the determination of carbonyl groups in cellulosics by fluorescence labeling. 1. Method development. Biomacromolecules 3:959–968
9. Bohrn R, Potthast A, Schiehser S, Rosenau T, Sixta H, Kosma P (2006) The FDAM method: determination of carboxyl profiles in cellulosic materials by combining group-selective fluorescence labeling with GPC. Biomacromolecules 7:1743–1750
10. Kamide K, Okajima K, Kowsaka K, Matsui T (1985) CP/MASS [cross-polarization/magic angle sample spinning] carbon-13 NMR spectra of cellulose solids: an explanation by the intramolecular hydrogen bond concept. Polym J 17:701–706 (Tokyo, Japan)
11. Liang CY, Marchessault RH (1959) Infrared spectra of crystalline polysaccharides. I. Hydrogen bonds in native celluloses. J Polym Sci 37:385–395
12. Michell AJ (1988) Second derivative FTIR spectra of celluloses I and II and related mono- and oligosaccharides. Carbohydr Res 173:185–195
13. Tashiro K, Kobayashi M (1991) Theoretical evaluation of three-dimensional elastic constants of native and regenerated celluloses: role of hydrogen bonds. Polymer 32:1516–1526
14. Gardner KH, Blackwell J (1974) Structure of native cellulose. Biopolymers 13:1975–2001

15. Nishiyama Y, Langan P, Chanzy H (2002) Crystal structure and hydrogen-bonding system in cellulose $I_\beta$ from synchrotron x-ray and neutron fiber diffraction. J Am Chem Soc 124:9074–9082
16. Irklei VM, Kleiner YY, Vavrinyuk OS, Gal'braikh LS (2005) Kinetics of degradation of cellulose in basic medium. Fibre Chem 37:452–458
17. El Seoud OA, Marson GA, Giacco GT, Frollini E (2000) An efficient, one-pot acylation of cellulose under homogeneous reaction conditions. Macromol Chem Phys 201:882–889
18. Zhang H, Wu J, Zhang J, He J (2005) 1-Allyl-3-methylimidazolium chloride room temperature ionic liquid: a new and powerful nonderivatizing solvent for cellulose. Macromolecules 38:8272–8277
19. Fidale LC, Possidonio S, El Seoud OA (2009) Application of 1-allyl-3-(1-butyl)imidazolium chloride in the synthesis of cellulose esters: properties of the ionic liquid, and comparison with other solvents. Macromol Biosci 9:813–821
20. Heinze T, Dorn S, Schoebitz M, Liebert T, Koehler S, Meister F (2008) Interactions of ionic liquids with polysaccharides—2: cellulose. Macromol Symp 262:8–22
21. Barnes HA, Hutton JF, Walters K (1989) An introduction to rheology. Elsevier, Amsterdam chapter 2
22. Wu C-S (ed) (1995) Handbook of size exclusion chromatography. Marcel Dekker, New York
23. Elias H-G (1997) An introduction to polymer science. VCH, Weinheim
24. Hunt BJ, James MI (eds) (1997) Polymer characterization. Chapman and Hall, London
25. Hiemenz PC, Rajagopalan R (1997) Principles of colloid and surface chemistry, 3rd edn. Marcel Dekker, New York, p 145, 193
26. Mori S, Barth HG (1999) Size exclusion chromatography. Springer, Berlin
27. Campbell D, Pethrick RA, White JR (2000) Polymer characterization: physical techniques, 2nd edn. Stanley Thornes, Cheltenham
28. Wu C (2008) In: Characterization and analysis of polymers. Wiley, New York, p 211
29. Dawkins JV (2008) Characterization and analysis of polymers. Wiley, New York, p 230
30. Rosen MR (1979) Characterization of non-Newtonian flow. Polym-Plast Technol Eng 12: 1–42
31. Aono H, Tatsumi D, Matsumoto T (2006) Scaling analysis of cotton cellulose/LiCl DMAc solution using light scattering and rheological measurements. J Polym Sci Part B Polym Phys 44:2155–2160
32. Kasaai MR (2002) Comparison of various solvents for determination of intrinsic viscosity and viscometric constants for cellulose. J Appl Polym Sci 86:2189–2193
33. Haward SJ, Sharma V, Butts CP, McKinley GH, Rahatekar SS (2012) Shear and extensional rheology of cellulose/ionic liquid solutions. Biomacromolecules 13:1688–1699
34. Possidonio S, Fidale LC, El Seoud OA (2010) Microwave-assisted derivatization of cellulose in an ionic liquid: an efficient, expedient synthesis of simple and mixed carboxylic esters. J Polym Sci Part A Polym Chem 48:134–143
35. Kadla JF, Korehei R (2010) Effect of hydrophilic and hydrophobic interactions on the rheological behavior and microstructure of a ternary cellulose acetate system. Biomacromolecules 11:1074–1081
36. Tamai N, Aono H, Tatsumi D, Matsumoto T (2003) Differences in rheological properties of solutions of plant and bacterial cellulose in LiCl/N, N-dimethylacetamide. J Soc Rheol 31:119–130
37. Kuang Q-L, Zhao J-C, Niu Y-H, Zhang J, Wang Z-H (2008) Celluloses in an ionic liquid: the rheological properties of the solutions spanning the dilute and semidilute regimes. J Phys Chem B 112:10234–10240
38. Gericke M, Schlufter K, Liebert T, Heinze T, Budtova T (2009) Rheological properties of cellulose/ionic liquid solutions: from dilute to concentrated states. Biomacromolecules 10:1188–1194
39. Standard Test Methods for Intrinsics Viscosity of Cellulose (2001) ASTM D1795–94

40. Kamide K, Miyazaki Y, Abe T (1979) Mark-Houwink-Sakurada equations of cellulose triacetate in various solvents. Makromol Chem 180:2801–2805
41. Kuhn W, Kuhn H (1943) The coiling of fiber molecules in flowing solutions. Helv Chim Acta 26:1394–1465
42. Kuhn W, Kuhn H (1945) Significance of limited free rotation for the viscosity and flow birefringence of solutions of fiber molecules. I Helv Chim Acta 28:1553–1579
43. Kuhn W, Kuhn H (1947) Diffusion, Sedimentation und Viskositat bei Losungen verzweigter Fadenmolekel. Helv Chim Acta 30:1233–1256
44. Jolley LJ (1939) The solution of chemically modified cotton cellulose in alkaline solutions. V. The solvent action of solutions of cupric hydroxide in aqueous ethylenediamine. J Text Inst 30:T22–T41
45. Lovell EL (1944) Viscometric chain length of wood cellulose in Triton F solution. Ind Eng Chem Anal Ed 16:683–685
46. Henley D (1960) The cellulose solvent Cadoxen, its preparation, and a viscometric relationship with cupriethylenediamine. Sven Papperstidn 63:143–146
47. Claesson S, Bergmann W, Jayme G (1959) Solutions of cellulose in an alkaline iron-tartaric acid-sodium complex. Sven Papperstidn 62:141–155
48. Strlic M, Kolar J, Zigon M, Pihlar B (1998) Evaluation of size-exclusion chromatography and viscometry for the determination of molecular masses of oxidized cellulose. J Chromatogr A 805:93–99
49. Marx-Figini M (1987) Evaluation of the accessibility of celluloses by the intrinsic viscosity ratio [η]cellulose nitrate acetone/[η]unsubstituted cellulose ethylenediamine-copper II-complex. Polym Bull 17:225–229
50. Burchard W, Husemann E (1961) A comparative structure analysis of cellulose and amylose tricarbanilates in solution. Makromol Chem 44–46:358–387
51. Philipp B, Linow KJ (1970) Interpretation of the chain length differences in the cuoxam and nitrate degree of polymerization of cellulose on the basis of absolute molecular weight determinations of some cellulose derivatives. Faserforsch Textiltech 21:13–20
52. Danhelka J, Kossler I, Bohackova V (1976) Determination of molecular weight distribution of cellulose by conversion into tricarbanilate and fractionation. J Polym Sci Polym Chem Ed 14:287–298
53. Marx-Figini M (1978) Significance of the intrinsic viscosity ratio of unsubstituted and nitrated cellulose in different solvents. Angew Makromol Chem 72:161–171
54. Terbojevich M, Cosani A, Conio G, Ciferri A, Bianchi E (1985) Mesophase formation and chain rigidity in cellulose and derivatives. 3. Aggregation of cellulose in N, N-dimethylacetamide-lithium chloride. Macromolecules 18:640–646
55. Ciacco GT, Morgado DL, Frollini E, Possidonio S, El Seoud OA (2010) Some aspects of acetylation of untreated and mercerized sisal cellulose. J Braz Chem Soc 21:71–77
56. Kuzmina O, Sashina E, Troshenkowa S, Wawro D (2010) Dissolved state of cellulose in ionic liquids—the impact of water. Fibres Text East Eur 18:32–37
57. Ramos LA, Morgado DL, El Seoud OA, da Silva VC, Frollini E (2011) Acetylation of cellulose in LiCl-N, N-dimethylacetamide: first report on the correlation between the reaction efficiency and the aggregation number of dissolved cellulose. Cellulose 18:385–392
58. McCormick CL, Callais PA, Hutchinson BH Jr (1985) Solution studies of cellulose in lithium chloride and N, N-dimethylacetamide. Macromolecules 18:2394–2401
59. Terbojevich M, Cosani A, Camilot M, Focher B (1995) Solution studies of cellulose tricarbanilates obtained in homogeneous phase. J Appl Polym Sci 55:1663–1671
60. Röder T, Moslinger R, Mais U, Morgenstern B, Glatter O (2003) Characterization of the solution structure of technical cellulose solutions. Lenzinger Ber 82:118–127
61. Kim SO, Shin WJ, Cho H, Kim BC, Chung IJ (1999) Rheological investigation on the anisotropic phase of cellulose-MMNO/$H_2O$ solution system. Polymer 40:6443–6450
62. Tswett M (1906) Physicochemical studies over the chlorophyll. The adsorptions. Ber Dtsch Bot Ges 24:316–323

63. Martin AJP (1957) In: Desty DH (ed) Vapour phase chromatography (1956 London symposium) Butterworth, London, p 1
64. Golay MJE (1957) In: Desty DH (ed) Vapour phase chromatography (1956 London Symposium) Butterworth, London, p 36
65. Lathe GH, Ruthven CRJ Jr (1956) Separation of substances and estimation of their relative molecular sizes by the use of columns of starch in water. Biochem J 62:665–674
66. Porath J, Flodin P (1959) Gel filtration: a method for desalting and group separation. Nature 183:1657–1659
67. Moore JC (1964) Gel permeation chromatography. I. New method for molecular-weight distribution of high polymers. J Polym Sci Part B 2:835–843
68. Gallot-Grubisic Z, Rempp P, Benoit H (1967) Universal calibration for gel permeation chromatography. J Polym Sci Polym Lett Ed 5:753–759
69. Dawkins JV (1984) Calibration of separation systems. In: Janca J (ed) Steric exclusion liquid chromatography of polymers. Marcel Dekker, New York, pp 53–116
70. Connor AH (1995) In: Wu C-S (ed) Handbook of size exclusion chromatography. Marcel Dekker, New York, pp 331–352
71. Bikova T, Treimanis A (2002) Problems of the MMD analysis of cellulose by SEC using DMA/LiCl: a review. Carbohydr Polym 48:23–28
72. Eremeeva T (2003) Size-exclusion chromatography of enzymatically treated cellulose and related polysaccharides: a review. J Biochem Biophys Methods 56:253–264 and references cited therein
73. Sollinger S, Diamantoglou M (1996) Spectroscopical characterization of cellulose derivatives. Papier (Darmstadt) 12:691–700
74. Bao YT, Bose A, Ladisch MR, Tsao GT (1980) New approach to aqueous gel permeation chromatography of nonderivatized cellulose. J Appl Polym Sci 25:263–275
75. Sjöholm E, Gustafsson K, Kolar J, Pettersson B (1994) Characterization of chemical pulps by SEC. In: Proceedings of the 3rd European workshop on lignocellulosics and pulp, Stockholm, pp 246–250
76. Hortling B, Färm P, Sundquist J (1994) Investigations of pulp components (polysaccharides, residual lignins) using HP/SEC system with viscometric RI and UV detectors. In: Proceedings of the 3rd European workshop on lignocellulosics and pulp, Stockholm, pp 256–259
77. Rahkamo L, Viikari L, Buchert J, Paakkari T, Suortti T (1998) Enzymic and alkaline treatments of hardwood dissolving pulp. Cellulose 5:79–88
78. Timpa JD (1991) Application of universal calibration in gel permeation chromatography for molecular weight determinations of plant cell wall polymers: cotton fiber. J Agric Food Chem 39:270–275
79. Silva AA, Laver ML (1997) Molecular weight characterization of wood pulp cellulose: dissolution and size exclusion chromatographic analysis. Tappi J 80:173–180
80. Kennedy JF, Rivera ZS, White CA, Lloyd LL, Warner FP (1990) Molecular weight characterization of underivatized cellulose by GPC using lithium chloride-dimethylacetamide solvent system. Cellul Chem Technol 24:319–325
81. Sjöholm E, Gustafsson K, Eriksson B, Brown W, Colmsjö A (2000) Aggregation of cellulose in lithium chloride/N, N-dimethylacetamide. Carbohydr Polym 41:153–161
82. Berthold F, Gustafsson K, Berggren R, Sjöholm E, Lindström M (2004) Dissolution of softwood kraft pulps by direct derivatization in lithium chloride/N, N-dimethylacetamide. J Appl Polym Sci 94:424–431
83. Striegel AM, Timpa JD (1995) Molecular characterization of polysaccharides dissolved in N, N-dimethylacetamide-lithium chloride by gel-permeation chromatography. Carbohydr Res 267:271–290
84. Sjöholm E, Gustafsson K, Berthold F, Colmsjö A (2000) Influence of the carbohydrate composition on the molecular weight distribution of kraft pulps. Carbohydr Polym 41:1–7

85. Brewer RJ, Tanghe LJ, Baily S (1969) Gel-permeation chromatography of cellulose esters. Effect of average degree of polymerization, degree of substitution, substituent size, and primary hydroxyl content. J Polym Sci Part A-1 Polym Chem 7:1635–1645
86. Schurz J, Haas J, Kraessig H (1971) Gel permeation chromatography of cellulose trinitrate in tetrahydrofuran. II Cellul Chem Technol 5:269–284
87. Kulicke WM, Clasen C, Lohman C (2005) Characterization of water-soluble cellulose derivatives in terms of the molar mass and particle size as well as their distribution. Macromol Symp 223:151–174
88. Ramos L (2005) Correlation between the physic-chemical properties of cellulose and its derivatization in LiCl/DMAc and DMSO/TBAF.3$H_2O$. Ph.D. thesis, University of São Paulo
89. Saake B, Horner S, Kruse T, Puls J, Liebert T, Heinze T (2000) Detailed investigation on the molecular structure of carboxymethyl cellulose with unusual substitution pattern by means of an enzyme-supported analysis. Macromol Chem Phys 201:1996–2002
90. Brown W, Henely D, Ohman J (1963) Studies on cellulose derivatives. I. The dimensions and configuration of sodium carboxymethyl cellulose in cadoxene and the influence of the degree of substitution. Makromol Chem 62:164–182
91. Eremeeva TE, Bykova TO (1998) SEC of mono-carboxymethyl cellulose (CMC) in a wide range of pH; Mark-Houwink constants. Carbohydr Polym 36:319–326
92. Rinaudo M, Danhelka J, Milas MA (1993) A new approach to characterizing carboxymethylcelluloses by size-exclusion chromatography. Carbohydr Polym 21:1–5
93. Wittgren B, Wahlund KG (2000) Size characterization of modified celluloses in various solvents using flow FFF-MALS and MB-MALS. Carbohydr Polym 43:63–73
94. Yokoyama W, Renner-Nantz JJ, Shoemaker CF (1998) Starch molecular mass and size by size-exclusion chromatography in DMSO-LiBr coupled with multiple angle laser light scattering. Cereal Chem 75:530–535
95. Berry GC (1966) Thermodynamic and conformational properties of polystyrene. I. Light-scattering studies on dilute solutions of linear polystyrenes. J Chem Phys 44:4550–4564
96. Andersson M, Wittgren B, Wahlund KG (2001) Ultrahigh molar mass component detected in ethyl hydroxyethyl cellulose by asymmetrical flow field-flow fractionation coupled to multi-angle light scattering. Anal Chem 73:4852–4861
97. Evans DF, Wennerström A (1999) The colloidal domain, 2nd edn. Weinheim, Wiley-VCH
98. Saalwaechter K, Burchard W, Kluefers P, Kettenbach G, Mayer P, Klemm D, Dugarmaa S (2000) Cellulose solutions in water containing metal complexes. Macromolecules 33:4094–4107
99. Röder T, Morgenstern B, Schelosky N, Glatter O (2001) Solutions of cellulose in N, N-dimethylacetamide/lithium chloride studied by light scattering methods. Polymer 42:6765–6773
100. Isogai A, Yanagisawa M (2008) In: Hu TQ (ed) Characterization of lignocellulosic materials. Blackwell Publishing, Oxford, pp 206–226
101. Fink HP, Weigel P, Purz HJ, Ganster J (2001) Structure formation of regenerated cellulose materials from NMMO-solutions. Prog Polym Sci 26:1473–1524 and references cited therein
102. Morgenstern B, Röder T (1998) Investigations on structures in the system cellulose/N-methylmorpholine N-oxide monohydrate by means of light scattering measurements. Papier (Heidelberg) 52:713–717
103. Röder T, Morgenstern B (1999) The influence of activation on the solution state of cellulose dissolved in N-methylmorpholine-N-oxide-monohydrate. Polymer 40:4143–4147
104. Trulove PC, Reichert WM, De Long HC, Kline SR, Rahatekar SS, Gilman JW, Muthukumar M (2009) The structure and dynamics of silk and cellulose dissolved in ionic liquids. ECS Trans 16:111–117
105. El Seoud OA, Heinze T (2005) Organic esters of cellulose: new perspectives for old polymers. Adv Polym Sci 186:103–149

106. Schulz L, Burchard W, Dönges R (1998) Evidence of supramolecular structures of cellulose derivatives in solution. In: Heinze T, Glasser WG (eds) Cellulose derivatives: modification, characterization, and nanostructures, ACS Symposium SERIES 688, Washington DC, pp 218–238
107. Morgenstern B, Kammer H-W (1998) On the particulate structure of cellulose solutions. Polymer 40:1299–1304
108. Menger FM (1993) Enzyme reactivity from an organic perspective. Acc Chem Res 26:206–212
109. Tsunashima Y, Kawanishi H, Horii F (2002) Reorganization of dynamic self-assemblies of cellulose diacetate in solution: dynamical critical-like fluctuations in the lower critical solution temperature system. Biomacromolecules 3:1276–1285
110. Schulz L, Seger B, Burchard W (2000) Structures of cellulose in solution. Macromol Chem Phys 201:2008–2022
111. Nilsson S, Sundeloef L-O, Bedrich Porsch (1995) On the characterization principles of some technically important water-soluble nonionic cellulose derivatives. Carbohydr Polym 28:265–275
112. Wittgren B, Porsch B (2002) Molar mass distribution of hydroxypropyl cellulose by size exclusion chromatography with dual light scattering and refractometric detection. Carbohydr Polym 49:457–469
113. Wittgren B, Stefansson M, Porsch B (2005) Interactions between sodium dodecyl sulphate and non-ionic cellulose derivatives studied by size exclusion chromatography with online multi-angle light scattering and refractometric detection. J Chromatogr A 1082:166–175
114. Dupont A-L, Mortha G (2006) Comparative evaluation of size-exclusion chromatography and viscometry for the characterisation of cellulose. J Chromatogr A 1026:129–141
115. Fukasawa M, Obara S (2004) Molecular weight determination of hypromellose acetate succinate (HPMCAS) using size exclusion chromatography with a multi-angle laser light scattering detector. Chem Pharm Bull 52:1391–1393
116. Schagerlöf H, Richardson S, Momcilovic D, Brinkmalm G, Wittgren B, Tjerneld F (2006) Characterization of chemical substitution of hydroxypropyl cellulose using enzymatic degradation. Biomacromolecules 7:80–85
117. Schittenhelm N, Kulicke W-M (2000) Producing homologous series of molar masses for establishing structure-property relationships with the aid of ultrasonic degradation. Macromol Chem Phys 201:1976–1984
118. Clasen C, Kulicke W-M (2001) Determination of viscoelastic and rheo-optical material functions of water-soluble cellulose derivatives. Prog Polym Sci 26:1839–1919 and references cited therein
119. Elias H-G (1997) An introduction to polymer science. VCH, p 275
120. Scherrer P (1918) Estimation of the size and internal structure of colloidal particles by means of Roentgen rays. Nachr Ges Wiss Gottingen 96–100, CAN 13:13268
121. Watanabe S, Hayashi J, Akahori T (1974) Molecular chain conformation and crystallite structure of cellulose. I. Fine structure of rayon fibers. J Polym Sci Polym Chem Ed 12:1065–1087
122. Hattula T (1987) Crystallization and disordering of cellulose in dissolving pulp during heterogeneous acid hydrolysis. Pap Puu 69:92–95
123. Lenz J, Schurz J (1990) Fibrillar structure and deformation behavior of regenerated cellulose fibers. I. Methods of investigation and crystallite dimensions. Cellul Chem Technol 24:3–21
124. Lenz J, Schurz J, Wrentschur E, Geymayer W (1986) Dimensions of crystalline regions in regenerated cellulosic fibers. Angew Makromol Chem 138:1–19
125. Ioyelovich MY (1991) Supermolecular structure of native and isolated cellulose. Polym Sci 33:1670–1676
126. Bansal P, Hall M, Realff MJ, Lee JH, Bommarius AS (2010) Multivariate statistical analysis of X-ray data from cellulose: a new method to determine degree of crystallinity and predict hydrolysis rates. Bioresour Technol 101:4461–4471

127. Driemeier C, Calligaris GA (2011) Theoretical and experimental developments for accurate determination of crystallinity of cellulose I materials. J Appl Crystallogr 44:184–192
128. Lenz J, Schurz J, Wrentschur E (1988) The length of the crystalline domains in fibers of regenerated cellulose. Determination of the crystallite length of cellulose II by means of wide-angle X-ray diffraction and transmission electron microscopy. Holzforschung 42:117–122
129. Krässig HA (1992) Cellulose: Structure, accessibility, and reactivity. Gordon and Breach, Yverdon, p 66
130. Ruland W (1961) X-ray determination of crystallinity and diffuse disorder scattering. Acta Crystallogr 14:1180–1185
131. Vonk CG (1973) Computerization of Ruland's x-ray method for determination of the crystallinity in polymers. J Appl Crystallogr 6:148–152
132. Segal L, Creely JJ, Markin AE Jr, Conrad CM (1959) An empirical method for estimating the degree of crystallinity of native cellulose using the x-ray diffractometer. Text Res J 29:786–794
133. Ant-Wuorinen O, Visapaa OA (1962) X-ray diffractometric method for determination of the crystallinity of cellulose. Norelco Rep 9:47–52
134. Buschle-Diller G, Zeronian SH (1992) Enhancing the reactivity and strength of cotton fibers. J Appl Polym Sci 45:967–979
135. Krischner H (1980) Einführung in die Röntgenfeinstrukturanalyse, Friedr. Wieweg Sohn, Braunschweig, p 28, 29, 43
136. Hofmann D, Fink HP, Philipp B (1989) Lateral crystallite size and lattice distortions in cellulose II samples of different origin. Polymer 30:237–241
137. Kasai K, Kakudo M (2005) X-ray diffraction by macromolcules. Springer, Berlin, p 163
138. Chandrasekaran R (1997) Molecular architecture of polysaccharide helices in oriented fibers. In: Horton D (ed) Advances in carbohydrate chemistry and biochemistry. Academic Press, San Diego, pp 311–439
139. Atalla RH, VanderHart DL (1984) Native cellulose: a composite of two distinct crystalline forms. Science (Washington, DC, United States) 223(4633):283–285
140. VanderHart DL, Atalla RH (1984) Studies of microstructure in native celluloses using solid-state carbon-13 NMR. Macromolecules 17:1465–1472
141. Belton PS, Tanner SF, Cartier N, Chanzy H (1989) High-resolution solid-state carbon-13 nuclear magnetic resonance spectroscopy of tunicin, an animal cellulose. Macromolecules 22:1615–1617
142. Nishiyama Y, Sugiyama J, Chanzy H, Langan P (2003) Crystal structure and hydrogen-bonding system in cellulose $I_\alpha$ from synchrotron X-ray and neutron fiber diffraction. J Am Chem Soc 125:14300–14306
143. Stipanovic A, Sarko A (1976) Packing analysis of carbohydrates and polysaccharides. 6. Molecular and crystal structure of regenerated cellulose II. Macromolecules 9:851–857
144. Kolpak FJ, Blackwell J (1976) Determination of the structure of cellulose II. Macromolecules 9:273–278
145. Dudley RL, Fyfe CA, Stephenson PJ, Deslandes Y, Hamer GK, Marchessault RH (1983) High-resolution carbon-13 CP/MAS NMR spectra of solid cellulose oligomers and the structure of cellulose II. J Am Chem Soc 105:2469–2472
146. Isogai A, Usuda M, Kato T, Uryu T, Atallah RH (1989) Solid-state CP/MAS carbon-13 NMR study of cellulose polymorphs. Macromolecules 22:3168–3172
147. Gessler K, Krauss N, Steiner T, Betzl C, Sarko A, Saenger W (1995) β-D-Cellotetraose hemihydrate as a structural model for cellulose II. An X-ray diffraction study. J Am Chem Soc 117:11397–11406
148. Raymond S, Henrissat B, Tran Qui D, Kvick A, Chanzy H (1995) The crystal structure of methyl β-cellotrioside monohydrate 0.25 ethanolate and its relationship to cellulose II. Carbohydr Res 277:209–229
149. Langan P, Nishiyama Y, Chanzy H (1999) A revised structure and hydrogen-bonding system in cellulose II from neutron fiber diffraction analysis. J Am Chem Soc 121:9940–9946

150. Wada M, Heux L, Isogai A, Nishiyama Y, Chanzy H, Sugiyama J (2001) Improved structural data of cellulose IIII prepared in supercritical ammonia. J Am Chem Soc 34:1237–1243
151. Takai M, Fukuda K, Murata M, Hayashi J (1987) Crystalline polymorphism of cellulose triacetate. In: Kennedy JF, Phillips GO, Williams PA (eds) Wood and cellulosics. Ellis Horwood, Chichester, pp 111–117
152. Kuppel A, Husemann E, Seifert E, Zugenmaier P (1973) Transformation of triacetyl cellulose I into triacetyl cellulose II and packing of cellulose in native fibers. Kolloid Z Z Polym 251:432–433
153. Zugenmaier P (2004) Characterization and physical properties of cellulose acetates. Macromol Symp 208:81–166
154. El Seoud OA, Fidale LC, Ruiz N, D'Almeida MLO, Frollini E (2008) Cellulose swelling by protic solvents: which properties of the biopolymer and the solvent matter? Cellulose 15:371–392
155. Shinouda HG, Kinawi A, Abdel-Moteleb MM (1978) X-ray diffraction and iodine adsorption of acid modified cellulose fibers. Makromol Chem 179:455–462
156. Revol JF, Dietrich A, Goring DAI (1987) Effect of mercerization on the crystallite size and crystallinity index in cellulose from different sources. Can J Chem 65:1724–1725
157. Sidiras DK, Koullas DP, Vgenopoulos AG, Koukios EG (1990) Cellulose crystallinity as affected by various technical processes. Cellul Chem Technol 24:309–317
158. Tang L-G, Hon DN-S, Pan S-H, Zhu Y-Q, Wang Z, Wag Z-Z (1996) Evaluation of microcrystalline cellulose. I. Changes in ultrastructural characteristics during preliminary acid hydrolysis. J Appl Polym Sci 59:483–488
159. Awadel-Karim S, Nazhad MM, Paszner L (1999) Factors affecting crystalline structure of cellulose during solvent purification treatment. Holzforschung 53:1–8
160. Chen Y, Stipanovic AJ, Winter WT, Wilson DB, Kim Y-J (2007) Effect of digestion by pure cellulases on crystallinity and average chain length for bacterial and microcrystalline celluloses. Cellulose 14:283–293
161. Liu Y, Hu H (2008) X-ray diffraction study of bamboo fibers treated with NaOH. Fibers Polym 9:735–739
162. Kim J, Chen Y, Kang K-S, Park Y-B, Schwartz M (2008) Magnetic field effect for cellulose nanofiber alignment. J Appl Phys. 104:096104/1–096104/3
163. Park S, Johnson DK, Ishizawa CI, Parilla PA, Davis MF (2009) Measuring the crystallinity index of cellulose by solid state $^{13}C$ nuclear magnetic resonance. Cellulose 16:641–647
164. Nishimura H, Sarko A (1987) Mercerization of cellulose. III. Changes in crystallite sizes. J Appl Polym Sci 33:855–866
165. Nishimura H, Sarko A (1987) Mercerization of cellulose. IV. Mechanism of mercerization and crystallite sizes. J Appl Polym Sci 33:867–874
166. Bober HL, Cuculo JA, Tucker PA (1987) Effects of ammonia/ammonium thiocyanate on cotton fabric. J Polym Sci Part A Polym Chem 25:2025–2032
167. Pavlov P, Makaztchieva V, Lozanov E (1992) High reactivity of cellulose after high temperature mercerization. Cellul Chem Technol 26:151–160
168. Fink HP, Philipp B, Zschunke C, Hayn M (1992) Structural changes of LODP cellulose in the original and mercerized state during enzymatic hydrolysis. Acta Polym 43:270–274
169. Sao KP, Samantaray BK, Bhattacherjee S (1996) X-ray line profile analysis in alkali-treated ramie fiber. J Appl Polym Sci 60:919–922
170. Ramos LA, Assaf JM, El Seoud OA, Frollini E (2005) Influence of the supramolecular structure and physicochemical properties of cellulose on its dissolution in a lithium chloride/N, N-dimethylacetamide solvent system. Biomacromolecules 6:2638–2647
171. Günzler H, Gremlich H-U (2002) IR Spectroscopy: an introduction. Wiley-VCH, New York
172. Wartewig S (2003) IR and Raman spectroscopy: fundamental processing. Wiley-VCH, New York
173. Krasovskii AN, Polyakov DN, Gorodneva EN, Varlamov AV, Mnatsakanov SS, Iskhakov DM (1992) IR spectra and structure of cellulose triacetate with low content of mono- and disubstituted glucopyranose units. Russ J Appl Chem 65:1528–1534

174. Krasovskii AN, Polyakov DN, Mnatsakanov SS (1993) Determination of the degree of substitution in highly substituted cellulose esters (acetates). Russ J Appl Chem 66:918–924
175. Polyakov DN, Krasovskii AN, Gorodneva EN, Varlamov AV, Mnatsakonov SS (1993) Effect of activation and acylation of cellulose on distribution of primary and secondary hydroxyl groups in cellulose triacetate with small content of partially substituted glucopyranose. Russ J Appl Chem 66:1944–1948
176. Krasovskii AN, Plodistyi AB, Polyakov DN (1996) Distribution of primary and secondary functional groups in highly substituted cellulose acetates, acetomaleates, and acetophthalates based IR absorption spectroscopy data. Russ J Appl Chem 69:1048–1054
177. Dominguez de Maria P, Martinsson A (2009) Ionic-liquid-based method to determine the degree of esterification in cellulose fibers. Analyst 134:493–496
178. Sollinger S, Diamantoglou M (1997) Determination of the degree of sulfonation of sulfonated poly(aryl ether) sulfone. J Raman Spectrosc 28:811–817
179. Robert P, Marquis M, Barron C, Guillon F, Saulnier L (2005) FT-IR investigation of cell wall polysaccharides from cereal grains. Arabinoxylan infrared assignment. J Agric Food Chem 53:7014–7018
180. O'Connor RT, DuPre EF, McCall ER (1957) Infrared spectrophotometric procedure for analysis of cellulose and modified cellulose. Anal Chem 29:998–1005
181. Fengel D, Ludwig M (1991) Possibilities and limits of FTIR spectroscopy for the characterization of cellulose. Part 1. Comparison of various cellulose fibers and bacterial-cellulose. Papier (Bingen, Germany) 45:45–51
182. Fengel D (1991) Possibilities and limits of FTIR spectroscopy for the characterization of cellulose. Part 2. Comparison of various pulps. Papier (Bingen, Germany) 45:97–102
183. Fengel D (1991) Possibilities and limits of FTIR spectroscopy for the characterization of cellulose. Part 3. Effect of accompanying compounds on the IR spectrum of cellulose. Papier (Bingen, Germany) 46:7–11
184. Richter U, Krause T, Schempp W (1991) Alkali treatment of cellulose fibers. I. Changes in order evaluated by IR spectroscopy and x-ray diffraction. Angew Makromol Chem 185/186:155–167
185. Marson GA, El Seoud OA (1999) Cellulose dissolution in lithium chloride/N, N-dimethylacetamide solvent system: relevance of kinetics of decrystallization to cellulose derivatization under homogeneous solution conditions. J Polym Sci Part A Polym Chem 37:3738–3744
186. Khalil EMA, El-Wakil NA (2001) Infrared absorption spectra of cyanoethylated cellulose fibres. Cellul Chem Technol 34:473–479
187. Xiao D, Hu J, Zhang M, Li M, Wang G, Yao H (2004) Synthesis and characterization of camphorsulfonyl acetate of cellulose. Carbohydr Res 339:1925–1931
188. Oh SY, Yoo DI, Shin Y, Kim HC, Kim HY, Chung YS, Park WH, Youk JH (2005) Crystalline structure analysis of cellulose treated with sodium hydroxide and carbon dioxide by means of X-ray diffraction and FTIR spectroscopy. Carbohydr Res 340:2376–2391
189. Fuller MP, Griffiths PR (1978) Diffuse reflectance measurements by infrared Fourier transform spectrometry. Anal Chem 50:1906–1910
190. Kubelka P (1948) New contributions to the optics of intensely light-scattering materials. J Opt Soc Am 38:448–457
191. Schultz TP, McGinnis GD, Bertran MS (1985) Estimation of cellulose crystallinity using Fourier transform infrared spectroscopy and dynamic thermogravimetry. J Wood Chem Technol 5:543–557
192. Hulleman SHD, van Hazendonk JM, van Dam JEG (1994) Determination of crystallinity in native cellulose from higher plants with diffuse reflectance Fourier-transform infrared spectroscopy. Carbohydr Res 261:163–172
193. Yang CQ, Wang X (1996) Infrared spectroscopy studies of the cyclic anhydride as the intermediate for the ester crosslinking of cotton cellulose by polycarboxylic acids. II. Comparison of different polycarboxylic acids. J Polym Sci Part A Polym Chem 34:1573–1580

194. Yang CQ, Wang X (1997) Infrared spectroscopy studies of the cyclic anhydride as the intermediate for the ester crosslinking of cotton cellulose by polycarboxylic acids. III. Molecular weight of a crosslinking agent. J Polym Sci Part A Polym Chem 35:557–564
195. Ogawa K, Hirai I, Shimasaki C, Yoshimura T, Ono S, Rengakuji S, Nakamura Y, Yamazaki I (1999) Simple determination method of degree of substitution for starch acetate. Bull Chem Soc Jpn 72:2785–2790
196. Jandura P, Kokta BV, Riedl B (2000) Fibrous long-chain organic acid cellulose esters and their characterization by diffuse reflectance FTIR spectroscopy, solid-state CP/MAS carbon-13 NMR, and x-ray diffraction. J Appl Polym Sci 78:1354–1365
197. Mao Z, Yang CQ (2001) IR spectroscopy study of cyclic anhydride as intermediate for ester crosslinking of cotton cellulose by polycarboxylic acids. V. Comparison of 1,2,4-butanetricarboxylic acid and 1,2,3-propanetricarboxylic acid. J Appl Polym Sci 81:2142–2150
198. Casarano R, Fidale LC, Lucheti CM, Heinze T, El Seoud OA (2010) Expedient, accurate methods for the determination of the degree of substitution of cellulose carboxylic esters: application of Uv-vis spectroscopy (dye solvatochromism) and FTIR. Carbohydr Polym 83:1285–1292
199. Crepy L, Chaveriat L, Banoub J, Martin P, Joly N (2009) Synthesis of cellulose fatty esters as plastics—influence of the degree of substitution and the fatty chain length on mechanical properties. Chemsuschem 2:165–170
200. El-Khouly AS, Kenawy E, Safaan AA, Takahashi Y, Hafiz YA, Sonomoto K, Zendo T (2011) Synthesis, characterization and antimicrobial activity of modified cellulose-graft-polyacrylonitrile with some aromatic aldehyde derivatives. Carbohydr Polym 83:346–353
201. Cheng HN, Biswas A (2011) Chemical modification of cotton-based natural materials: products from carboxymethylation. Carbohydr Polym 84:1004–1010
202. Kaur B, Gur IS, Bhatnagar HL (1987) Thermal degradation studies of cellulose phosphates and cellulose thiophosphates. Angew Makromol Chem 147:157–183
203. Pohl M, Heinze T (2008) Novel biopolymer structures synthesized by dendronization of 6-deoxy-6-aminopropargyl cellulose. Macromol Rapid Commun 29:1739–1745
204. Hasani M, Westman G, Potthast A, Rosenau T (2009) Cationization of cellulose by using N-oxiranylmethyl-N-methylmorpholinium chloride and 2-oxiranylpyridine as etherfication agents. J Appl Polym Sci 114:1449–1456
205. Zhang C, Price LM, Daly WH (2006) Synthesis and characterization of a trifunctional aminoamide cellulose derivative. Biomacromolecules 7:139–145
206. Kostag M, Koehler S, Liebert T, Heinze T (2010) Pure cellulose nanoparticles from trimethylsilyl cellulose. Macromol Symp 294-II:96–106
207. Kondo T, Sawatari C (1996) A Fourier transform infrared spectroscopic analysis of the character of hydrogen bonds in amorphous cellulose. Polymer 37:393–399
208. Schwanninger M, Rodrigues JC, Pereira H, Hinterstoisser B (2004) Effects of short-time vibratory ball milling on the shape of FT-IR spectra of wood and cellulose. Vib Spectrosc 36:23–40
209. Gavira JM, Hernanz A, Bratu I (2003) Dehydration of & β-cyclodextrin: an IR & ν(OH) band profile analysis. Vib Spectrosc 32:137–146
210. Hurtubise F, Krässig H (1960) Classification of fine structural characteristics in cellulose by infrared spectroscopy. Anal Chem 32:177–181
211. Nelson ML, O'Connor RT (1964) Relation of certain infrared bands to cellulose crystallinity and crystal lattice type. II. A new infrared ratio for estimation of crystallinity in celluloses I and II. J Appl Polym Sci 8:1325–1341
212. El-Saied H, Hanna AA, Ibrahem AA (1985) Comparative study of various physical methods for the determination of cellulose crystallinity. Indian Pulp Pap 40:7, 9–10, 24
213. Iyer PB, Sreenivasan S, Chidambareswaran PK, Patil NB, Sundaram V (1991) Induced crystallization of cellulose in never-dried cotton fibers. J Appl Polym Sci 42:1751–1757

214. He J, Cui S, Wang S-Y (2008) Preparation and crystalline analysis of high-grade bamboo dissolving pulp for cellulose acetate. J Appl Polym Sci 107:1029–1038
215. Puleo AC, Paul DR, Kelly SS (1989) The effect of degree of acetylation on gas sorption and transport behavior in cellulose acetate. J Membr Sci 47:301–332
216. Normakhamatov NS, Turaev AS, Burkhanova ND (2009) Cellulose supramolecular structure changes during chemical activation and sulfation. Holzforschung 63:40–46
217. Miyamoto T, Sato Y, Shibata T, Tanahashi M, Inagaki H (1985) Carbon-13 NMR spectral studies on the distribution of substituents in water-soluble cellulose acetate. J Polym Sci Polym Chem Ed 23:1373–1383
218. Krasovskii AN, Polyakov DN, Mnatsakanov SS (1993) Determination of the degree of substitution in highly substituted cellulose esters (acetates). Zh Prikl Khim 66:1118–1126
219. Krasovskii AN, Plodistyi AB, Polyakov DN (1996) Distribution of primary and secondary functional groups in highly substituted cellulose acetates, acetomaleates, and acetophthalates based IR absorption spectroscopy data. Zh Prikl Khim 69:1183–1189
220. Braun S, Kalinowski HO, Berger S (2004) 200 and more basic NMR experiments. Wiley-VCH, Weinheim, p 128
221. Sei T, Ishitani K, Suzuki R, Ikematsu K (1985) Distribution of acetyl group in cellulose acetate as determined by nuclear magnetic resonance analysis. Polym J 17:1065–1069
222. Iyer PB, Iyer KRK, Patil NB (1976) An infrared technique for the quick analysis of cotton-polyester. J Appl Polym Sci 20:591–595
223. Iyer PB, Iyer KRK, Patil NB (1978) Quantitative analysis of wool/cotton blends: an infrared method. J Appl Polym Sci 22:2677–2683
224. Fidale LC, Lima PM Jr, Hortencio LMA, Pires PAR, Heinze T, El Seoud OA (2012) Employing perichromism for probing the properties of carboxymethyl cellulose films: an expedient, accurate method for the determination of the degree of substitution of the biopolymer derivative. Cellulose 19:151–159
225. Becker ED (1999) High resolution NMR, 3rd edn. Academic Press, New York, NY, p 424
226. Ernst RR, Bodenhausen G, Wokaun A (1990) Principles of nuclear magnetic resonance in one and two dimensions. Oxford University Press, USA
227. Günther H (1995) NMR spectroscopy: basic principles, concepts, and applications in chemistry, 2nd edn. Wiley, USA
228. http://www.cis.rit.edu/htbooks/nmr/ by Joseph P. Hornak
229. Sternberg U, Koch FT, Prieß W, Witter R (2003) Crystal structure refinements of cellulose polymorphs using solid state $^{13}C$ chemical shifts. Cellulose 10:189–199
230. Witter R, Sternberg U, Hesse S, Kondo T, Koch FT, Ulrich AS (2006) 13C chemical shift constrained crystal structure refinement of cellulose $I_\alpha$ and its verification by NMR anisotropy experiments. Macromolecules 39:6125–6132
231. Unger EW, Fink HP, Philipp B (1995) Morphometric investigation of the swelling dissolution process of cellulose fibers in FeTNa and LiCl/dimethylacetamide. Papier (Darmstadt) 49(6):297–307
232. Evans R, Newman RH, Roick UC, Suckling ID, Wallis AFA (1995) Changes in cellulose crystallinity during kraft pulping. Comparison of infrared, x-ray diffraction and solid state NMR results. Holzforschung 49:498–504
233. Hesse S (2005) Strukturanalyse modifizierter Bakteriencellulosen verschiedener Subspezies des A. xylinum mittels Festkörper-Kernresonanz-Spektroskopie. Ph.D. thesis, University of Jena, Germany
234. Debzi EM, Chanzy H, Sugiyama J, Tekely P, Excoffier G (1991) The $I_\alpha \rightarrow I_\beta$ transformation of highly crystalline cellulose by annealing in various mediums. Macromolecules 24:6816–6822
235. Yamamoto H, Horii F (1993) CPMAS carbon-13 NMR analysis of the crystal transformation induced for Valonia cellulose by annealing at high temperatures. Macromolecules 26:1313–1317
236. Yamamoto H, Horii F (1994) In situ crystallization of bacterial cellulose. I. Influences of polymeric additives, stirring and temperature on the formation of celluloses $I_\alpha$ and $I_\beta$ as

revealed by cross polarization/magic angle spinning (CP/MAS) carbon-13 NMR spectroscopy. Cellulose 1:57–60
237. Larsson PT, Westermark U, Iversen T (1995) Determination of the cellulose $I_\alpha$ allomorph content in a tunicate cellulose by CP/MAS $^{13}$C-NMR spectroscopy. Carbohydr Res 278:339–343
238. Newman RH (1999) Estimation of the relative proportions of cellulose $I_\alpha$ and $I_\beta$ in wood by carbon-13 NMR spectroscopy. Holzforschung 53:335–340
239. Horii F, Yamamoto H, Kitamaru R (1987) Transformation of native cellulose crystals induced by saturated steam at high temperatures. Macromolecules 20:2946–2949
240. Sugiyama J, Okano T, Yamamoto H, Horii F (1990) Transformation of Valonia cellulose crystals by an alkaline hydrothermal treatment. Macromolecules 23:3196–3198
241. Kono H, Erata T, Takai M (2003) Determination of the through-bond carbon-carbon and carbon-proton connectivities of the native celluloses in the solid state. Macromolecules 36:5131–5138
242. Kono H, Numata Y (2006) Structural investigation of cellulose $I_\alpha$ and $I_\beta$ by two-dimensional RFDR NMR spectroscopy: determination of sequence of magnetically inequivalent d-glucose units along cellulose chain. Cellulose 13:317–326
243. Horii F, Hirai A, Kitamaru R (1982) Solid-state high-resolution carbon-13 NMR studies of regenerated cellulose samples with different crystallinities. Polym Bull 8:163–170
244. Kunze J, Fink HP (1999) Characterization of cellulose and cellulose derivatives by high resolution solid state $^{13}$C-NMR spectroscopy. Papier (Bingen, Germany) 53:753–764
245. Atalla RH, VanderHart DL (1999) The role of solid-state carbon-13 NMR spectroscopy in studies of the nature of native celluloses. Solid State Nucl Magn Reson 15:1–19
246. VanderHart DL, Campbell GC (1998) Off-resonance proton decoupling on-resonance and near-resonance. A close look at $^{13}$C CPMAS linewidths in solids for rigid, strongly coupled carbons under CW proton decoupling. J Magn Reson 134:88–112
247. Yamamoto H, Horii F, Hirai A (2006) Structural studies of bacterial cellulose through the solid-phase nitration and acetylation by CP/MAS $^{13}$C NMR spectroscopy. Cellulose 13:327–342
248. Tokoh C, Takabe K, Sugiyama J, Fujita M (2002) CP/MAS 13C-NMR and electron diffraction study of bacterial cellulose structure affected by cell wall polysaccharides. Cellulose 9:351–360
249. Larsson PT, Wickholm K, Iversen T (1997) A CP/MAS carbon-13 NMR investigation of molecular ordering in celluloses. Carbohydr Res 302:19–25
250. Larsson PT, Hult EL, Wickholm K, Pettersson E, Iversen T (1999) CP/MAS carbon-13 NMR spectroscopy applied to structure and interaction studies on cellulose I. Solid State Nucl Magn Reson 15:31–40
251. Newman RH (1999) Estimation of the lateral dimensions of cellulose crystallites using carbon-13 NMR signal strengths. Solid State Nucl Magn Reson 15:21–29
252. Kono H, Erata T, Takai M (2002) CP/MAS $^{13}$C NMR study of cellulose and cellulose derivatives. 2. Complete assignment of the $^{13}$C resonance for the ring carbons of cellulose triacetate polymorphs. J Am Chem Soc 124:7512–7518
253. Hesse-Ertelt S, Witter R, Ulrich AS, Kondo T, Heinze T (2008) Spectral assignments and anisotropy data of cellulose $I_\alpha$: $^{13}$C-NMR chemical shift data of cellulose $I_\alpha$ determined by INADEQUATE and RAI techniques applied to uniformly 13C-labeled bacterial celluloses of different Gluconacetobacter xylinus strains. Magn Reson Chem 46:1030–1036
254. Hesse S, Kondo T (2005) Behavior of cellulose production of Acetobacter xylinum in $^{13}$C-enriched cultivation media including movements on nematic ordered cellulose templates. Carbohydr Polym 60:457–465
255. Hesse-Ertelt S, Heinze T, Togawa E, Kondo T (2010) Structure elucidation of uniformly 13C-labeled bacterial celluloses from different Gluconacetobacter xylinus strains. Cellulose 17:139–151
256. Fyfe CA, Dudley RL, Stephenson PJ, Deslandes Y, Hamer GK, Marchessault RH (1983) Application of high-resolution solid-state NMR with cross-polarization magic-angle

spinning (CP/MAS) techniques to cellulose chemistry. J Macromol Sci Rev Macromol Chem Phys C23:187–216
257. Kono H, Erata T, Takai M (2003) Complete assignment of the CP/MAS $^{13}C$ NMR spectrum of cellulose IIII. Macromolecules 36:3589–3592
258. Kono H, Numata Y, Erata T, Takai M (2004) $^{13}C$ and $^{1}H$ resonance assignment of mercerized cellulose II by two-dimensional MAS NMR spectroscopies. Macromolecules 37:5310–5316
259. Wada M, Heux L, Nishiyama Y, Langan P (2009) X-ray crystallographic, scanning microprobe X-ray diffraction, and cross-polarized/magic angle spinning $^{13}C$ NMR studies of the structure of cellulose $III_{II}$. Biomacromolecules 10:302–309
260. Heinze T, Dicke R, Koschella A, Kull AH, Klohr E-A, Koch W (2000) Effective preparation of cellulose derivatives in a new simple cellulose solvent. Macromol Chem Phys 201:627–631
261. Heinze T, Schwikal K, Barthel S (2005) Ionic liquids as reaction medium in cellulose functionalization. Macromol Biosci 5:520–525
262. Fischer S, Voigt W, Fischer K (1999) The behavior of cellulose in hydrated melts of the composition $LiX{\bullet}nH_2O$ ($X = I^-$, $NO_3^-$, $CH_3COO^-$, $ClO_4^-$). Cellulose 6:213–219
263. Nehls I, Wagenknecht W, Philipp B, Stscherbina D (1994) Characterization of cellulose and cellulose derivatives in solution by high resolution carbon-13 NMR spectrometry. Prog Polym Sci 19:29–78
264. Hasegawa M, Isogai A, Onabe F, Usada M (1992) Dissolving states of cellulose and chitosan in trifluoroacetic acid. J Appl Polym Sci 45:1857–1863
265. Yanagisawa M, Shibata I, Isogai A (2004) SEC-MALLS analysis of cellulose using LiCl/1,3-dimethyl-2-imidazolidinone as an eluent. Cellulose 11:169–176
266. Fujimoto T, Takahashi S, Tsuji M, Miyamoto T, Inagaki H (1986) Reaction of cellulose with formic acid and stability of cellulose formate. J Polym Sci Part C Polym Lett 24:495–501
267. Koehler S, Liebert T, Heinze T (2009) Ammonium-based cellulose solvents suitable for homogeneous etherification. Macromol Biosci 9:836–841
268. Meiland M, Heinze T, Guenther W, Liebert T (2010) Studies on the boronation of methyl-β-D-cellobioside—a cellulose model. Carbohydr Res 345:257–263
269. Meiland M, Heinze T, Guenther W, Liebert T (2009) Seven membered ring boronates at trans-diol moieties of carbohydrates. Tetrahedron Lett 50:469–472
270. Flugge LA, Blank JT, Petillo PA (1999) Isolation, modification, and NMR assignments of a series of cellulose oligomers. J Am Chem Soc 121:7228–7238
271. Jiang N, Pu Y, Ragauskas AJ (2010) Rapid determination of lignin content via direct dissolution and $^{1}H$ NMR analysis of plant cell. Chemsuschem 3:1285–1289
272. Remsing RC, Swatloski RP, Rogers RD, Moyna G (2006) Mechanism of cellulose dissolution in the ionic liquid 1-N-butyl-3-methylimidazolium chloride: a $^{13}C$ and $^{35/37}Cl$ NMR relaxation study on model systems. Chem Commun 1271–1273
273. www.otto-diels-institut.de/studium/spektroskopie/FDS_2D-NMR1–08.pdf: 2 dimensionale-NMR Spektroskopie F.D. Sönnichsen Mittwoch, 22 Oct 2008
274. Fischer S, Leipner H, Thümmler K, Brendler E, Peters J (2003) Inorganic molten salts as solvents for cellulose. Cellulose 10:227–236
275. Heinze T, Liebert T, Koschella A (2006) Esterification of polysaccharides. Structure analysis of polysaccharide esters
276. Goodlett VW, Dougherty JF, Patton HW(1971) Characterization of cellulose acetates by nuclear magnetic resonance. J Polym Sci Part A-1 Polym Chem 9:155–161
277. Kamide K, Okajima K (1981) Determination of distribution of O-acetyl group in trihydric alcohol units of cellulose acetate by carbon-13 nuclear magnetic resonance analysis. Polym J (Tokyo) 13:127–133
278. Hikichi K, Kakuta Y, Katoh T (1995) $^{1}H$ NMR study on substituent distribution of cellulose diacetate. Polym J (Tokyo) 27:659–663
279. Buchanan CM, Hyatt JA, Lowman DW (1987) 2D-NMR of polysaccharides: spectral assignments of cellulose triesters. Macromolecules 20:2750–2754

280. Gagnaire DY, Taravel FR, Vignon MR (1976) Attribution of carbon-13 nuclear magnetic resonance signals to peracetyl disaccharides in the D-glucose series. Carbohydr Res 51:157–168
281. Gagnaire DY, Taravel FR, Vignon MR (1982) Two-dimensional J spectroscopy: proton NMR of polysaccharides. Application to capsular heteroglycans and labeled cellulose triacetate. Macromolecules 15:126–129
282. Capon B, Rycroft DS, Thomson JW (1979) The carbon-13 NMR spectra of peracetylated cello-oligosaccharides. Carbohydr Res 70:145–149
283. Miyamoto T, Sato Y, Shibata T, Inagaki H, Tanahashi M (1984) Carbon-13 nuclear magnetic resonance studies of cellulose acetate. J Polym Sci Polym Chem Ed 22:2363–2370
284. Kamide K, Okajima K, Kowsaka K, Matsui T (1987) Solubility of cellulose acetate prepared by different methods and its correlationships with average acetyl group distribution on glucopyranose units. Polym J (Tokyo) 19:1405–1412
285. Kowsaka K, Okajima K, Kamide K (1986) Further study on the distribution of substituent group in cellulose acetate by carbon-13 and proton NMR analysis: assignment of carbonyl carbon peaks. Polym J (Tokyo) 18:843–849
286. Kamide K, Saito M (1994) Recent advances in molecular and supermolecular characterization of cellulose and cellulose derivatives. Macromol Symp 83:233–271
287. Buchanan CM, Edgar KJ, Hyatt JA, Wilson AK (1991) Preparation of cellulose [1-carbon-13]acetates and determination of monomer composition by NMR spectroscopy. Macromolecules 24:3050–3059
288. Reuben J, Conner HT (1983) Analysis of the carbon-13 NMR spectrum of hydrolyzed O-(carboxymethyl)cellulose: monomer composition and substitution patterns. Carbohydr Res 115:1–13
289. Tezuka Y, Tsuchiya Y, Shiomi T (1996) Proton and carbon-13 NMR structural study on cellulose and polysaccharide derivatives with carbonyl groups as a sensitive probe. Part II. Carbon-13 NMR determination of substituent distribution in carboxymethyl cellulose by use of its peresterified derivatives. Carbohydr Res 291:99–108
290. Capitani D, Porro F, Segre AL (2000) High field NMR analysis of the degree of substitution in carboxymethyl cellulose sodium salt. Carbohydr Polym 42:283–286
291. Tezuka Y, Tsuchiya Y (1995) Determination of substituent distribution in cellulose acetate by means of a carbon-13 NMR study on its propanoated derivative. Carbohydr Res 273:83–91
292. Deus C, Friebolin H, Siefert E (1991) Partially acetylated cellulose. Synthesis and determination of the substituent distribution via proton NMR spectroscopy. Makromol Chem 192:75–83
293. Lee CK, Gray GR (1995) Analysis of positions of substitution of O-acetyl groups in partially O-acetylated cellulose by the reductive-cleavage method. Carbohydr Res 269:167–174
294. Schaller J, Heinze T (2005) Studies on the synthesis of 2,3-O-hydroxyalkyl ethers of cellulose. Macromol Biosci 5:58–63
295. Grote C, Heinze T (2005) Starch derivatives of high degree of functionalization 11: studies on alternative acylation of starch with long-chain fatty acids homogeneously in N, N-dimethyl acetamide/LiCl. Cellulose 12:435–444
296. Hornig S (2005) Selbststrukturierende Funktionspolymere durch chemische Modifizierung von Dextranen. Diploma thesis, University of Jena
297. Hussain MA, Liebert T, Heinze T (2004) Acylation of cellulose with N, N′-carbonyldiimidazole-activated acids in the novel solvent dimethyl sulfoxide/tetrabutylammonium fluoride. Macromol Rapid Commun 25:916–920
298. Liebert T, Hussain MA, Heinze T (2005) Structure determination of cellulose esters via subsequent functionalization and NMR spectroscopy. Macromol Symp 223:79–92
299. Hedenström M, Wiklund-Lindström S, Öman T, Lu F, Gerber L, Schatz P, Sundberg B, Ralph J (2009) Identification of lignin and polysaccharide modifications in Populus wood by chemometric analysis of 2D NMR spectra from dissolved cell walls. Mol Plant 2(933):942

300. Lu F, Ralph J (2003) Non-degradative dissolution and acetylation of ball-milled plant cell walls: high-resolution solution-state NMR. Plant J 35:535–544
301. Baar A, Kulicke W-M, Szablikowski K, Kiesewetter R (1994) Nuclear magnetic resonance spectroscopic characterization of carboxymethyl cellulose. Macromol Chem Phys 195:1483–1492
302. Buchanan CM, Hyatt JA, Lowman DW (1989) Supramolecular structure and microscopic conformation of cellulose esters. J Am Chem Soc 111:7312–7319
303. Nunes T, Burrows HD, Bastos M, Feio G, Gil MH (1995) $^{13}C$ nuclear magnetic resonance studies of cellulose ester derivatives in solution, powder and membranes. Polymer 36:479–485
304. Iijima H, Kowsaka K, Kamide K (1992) Determination of sequence distribution of substituted and unsubstituted glucopyranose units in water-soluble cellulose acetate chain as revealed by enzymic degradation. Polym J (Tokyo) 24:1077–1097
305. King AWT, Jalomäki J, Granström M, Argyropoulos DS, Heikkinen S, Kilpelainen I (2010) A new method for rapid degree of substitution and purity determination of chloroform-soluble cellulose esters, using 31P NMR. Anal Methods 2:1499–1505
306. KulickeW-M Otto M, Baar A (1993) Improved NMR characterization of high-molecular-weight polymers and polyelectrolytes through the use of preliminary ultrasonic degradation. Makromol Chem 194:751–765
307. Iwata T, Azuma J, Okamura K, Muramoto M, Chun B (1992) Preparation and NMR assignments of cellulose mixed esters regioselectively substituted by acetyl and propanoyl groups. Carbohydr Res 224:277–283
308. McNair HM, Miller JM (1997) Basic gas chromatography. Wiley-Interscience, New York. ISBN 0–471-17260-X
309. Snyder LR, Kirkland JJ, Dolan JW (2010) Introduction to modern liquid chromatography, 3rd edn. Wiley. ISBN: 978–0-470-16754-0
310. Snyder LT, Glajch JL, Kirkland JJ (1988) Practical HPLC method development, 2nd edn. Wiley, USA
311. Cunico RL, Gooding KM, Wehr T (1998) Basic HPLC and CE of biomolecules. Bay Bioanalytical Laboratory
312. Dong MW (2006) Modern HPLC for practicing scientists. Wiley. ISBN 978–0-471-72789-7
313. Mischnick P, Momcilovic D (2010) Chemical structure analysis of starch and cellulose derivatives. In: Horton D (ed) Advances in carbohydrate chemistry and biochemistry, vol 64. Elsevier, Oxford, pp 117–210
314. Rolf D, Gray GR (1982) Reductive cleavage of glycosides. J Am Chem Soc 104:3539–3541
315. Rosell K-G (1988) Distribution of substituents in methylcellulose. J Carbohydr Chem 7:525–536
316. Erler U, Mischnick P, Stein A, Klemm D (1992) Determination of the substitution patterns of cellulose methyl ethers by HPLC and gas-liquid chromatography—comparison of methods. Polym Bull 29:349–356
317. Gohdes M, Mischnick P, Wagenknecht W (1997) Methylation analysis of cellulose sulfates. Carbohydr Polym 33:163–168
318. Gohdes M, Mischnick P (1998) Determination of the substitution pattern in the polymer chain of cellulose sulfates. Carbohydr Res 309:109–115
319. Kragten EA, Kamerling JP, Vliegenthart JFG (1992) Composition analysis of carboxymethylcellulose by high-pH anion-exchange chromatography with pulsed amperometric detection. J Chromatogr 623:49–53
320. Kragten EA, Kamerling JP, Vliegenthart JFG, Botter H, Batelaan JG (1992) Composition analysis of sulfoethylcelluloses by high-pH anion exchange chromatography with pulsed amperometric detection. Carbohydr Res 233:81–86
321. Lee DS, Perlin AS (1984) Formation, and stereochemistry, of 1,2-O-(1-methyl-1,2-ethanediyl)-D-glucose acetals formed in the acid-catalyzed hydrolysis of O-(2-hydroxypropyl)cellulose. Carbohydr Res 126:101–114

322. Arisz PW, Kauw HJJ, Boon JJ (1995) Substituent distribution along the cellulose backbone in O-methylcelluloses using GC and FAB-MS for monomer and oligomer analysis. Carbohydr Res 271:1–14
323. Heinze T (1998) Neue Funktionspolymere aus Cellulose: neue Synthesekonzepte, Strukturaufklärung und Eigenschaften. Shaker Verlag, Aachen, Germany. ISBN 3-8265-3300-3
324. Heinze T, Erler U, Nehls I, Klemm D (1994) Determination of the substituent pattern of heterogeneously and homogeneously synthesized carboxymethyl cellulose by using high-performance liquid chromatography. Angew Makromol Chem 215:93–106
325. Heinze T, Pfeiffer K, Liebert T, Heinze U (1999) Effective approaches for estimating the functionalization pattern of carboxymethyl starch of different origin. Starch/Staerke 51:11–16
326. Gelman RA (1982) Characterization of carboxymethylcellulose: distribution of substituent groups along the chain. J Appl Polym Sci 27:2957–2964
327. Ma Z, Zhang W, Li Z (1989) Study on the characterization of distribution of substituents along the chain of carboxymethyl cellulose. Chin J Polym Sci 7:45–53
328. Martinez-Richa A, Munoz-Alarcon H, Joseph-Nathan P (1991) Studies on enzymatic resistance and molecular structure by carbon-13 NMR of cellulosic ethers. J Appl Polym Sci 44:347–352
329. Heinze U, Schaller J, Heinze T, Horner S, Saake B, Puls J (2000) Characterization of regioselectively functionalized 2,3-O-carboxymethyl cellulose by enzymic and chemical methods. Cellulose 7:161–175
330. Horner S, Puls J, Saake B, Klohr E-A, Thielking H (1999) Enzyme-aided characterization of carboxymethyl cellulose. Carbohydr Polym 40:1–7
331. Puls J, Horner S, Kruse T, Saake B, Heinze T (1998) Enzyme-aided characterization of carboxymethyl cellulose with conventional and novel distribution of functional groups. Papier (Heidelberg, Germany) 52:743–748
332. Urbanski J (1992) Analysis and characterization of cellulose and its derivatives. Appl Polym Anal Charact 2:345–361
333. Mischnick P, Heinrich J, Gohdes M, Wilke O, Rogmann N (2000) Structure analysis of 1,4-glucan derivatives. Macromol Chem Phys 201:1985–1986
334. De Belder AN, Norrman B (1968) The distribution of substituents in partially acetylated dextran. Carbohydr Res 8:1–6
335. Bouveng HO (1961) Arabinogalactoglycans. V. Barry degradation of the arabinogalactoglycans from Western larch—a kinetic study of the mild acid hydrolysis of arabinogalactoglycan A. Acta Chem Scand 15:78–86
336. Liebert T, Pfeiffer K, Heinze T (2005) Carbamoylation applied for structure determination of cellulose derivatives. Macromol Symp 223:93–108
337. Bjorndal H, Lindberg B, Rosell KG (1971) Distribution of substituents in partially acetylated cellulose. J Polym Sci Polym Symp 36:523–527
338. Franz G (1991) Polysaccharide. Springer, Berlin
339. Prehm P (1980) Methylation of carbohydrates by methyl trifluoromethanesulfonate in trimethyl phosphate. Carbohydr Res 78:372–374
340. Mischnick P (1991) Determination of the substitution pattern of cellulose acetates. J Carbohydr Chem 10:711–722
341. Yu N, Gray GR (1998) Analysis of the positions of substitution of acetate and propionate groups in cellulose acetate-propionate by the reductive-cleavage method. Carbohydr Res 313:29–36
342. Yu N, Gray GR (1998) Analysis of the positions of substitution of acetate and butyrate groups in cellulose acetate butyrate by the reductive-cleavage method. Carbohydr Res 312:225–231
343. D'Ambra AJ, Rice MJ, Zeller SG, Gruber PR, Gray GR (1988) Analysis of positions of substitution of O-methyl or O-ethyl groups in partially methylated or ethylated cellulose by the reductive-cleavage method. Carbohydr Res 177:111–116

344. Garegg PJ, Lindberg B, Konradsson P, Kvarnstrom I (1988) Hydrolysis of glycosides under reducing conditions. Carbohydr Res 176:145–148
345. Stevenson TT, Furneaux RH (1991) Chemical methods for the analysis of sulfated galactans from red algae. Carbohydr Res 210:277–298
346. Liebert T, Schnabelrauch M, Klemm D, Erler U (1994) Readily hydrolyzable cellulose esters as intermediates for the regioselective derivatization of cellulose. Part II Soluble, highly substituted cellulose trifluoroacetates. Cellulose 1:249–258
347. Mischnick-Lubbecke P, König WA (1989) Determination of the substitution pattern of modified polysaccharides. Part I. Benzyl starches. Carbohydr Res 185:113–118
348. Mischnick P, Lange M, Gohdes M, Stein A, Petzold K (1995) Trialkylsilyl derivatives of cyclomaltoheptaose, cellulose, and amylose: rearrangement during methylation analysis. Carbohydr Res 277:179–187
349. Gross JH (2004) Mass spectrometry: a textbook. Springer, Heidelberg. ISBN 3-540-40739
350. Liebert T, Seifert M, Heinze T (2008) Efficient method for the preparation of pure, water-soluble cellodextrines. Macromol Symp 262:140–149
351. Hofmeister GE, Zhou Z, Leary JA (1991) Linkage position determination in lithium-cationized disaccharides: tandem mass spectrometry and semiempirical calculations. J Am Chem Soc 113:5964–5970
352. Adden R, Mischnick P (2005) A novel method for the analysis of the substitution pattern of O-methyl-α- and β-1,4-glucans by means of electrospray ionization-mass spectrometry/collision induced dissociation. Int J Mass Spectrom 242:63–73
353. Ciucanu I (2006) Per-O-methylation reaction for structural analysis of carbohydrates by mass spectrometry. Anal Chim Acta 576:147–155
354. Domon B, Costello CE (1988) A systematic nomenclature for carbohydrate fragmentations in FAB-MS/MS spectra of glycoconjugates. Glycoconjugate J 5:397–409
355. Arisz PW, Boon J (1995) Pyrolysis chemical ionization mass spectrometry of cellulose ethers. J Polym Sci Part A Polym Chem 33:2855–2864
356. Heinrich J, Mischnick P (1999) Determination of the substitution pattern in the polymer chain of cellulose acetates. J Polym Sci Part A Polym Chem 37:3011–3016
357. Mischnick P, Niedner W, Adden R (2005) Possibilities of mass spectrometry and tandem-mass spectrometry in the analysis of cellulose ethers. Macromol Symp 223:67–77
358. Adden R, Müller R, Brinkmalm G, Ehrler R, Mischnick P (2006) Comprehensive analysis of the substituent distribution in hydroxyethyl celluloses by quantitative MALDI-ToF-MS. Macromol Biosci 6:435–444
359. Pastorova I, Botto RE, Arisz PW, Boon JJ (1994) Cellulose char structures: a combined analytical Py-GC-MS, FTIR, and NMR study. Carbohydr Res 262:27–47
360. Carollo P, Grospietro B (2004) Plastic materials. Macromol Symp 208:335–351
361. Kamide K, Terakawa T, Miyazaki Y (1979) The viscometric and light-scattering determination of dilute solution properties of cellulose diacetate. Polym J 11:285–298
362. Kamide K, Miyazaki Y, Abe T (1979) Dilute solution properties and unperturbed chain dimension of cellulose triacetate. Polym J 11:523–538
363. Glasser WG, Samaranayake G, Dumay M, Dave V (1995) Novel cellulose derivatives. III. Thermal analysis of mixed esters with butyric and hexanois acid. J Polym Sci Part B Polym Phys 33:2045–2054
364. Sealey JS, Samaranayake G, Todd JG, Glasser WG (1996) Novel cellulose derivatives. IV. Preparation and thermal analysis of waxy esters of cellulose. J Polym Sci Part B Polym Phys 34:1613–1620
365. Fidale LC, Iβbrücker C, Silva PL, Lucheti CM, Heinze T, El Seoud OA (2010) Probing the dependence of the properties of cellulose acetates and their films on the degree of biopolymer substitution: use of solvatochromic indicators and thermal analysis. Cellulose 17:937–951
366. Crompton TR (1993) Practical polymer analysis. Plenum Press, New York, pp 595–664
367. Campbell D, Pethrich RA, White JR (2000) Polymer characterization: physical techniques. Stanley Thornes, Cheltenham, pp 362–407

368. Chartoff RP (2008) Thermal analysis of polymers. Characterization and analysis of polmers. Wiley Interscience, Hoboken, pp 805–881
369. Hill JO (1991) For better thermal analysis and calorimetry, ICTA, 3rd edn. CPC Reprographics, Portsmouth
370. Sircar AK (1982) Characterization of elastomers by thermal analysis. J Sci Ind Res 41:536–560
371. Savasci OT, Petkim Baysal SM (1986) Determination of effectivenesses of 2,6-di-tert-butyl-p-catechecol, mixed tri(mono- and dinonylphenyl) phosphite and their mixtures as antioxidants for CBR [cis-butadiene rubber] by DSC. J Appl Polym Sci 31:2157–2169
372. Gallagher PK (1993) Thermal analysis. Adv Anal Geochem 1:211–257
373. Brown ME (1988) Introduction to thermal analysis. Chapman and Hall, London
374. Häggkvist M, Li T-Q, Ödberg L (1998) Effects of drying and pressing on the pore structure in the cellulose fiber wall studied by proton and deuteron NMR relaxation. Cellulose 5:33–49
375. Crawshaw J, Cameron RE (2000) A small X-ray scattering study of pore structure in Tencel cellulose fibres and the effects of physical treatments. Polymer 41:4691–4698
376. Berggren J, Alderborn G (2001) Drying behavior of two sets of microcrystalline cellulose pellets. Int J Pharm 219:113–126
377. Rosenau T, Potthast A, Sixta H, Kosma P (2001) The chemistry of side reactions and byproduct formation in the system NMMO/cellulose (Lyocell process). Progr Polym Sci 26:1763–1837
378. Dorn S, Wendler F, Meister F, Heinze T (2008) Interactions of ionic liquids with polysaccharides—7: Thermal stability of cellulose in ionic liquids and N-methylmorpholine-N-oxide. Macromol Mater Eng 293:907–913
379. Wendler F, Konkin A, Heinze T (2008) Studies on the stabilization of modified Lyocell solutions. Macromol Symp 262:72–84
380. Hatakeyama H, Hatakeyama T (1998) Interactions between water and hydrophilic polymers. Thermochim Acta 308:3–22
381. Horbach A (1987) Thermoanalytical possibilities for characterization of cellulose and cellulose derivatives. Papier (Bingen, Germany) 41:652–657
382. Ruseckaite RA, Jiménez A (2003) Thermal degradation of mixtures of polycaprolactone with cellulose derivatives. Polym Degrad Stab 81:353–358
383. Hassan ML, Moorefield CN, Kotta K, Newkome GR (2005) Regioselective combinational-type synthesis, characterization, and physical properties of dendronized cellulose. Polymer 46:8947–8955
384. Heinze T, Rahn K, Jaspers M, Berghmans H (1996) Thermal studies on homogeneously synthesized cellulose p-toluenesulfonates. J Appl Polym Sci 60:1891–1900
385. Gaan S, Rupper P, Salimova V, Heuberger M, Rabe S, Vogel F (2009) Thermal decomposition and burning behavior of cellulose treated with ethyl ester phosphoramidates: effect of alkyl substituent on nitrogen atom. Polym Degrad Stab 94:1125–1134
386. Alvarez VA, Vásquez A (2004) Thermal degradation of cellulose derivatives/starch blends and sisal biocomposites. Polym Degrad Stab 84:13–21
387. El-Kalyoubi SF, El-Shinnawy NA (1985) Thermogravimetric analysis of some chemically modified celluloses. J Appl Polym Sci 30:4793–4799
388. Nada AMA, Hassan ML (1999/2000) Thermal behavior of cellulose and some cellulose derivatives. Polym Degrad Stab 67:111–115
389. Jain RK, Lal K, Bhatnagar HL (1989) Thermal degradation of cellulose esters and their tosylated products in air. Polym Degrad Stab 26:101–112
390. Kaloustian J, Pauli AM, Pastor J (1997) Thermal analysis of cellulose and some etherified and esterified derivatives. J Therm Anal 48:791–804
391. Jandura P, Riedl B, Kokta BV (2000) Thermal degradation behavior of cellulose fibers partially esterified with some long chain organic acids. Polym Degrad Stab 70:387–394
392. Berthold J, Rinaudo M, Salmen L (1996) Association of water to polar groups; estimations by an adsorption model for ligno-cellulosic materials. Colloids Surf A 112:117–129

393. Mizutani C, Inagaki H, Bertoniere NR (1999) Water absorbancy of never-dried cotton fibers. Cellulose 6:167–176
394. Hatakeyama T, Nakamura K, Hatakeyama H (2000) Vaporization of bound water associated with cellulose fibers. Thermochim Acta 352–353:233–239
395. Nakamura K, Hatakeyama T, Hatakeyama H (1981) Studies on bound water of cellulose by differential scanning calorimetry. Text Res J 51:607–613
396. Kaloustian J, Pauli AM, Pastor J (1996) Characterization by thermal analysis of lignin, cellulose, and some of its etherified derivatives. J Therm Anal 46:91–104
397. Ciesla K, Rahier H, Zakrzewska-Trznadel G (2004) Interaction of water with the regenerated cellulose membrane studied by DSC. J Therm Anal Calorim 77:279–293
398. Park S, Venditti RA, Jameel H, Pawlak JJ (2006) Changes in pore size distribution during the drying of cellulose fibers as measured by differential scanning calorimetry. Carbohydr Polym 66:97–103
399. Edgar KJ, Pecorini TJ, Glasser WG (1998) Long-chain cellulose esters: preparation, properties, and perspective. ACS Symp Ser 688:38–60
400. Takahashi A, Kawaharada T, Kato T (1979) Melting temperature of thermally reversible gel. V. Heat of fusion of cellulose triacetate and the melting of cellulose diacetate-benzyl alcohol gel. Polym J 11:671–675
401. Kamide K, Saito M (1985) Thermal analysis of cellulose acetate solids with total degrees of substitution of 0.49, 1.75, 2.46, and 2.92. Polym J 17:919–928
402. Joly N, Granet R, Krausz P (2004/2005) Olefin metathesis applied to cellulose derivatives: synthesis, analysis, and properties of new cross-linked cellulose plastic films. J Polym Chem A 43:407–418
403. Tosh BN, Saikia CN (1998) Thermal degradation of some homogeneously esterified products prepared from different molecular weight fractions of high α-cellulose pulp. J Polym Mater 15:185–195
404. Uryash VF, Rabinovich IB, Mochalov AN, Khlyustova TB (1985) Thermal and calorimetric analysis of cellulose, its derivatives and their mixtures with plasticizers. Termochim Acta 93:409–412
405. Cooney JD, Day M, Wiles DM (1984) Kinetic and thermogravimetric analysis of the thermal oxidative degradation of flame-retardant polyesters. J Appl Polym Sci 29:911–923
406. Cooney JD, Day M, Wiles DM (1983) Thermal degradation of poly(ethylene terephthalate): a kinetic analysis of thermogravimetric data. J Appl Polym Sci 50:2887–2892
407. Yao F, Wu Q, Lei Y, Guo W, Xu Y (2008) Thermal decomposition kinetics of natural fibers: activation energy with dynamic thermogravimetric analysis. Polym Degrad Stab 93:90–98

# Chapter 3
# Cellulose Activation and Dissolution

## 3.1 Activation of Cellulose

### *3.1.1 Introduction*

It is well known that controlling the reactions of cellulose, e.g., its transformation into esters or ethers is not trivial. The products obtained may exhibit unpredictable, and often irreproducible DS. The reason may be the accessibility of the hydroxyl groups of the AGUs. The hydroxyl groups on the surface of the fiber or in the amorphous regions of the biopolymer are more accessible to the reagent than those in the crystalline regions that may lead to an inhomogeneous reaction at the molecular level. Therefore, cellulose is customarily subjected to a pretreatment or an activation step before it is submitted to a chemical reaction. This strategy is employed both in the industry and in the laboratory. A comment concerning the use of the term "activation" is in order, as there are a few examples where "classic" pretreatments of cellulose, e.g., mercerization and regeneration, do not lead to the desired effect. For example, the reactivity of some mercerized celluloses by ammonia or aqueous NaOH toward heterogeneous acetylation or nitration was found to be either equal [1], or even less than that of the corresponding untreated cellulose [2]. Whereas native cellulose samples dissolve in $SO_2$–diethylamine–DMSO mixture, their regenerated counterparts did not [3, 4]. Nevertheless, the term activation will be employed in order to describe any pretreatment intended to make the cellulose more accessible, e.g., increase its solubility in specific media (alkali solution, DMAc/LiCl, etc.) and/or increase its reactivity in chemical reactions. Note that in some strongly polar media, e.g., NMMO, urea/alkali, and ionic liquids, the initial strong swelling of cellulose leads to its dissolution. The mechanisms of action of these media are discussed in Sect. 3.2.

The activation procedure most extensively employed in the industry involves treatment of cellulose with aqueous alkali. Depending on the concentration of this swelling agent, such treatments cause extensive disruption of the inter- and



T. Heinze et al., *Cellulose Derivatives*, Springer Series on Polymer and Composite Materials, https://doi.org/10.1007/978-3-319-73168-1_3

intramolecular interactions, and may eventually lead to the dissolution of the biopolymer. Cellulose may be shredded and added to an alkaline bath (most commonly sodium hydroxide solution) before an alkyl halide or chloroacetate is added to form the corresponding cellulose ethers [5].

Activation of cellulose can be caused by treatment with solvents that disrupts essentially intermolecular interactions including hydrogen bonding and leads to cellulose swelling, but not dissolution. The effect of intercrystalline swelling on the accessibility of cellulose is shown by the observation that the following solvent exchange (water → acetone → DMAc) resulted in enhanced solubility of softwood pulp in DMAc/LiCl, without changing the crystalline structure of the biopolymer, on one hand. On the other hand, milling did not enhance dissolution of the same cellulose, although its crystalline structure was almost destroyed [6]. Additionally, cellulose samples treated with DMAc dissolve in DMAc/LiCl faster than samples treated with acetone, and much faster than untreated samples. Relative to samples treated with acetone, those pre-swollen by DMAc exhibit larger fractal dimensions and shorter longitudinal relaxation time, $T_1$, both for $^{1}$H- and $^{13}$C NMR measurements. This indicates that the latter cellulose exhibit larger surface roughness, larger segmental mobility, and larger molecular heterogeneity at the 100 nm scale. Such length corresponds to LODP of cellulose [7] that is a measure of dynamic heterogeneity of the biopolymer [8]. Considering that the main objective of cellulose activation is to increase the accessibility of its hydroxyl groups, hence solubility in different media for subsequent regeneration, or chemical modification, the discussion below addresses accessibility and its methods of determination. Moreover, the different methods of activation, including mechanical, intercrystalline solvent-mediated swelling, and, finally, intracrystalline swelling are considered.

### *3.1.2 Accessibility and Its Methods of Determination*

The initial step of any processing of cellulose, dissolution or derivatization, proceeds under heterogeneous (solid/liquid) conditions. The rate and yield of the reaction (in terms of targeted versus obtained DS) are strongly dependent on the availability, i.e., accessibility of the OH groups of the biopolymer. The elementary crystallites, which form the basic fibrillar structure, are involved in the intermolecular hydrogen-bond network, coupled to dipolar and van der Waals interactions. These forces are strong enough to limit the penetration of the crystalline regions of cellulose, even by small, hydrophilic molecules like water. A few examples suffice to demonstrate that strenuous conditions are required in order to access the hydroxyl groups of the crystalline region. One hundred cycles of treatment of wood cellulose with hot $D_2O$ were required in order to achieve nearly complete OH/OD exchange [9]. High temperature (>300 °C) and high pressure (>11 MPa) were necessary in order to dissolve even the MCC with relatively low

**Table 3.1** Main methods employed for the determination of the accessibility of cellulose

| Method | Examples |
|---|---|
| *Sorption techniques* | |
| Sorption of gases | Sorption of argon, helium, or nitrogen |
| Sorption of vapors | Sorption of $H_2O$ or $D_2O$ vapor |
| Sorption from solution | Sorption of iodine from aqueous solution of $I_2$/KI |
| *Purely physical interaction with liquids (justify liquids)* | |
| Swelling of liquids | Water, organic solvents, or solvent mixtures |
| Isotope exchange | H/D exchange by interaction with $D_2O$ |
| *Chemical reactions* | |
| Alcoholysis | Ethanolysis of the glycosidic bonds |
| Chemical derivatization | Transformation into xanthates, formats, acetates, and trifluoroacetates |
| Other chemical reactions | Oxidation, e.g., by $N_2O_4/CCl_4$ and $HIO_4$ |

DP in sub- and supercritical water [10]. That is, the accessibility of the crystalline regions to many solvents and chemical reagents is severely limited. Only the hydroxyl groups that are are readily accessible, which are located at the surface of the elementary fibrils or in the (amorphous) segments of cellulose in the interlinking regions between the crystallites. For liquids, which do not perturb the intermolecular hydrogen bonding of cellulose, the accessibility depends on the available inner surface of the pore and void systems, on the supramolecular order, and on the fibrillar architecture of the biopolymer. The methods most frequently employed to determine cellulose accessibility are summarized in Table 3.1.

Sorption of gases and vapors

Sorption of gases like Ar, He, $N_2$, or water vapor by cellulose is usually employed in order to determine some fundamental properties that bear on accessibility, namely the total surface area, the total pore volume, and pore diameter distribution. This is carried out by applying the BET and BJH equations to the experimental adsorption isotherm [11]. Briefly, the uptake of a gas is the relationship between the gas molecules that adsorb on the surface of a substrate (inside a sealed container) and those in the gas phase. The free gas exerts a measurable pressure, whereas that adsorbed does not. Therefore, the amount of gas adsorbed by the sample can be deduced from $p/p^\circ$, the equilibrium gas pressure, and the starting one, respectively. For water vapor sorption, the relationship is between the moisture content of cellulose and the relative humidity (RH) of air above the biopolymer. The adsorption isotherm gives information about the surface characteristics of the substrate; porous materials display characteristic hysteresis curves. The latter behavior means that once a relative pressure (or RH for water vapor) of 1.0 has been reached, a slow reduction of pressure (or of RH) produces a curve (the desorption curve) that is different from its sorption counterpart, because of the way that the micropores empty. The five classes of sorption/desorption curves that are

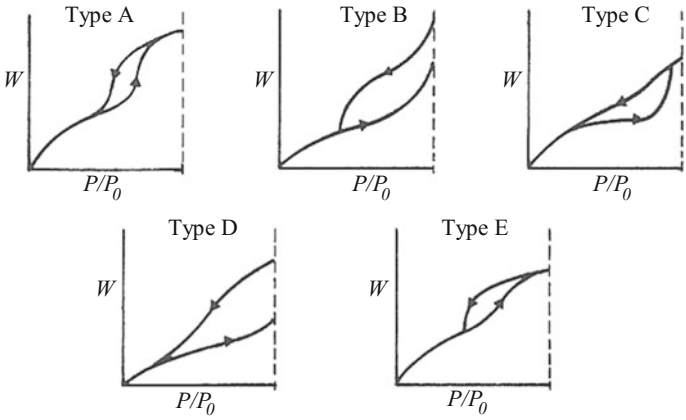


**Fig. 3.1** Types of adsorption/desorption curves for surfaces with different porosities. Type (A) to (E) are hysteresis curves caused by adsorbent condensation in cylindrical-shaped; slit-shaped; wedge-shaped; wedge-shaped with narrow neck, and "bottle-neck" pores, respectively (Reproduced from [11] with permission from Springer)

characteristic for relatively porous materials are shown in Fig. 3.1. Cellulose is expected to give Type A curve (see, e.g., [12]).

A comment on the adsorption of inert gases is worthwhile because this is relevant to the surface area calculated. In order to ensure proper adsorption, the surface studied should be clean and dry. Cleaning requires removal of strongly adsorbed water, either by extensive heating [13–15], or by (tedious) solvent exchange, e.g., methanol is exchanged for water, *n*-pentane is exchanged for methanol, the alkane is removed by purging with He gas during 1 week [16]. Sample drying under reduced pressure is used by most researchers; this treatment leads to a marked decrease in the sorptivity of cellulose due to degradation [13, 14] or "hornification" [17]. Hornification refers to the remarkable decrease in cellulose accessibility, hence reactivity due to the formation of hydrogen bonds between the surface hydroxyl groups, i.e., "fusion" of the fibrillar structure, on one hand [18]. On the other hand, incomplete drying may lead to unexpected results, e.g., gas desorption curve ahead of, not lagging behind, the sorption "arm", at least in a part of the adsorption isotherm [19]. The occurrence of the last problem may go unnoticed because, in principle, the sorption arm of the isotherm is sufficient to calculate the surface area (see, e.g., [20–22]). Hornification results in the calculation of smaller surface areas, whereas the meaning, hence interpretation, of gas desorption ahead of its sorption is not clear. Therefore, the effect of the procedure employed for water removal on the surface area of cellulose should not be underestimated; both arms of the gas adsorption isotherm should be determined and reported.

For type II isotherms, application of the BET model is limited to the lower range of relative pressure, i.e., below ($p/p°$) of 0.3. A description of isotherms that covers the whole range of relative pressure (or RH) for nonporous and porous surfaces has

been introduced. The most relevant quantities are the excess surface work (ESW) and the sorbed mass at ESW-minimum, Φ, defined by Eq. 3.1

$$\Phi = n_{\text{ads}} \cdot \Delta\mu = \left(\frac{M_\infty}{M_{\text{mol}}}\right) \cdot RT \ln \frac{p}{p^\circ}, \tag{3.1}$$

where $n_{\text{ads}}$ = number of sorbed molecules; $\Delta\mu$ = change in the chemical potential; $M_\infty$ and $M_{\text{mol}}$ refer to sorbate mass at equilibrium and the molar mass of the sorbate, $R$ and $T$ have their usual meaning; $(p/p^\circ)$ = (RH/100) = equilibrium partial pressure of the vapor [23].

A related experiment, which is based on sorption/desorption of a substance on the surface of cellulose, involves the determination of the dispersive component (London interactions) of the surface free energy of the biopolymer by inverse gas chromatography. The retention time of alkanes of increasing molecular volume, e.g., *n*-hexane to *n*-decane in a column packed with a biopolymer is determined. This is converted to retention volume; the latter is employed in the calculation of the above-mentioned component, since alkanes interact with biopolymers essentially by dispersive interactions [24].

An easier approach for the determination of the specific surface area of cellulose is dye adsorption from aqueous solution. The information obtained (specific area of wet biopolymer) is of fundamental practical importance because cellulose is usually processed wet, e.g., during dyeing. The dye is adsorbed under specified experimental conditions and the surface area of the biopolymer is calculated from the adsorption isotherm obtained, the surface area of the dye, and Avogadro's number [25, 26]. Figure 3.2 shows a typical plot for the adsorption of Congo red on fibrous celluloses and their mercerized counterparts. The cellulose samples tested showed Langmuir-type adsorption isotherm. As expected, the mercerized samples adsorb much more dye than their native counterparts due to the enhanced accessibility.

Two factors should be considered when dye adsorption data are manipulated, namely, dye distribution on the fiber, and the area of contact dye/cellulose. Molecular modeling of cellulose/dye (C. I. Reactive Red 2)/water assemblies has indicated that there is no apparent specificity in the initial dye–cellulose binding process, although stronger interactions, e.g., in the amorphous regions cannot be ruled out [28]. Thus, preferential dye adsorption is not a problem, provided that Langmuir-type adsorption isotherm of the dye is exhibited. An "operational" solution to the question of the area of contact dye/cellulose is based on the fact that the AFM images of cellulose surfaces show periodicities at 1.07 and 0.53 nm, attributed to fiber-repeat and glucose unit-repeat, respectively [29]. This repetitive morphology ensures an even deposition of the dye on the fiber surface. Most of the dyes employed in this measurement are aromatic, i.e., their structure is rigid. It is plausible, therefore, that the dye is adsorbed "flat" on the surface of the fiber [30]. The area of contact can then be taken as equal to the surface area of the dye molecule. The latter is readily calculated by commercial software, employed for geometry optimization in gas phase, followed by solvation in water. The result of such calculation for Congo red is shown in Fig. 3.3.

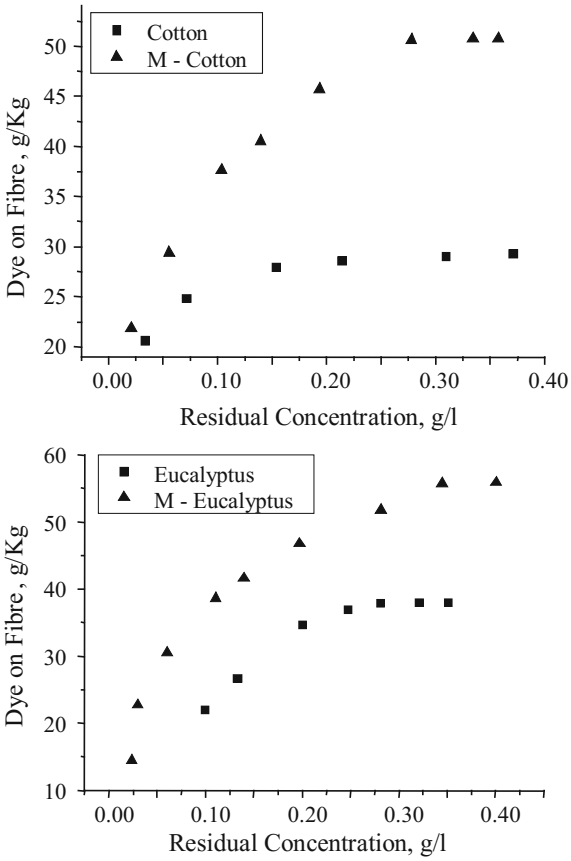


**Fig. 3.2** Interaction of Congo red with the fibers of cotton, eucalyptus, and their mercerized counterparts (marked by M). The plots show the dependence of the amount of dye adsorbed by the fiber on dye concentration in the bath (Reproduced from [27] with permission from John Wiley and Sons)

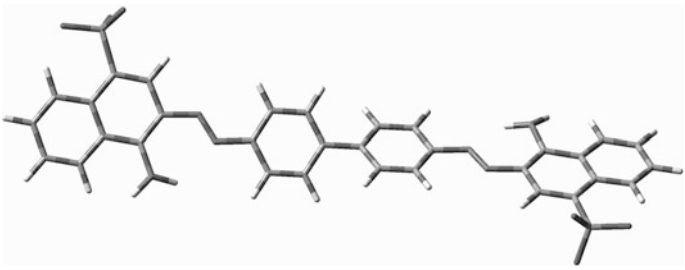

**Fig. 3.3** Minimum-energy conformation of Congo red dye solvated in water, as calculated by the AMSOL program package (version 7.0), the PM3 semi-empirical method and the SM 5.4 solvation model

An application that is related to dye adsorption is volume-dependent solute exclusion from cellulose yielding information on the average and maximum pore size and internal surface area. Solutions of solutes (probes) of increasing molar volumes (mono- to tetrasaccharides; mono- to tetraethylene glycols, and commercial "Carbowaxes") are brought into contact with wet cellulose of known water content. The concentration of the probe in the solution is measured before and after contact with the biopolymer. Thus, the solution will be diluted but not as much as if it had complete access to all water in cellulose. From the resultant change in mass, the amount of "inaccessible" water can be calculated. This amount will increase as a function of increasing the molar volume of the probe until a maximum, where all solute molecules are excluded from cellulose. At this stage, a plot between the amount of inaccessible water versus probe molar volume or diameter levels off. Thus, the amount of inaccessible water, with respect to a specific probe molecule, can be calculated from the total amount of water present in cellulose, and the dilution of the probe solution [31]. This technique has been employed, e.g., in order to show the remarkably higher accessibility of never-dried cellulose compared to samples that have been dried and then re-swollen. The deleterious effect of drying on micropore size (due to hornification) has also been demonstrated by this technique [32–34].

The adsorption of water vapor is interesting because the cellulose sample does not have to be dried, hence hornification is not an issue. The experiment is carried out by maintaining cellulose in an atmosphere of known RH, at a fixed temperature, until equilibrium is attained (as evidenced by the constancy of sample mass). The value of RH can be controlled either by a static or a dynamic method. In the former, cellulose is stored in a closed container, e.g., a desiccator, over a supersaturated aqueous solution of an electrolyte. For example, the values of RH over saturated solutions of LiCl, $CH_3CO_2K$, $K_2CO_3$, NaBr, NaCl, and $KNO_3$ are 11, 25, 40, 63, 75, and 96% RH, respectively, at 25 °C [35, 36]. Although convenient and widely employed, this method is relatively slow and several days may be required in order to attain sorption equilibrium. At high RH, this time scale may lead to bacterial growth, which invalidates the results [37].

Water sorption can be more conveniently measured under dynamic conditions. Briefly, this apparatus is composed of a Cahn-type microbalance inserted in a chamber with controlled temperature and humidity. The latter is achieved by mixing streams of nitrogen, dry and saturated with water vapor; the proportions of both are fixed by gas flow controllers. The variation in sample mass is then determined as a function of time. A comparison between the static and dynamic water vapor sorption has shown that the results of both are consistent as long as the diffusion coefficient of water vapor in the material is high as, e.g., in the case of MCC. When the diffusion coefficient becomes small, the static method is very slow because of the difficulty to reach thermodynamic equilibrium. Thus, the dynamic method is more expedient [38].

The kinetics of water sorption/desorption has been conveniently reproduced by employing a "partial exponential model", where the change in mass as a function of

time is described in terms of two time domains, for fast and slow water sorption, probably related to the formation of "bound" and "free" water [39].

Surface areas calculated by water or gas adsorption are usually largely different. For example, the specific surface areas of different celluloses, calculated by the BET method, are typically <10 $m^2/g$ (see, e.g., [12, 19, 40]). The range is much smaller than that calculated from water vapor sorption (130–160 $m^2/g$) [41]. This discrepancy indicates a fundamental difference in the adsorption mechanism between the two cases. This can be rationalized if it is assumed that the adsorption of nitrogen occurs on the surface of cellulose particles (which have sizes in the micron range), whereas the adsorption of water also occurs inside the particles. In the latter case, adsorption would also occur on the interfaces between the structural units of cellulose with sizes in the range from 2 to 5 nm [42, 43], or more, e.g., 7–8 nm for cotton [44]. That is, water adsorption occurs on a much larger surface area of cellulose as shown in Fig. 3.4.

The presence of multilayers of adsorbed water, as shown in Fig. 3.4, is in agreement with the observation that water vapor sorption isotherm is almost linear up to RH of ca. 50–60%, but increases much faster at higher values. The latter increase has been attributed to capillary condensation; adsorption in multilayers; or increase in cellulose surface that is exposed to water vapor, due to either swelling or temperature fluctuations [41, 45].

It is also possible to adsorb $D_2O$ (or $T_2O$). The hydroxyl groups that are located in the less-ordered regions of the biopolymer will exchange their H with D (or T) [46]. The isotope exchange can be most readily studied by measuring sample radioactivity (tritium) or by several methods for $D_2O$, including change in sample mass [47], change in areas of the appropriate IR bands, 3200–3500 $cm^{-1}$ ($\nu_{OH}$), 2600–2400 $cm^{-1}$ ($\nu_{OD}$) [48], change in peak areas in NIR (6000–7200 $cm^{-1}$, overtone of $\nu_{OH}$) [49], and $^{13}C$ CP/MAS NMR (55–110 ppm, different carbons of the AGU) [50].

In principle, the isotope exchange method can be employed as a measure of crystallinity, because the reaction rate is fast for accessible OH groups. Some

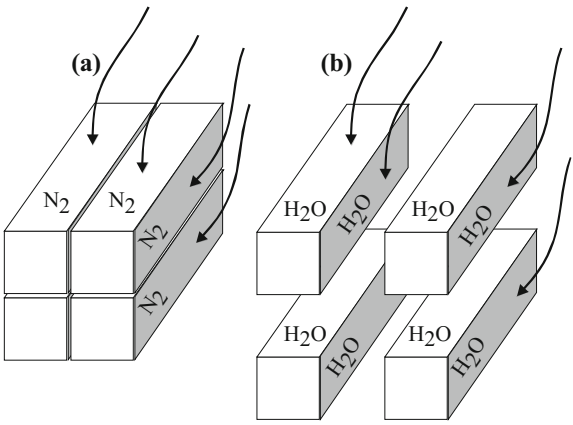


**Fig. 3.4** Schematic representation of **a** $N_2$ and **b** water vapor sorption by cellulose (Reprinted from [19], copyright (©2004) with permission from Elsevier)

(slower) exchange also takes place at the outer fringe of the well-ordered crystalline regions. An indication of the penetration of $D_2O$ vapor into the (ordered) outer layers of the crystallites is the persistence of some OD groups after the sample has been rehydrated with $H_2O$ [51]. Therefore, $I_c$ values obtained by D/H exchange are always appreciably lower than those derived from WAXS. Consequently, the results of isotopic exchange experiments should be considered as "accessibilities", or as "percentage of hydrogen bond order", rather than crystallinity [47]. A scheme for explaining the reason for the difference between crystallinity and accessibility, as measured by WAXS and $D_2O$ vapor sorption, respectively, is presented in Fig. 3.5. Part (a) depicts a cross section of a crystallite, composed (arbitrarily) of 256 cellulose molecules ($16 \times 16$) in a crystalline domain, surrounded by 64 cellulose molecules in an amorphous region; this arrangement corresponds to 25% accessible OH groups. In part (b), D/H exchange was assumed to occur in the amorphous region (i.e., the 64 molecules) plus in the peripheral molecules of the crystalline region, an additional 64 molecules, leading to an increase in the (apparent) percentage of accessible OH groups from 25 to 35%.

The iodine sorption is usually carried out by adding a concentrated $I_2$/KI solution to a known weight of cellulose. After 3 min, the excess of iodine is displaced by

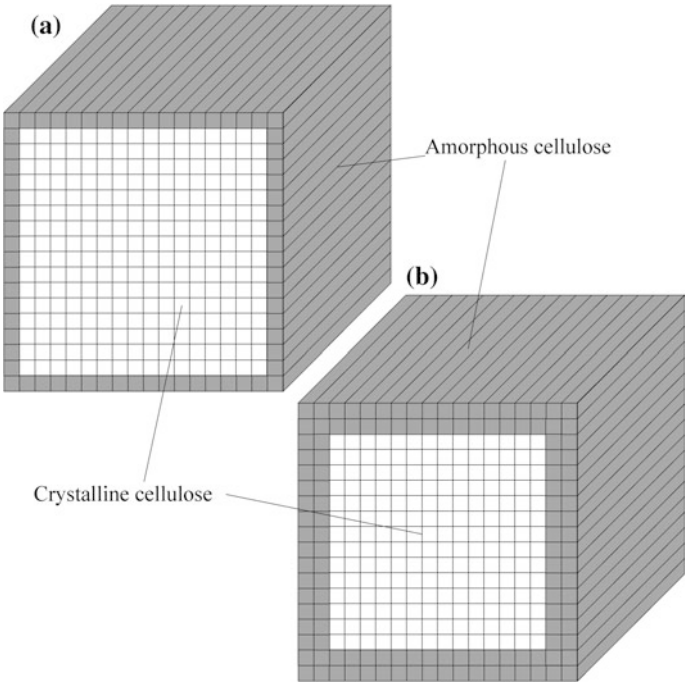


**Fig. 3.5** Schematic representation of a concept for a possible explanation of the difference between crystallinity and accessibility of cellulosic fibre substrates. Cellulose crystallite before (**a**) and after D/H exchange (**b**)

**Table 3.2** Percentage of amorphous material in cellulose samples calculated by different techniques [60]

| Technique | Cotton | Mercerized cotton | Wood pulp | Regenerated cellulose |
|---|---|---|---|---|
| X-ray diffraction | 27 | 49 | 40 | 65 |
| Density | 36 | 64 | 50 | 65 |
| Moisture regain (sorption ratio) | 42 | 62 | 49 | 77 |
| Deuteration | 42 | 59 | 55 | 72 |
| Acid hydrolysis | 10 | 20 | 14 | 28 |
| Formylation | 21 | 35 | 31 | 63 |
| Periodate oxidation | 8 | 10 | 8 | 20 |
| Iodine sorption | 13 | 32 | 27 | 52 |

adding a large volume of saturated $Na_2SO_4$ solution. After standing and frequent agitation, the iodine content of the aqueous solution is determined by titration. The ISV calculated is a measure of cellulose accessibility [52–55]. The isotherms reported for iodine adsorption include Freundlich [56]; Langmuir [57], and Fowler–Guggenheim types [58]. A detailed study of this technique, where the variables, namely, concentration of iodine reagent, of $Na_2SO_4$, iodine reagent/cellulose ratio, mixing time, and agitation were carefully controlled, has shown that the results of this method are reproducible. Titration of the iodine in the supernatant or that adsorbed on cellulose gives the same ISV. The adsorption isotherms are of Langmuir type [59].

Considering the above discussion, it is obvious that the agreement between cellulose accessibility and crystallinity index, as determined by different experimental approaches, is more qualitative than quantitative (Table 3.2).It should be mentioned that accessibility is affected by the size of the crystallites and their distribution and is not available from analysis of crystallinity by X-ray, IR, or Raman spectroscopy because these techniques focus on the amorphous/crystalline ratio only [61]. The accessibility also depends on the size of the probe molecule because the linking regions of the crystallites are more accessible to relatively small molecules, e.g., water. The effect of pretreatments on cellulose accessibility is clear and consistent. That is, the induced transformation of cellulose I → cellulose II (by mercerization or regeneration from the dissolved state) increases the accessibility, independent of the method employed to express this property.

### *3.1.3 Activation by Intercrystalline Swelling*

Activation is most conveniently discussed on the basis of the structural modification of cellulose caused by the method employed. These strategies are shown in the scheme below (Fig. 3.6).

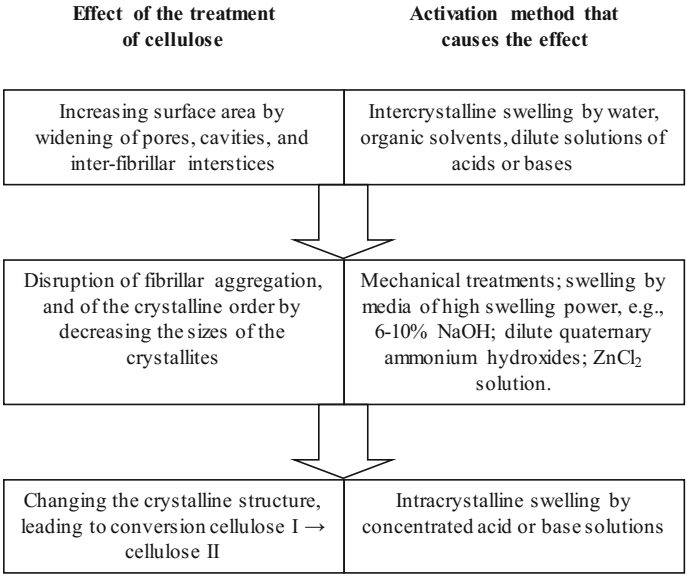


**Fig. 3.6** Treatment of cellulose in order to activate the polymer

There are several reasons for the continued interest in studying intercrystalline swelling of cellulose: From the point of view of application (e.g., fiber dyeing), the accessibility of wet cellulose is far more important than the accessibility of its dry counterpart. Intercrystalline swelling of cellulose and its dissolution have many common features, hence are controlled by the same solvent–biopolymer interactions. The underlying cause of the similarity is that both processes disrupt the strong hydrogen bonding to a varying extent, or even eliminate cellulose supramolecular structure. The intimate relationship between cellulose intercrystalline swelling and dissolution can be shown by examining the results of treatment with solutions of bases, e.g., $(C_2H_5)_4NOH$ or NMMO dissolved in water or in DMSO. Up to the base concentration of 1.7 mol/L, solutions of $(C_2H_5)_4NOH$ cause a rapid and limited swelling of spruce pulp. However, NMMO dissolves in 1.8 mol/L base [62]. A 20% (w/w) NMMO/DMSO causes swelling of ca. 60% of untreated beech cellulose, whereas pretreatment of the cellulose with ammonia, followed by NMMO/DMSO results in complete dissolution [63]. The effect of aqueous NMMO on cellulose depends on the water content of the medium (see Sect. 3.1.4) [64]. Because the physical integrity of the biopolymer is maintained during intercrystalline swelling, it gives more insight into the interaction mechanisms between cellulose and the medium, hence sheds light on what controls dissolution.

Solvents that yield intercrystalline swelling are water, alcohols, and other organic solvents, or their mixtures. Akin to the mechanism of water vapor sorption, the solvent is expected to penetrate into the interstices between the fibrillar structural units and swells their less-ordered surface areas, and possibly the less-ordered

interlinking areas between the elementary crystallites in the basic fibrils. Swelling can be determined from the gain in mass of cellulose under specified experimental conditions. This method is simple, accurate, and widely used for determining swelling by water [65] and organic solvents, including relatively viscous ones, e.g., 1-octanol and DMSO, provided that the experimental conditions, in particular, those of centrifugation of the sample after swelling, are adjusted in order to obtain reproducible results.

The extent of intercrystalline swelling by a given solvent can be enhanced by solvent exchange. Cellulose is first swollen by a small, dipolar solvent, followed by an exchange with the solvent desired. For example, swelling by DMF increased to 61, 45, 81, 65, and 62%, when cellulose was pre-swollen with water, ethanol, ethanolamine, DMSO, and formamide, respectively [66]. MCC and fibrous celluloses, including cotton, dissolve easily in DMAc/LiCl after the following sequence of solvent exchange: water → methanol → DMAc [67–70]. The exchange of DMAc for water has also been carried out in a single step, by suspending the cellulose in this solvent followed by distillation of 25% of solvent volume [71]. The effect of solvent exchange on acetylation of cellulose wetted with water, then dried under reduced pressure was compared with samples where the water was displaced by pyridine or by solvent exchange (ethanol → diethyl ether → cyclohexane, ethanol → diethyl ether → $CCl_4$). In all cases, the solvent-exchanged samples, even when dried under reduced pressure, gave higher acetyl content than untreated samples, or those treated only with water and dried [72–74]. Similar results were reported for cotton fibers that were kept in the never-dried state after the swelling treatment. Extraction by organic solvents is preferred over washing with water in order to remove the swelling agent. The greatest modifications of the crystal structure of cotton were obtained by treatment with anhydrous methylamine, followed by washing with chloroform and pyridine, and acetylation, as well as by alcoholic mercerization followed by washing with ethanol then pyridine, and acetylation [75].

In many cases, it is not possible to remove the organic solvent completely from cellulose, even after heating for an extended time under reduced pressure. Solvent "entrapment" in the interfibrillar interstices prevents the reformation of hydrogen bonds during fiber collapse, i.e., it prevents hornification, this leads to enhanced reactivity. Table 3.3 shows the amount of solvent entrapment in native and M-cotton, and the subsequent effect on the DS of the product. The biopolymer samples were heated at 100 °C for 2 days, at 0.1 mm Hg and acetylated by acetic anhydride in pyridine. As expected, solvent entrapment is different for native and M-cellulose that is more reactive. The relevant points here are that volatile, weakly polar solvents like acetone (b.p. 56 °C) or THF (b.p. 66 °C) are not completely removed from cellulose after such strenuous treatment, and that the trace amounts of residual solvents have an important effect on acetylation. Entrapment of *n*-hexane, benzene, and toluene shows that solvent polarity and hydrogen-bonding ability do not seem to be important to solvent inclusion in cellulose. Almost any solvent employed penetrated the biopolymer provided that the cellulose is sufficiently swollen [72–74].

**Table 3.3** Amount of solvents entrapped in cellulose and their effect on the DS after acetylation of cellulose[a]

| Solvent entrapped | Native cotton | | M-cotton | |
|---|---|---|---|---|
| | Ratio solvent/AGU[b] | DS[b] | Ratio solvent/AGU[b] | DS[b] |
| Water | 0 | 0.16 | 0 | 0.02 |
| Methanol | 0.04 | 0.73 | 0.02 | 0.09 |
| Ethanol | 0.06 | 0.62 | 0.09 | 1.45 |
| 1-Propanol | 0.09 | 0.70 | 0.10 | 1.57 |
| Acetone | 0.06 | 0.73 | 0.07 | 1.46 |
| Pyridine | 0.06 | 0.75 | 0.14 | 1.62 |
| THF | 0.16 | 0.60 | 0.08 | 1.41 |
| *n*-Hexane | 0.10 | 0.79 | 0.07 | 1.36 |
| Benzene | 0.06 | 0.69 | 0.08 | 1.31 |
| Toluene | 0.05 | 0.62 | 0.08 | 1.39 |

[a]After solvent exchange, the cellulose samples were heated under reduced pressure, and then submitted to acetylation; see text for details

[b]In the original literature, these values were reported as a number of AGU/mole of solvent entrapped, and acetyl %, respectively. For ease of reading, these figures were recalculated as number of solvent molecules per AGU, and DS, respectively

The data of swelling are usually reported as percent swelling (%Sw) [76]. This scale is also employed when the extent of swelling is correlated with the physicochemical properties of a series of solvents. The following simple calculation demonstrates that %Sw is appropriate for comparing the swelling of different cellulose samples by the same solvent, or by solvents whose molecular masses are not very different. Consider a 50% increase in cellulose mass due to swelling (=81.026 g, based on one AGU); this mass gain corresponds to the very different number of moles of solvent molecules/AGU, *n*Sw, 2.53, 0.63, 2.0, and 0.45 for methanol, 1-octanol, acetonitrile, and HMPA, respectively. It follows, therefore, that it is more appropriate to compare the efficiencies of solvents in terms of *n*Sw, rather than %Sw. The reason is that the former scale is directly related to the number of solvent molecules per OH group of the AGU. Indeed, the use of *n*Sw has solved an apparent discrepancy between the swelling power of two homologous series of structurally related protic solvents, namely alcohols (methanol to 1-octanol) and 2-$ROCH_2CH_2OH$ (R = methyl to 1-butyl) [40]. The use of *n*Sw instead of %Sw also leads to better correlations between the swelling by a series of aprotic solvents and their physicochemical properties [27].

Cellulose–solvent interactions depend on several factors, those of the biopolymer (e.g., its supramolecular structure), of the solvent (e.g., $pK_a$ and molar volume), as well as experimental variables, e.g., the temperature. With regard to the biopolymer, there is a general agreement that celluloses with different DP, $I_c$, α-cellulose contents, and pore volume distribution are expected to give different degrees of swelling [77, 78]. Specifically, the swelling of the biopolymer decreases as a function of increasing its $I_c$, DP, α-cellulose content [79] and decreasing its

surface area [80]. For example, the ease of solvent uptake and dissolution of highly crystalline MCC relative to fibrous celluloses can be traced to its low DP, and mesoporous nature, compared with microporous celluloses of high DP [19, 81]. Whereas $I_c$ plays a minor role in the dissolution of non-fibrous cellulose of low DP in aqueous NaOH [82], it is a determinant structural feature, along with DP, the total volume, and size distribution of the micropores for the processing of fibrous celluloses [70, 75, 81, 83, 84].

Mercerization and other treatments (e.g., cellulose regeneration by hydrolysis of its carboxylic acid esters) lead to cellulose that shows a noticeable increase in swelling. The following are examples of the ratios of WRV, of two related celluloses; listed as cellulose type and treatment employed, followed by ratio of the two WRV (pretreated/air-dried celluloses): (spruce sulfite pulp; decrystallized), 1.38; (pine sulfate pulp; never dried), 1.61; (Rayon staple; never dried), 1.12; (cotton; NaOH-mercerized), 2.43; (eucalyptus; NaOH-mercerized), 1.73 [85]. The effect of cellulose mercerization on its swelling can be demonstrated by examining the values of *n*Sw for a series of aliphatic alcohols, from methanol to 1-octanol. The ratios *n*Sw(water)/(*n*Sw(protic solvent) were recalculated from published data for MCC, cotton, M-cotton, cellulose from eucalyptus, and M-eucalyptus, respectively [40]. These ratios show perfect linear dependence on the number of carbon atoms in the alcohol; the corresponding slopes are 9.01 ($r = 0.9954$), 2.49 ($r = 0.9952$), 11.65 ($r = 0.9988$), and 3.09 ($r = 0.9965$), respectively (Fig. 3.7). The large differences between the slopes of native celluloses and mercerized counterparts clearly show the important effects of alkali treatment on the biopolymer supramolecular structure, i.e.,

- an increase in cellulose accessibility due to increase in surface areas (between 47 and 74%)
- an increase in pore volume due to the expansion of the pores, and unification of adjacent ones [86]
- a decrease in the size of the crystallites [87]
- an increase in the degree of disorder of the hydroxymethyl groups [88].

These modifications in the supramolecular structure tend to “attenuate” the dependence of *n*Sw of mercerized celluloses on the molecular properties of the solvent, e.g., the molar volume of the alcohols.

There are also effects of the properties of the solvent employed. First, correlations between solvent properties and their power of swelling are presented, followed by a discussion of the results of water and DMSO, two particularly efficient solvents for swelling of cellulose. Several properties have been employed in order to explain the swelling efficiency of solvents, including the molar volume ($V_S$), where the subscript (S) refers to solvent [89, 90], and Hildebrand’s or Hansen’s solubility parameters [91–93]. The fact that some swelling data of cellulose and wood did not correlate with Hildebrand’s solubility parameter ($\delta_{Hildebrand}$), and that $\delta_{Hildebrand}$ can be split into three components, namely $\delta_D$ (van der Waals dispersion forces), $\delta_H$ (hydrogen bonding), and $\delta_P$ (Keesom’s dipole interactions) prompted

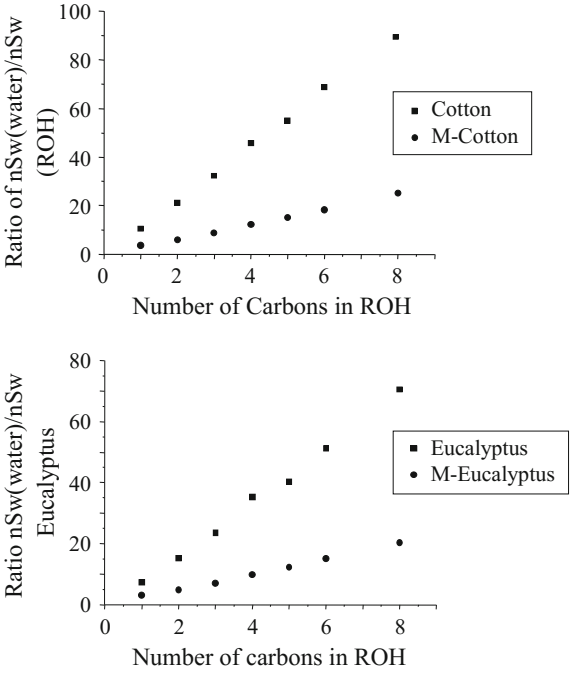


**Fig. 3.7** Dependence of *n*Sw(water)/(*n*Sw(protic solvent) on the number of carbon atoms of aliphatic alcohols (ROH) calculated based on published *n*Sw data [40]

some authors to use the latter quantities, in addition to $V_S$, in order to correlate swelling with the molecular properties of the solvent [77, 79, 80, 94–98]. A different approach used was to substitute $\delta_H$ by Gutmann's acceptor (AN) and donor (DN) numbers of the solvent [99]. These data indicate that swelling is a complex process and cannot be correlated by a single solvent property unless the other structural parameters are held practically constant as in the case of using a homologous series of alkylamines or aliphatic alcohols (of practically constant $pK_a$). A more appropriate approach is to use a linear combination of solvent properties.

Appropriate statistical criteria [100] have been applied to study swelling of MCC, cotton, M-cotton, cellulose from eucalyptus, and M-eucalyptus by 20 proptic- and 16 aprotic solvents. Solvatochromic properties were employed as solvent descriptors. These are obtained by the use of solvatochromic probes, i.e., substances that exhibit solvent-sensitive intramolecular charge-transfer (CT) bands as shown in Fig. 3.8, where the CT in the dye is from its phenolate oxygen to the heterocyclic nitrogen [101, 102]. Figure 3.9 shows the phenomenon of solvatochromism for the merocyanine probe 2,6-dibromo-4-[(*E*)-2-(1-methylpyridinium-4-yl)ethenyl] phenolate, $MePMBr_2$ [103]. The solvent properties, which are determined by use of these probes, are solvent "acidity", $\alpha_S$; "basicity", $\beta_S$; and dipolarity/polarizability, $\pi$ * S. Regression analyses of *n*Sw for both classes of solvents (protic and aprotic) versus

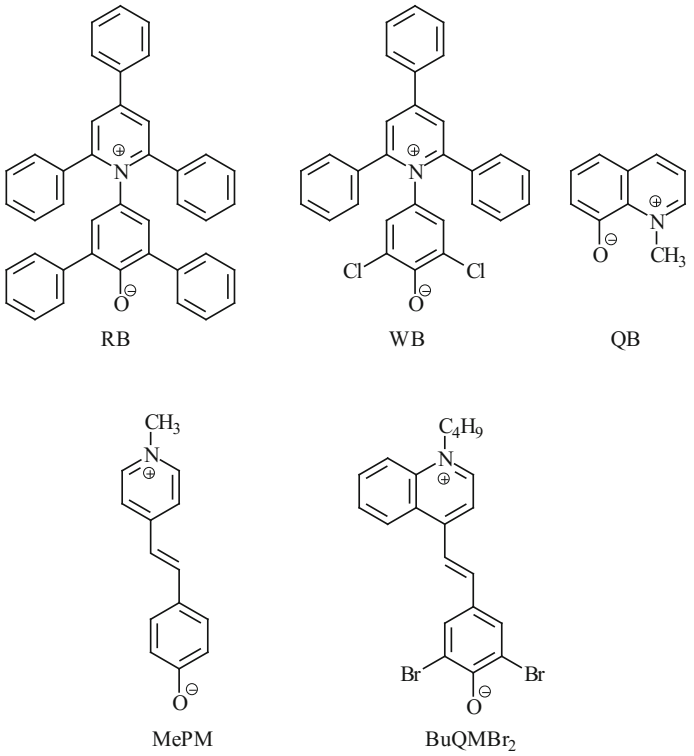


**Fig. 3.8** Molecular structures and acronyms of some solvatochromic probes

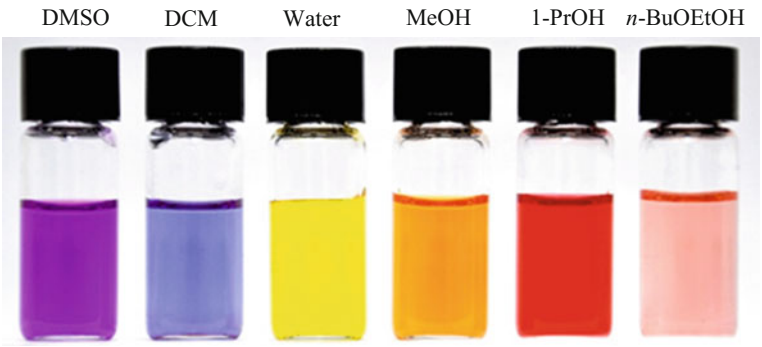


**Fig. 3.9** Demonstration of the phenomenon of solvatochromism. The solvatochromic indicator $MePMBr_2$ shows distinct colors in different solvents

solvent properties have indicated that the swelling is affected by the structure (DP), supramolecular parameters ($I_c$ and accessibility), and morphology (total pore volume, pore volume distribution) of the celluloses employed. The use of solvatochromic parameters as descriptors is superior to that of other parameters, e.g., Hildebrand solubility parameters and Gutmann's AN and DN [27, 40].

Three parameters, molar volume, acidity, and dipolarity/polarizability of the solvent satisfactorily correlate with cellulose swelling in protic solvents. The inclusion of solvent basicity leads to better correlations. These results are in agreement with the expectation that cellulose accessibility decreases as a function of increasing the volume of the solvent, as mentioned above for swelling by aliphatic amines and aliphatic alcohols [89, 90]. Correlation with both solvent acidity and basicity agrees with the fact that an alcohol acts as hydrogen-bond donor and acceptor. An important result of the correlations of *n*Sw with the solvatochromic properties of both classes of solvents is that solvent dipolarity/polarizability is either statistically significant or is the most statistically significant descriptor. Thus, dipolar interactions and, possibly, London dispersion forces are quite important for intercrystalline swelling [104]. Massive rupture of the existing hydrogen-bond network is not required for efficient swelling.

The data of swelling of cellulose by water and DMSO were excluded from the correlations between *n*Sw and the properties of protic and aprotic solvents, respectively [27, 40]. The efficiency of water is due to the combined effects of its unique three-dimensional structure and the ability to maintain its (bulk) geometry within cellulose as well as the incorporation of additional water molecules, not directly bonded to cellulose.

As shown by molecular modeling calculations, water present in cellulose is akin to that adsorbed on other polar surfaces, i.e., it can be pictured as present in "layers" of different degrees of order. The water bound to cellulose is probably oriented by dipole–dipole interactions [105, 106] and can be divided into bound water and free, bulk-like, water [28, 107–109]. The existence of different types of water has been investigated by NMR spectroscopy. Determination of the transverse-relaxation time, $T_{2,}$ in suspensions of cellulose (MCC) in water as a function of the concentration of cellulose revealed a large decrease of the relaxation time, e.g., from 0.43 to 0.045 s as cellulose was increased in the suspension from 1 to 10% (w/w). By using a two-site analysis (bound and free water), $T_2$ of bound water was calculated to 0.005 s that is much smaller than that of free water, 3 s, at 25 °C, showing the high immobility of the former type [110]. Qualitatively similar results were obtained when $T_2$ of water in soft- and hardwood celluloses (4–19% (w/w) water) was measured. Values of $T_2$ were found to increase as a function of increasing concentration of water. Values of $T_2$ were greater for mercerized celluloses [111].

In summary, water inside cellulose appears to maintain its tetrahedral structure to a large extent. The network formed includes both water–cellulose and water–water molecules, as depicted in Fig. 3.10. The consequence is an enhanced *n*Sw that cannot be simply related to the physicochemical properties of the solvent [40, 112].

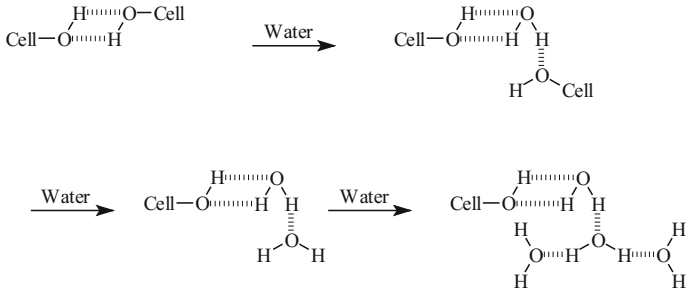


**Fig. 3.10** Scheme for the progressive hydration of cellulose

Expressed as %Sw, DMSO is even more efficient than water; expressed as *n*Sw it is more efficient than methanol. This enhanced efficiency is explained by considering data of solutions of carbohydrates in DMSO, and data of well-documented DMSO–water binary mixtures. Several pieces of evidence, including theoretical calculations [113], IR and NMR spectroscopy [114], and electron-spray mass spectroscopy [115] have shown that DMSO–water interactions are stronger than water–water interactions and that DMSO form complexes with one, or two water molecules. Likewise, IR, NMR, and thermochemical data have shown that DMSO forms strong hydrogen bonds with mono- and disaccharides, oligomers (e.g., oligodextrins), and cellulose. Additionally, DMSO may form one, or several hydrogen bonds with the same sugar moiety and, presumably, with several AGU of cellulose [116–120]. Therefore, a combination of high dipole moment and relatively small volume enhance the efficiency of DMSO in forming hydrogen bonds with the OH groups of one, or more AGU of cellulose, this leads to its exceptional swelling power.

It is possible to correlate solvent swelling with aprotic and protic solvents simultaneously, as shown in Fig. 3.11. The latter shows the correlation between experimental *n*Sw and those calculated based on solvent basicity, molar volume, and dipolarity/polarizability. These linear correlations are remarkable; swelling by hydrogen-bond donation of the solvent does not occur because aprotic solvents do not act as hydrogen-bond donors. The good linear fit results partly from the influence of solvent dipolarity/polarizability on the swelling of cellulose.

The swelling of cellulose and wood by binary solvent mixtures of water and methanol, ethanol, acetonitrile [50% (w/w)], and 1,4-dioxane [25 and 40% (w/w)] was carried out. The cellulose (MCC) from different suppliers was employed either as received, or after heating overnight in air, or under an $N_2$ atmosphere at 80 °C. The absorption of the biopolymer depended on its pretreatment and on the organic component of the binary solvent mixture. For example, all samples absorb methanol preferentially. The same behavior was observed for ethanol, except for one sample. A combination of the small molar volume of acetonitrile and its relatively large dipole moment (4.1 D, compared with 1.76 D for water) probably explains the preferential swelling by this solvent relative to water. However, cellulose swelling

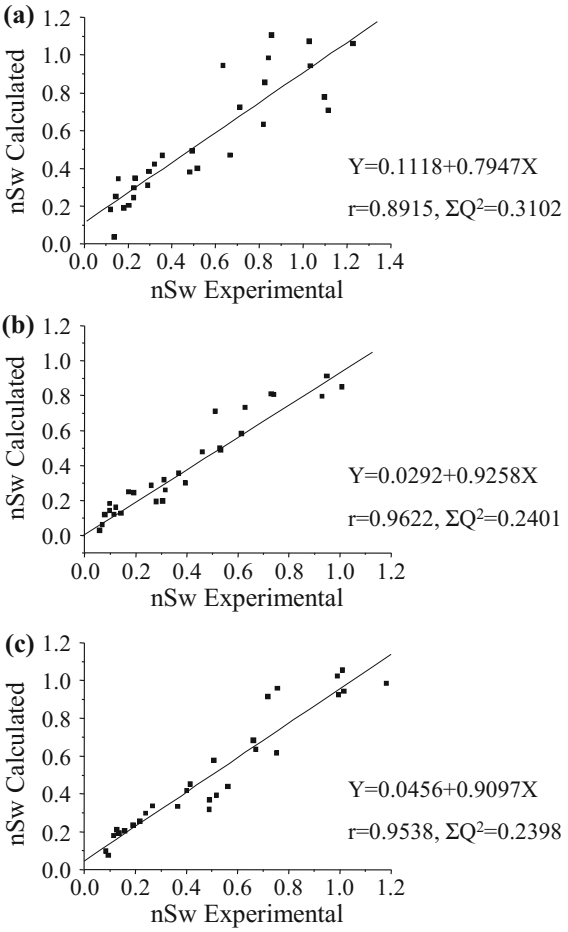


**Fig. 3.11** Correlation between calculated *n*Sw and experimentally determined ones for the swelling of MCC, cotton, and eucalyptus celluloses by 28 solvents; 16 protic and 12 aprotic. Calculated nSw are based on the solvent descriptors $V_S$, $\pi^*_S$, and $\beta_S$ (Reprinted from [27] with permission from John Wiley and Sons)

by aqueous 1,4-dioxane showed no preference for the organic component, probably because of its large molecular volume and very small polarity (dipole moment = 0.45 D) [121].

### *3.1.4 Activation by Intracrystalline Swelling*

The accessibility of cellulose depends on the molecular, supramolecular, and morphological structures, on one hand. On the other, the physicochemical properties (e.g., $pK_a$ value, molar volume) of the swelling agent and the experimental conditions (e.g., time, temperature, stirring) influence the accessibility. Intercrystalline swelling, e.g., by water, or diluted solutions of acids and bases opens and widens the existing

micropores. Increasing the concentration of the swelling solution, e.g., 4–8% aqueous NaOH or aqueous solutions of quaternary ammonium hydroxides causes further increases in accessibility due to splitting up of the fibrillar aggregates. Finally, treatment with alkali solutions of mercerization strength, e.g., 12% aqueous NaOH, or with liquid ammonia causes a change in the unit cell structure by transformation of cellulose I into cellulose II (after regeneration).

Solvent penetration into mercerized celluloses is expected to be larger than that in native cellulose because of:

- Favorable modifications of supramolecular structure due to the combined effects of decrease in crystallite size; increase in pore volume, and increase in disorder of the hydroxymethyl groups;
- Less hydrogen bonding.

Cellulose I possesses different conformations of the hydroxymethyl groups and an additional intramolecular hydrogen bond along the chain axis that does not exist in cellulose II (Fig. 3.12) [88, 122–126]. The solvent has to compete (for the OH groups of cellulose) with less intramolecular hydrogen bonds in case of M-cellulose, than in case of native cellulose. This contributes to the observed order of swelling.

Swelling of cellulose by mineral acids

Treatment of cellulose with sulfuric acid up to concentrations of 59% causes swelling slightly higher than water. Treatment with 62.5% acid at 0–20 °C for relatively short times ($\leq 30$ min) causes optimum swelling, whereas rapid dissolution occurs at acid concentrations >71% [127, 128]. It has been claimed that

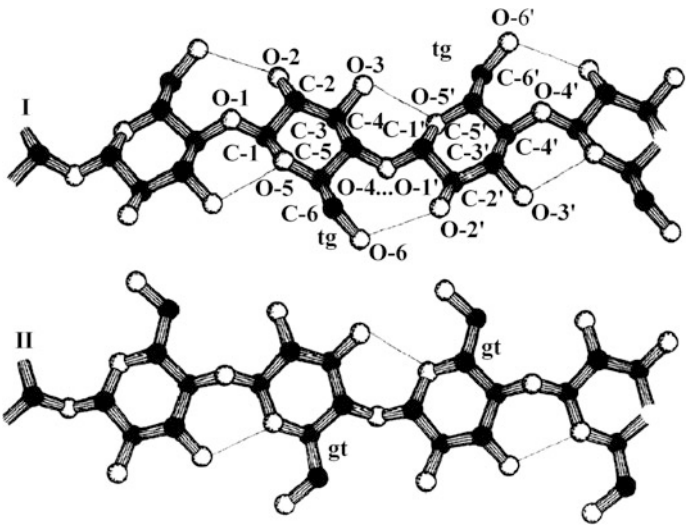


**Fig. 3.12** Hydrogen bonding in cellulose I and cellulose II

conversion of cellulose I → cellulose II occurs during the treatment with 62.5% acid [129]. However, the swelling at this acid concentration is intercrystalline. Cellulose crystal structure conversion can be induced, however, by treatment with higher acid concentrations (63–74%) for a very short time. The conversion possibly originates from the re-precipitation of dissolved cellulose [130].

Little swelling occurs upon treatment with phosphoric acid up to 70%. The degree of swelling increases at an acid concentration ranging from 70 to 81%, whereas cellulose dissolves at higher concentrations [127, 128]. Swelling by phosphoric acid causes an increase in the ISV and partial conversion of cellulose I → cellulose II [131, 132].

Whereas there is little swelling by nitric acid, above that by water, up to concentrations of 60%, cellulose swelling changes from inter- to intracrystalline swelling between acid concentrations from 59 to 69% [133]. The products of such treatment show high sorption of moisture, high ISV, and dye uptake [134]. Nitration of cellulose occurs above 69% nitric acid, whereas cotton and M-cotton dissolve at a concentration of nitric acid >80% [127].

Up to a concentration of HCl < 35%, the swelling of cotton is not different from that by water. Optimum swelling and cellulose I → cellulose II transformation are achieved by acid concentrations of 37–38%. The biopolymer is soluble at HCl concentrations 40–42% [135, 136].

Swelling of cellulose by organic bases—ammonia, amines, amine complexes, and amine oxides

Treatment with liquid ammonia, e.g., the ammonia/dry steaming process employed in the textile finishing industry, leads to improved softness, flexibility, resilience, and less fiber damage compared with conventionally mercerized fabrics. The higher resilience allows using less cross-linking agents in easy-care treatments resulting in a better preservation of the fabric strength and abrasion resistance [137–140].

The lone electron pair of ammonia makes it an efficient swelling agent for cellulose. This leads to penetration into the crystalline region and formation of relatively unstable ammonia–cellulose complexes that decompose on heating the swollen cellulose or on washing with water, alcohol, acetone, or THF [141]. Ammonia treatment does not cause irreversible rearrangement of the hydrogen bonding that occurs when native cellulose is converted to cellulose II by aqueous NaOH. Cotton fibers treated with liquid ammonia (cellulose III) are readily converted back to native cellulose I lattice when ammonia is removed from the fibers by washing with water [142]. Depending on the cellulose and the conditions employed, treatment with liquid ammonia may lead to partial or complete change from cellulose I → cellulose III [143]. This treatment leads to an increase in cellulose accessibility as measured by moisture regain and by the effect on biopolymer reactivity [144]. Whereas mercerization of untreated pine cellulose occurs at a concentration of aqueous NaOH of 10–15%, that of liquid ammonia pretreated sample occurred at 7–8% inorganic base, and already showed the substantial

conversion of cellulose I → cellulose II (50%) at 2.5% aqueous NaOH [145]. The advantages of pretreatment with liquid ammonia, aqueous ammonia, or $NH_3$-ethanolamine has been demonstrated for several reactions of cellulose. For example, they lower the LODP in heterogeneous acetylation that indicates the breaking of fibrillar aggregations with a concomitant increase in reactivity. Whereas it is not simple to obtain alkali- and water-soluble cyanoethyl cellulose from native celluloses, the pretreatment gave alkali-soluble cyanoethylated products that may be converted into water-soluble products (DS of 0.7–1.0) by further reaction under homogeneous conditions [146].

Aliphatic amines are efficient swelling agents for cellulose. They form 1:1 amine–AGU complexes. As a function of increasing chain length of the amine, i.e., its molecular volume, the 101-lattice distance increases, whereas the swelling efficiency decreases. For example, the swelling of cotton fibers with methylamine at −10 °C is stronger than that by ethylamine at 0 °C [147, 148]. The penetration of cellulose by voluminous amines, e.g., pentylamine is only possible if the biopolymer is pretreated with ammonia or a small amine [149–151]. Compared to untreated, native cellulose, treatment with ethylamine lowers the LODP [152]. Slow evaporation of the amine induces conversion of cellulose I (but not cellulose II) → cellulose III [153]. Compared to native or mercerized cellulose, the acetylation of ethylamine treated, and pyridine extracted, but never-dried cotton is greatly enhanced [154]. The reactivity toward acetylation with acetic anhydride in pyridine can be further enhanced if the swelling agent, i.e., ethylamine or NaOH is extracted with water, followed by solvent exchange with pyridine [155].

Compared with monoamines, cellulose complexes with aliphatic diamines are formed at a faster rate and are more thermally stable. It is possible to evaporate the excess base without decomposing the biopolymer–diamine complex [156, 157]. An aqueous solution of aliphatic amines and diamines also swell cellulose. Intracrystalline swelling occurs at high base concentrations, i.e., where the base is less hydrated [154, 156].

Due to their high basicity and ability to form hydrated ion dipoles, aqueous tetraalkylammonium hydroxides interact with cellulose similar to alkali hydroxides. The solubilizing power depends on the structure and concentration of the quaternary ammonium compound. A suggested solvation model is based on the sheet lattice structure of the crystalline regions of native cellulose. The polar moiety of the tetraalkylammonium base disrupts the inter-sheet hydrogen bonds, whereas the nonpolar part penetrates between the cellulose chains within each sheet and keep them separated [158]. This steric interaction explains several experimental results. The concentration of $R_4NOH$ necessary to dissolve cellulose decreases as a function of increasing the size of the R group [159–161]. As a swelling agent for cotton, tetramethylammonium hydroxide is more efficient than NaOH (under comparable conditions), especially above 2 mol base per liter [20].

Metal–amine complexes easily swell and may dissolve celluloses, even those with high DP. The resulting solutions are employed for the determination of viscosity-based molar mass. The complexes of copper with ammonium hydroxide, those of cadmium, copper, nickel, and zinc with ethylenediamine also dissolve

cellulose. These complexes are more interesting as solubilizing agents for cellulose, therefore details of their structure and mechanism of action are addressed in Sect. 3.2.

With regard to swelling by amine oxides, NMMO hydrates are employed in the commercial production of the generic Lyocell cellulose fibers [162, 163], Alceru [164], Lyocell [165], and Tencel processes [166]. The Lyocell fiber complements the Rayon fiber and may substitute it to a certain extent because it is produced by an environmentally attractive process. The characteristics of the produced fiber are very convenient, in particular with regard to fiber strength when wet, and ease of spinning and dying [167]. Continuous filaments were also obtained by the spinning of NMMO solutions of wood steam-exploded fibers [168, 169]. This solvent has been employed for the synthesis of cellulose derivatives, e.g., CMC, however with low efficiency [170] and for upgrading the quality of ramie fibers with respect to uptake of reactive dyes, and dye fastness [171]. Additionally, the thickness, morphology, and porosity of dry cellulose membranes can be adjusted by wet spinning from its solutions in NMMO–DMSO [172] or by regeneration of cellulose solution in NMMO in a suitable solvent [173]. For example, regeneration in water, methanol, and ethanol produce dense and highly porous membranes [174]. This control of the properties of the cellulose membranes renders feasible several important applications, e.g., very efficient dehydration of aqueous 2-propanol, in comparison with membranes from other natural raw materials (chitosan and sodium alginate) as well as synthetic membranes (poly(vinyl alcohol) and polyimide and polyetherimide) [175]. Additionally, the efficiency of enzymatic hydrolysis of cellulose to produce ethanol, or its anaerobic digestion to biogas (methane) is enhanced by controlling the swelling of the biopolymer before being submitted to degradation treatments [176].

Swelling of cellulose by alkali hydroxides

Interest in studying the effects of treatment of cellulose by alkali metal hydroxides dates back more than a century ago when Mercer and Lowe have shown the beneficial effects of treatment of slack or stretched cotton fabrics by concentrated aqueous NaOH [177, 178]. The textile industry has employed mercerization in order to increase dye affinity, to improve luster and smoothness, to achieve dimensional stability, and to raise tensile strength [179–181].

Systematic studies on the mercerization of cellulose have indicated that the extent of swelling depends on the cellulose and the experimental conditions including the concentration of the swelling agent and the temperature. Considering first the biopolymer, fibers shrink when placed in alkaline solutions while fiber width or cross-sectional area increases. The changes of fiber observed depend on the concentration of the alkali [182]. The dimensional changes of whole fibers were studied in 5.4 mol/L aqueous NaOH. The length shrank by ca. 13%, the diameter increased by ca. 20%, and the cross section became more circular. The length shrinkage increased to ca. 20%, the width increased to ca. 65% when the primary wall of the fiber was mechanically removed. Thus, the primary wall has a restrictive

effect on the swelling of the fiber during mercerization; this is the reason that the perimeter of the fibers does not change appreciably [183, 184]. An interesting "structure" is formed when mercerization is carried out not on whole fibers, i.e., on assemblies of a large number of organized microfibriles, but on isolated microfibriles. Upon partial mercerization by sodium ethoxide, the microfibrils suffer drastic morphological modification. The cellulose chains, which had been disturbed during the alkali treatments, recrystallize on the top of the underlying undisturbed microfibrils. When examined by microscopy, the morphology formed resemble "shish-kebab", where recrystallized cellulose II lamellae (the "kebab") are deposited on the intact microfibrils of cellulose I (the "shish") [185, 186]. The high susceptibility of cellulose from the primary wall of microfibrils toward intracrystalline swelling, as compared to that of celluloses from the secondary wall may be related to two factors: The loose organization of the primary wall, leading to a free swelling of the microfibrils [187] and the slightly narrower lateral size of the crystalline microfibrils, ca. 3 nm, which governs the number of lattice units that have to be swollen for NaOH penetration to occur [186].

Cellulose swells much more than it does in water once the alkali concentration reaches a threshold value. The swelling depends on the cellulose type, e.g., Fig. 3.13a and, for the same cellulose, on the temperature, Fig. 3.13b. Plots of the degree of swelling of cotton cellulose versus concentration of NaOH showed a clear maximum at 0 °C at ca. 3 mol/L, whereas at 25 and 100 °C these maxima are poorly defined and appear at ca. 4 mol/L base [130].

In view of the base concentrations at which these maxima occur, the reason for using [NaOH] > 17% is not clear, especially because some α-cellulose will dissolve at room temperature at [NaOH] > 17.5% [189]. The transformation of cellulose I to cellulose II appears to be complete after treatment with 14% aqueous NaOH for 2 h at room temperature [186]. Therefore, carrying out this treatment for a long time even days may not be warranted [190].

Unless intended, mercerization can lead to a drastic decrease of DP due to oxidative degradation, a reaction of rather low energy of activation (91.7 kJ/mol)

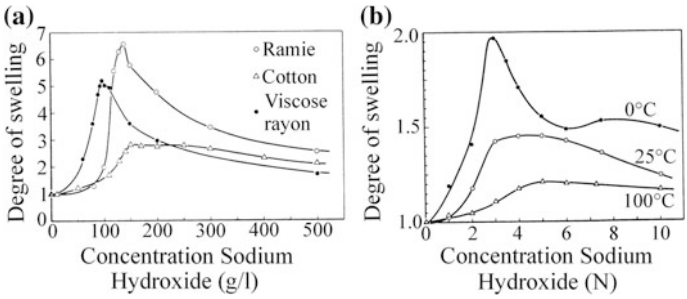


**Fig. 3.13** Relationship between degree of swelling and the concentration of NaOH. Part **a** shows the dependence of cross-sectional swelling on the type of cellulose (compiled from [188]). Part **b** the dependence of swelling of cotton on the temperature (reproduced from [130] with permission of John Wiley and Sons)

[191]. This degradation is problematic when the behavior of cellulose (starting and mercerized cellulose) are to be compared, e.g., with regard to accessibility or reactivity in a chemical reaction. The reason is that both properties are sensitively dependent on DP of the biopolymer. Consequently, comparison of the results of two samples of very different DP may not be warranted. Oxidative degradation during mercerization can be avoided by carrying out the steps involved (treatment with base and washing) under reducing/inert conditions, e.g., by use of $NaBH_4$/NaOH for mercerization, and by carrying out the whole process (base treatment and subsequent washing and filtering) under an inert atmosphere.

X-ray-based schematic representation of the mechanisms of the transition of cellulose I → cellulose II in cotton linters and bacterial cellulose is shown in Fig. 3.14. The difference between the schemes of cotton and bacterial celluloses stems from the observation that the transformation of bacterial cellulose is much slower and the LODP is much smaller than that for cotton linters. When treated with aqueous NaOH, the crystallites composed of parallel cellulose chains (part a) incorporate hydrated NaOH, forming "alkali cellulose"; this is considered to be highly mobile state of cellulose, retaining its macroscopic structure (part b) [193]. For the transition of parallel to the antiparallel chain, which takes place through interdigitation without folding, there must be close contacts between neighboring microfibrils with opposite chain polarities (Fig. 3.14c). Such condition is likely to be met in case of higher plant cellulose, which may be formed as lamellae composed of microfibrils with opposite chain directions, composed of ca. 30–40 cellulose chains [194]. On the contrary, bacterial cellulose microfibrils are typically composed of 1000–2000 units of the same polarity [195, 196]. Consequently, the structure is shown in Fig. 3.14c is not easily attainable. If the sample is washed after a short treatment time, nearly amorphous cellulose is obtained, part (Fig. 3.14g). However, if the alkali treatment is continued for several days, random chain folding occurs leading to the extensive formation of folded-chain crystallites, part (h) [192, 197].

The degree of swelling also depends on the alkali metal hydroxide used. The order of swelling LiOH > NaOH > KOH > RbOH > CsOH has been reported for cotton fibers [198]. At 21 °C and 5 mol/L alkali, the order of swelling of cotton was reported to be NaOH > LiOH > KOH. Although the discrepancy between these orders of efficiency has been attributed to differences in the experimental techniques and conditions used [199], the order LiOH > NaOH > KOH has been more recently reported for swelling of flax cellulose [200]. This order is related to the extent of hydration of the alkali metal ion. The structures of hydrated $Li^+$, $Na^+$, and $K^+$ ions are tetrahedral, i.e., their primary hydration shells consist of four water molecules. For these ions, electrostatic forces operate beyond the first shell and additional water molecules are bound in layers of decreasing firmness. The larger the cation, the less it binds an outer layer of water, i.e., although the crystallographic radii increase, the hydrated radii decrease. The total hydration numbers are ca. 25, 16, and 10 water molecules for LiOH, NaOH, and KOH, respectively [201]. Based on this information, the base concentrations at which all water present is involved in solvation shells are ca. 2.2, 3.5, and 5.5 mol/L for LiOH, NaOH, and

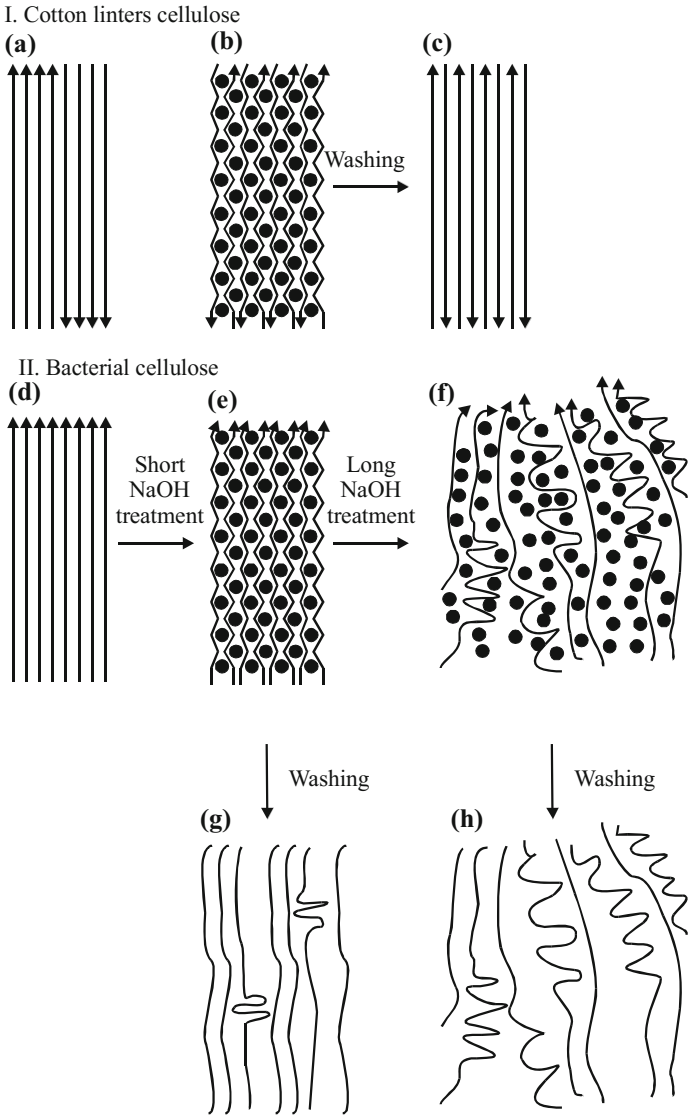


**Fig. 3.14** Suggested mechanisms for the molecular arrangements of cellulose chains during mercerization of cotton (sequence **a–c**) and bacterial cellulose (sequence **d–h**) (reproduced from [192] with permission from Springer)

KOH, respectively. These figures are similar to those calculated elsewhere, 3.2, 3.1, and 6.5 mol/L for LiOH, NaOH, and KOH, respectively, in agreement with the above-mentioned mercerization efficiency order of alkali metal hydroxides [200].

The important effects of medium composition on the conversion of cellulose I to cellulose II has been followed by measuring X-ray diffraction of cotton linters with

NaOH in aqueous ethanol, aqueous 2-propanol, and mixtures of ethanol-2-propanol-water. The dependence of the percentage of cellulose II on medium composition is complex, and showed maxima at certain alcohol concentrations. As expected, the cellulose II content increased as a function of increasing temperature and mercerization time, at a constant concentration of base and medium composition. The dependence of the conversion on the concentration of NaOH showed maxima because of the balance between increasing base concentration and the accompanied decrease of concentration of water that leads to base precipitation [202]. The same technique, X-ray diffraction, has been employed in order to investigate the effect of microwave heating of solutions of cotton powder, at different powers, 400 and 900 W, from 10 to 40 min. It was found that microwave heating has no effect on the mechanism of (cellulose I → cellulose II) transformation; it reduces the length of time, and the NaOH concentration required for mercerization, both variables are dependent on the applied power [203]. A more thorough evaluation of the effect of this relatively energetic treatment on the DP of cellulose is certainly required.

The decrease in alkali concentration caused by adding a certain mass of cellulose to the solution has been measured. A plot between alkali uptake and the original alkali concentration is shown in part (a) of Fig. 3.15, where a two-step process is clearly seen [132, 204, 205]. The absence of a clear adsorption isotherm (e.g., that of Langmuir) and the fact that this absorption is not reversible has been explained based on a chemical reaction between cellulose and the base. However, this behavior can be explained by a preferential uptake of the components of the alkali solution and unequal accessibility of the sites in particular during the initial base uptake. With regard to the first, an experimental procedure was employed in order to separate cellulose uptake of water from that of alkali yielding the corresponding plot depicted in Fig. 3.15b [206, 207]. Whereas the water uptake by cellulose goes through a maximum, that of NaOH increases over the entire base concentration

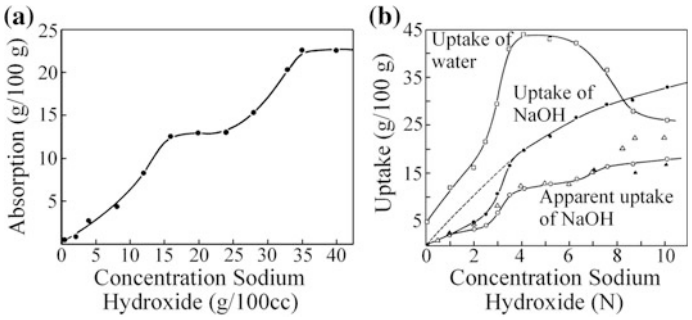


**Fig. 3.15** **a** Apparent uptake of NaOH by cotton determined by the "change-in-titer" method (compiled from [204]); **b** Separated uptake of NaOH and water (compiled from [205, 206]). The dashed part of the sodium hydroxide curve shows the correction made for the initial inaccessibility of cellulose [130]

range, in an approximately (S)-shaped manner. This shape can be due to the initial inaccessibility of sites that are made later available for swelling. These mechanisms, however, are not operative for regenerated cellulose. Indeed, the latter shows the expected adsorption isotherms, from low to high alkali concentrations and the process is practically reversible [208, 209]. Therefore, the S-shaped part of the NaOH uptake should be corrected for the change in accessibility during mercerization leading to the dashed part of the curve (Fig. 3.15b). That is, the uptake of alkali hydroxides by cellulose is not a chemical process in a strict sense; it is an adsorption phenomenon governed by the Donnan equilibrium. This, however, does not exclude that the base uptake involves complex formation between the cations and the OH groups of the AGU.

Several techniques have been employed in order to study different aspects of mercerization; including $^{23}$Na- and $^{13}$C NMR spectroscopy, electron microscopy, X-ray diffraction [189], IR [210, 211], and Raman spectroscopy [212]. The use of environmental scanning electron microscopy is interesting because water vapor pressure inside the specimen chamber is kept equal to that of the laboratory [213]. Consequently, the sample can be examined without any previous preparation (versus the extreme drying in SEM); the micrographs obtained represent the actual sample and not a "ghost" copy, as in SEM. The results of the above-mentioned studies, and those of Philipp et al. [214, 215] lead to the following conclusions about mercerization by aqueous NaOH solutions: Akin to swelling by water, NaOH exists in two states of binding to cellulose, tight, and relatively free. At higher base concentrations, 15–25%, sodium–cellulose is formed, by attachment of one NaOH molecule and water to each AGU. The observed fast exchange between free and bound sodium ions shows the formation of an addition compound between NaOH and cellulose, rather than the formation of sodium alcoholate. $^{23}$Na NMR spectroscopy line width indicates the existence of defined states of $Na^+$ ion hydration; $^{13}$C NMR spectroscopy indicates that at low alkali concentration, position 2 and/or position 3 of the AGU interact preferentially with the base.

The conditions required in order to secure good cellulose reactivity in chemical reactions include weakening of the primary wall of native celluloses; widening of the existing capillaries, voids, or fibrillar interstices in fiber morphology. These changes can be accomplished by use of cellulose-included inert compounds; by keeping the cellulose in the never-dried state; by increasing the accessible internal surface by swelling and/or activation treatments, in particular, mercerization. Finally, it is clear that there is no "universal" reactivity scale for cellulose; it is dependent on the reaction carried out. Therefore, it is unrealistic to expect that the same cellulose will show similar reactivities in diverse reactions, e.g., acylation, xanthation, or etherification, because of different reaction mechanisms. Likewise, reactivity of the same cellulose in reactions that occur by the same mechanism (e.g., acylation) maybe be different, because of differences between the properties of the attacking reagent including, inter alia, reactivity (acyl chloride vs. the corresponding anhydride), use of catalyst, and molecular volume (e.g., acetic versus butyric anhydride).

## 3.2 Dissolution of Cellulose

Cellulose is insoluble in water and common organic solvents due to the intensive supramolecular interactions, in particular, the hydrogen bonding within and between the macromolecules, as well as to hydrophobic interactions (see Chap. 2.1). However, dissolution of cellulose is an unambiguous prerequisite for

1. characterization (e.g., determination of molar mass and molar mass distribution)
2. shaping (e.g., preparation of fibers and membranes) and
3. homogeneous chemistry (as one of the most important paths to design novel functional polymers and materials based on this renewable resource)

To classify cellulose solvents, it is appropriate to divide them into non-derivatizing and derivatizing solvents [216].

### *3.2.1 Non-derivatizing Solvents*

Aqueous metal–complex solvents

Solvents for cellulose based on aqueous metal–complexes are known for a long time. Prominent examples are cuprammonium hydroxide (Cuam), cupriethylene diamine (Cuen), cadmiumethylene diamine (Cadoxen), and a ferric tartaric acid sodium salt (FeTNa) [217]. Table 3.4 gives a variety of examples of this type of solvents.

**Table 3.4** Examples of aqueous cellulose solvents (Reprinted/adapted from [216], copyright (©2001) with permission from Elsevier)

| Type of compound | Solvent abbreviation | Active species |
|---|---|---|
| Transition metal complexes with amines or $NH_3$ | Cadoxen | $[Cd(H_2N)–(CH_2)_2–NH_2)_3](OH)_2$ |
| | Cdtren | $[Cd(NH_2(CH_2)_2)_3N](OH)_2$ |
| | Cooxen | $[Co(H_2N–(CH_2)_2–NH_2)_2](OH)_2$ |
| | Cupren | $[Cu(H_2N–(CH_2)_3–NH_2)_2](OH)_2$ |
| | Cuam | $[Cu(NH_3)_4](OH)_2$ |
| | Cuen | $[Cu(H_2N–(CH_2)NH_2)_2](OH)_2$ |
| | Nioxam | $[Ni(NH_3)_6](OH)_2$ |
| | Nioxen | $[Ni(H_2N–(CH_2)_2–NH_2)_3](OH)_2$ |
| | Nitren | $[Ni(H_2N(CH_2)_2)_3N](OH)_2$ |
| | Pden | $[Pd(H_2N–(CH_2)_2–NH_2](OH)_2$ |
| | Zincoxen | $[Zn(H_2N–(CH_2)_2–NH_2)_2](OH)_2$ |
| Transition metal complexes with tartaric acid | FeTNa | $Na_6[Fe(C_4H_3O_6)_3]$ |

The aqueous solution of cellulose in $Cu(OH)_2/NH_3$ (Cuam, Schweizer reagent) was discovered as early as 1857 and still plays an important role in cellulose analysis (determination of DP) and cellulose processing, like membrane formation. Membranes regenerated from Cuam solution provide high-quality products for haemodialysis [218].

The $[Cu(NH_3)_4](OH)_2$ interacts strongly with the hydroxyl groups of the polymer backbone at position 2 and 3 of the AGU (Fig. 3.16, [219]). At copper concentration from 15 to 30 g/L and ammonia concentration above 15% even high DP cellulose can be dissolved completely in a short time.

The formation of polyolato complexes occurs not only with Cuam but also other amines like ethylene diamine (en) and 1,3-diaminopropane (pren) that are efficient ligands for copper, the complexes formed dissolve the biopolymer [220]. Cuen, has also been known for a very long time [221]. The active species is $[Cu(en)_2](OH)_2$, i.e., it does not contain an excess of amine as in case of $NH_3$ for Cuam.

Cadoxen, $[Cd(H_2N–(CH_2)_2–NH_2)_3](OH)_2$, is a colorless solvent of fairly high solvent power. Based on $^{13}C$- and $^{113}Cd$ NMR studies it was found that Cadoxen does not coordinate with cellulose but interacts with cellulose according to an acid–base principle similar to aqueous sodium hydroxide [222, 223]. The solvent power is increased with increasing concentration of Cd ions and by addition of NaOH [224].

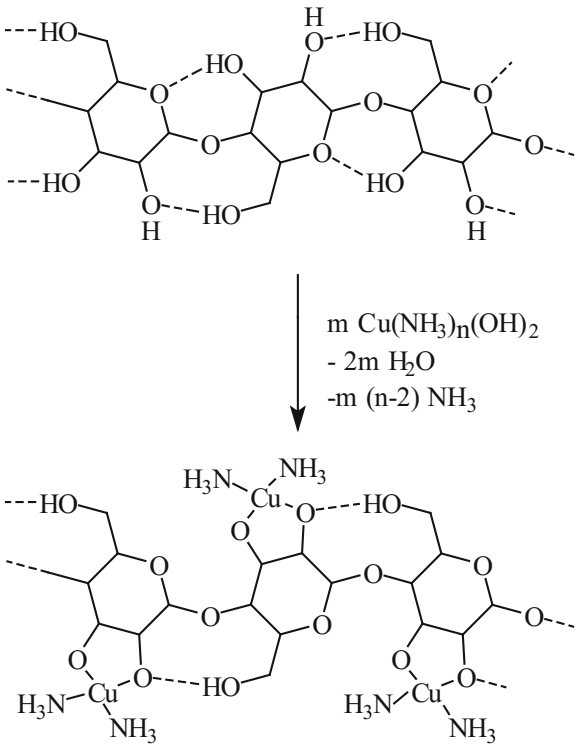


**Fig. 3.16** Scheme of Cuam–cellulose complex structure

However, there is still a controversial discussion if the cellulose solvent interacts with the polymer forming diolato complexes of the hydroxyl groups at position 2 and 3 of the AGU or if an acid-–base interaction is more likely leading to additional chain separation due to the voluminous amine-complexed cation persisting as a homoleptic cationic complex in the system.

Further metal complex solvents are Nitren, $[Ni(tren)(OH)_2]$ (tren = tris (2-aminoethyl)amine) and $[Pd(II)(en)](OH)_2$ as active species [224, 225]. An acid–base interaction seems to be appropriate to describe the solution complex (Fig. 3.17).Solutions of cellulose in $[Pd(II)(en)](OH)_2$ are colorless and have been studied by means of NMR spectroscopy and light scattering [224, 226].

Aqueous alkali hydroxides

As discussed above, solutions of alkali hydroxides in water cause strong swelling of cellulose. Under certain conditions, they may cause even dissolution of the biopolymer. The degree of swelling of cellulose in aqueous sodium hydroxide depends on the concentration of the base, the temperature, the structure of cellulose (accessibility), and in particular on the DP of the biopolymer. Decreasing of the temperature generally results in higher swelling and favors the dissolution of low DP cellulose [227]. Solutions of cellulose (up to 5%) could be obtained with samples of a DP of up to 200 applying 9–10% aqueous NaOH at about 10 °C. Samples of higher DP dissolve only partially. Thus, regarding the DP, aqueous NaOH represents a borderline solvent.

Studies on the dissolution of different cellulose samples by aqueous NaOH regarding the DP, degree of crystallinity, crystalline form, and lignin content, have indicated that optimal conditions for dissolution involve swelling of the biopolymer in 8–9% (w/w) aqueous NaOH and subsequently freezing it into a solid at −20 °C followed by thawing at room temperature and dilution with water to a 5% aqueous base [82]. Changes in the $^{13}C$ NMR chemical shifts of cellulose dissolved in NaOD/$D_2O$ indicated that the hydroxyl groups at position 3 have the highest resistance to dissociation compared to those at position 2 and 6 in accordance with the documented lowest reactivity of the hydroxyl group at position 3 after mercerization [228]. The ratio between the NaOH molecules to AGU must be at least 4 to 1 in

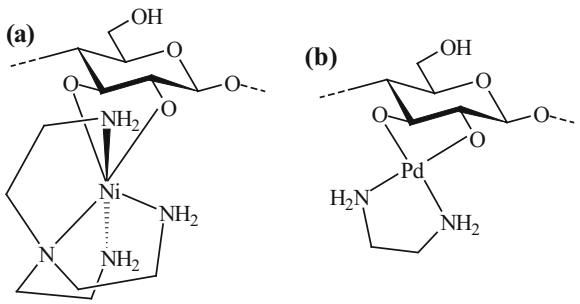


**Fig. 3.17** Structure of cellulose units in **a** Nitren and **b** Pden

order to dissolve the biopolymer [229]. The dissolved cellulose forms coherent gels on standing that impedes technical application of the solvent. Completeness of dissolution and stability of the solutions could be enhanced with zinc oxide and/or urea [230].

Dissolution of cellulose could be realized with aqueous NaOH in combination with urea or thiourea as well as with aqueous LiOH in combination with urea. Cellulose with viscosity-average molecular weight values of $11.4 \times 10^4$ g/mol (DP 703) and $37.2 \times 10^4$ g/mol (DP 2282) are soluble in aqueous 7% NaOH/12% urea or 4.2% LiOH/12% urea cooled to −10 °C within 2 min while aqueous KOH/urea does not dissolve the biopolymer [231, 232]. The urea hydrates could possibly be self-assembled at the surface of the NaOH hydrogen-bonded cellulose [233]. The solutions are rather unstable and sensitive to temperature, polymer concentration, and storage time [231, 234].

Transmission electron microscopic (TEM) images and WAXD provided experimental evidence on the formation of a wormlike cellulose inclusion complex being surrounded with urea (Fig. 3.18) [236].

A material with a very high inner surface, so-called aerogels, is accessible from NaOH-based solvents. Although NaOH/$H_2O$ can only dissolve cellulose with both low crystallinity and degree of polymerization, it may be exploited for the defined shaping of the polymer. It was shown that irreversible gelation may lead to such aerogels. Cylindrical gels were regenerated in water (Fig. 3.19). Regenerated swollen-in-water cellulose samples kept their cylindrical shape upon drying with a very slight volume decrease of less than 10% [237].Cellulose materials with a huge surface were accessible via this path using LiOH/urea as solvent showing different morphologies depending on the workup (Fig. 3.20) [238].

It should be mentioned that recently comparable aerogels were prepared from bacterial cellulose hydrogels by a simple solvent exchange and subsequent drying with supercritical carbon dioxide. The average density of the obtained dry cellulose aerogels is only about 8 mg/cm$^{-3}$, which is comparable to the most lightweight silica aerogels [239].

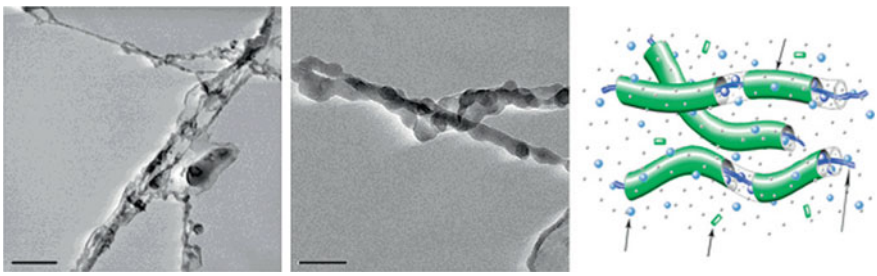

**Fig. 3.18** TEM images of cellulose at $4.0 \times 10^{-4}$ g ml$^{-1}$ in aqueous LiOH/urea (4.7/15%, w/w) (left and middle) and (right) schematic inclusion complex model showing channel inclusion complexes (tubes), LiOH-hydrate (large spheres), urea hydrate (sticks), and water (small spheres) (Reproduced from [235] with permission from John Wiley and Sons)

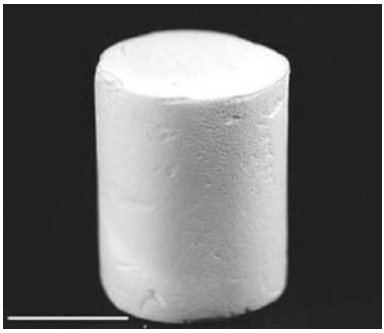

**Fig. 3.19** Example of a cylindrical aerocellulose sample obtained from 5% Avicel/NaOH/water gel (Reprinted and permission from [237], copyright (©2008) American Chemical Society)

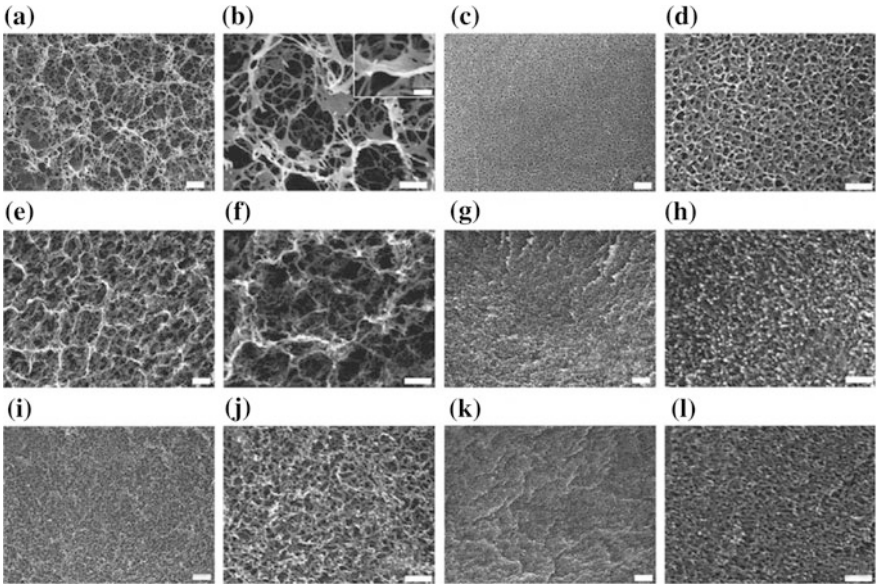


**Fig. 3.20** SEM images of aerogels prepared from 4% (w/w) cellulose in aqueous LiOH/urea solution, regenerated with EtOH, and freeze-dried from either $H_2O$ (**a–d**) or t–BuOH (**e–h**), or dried from $CO_2$ (**i–l**) as indicated. Low-magnification (**a**, **e**, **i**) and high-magnification (**b**, **f**, **j**) images of the surface. Low-magnification (**c**, **g**, **k**) and high-magnification (**d**, **h**, **l**) images of the cross sections of the aerogels. The inset in part **b** shows the SEM image of a tilted sample (Reproduced from [238] with permission of John Wiley and Sons)

### Electrolytes in dipolar aprotic solvents

Many dipolar aprotic solvents cause cellulose swelling, sometimes extensively, but do not dissolve the biopolymer, on one hand. On the other hand, there are several solvents, in many cases called "solvent systems" (e.g., solutions of strong

electrolytes in dipolar aprotic solvents) that physically dissolve cellulose, i.e., without formation of covalent bonds. As discussed before (Sect. 3.1.4), cellulose swelling and dissolution are interrelated because both processes disrupt the strong intermolecular hydrogen bonding to varying degrees, in particular, the OH(6)–O (3″) link between the chains and solvophobic interactions leading eventually to elimination of the cellulose supramolecular structure [240]. Whether the biopolymer shows swelling only or dissolves partially or completely in a given medium depend on the extent of these interactions and the region(s) that the solvent is able to penetrate into the biopolymer supramolecular structure. Weak-to-moderate cellulose–solvent interactions coupled with limited solvent access (i.e., restricted to the amorphous regions) lead to swelling; strong interactions in all biopolymer domains lead to dissolution.

Solutions of some strong electrolytes, e.g., LiCl, LiBr, TBAF × $3H_2O$, TAAF × $H_2O$, BMAF × $0.1H_2O$ in dipolar aprotic solvents, e.g., DMF, DMAc, NMP, HMPA, DMSO may dissolve cellulose even of high DP and $I_c$, e.g., bacterial cellulose and wood [84, 241, 242]. The cellulose solutions formed have attracted much attention for controlled regeneration of fibers or functionalization of the biopolymer into a myriad of derivatives like inorganic and organic esters, ethers etc. [240] and in the analysis of cellulose (and its derivatives) [243–245].

For dissolution of cellulose in DMAc/LiCl the biopolymer is subjected to "activation", i.e., pretreatment step before its dissolution is attempted. The objective of activation is to increase the diffusion of solvent components into the supramolecular structure of cellulose, by making the crystallite surfaces and the crystalline regions more accessible. This is achieved by inter- and intracrystalline penetration of the activating agent into cellulose, which disrupts the strong, water-mediated hydrogen bonding between the biopolymer chains [246, 247]. The relevance of this step may be demonstrated by the erratic results that may be obtained if it is not carried out properly. The following data on percentage of acetyl content of cellulose acetate after one day of treatment with 50% (w/w) acetic anhydride in pyridine at 30 °C, emphasize this circumstance: No activation, 8.8%; pretreatment with chloroform/pyridine, 26.4%; same pretreatment with ethanol/chloroform, 27.6% [248].

Alkali treatment has been extensively employed for activation of cellulose. Mercerization followed by washing of the residual base has been employed. As discussed above, this treatment results in the irreversible transformation of cellulose I into the less ordered (hence more reactive) cellulose II (after regeneration). Another consequence of mercerization may be an increase of the α-cellulose content due to the extraction of the hemicellulose and other residual non-cellulosic material, e.g., wax. Therefore, this activation procedure has been routinely employed with cellulose samples of high $I_c$ and DP, in particular, cotton linters.

Another activation treatment is displacement of solvent at room temperature. The polymer is treated with a series of solvents ending with the one that will be employed in the dissolution step. Thus, cellulose was treated with the following sequence of solvents, before it is dissolved in DMAc/LiCl (water → methanol → DMAc) [67, 70, 249]. This method is both laborious (needs ca. 1 day) and expensive since 25 mL of water, 64 mL of methanol, and

80 mL of DMAc are required to activate one gram of MCC. Its use may be recommended for special cases, e.g., where cellulose dissolution with almost no degradation is sought [250].

Several procedures have been suggested for heat-mediated cellulose activation, e.g., by heating solid cellulose or by using the solvent itself as the heat-transfer agent. The latter approach is based on the fact that the vapor pressure of DMAc near or at its boiling point is sufficiently high to induce efficient fiber penetration and swelling [251]. Relative to solvent exchange, heat activation is an expedient scheme that requires less LiCl in subsequent dissolution [250]. As mentioned above, water can be removed from cellulose by heating the polymer/DMAc slurry at 150 °C for 1 hour, then to the boiling point of the solvent followed by distillation of 25% of the volume of the latter [71, 252]. Although convenient, this activation may be problematic. First, it does not lead to a complete drying of the system, probably because residual water is tightly bound to the biopolymer [253]. More importantly, however, is that the solutions usually become yellowish, sometimes brownish, indicating side reactions. Refluxing celluloses in DMAc/LiCl may lead to oxidative degradation of the polymer. Polymer degradation may take place by two processes: The first one occurs at temperatures above ca. 80 °C, and involves *N,N*-dimethylacetoacetamide, $CH_3CO–CH_2CON(CH_3)_2$, a primary auto-condensation product of DMAc:

$$(2\ CH_3CON(CH_3)_2 \rightarrow CH_3CO-CH_2CON(CH_3)_2\ +\ HN(CH_3)_2).$$

Its formation leads to a slow, thermal degradation of cellulose, due to its reaction with the reducing end of the biopolymer, to produce furan structures, see, e.g., Fig. 3.21 for the reaction with glucose [254].The formation of this furan intermediate leads to cellulose chain degradation by an endwise peeling mechanism via neighboring-group participation (Fig. 3.22).

The other (faster) reaction involves the *N,N*-dimethylketeniminium ion ($CH_2=C=N^+(Me)_2$), whose precursor is the enol tautomer of DMAc, $CH_2=C(OH)N(Me)_2$. Formation of the latter is facilitated by coordination of the $Li^+$ to the oxygen of the solvent C=O group; in a typical acylation reaction, DMAc enolization will be catalyzed by the acid produced:

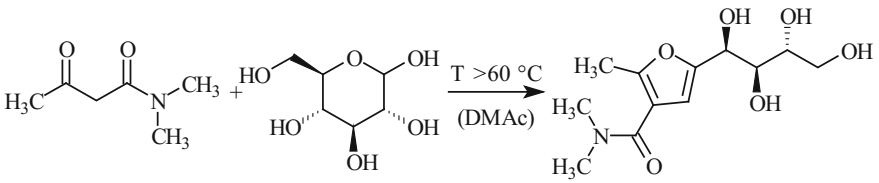


**Fig. 3.21** Production of furan derivatives by prolonged heating of glucose with DMAc

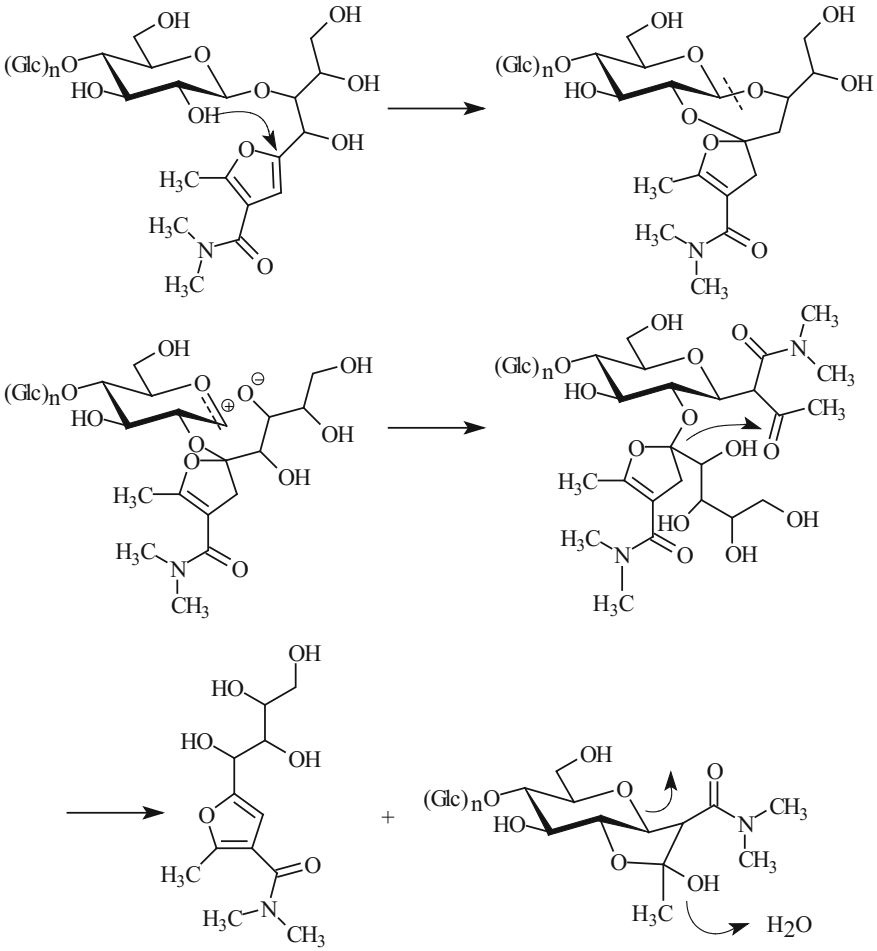

**Fig. 3.22** Mechanism of cellulose degradation by an endwise peeling mechanism, involving neighboring-group participation (adapted from [254])

This solvent-generated cation is an extremely reactive species, more electrophilic than ketenes, and does not dimerize as ketenes do [255]. Its formation leads to random cleavage of the cellulosic chains resulting in pronounced and rather fast changes in the molar mass distribution of the biopolymer (Figs. 3.23 and 3.24).

In order to avoid degradation, activation by solvent distillation may be carried out under reduced pressure, hence, at a lower temperature. However, this may result in the incomplete dissolution of fibrous celluloses, e.g., bagasse and sisal [256]. Therefore, it is safer to keep the temperature of the cellulose slurry as low as practical and to suspect extensive degradation if the color of the solution becomes dark amber or brownish [250].

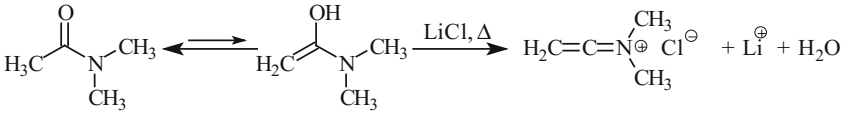


**Fig. 3.23** Mechanism of formation *N,N*-dimethylketeniminium ion from enolized DMAc [254]

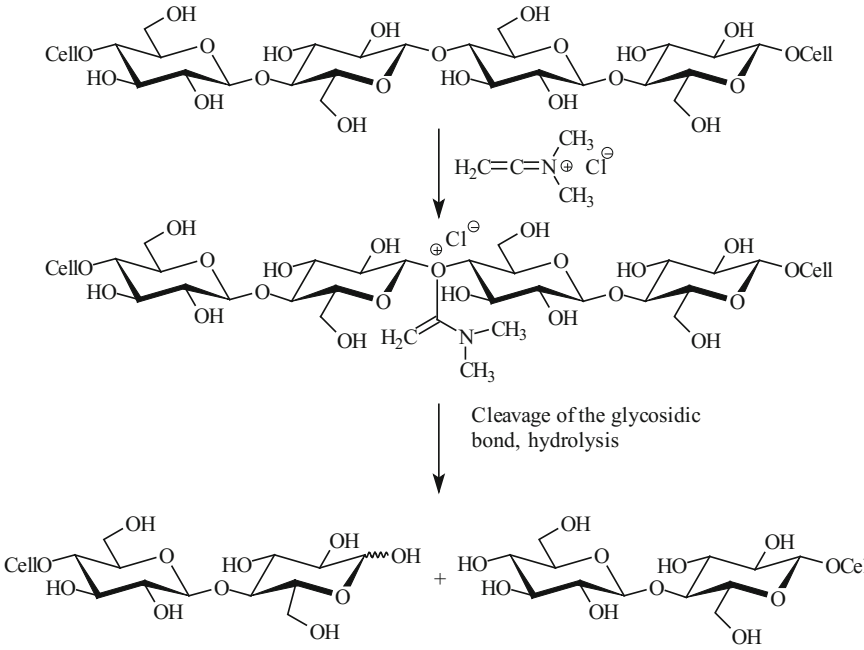


**Fig. 3.24** Cleavage of the glycosidic bonds in cellulose by the *N,N*-dimethylketeniminium ion [254]

Cellulose activation has been achieved by heating the polymer with dry LiCl at 110 °C under reduced pressure followed by addition of DMAc before atmospheric pressure is restored [257]. In addition to avoiding the above-mentioned DMAc-mediated side reactions, this solubilization procedure causes very little change in DP of the starting cellulose ($\leq 6\%$) for microcrystalline cellulose, bagasse, and cotton linters [258]. Note that some solvents, in particular, $R_4NF \times nH_2O$/dipolar aprotic solvent dissolve MCC and fibrous cellulose without activation pretreatment [242, 259].

Activation is followed by biopolymer dissolution. That the latter step is intimately dependent on the solvent system employed. The structural characteristics of the biopolymer can be clearly inferred from the following representative results:

- Whereas lithium salts in dipolar aproptic solvents dissolve cellulose, the corresponding sodium or potassium salts do not; LiCl is more effective than LiBr in the same dipolar aprotic solvent applied;
- TBAF × $3H_2O$/DMSO dissolves cellulose at room temperature; the corresponding tetramethylammonium fluoride is ineffective; benzyltrimethylammonium fluoride × $H_2O$ is only partially satisfactory, whereas BMAF × $0.1H_2O$ is at least as efficient as BMAF × $3H_2O$ [260, 261];
- MCC dissolves in DMAc/LiCl more readily than fibrous celluloses; dissolution of the latter depends on their DP and $I_c$; cotton is frequently mercerized in order to facilitate its dissolution [257, 258].

The results mentioned above raise a question about the pre-requirements for cellulose dissolution. These will be addressed for the solvents first. The effects of the structural characteristics of cellulose will be examined later. The dependence on the nature of the strong electrolytes is a combination of factors, including its solubility in the medium, the strength of the interaction between its ions, between the ions and the solvent, and the ions and the AGU of cellulose. For example, the efficiency of cellulose solubilization is TBAF × $3H_2O$ > benzyltrimethylammonium fluoride × $H_2O$, this is parallel to their solubility in DMSO, 0.94 and 0.025 mol/L, respectively; $(CH_3)_4NF$ is practically insoluble in DMSO and its suspension does not dissolve cellulose [260]. Solubility in the solvent, however, is necessary, but not sufficient condition for cellulose dissolution; tetra(1-butyl)ammonium chloride and bromide are soluble in DMSO but do not dissolve cellulose [259].

A combination of techniques and physicochemical properties has been employed in order to quantify the interactions of electrolytes with the dipolar aprotic solvent proper; with carbohydrates solubilized in the dipolar aprotic solvents, and to rationalize the dependence of solubilization on the electrolyte and the characteristics of cellulose. Thus, the free energies of transfer, $\Delta G_{tr}$, from water to 5–60% (w/w) DMSO are positive for LiCl, NaCl, and KCl (unfavorable transfer), but $\Delta G_{tr}$ for the last two electrolytes are ca. twice that of LiCl [262]. The free energies of solvation of some cations and anions in acetonitrile and DMSO (these refer to attachment of the dipolar aprotic solvent molecules to the ions in the gas phase) are favorable (i.e., negative); the orders of $\left|\Delta G^{\circ}_{solvation}\right|$ for both solvents are: $Li^+ > Na^+ > K^+$; $F^- > Cl^- > Br^-$ [263]. Therefore, it is easier to dissolve a lithium salt than its sodium or potassium counterpart in dipolar aprotic solvents; solvation of $Li^+$, $F^-$, and $Cl^-$ ions are favorable leading to more efficient interaction with the OH groups of the AGU.

The abilities of the strong electrolytes to complex with dipolar aprotic solvents have been assessed by electrospray mass spectra. For example, for electrolyte/DMAc the ratio of the peak intensities [alkali metal$^+$ + DMAc] were 10, 4.2, 1.0, and 1.2, for $Li^+$, $Na^+$, $K^+$, and $Cs^+$, respectively, indicating that $Li^+$ is solvated by DMAc more strongly than other alkali metals. The complexation of $Li^+$ with the *N, N*-dimethylamide of carboxylic acids increases as a function of the increasing length of the acyl group from formic to pentanoic acid. This order indicates that the

$Li^+$ is essentially coordinated to the oxygen atom of the amide group, whose basicity increases (due to the inductive effect of the attached moiety, H or R) from −0.38 to −0.43 e for DMF and *N,N*-dimethylpentamide, respectively [243]. A similar conclusion has been reached from $^7Li$ and $^{13}C$ NMR investigation of solutions of LiCl and LiBr in DMF, DMAc, *N,N*-dimethylpropionamide, and NMP. That is, LiCl interacts with the dipolar aproptic solvent more strongly than LiBr; the interaction of LiCl with the carbonyl group of the amide increases as a function of the increasing basicity of the amide [264].

Several schemes have been employed in order to describe the structure of cellulose/solvent complexes. These differ essentially in the role played by the $Li^+$ and $Cl^-$ (Fig. 3.25). In structure (A), the complex between $Li^+$ and the oxygen of the solvent C=O group results in the formation of a macro-cation [Li (DMAc)]$^+$ leaving the $Cl^-$ free to form hydrogen bonding with the OH group of the AGU. The repulsion among macro-cations formed allows solvent penetration within the natural polymer chains [67]. Alternatively, the $Li^+$ binds simultaneously to the OH group of cellulose and the solvent, the latter binding can occur either with the C=O group of DMAc, structure (B) [264], or with the C=O group and the amide nitrogen, structure (C) [266], LiCl may be also present in an undissociated form, as shown in structures (D), and (E). In the former, the electrolyte is bound to DMAc and the cellulose OH groups, forming a sandwich-type structure [267, 268]. In the latter (suggested for dissolution in DMSO/LiCl), only $Li^+$ is bound to the S=O dipole of the solvent and the oxygen atom of the OH groups, whereas the $Cl^-$ is not involved in bonding [269]. Structure (F) shows a possibility for TBAF–DMSO interactions [265].

These structures suggested will now be examined comparatively. In addition to the above-mentioned NMR results, the protonation of amides provides additional support for the association of the $Li^+$ ion, a hard acid, with the oxygen atom of the amide C=O group, since very little *N*-protonation has been detected [270, 271].

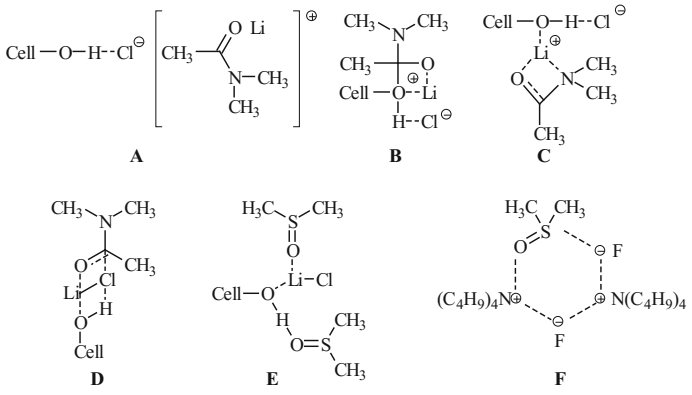


**Fig. 3.25** Structures suggested for explaining the interactions of cellulose with aprotic solvent/LiCl systems (A–E) and DMSO/TBAF (F) [84, 265]

Therefore, structures A and C are not very different because the $Li^+$–N association, if it occurs, is probably weak. There are problems associated with structures (D) and (E) in which the chloride ion plays a minor role (D), or no role (E) in cellulose dissolution. In view of the enhanced nucleophilicity of halides ions in dipolar aprotic solvents [272], and due to the fact that cellulose dissolution depends on the anion, being more efficient for LiCl than for LiBr, i.e., more efficient for the harder base [273], it may be concluded that the chloride ion is the strongest general base present in the electrolyte/DMAc solvent system. This conclusion does not agree with (E), which shows that the cellulose OH groups interact with the solvent S=O dipole, but not with the chloride ion. The relative importance of the halide anion-HO–Cell interactions can be inferred from the application of solvation free energy relationships, e.g., the Taft–Kamlet–Abboud equation [274] to solutions of cellulose in DMAc/LiCl and NMP/LiCl. The most important factors in these solutions are the acidic character of cellulose and basic character of the solvent system. Therefore, the most dominant interaction is the $Cl^-$-HO–Cell [275], a conclusion that is in variance with structures (D) and (E). The symmetrical, cyclic structure (F) may be an oversimplifaction because of the associated steric crowding in the $TBA^+$ cation. An open structure of electrolyte/dipolar aprotic solvent may be envisaged as it has been inferred from quantum chemical calculations on cellobiose/$R_4NF$/DMSO [276].

The above-mentioned techniques have been employed in order to study the interactions of lithium salts with cellulose solutions in dipolar aprotic solvents. Measurement of the longitudinal relaxation time ($T_1$) of the $^{13}C$ NMR peak of C=O group, in the presence of 6% (w/w) and 11.2% (w/w) cellulose (DP = 500) has indicated that the interaction between LiCl and DMAc is stronger than that with NMP [264]. Whereas the chemical shift of the $^7Li$ NMR peak did not change between 0.4 and 2.4 mol/L LiCl in DMAc (indicating strong electrolyte–dipolar aprotic solvent association), co-solubilization of cellulose decreased the chemical shift and increased the line width of the $^7Li^+$ peak, indicating its interaction with the biopolymer. It was concluded that one DMAc molecule in the inner coordination sphere of the $Li^+$ is replaced by one cellulosic OH group, e.g., as shown by the following equilibrium (Fig. 3.26) [273, 277].

Electrospray ionization mass spectroscopy has been employed in order to investigate the (average) structure of the associated species of strong electrolytes (LiF, LiCl, LiBr, NaCl, KCl, and CsCl) and oligosaccharides (maltose, maltotetraose; maltopentaose, maltohexaose, and maltoheptaose) in DMAc. The special efficiency of LiCl is indicated by the formation of a series of ions $[M_x^+Li^+nLiCl]^+$

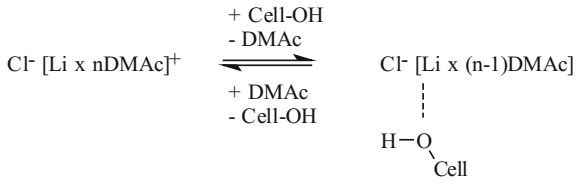


**Fig. 3.26** Ligand exchange reaction in solution of cellulose (Cell–OH) in *N,N*-dimethyl acetamide (DMAc)/LiCl mixtures according to [273]

and $[2M_x + Li^+nLiCl]^+$, where (M, $x$, $n$) refer to maltose unit whose number is equal to $x$, and LiCl molecules (from 1 to 7), respectively. The propensity toward attachment increases as a function of the increasing value of $x$. Neutral electrolyte attachment was observed with LiCl, to a lower extent with LiBr, but not with LiF, NaCl, KCl, or CsCl [278].

$^{19}F$ and $^{1}H$ NMR spectroscopic studies (chemical shifts and line widths) have been employed in order to investigate the interactions in cellulose (MCC) and TBAF in DMSO. The results indicated that the strongly electronegative $F^-$ ions act as hydrogen-bond acceptors to cellulose OH groups that break the intermolecular hydrogen bonds between the cellulose chains leading to the dissolution of the biopolymer. Solubilization is enhanced by electrostatic repulsion between the negatively charged cellulose chains due to the condensation of $F^-$ [279]. This picture is corroborated by an FTIR spectroscopic study on the dissolution of 2,2-bis (hydroxymethyl)-1,3-propanediol (model for the AGU) by a series of electrolytes and ionic liquids in DMSO, including TBAF and TMAF. This study showed the importance of the sizes of the electrolyte ions, and the charge density of the anion for efficient dissolution of the above-mentioned polyol. Thus, electrolytes with small, strongly interacting ions, e.g., TMAF, are not good solvents for the polyol because the negative charge of the anion is transferred to the cation rather than into the OH antibonding orbitals of the polyol [280].

It is common knowledge that the conditions to dissolve fibrous celluloses are more energetic than those required for MCC. Consequently, for fibrous cellulose it is common to use a higher temperature, longer reaction times, and higher molar ratio of the derivatizing agent per AGU. This is interesting in view of the fact that the rate constants and activation parameters for the decrystallization of cellulose, an important step in its dissolution, are practically the same for MCC and fibrous celluloses [81, 281]. Although surprising, this result indicates that decrystallization of cellulose is not rate limiting to its dissolution. The effects of other factors, e.g., $I_c$ and DP, should be sought. For example, the dissolution of several cellulose samples in aqueous NaOH depends on their DP and the corresponding supramolecular structure. Low DP and the absence of a non-fibrous structure contribute to the ease of dissolution of microcrystalline cellulose, whereas $I_c$ plays a minor role [82]. Focusing on DMAc/LiCl, the literature describes some results in which both the solubility and the reactivity of cellulose increase as $I_c$ decreases [70, 282]. However, Kraft pulp of low crystallinity dissolved slower than highly crystalline linters [83, 283]. Celluloses of low crystallinity dissolved in this solvent only after cellulose activation by solvent exchange [284].

Based on the preceding discussion, three factors affecting solubilization must be considered:

- the supramolecular structure,
- the DP, and
- the physical state of cellulose.

With regard to supramolecular structure, Fig. 3.27 shows the pore size distribution of MCC, untreated and mercerized sisal cellulose. The pores of MCC are much larger in diameter (between $6 \times 10^2$ and $2 \times 10^3$ nm) than those of fibrous celluloses. Mercerization of the latter leads to a decrease in the volume/radius ratios of the pores, and more homogeneous distribution of pore sizes. Thus, the much larger pore size of MCC explains, in part, its ease of solubilization because the penetration of the solvent into its crystalline structure should be much easier. The effect of mercerization on the ease of solubility cannot be explained on the bases of changes in pore size distribution alone; the concomitant cellulose I → cellulose II change, and the (mercerization-induced) removal of hemicelluloses and other alkali-soluble extractives play a role.

It is known that a clear cellulose solution is a necessary, but not sufficient condition for the success of derivatization. The reason is that at moderate concentrations, namely those employed in derivatization, the biopolymer chains are not molecularly dispersed, but most certainly contain aggregates of still ordered cellulose molecules [285, 286]. In fact, aggregate-free solutions of cellulose are hard to prepare [287]. The state of these aggregates depends on the concentration of LiCl and the method of solution preparation [288, 289].

The structure of these aggregates has been described in terms of a "fringed" micellar structure. Figure 3.28a shows a schematic possibility for such aggregate, composed of laterally aligned chains, forming a rather compact and probably geometrically anisotropic core, surrounded by disordered regions that give rise to the formation of solvent-separated "coronas". For different celluloses, at the same concentration, only the outer surface of the fringed micellar core is accessible, the area of this part decreases as a function of increasing DP. Formation of a fringed micellar structure is backed by theoretical calculations [290] and experimental evidence. For example, increasing cellulose concentration results in a pronounced increase in the molar mass of the particle, although its dimensions increase only slightly [291]. Parts (b) and (c) of Fig. 3.28 refer to monodisperse solutions of a small DP (b) and large DP (c) cellulose. The former part shows that the length of the short cellulosic chain is practically equal to its persistent length, i.e., there is neither coiling, nor interactions between the chains. The flexibility of the long-chain polymer (part c) permits the formation of strong intramolecular hydrogen bonds. Consequently, the properties of cellulose, in particular, its DP and concentration, affect its state of solution, hence, its dissolution/derivatization.

LS data have indicated the presence of aggregates in the DMAc/LiCl, whose size depends on the pretreatment employed, DP, concentration of LiCl, and presence of water. Molecularly dispersed cellulose solutions were not observed at the lowest concentration employed [0.2–0.3% (w/w)] softwood cellulose in the presence of 6–9% (w/w) LiCl [292, 293]. Non-cellulosic material may lead to further aggregation. Whereas hardwood Kraft pulps were found to be completely soluble in this solvent system, softwood Kraft pulps were not, due to relatively higher contents of mannan-, lignin-, and nitrogen-containing compounds (originated from degraded proteins) [288]. Therefore, one of the reasons that mercerization may lead to better results in dissolution is the effect of alkali-mediated removal of non-cellulosic material on the

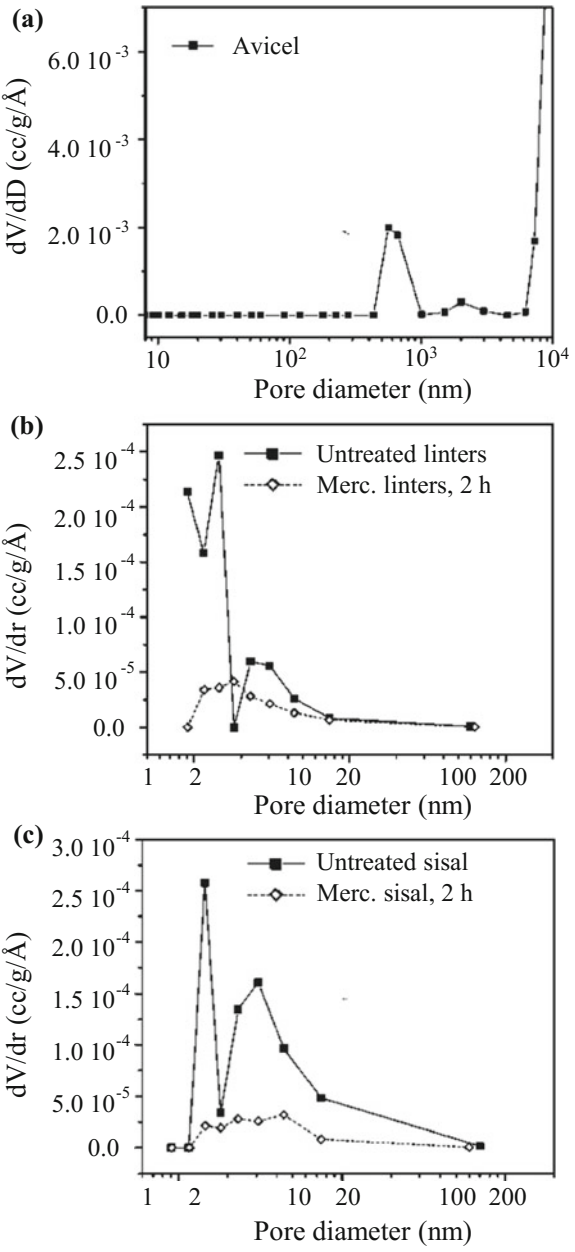


**Fig. 3.27** Pore size distribution of MCC (**a**), untreated and mercerized linters (**b**), untreated and mercerized sisal cellulose (**c**) (Reprinted from [81], copyright (©2005) American Chemical Society)

physical state of cellulose in solution. In addition to light scattering, SEC experiments on solutions of different celluloses in DMAc/LiCl have indicated the presence of large aggregates [288, 294–296]. The solvent 1,3-dimethyl-2-imidazolidinone/LiCl seems to be superior to DMAc/LiCl for cellulose dissolution, although the polymer

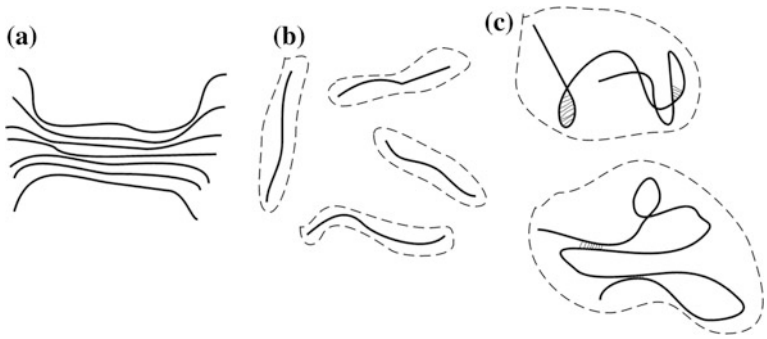


**Fig. 3.28** Schematic representation of cellulose structures in solution: Part **a** shows the "fringed" micellar structure. Parts **b** and **c** show possible chain conformations of celluloses of different DP. For high molecular weight cellulose (**c**), intramolecular hydrogen bonding is possible

concentration studied, 0.4% (w/w), is smaller than that usually employed in the synthesis of esters [297].

The presence of adventitious water in the medium is important because the efficiency of electrolytes depends on their state of hydration, a consequence of their strong hygroscopic character. Thus TBAF is very hygroscopic, i.e., absorbs water well beyond the trihydrate [298], LiCl forms stable LiCl × $2H_2O$ hydrate [299]. Analysis of the effect of water on cellulose/DMAc/LiCl indicated that the molar ratio $H_2O$/LiCl must be less than 2. Otherwise, complete dissolution cannot be achieved [300]. The effect of water on cellulose/TBAF/DMSO has been studied by $^{1}H$ and $^{19}F$ NMR chemical shifts and line widths. Because $F^-$ interacts strongly with both cellulose and water, the presence of the latter decreases the solubility of cellulose and, finally, leads to gel formation, as shown schematically in Fig. 3.29 [279]. Thus, it may be advantageous to synthesize the $R_4NF \times H_2O$, not only because some are not commercially available (BMAF), but also because the water content of the strong electrolyte/dipolar aprotic solvent solution can be controlled [301].

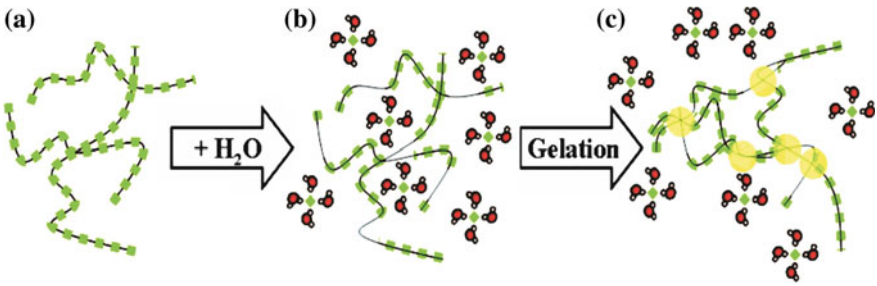


**Fig. 3.29** A schematic representation of the effect of water on the cellulose chains solubilized in a TBAF/DMSO solution. Due to the strong solvation of the $F^-$ by water, addition of the latter compete effectively for TBAF, leading to phase separation of the polymer (gelation) (Reprinted from [279], copyright (©2009) American Chemical Society)

From the thermodynamic point of view, the requirement for cellulose dissolution is that the free energy of the process is negative, i.e., $\Delta G_{\text{Dissolution}} < 0$. This condition can be achieved by a combination of a small, or negative enthalpy term $\Delta H_{\text{Dissolution}}$, a positive entropy term $\Delta S_{\text{Dissolution}}$, or both [273]. Operationally, the essential factors required for dissolution of cellulose in any solvent include:

1. Adequate stability of the electrolyte/solvent complex
2. Cooperative action of the solvated ion pair on hydrogen bonding of cellulose
3. Sufficient basicity (hardness or charge density) of the anion
4. Adequate volume of the electrolyte/solvent complex [273, 302].

Adequate stability of the strong electrolyte/dipolar aprotic solvent complex is important because exceedingly stable or unstable complexes do not dissolve cellulose [277], e.g., the stronger complex DMAc/LiCl is more effective than its weaker DMAc/LiBr and DMF/LiCl counterparts [303, 304], on one hand. On the other hand, the ions of TMAF associate very strongly, so that this strong electrolyte is insoluble in DMSO, hence, does not dissolve cellulose or polyols in general [280]. Cooperative action of the solvated ion pair on hydrogen bonding should occur, e.g., by bonding of the $Li^+$ and $Cl^-$, respectively, to the oxygen and hydrogen atoms of the cellulose OH group [266, 303]. Points (1) to (3) above ensure a negative $\Delta H_{\text{Dissolution}}$, whereas points (2) and (4) ensure that $\Delta S_{\text{Dissolution}}$ is positive. As mentioned above, electrostatic repulsion, due to condensation of the anions on the cellulosic chain, most certainly contributes to the stability of the dissolved biopolymer. For $R_4NF \times H_2O$/dipolar aprotic solvent, the cations are voluminous and interact much less with the hydroxyl groups of the AGU than the strongly basic and small $F^-$.

To summarize, cellulose samples including bacterial cellulose of high DP and crystallinity can be dissolved either directly, or after activation in strong electrolyte/dipolar aprotic solvent; the ease of dissolution depends on the electrolyte/dipolar aprotic solvent pair, the structural characteristics of cellulose, the temperature and dissolution time (up to 1 week at low temperature) [255, 288]. Some activation procedures may lead to cellulose degradation. The presence of adventitious water should be minimized and controlled. Because its molecular weight is only 11% of that of the AGU, even small amount of water (originated from cellulose, the electrolyte, or the dipolar aprotic solvent) may adversely affect the outcome of, e.g., esterification reaction by impairing the efficiency of the electrolyte. In particular, due to anion hydration; hydrolysis of the acylating reagent, participation in side reactions (vide supra, DMAc), and decreasing the accessibility of cellulose because of the enhanced aggregate formation.

It has been recently demonstrated that solutions of quaternary tetraalkylammonium chlorides with one long alkyl chain in various organic solvents constitute a new class of cellulose solvents. Contrary to the well-established solvent DMAc/LiCl, cellulose dissolves in DMAc/quaternary ammonium chlorides without any pretreatment [305]. Surprisingly, even acetone containing tetraalkylammonium chloride is an efficient solvent for cellulose. The addition of an amount of 10 mol% (based on acetone) of well soluble salt triethyloctylammonium chloride adjusts the solvent's properties (increases the polarity) to promote cellulose dissolution. It is

worth to note that the dissolved cellulose in acetone/$Et_3OctNCl$ possesses the lowest viscosity reported for comparable aprotic solutions making it a promising system for shaping processes and homogenous chemical modification of the biopolymer [306]. It is expected that further solvents for cellulose will be designed based on this concept.

Melts of inorganic salt hydrates

Inorganic molten salt hydrates or mixtures of these compounds have attracted attention as solvents of the biopolymer. Dissolution of cellulose in $Ca(SCN)_2 \times 3H_2O$ occurs in the temperature range from 120 to 140 °C within 40 min [307]. Coordination of $Ca^{2+}$ at *O*6 and *O*5 of cellulose backbone is reported [308–310]. Representative examples of molten salt hydrates that dissolve cellulose are listed below in the following order: Pure salt hydrate melts (the first compound in the row) or mixtures (second compound in the row):

$ZnCl_2 \times 3$ - $4H_2O$; ($LiClO_4 \times 3H_2O$ + $\leq 25\%$/w/w) $Mg(ClO_4)_2/H_2O$)
$LiClO_4 \times 3H_2O$; ($LiClO_4 \times 3H_2O$ + $\leq 10\%$(w/w) $NaClO_4/H_2O$)
$FeCl_3 \times 6H_2O$; ($LiClO_4 \times 3H_2O$ + $MgCl_2 \times 6H_2O$)
(NaSCN/KSCN (eutectic) + LiSCN $\times 2H_2O$)
$LiCl_2$ $ZnCl_2/H_2O$

Very effective is $LiClO_4 \times 3H_2O$ yielding transparent cellulose solutions within a few minutes. Furthermore, mixtures of $LiClO_4 \times 3H_2O$ with $Mg(ClO_4)_2 \times H_2O$ or the eutectic mixture of NaSCN/KSCN/$H_2O$ with different amounts of $LiSCN \times 2H_2O$ dissolve cellulose. In case of $LiI \times 2H_2O$, the dissolution is explained on the basis of the salt composition consisting of a soft polarizing anion and a small polarizing cation. In this regard, it is surprising that $LiClO_4 \times 3H_2O$ gave best results. The reason should be the strong interaction of cellulose with the hydrated $Li^+$ and the structure of the molten $LiClO_4 \times 3H_2O$ as revealed by X-ray scattering. It is possible to acquire NMR spectra in these systems and to regenerate cellulose II from them [311–313].

Ionic Liquids

The current convention is that an electrolyte melting below 100 °C is called ionic liquid. With this proviso, the acronym RTIL (room temperature ionic liquid) is redundant. ILs have also been termed ionic fluids, molten salts, fused salts, or neoteric solvents. These electrolytes are liquids because their Gibbs free energies of solvation are negative. That is, the liquid state is thermodynamically favorable, due to the large size and conformational flexibility of the ions, which leads to small lattice enthalpies and large entropy changes that favor the liquid state [314]. Figure 3.30 shows the structure of cations and anions of ILs that are most employed with cellulose [315–320].

We refer to the structural moieties present by using Me, Et, Pr, Bu, Al, Hx, Oc, Ac, Py, and Im. These abbreviations refer to methyl, ethyl, 1-propyl, 1-butyl, allyl, 1-hexyl, 1-octyl, acetate, pyridine, and imidazole, respectively. Unless specified otherwise, the alkyl groups are 1-alkyl; the acronyms for the cation and anion are

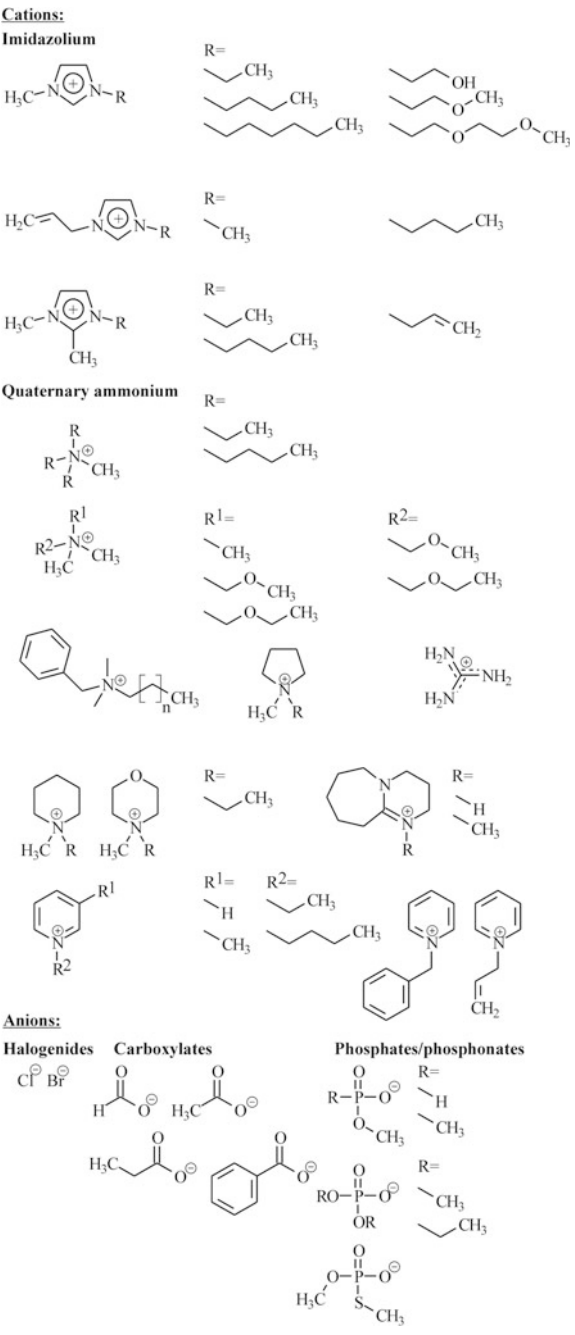


**Fig. 3.30** Structure of anions and cations of ILs employed for cellulose dissolution [315]

placed next to each other, without showing the corresponding charges. Unless specified otherwise, the substitution is on the two nitrogen atoms of imidazole, i.e., 1,3. Therefore, $Me_2ImCl$; $BuMeImBF_4$; Bu-2,3-$Me_2ImCl$, and BuPyAc refer to 1,3-dimethylimidazolium chloride, 1-(1-butyl)-3-methylimidazolium tetrafluoroborate, 1-(1-butyl)-2,3-dimethyl-imidazolium chloride, and *N*-(1-butyl)pyridinium acetate, respectively.

Most imidazole-based ILs are synthesized directly by an $S_N$ (Mentschutkin) reaction of, e.g., 1-methylimidazole, and alkyl halide, dialkylsulfate, or alkyl methanesulfonate to yield ILs with halides, alkylsulfate, or methanesulfonate, respectively, as counterions. These are termed "first generation" ILs. Two alternatives are available to convert the first generation into "second generation" ILs containing bulkier anions, e.g., $BF_4^-$, $PF_6^-$, $C_6H_5CO_2^-$, and $(F_3CSO_2)_2N^-$ having interesting properties such as lower melting points, different solubilities, and viscosities. Metathesis of the counterion can be performed in one- or two-phase system (Finkelstein reaction), or by ion exchange usually by using macroporous resin in its OH form followed by neutralization by the acid (Fig. 3.31) [316]. Alternatively, second-generation ILs can be synthesized directly by the reaction of the heterocyclic base (imidazole, pyridine, *N*-methylpyrrole) with an alkyl halide in the presence of an electrolyte, e.g., $KBF_4$. These reactions are assisted by a combination of ultrasound and microwave; for 1-methylimidazole the yields are from 65 to 98%, depending on the counterion [321]. Depending on the method of synthesis, the impurities may include water, excess tertiary amine, excess alkyl halide, sulfate, or sulfonate and, after metathesis, residual halide, $RSO_3^-$, or $RSO_4$. Because ILs have an extremely low vapor pressure, they cannot be purified by the most employed technique for the purification of organic compounds, i.e., fractional distillation. They are purified by solvent extraction or chromatography instead.

The purity of IL is important for using these solvents in cellulose chemistry. Because the purification of ILs can be laborious, it is expedient to use commercial samples of 95–98% purity. Several practical problems may result, however, from this use, including conflicting physicochemical properties that are important for

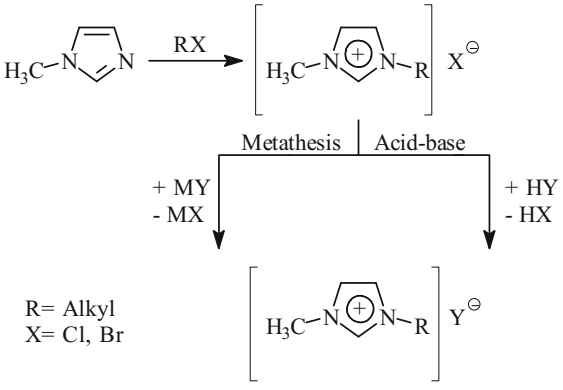


**Fig. 3.31** Schematic routes for the synthesis of the first generation IL by $S_N$ reaction of 1-methylimidazole with an alkyl halide RX and the second-generation IL either by metathesis with the inorganic compound (MY), or via conversion of RMeImX with the acid HY [318]

their applications. Examples are the published data on the m.p., e.g., $EtMeImBF_4$, 5.8 °C [322]; 11 °C [323]; 12.0–12.5 °C [324]; 6 °C [325], and 15 °C [326]. AlMeImCl, 17 °C [327]; 52–53 °C [328]. Viscosities in mPas: 37 and 66.5 for $EtMeImBF_4$; 691 and 866 for $OcMeImPF_6$; 67 and 222.7 for $BuMeImNO_3$; and 1238 and 8465 for $OcMeImNO_3$ [329–332], and thermal stabilities [333].

The presence of water (a typical, difficult to remove impurity) bears on the solubility of cellulose in the Ils and its subsequent reactions. Whereas 3–10% (w/w) cellulose solutions can be easily prepared in BuMeImCl, the biopolymer is insoluble in the presence of 1% water [334]. This surprisingly strong adverse effect may be traced to the deterioration of solvent quality in the presence of water and water-mediated increase in cellulose aggregation. Thus, similar to cellulose solutions in strong electrolyte/dipolar aprotic solvents, the biopolymer auto-aggregates in ILs, even the ones that are known to be efficient solvents, e.g., BuMeImCl and EtMeImAc, as shown by SLS, DLS, and SANS data [335, 336]. In the latter IL, cellulose (DP = 494) forms 21-mer. The aggregation number, hence $R_h$ is a function of cellulose concentration, as shown in part (a) of Fig. 3.32. Water increases noticeably the value of $R_h$, e.g., from ca. 150 to 550 nm in the presence of ca. 7% (w/w) water, see the upper curve of part (b) below [336].

The yields of spontaneous (no added acid) conversion of cellulose into sugars in water-ILs mixtures depend on the purity of the IL. Residual base impurity increases the effective pH value of the medium, hence decreases the yield [337]. Incomplete ion exchange can also be problematic, as shown by the following example: $HxMeImN(TFMS)_2$ has been synthesized from the corresponding chloride by metathesis. The yield of a typical carbohydrate reaction, glycosylation of cyclohexylmethanol, in $HxMeImN(TFMS)_2$ is reduced from 90 to 6% when the efficiency of the anion exchange was reduced from 100 to 95%; the reaction ceased to occur when the exchange was 90% complete [338]! Additionally, initially present basic impurities and those generated by heat-mediated side reactions catalyze IL-cellulose side reactions, e.g., the addition of the IL cation to the reducing end of the sugar or cellulose (Figs. 3.33, 3.34 and 3.35) [339].

Therefore, using ILs of high purity is recommended in order to obtain reproducible cellulose solubilization/derivatization results. Commercial ILs can be employed without overlooking the possible effects of the impurities present. Some older data in the literature, when the consequences of IL purity were not fully appreciated should be evaluated with some reserve [340].

The use of ILs for cellulose dissolution and subsequent regeneration or derivatization has generated intense interest because being ionic, they disrupt the strong hydrogen bonding present in cellulose leading to its fast dissolution and no additional electrolyte is required. The most important aspect, however, is their structural versatility. This entails that their physicochemical properties (viscosity, miscibility with molecular solvents, etc.) that are relevant to cellulose processing and transformation covers a range much wider than that of molecular solvents. After the initial interest in verifying their efficiency as solvents for cellulose and

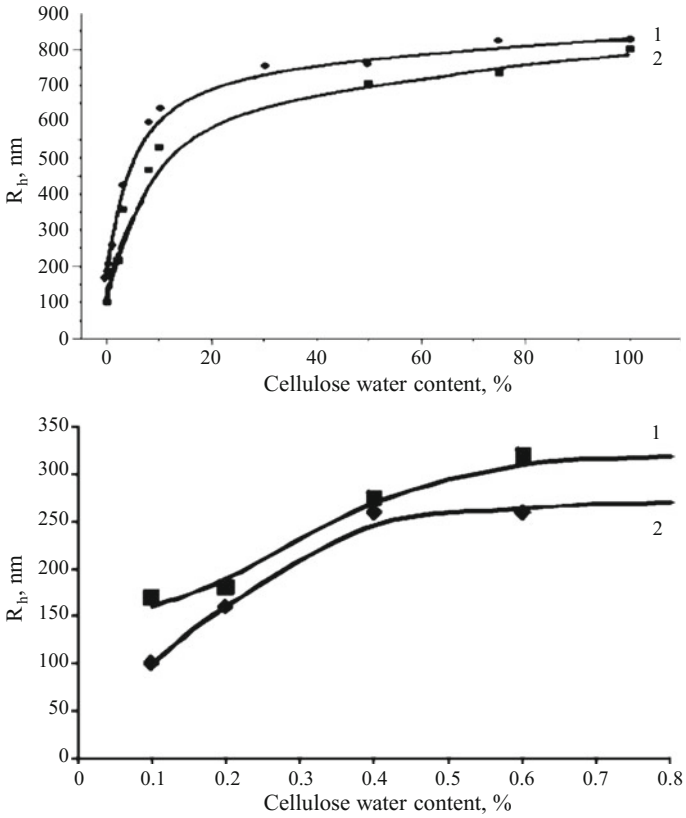


**Fig. 3.32** SLS results (hydrodynamic radii) for solutions of cellulose (DP = 494) in the ILs EtMeImAc (1) and BuMeImCl (2), in the absence (top) and presence (bottom) of added water

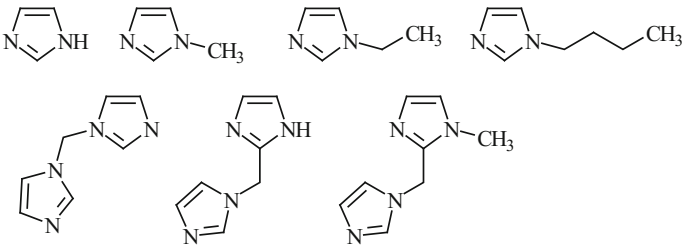

**Fig. 3.33** Thermal degradation products of ILs (3-R-1-MeImX, R = ethyl or butyl, X = $Cl^-$ or $CH_3CO_2^-$) formed after heating for 24 h at 200 °C, under inert atmosphere (adapted from [339])

other carbohydrates, the focus has shifted to the study of the relationship between the molecular structure of the IL and its efficiency to dissolve cellulose and the search for novel, more convenient ILs.

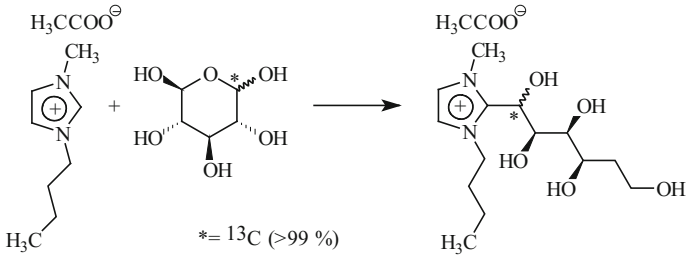


**Fig. 3.34** Reaction of BuMeImAc with $^{13}$C-enriched glucose leading to condensation of the cation with the aldehyde group of the sugar

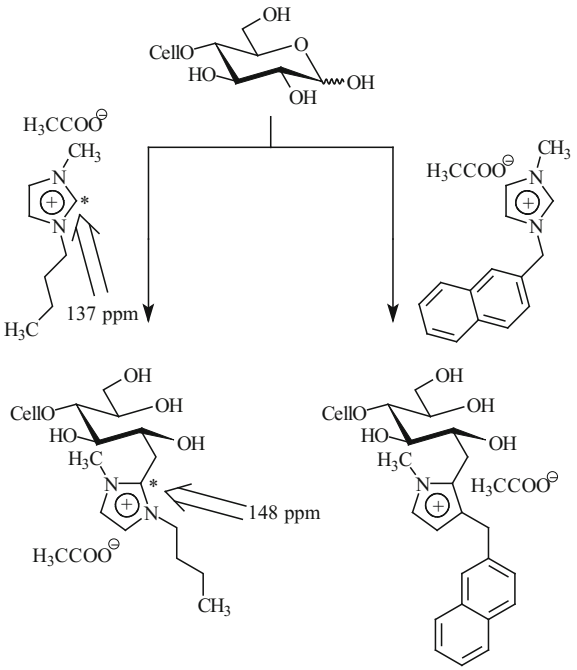


**Fig. 3.35** Reaction of $^{13}$C-enriched BuMeImAc with cellulose (Cell) showing the condensation of the IL cation with the reducing end of cellulose

The relationship between the structure of the IL and the efficiency to dissolve cellulose bears on biopolymer accessibility. This conclusion is based on the fact that the anion and cation of the IL interact with cellulose [341], this leads to enhanced reactivity due to biopolymer chain separation (entropy effect) and increase in the nucleophilicity of the OH groups of the AGU (enthalpy effect). A systematic approach to select an IL is to search for one with appropriate physicochemical properties, in particular, low m.p. and viscosity. Physicochemical data ($T_g$, $T_m$, $T_{Decomp}$, density, viscosity, surface tension, and polarity) have been collected for 588 ILs. From this compilation, the dependence on the structure of the IL of several

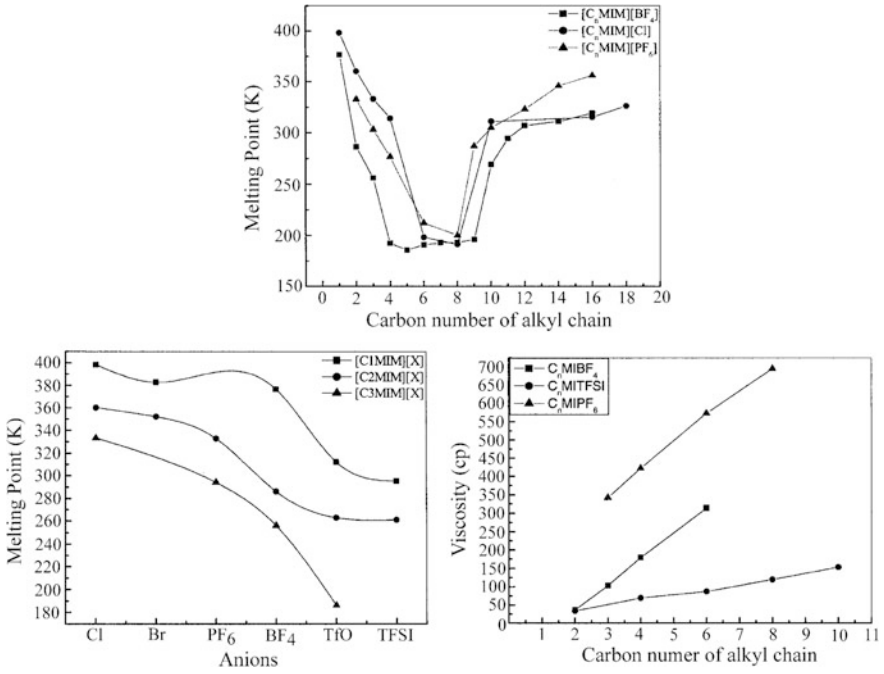


**Fig. 3.36** Dependence of the melting points, densities, and viscosities of some ILs on their molecular structures (Reprinted from [342] with permission from AIP Publishing)

properties that are relevant to cellulose chemistry becomes apparent, as shown in Fig. 3.36 [342].

From these, and similar data it is possible to decide on the IL structures that are appropriate for use with cellulose. The second step is to determine the solubility of different celluloses in the chosen ILs, as shown by the example of Table 3.5 [343]. This solubility can be judged either visually or better, by using a microscope with plan-polarized light.

Understanding why some ILs are efficient solvents for cellulose whereas others do not require insight into the roles of the solvent anion and cation. Both the cation and anion are involved, as shown schematically in Fig. 3.37 for BuMeImCl and BuMeImAc. An odd–even effect was found for different alkyl side-chain lengths of the imidazolium chlorides which could not be observed for the bromides [344]. Furthermore, 1-ethyl-3-methylimidazolium diethyl phosphate was found to exhibit the best dissolution capability for cellulose.

An interesting feature is the association of the anion with two hydroxyl groups of the AGU simultaneously, which explains hydrogen-bonding disruption efficiency of ILs. This schematic representation is in agreement with molecular dynamics simulations for the dissolution of glucose dodecamer (oligomer) in AlMeImCl/DMAc, Fig. 3.38. Thus, the structure of the cation and the basicity of the anion are

**Table 3.5** Solubility of cellulose in ionic liquids

| Ionic liquid | Solubility |
|---|---|
| 1-Butyl-3-methylimidazolium chloride | Soluble[a] |
| 1-Allyl-3-methylimidazolium chloride | Soluble |
| 1-Allyl-3-butylimidazolium chloride | Soluble |
| 1,3-Diallylimidazolium chloride | Soluble |
| 1-Butyl-2,3-dimethylimidazolium chloride | Dissolves slowly |
| 1-Allyl-3-propargylimidazolium chloride | Dissolves slowly |
| 1-Butyl-2,3-dimethylimidazolium thiocyanate | Insoluble |
| 1-Butyl-3-methylimidazolium saccharinate | Insoluble |
| 1-Butyl-3-methylimidazolium tosylate | Insoluble |
| 1-Butyl-3-methylimidazolium hydrogen sulfate | Insoluble |
| 1-Allyl-3-methylimidazolium dicyanamide | Insoluble |
| 1-Allyl-3-butylimidazolium dicyanamide | Insoluble |
| 1-Allyloxy-3-methylimidazolium dicyanamide | Insoluble |
| 1-Allyloxy-3-methylimidazolium chloride | Insoluble |

[a]Cellulose is considered as soluble if the attained concentration in the given solvent is $\geq 3\%$

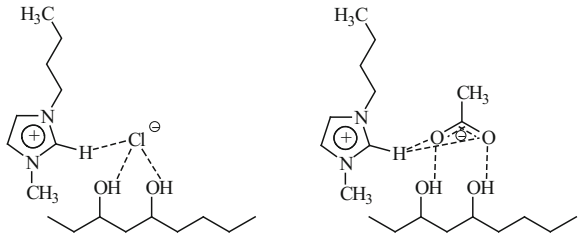


**Fig. 3.37** Schematic representations of the association of cellulose with the cation and anion of BuMeImX, X = chloride or acetate

determinant for cellulose dissolution, ILs with small cations and basic anions are efficient.

Figures 3.37 and 3.38 agree with the results of NMR spectroscopy. The $^{13}C$ NMR signals of cellulose dissolved in BuMeImCl were recorded, and the spectrum was compared with that of the same cellulose in DMSO/TBAF. The similarity of the chemical shifts of the AGU carbon atoms indicated that the IL is a non-derivatizing solvent for cellulose [346]. NMR spectroscopy has been applied to solutions of celluloses (DP 400–1000), and the oligomers cellobiose, cellotriose, and cellohexaose in $D_2O$ (where the carbohydrates are soluble) and in BuMeImCl containing DMSO-$d_6$ (in order to reduce solution viscosity). The spectra recorded indicated that cellulose oligomers are disordered in the IL-DMSO solution. This result is similar to that observed for the corresponding aqueous solutions, despite the considerable differences between the two media [347]. The NMR ($T_1$) and ($T_2$)

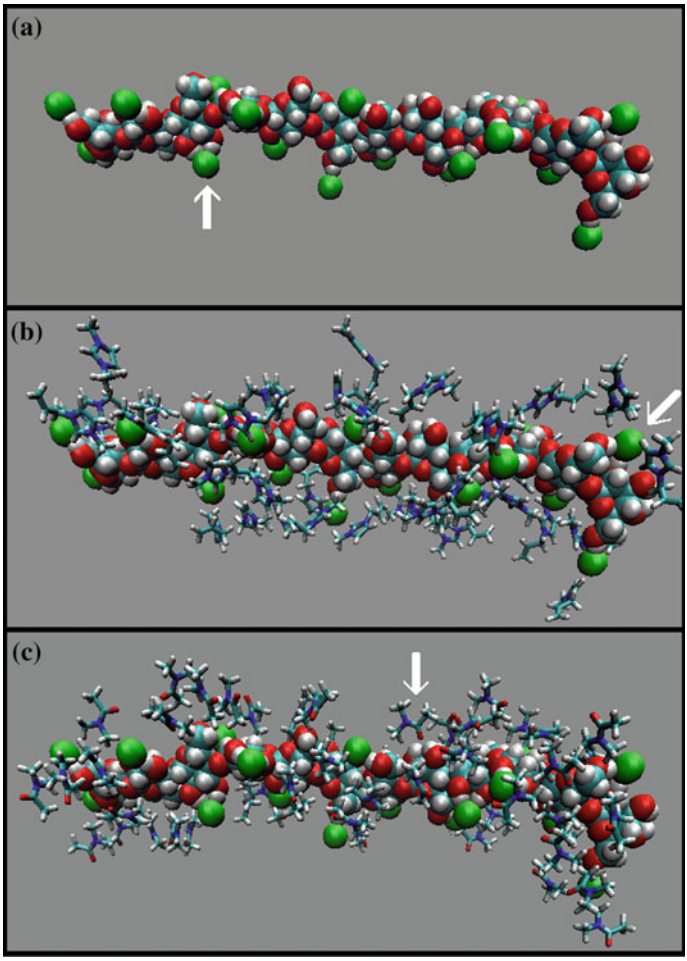


**Fig. 3.38** Snapshot of an MD simulation frame showing the cellulose oligomer and its first solvation shell (0.47 nm). Part **a** shows the oligomer plus ($Cl^-$). The arrow shows that this anion forms simultaneous hydrogen bonds to two OH groups of the AGU. Part **b** shows the oligomer plus ($Cl^-$) and $Imz^+$. The arrow shows two $Imz^+$ hydrogen bonded to a single ($Cl^-$) via their C2–H. Part **c** shows the oligomer plus ($Cl^-$) and DMAc. The arrow indicates the hydrogen bonding between C=O of DMAc and the OH of the AGU (Reproduced from [345] with permission of Springer)

relaxation times of BuMeImCl, both for the cation ($^{13}C$), and the anion ($^{35/37}Cl$) were determined as a function of the concentrations of cellobiose (model for cellulose), glucose and glucose pentaacetate, which lacks hydrogen-bond donors due to the acetylation of all OH groups. The effects of increasing temperature (from 40 to 90 °C) on $T_1$ and $T_2$ of both nuclei ($^{13}C$ and $^{35/37}Cl$) of the pure IL indicated the expected weakening of ion–pair interactions. Investigation of the relaxation times as a function of increasing cellobiose concentration has indicated that the interactions with the anion are very strong. These interactions are due to hydrogen bonding

of $Cl^-$ to the OH groups of the sugar that were confirmed by studying the dependence of relaxation times on the concentrations of glucose and glucose pentaacetate. Whereas the former interacted strongly with the anion, the latter showed almost no effect on the relaxation rate of $^{35}Cl$. The stoichiometry of the interaction was calculated to be 7.8 and 4.9, for cellobiose and glucose, respectively, corresponding to one IL molecule/sugar OH group [348].

The effect of IL structure can, in principle, be rationalized by employing a free-energy relationship according to Eq. 3.2,

$$\text{Solvent dependent phenomenon} = \text{a SA} + \text{b SB} + \text{d SD} + \text{p SP}, \tag{3.2}$$

where the phenomenon of interest is cellulose dissolution. (S) refers to solvent, (SA, SB, SD, and SP) refer to Lewis acidity and basicity, dipolarity and polarizability, respectively. The result of an early application of this approach to the dissolution of macromolecules is shown in Fig. 3.39 [349].

As discussed above, cellulose dissolves in strong electrolyte/dipolar aprotic solvent due to the combined effect of efficient swelling of the biopolymer and disruption of the present inter- and intramolecular hydrogen bonding. It is not surprising, therefore, that ILs are expected to dissolve cellulose efficiently due to a combination of favorable solvent properties and IL-cellulose-specific interactions. With regard to the first criterion, the overall polarity of ILs, as measured by

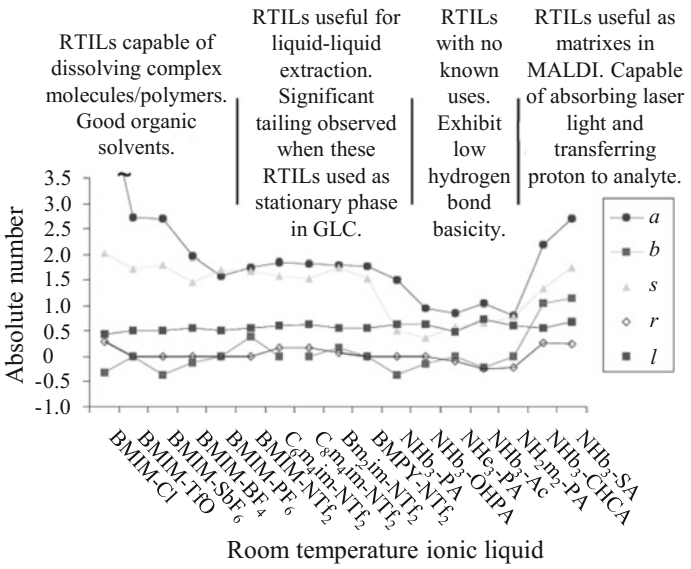


**Fig. 3.39** Plot illustrating the magnitude of each interaction parameter at 70 °C: hydrogen-bond basicity (a), hydrogen-bond acidity (b), interaction via nonbonding and π-electrons (r), dipolarity/polarizability (s), and dispersion forces (l) (Reprinted (adapted) with permission from [349], copyright (©2002) American Chemical Society)

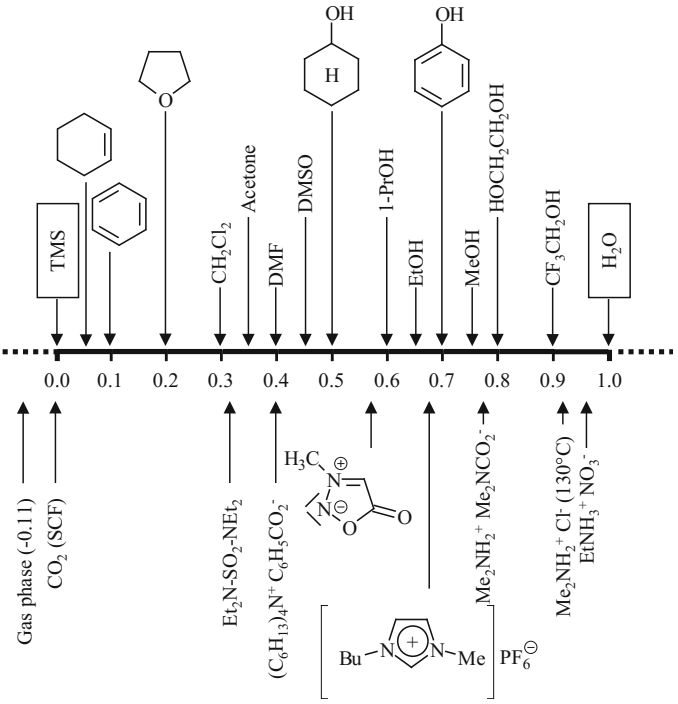


**Fig. 3.40** Reduced empirical solvent polarities for a collection of molecular solvents and ILs [350]

solvatochromic probes, are in the same range as dipolar aprotic solvents, where the solvent empirical polarity is defined according to a reduced scale that ranges (arbitrarily) from zero (tetramethylsilane, TMS) to unity (water, Fig. 3.40).

According to Eq. 3.2, substituting empirical solvent polarity for the left-hand side, ILs, which are relatively basic and strongly dipolar, should be efficient solvent for cellulose. The basicity is sensitively dependent on the counterion, e.g., for HeMeImX, $Cl^- > Br^- > MeSO_4^- > BF_4^- > PF_6^-$ [351]. This basicity/dipolarity combination is shown in Fig. 3.41. The IL number 10, BuMeImCl, that is being extensively employed for dissolving cellulose possesses the largest basicity and dipolarity/polarizability among 17 ILs tested [349]. It should be noticed that ILs show some acidic character, due to the relatively acidic C2–H of the imidazolium ring [352].

The ideas in the discussion above have been developed further in the direction that efficient ILs for cellulose dissolution are those that possess high basicity and low acidity. This is shown in Fig. 3.42 where $\beta$–$\alpha$ is plotted against $\beta$. The compounds within the hatched rectangle are efficient solvents for cellulose [353].

Table 3.6 shows the solubility of representative cellulose samples in ILs [320, 354].

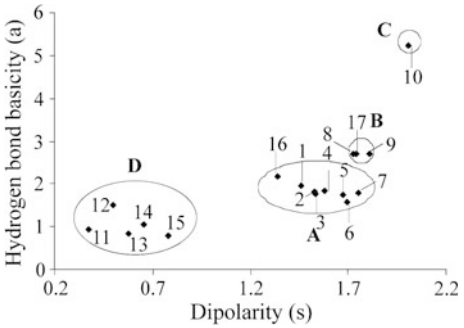


**Fig. 3.41** Correlation between the basicity and dipolarity/polarizability for 17 ILs, consisting of BuMeImX (5); other 1,3-dialkylImX (4); alkylammoniumX (8) with different counterions (X), including $Cl^-$, $BF_4^-$, $PF_6^-$, carboxylates, etc. The IL number 10 is BuMeImCl (Reprinted (adapted) with permission from [349], copyright (©2002) American Chemical Society)

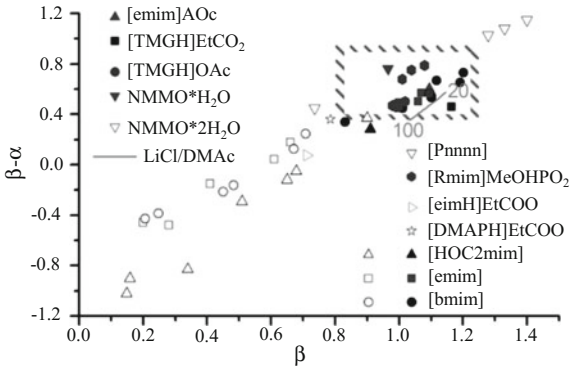


**Fig. 3.42** Dependence of cellulose solubility on the basicity and acidity of cellulose solvents, including NMMO, DMAc/LiCl, and ILs. Solvents with large basicity ($\beta$) and small acidity ($\alpha$), i.e., relatively large ($\beta - \alpha$) are efficient for cellulose dissolution (Reprinted (adapted) from [353], copyright (©2012) American Chemical Society)

The role of the cation, in particular, the relatively strongly acidic C2–H of the imidazolium ring [355], became clear from a $^{13}C$ NMR study of the solutions of cellulose oligomers (DP 6–10) in EtMeImAc. The results have led to the conclusion that a covalent bond is formed between C1 of the AGU and C2 of the imidazolium ring, see Fig. 3.43. This covalent bond formation may be related to the acetate-mediated formation of carbene from the imidazolium cation [357].

Concurrently, the search for new, convenient ILs as solvents for cellulose, wood, and other lignocellulosic raw material has continued [358, 359]. For example, the fairly corrosive halide anions of imidazolium ILs have been substituted with carboxylate, dialkyl phosphonates, dialkyl phosphates, and tosylates. The interaction

**Table 3.6** Representative examples of solubility of sugars, cellulose, wood, and other carbohydrates in molecular solvents and ionic liquids

| Cellulose source | DP | IL | Concentration, wt% | T, °C |
|---|---|---|---|---|
| MCC | 286 | BuMeImCl | 18 | 85 |
| Spruce | 593 | BuMePyCl | 13 | 105 |
| Linter | 1198 | [BMIM]Cl | 10 | 83 |
| Norway spruce | – | [BMIM]Cl | 7 | 130 |
| MCC;spruce; beech; chestnut | – | AlMeImCl; BuMeImBr; BuMeImCl | $\leq 6$ | 90 |
| MCC | 220 | AMIMCl | 14.5 | 80 |
| Dissolving pulp | 1000 | BuMeImCl<br>HxMeImCl | 10<br>5 | 100<br>100 |
| Spruce chips | – | EtMeImCl | 5 | 90 |
| Yellow pine | – | EtMeImAc | 92.6 | 110 |
| Pine | – | BuMeImCl | 67 | 100 |
| Oak | – | BuMeImCl | 56 | 100 |

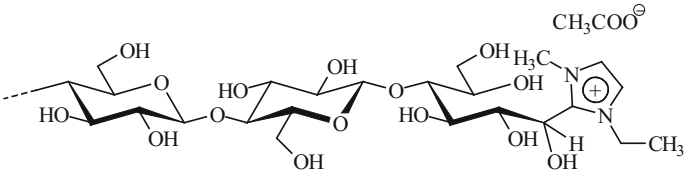


**Fig. 3.43** Formation of a covalent bond between the cation of the IL EtMeImAc and the reducing end of oligomer (Reproduced from [356] with permission from John Wiley and Sons)

between the 1,3-dialkylimidazolium cation and cellulose has been modified by using the (polyoxa-) side chain instead of its alkyl counterpart [320]. Quaternary ammonium and quaternary phosphonium cations have replaced the dialkylimidazolium cation [305, 360, 361] and microwave-assisted cellulose esterification has proved to be faster compared with reactions under conventional heating, i.e., convection [362–364].

As in case of other non-derivatizing solvents for cellulose, the biopolymer has been regenerated in different forms from its solutions in ILs. Figure 3.44; (a) shows a schematic representation of a dry–wet spinning process for regeneration of cellulose fibers from its solutions in ILs, whereas part (b) shows regenerated cellulose fibers, as well as those containing embedded multiwalled carbon nanotubes (composite fibers) [319].

*N*-Oxides of tertiary amines

Typical structures of this type of solvents are *N*-oxides of tertiary amines and *N*-alkylpyridinium halides as shown in Fig. 3.45 with NMMO being the most

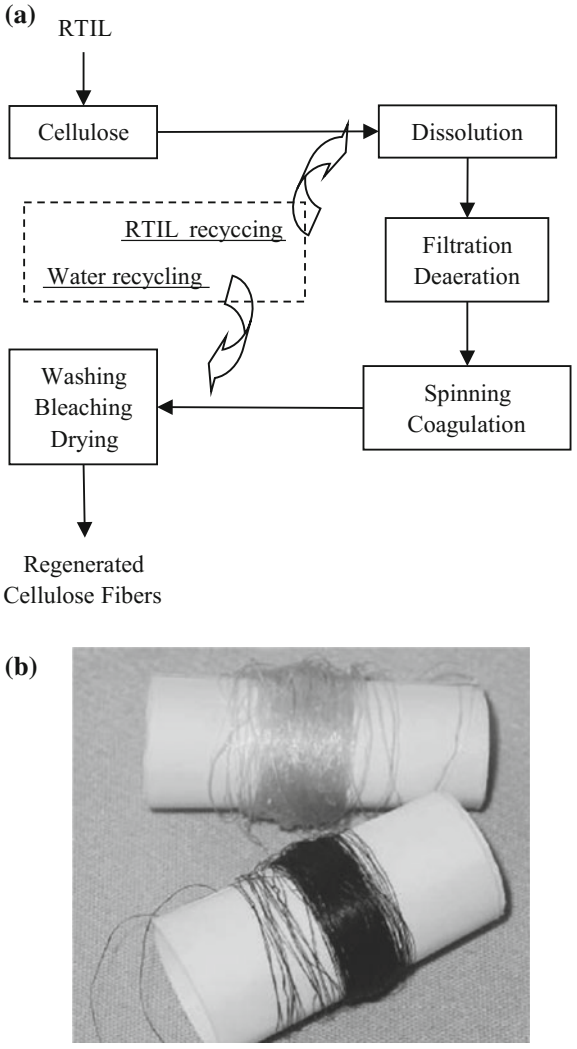


**Fig. 3.44** **a** A schematic representation of a dry–wet spinning process for regeneration of cellulose fibers from their solutions in ILs and **b** cellulose fibers and composite fibers regenerated from their solutions in ILs (Reprinted from [319], copyright (©2009) with permission from Elsevier)

powerful one. Typically, NMMO is used as monohydrate that dissolves cellulose, even of high DP, at about 100 °C rather quickly. $^{13}C$ NMR spectroscopy and microscopy have indicated that NMMO is able to break hydrogen bonds, in particular at *O*-6 and, hence, chain aggregates and even individual chains are sufficiently liberated leading to the dissolution of the cellulose sheets [365]. In the dissolved state, cellulose interacts with the NMMO via hydrogen bonds superimposed by ionic interactions (Fig. 3.46) [366, 367]. NMMO has gained enormous attention for cellulose regeneration regarding a fiber spinning process, the Lyocell process that is industrially realized.

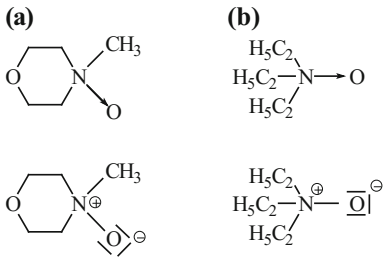


**Fig. 3.45** Structures of typical single component solvents of cellulose: **a** *N*-methylmorpholine-*N*-oxide and **b** triethylamine-*N*-oxide

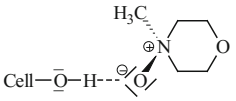

**Fig. 3.46** Interaction of cellulose (Cell) with NMMO

In the context of cellulose chemistry, it is worth mentioning that cellulose/NMMO solution could be diluted with organic solvents including DMSO and DMF down to a ratio of about 1:1 without precipitating the biopolymer [63, 368]. As a consequence, the viscosity could be decreased and a mixing during a chemical modification is improved.

A major drawback of NMMO is the instability of the solvent at high temperature, at water content less than the monohydrate, and in the presence of various compounds including heavy metal ions, polyelectrolytes, and charcoal [367, 369–371].

*N*-Methylmorpholine-*N*-oxide

Due to its high technical importance, it is appropriate to discuss this solvent in some more detail. The strength of interaction of NMMO and cellulose, hence, the outcome of solute–solvent interactions (little interaction; weak or strong swelling; dissolution) depends on the water content in the ternary system, amine oxide/water/biopolymer. The melting points and composition diagrams of both binary (NMMO + water) and ternary (NMMO + water + cellulose) systems have been studied (Fig. 3.47). At low water contents and higher temperatures, rapid dissolution of the fibers occurs without any pre-swelling. At a water content of 17–20% (w/w) in NMMO and a temperature of 60–70 °C, the fibers swell extensively but do not dissolve. At still higher water content no interaction was detected at any temperature [372].

More elaborated phase diagrams of the system NMMO/water/cellulose (DP = 96, 169, 228, and 536) have been constructed. The experiment was accomplished at 80 °C by employing a special procedure in order to ensure solution homogeneity at elevated viscosities. After thermal equilibration the solution was centrifuged in order to separate highly viscous cellulose-rich gel phase from cellulose-lean sol phase. The compositions of both phases (cellulose, NMMO, and water) were then determined. The results showed a continuous reduction of the two-phase area of the subsystem $H_2O$/cellulose upon the addition of NMMO;

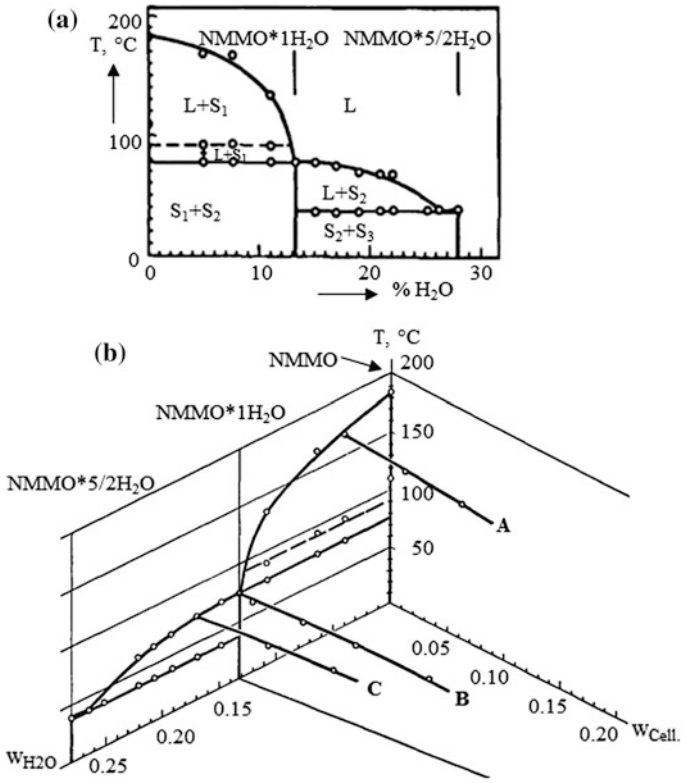


**Fig. 3.47** Melting point and composition diagram of the binary system NMMO + water, part **a**, where $S_1$, $S_2$, and $S_3$ refer to solid NMMO and two of its hydrates, respectively. The ternary system NMMO + water + cellulose is shown in part **b** (Reprinted from [372], copyright (©1982) with permission from Elsevier)

complete dissolution of the sample with DP = 169 was reached at 75% (w/w) NMMO. All experimental observations can be well modeled on the basis of composition-dependent binary interaction parameters [373].

One of the most interesting and relevant aspects from the application point of view is that swelling and dissolution of cellulose in NMMO depends on the origin of the fiber. For example, flax fibers undergo dissolution through "disintegration" into a series of spindle-like fragments, without swelling [374]. Cotton and wood cellulose fibers, on the other hand, show the so-called "ballooning" effect, which occurs at certain regions along the fiber giving the impression of having "balloons" growing [64]. This phenomenon has been explained as a result of much more swelling along the fiber transverse plan than its longitudinal counterpart [375]. Consequently, the radial expansion of cellulose in the secondary wall causes the primary wall to burst. As the expanding swollen cellulose pushes its way through these tears in the primary wall, the latter rolls back in the form of collars, rings or

spirals which restrict the uniform expansion of the fiber; under the microscope, the structures formed appear as balloons [376].

Microscopy has been employed in order to observe the formation of balloons and measure their dimensions (length and diameter). Five modes of behavior were described when cellulose samples get into contact with aqueous NMMO, these are [64]:

***Mode 1***: Is where there is fast dissolution by disintegration into rod-like fragments without noticeable swelling. This occurs when the solvent is efficient, i.e., interacts very strongly with cellulose, where the water content is low, namely, between 13 (NMMO monohydrate) and 17% (w/w). See part Fig. 3.48a and the schematic representation (b), suggested for the dissolution of *Valonia* cellulose. The fragmentation is essentially due to the attack of solvent on the amorphous regions. Dissolution occurs from the surface of the fragment.

***Modes 2 and 3***: These have a common feature, namely swelling by ballooning. Depending on the water content this swelling leads to complete dissolution [mode 2, water 19–24% (w/w)] or only to partial one [mode 3, water 25–30% (w/w)], see part (b) of Fig. 3.48.

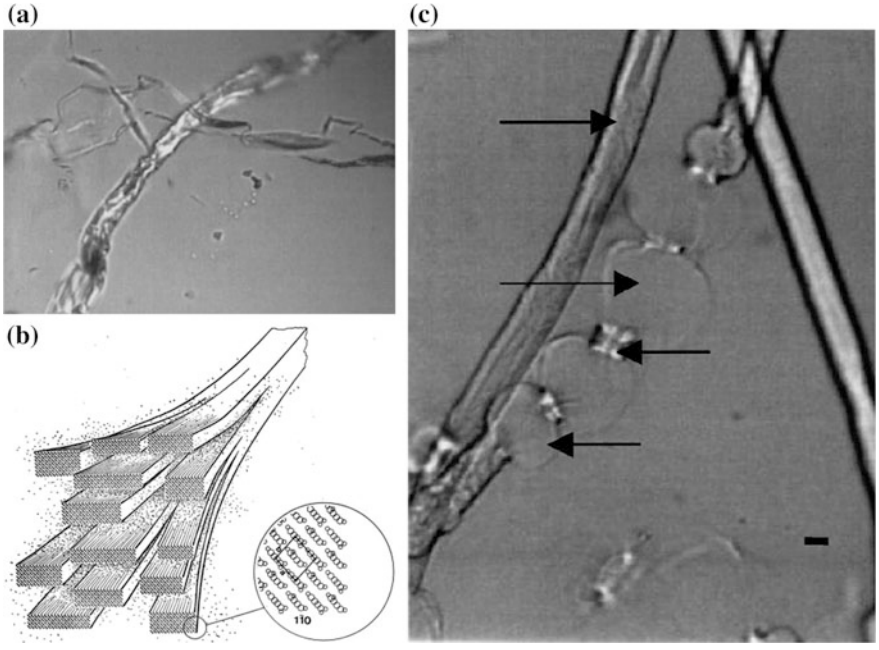


**Fig. 3.48** Effects of the water content of NMMO baths on the swelling and dissolution of cellulose for Borregaard cotton fibers (DP 942). Part **a** shows the disintegration into rod-like fragments without swelling in 17% (w/w) water in NMMO (part **a** and **c** reproduced from [64] with permission of John Wiley and Sons). The same process is represented schematically in (**b**) for the dissolution of *Valonia* cellulose (reproduced from [377], ©2008, Canadian Science Publishing or its licensors, reproduced with permission). Part **c** swelling by 23.5% (w/w) water in NMMO

***Mode 4***: At still higher water content, the fiber only swells homogenously without dissolution of any part of the fiber.

***Mode 5***: When more water is added, there is no detectable fiber–solvent interaction as evidenced by absence of either swelling or dissolution. This is akin to contact of cellulose with a non-solvent. Interestingly, NMMO was found to act as an inhibitor for the dissolution of cotton cellulose in NaOH solutions [378].

The swelling/dissolution mechanisms are not restricted to cellulose. Several biopolymer derivatives (cellulose nitrate, cyanoethyl cellulose, and xanthate fibers) in aqueous NMMO and in imidazole-based ionic liquids showed the same modes observed for cotton and wood fibers. The observed swelling by ballooning shows that this phenomenon is linked to fiber morphology, which is retained after undergoing derivatization [379].

### 3.2.2 *Derivatizing Solvents*

Cellulose may dissolve by the formation of covalent bonds. Examples of these "derivatizing solvents" are (solvent, cellulose derivative formed): $N_2O_4$/DMF, nitrite; HCOOH/$H_2SO_4$, formate; $F_3CCOOH$, trifluoroacetate; $Cl_2CHCOOH$, dichloroacetate; paraformaldehyde/DMSO, hydroxymethyl; and $ClSi(CH_3)_3$, trimethylsilyl ether. There are several reasons for the interest in this type of dissolution, e.g., cellulose with different physicochemical properties and shapes can be regenerated from these solutions [380–383]. The dissolved biopolymer ("first generation" derivative) can be further derivatized into several important end products ("second generation" derivatives) [384, 385], e.g., carboxylic acid esters [386, 387].

The relatively strong dichloroacetic acid may be employed as a solvent for cellulose. Thus, a mixture of this acid and the corresponding anhydride reacts slowly with cellulose to generate dichloroacetate esters with DS from 1.6 to 1.9, in which position 6 is almost completely functionalized. These products are soluble in DMF, DMSO, pyridine, and THF, and are thermally stable up to 280 °C, but become insoluble at temperatures >150 °C [388].

The introduction of the solubilizing substituent occurs in many cases by a preferred reaction at position 6 of the AGU. Under certain conditions (in particular water-free organic media), the substituent introduced during the dissolution may act as a protecting group during a subsequent reaction. Therefore, an inverse pattern of functionalization is achieved after the workup procedure, which yields a removal of the solubilizing substituent in aqueous solution. An example is the formation of cellulose nitrite and its conversion into other derivatives. Soluble trimethylsilyl cellulose may be modified by acylation leading to a product with an inverse pattern of functionalization (after desilylation) on one hand. On the other hand, the silyloxy moiety may act as activation group being the more reactive function compared to the remaining OH moieties. Thus, the novel substituent is introduced only at positions, where the silyloxy groups were located [389].

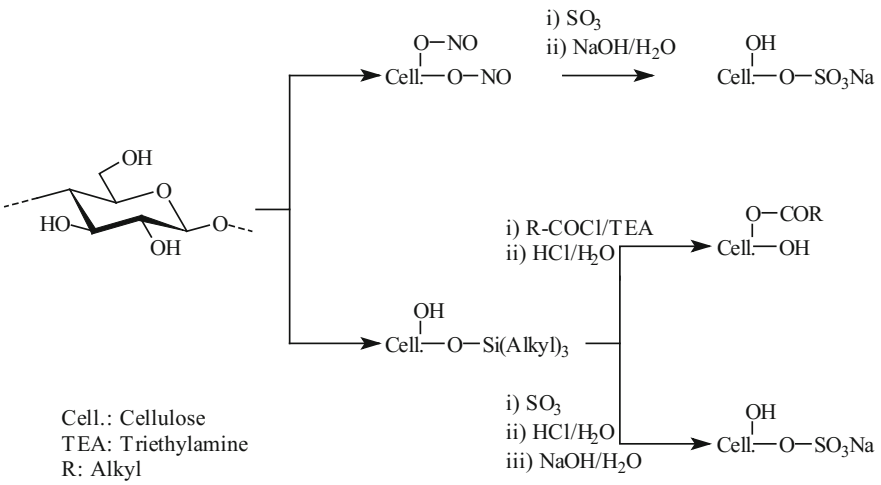


**Fig. 3.49** Examples of regioselectively substituted cellulose derivatives obtained in derivatizing solvents

Examples of employed derivatizing solvents for a selective derivatization of cellulose are shown in Fig. 3.49. More information on cellulose nitrite is found in Chap. 4 on cellulose derivatization.

Methylol cellulose

Paraformaldehyde/DMSO dissolves cellulose rapidly with negligible degradation forming hydroxymethyl (methylol) moieties mainly at position 6 as found by $^{13}C$ NMR studies [390–394]. Therefore, cellulose derivatives at the secondary carbon atoms are easily obtained after (ready) hydrolysis of the methylol residue. Additionally, fresh formaldehyde may be added to the methylol group, resulting in longer methylene oxide chains. The latter can be functionalized at the terminal OH group, akin to nonionic, ethylene oxide-based surfactants [395, 396]. The methylol derivative can also be further derivatized, e.g., into esters [397–399].

Cellulose formate

Cellulose formate is obtained by the dissolution of the biopolymer in formic acid only, or, more efficiently in the presence of a mineral acid as catalyst, e.g., sulfuric or phosphoric acid. The uncatalyzed reaction rate is very slow, taking hours to days to be completed, depending on the DP and $I_c$ of the starting cellulose. The rate can be enhanced in the presence of phosphoric acid or sulfuric acid (from 18 to 3 d for birch cellulose at 25 °C). The cellulose formate dissolved possesses a DS of 2.5. Faster reactions and even higher DS were obtained in the presence of a mixture of $H_3PO_4/H_2SO_4$, although this condition led to biopolymer degradation.

Applying of $SOCl_2$ in DMF produces the Vilsmeier–Haack adduct ($HC(Cl)=N^+(CH_3)_2Cl^-$). In the presence of a base, cellulose reacts with this adduct to form

the unstable intermediate (Cell–O–CH=$N^+(CH_3)_2Cl^-$) from which cellulose formate is obtained by hydrolysis [400]. Products with DS from 1.2 to 2.5 have been obtained. Based on $^{13}C$ NMR spectral data, the order of reactivity is position 6 > position 2 > position 3. The formyl group can be slowly removed by heating with water at 100 °C, and incompletely by dry heating [386]. Cellulose formate can be converted into other derivatives, e.g., cellulose sulfate by the reaction with $SO_3$/DMF [387, 392, 393, 401, 402].

Cellulose trifluoroacetate

Treatment of cellulose with trifluoroacetic acid alone or in the presence of the corresponding anhydride leads to dissolution of the biopolymer with the formation of cellulose trifluoroacetates [403]. The reaction can be carried out in organic solvents, e.g., chlorinated solvents [404]. The rates of cellulose dissolutions in TFA plus $H_2SO_4$, and TFAA have been studied by turbidimetry, optical microscopy, and high-frequency conductimetry. The kinetics is influenced by the electron-acceptor power of the solvent mixture. Maximum cellulose dissolution was observed in the presence of $H_2SO_4$ [405].

Cellulose trifluoroacetates are thermally stable up to 250 °C, easily hydrolyzable with water (few minutes), and the primary OH groups are almost completely derivatized [387, 406, 407]. Provided that extensive polymer degradation does not take place during dissolution, cellulose trifluoroacetates serve as attractive starting material for derivatization at the secondary OH groups. Additionally, they form mesophases at a relatively low polymer concentration (4% (w/w)), and hence may be employed for regeneration of strong cellulose fibers [404, 408]. TFA can be employed as a reaction medium, e.g., for the esterification of the cellulose trifluoroacetates (acetate to decanoate) and/or mixed esters of cellulose, of high DS, by the reaction with carboxylic acid anhydrides [406].

Viscose

From a commercial point of view, the viscose process, i.e., dissolution of the biopolymer as cellulose xanthate in $CS_2$/NaOH is widely applied and still most important technical process to produce cellulose fibers and other shapes. The viscose process is practiced today with an output of about 3–4 million tons annually worldwide [162].

The first patent on the viscose process was granted to Cross and Bevan in 1893 [409]. In 1904 scientists at the Donnersmarck's plant in Germany developed a spinning bath containing a mixture of sulfuric acid and a salt, known as Mueller spin bath [410]. Although the process has undergone many refinements over the past 100 years, the basic chemistry is still the same. A combination of $CS_2$ and aqueous NaOH is used to prepare an alkali-soluble anionic cellulose xanthate (xanthogenate, Fig. 3.50), which is subsequently decomposed in an acidic bath leading to regenerated cellulose.

The pulp is steeped in an aqueous solution of sodium hydroxide, which causes swelling and formation of alkali cellulose. The swollen mass is pressed to adjust the

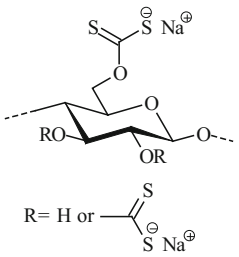


**Fig. 3.50** Cellulose xanthate, the intermediate formed during the viscose process

ratio of alkali to cellulose. The alkali cellulose is aged under controlled time and temperature to adjust the DP of the cellulose (DP 270–350) prior the reaction with $CS_2$ is carried out. A so-called ripening appears, i.e., transesterification yields to an even distribution of the ester moieties along the polymer chain, the cellulose xanthate formed is dissolved by diluting the aqueous NaOH. Finally, the filaments are formed, i.e., the viscose solution is extruded through the very small holes of a spinneret (Fig. 3.51) into a spin bath consisting basically of $H_2SO_4$, $Na_2SO_4$, and $H_2O$ (Fig. 3.52).

Viscose can also be applied to convert the polymer into sponges and chest-like forms after previous addition of $NaHCO_3$ [411]. Viscose sponges are used to a large extent for cleaning, for cosmetic purposes or in printing machines. Additionally, it was shown that they are suitable for tissue engineering [412].

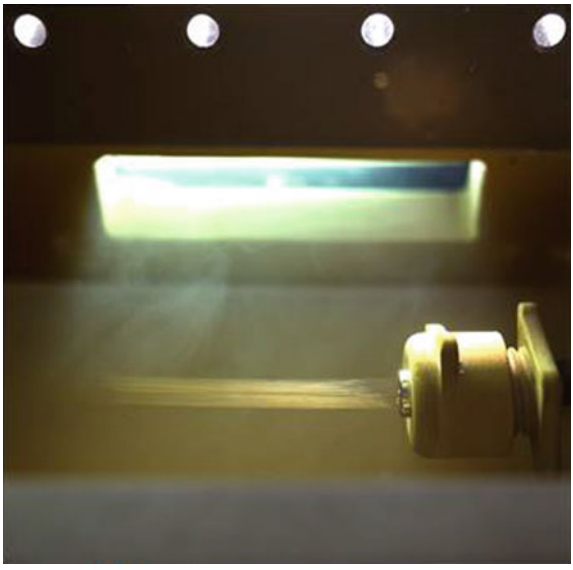

**Fig. 3.51** Viscose fibers extruded through a spinneret with 120 holes of a pilot plant (Courtesy of the Thuringian Institute for Textiles and Plastics Research, TITK, Rudolstadt, Germany)

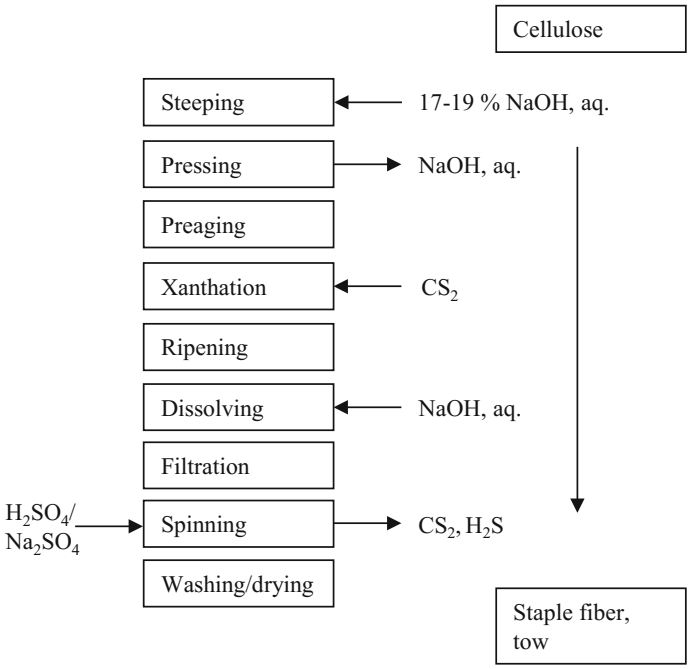


**Fig. 3.52** Schematic representation of the viscose process

## References

1. Philipp B (1983) Role of supermolecular structure and morphology in heterogeneous reactions of cellulose. Acta Chim Hung 112:445–459
2. Shimizu Y, Kimura K, Masuda S, Hayashi J (1993) Supermolecular structure of cellulose suggested from the behavior of chemical reactions. In: Kennedy JF, Phillips GO, Williams PA (eds) Cellulosics: Chemical, Biochemical and Material Aspects. Ellis Horwood, Chichester, pp 67–73
3. Yamazaki S, Nakao O (1974) Dissolution of cellulose in organic solvents in the presence of small amounts of amines and sulfur dioxide. Sen'i Gakkaishi 30:T234–T244
4. Kamide K, Okajima K, Matsui T, Kowsaka K (1984) Study on the solubility of cellulose in aqueous alkali solution by deuteration IR and carbon-13 NMR. Polym J 16:857–866
5. Klemm D, Philipp B, Heinze T, Heinze U, Wagenknecht W (1998) Comprehensive cellulose chemistry, vol 1. Wiley-VCH, Weinheim, p 130
6. Ishii D, Tatsumi D, Matsumoto T (2003) Effect of solvent exchange on the solid structure and dissolution behavior of cellulose. Biomacromol 4:1238–1243
7. Philipp HJ, Nelson ML, Ziifle HM (1947) Crystallinity of cellulose fibers as determined by acid hydrolysis. Text Res J 17:585–596
8. Ishii D, Tatsumi D, Matsumoto T (2008) Effect of solvent exchange on the supramolecular structure, the molecular mobility and the dissolution behavior of cellulose in LiCl/DMAc. Carbohydr Res 343:919–928
9. Sepall O, Mason SG (1961) Hydrogen exchange between cellulose and water. II. Interconversion of accessible and inaccessible regions. Can J Chem 39:1944–1955

10. Ogihara Y, Smith RL Jr, Inomata H, Arai K (2005) Direct observation of cellulose dissolution in subcritical and supercritical water over a wide range of water densities (550-1000 kg/m$^3$). Cellulose 12:595–606
11. Lowell S, Shields JE (1991) Powder surface area and porosity, 3rd edn. Chapman and Hall, London, p 52
12. Bismarck A, Aranberri-Askargorta I, Springer J, Lampke T, Wielage B, Stamboulis A, Shenderovich I, Limbach HH (2002) Surface characterization of flax, hemp and cellulose fibers; surface properties and the water uptake behavior. Polym Compos 23:872–894
13. Jeffries R (1960) The sorption of water by cellulose and eight other textile polymers. I. The sorption of water by celluloses below 100°. J Text Inst 51:T339–T374
14. Jeffries R (1960) Sorption of water by cellulose and eight other textile polymers. III. Sorption of water vapor by textile polymers at 120 and 150°. J Text Inst 51:T441–T457
15. Park S, Venditti RA, Jameel H, Pawlak JJ (2006) Hard to remove water in cellulose fibers characterized by high resolution thermogravimetric analysis—methods development. Cellulose 13:23–30
16. Merchant MV (1957) A study of water-swollen cellulose fibers which have been liquid-exchanged and dried from hydrocarbons. Tappi 40:771–781
17. Porter BR, Rollins ML (1972) Changes in porosity of treated lint cotton fibers. I. Purification and swelling treatments. J Appl Polym Sci 16:217–236
18. Arthur JC Jr (1966) Photooxidation of chemically modified celluloses and free radical formation. In: Phillips GO (ed) Energy transfer in radiation processes. Elsevier, Amesterdam, pp 29–36
19. Mihranyan A, Llagostera AP, Karmhag R, Stromme M, Ek R (2004) Moisture sorption by cellulose powders of varying crystallinity. Int J Pharm 269:433–442
20. Tanczos I, Borsa J, Sajó I, László K, Juhász ZA, Tóth T (2000) Effect of tetramethylammonium hydroxide on cotton cellulose compared to sodium hydroxide. Macromol Chem Phys 201:2550–2556
21. Strømme M, Mihranyan A, Ek R, Niklasson GA (2003) Fractal dimension of cellulose powders analyzed by multilayer BET adsorption of water and nitrogen. J Phys Chem B 107:14378–14382
22. Kocherbitov V, Ulvenlund S, Kober M, Jarring K, Arnebrant T (2008) Hydration of microcrystalline cellulose and milled cellulose studied by sorption calorimetry. J Phys Chem B 112:3728–3734
23. Adolphs J, Setzer JM (1998) Description of gas adsorption isotherms on porous and dispersed systems with the excess surface work model. J Colloid Interface Sci 207:349–354
24. Belgacem MN, Blayo A, Gandini A (1996) Surface characterization of polysaccharides, lignins, printing ink pigments, and ink fillers by inverse gas chromatography. J Colloid Interface Sci 182:431–436
25. Inglesby MK, Zeronian SH (1996) The accessibility of cellulose as determined by dye adsorption. Cellulose 3:165–181
26. Inglesby MK, Zeronian SH (2002) Direct dyes as molecular sensors to characterize cellulose substrates. Cellulose 9:19–29
27. Fidale LC, Ruiz N, Heinze T, El Seoud OA (2008) Cellulose swelling by aprotic and protic solvents: what are the similarities and differences? Macromol Chem Phys 209:1240–1254
28. Baird MS, Hamlin JD, O'Sullivan A, Whiting A (2008) An insight into the mechanism of the cellulose dyeing process: molecular modelling and simulations of cellulose and its interactions with water, urea, aromatic azo-dyes and aryl ammonium compounds. Dyes Pigm 76:406–416
29. Hanley SJ, Giasson J, Revol J-F, Gray DG (1992) Atomic force microscopy of cellulose microfibrils: comparison with transmission electron microscopy. Polymer 33:4639–4642
30. Zollinger H (1960) Dyeing mechanisms and molecular shape. Am Dyest Rep 49:29–36

31. Rowland SP (1979) Solid-liquid interactions: inter- and intracrystalline reactions in cellulose fibers. In: Happey F (ed) Applied Fibre Science, vol 2. Academic Press, London, pp 205–237
32. Stone JE, Treiber E, Abrahamson B (1969) Accessibility of regenerated cellulose to solute molecules of a molecular weight of 180 to 2 × 106. Tappi 52:108–110
33. Scallan AM, Carles JE (1972) Correlation of the water retention value with the fiber saturation point. Sven Papperstidn 75:699–703
34. Stone JE, Scallan AM, Donefer E, Ahlgren E (1969) Digestibility as a simple function of a molecule of similar size to a cellulase enzyme. Adv Chem Ser 95:219–241
35. Nyqvist H (1983) Saturated salt solutions for maintaining specified relative humidities. Int J Pharm Technol Prod Manuf 4:47–48
36. ASTM E104—02 (2012) Standard practice for maintaining constant relative humidity by means of aqueous solutions
37. Rahman MS, Matin N, Majid MA, Sheikh MAS (1997) Swelling characteristics of jute fiber with water and different organic and inorganic vapors and liquids. Cellul Chem Technol 31:87–92
38. Arlabosse P, Rodier E, Ferrasse JH, Chavez S, Lecomte D (2003) Comparison between static and dynamic methods for sorption isotherm measurements. Drying Technol 21:479–497
39. Kohler R, Alex R, Brielmann R, Ausperger B (2006) A new kinetic model for water sorption isotherms of cellulosic materials. Macromol Symp 244:89–96
40. El Seoud OA, Fidale LC, Ruiz N, D'Almeida MLO, Frollini E (2008) Cellulose swelling by protic solvents: which properties of the biopolymer and the solvent matter? Cellulose 15:371–392
41. Krässig HA (1993) Cellulose: structure, accessibility and reactivity. Gordon and Breach, Yverdon, p 167
42. O'Sullivan AC (1997) Cellulose: the structure slowly unravels. Cellulose 4:173–207
43. Heux L, Dinand E, Vignon MR (1999) Structural aspects in ultrathin cellulose microfibrils followed by 13C CP-MAS NMR. Carbohydr Polym 40:115–124
44. Newman RH (1999) Estimation of the lateral dimensions of cellulose crystallites using carbon-13 NMR signal strengths. Solid State Nucl Magn Reson 15:21–29
45. Zografi G, Kontny MJ, Yang AYS, Brenner GS (1984) Surface area and water vapor sorption of microcrystalline cellulose. Int J Pharm 18:99–116
46. Sepall O, Mason SG (1961) Hydrogen exchange between cellulose and water. I. Measurement of accessibility. Can J Chem 39:1934–1943
47. Jeffries R (1964) The amorphous fraction of cellulose and its relation to moisture sorption. J Appl Polym Sci 8:1213–1220
48. Nishiyama Y, Isogai A, Okano T, Müller M, Chanzy H (1999) Intracrystalline deuteration of native cellulose. Macromolecules 32:2078–2081
49. Tsuchikawa S, Siesler HW (2003) Near-infrared spectroscopic monitoring of the diffusion process of deuterium-labeled molecules in wood. Part I: Softwood. Appl Spectrosc 57:667–674
50. Wickholm K, Hult E-L, Larsson PT, Iversen T, Lennholm H (2001) Quantification of cellulose forms in complex cellulose materials: a chemometric model. Cellulose 8:139–148
51. Mann J, Marrinan HJ (1956) Reaction between cellulose and heavy water. I. Qualitative study by infrared spectroscopy. Trans Faraday Soc 52:481–487
52. Schwertassek K (1931) Method for determining the degree of mercerization of cotton. Melliand Textilber 12:457–458
53. Bailey AV, Honold E, Skau EL (1958) Topochemical mechanisms involved in the preparation and deacetylation of partially acetylated cottons. Text Res J 28:861–873
54. Hessler LE, Power RE (1954) The use of iodine adsorption as a measure of cellulose fiber crystallinity. Text Res J 24:822–827
55. Nelson ML, MaresT (1965) Accessibility and lateral order distribution of the cellulose in the developing cotton fiber1. Text Res J 35:592–603

56. Bréguet A, Chareyron C (1952) Adsorption of iodine from its solutions by viscose rayon. Relation between orientation and crystalline state of the fibers. Meml Serv Chim Etat 37:249–263
57. Tanzawa H (1960) Iodine sorption on cellulose fibers. Sen-I Gakkaishi 16:373–380
58. Doppert HL (1967) Adsorption of iodine from aqueous solutions by samples of tire yarn from regenerated cellulose. J Polym Sci Polym Phys Ed 5:263–270
59. Nelson ML, Rousselle MA, Cangemi SJ, Trouard P (1970) Iodine sorption test. Factors affecting reproducibility and a semimicro adaptation. Text Res J 40:872–880
60. Jeffries R, Jones DM, Roberts JG, Selby K, Simmens SC, Warwicker JO (1969) Current ideas on the structure of cotton. Cellul Chem Technol 3:255–274
61. Röder T, Moosbauer J, Fasching M, Bohn A, Fink H-P, Baldinger T, Sixta H (2006) Crystallinity determination of native cellulose-comparison of analytical methods. Lenzinger Ber 86:85–89
62. Schwabe K, Phillip B (1955) Interaction of cellulose with tetraethylammonium hydroxide. Holzforschung 9:104–109
63. Berger W, Keck M, Kabrelian V, Mun Song U, Phillip B, Zenke I (1989) Solution of cellulose in aprotic mixed solvents. 2. Effect of the physical structure of the cellulose on the dissolution process. Acta Polym 40:351–358
64. Cuissinat C, Navard P (2006) Swelling and dissolution of cellulose part 1: free floating cotton and wood fibers in N-methylmorpholine-N-oxide-water mixtures. Macromol Symp 244:1–18
65. Jayme G, Rothamel L (1948) Development of a standard centrifugal method for determining the swelling values of pulps. Papier (Bingen, Germany) 2:7–18
66. Schleicher H, Philipp B (1980) Effect of activation on the reactivity of cellulose. Papier (Bingen, Germany) 34:550–555
67. McCormick CL, Callais PA, Hutchinson BH (1985) Solution studies of cellulose in lithium chloride and N,N-dimethylacetamide. Macromolecules 18:2394–2401
68. McCormick CL, Callais PA (1986) Derivatization of cellulose in lithium chloride and N, N-dimethylacetamide solutions. Polym Prepr 27:91–92
69. McCormick CL, Callais PA (1987) Derivatization of cellulose in lithium chloride and N, N-dimethylacetamide solutions. Polymer 28:2317–2323
70. Suzuki K, Kurata S, Ikeda I (1992) Homogeneous acetalization of cellulose in lithium chloride and dimethylacetamide. Polym Int 29:1–6
71. Edgar KJ, Arnold KM, Blount WW, Lawniczak JE, Lowman DW (1995) Synthesis and properties of cellulose acetoacetates. Macromolecules 28:4122–4128
72. Staudinger H, Döhle W (1942) Macromolecular compounds. CCCX. Cellulose. 85. Inclusion cellulose. J Prakt Chem (Leipzig, Germany) 161:219–240
73. Staudinger H, Döhle W (1953) The acetylation of inclusion celluloses. Makromol Chem 9:188–189
74. Staudinger H, Eicher T (1953) Macromolecular compounds. CCCLXXXVI. The swelling and inclusion of cellulose with lower fatty acids. Makromol Chem 10:254–260
75. Buschle-Diller G, Zeronian SH (1992) Enhancing the reactivity and strength of cotton fibers. J Appl Polym Sci 45:967–979
76. ASTM-D3616—95 (2009) Standard test method for rubber-Determination of gel, swelling index, and dilute solution viscosity
77. Mantanis GI, Young RA, Rowell RM (1995) Swelling of compressed cellulose fiber webs in organic liquids. Cellulose 2:1–22
78. Eckelt J, Richardt D, Schuster KC, Wolf BA (2010) Thermodynamic interactions of natural and of man-made cellulose fibers with water. Cellulose 17:1079–1093
79. Philipp B, Schleicher H, Wagenknecht W (1973) The influence of cellulose structure on the swelling of cellulose in organic liquids. J Polym Sci Part C Polym Symp 42:1531–1543
80. Thode EF, Guide RG (1959) A thermodynamic interpretation of the swelling of cellulose in organic liquids: the relations among solubility parameter, swelling, and internal surface. Tappi 42:35–39

81. Ramos LA, Assaf JM, El Seoud OA, Frollini E (2005) Influence of the supra-molecular structure and physico-chemical properties of cellulose on its dissolution in the lithium chloride/N,N-dimethylacetamide solvent system. Biomacromol 6:2638–2647
82. Isogai A, Atalla RH (1998) Dissolution of cellulose in aqueous NaOH solutions. Cellulose 5:309–319
83. Schult T, Hjerde T, Optun OI, Kleppe PJ, Moe S (2002) Characterization of cellulose by SEC-MALLS. Cellulose 9:149–158
84. El Seoud OA, Heinze T (2005) Organic esters of cellulose: new perspectives for old polymers. Adv Polym Sci 186:103–149
85. Koblitz W, Kiessig H (1960) Role of water sorption in the swelling of cellulose fibers. Papier (Bingen, Germany) 14:179–185
86. Stone JE, Scallan AM (1968) Structural model for the cell wall of water-swollen wood pulp fibers based on their accessibility to macromolecules. Cellul Chem Technol 2:343–358
87. Yachi T, Hayashi J, Shimizu Y (1983) Supermolecular structure of cellulose: stepwise decrease in LODP and particle size of cellulose hydrolyzed after chemical treatment. J Appl Polym Sci: Appl Polym Symp 37:325–343
88. Langan P, Nishiyama Y, Chanzy H (2001) X-ray structure of mercerized cellulose II at 1 Å resolution. Biomacromol 2:410–416
89. Davis WE, Barry AJ, Peterson FC, King AJ (1943) X-ray studies of reactions of cellulose in nonaqueous systems. II. Interaction of cellulose and primary amines. J Am Chem Soc 65:1294–1299
90. Creely JJ, Wade RH (1978) Complexes of cellulose with sterically hindered amines. J Polym Sci Polym Lett Ed 16:477–480
91. Barton AFM (1991) Handbook of solubility parameters and other cohesion parameters. CRC Press, Boca Raton
92. Hansen CM, Bjoerkman A (1998) The ultrastructure of wood from a solubility parameter point of view. Holzforschung 52:335–344
93. Hansen CM (2004) 50 Years with solubility parameters-past and future. Prog Org Coat 51:77–84
94. Robertson AA (1970) Interactions of liquids with cellulose. Tappi 53:1331–1339
95. Chitumbo K, Brown W, De Ruvo A (1974) Swelling of cellulosic gels. J Polym Sci Polym Symp 47:261–268
96. Schleicher H (1983) Relation of cellulose swelling to the donor and acceptor numbers of the swelling agent. Acta Polym 34:63–64
97. Mantanis GI, Young RA, Rowell RM (1994) Swelling of wood. Part 1. Swelling in water. Wood Sci Technol 28:119–134
98. Mantanis GI, Young RA, Rowell RM (1994) Swelling of wood. Part II. Swelling in organic liquids. Holzforschung 48:480–490
99. Gutmann V (1978) The donor-acceptor approach to molecular interaction. Plenum Press, New York
100. Hill T, Lewicki P (2006) A comprehensive reference for science, industry and data mining: statics methods and applications. Tulsa, StatSoft
101. Reichardt C (2003) Solvents and solvent effects in organic chemistry, 3rd edn. Wiley-VCH, Weinheim
102. El Seoud OA (2007) Solvation in pure and mixed solvents: some recent developments. Pure Appl Chem 79:1135–1151
103. Martins CT, Lima MS, El Seoud OA (2006) Thermo-solvatochromism of merocyanine polarity indicators in pure and aqueous solvents: relevance of solvent lipophilicity. J Org Chem 71:9068–9079
104. Medronho B, Romano A, Miguel MG, Stigsson L, Lindman B (2012) Rationalizing cellulose (in)solubility: reviewing basic physicochemical aspects and role of hydrophobic interactions. Cellulose 19:581–587
105. Drost-Hansen W (1969) Structure of water near solid interfaces. Ind Eng Chem 61:10–47

106. Hartley ID, Kamke FA, Peemoeller H (1992) Cluster theory for water sorption in wood. Wood Sci Technol 26:83–99
107. Baird MS, O'Sullivan AC, Banks WB (1998) A native cellulose microfibril model. Cellulose 5:89–111
108. Despond S, Espuche E, Cartier N, Domard A (2005) Hydration mechanism of polysaccharides: a comparative study. J Polym Sci Part B: Polym Phys 43:48–58
109. Humeres E, Mascayano C, Riadi G, Gonzalez-Nilo F (2006) Molecular dynamics simulation of the aqueous solvation shell of cellulose and xanthate ester derivatives. J Phys Org Chem 19:896–901
110. Ono H, Yamada H, Matsuda S, Okajima K, Kawamoto T, Iijima H (1998) Proton-NMR relaxation of water molecules in the aqueous microcrystalline cellulose suspension systems and their viscosity. Cellulose 5:231–247
111. Smirnova LG, Grunin YB, Krasil'nikova SV, Zaverkina MA, Bakieva DR, Smirnov EV (2003) Study of the structure and sorption properties of some types of cellulose. Colloid J 65:778–781
112. Klemm D, Philipp B, Heinze T, Heinze U, Wagenknecht W (1998) Comprehensive cellulose chemistry. Wiley-VCH, Weinheim, p 44
113. Borin IA, Skaf MS (1999) Molecular association between water and dimethyl sulfoxide in solution: a molecular dynamics simulation study. J Chem Phys 110:6412–6420
114. Mizuno K, Imafuji S, Ochi T, Ohta T, Maeda S (2000) Hydration of the CH groups in dimethyl sulfoxide probed by NMR and IR. J Phys Chem B 104:11001–11005
115. Shin DN, Wijnen JW, Engberts JBFN, Wakisaka A (2001) On the origin of microheterogeneity: a mass spectrometric study of dimethyl sulfoxide-water binary mixture. J Phys Chem B 105:6759–6762
116. Rao VSR, Foster JF (1965) Addition complex between carbohydrates and dimethyl sulfoxide as revealed by proton magnetic resonance. J Phys Chem 69:656–658
117. Casu B, Reggiani M, Gallo GG, Vigevani A (1966) Hydrogen bonding and conformation of D-glucose and polyglucoses in dimethyl sulfoxide solution. Tetrahedron 22:3061–3081
118. Basedow AM, Ebert KH, Feigenbutz W (1980) Polymer-solvent interactions: dextrans in water and DMSO. Makromol Chem 181:1071–1080
119. Fernandez-Bertran J, Reguera E, Ortiz P (2001) Spectroscopic study of the interactions of alkali fluorides with D-xylose. Spectrochim Acta, Part A 57A:2607–2615
120. Ko H, Shim G, Kim Y (2005) Evidences that β-lactose forms hydrogen bonds in DMSO. Bull Korean Chem Soc 26:2001–2006
121. Ardizzone S, Dioguardi FS, Mussini PR, Mussini T, Rondinini S, Vercelli B, Vertova A (1999) Batch effects, water content, and aqueous/organic solvent reactivity of microcrystalline cellulose samples. Int J Biol Macromol 26:269–277
122. Gardner KH, Blackwell J (1974) Structure of native cellulose. Biopolymers 13:1975–2001
123. Kolpak FJ, Blackwell J (1976) Determination of the structure of cellulose II. Macromolecules 9:273–278
124. Northolt MG, De Vries H (1985) Tensile deformation of regenerated and native cellulose fibers. Angew Makromol Chem 133:183–203
125. Northolt MG, Hout RVD (1985) Elastic extension of an oriented crystalline fiber. Polymer 26:310–316
126. Kroon-Batenburg LMJ, Kroon J, Northolt MG (1986) Chain modulus and intramolecular hydrogen bonding in native and regenerated cellulose fibers. Polym Commun 27:290–292
127. Kasbekar GS, Neale SM (1947) Swelling of cellulose in aqueous solutions of certain acids and salts with measurements of the vapor pressures, densities, and viscosities of these solutions Trans Faraday Soc 43:517–528
128. Warwicker JO, Clayton JW (1969) Reactivity of cotton after treatment in alkaline and acid swelling agents. J Appl Polym Sci 13:1037–1048
129. Bucher H (1957) Reactions during pulp parchmentization. Papier 11:125–133
130. Warwicker JO (1969) Swelling of cotton in alkalis and acids. J Appl Polym Sci 13:41–54
131. Champetier G (1933) Addition compounds of cellulose. Ann Chim Appl 20:5–96

132. Warwicker JO (1967) Effect of chemical reagents on the fine structure of cellulose. IV. Action of caustic soda on the fine structure of cotton and ramie J Polym Sci Part A-1 Polym Chem 5:2579–2593
133. Chedin J, Marsaudon A (1954) Progress in the understanding of liquid reaction mediums, and interpretation of their reactions with cellulosic fibers: mercerization-nitration. Chim Ind (Paris) 71:55–68
134. Knecht E, Lipschitz A (1914) Action of strong nitric acid on cotton cellulose. J Soc Chem Ind (London) 33:116–122
135. Ellefsen Ø, Gjönnes J, Norman N (1959) Changes in the crystalline structure of cellulose caused by treatment of cotton and wood pulps with concentrated hydrochloric acid. Nor Skogind 13:411–421
136. Bartunek R (1953) The reactions, swelling and solution of cellulose in solutions of electrolytes. Papier (Bingen) 7:153–158
137. Danielowski G (1977) Ammonia in yarn processing. Lenzinger Ber 42:90–96
138. Troope WS (1980) Improved ammonia finishing of corduroys. Text Res J 50:162–165
139. Heap SA (1978) Liquid ammonia treatment of cotton fabrics, especially as a pretreatment for easy-care finishing. Text Inst Ind 16:387–390
140. Cheek L, Struszczyk H (1980) Effect of anhydrous liquid ammonia and sodium hydroxide on viscose fabric. Cellul Chem Technol 14:893–904
141. Hess K, Gundermann J (1937) The influence of liquid ammonia on cellulose fibers (formation of ammonia-cellulose I, ammonia-cellulose II and cellulose III). Ber Dtsch Chem Gesellschaft B 70B:1788–1799
142. Vigo TL (1994) Textile processing and properties. Elsevier, Amsterdam, p 43
143. Calamari TA Jr, Schreiber SP, Cooper AS Jr, Reeves WA (1971) Liquid ammonia modification of cellulose in cotton and polyester/cotton textiles. Text Chem Color 3:234–238
144. Rousselle MA, Nelson ML (1976) Reactivity and fine structure of cotton mercerized in sodium hydroxide or liquid ammonia. Text Res J 46:648–653
145. Koura A, Schleicher H, Philipp B (1973) Swelling and dissolution of cellulose in amine-containing solvent mixtures. 6. Structural changes of cellulose caused by amines and amine solutions. Faserforsch Textiltech 24:187–194
146. Koura A, Lukanoff B, Philipp B, Schleicher H (1977) Preparation of alkali-soluble cyanoethyl cellulose from preactivated cellulose. Faserforsch Textiltech 28:63–65
147. Klenkova NI, Matveeva NA, Volkova L (1967) Effect of amines on structure and properties of cellulose fibers. IV. Effect of amines on hydrated cellulose fibers. J Appl Chem (USSR) 40:121–123
148. Klenkova NI, Matveeva NA, Kulakova OM, Volkova LA (1967) Additional data on the activation of cellulose by amines. J Appl Chem (USSR) 40:2113–2120
149. Zeronian SH (1985) In: Nevell TP, Zeronian SH (eds) Cellulose chemistry and its applications. Ellis Howard, Chichester, p 171
150. Warwicker JO, Wright AC (1976) Function of sheets of cellulose chains in swelling reactions on cellulose. J Appl Polym Sci 11:659–671
151. Creely JJ, Segal L, Loeb L (1959) X-ray study of new cellulose complexes with diamines containing three, five, six, seven, and eight carbon atoms. J Polym Sci 36:205–214
152. Warwicker JO, Jeffries R, Colbran RL, Robinson RN (1966) A review of the literature on the effect of caustic soda and other swelling agents on the fine structure of cotton. Shirley Institute Pamphlet No. 93, Shirley Institute, Didsbury, Manchester
153. Haydel CH, Seal JF, Janssen HJ, Vix HLE (1958) Decrystallization of cotton cellulose. Ind Eng Chem 50:74–75
154. Loeb L, Segal L (1955) The treatment of cotton cellulose with aqueous solutions of ethylamine. Text Res J 25:516–519
155. Nevell TP, Zeronian SH (1962) Action of ethylamine on cellulose. I. Acetylation of ethylamine-treated cotton. Polymer 3:187–194

156. Segal L, Creely JJ (1961) The ethylenediamine-cellulose complex. III. Factors in the formation of the complex. J Polym Sci 50:451–465
157. Hennige E (1963) The structural change in cotton caused by treatment with diamines and caustic soda. Melliand Textilber 44:1350–1352
158. Pasteka M (1984) Dissolution of cellulose materials in aqueous solutions of benzyltriethylammonium hydroxide. Cellul Chem Technol 18:379–387
159. Lieser T, Leckzych E (1936) Constitution of cellulose xanthates IV. Justus Liebigs Ann Chem 522:56–65
160. Lieser T, Ebert R (1937) Carbohydrates. VIII. Cellulose and its solutions. Justus Liebigs Ann Chem 528:276–295
161. Strepikheev AA, Knunyants IL, Nikolaeva NS, Mogilevskii EM (1957) Solution of cellulose in quaternary ammonium bases. Izv Akad Nauk SSSR Ser Khim 750–753
162. Fink HP, Weigel P, Purz HJ, Ganster J (2001) Structure formation of regenerated cellulose materials from Nmmo solutions. Prog Polym Sci 26:1473–1524
163. Chavan RB, Patra AK (2004) Development and processing of lyocell. Indian J Fibre Text Res 29:483–492
164. Berger W (1994) Possibilities and limits of alternative methods for cellulose dissolution and regeneration. Lenzinger Ber 74:11–18
165. Eibl M, Eichinger D, Lotz C (1997) Lyocell—the cellulosic fiber chameleon. Lenzinger Ber 76:89–91
166. Taylor J (1998) Tencel—a unique cellulosic fiber. J Soc Dyers Colour 114:191–193
167. Woodings CR (1995) The development of advanced cellulosic fibres. Int J Biol Macromol 17:305–309
168. Chanzy H, Paillet M, Peguy A (1986) Spinning of exploded wood from amine oxide solutions. Polym Commun 27:171–172
169. Chanzy H, Paillet M, Peguy A, Vuong R (1987) Dissolution and spinning of exploded wood in amine oxide systems. In: Kennedy JF, Phillips GO, Williams PA (eds) Wood Cellul 573–579
170. Heinze T, Liebert T, Klüfers P, Meister F (1999) Carboxymethylation of cellulose in unconventional media. Cellulose 6:153–165
171. Gao M, Chen S, Han J, Luo D, Zhao L, Zheng Q (2010) Effects of a pretreatment with N-methylmorpholine-N-oxide on the structures and properties of ramie. J Appl Polym Sci 117:2241–2250
172. Faelt S, Wagberg L, Vesterlind E-L, Larsson PT (2004) Model films of cellulose II—improved preparation method and characterization of the cellulose film. Cellulose 11:151–162
173. Le Moigne N, Bikard J, Navard P (2010) Rotation and contraction of native and regenerated cellulose fibers upon swelling and dissolution: the role of morphological and stress unbalances. Cellulose 17:507–519
174. Lu Y, Wu Y (2008) Influence of coagulation bath on morphology of cellulose membranes prepared by NMMO method. Front Chem Eng China 2:204–208
175. Mao Z, Cao Y, Jie X, Kang G, Zhou M, Yuan Q (2010) Dehydration of isopropanol–water mixtures using a novel cellulose membrane prepared from cellulose/N-methylmorpholine-N-oxide/$H_2O$ solution. Sep Purif Technol 72:28–33
176. Jeihanipour A, Karimi K, Taherzadeh MJ (2010) Enhancement of ethanol and biogas production from high-crystalline cellulose by different modes of NMO pretreatment. Biotechnol Bioeng 105:469–476
177. Mercer J (1851) Improvement in chemical process for fulling vegetable and other textures. US 8303 A, 19 Aug 1851
178. Gardner WM (1898) Properties of mercerized cotton. J Soc Dyers Colour 14:186–190
179. Bechter D (1981) Mercerization of cotton. Dtsch Faerber-Kal 85:82–100
180. Iyer ND (2000) Cotton—the king of fibres -V. Colourage 47:75–76
181. Saravanan D, Ramachandran T (2007) Forgotten fundamentals of mercerisation. Asian Dyer 4:35–40

182. Warwicker JO (1971) Cellulose swelling. In Bikales NM, Segal L (ed) Cellulose and cellulose derivatives, Part IV. Wiley-Interscience, New York, pp 344–349
183. Tripp VW, Moore AT, Rollins ML (1954) A microscopical study of the effects of some typical chemical environments on the primary wall of the cotton fiber. Text Res J 24:956–970
184. Rollins ML (1954) Some aspects of microscopy in cellulose research. Anal Chem 26:718–724
185. Chanzy HD, Roche EJ (1976) Fibrous transformations of Valonia cellulose I into cellulose II. Appl Polym Symp 28:701–711
186. Dinand E, Vignon M, Chanzy H, Heux L (2002) Mercerization of primary wall cellulose and its implication for the conversion of cellulose I → cellulose II. Cellulose 9:7–18
187. Roelofsen PA (1959) The plant cell wall. Gebrüder Bornträger, Berlin-Nikolassee, p 126
188. Saito G (1939) Das Verhalten der Zellulose in Alkalilösungen. 1. Mitteilung. Kolloid-Beih 49:365–454
189. Colom X, Carrillo F (2002) Crystallinity changes in lyocell and viscose-type fibres by caustic treatment. Eur Polym J 38:2225–2230
190. Nishimura H, Sarko A (1987) Mercerization of cellulose. IV. Mechanism of mercerization and crystallite sizes. J Appl Polym Sci 33:867–874
191. Irklei VM, Kleiner YY, Vavrinyuk OS, Gal'braikh LS (2005) Kinetics of degradation of cellulose in basic medium. Fibre Chem 37:452–458
192. Shibazaki H, Kuga S, Okano T (1997) Mercerization and acid hydrolysis of bacterial cellulose. Cellulose 4:75–87
193. Yokota H, Sei T, Horii F, Kitamaru R (1990) Carbon-13 CPMAS NMR study on alkali cellulose. J Appl Polym Sci 41:783–791
194. Dolmetsch H (1970) Regular physical changes of the fibrillar-structure in spun fibers of cellulose and synthetic polymers. Melliand Textilber 51:182–190
195. Brown RM Jr, Haigler CH, Suttie J, White AR, Roberts E, Smith C, Itoh T, Cooper K (1983) The biosynthesis and degradation of cellulose. J Appl Polym Sci: Appl Polym Symp 37:33–78
196. Haigler CH (1985) The functions and biogenesis of native cellulose. In Nevell TP, Zeronian SH (eds) Cellulose chemistry and its applications. Ellis Horwood, Chichester, UK, pp 30–83
197. Nishiyama Y, Kuga S, Okano T (2000) Mechanism of mercerization revealed by X-ray diffraction. J Wood Sci 46:452–457
198. Heuser E, Bartunek R (1925) Alkali cellulose II. Cellul-Chem 6:19–26
199. Zeronian SH, Cabradilla KE (1972) Action of alkali metal hydroxides on cotton. J Appl Polym Sci 16:113–128
200. Voronova MI, Petrova SN, Lebedeva TN, Ivanova ON, Prusov AN, Zakharov AG (2004) Changes in the structure of flax cellulose induced by solutions of lithium, sodium, and potassium hydroxides. Fibre Chem 36:408–412
201. Cotton FA, Wilkenson G, Murillo CA, Bochmann M (1999) Advanced inorganic chemistry, 6th edn. Wiley, New York, p 92
202. Mansikkamaeki P, Lahtinen M, Rissanen K (2007) The conversion from cellulose I to cellulose II in NaOH mercerization performed in alcohol-water systems: an X-ray powder diffraction study. Carbohydr Polym 68:35–43
203. Moharram MA, Mahmoud OM (2007) X-ray diffraction methods in the study of the effect of microwave heating on the transformation of cellulose I into cellulose II during mercerization. J Appl Polym Sci 105:2978–2983
204. Vieweg W (1924) The absorption of sodium hydroxide from solutions by cellulose. Angew Chem 37:1008–1010
205. Leighton A (1916) Adsorption of caustic soda by cellulose. J Phys Chem 20:32–50
206. Coward HF, Spencer L (1923) Efficacy of a centrifuge for removing surface liquids from cotton hairs. J Text Inst 14:28–32T

207. Marsh PB, Barker HD, Kerr T, Butler ML (1950) Wax content as related to surface area of cotton fibers. Text Res J 20:288–297
208. Neale SM (1929) Swelling of cellulose and its affinity relations with aqueous solutions. I. Experiments on the behavior of cotton cellulose and regenerated cellulose in sodium hydroxide solution, and their theoretical interpretation. J Text Inst 20:373–400T
209. Hess K, Trogus C, Schwarzkopf O (1932) Alkali cellulose. II. Phase-theory treatment of gel reactions. Z Phys Chem (Leipzig, Germany) A162:187–215
210. Fengel D (1994) FTIR spectroscopic studies on the heterogeneous transformation of cellulose I into cellulose II. Acta Polym 45:319–324
211. Gilbert RD, Kadla JF (1998) Polysacchrides—Cellulose In: Kaplan DL (ed) Biopolymers from renewable resources. Springer, Heidelberg, pp 47–95
212. Schenzel K, Fischer S (2001) NIR FT Raman spectroscopy—a rapid analytical tool for detecting the transformation of cellulose polymorphs. Cellulose 8:49–57
213. Jähn A, Schröder MW, Füting M, Schenzel K, Diepenbrock W (2002) Characterization of alkali treated flax fibres by means of FT Raman spectroscopy and environmental scanning electron microscopy. Spectrochim Acta, Part A 58A:2271–2279
214. Kunze J, Ebert A, Frigge K, Philipp B (1981) Sodium-23 NMR investigation of the sodium bond in the treatment of cotton with aqueous sodium hydroxide. Acta Polym 32:179–181
215. Kunze J, Schröter B, Scheler G, Philipp B (1983) High-resolution solid-state carbon-13 NMR studies of the formation of alkali cellulose from different treated celluloses. Acta Polym 34:248–254
216. Heinze T, Liebert T (2001) Unconventional methods in cellulose functionalization. Prog Polym Sci 26:1689–1762
217. Jayme G (1978) New publications about applicabilities of EWNN and cadoxene in cellulose chemistry. Papier (Bingen, Germany) 32:145–149
218. Hoenich NA, Woffidin C, Stamp S, Roberts SJ, Turnbull J (1997) Synthetically modified cellulose: an alternative to synthetic membranes for use in haemodialysis. Biomaterials 18:1299–1303
219. Burchard W, Habermann N, Kluefers P, Seger B, Wilhelm U (1994) Polyol-metal complexes. 7. Cellulose in Schweizer's reagent: a stable, polymeric metal complex with high chain rigidity. Angew Chem 106:936–939
220. Gadd KF (1982) A new solvent for cellulose. Polymer 23:1867–1869
221. Traube W (1912) Behavior of metallic hydroxides to alkylenediamino solutions. Ber Dtsch Chem Ges 44:3319–3324
222. Bain AD (1980) An NMR-study of the interactions between cadoxen and saccharides. Carbohydr Res 84:1–12
223. Nehls I, Wagenknecht W, Philipp B (1995) Carbon-13 NMR spectroscopic studies of cellulose in various solvent systems. Cellul Chem Technol 29:243–251
224. Burger J, Kettenbach G, Klüfers P (1995) Coordination equilibria in transition-metal based cellulose solvents. Macromol Symp 95:113–126
225. Ahlrichs R, Ballauff M, Eichkorn K, Hanemann O, Kettenbach G, Klufers P (1998) Polyol metal complexes. Part 30. Aqueous ethylenediamine dihydroxo palladium(II): A coordinating agent for low- and high-molecular weight carbohydrates. Chem Eur J 4:835–844
226. Saalwächter K, Burchard W, Klüfers P, Kettenbach G, Mayer P, Klemm D, Dugarmaa S (2000) Cellulose solutions in water containing metal complexes. Macromolecules 33:4094–4107
227. Kamide K, Yasuda K, Matsui T, Okajima K, Yamashiki T (1990) Structural change in alkali-soluble cellulose solid during its dissolution into aqueous alkaline solution. Cellul Chem Technol 24:23–31
228. Isogai A (1997) NMR analysis of cellulose dissolved in aqueous NaOH solutions. Cellulose 4:99–107
229. Egal M, Budtova T, Navard P (2007) Structure of aqueous solutions of microcrystalline cellulose/sodium hydroxide below 0 °C and the limit of cellulose dissolution. Biomacromol 8:2282–2287

230. Lang H, Laskowski I (1991) Pulp solubility in sodium hydroxide. Cellul Chem Technol 25:143–153
231. Cai J, Zhang L (2006) Unique gelation behavior of cellulose in NaOH/Urea aqueous solution. Biomacromol 7:183–189
232. Cai J, Zhang L (2005) Rapid dissolution of cellulose in LiOH/urea and NaOH/urea aqueous solutions. Macromol Biosci 5:539–548
233. Cai J, Zhang L, Liu S, Liu Y, Xu X, Chen X, Chu B, Guo X, Xu J, Cheng H (2008) Dynamic self-assembly induced rapid dissolution of cellulose at low temperatures. Macromolecules 41:9345–9351
234. Qi H, Chang C, Zhang L (2008) Effects of temperature and molecular weight on dissolution of cellulose in NaOH/urea aqueous solution. Cellulose 15:779–787
235. Cai J, Zhang L, Chang C, Cheng G, Chen X, Chu B (2007) Hydrogen-bond-induced inclusion complex in aqueous cellulose/LiOH/urea solution at low temperature. ChemPhysChem 8:1572–1579
236. Liu S, Zhang L (2009) Effects of polymer concentration and coagulation temperature on the properties of regenerated cellulose films prepared from LiOH/urea solution. Cellulose 16:189–198
237. Gavillon R, Budtova T (2008) Aerocellulose: new highly porous cellulose prepared from cellulose-NaOH aqueous solutions. Biomacromol 9:269–277
238. Cai J, Kimura S, Wada M, Kuga S, Zhang L (2008) Cellulose aerogels from aqueous alkali hydroxide-urea solution. Chemsuschem 1:149–154
239. Liebner F, Haimer E, Wendland M, Neouze MA, Schlufter K, Miethe P, Heinze T, Potthast A, Rosenau T (2010) Aerogels from unaltered bacterial cellulose: application of $scCO_2$ drying for the preparation of shaped, ultra-lightweight cellulosic aerogels. Macromol Biosci 10:349–352
240. Philipp B (1993) Organic solvents for cellulose as a biodegradable polymer and their applicability for cellulose spinning and derivatization. J Macromol Sci Pure Appl Chem A30:703–714
241. Wang Z, Yokoyama T, Chang H-M, Matsumoto Y (2009) Dissolution of beech and spruce milled woods in LiCl/DMSO. J Agric Food Chem 57:6167–6170
242. El Seoud OA, Nawaz H, Arêas EPG (2013) Chemistry and applications of polysaccharide solutions in strong electrolytes/dipolar aprotic solvents: an overview. Molecules 18:1270–1313
243. Striegel AM (1997) Theory and applications of DMAC/LICL in the analysis of polysaccharides. Carbohydr Polym 34:267–274
244. Strlic M, Kolar J (2003) Size exclusion chromatography of cellulose in LiCl/N, N-dimethylacetamide. J Biochem Biophys Methods 56:265–279
245. Zugenmaier P (2004) Characterization and physical properties of cellulose acetates. Macromol Symp 208:81–166
246. Callais PA (1986) Derivatzation and characterization of cellulose in lithium chloride and N, N-dimethylacetamide solutions. Ph.D. thesis, University of Southern Mississippi, University Microfilms, DA8626439, CAN 106:121612
247. Klemm D, Phillip B, Heinze T, Heinze U, Wagenknecht W (1998) Comprehensive cellulose chemistry, vol 1. Wiley-VCH, Weinheim
248. Krässig H, Schurz J, Steadman RG, Schliefer K, Albrecht W, Mohring M, Schlosser H (2008) Cellulose. Ullmann's fibers, 1. Wiley-VCH, Weinheim, pp 335–389
249. Ibrahim AA, Nada AMA, Hagemann U, El Seoud OA (1996) Preparation of dissolving pulp from sugar cane bagasse, and its acetylation under homogeneous solution condition. Holzforschung 50:221–225
250. Dupont A-L (2003) Cellulose in lithium chloride/N,N-dimethylacetamide, optimization of a dissolution method using paper substrate and stability of the solutions. Polymer 44:4117–4126
251. Ekmanis JL (1987) Gel permeation chromatographic analysis of cellulose. Am Lab News 19:10–11

252. Tosh B, Saikia CN, Dass NN (2000) Homogeneous esterification of cellulose in the lithium chloride-N,N-dimethylacetamide solvent system: effect of temperature and catalyst. Carbohydr Res 327:345–352
253. Regiani AM, Frollini E, Marson GA, Arantes GM, El Seoud OA (1999) Some aspects of acylation of cellulose under homogeneous solution conditions. J Polym Sci Part A: Polym Chem 37:1357–1363
254. Rosenau T, Potthast A, Kosma P (2006) Trapping of reactive intermediates to study reaction mechanisms in cellulose chemistry. Adv Polym Sci 205:153–197
255. Falmagne JB, Escudero J, Taleb-Sahraoui S, Ghosez L (1981) Cyclobutanone and cyclobutenone derivatives by reaction of tertiary amides with alkenes and alkynes. Angew Chem 93:926–931
256. Marson GA (1999) Acylation of cellulose in homogeneous medium, M.Sc. thesis, University of São Paulo, Brazil
257. Marson GA, El Seoud OA (1999) A novel, efficient procedure for acylation of cellulose under homogeneous solution conditions. J Appl Polym Sci 74:1355–1360
258. El Seoud OA, Marson GA, Ciacco GT, Frollini E (2000) An efficient, one-pot acylation of cellulose under homogeneous reaction conditions. Macromol Chem Phys 201:882–889
259. Heinze T, Dicke R, Koschella A, Kull A-H, Klohr E-A, Koch W (2000) Effective preparation of cellulose derivatives in a new simple cellulose solvent. Macromol Chem Phys 201:627–631
260. Köhler S, Heinze T (2007) New solvents for cellulose: Dimethyl sulfoxide/ammonium fluorides. Macromol Biosci 7:307–314
261. Casarano R, Pires PAR, El Seoud OA (2014) Acylation of cellulose in a novel solvent system: solution of dibenzyldimethylammonium fluoride in DMSO. Carbohydr Polym 101:444–450
262. Elsemongy MM, Reicha FM (1986) Absolute electrode potentials in dimethyl sulfoxide-water mixtures and transfer free energies of individual ions. Thermochim Acta 108:115–131
263. Kelly CP, Cramer CJ, Truhlar DG (2007) Single-ion solvation free energies and the normal hydrogen electrode potential in methanol, acetonitrile, and dimethyl sulfoxide. J Phys Chem B 111:408–422
264. El-Kafrawy A (1982) Investigation of the cellulose/lithium chloride/dimethylacetamide and cellulose/lithium chloride/N-methyl-2-pyrrolidinone solutions by 13C NMR spectroscopy. J Appl Polym Sci 27:2435–2443
265. Pinkert A, Marsh KN, Pang S (2010) Reflections on the solubility of cellulose. Ind Eng Chem Res 49:11121–11130
266. Turbak AS (1984) Recent developments in cellulose solvent systems. Tappi J 67:94–96
267. Gagnaire D, Saint-Germain J, Vincendon M (1983) NMR evidence of hydrogen bonds in cellulose solutions. J Appl Polym Sci: Appl Polym Symp 37:261–275
268. Vincendon M (1985) Proton NMR study of the chitin dissolution mechanism. Makromol Chem 186:1787–1795
269. Petrus L, Gray DG, BeMiller JN (1995) Homogeneous alkylation of cellulose in lithium chloride/dimethyl sulfoxide solvent with dimsyl sodium activation. A proposal for the mechanism of cellulose dissolution in lithium chloride/DMSO. Carbohydr Res 268:319–323
270. Fersht AR (1971) Acyl-transfer reactions of amides and esters with alcohols and thiols. Reference system for the serine and cysteine proteinases. Nitrogen protonation of amides and amide-imidate equilibriums. J Am Chem Soc 93:3504–3515
271. Kresge AJ, Fitzgerald PH, Chiang Y (1974) Position of protonation and mechanism of hydrolysis of simple amides. J Am Chem Soc 96:4698–4699
272. Cary FA, Sundberg RJ (1990) Advanced organic chemistry, 3rd edn. Part A, Plenum Press, New York, p 257
273. Morgenstern B, Kammer H-W (1996) Solvation in cellulose-LiCl-DMAc solutions. Trends Polym Sci 4:87–92
274. El Seoud OA (2009) Understanding solvation. Pure Appl Chem 81:697–707

275. Spange S, Reuter A, Vilsmeier E, Heinze T, Keutel D, Linert W (1998) Determination of empirical polarity parameters of the cellulose solvent N,N-dimethylacetamide/LiCl by means of the solvatochromic technique. J Polym Scie Part A Polym Chem 36:1945–1955
276. Casarano R, Pires PAR, Borin AC, El Seoud OA (2014) Novel solvents for cellulose: use of dibenzyldimethylammonium fluoride/dimethyl sulfoxide (DMSO) as solvent for the etherification of the biopolymer and comparison with tetra(1-butyl)ammonium fluoride/DMSO. Ind Crops Prod 54:185–191
277. Morgenstern B, Kammer HW, Berger W, Skrabal P (1992) 7Li-NMR study on cellulose/LiCl/N,N-dimethylacetamide solutions. Acta Polym 43:356–357
278. Striegel AM, Timpa JD, Piotrowiak P, Cole RB (1997) Multiple neutral alkali halide attachments onto oligosaccharides in electrospray ionization mass spectrometry. Int J Mass Spectrom Ion Processes 162:45–53
279. Östlund A, Lundberg D, Nordstierna L, Holmberg K, Nydén M (2009) Dissolution and gelation in TBAF/DMSO solutions: the roles of fluoride ions and water. Biomacromol 10:2401–2407
280. Papanyan Z, Roth C, Wittler K, Reimann S, Ludwig R (2013) The dissolution of polyols in salt solutions and ionic liquids at molecular level: ions, counter ions, and Hofmeister effects. ChemPhysChem 14:3667–3671
281. Marson GA, El Seoud OA (1999) Cellulose dissolution in lithium chloride/N,N-dimethylacetamide solvent system: relevance of kinetics of decrystallization to cellulose derivatization under homogeneous solution conditions. J Polym Sci, Part A: Polym Chem 37:3738–3744
282. Wu J, Zhang J, Zhang H, He J, Ren Q, Guo M (2004) Homogeneous acetylation of cellulose in a new ionic liquid. Biomacromol 5:266–268
283. Silva AA, Laver ML (1997) Molecular weight characterization of wood pulp cellulose: dissolution and size exclusion chromatographic analysis. Tappi J 80:173–180
284. Matsumoto T, Tatsumi D, Tamai N, Takaki T (2001) Solution properties of celluloses from different biological origins in LiCl.DMAc. Cellulose 8:275–282
285. Buchard W (1993) Macromolecular association phenomena. A neglected field of research? Trends Polym Sci 1:192–198
286. Ramos LA, Morgado DL, El Seoud OA, da Silva VC, Frollini E (2011) Acetylation of cellulose in LiCl-N,N-dimethylacetamide: first report on the correlation between the reaction efficiency and the aggregation number of dissolved cellulose. Cellulose 18:385–392
287. Rinaudo M (1993) Polysaccharide characterization in relation with some original properties. J Appl Polym Sci: Appl Polym Symp 52:11–17
288. Sjöholm E, Gustafsson K, Pettersson B, Colmsjö A (1997) Characterization of the cellulosic residues from lithium chloride/N,N-dimethylacetamide dissolution of softwood kraft pulp. Carbohydr Polym 32:57–63
289. Ciacco GT, Morgado DL, Frollini E, Possidonio S, El Seoud OA (2010) Some aspects of acetylation of untreated and mercerized sisal cellulose. J Braz Chem Soc 21:71–77
290. Morgenstern B, Kammer H-W (1999) On the particulate structure of cellulose solutions. Polymer 40:1299–1304
291. Schulz L, Burchard W, Dönges R (1998) Evidence of supramolecular structures of cellulose derivatives in solution. In: Heinze T, Glasser WG (eds) Cellulose derivatives: modification, characterization, and nanostructures. ACS Symposium Series 688, Washington, DC, US, pp 218–238
292. Röder T, Morgenstern B, Glatter O (2000) Light-scattering studies on solutions of cellulose in N,N-dimethylacetamide/lithium chloride. Lenzinger Ber 79:97–101
293. Röder T, Morgenstern B, Schelosky N, Glatter O (2001) Solutions of cellulose in N,N-dimethylacetamide/lithium chloride studied by light scattering methods. Polymer 42:6765–6773
294. Striegel AM, Timpa JD (1995) Molecular characterization of polysaccharides dissolved in N,N-dimethylacetamide-lithium chloride by gel-permeation chromatography. Carbohydr Res 267:271–290

295. Hasegawa M, Isogai A, Onabe F (1993) Size-exclusion chromatography of cellulose and chitin using lithium chloride-N,N-dimethylacetamide as a mobile phase. J Chromatogr 635:334–337
296. Dupont A-L, Harrison G (2004) Conformation and dn/dc determination of cellulose in N, N-dimethylacetamide containing lithium chloride. Carbohydr Polym 58:233–243
297. Yanagisawa M, Shibata I, Isogai A (2004) SEC-MALLS analysis of cellulose using LiCl/1,3-dimethyl-2-imidazolidinone as an eluent. Cellulose 11:169–176
298. Fidale LC, Köhler S, Prechtl MHG, Heinze T, El Seoud OA (2006) Simple, expedient methods for the determination of water and electrolyte contents of cellulose solvent systems. Cellulose 13:581–592
299. Moran HE Jr (1956) System lithium chloride-water. J Phys Chem 60:1666–1667
300. Chrapava S, Touraud D, Rosenau T, Potthast A, Kunz W (2003) The investigation of the influence of water and temperature on the LiCl/DMAc/cellulose system. Phys Chem Chem Phys 5:1842–1847
301. Casarano R, El Seoud OA (2013) A novel route to obtaining stable quaternary ammonium fluoride solutions in DMSO: application in microwave-assisted acylation of cellulose. Lenzinger Ber 91:112–121
302. Berger W, Keck M, Philipp B (1988) On the mechanism of cellulose dissolution in non-aqueous solvents, especially in O-basic systems. Cellul Chem Technol 22:387–397
303. Yakimanskii AV, Bochek AM, Zubkov VA, Petropavloskie GA (1993) Quantum-chemical analysis of electronic structure parameters of dimethylacetamide and dimethylformamide complexes with lithium chloride additives. Russ J Appl Chem 66:2129–2132
304. Morgenstern B, Berger W (1993) Investigations about dissolution of cellulose in the lithium chloride/N,N-dimethylformamide system. Acta Polym 44:100–102
305. Kostag M, Liebert T, El Seoud OA, Heinze T (2013) Efficient cellulose solvent: quaternary ammonium chlorides. Macromol Rapid Commun 34:1580–1584
306. Kostag M, Liebert T, Heinze T (2014) Acetone based cellulose solvent. Macromol Rapid Commun. https://doi.org/10.1002/marc.201400211
307. Kuga S (1980) The porous structure of cellulose gel regenerated from calcium thiocyanate solution. J Colloid Interface Sci 77:413–417
308. Hattori M, Shimaya Y, Saito M (1998) Structural changes in wood pulp treated by 55 wt% aqueous calcium thiocyanate solution. Polym J 30:37–42
309. Hattori M, Koga T, Shimaya Y, Saito M (1998) Aqueous calcium thiocyanate solution as a cellulose solvent. Structure and interactions with cellulose. Polym J 30:43–48
310. Hattori M, Shimaya Y, Saito M (1998) Solubility and dissolved cellulose in aqueous calcium and sodium thiocyanate solution. Polym J 30:49–55
311. Fischer S, Voigt W, Fischer K (1999) The behaviour of cellulose in hydrated melts of the composition $LiX \cdot nH_2O$ ($X^- = I^-$, $NO_3^-$, $CH_3COO^-$, $ClO_4^-$). Cellulose 6:213–219
312. Fischer S, Leipner H, Brendler E, Voigt W, Fischer K (1999) Molten inorganic salt hydrates as cellulose solvents. In: El-Nokaly MA, Soini HA (eds) Polysaccharide applications, cosmetics and pharmaceuticals. ACS Symposium Series 737, Washington, DC, USA, p 143
313. Leipner H, Fischer S, Brendler E, Voigt W (2000) Structural changes of cellulose dissolved in molten salt hydrates. Macromol Chem Phys 201:2041–2049
314. Krossing I, Slattery JM, Daguenet C, Dyson PJ, Oleinikova A, Weingaertner H (2006) Why are ionic liquids liquid? A simple explanation based on lattice and solvation energies. J Am Chem Soc 128:13427–13434
315. Gericke M, Fardim P, Heinze T (2012) Ionic liquids-promising but challenging solvents for homogeneous derivatization of cellulose. Molecules 17:7458–7502
316. El Seoud OA, Koschella A, Fidale LC, Dorn S, Heinze T (2007) Applications of ionic liquids in carbohydrate chemistry: a window of opportunities. Biomacromol 8:2629–2647
317. Liebert T, Heinze T (2008) Interactions of ionic liquids with polysaccharides 5. Solvents and reaction media for the modification of cellulose. BioResources 3:576–601
318. Pinkert A, Marsh KN, Pang S, Staiger MP (2009) Ionic liquids and their interaction with cellulose. Chem Rev 109:6712–6728

319. Cao Y, Wu J, Zhang J, Li H, Zhang Y, He J (2009) Room temperature ionic liquids (RTILs): a new and versatile platform for cellulose processing and derivatization. Chem Eng J 147:13–21
320. Mäki-Arvela P, Anugwom I, Virtanen P, Sjöholm R, Mikkola JP (2010) Dissolution of lignocellulosic materials and its constituents using ionic liquids-a review. Ind Crops Prod 32:175–201
321. Cravotto G, Gaudino EC, Boffa L, Levêque J-M, Estager J, Bonrath W (2008) Preparation of second generation ionic liquids by efficient solvent-free alkylation of N-heterocycles with chloroalkanes. Molecules 13:149–156
322. Holbrey JD, Seddon KR (1999) The phase behaviour of 1-alkyl-3-methylimidazolium tetrafluoroborates; ionic liquids and ionic liquid crystals. J Chem Soc Dalton Trans 2133–2140
323. McEwen AB, Ngo EL, LeCompte K, Goldman JL (1999) Electrochemical properties of imidazolium salt electrolytes for electrochemical capacitor applications. J Electrochem Soc 146:1687–1695
324. Fuller J, Carlin RT, Osteryoung RA (1997) The room-temperature ionic liquid 1-ethyl-3-methylimidazolium tetrafluoroborate: electrochemical couples and physical properties. J Electrochem Soc 144:3881–3886
325. Noda A, Watanabe M (2000) Highly conductive polymer electrolytes prepared by in situ polymerization of vinyl monomers in room temperature molten salts. Electrochim Acta 45:1265–1270
326. Wilkes JS, Zaworotko MJ (1992) Air and water stable 1-ethyl-3-methylimidazolium based ionic liquids. J Chem Soc Chem Commun 965–967
327. Zhang H, Wu J, Zhang J, He J (2005) 1-Allyl-3-methylimidazolium chloride room temperature ionic liquid: a new and powerful nonderivatizing solvent for cellulose. Macromolecules 38:8272–8277
328. Fidale LC, Possidonio S, El Seoud OA (2009) Application of 1-allyl-3-(1-butyl)imidazolium chloride in the synthesis of cellulose esters: properties of the ionic liquid, and comparison with other solvents. Macromol Biosci 9:813–821
329. Seddon KR, Stark A, Torres M-J (2000) Influence of chloride, water, and organic solvents on the physical properties of ionic liquids. Pure Appl Chem 72:2275–2287
330. Poole CF (2004) Chromatographic and spectroscopic methods for the determination of solvent properties of room temperature ionic liquids. J Chromatogr A 1037:49–82
331. Nishida T, Tashiro Y, Yamamoto M (2003) Physical and electrochemical properties of 1-alkyl-3-methylimidazolium tetrafluoroborate for electrolyte. J Fluorine Chem 120:135–141
332. Aparicio S, Atilhan M, Karadas F (2010) Thermophysical properties of pure ionic liquids: review of present situation. Ind Eng Chem Res 49:9580–9595
333. Ngo HL, LeCompte K, Hargens L, McEwen AB (2000) Thermal properties of imidazolium ionic liquids. Thermochim Acta 357–358:97–102
334. Swatloski RP, Spear SK, Holbrey JD, Rogers RD (2002) Disolution of cellulose with ionic liquids. J Am Chem Soc 124:4974–4975
335. Trulove PC, Reichert WM, De Long HC, Kline SR, Rahatekar SS, Gilman JW, Muthukumar M (2009) The structure and dynamics of silk and cellulose dissolved in ionic liquids. ECS Trans 16:111–117
336. Kuzmina O, Sashina E, Troshenkowa S, Wawro D (2010) Dissolved state of cellulose in ionic liquids—the impact of water. Fibres Text East Eur 18:32–37
337. Zhang Y, Du H, Qian X, Chen EY-X (2010) Ionic liquid-water mixtures: enhanced Kw for efficient cellulosic biomass conversion. Energy Fuels 24:2410–2417
338. Sasaki K, Nagai H, Matsumura S, Toshima K (2003) A novel greener glycosidation using an acid-ionic liquid containing a protic acid. Tetrahedron Lett 44:5605–5608
339. Liebner F, Patel I, Ebner G, Becker E, Horix M, Potthast A, Rosenau T (2010) Thermal aging of 1-alkyl-3-methylimidazolium ionic liquids and its effect on dissolved cellulose. Holzforschung 64:161–166

340. Stark A, Behrend P, Braun O, Müller A, Ranke J, Ondruschka B, Jastorff B (2008) Purity specification methods for ionic liquids. Green Chem 10:1152–1161
341. Liu H, Sale KL, Holmes BM, Simmons BA, Singh S (2010) Understanding the interactions of cellulose with ionic liquids: a molecular dynamics study. J Phys Chem B 114:4293–4301
342. Zhang S, Sun N, He X, Lu X, Zhang X (2006) Physical properties of ionic liquids: database and evaluation. J Phys Chem Ref Data 35:1475–1517
343. Laus G, Bentivoglio G, Schottenberger H, Kahlenberg V, Kopacka H, Roeder T, Sixta H (2005) Ionic liquids: current developments, potential and drawbacks for industrial applications. Lenzinger Ber 84:71–85
344. Vitz J, Erdmenger T, Haensch C, Schubert US (2009) Extended dissolution studies of cellulose in imidazolium based ionic liquids. Green Chem 11:417–424
345. Nawaz H, Pires PAR, Bioni TA, Areas EPG, El Seoud OA (2014) Mixed solvents for cellulose derivatization under homogeneous conditions: kinetic, spectroscopic, and theoretical studies on the acetylation of the biopolymer in binary mixtures of an ionic liquid and molecular solvents. Cellulose 21:1193–1204
346. Heinze T, Schwikal K, Barthel S (2005) Ionic liquids as reaction medium in cellulose functionalization. Macromol Biosci 5:520–525
347. Moulthrop JS, Swatloski RP, Moyna G, Rogers RD (2005) High-resolution $^{13}C$ NMR studies of cellulose and cellulose oligomers in ionic liquid solutions. Chem Commun 1557–1559
348. Remsing RC, Swatloski RP, Rogers RD, Moyna G (2006) Mechanism of cellulose dissolution in the ionic liquid 1-n-butyl-3-methylimidazolium chloride: a $^{13}C$ and $^{35/37}Cl$ NMR relaxation study on model systems. Chem Commun 1271–1273
349. Anderson JL, Ding J, Welton T, Armstrong DW (2002) Characterizing ionic liquids on the basis of multiple solvation interactions. J Am Chem Soc 124:14247–14254
350. Reichardt C (2004) Pyridinium N-phenoxide betaine dyes and their application to the determination of solvent polarities. Part XXVIII. Pure Appl Chem 76:1903–1919
351. Oehlke A, Hofmann K, Spange S (2006) New aspects on polarity of 1-alkyl-3-methylimidazolium salts as measured by solvatochromic probes. New J Chem 30:533–536
352. Fortunato GG, Mancini PM, Bravo MV, Adam CG (2010) New solvents designed on the basis of the molecular-microscopic properties of binary mixtures of the type (protic molecular solvent + 1-butyl-3-methylimidazolium-based ionic liquid). J Phys Chem B 114:11804–11819
353. Hauru LKJ, Hummel M, King AWT, Kilpeläinen I, Sixta H (2012) Role of solvent parameters in the regeneration of cellulose from ionic liquid solutions. Biomacromol 13:2896–2905
354. Zakrzewska ME, Bogel-Lukasik E, Bogel-Lukasik R (2010) Solubility of carbohydrates in ionic liquids. Energy Fuels 24:737–745
355. Novoselov NP, Sashina ES, Kuz'mina OG, Troshenkova SV (2007) Ionic liquids and their use for the dissolution of natural polymers. Russ J Gen Chem 77:1395–1405
356. Heinze T, Dorn S, Schoebitz M, Liebert T, Koehler S, Meister F (2008) Interactions of ionic liquids with polysaccharides—2: cellulose. Macromol Symp 262:8–22
357. Hollóczki O, Gerhard D, Massone K, Szarvas L, Németh B, Veszprémi T, Nyulászi L (2010) Carbenes in ionic liquids. New J Chem 34:3004–3009
358. Fort DA, Remsing RC, Swatloski RP, Moyna P, Moyna G, Rogers RD (2007) Can ionic liquids dissolve wood? Processing and analysis of lignocellulosic materials with 1-n-butyl-3-methylimidazolium chloride. Green Chem 9:63–69
359. Han S, Li J, Zhu S, Chen R, Wu Y, Zhang X, Yu Z (2009) Potential applications of ionic liquids in wood related industries. BioResources 4:825–834
360. Chen Z, Liu S, Li Z, Zhang Q, Deng Y (2011) Dialkoxy functionalized quaternary ammonium ionic liquids as potential electrolytes and cellulose solvents. New J Chem 35:1596–1606

361. Kong F, Song J, Cheng B, Zheng Y (2014) Synthesis and characterization of cellulose/quaternary phosphonium salt. Adv Mater Res 842:138–141
362. Ratanakamnuan U, Atong D, Aht-Ong D (2007) Microwave assisted esterification of waste cotton fabrics for biodegradation films preparation. Adv Mater Res 26–28:457–460
363. Semsarilar M, Perrier S (2009) Solubilization and functionalization of cellulose assisted by microwave irradiation. Aust J Chem 62:223–226
364. Possidonio S, Fidale LC, El Seoud OA (2010) Microwave-assisted derivatization of cellulose in an ionic liquid: An efficient, expedient synthesis of simple and mixed carboxylic esters. J Polym Sci, Part A: Polym Chem 48:134–143
365. Michael M, Ibbett RN, Howarth OW (2000) Interaction of cellulose with amine oxide solvents. Cellulose 7:21–33
366. Maia ER, Perez S (1983) Organic solvents for cellulose. IV. Modeling of the interaction between N-methylmorpholine N-oxide (MMNO) molecules and a cellulose chain. Nov J Chim 7:89–100
367. Rosenau T, Potthast A, Sixta H, Kosma P (2001) The chemistry of side reactions and byproduct formation in the system NMMO/cellulose (Lyocell process). Prog Polym Sci 26:1763–1837
368. Kabrelian V, Berger W, Keck M, Philipp B (1988) Investigation of the dissolution of cellulose in binary aprotic systems. 1. Solubility and decrease in degree of polymerization of a textile pulp in binary systems with N-methylmorpholine N-oxide as one component. Acta Polym 39:710–714
369. Wendler F, Graneß G, Büttner R, Meister F, Heinze T (2006) A novel polymeric stabilizing system for modified Lyocell solutions. J Polym Sci, Part B: Polym Phys 44:1702–1713
370. Wendler F, Graneß G, Heinze T (2005) Characterization of autocatalytic reactions in modified cellulose/NMMO solutions by thermal analysis and UV/VIS spectroscopy. Cellulose 12:411–422
371. Wendler F, Meister F, Heinze T (2005) Thermostability of Lyocell dopes modified with surface-active additives. Macromol Mater Eng 290:826–832
372. Chanzy H (1982) Cellulose-amine oxide systems. Carbohydr Polym 2:229–231
373. Eckelt J, Eich T, Röder T, Rüf H, Sixta H, Wolf BA (2009) Phase diagram of the ternary system NMMO/water/cellulose. Cellulose 16:373–379
374. Chanzy H, Noe P, Paillet M, Smith P (1983) Swelling and dissolution of cellulose in amine oxide/water systems. J Appl Polym Sci: Appl Polym Symp 37:239–259
375. Bushnel F, Baley C, Grohens Y (2004) Composites materials reinforced by flax fibers correlation between adhesion of fiber/matrix and mechanicals properties of laminates according to chemicals treatments of fibers. Proc Am Soc Compos, 19th Technical Conference, MP1/1-MP1/12
376. Otto E, Spurlin HM, Grafflin MW (1954) 'Cellulose and cellulose derivatives (Part 1). Interscience, New York
377. Noé P, Chanzy H (2008) Swelling of *Valonia* cellulose microfibrils in amine oxide systems. Can J Chem 86:520–524
378. Cuissinat C, Navard P (2006) Swelling and dissolution of cellulose. Part II: free floating cotton and wood fibres in NaOH-water-additives systems. Macromol Symp 244:19–30
379. Cuissinat C, Navard P, Heinze T (2008) Swelling and dissolution of cellulose. Part V: cellulose derivatives fibres in aqueous systems and ionic liquids. Cellulose 15:75–80
380. Hammer RB, O'Shaughnessy ME, Strauch ER, Turbak AF (1979) Process and fiber spinning studies for the cellulose/paraformaldehyde/dimethyl sulfoxide system. J Appl Polym Sci 23:485–494
381. Kudlacek L, Kacetl L, Kasparova Z, Krejci F (1982) Production of fibers from cellulose solutions in the dimethyl sulfoxide-paraformaldehyde system. Khim Volokna 3:47–49
382. Yang ZL, Wu GM, Mei CF, Gao G, Lin S, Liu HM, Zou JH (1987) Study on the manufacture of rayon fiber from a paraformaldehyde/DMSO solvent system. Cellul Chem Technol 21:493–505

383. Kostag M, Koehler S, Liebert T, Heinze T (2010) Pure cellulose nanoparticles from trimethylsilyl cellulose. Macromol Symp 294:96–106
384. Koura A, Krause T (1985) Effect of weak cyanoethylation of initially wet cellulose on its reactivity after drying. Cellul Chem Technol 19:497–504
385. Volkert B, Wagenknecht W, Mai M (2010) Structure-property relationship of cellulose ethers: influence of the synthestic pathway on cyanoethylation. ACS Symp Ser 1033:319–341
386. Fujimoto T, Takahashi S, Tsuji M, Miyamoto T, Inagaki H (1986) Reaction of cellulose with formic acid and stability of cellulose formate. J Polym Sci, Part C: Polym Lett 24:495–501
387. Liebert T, Klemm D, Heinze T (1996) Synthesis and carboxymethylation of organo-soluble trifluoroacetates and formates of cellulose. J Macromol Sci, Pure Appl Chem A33:613–626
388. Liebert T, Klemm D (1998) A new soluble and hydrolytically cleavable intermediate in cellulose functionalization. Cellulose dichloroacetate (CDCA). Acta Polym 49:124–128
389. Klemm D, Heinze T, Philipp B, Wagenknecht W (1997) New approaches to advanced polymers by selective cellulose functionalization. Acta Polym 48:277–297
390. Aaltonen O, Alkio M (1983) Pulp solubility in DMSO/PF [DMSO/paraformaldehyde] solvent. Effect of pulp pH. Cellul Chem Technol 17:695–698
391. Schroeder LR, Gentile VM, Atalla RH (1986) Nondegradative preparation of amorphous cellulose. J Wood Chem Technol 6:1–14
392. Schnabelrauch M, Vogt S, Klemm D, Nehls I, Philipp B (1992) Readily hydrolyzable cellulose esters as intermediates for the regioselective derivatization of cellulose. 1-Synthesis and characterization of soluble, low-substituted cellulose formates. Angew Makromol Chem 198:155–164
393. Philipp B, Wagenknecht W, Nehls I, Ludwig J, Schnabelrauch M, Kim HR, Klemm D (1990) Comparison of cellulose formate and cellulose acetate under homogeneous reaction conditions. Cellul Chem Technol 24:667–678
394. Bosso C, Defaye J, Gadelle A, Wong CC, Pedersen C (1982) Homopolysaccharides interaction with the dimethyl sulphoxide-paraformaldehyde cellulose solvent system. Selective oxidation of amylose and cellulose at secondary alcohol groups. J Chem Soc Perkin Trans 1579–1585
395. Gagnaire D, Mancier D, Vincendon M (1980) Cellulose organic solutions: a nuclear magnetic resonance investigation. J Polym Sci Polym Chem Ed 18:13–25
396. Hiemenz PC, Rajagopalan R (1997) Principles of colloid and surface chemistry, 3rd edn. Marcel Dekker, New York, p 297, 355
397. Kinstle JF, Irving NM (1981) Selected chemical modifications, including grafting, on cellulosics. Org Coat Appl Polym Sci Proc 46:262–265
398. Morooka T, Norimoto M, Yamada T (1986) Cyanoethylated cellulose prepared by homogeneous reaction in paraformaldehyde-DMSO system. J Appl Polym Sci 32:3575–3587
399. Tosh B, Saikia CN (1999) Homogeneous esterification of fractionated cellulose in dimethyl sulfoxide/paraformaldehyde solvent system: characterization of esterified products. Trends Carbohydr Chem 4:55–67
400. Vigo TL, Daigle DJ (1972) Preparation of fibrous cellulose formate by the action of thionyl chloride in N,N-dimethylformamide. Carbohydr Res 21:369–377
401. Vigo TL, Daigle DJ, Welch CM (1972) Reaction of cellulose with chlorodimethylformiminium chloride and subsequent reaction with halide ions. J Polym Sci Polym Lett Ed 10:397–406
402. Wagenknecht W, Philipp B, Schleicher H (1979) The esterification and dissolution of cellulose with sulfur and phosphorous acid anhydrides and acid chlorides. Acta Polym 30:108–112
403. Liebert T, Schnabelrauch M, Klemm D, Erler U (1994) Readily hydrolyzable cellulose esters as intermediates for the regioselective derivatization of cellulose. Part II Soluble, highly substituted cellulose trifluoroacetates. Cellulose 1:249–258

404. Hawkinson DE, Kohout E, Fornes RE, Gilbert RD (1991) Some further observations on the systems cellulose/trifluoroacetic acid/dichloromethane and cellulose triacetate/trifluoroacetic acid/dichloromethane. J Polym Sci B Polym Phys 29:1599–1605
405. Cemeris M, Mus'ko NP, Cemeris N (1986) Mechanism of cellulose dissolution in trifluoroacetic acid. 2. Interaction of cellulose with trifluoroacetic acid. Koksnes Kim 29–33
406. Salin BN, Cemeris M, Mironov DP, Zatsepin AG (1991) Trifluoroacetic acid as solvent for the synthesis of cellulose esters. 1. Synthesis of triesters of cellulose and aliphatic carboxylic acids. Koksnes Kim 65–69
407. Salin BN, Chemeris MM, Malikova OL (1993) Trifluoroacetic acid as a solvent for the synthesis of cellulose esters. 3. Synthesis of mixed cellulose esters. Koksnes Kim 3–7
408. Hong YK, Hawkinson DE, Kohout E, Garrard A, Fornes RE, Gilbert RD (1989) Cellulose and cellulose triacetate mesophases. Ternary mixtures with polyesters in trifluoroacetic acid-methylene chloride solutions. ACS Symp Ser 384:184–203
409. Cross CF, Bevan EJ, Beadle C (1892) Improvements in the dissolution of cellulose. British Patent 8,700
410. Mueller M (1906) British Patent 10094
411. Askew GJ, Bahia HS, Foxall CW, Law SJ, Street H (1998) Cellulose sponges. WO 9828360 A1
412. Pajulo O, Viljanto J, Lönnberg B, Hurme T, Lonnqvist K, Saukko P (1996) Viscose cellulose sponge as an implantable matrix: changes in the structure increase the production of granulation tissue. J Biomed Mater Res 32:439–446

# Chapter 4
# Principles of Cellulose Derivatization

The reactions known in organic chemistry can, in principle, be applied to polymers carrying the same functional groups. However, there are characteristics that should be kept in mind:

- The limitation of the completeness of the reactions and of the purity of product, due to the formation of side products that cannot be easily removed because they are embedded in the polymer produced,
- The high relevance of inter- and intramolecular interactions in the course of polymer reactions,
- The number of phases during the course of the reaction. The reaction may occur in one phase, or the number of phases may change, e.g., from two- to a one-phase system.

The influence of the reaction phase on product structure and the efficiency of the reaction is a very important issue in cellulose chemistry. It is instructive to consider separately chemical reactions starting from the dissolved biopolymer and those involving solid cellulose in a swollen state. In the latter case, the supramolecular structure and the morphology can be decisive regarding the rate of the reaction and its yield. In many cases, however, the number of phases may change during the reaction, a phenomenon that is observed both in industrial processes and in reactions carried out in the laboratory. From the authors' point of view, it is important to distinguish between homogeneous and heterogeneous reactions that will be discussed below for various cellulose derivatives.

Cellulose can be converted into a myriad of derivatives involving different functionalities. Some of the commercially available ones are shown in Fig. 4.1. These include esters of inorganic acids (e.g., cellulose nitrates), of organic acids (e.g., acetates), and ionic and nonionic ethers (e.g., CMC, alkyl-, 2-hydroxyethyl- and 2-hydroxypropyl cellulose). They also include products with "mixed" functional groups pertaining to the same chemical class e.g., acetate/propionate and acetate/butyrate, or distinct classes, e.g., ether and ester like carboxymethyl cellulose acetate butyrate.



T. Heinze et al., *Cellulose Derivatives*, Springer Series on Polymer and Composite Materials, https://doi.org/10.1007/978-3-319-73168-1_4

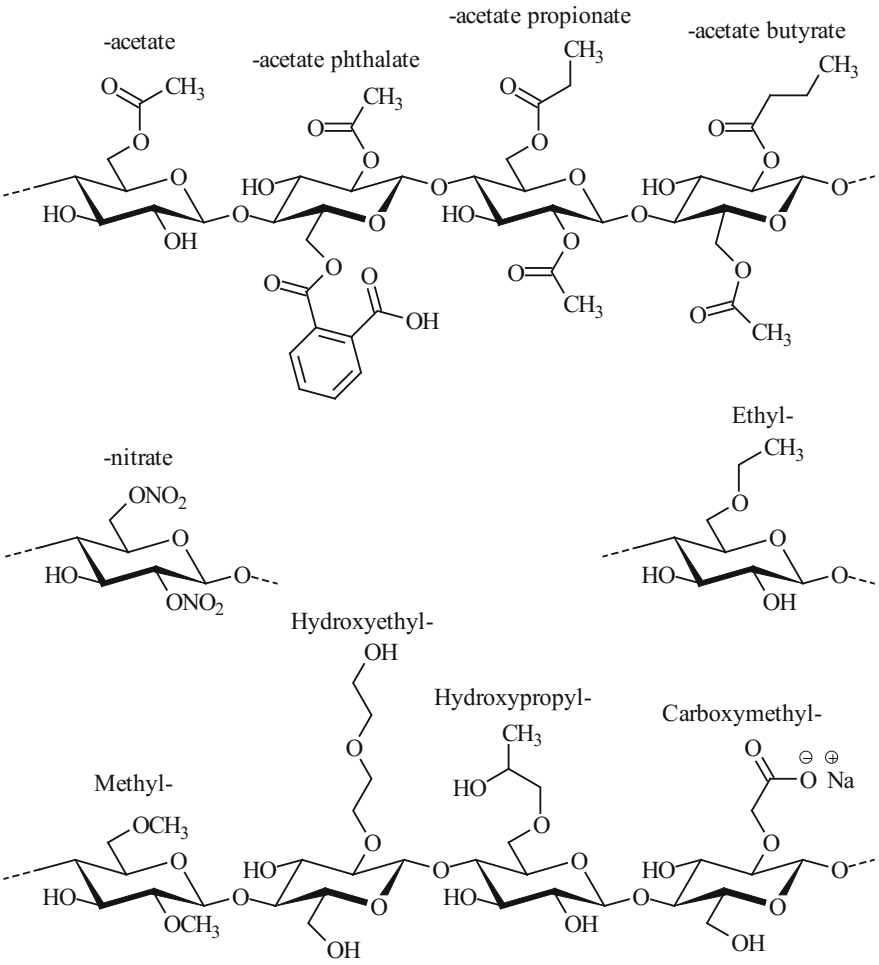


**Fig. 4.1** Schematic representation of some commercially available cellulose derivatives

There are many examples where the derivative obtained is not the end product. That is, the derivatizing group introduced is either substituted or removed (protecting group). Thus, the introduction of a good leaving group into the AGU, in particular, sulfonates (tosylate; brosylate; mesylate; triflate), followed by $S_N$ displacement reactions yield several soluble deoxycellulose derivatives with interesting properties/applications [1, 2]. In fact, cellulose tosylates are usually associated with some deoxy-chloro derivatives because of the $S_N$ displacement of the tosylate group by $Cl^-$ formed during the reaction of cellulose and TsCl/base, on one hand [3]. On the other hand, the (readily cleavable) thexyldimethylsilyl- and trityl group have been employed in product regioselectivity control, e.g., cellulose ethers and esters substituted highly or exclusively at one or two of the AGU positions [4, 5].

## 4.1 The Heterogeneous Versus the Homogeneous Reaction Path: Advantages and Limitations

The reaction of cellulose may occur in one phase or the phases may change during its derivatization. For example, the reaction of cellulose dissolved in DMAc/LiCl or $R_4NF \times H_2O$/DMSO, i.e., the cellulose is dissolved prior the reaction with carboxylic acid anhydrides or acyl chlorides together with tertiary amine starts and remains homogenously until the end of the reaction. The other extreme is the completely heterogeneous reaction, e.g., the process for manufacturing cellulose triacetate applying slurry medium. Cellulose may be treated with acetic anhydride and a catalyst (usually sulfuric acid) in the presence of a non-solvent for the starting cellulose, any intermediated state of derivatization and for the product, e.g., acetic acid and organic solvents like petroleum ether or toluene. The resultant triacetate flakes obtained are recovered in a fibrous state. CMC is also produced by the heterogeneous process. Suspension of the biopolymer is treated with a base in an aqueous alcohol, like 2-propanol, then react with sodium chloroacetate [6].

In many cases, however, the number of phases changes during the reaction. In another process of the industrial acetylation, cellulose is treated with a mixture of acetic acid, acetic anhydride, mineral acid catalyst, and an organic solvent that dissolves the product. As the reaction progresses, the cellulose/acetylating slurry turns homogeneous because the triacetate formed dissolves in the medium [7]. Likewise, the swollen, solid alkali cellulose is allowed to react with $CS_2$ heterogeneously forming alkali-soluble cellulose xanthate that is dissolved by the addition of additional lye [8]. Even cellulose solutions in solvents like electrolytes/dipolar aprotic solvents and in ILs are subjected to phase separation problems due to several reasons, as shown in Fig. 4.2 (see Figure legend for details) [9, 10].

As an operational definition, we will describe a reaction as homogeneous one if it stays in one phase from the start until the workup of the product. Homogeneous phase chemistry with cellulose means dissolution of the biopolymer prior to the chemical reaction in either non-derivatizing or derivatizing solvents. The latter approach includes cellulose dissolution due to its transformation into a derivative, as well as modification of this intermediate, *in situ*, or after isolation and re-dissolution in an organic solvent (DMSO, DMF). Conversely, the chemical modification of soluble but "stable" cellulose derivatives like cellulose acetate in DMSO, as well as the chemical modification of cellulose under dissolution of the cellulose derivative formed, as a result of the conversion, is not included in the context of cellulose homogeneous phase chemistry.

The reaction will be considered heterogeneous if there is no change in the number of phases present (at least two). Reactions where the number of phases changes during their course will be indicated, where appropriate.

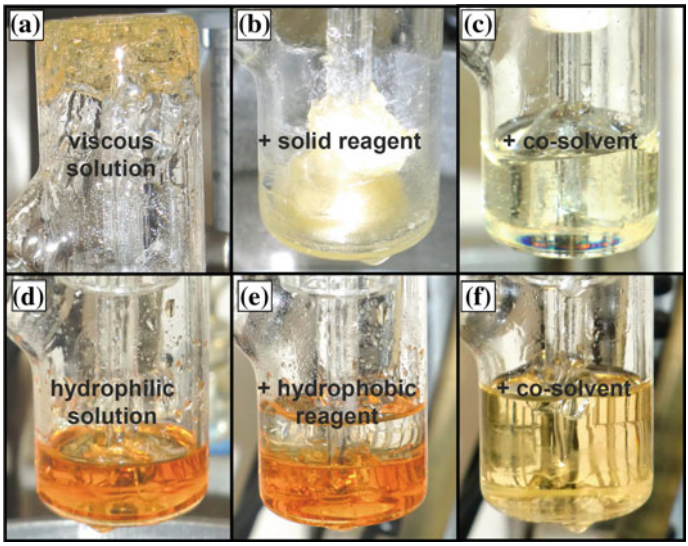


**Fig. 4.2** Examples of inhomogeneity and phase number changes in the reaction of cellulose dissolved in the IL BuMeImCl. Part **b** shows an attempt to mix solid $SO_3$/pyridine (used for biopolymer sulfation) with the viscous cellulose/IL solution shown in part (**a**; 10% (w/w) cellulose, 25 °C). The pasty mixture is difficult to handle. Parts **d** and **e** show that the hydrophilic solution of cellulose in EtMeImAc (**d)** is immiscible with the hydrophobic silylating reagent, hexamethydisilazane (**e**). Parts **c** and **f** show that these problems can be solved by addition of the molecular co-solvents DMF and $CH_2Cl_2$, respectively. Reprinted from [11] with permission from Springer

## 4.2 Esterification of Cellulose—General Comments

The industrially established production of cellulose esters and mixed esters is carried by heterogeneous processes exclusively, or those where the ester formed dissolves in the medium during the course of the reaction. As a consequence of the semi-crystalline nature of cellulose, esters with intermediate average DS, i.e., those with a DS below 2.9 are not commercially produced directly. The reason is that these products will be unevenly substituted, both within the individual AGUs, and along the polymer backbone, with the average DS in the amorphous regions higher than that in their crystalline counterparts. This heterogeneity of substitution leads to problems, in particular, irreproducible product characteristics (e.g., viscosity of the derivative solution) and formation of gel particles in the solvent employed. The latter is problematic in the production of cellulose acetate fibers and filter-tow, due to clogging of the nozzles during fiber precipitation [12, 13].

For cellulose esters that are susceptible to hydrolysis, in particular, the esters of carboxylic acids, the solution to this problem is to derivatize the biopolymer almost fully, then to obtain the required average DS by (heterogeneous) partial hydrolysis. Due to the difference in reactivity between the three OH groups of the AGU, this

hydrolysis occurs preferentially at position 6 (reactivity of position 6 is 4 ± 1 compared to those of positions 2 or 3), leading to certain "homogeneity" of product characteristics [14–16].

However, it is shown that it is possible to obtain directly partially substituted cellulose esters and mixed esters, including those of long-chain acids (CAP, CA/hexanoate, nonanoate, and laurate) under heterogeneous conditions. The solvents employed include DMAc and DMI and the catalysts in particular sulfonated polystyrene resin and titanium isopropoxide. The cellulose esters contained, however, material from the catalysts employed, e.g., 1000 ppm Ti, and 200–300 ppm sulfur. These impurities do not seem to affect the performance of the products. The latter element comes from cellulose sulfate, formed by sulfation of the biopolymer by the sulfuric acid produced by partial desulfurization of the catalyst at the high reaction temperatures employed (120–160 °C) [17]. It is also worth mentioning that cellulose acetate has been prepared under heterogeneous conditions by using solid super-acid catalyst ($SO_4^{2-}/ZrO_2$) and milling to activate the cellulose (Fig. 4.3) [18].

The commercial production of cellulose esters is a well-established process although limited to some types only (CA, CAP, CAB, CAPh of different total DS) applying the carboxylic acid anhydrides as reagent. The insufficient reactivity of the

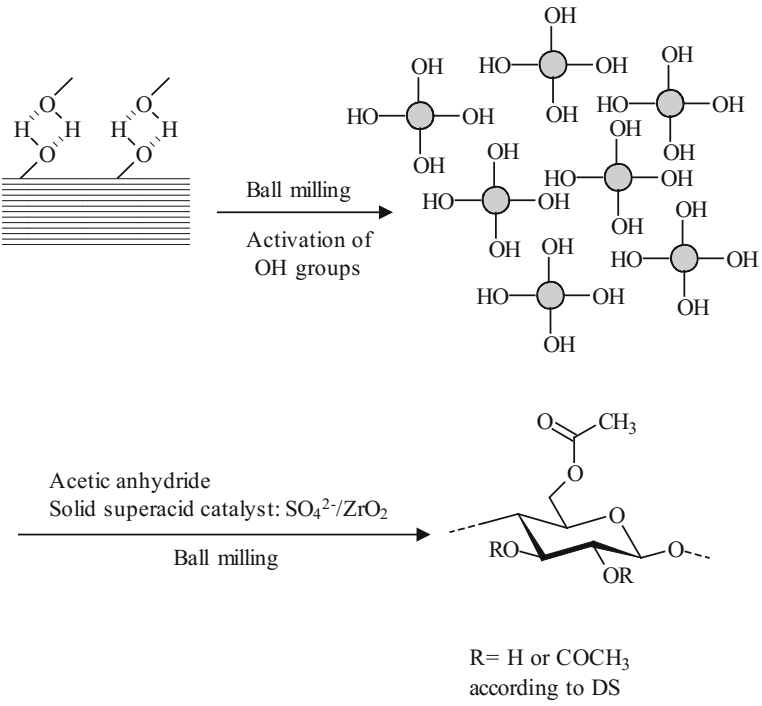


**Fig. 4.3** Cellulose activation by ball milling and subsequent solvent-free acetylation. Adapted from [18]

anhydrides of other carboxylic acids is one of the most important issues for this limitation in commercially accessible ester structures. Due to long-standing process developments (e.g., the fast acetylation/fast hydrolysis process for cellulose acetates), these processes are cost effective; there is no immediate need for major changes in the industrial plants. The (unavoidable) decrease of DP during the reaction (due to acid- or base-catalyzed degradation) can be controlled. In some cases, this degradation is intentional, e.g., in order to decrease solution viscosity of the product. Blending of the products of several batches leads to products with acceptably reproducible performance. A noticeable limitation is that heterogeneous reactions cannot be employed commercially for the preparation of carboxylic acid ester with moieties containing more than 4 carbon atoms. Cellulose esters of long-chain acids are important because of their lower $T_m$, (leading to less drastic extrusion conditions), solubility in common organic solvents, and compatibility in blends with hydrophobic polymers [19–21]. Another problem is connected with the simultaneous acylation of cellulose with acetic- and butyric anhydride due to the intrinsic difficulty of controlling the reactivity of two competing reagents under heterogeneous conditions.

On the other end of the spectrum is the homogeneous reaction scheme (HRS) in which cellulose is dissolved in a non-derivatizing solvent, followed by reaction with the reagent (carboxylic acid anhydride; acyl chloride/base; TsCl/base and many others. In principle, the HRS is largely free of the consequences of the cellulose semi-crystalline nature on reactivity because the biopolymer is decrystallized upon solubilization [22]. Therefore, the products are expected to be essentially evenly substituted, both within the AGU and along the biopolymer backbone. Additional advantages of the HRS include the following:

- little degradation of the starting polymer;
- high reproducibility;
- better control of the reactions with two competing reagents (e.g., acetic- and butyric anhydride), and,
- at least to a certain extent, control of regioselectivity [23].

Whereas the relevance to the industrial application of negligible cellulose degradation may be open to question, the HRS is definitely superior in terms of much better control of the product characteristics. The latter fact is the impetus of the continued intense interest in pursuing different aspects of homogeneous cellulose chemistry.

In a homogeneous reaction, the (visual) homogeneity of the solution does not necessarily mean that the biopolymer chains are well dispersed. As shown in Sect. 3.2, solutions of cellulose in electrolyte/dipolar aprotic solvent, and in ILs in the range of concentration employed in synthesis (1–10% (w/w) cellulose), even those of MCC, may contain aggregates [24–26]. Therefore, the problem of accessibility is not entirely eliminated, as can be deduced from the observed high reactivity of MCC, relative to that of fibrous celluloses; the easier reaction and better yields obtained with mercerized celluloses, and the dependence of DS on the

characteristics of the starting cellulose, in particular its DP, α-cellulose content, and degree of aggregation in solution [26]. Nevertheless, very many examples show that homogeneous chemical modification of cellulose leads to consistent results, in particular with regard to the reproducibility of the DS and the distribution of substituents within the AGU and along the polymer chains of the products. This indicates that the cellulose aggregates formed are extensively swollen, so that the hydroxyl groups of the AGU within the aggregates are much more accessible, as compared with their counterparts within solvent-swollen cellulose in the heterogeneous esterification reaction.

The main limitations of the HRS are the low cellulose charge in the reaction (about 10% (w/w) for isotropic solutions, higher cellulose concentrations may lead to anisotropic solutions) and the high cost of the solvents. The former aspect is especially problematic in certain ILs, where the solution undergoes the following transformations as a function of increasing cellulose concentration: viscous/isotropic → very viscous/anisotropic → gel. The content of cellulose at which these transformations occur depends on the characteristics of the cellulose used, in particular, its DP, the structure of the IL, the temperature, and the effect of shear (solution agitation). For example, for the same cation, 1,3-dialkylimidazolium, the acetates have lower viscosities than the corresponding chlorides; the same order of viscosity is observed for solutions of different cellulose samples in these ILs [27, 28]. Whereas temperature increase leads to (expected) decrease in solution viscosity, the Arrhenius-type energy of viscous flow, hence the dependence of solution viscosity (at zero shear) on temperature depends on the cellulose and the molecular structure of the IL. With regard to the effect of shear, many cellulose solutions in ILs show Newtonian behavior at low temperatures, i.e., shear rate-independent viscosity [29]. At higher temperatures, however, they usually display shear-thinning, although cases are known where the behavior continues to be Newtonian [30]. Therefore, higher cellulose content can be employed in the process by applying high temperature and strong, steady shear. Little is known, however, on how much of the above-mentioned advantages of the HRS will be maintained when the cellulose/IL solution is moderately or highly viscous and anisotropic. In this regard, the addition of a molecular solvent, e.g., chlorinated solvent, DMSO, or DMAc as diluent for the solution attenuates the high viscosity problem, and leads to better heat and mass transfer in the solution [10]. However, more work is needed on the effect of the diluents on cellulose solubility; the outcome of the reaction, in particular, DS, and the distribution of the substituents in the AGU and along the biopolymer backbone. Figure 4.4 shows the dependence of solubility and conductivity of the dissolved cellulose on the molar ratio ($R_{DMSO}$ = DMSO/BuMeImAc). Both plots are not linear functions in $R_{DMSO}$, presumably because of the interactions between the two solvent components and between these and cellulose [31].

Diluents have been employed in order to avoid phase separation of the reagents in or the products from the cellulose/IL solution [10]. The rate of acylation reaction depends on the dipolar aprotic solvent. The following order of rate constants has been observed for AlMeImCl/dipolar aprotic solvent: IL/DMAc>DMAc/LiCl>IL/

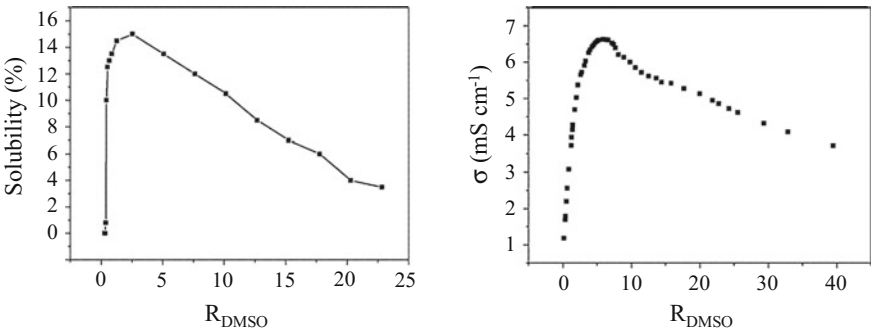


**Fig. 4.4** Dependence of cellulose solubility (%, w/w, left) and cellulose solution conductivity on the molar ratio ($R_{DMSO}$ = DMSO/BuMeImAc). Reprinted from [31], copyright (©2013) with permission from Elsevier

MeCN. This order of reactivity has been attributed to differences in the activation enthalpy and entropy [32].

Several aspects can be raised with regard to the cost issue. First, regeneration is relatively simple. For example, DMAc, unreacted acetic anhydride, and produced acetic acid have been recovered, essentially pure, from the reaction mixture by fractional distillation under reduced pressure [33]. LiCl can be precipitated by addition of a less polar solvent. Because most ILs are chemically and thermally stable, and possess extremely low vapor pressure, they can be readily recovered by evaporating the volatiles after the reaction is completed, e.g., ethanol, carboxylic acid, alkyl or benzyl halide, etc. A less energy consuming strategy is to separate the IL from the aqueous mixture by salting-out, i.e., by adding inorganic electrolytes, e.g., phosphates. The IL separated by this procedure has been successfully recycled into the process several times, without loss of efficiency [34]. Although ILs are much more expensive than molecular solvents, this price disadvantage might be decreasing due to their preparation in increasingly larger scale. Additionally, cellulose dissolution does not need an extra electrolyte, e.g., LiCl or $R_4NF$. Further discussion on the advantages and limitations of ILs as solvents for cellulose derivatization has recently been published [35].

The research on the application of the HRS to the derivatization of cellulose has been focused on the different aspects of the following experimental procedures:

1. Activation of cellulose prior the dissolution
2. Characteristics of the regenerated cellulose
3. The nature of the derivatizing agent, and its ratio to AGU
4. Characteristics of the products.

(Point 1): In addition to the discussion in Sect. 3.2, it suffices to mention that cellulose activation has been done by solvent exchange, ending with the one employed in cellulose derivatization, e.g., water → methanol → DMAc; water removal by distillation of a fraction of the reaction solvent; by conventional

(i.e., convection) heating under reduced pressure, and by MW heating [36, 37]. It is important to note that a pretreatment is not required for solvents like DMSO/$R_4NCl$ [38], and ILs [5]. Thus, a sample of cellulose acetate with the same DS were obtained by acetylation of MCC by acetic anhydride in AlBuImCl without and with prior activation (2 h at 110 °C under reduced pressure) [34]. There are examples where even the removal of water is not essential for the success of the reaction because the water activity in IL is greatly reduced [39].

Point (2): The few reports available on the effects of cellulose dissolution on its phyiscochemical properties show that the decrease in its DP is relatively small, $\leq 8\%$ in DMAc/LiCl, or ILs [33, 40, 41] although more degradation has also been reported [42]. Analysis of cellulose regenerated from DMAc/LiCl, $R_4NF \times H_2O$/DMSO and BuMeImCl by X-ray scattering has shown relatively large decreases in $I_c$ [43]. As it is expected, SEM micrographs have indicated large texture differences between the starting and regenerated cellulose samples, including those dissolved by employing conventional and MW heating, and a different distribution of the "micro-pores" in its structure (Fig. 4.5).

Point (3): A broad variety of reagents have been employed in order to prepare cellulose esters. The DS of the products depends on the ratio of the reagent/AGU. For example, carboxylic acid esters have been produced by reacting dissolved cellulose with acid anhydrides alone, or in the presence of a tertiary base, e.g., pyridine or triethylamine; acyl chloride/tertiary base; carboxylic acids activated by a variety of reagents, e.g., *N,N′*-carbonyldiimidazole, and vinyl esters of carboxylic acids. The transesterification reaction of cellulose (an alcohol) with vinyl esters of

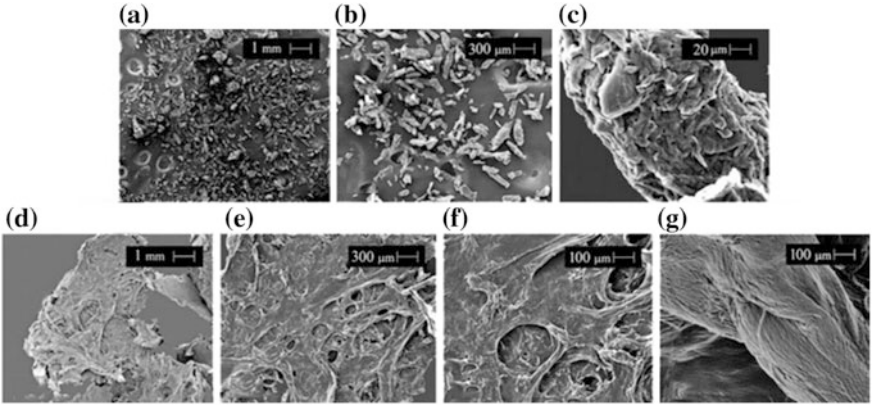


**Fig. 4.5** SEM micrographs showing the treatment-induced morphological changes of MCC. Micrographs **a–c** are for MCC after swelling by water for 10 min, at 80 °C (conventional heating), (×100), (×300), and (×5000), respectively, (reprinted from Ref. [34] with permission from John Wiley & Sons). Micrographs **d–f** are for regenerated MCC after MW-assisted dissolution in AlBuImCl (10 min, 30 W, 80 °C), (×100), (×300), and (×1000), respectively. Micrograph **g** (×1000) is for MCC regenerated after conventional heating dissolution in AlBuImCl (1 h, 80 °C reprinted from [41], with permission from John Wiley & Sons)

carboxylic acids displaces vinyl alcohol. The equilibrium is shifted to product (cellulose ester) by volatilization of acetaldehyde (keto tautomer of the produced vinyl alcohol). Tosylates have been obtained by the reaction with TsCl/tertiary base, whereas deoxycellulose derivatives like chlorodeoxy cellulose have been obtained from the cellulose tosylates by $S_N$ reactions. Examples include the reaction of tosyl cellulose with halides (deoxyhalogeno celluloses); ammonia (cross-linked, hence water-insoluble deoxyaminocelluloses) or amines (water-soluble deoxyamino celluloses); azide followed by reduction of the azide moiety (deoxyazido → deoxyamino cellulose).

The HRS conforms to the principles of green chemistry because the reaction can be carried out with or without catalyst, under essentially equimolar, or quasi equimolar derivatizing agent/OH of AGU. An acceptable excess of acid anhydride (1.5 anhydride/OH of the AGU) is routinely employed for the acylation of fibrous celluloses, including cotton linters in electrolyte/dipolar aprotic solvent and ILs. These ratios compare favorably with those employed for the acetylation under heterogeneous conditions, e.g., of sisal fibers (3.8 $Ac_2O$/OH of the AGU) [44] and bamboo cellulose (3.3 AcOH and 2.3 $Ac_2O$/OH of the AGU) [45]. The quasi-equimolar acylating agent/OH of AGU employed in the HRS means that no recovery of the derivatizing agent is required. Relative to some electrolyte/dipolar aprotic solvent solvents, the dissolution of cellulose is faster, and its reaction time is shorter in ILs, especially if microwave heating is employed [41]. Therefore, synthesis of cellulose derivatives is less energy demanding in electrolyte/dipolar aprotic solvent and IL than the heterogeneous reaction. These features are part of the reason that extensive effort has, and still is being put into optimizing the homogeneous chemical modification of cellulose.

Point (4): Regarding the properties of the products, the emphasis has been on their DP, reproducibility of the total DS, the partial DS at positions 2, 3, and 6 of the AGU, and the regularity of substitution within the AGU and along the biopolymer backbone. Due to the less energetic conditions employed in the HRS, relative to those of the heterogeneous reaction, the decrease in the DP of the products is acceptably small. In addition to high reproducibility of the total DS, the order reactivity is very often: position 6 > 2 and 3. The preference for substitution on position 6 is parallel to that observed for many cellulose esters. A kinetic study on the acylation of cyclohexylmethanol (a model for OH of the AGU) and trans-1,2-cyclohexane diol (a model for OH at positions 2 and 3), and of MCC in DMAc/LiCl has shown that the preference for C6-OH is due to a combination of activation enthalpy and entropy. The same factors also explain the dependence of DS on the length of the acyl group of the anhydride, *vide infra* [46]. Although it is expected that the order of substitution is position 6 > 2 and 3, this difference may not be apparent if the reaction conditions "level off" the differences between the hydroxyl groups, e.g., when cellulose is reacted with a large excess of the derivatizing agent for a long time (typically overnight) [33].

From the above discussion, it becomes clearly obvious that the HRS is suitable for the synthesis of specialty products where the molecular structure (type of

**Table 4.1** Solubility (−insoluble, +soluble) of cellulose acetate (obtained by hydrolysis of cellulose triacetate) depending on the degree of substitution (DS)

| DS | Solvent | | | |
|---|---|---|---|---|
| | Chloroform | Acetone | 2-Methoxy-ethanol | Water |
| 2.8–3.0 | + | − | − | − |
| 2.2–2.7 | − | + | − | − |
| 1.2–1.8 | − | − | + | − |
| 0.6–0.9 | − | − | − | + |
| <0.6 | − | − | − | − |

Reprinted from [47] with permission from Springer

substituent, DS, regularity of substitution; selectivity) is important in order to control product properties and performance, hence its applications. A classic example is hemodialysis membranes whose biocompatibility with the blood depends on total DS and the substitution pattern present [46]. The potential industrial use of the HRS requires optimization of several aspects of the process, in particular recovery and recycling of the solvents.

Esterification of cellulose is a vast subject that can be presented in different ways, according to the specific field(s) of interest. Although all derivatizations involve the transformation of the OH group of the AGU into other functionalities, the approaches employed differ widely. Therefore, the industrial production of cellulose carboxylic acid esters is discussed first, followed by methods that are employed in the laboratory in order to obtain these derivatives with high efficiency, derivatives with controlled substitution patterns, and novel cellulose products. In addition to the thermal properties, including $T_g$, $T_m$, and $T_{Decomp}$, solubility in different solvents is very important for processing, therefore this property is almost always tested. Unexpected insolubility in a certain solvent may indicate irregular substitution in the AGU or along the biopolymer backbone. As an example, the relationship between DS of CAs and their solubility in common solvents can be mentioned (Table 4.1).

## 4.3 Etherification of Cellulose—Overview

The majority of the commercial cellulose ethers are well soluble in water and are not toxic. Consequently, they are employed in diverse applications as protective colloids, thickeners, suspending aids, flow-control agents, water binders, liquid crystals, film formers, or glues. The cellulose ethers are used in diverse industries as food, paint, oil recovery, paper, cosmetics, pharmaceuticals, adhesives, printing, agriculture, ceramics, textiles, and building materials (Table 4.2). The production of cellulose ethers worldwide is estimated in the range of about 650,000 t (Fig. 4.6).

**Table 4.2** Applications of nonionic cellulose ethers

| Use in | For/as |
|---|---|
| Ceramics | Water retention, lubricity |
| Construction products | Water retention, workability |
| Cosmetics | Rheology control, emulsification, foam stabilization |
| Foods | Thickener, binder, emulsification |
| Paint | Protective colloid, thickener, suspending aid |
| Paper | Film formation, adhesive |
| Pharmaceuticals | Binder, granulating agent, film former, stabilizer |
| Polymerization (HEC) | Protective colloid for polymerization of vinyl acetate and vinyl chloride |
| Printing inks | Thickener, suspending agent |
| Textile | Binder, sizing agents, coating |
| Tobacco | Thickener, film former, adhesive |

**Ionic products**

- Carboxymethyl cellulose, CMC
- Carboxymethylhydroxyethyl cellulose, CMHEC

**Non-ionic products**

*Alkyl ethers*

- Methyl cellulose, MC
- Ethyl cellulose, EC

*Hydroxyalkyl ethers*

- Hydroxyethyl cellulose, HEC
- Hydroxypropyl cellulose, HPC

*Mixed ethers of cellulose*

- Hydroxyethylmethyl cellulose, HEMC
- Hydroxypropylhydroxyethyl cellulose, HPHEC
- Ethylhydroxyethyl cellulose, EHEC
- Hydroxybutylmethyl cellulose, HBMC
- Hydrophobically modified hydroxyethyl cellulose, HMHEC

**Fig. 4.6** Important neutral, anionic, and cationic cellulose ethers, along with their acronyms

Moreover, cellulose ethers with low amounts of functional groups are prepared, that swells in common organic solvents and water. Cationic derivatives (e.g. diethylaminoethyl cellulose, DEAE cellulose) are produced, which can be used as ion exchanger. Many derivatives are exploited frequently in research and

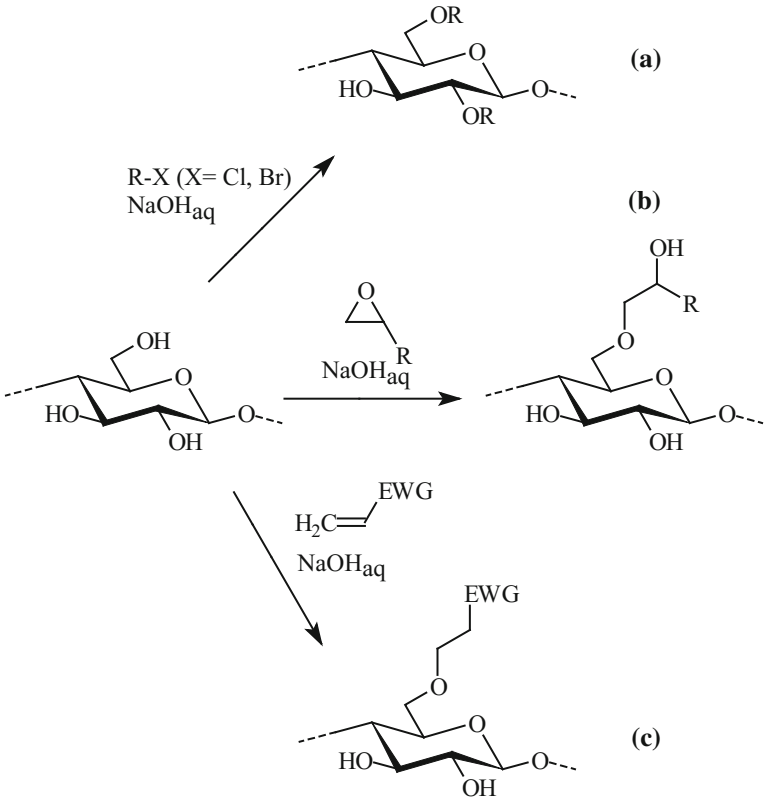


**Fig. 4.7** Synthesis pathways for commercial cellulose ethers

development, e.g., in regiochemistry of cellulose applying protecting groups technique (see Sects. 4.4.1 and 4.4.2).

The syntheses of commercial cellulose ethers are classical organic reactions, i.e., nucleophilic reaction of cellulose under alkaline conditions with one of the following reagents (Fig. 4.7):

- Alkyl or aryl halides (Williamson ether synthesis, A)
- Epoxides (Ring-opening reaction, B)
- Activated double bonds (Michael addition-type reactions, C)

The alkylation may be carried out homogeneously or heterogeneously. Commercially only the heterogeneous processes have gained relevance. Two paths are applied, which differ in terms of media used. One type is the diluent-free process in batch or continuous operation. The second is an organic diluent-mediated method. During these processes, the cellulose ethers remain in a fibrous or particulate state throughout the reaction.

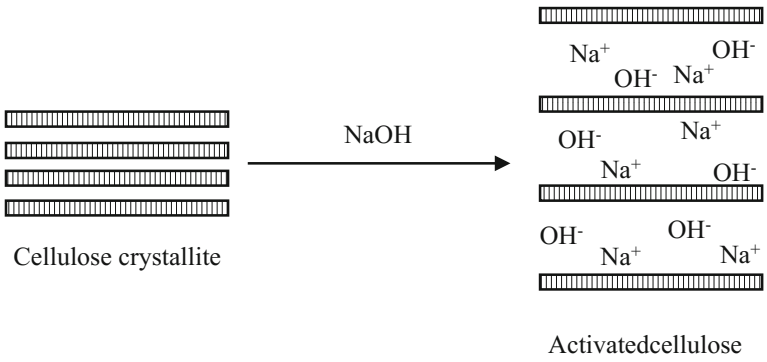


**Fig. 4.8** Activation of cellulose by conversion of cellulose crystallites with aqueous sodium hydroxide

To promote a uniform reaction, the cellulose has to be activated, generally *in situ*, before reaction with the etherifying reagent. In almost all cases, an activation of the cellulose with aqueous NaOH of different concentration (15–50%) is carried out that disrupts the hydrogen bonds present due to strong cellulose swelling (see Fig. 4.8). In lab-scale chemistry, not only alkali metal hydroxide solutions are employed, but also liquid ammonia, amines, dialkylformamides, dimethyl sulfoxides, strong carboxylic acids, and aqueous solutions of ammonium hydroxides.

The second process employs an organic diluent in the activation step and was first applied for the preparation of high-grade carboxymethyl cellulose [48]. Today, it is the dominant process for the manufacture of CMC, HEC, EHEC, and MC for technical use. The cellulose is added, after shredding or grinding, to an organic diluent containing aqueous sodium hydroxide.

The organic diluent has a number of significant advantages:

- it effectively suspends and disperses the polymer
- it promotes mass transfer, which allows the work with smaller quantities
- it acts as a heat-transfer medium, which is necessary for the reaction control
- it renders recovery of the reaction product easier.

It is essential that the organic diluent does not react during the alkylation reaction, i.e. the reaction exclusively occurs with the polymer, and that the medium does not dissolve the cellulose ether during the process. After formation of the alkali cellulose and addition of the alkylating agent, the reaction is initiated by heating. The following variables are important for reaction control: water content, sodium hydroxide concentration, temperature, slurry concentration, agitation, and the type of organic diluent applied. Diluents frequently used today are isopropyl or tert-butyl alcohol, acetone, toluene, and dimethoxyethane [48–50]. Uniformity of the formation of the alkali cellulose during the heterogeneous processes is usually proven by the excellent solubility of commercially obtained cellulose ethers.

Regarding lab-scale syntheses, homogeneous etherification is not as important as homogeneous esterification that has been, and is still being considered by the cellulose derivatives industry. One of the most important problems with homogeneous etherification is the solubility of the activating agent, e.g., NaOH or NaH, that are needed to increase the nucleophilicity of the hydroxyl groups. Moreover, during the etherification by alkyl, aralkyl, and aryl moieties, the very polar polymer cellulose is transferred to a less polar counterpart. As a consequence, the polar solvents usually used for cellulose dissolution (DMAc/LiC or ILs) cannot interact sufficiently with the polymer backbone and hence gelation or even precipitation occurs. Nevertheless, there are some examples of homogeneous etherification that show the effectiveness of this path.

Thus, homogeneous preparation of nonionic cellulose ethers could be realized by reaction of cellulose dissolved in DMSO/$SO_2$/DEA with solid NaOH and alkyl- and aralkyl halides [51–54]. Various completely functionalized cellulose ethers bearing alkyl- and aryl substituents as well as functions containing double bonds could be obtained. Tri-*O*-isopentyl cellulose is capable to form ultrathin layers and supramolecular architectures [55–57].

Cellulose dissolved in DMSO/LiCl (after activation) was treated with NaH forming dimsyl sodium [58]. Iodomethane, iodoethane, bromoethane, 1-bromopropane and 1-bromobutane were utilized as etherifying agents. An alternative route for a complete methylation is the reaction of cellulose in DMI/LiCl [59]. Tri-*O*-methyl cellulose was obtained in a one-step conversion. An interesting procedure for the preparation of tri-*O*-allyl- and tri-*O*-crotyl cellulose was described using cellulose dissolved in DMAc/LiCl, allyl- and crotyl chloride and powdered NaOH. However, by adding the powdered NaOH the reaction system becomes heterogeneous.

The selective synthesis of different cellulose ethers like MC showing different patterns of functionalization were carried out by alkylation of cellulose in DMAc/LiCl with dimethyl sulfate or methyl iodide starting from cellulose acetate after treatment with sodium naphthalenide and subsequent deacylation [60] The regioselective synthesis of 6-mono-*O*-methyl-, 2,3-di-*O*-methyl-, 2,3-di-*O*-benzyl-, and of 6-mono-*O*-benzyl cellulose was carried out [61–64]. In addition, 6-mono-*O*-trityl-2,3-di-*O*-butyl-, 6-mono-*O*-trityl-2,3-di-*O*-pentyl-, and 6-mono-*O*-trityl-2,3-di-*O*-hexyl cellulose were obtained by subsequent modification of tritylated cellulose (see Sect. 4.4.1) [65].

Besides cellulose ether with one type of function like methyl, ethyl, or hydroxyethyl moieties, mixed nonionic ethers, e.g., MHEC or EHEC are prepared basically for an adjustment of properties applying the above-mentioned synthesis routes.

Subsequent modification of water-soluble cellulose derivatives has attracted considerable attention. HE, HP, and MC were modified by reacting the remaining hydroxyl groups with long-chain aliphatic compounds carrying reactive functions such as epoxide, chloride, isocyanate, acid chloride, and acid anhydride moieties [66, 67]. The solutions of the hydrophobically modified cellulose ethers possess enhanced viscosity efficiency, improved shear and salt stability, and shear-thickening rheology compared to the starting cellulose ethers [68–73].

Cellulose can be silylated in a various media using different reagents. Thus, a mixture consisting of cellulose, THF, pyridine, and trimethylsilyl chloride yields trimethylsilyl celluloses (TMSC). This reaction starts heterogeneously and becomes homogeneous starting from a DS value of about 2. Homogeneous synthesis in the solvent DMAc/LiCl using hexamethyldisilazane gives products with an almost complete silylation (DS 2.7–2.9) [74] or with a broad range of DS values yielding the soluble trimethylsilyl ether. The reaction starts homogeneous and becomes heterogeneous after a certain time because the product formed is insoluble. The TMSC obtained were extensively studied because of their potential to regenerate cellulose simply by treatment with acids and to obtain thereby cellulose fibers, films, micro- and nanoparticles [75] as well as ultrathin films applying Langmuir–Blodgett (LB) technique [76]. The etherification of cellulose with reagents containing bulky groups is the most important path of regiochemistry up to now.

## 4.4 Regioselective Synthesis of Cellulose Derivatives Using Protecting Groups

Cellulose derivatives prepared under conventional conditions can be composed of up to eight different repeating units: non-functionalized AGU and 2,3,6-tri-*O*-functionalized AGU as well as 3 modified AGUs bearing one substituent at position 2, 3, or 6, and 3 modified AGUs bearing two substituents at position 2,3, 2,6, and 3,6. These different repeating units are shown in Fig. 4.9.

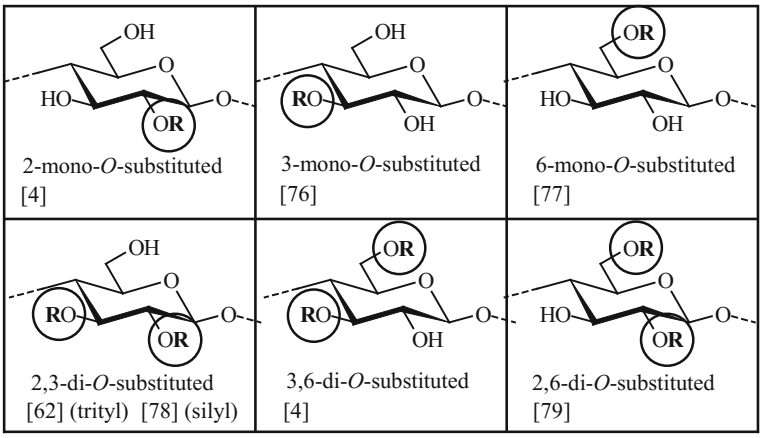


**Fig. 4.9** Differently functionalized repeating units that may occur in cellulose derivatives (non-functionalized and tri-*O*-functionalized compounds are not shown). Relevant references are given in brackets. 2,3-di-*O*-substituted cellulose derivatives have been prepared via 6-*O*-triphenylmethyl (trityl)- or 6-*O*-TDMS ethers (silyl)

It is generally accepted that the properties of cellulose derivatives are not only determined by the type of substituent and its degree of substitution but also by the functionalization pattern within the repeating unit and along the polymer chain. Understanding the properties in relation to the functionalization pattern in details requires:

- synthesis of cellulose derivatives with a well-defined structure
- proof of desired structure
- evaluation of properties.

Such information is a prerequisite for the establishment of structure–property relationships. Of particular interest are rheological and thermal properties (thermoreversible flocculation) of cellulose ethers in aqueous solution due to their applications, e.g., as thickeners. Consequently, their performance can be improved by changing the functionalization pattern.

With regard to the synthesis of regioselectively functionalized cellulose derivatives, a distinction should be made between a bottom-up synthesis by polymerization of the sugar units with a regiocontrolled functionalization pattern and a polymer-analogous reaction. Despite their high selectivity and versatility, the bottom-up approach, i.e., the ring-opening polymerization of glucose derivatives, yields samples of low DP as well as the need for many reaction steps including the regio- and stereospecific formation of the glycosidic bonds [77–81].

The preparation of regioselectively functionalized cellulose ethers is still a challenging goal in polysaccharide chemistry. Up to now, the most important approach for the synthesis of cellulose derivatives with controlled functionalization pattern is the application of protecting groups (Fig. 4.10a). To ensure a highly selective introduction, blocking group reagents must consist of at least one bulky (i. e., branched) alkyl or aryl moiety. In this regard, triphenylmethyl and trialkylsilyl ethers are of special interest [82]. As is usual in this approach, the blocking group must meet requirements related to the selective introduction, stability during subsequent reactions, and removability without loss of other substituents [83].

Other methods comprising, e.g., selective cleavage of primary substituents play a minor role. Examples are the deacetylation of cellulose acetate under aqueous acidic or alkaline conditions or in the presence of amines (Fig. 4.10b) [84, 85]. A certain regioselectivity of enzymes toward deacetylation of cellulose acetate has been observed as well [86].

Recently, tetrabutylammonium fluoride has been found to catalyze the deacylation of cellulose esters. The deacylation is highly regioselective, on one hand. On the other, in contrast to the regioselectivity of other reactions of cellulose and its derivatives towards position 6, this deacylation shows substantial selectivity for the removal of the acyl groups from the esters of the secondary positions, affording 6-*O*-esters of cellulose with high regioselectivity by a simple one-step process employing no protecting groups [87]. Additionally, tetraalkylammonium hydroxides have been found to mediate regioselective deacylation of cellulose esters.

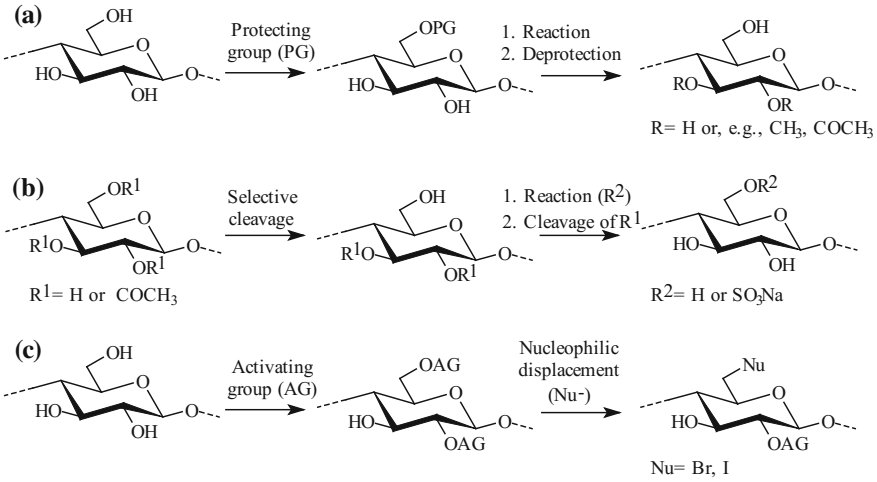


**Fig. 4.10** Pathways for the regioselective functionalization: **a** protecting group technique, **b** selective cleavage of primary substituents, and **c** activating groups. Reproduced from [83] with permission from John Wiley and Sons

This deacylation occurs selectively at position 2 and 3, affording cellulose-6-*O*-esters by a simple, efficient one-step process [88].

In addition, activating groups may also be exploited for selective reactions (Fig. 4.10c). The introduction of sulfonic acid ester moieties may be an appropriate path. Tosylation occurs faster at the primary position. Thus, there is a certain regioselectivity.

Regioselectively functionalized cellulose derivatives may be worthy in the context of clarifying reaction mechanism and unexpected side reactions. For instance, during subsequent nucleophilic displacement reaction, cross-linking of cellulose p-$NO_2$-phenyl carbonate with a low DS of about 1 has been observed. In order to clarify the reason for this side reaction, the protection of the primary hydroxyl group at position 6 of cellulose by 6-*O*-triphenylmethyl (trityl) moiety was carried out and thus soluble cellulose aryl carbonates of low DS were obtained that do not contain any carbonate moieties at the primary position. The subsequent $S_N$ reaction with amines yields soluble products, i.e., no cross-linking occurred. Thus, the primary carbonates are mainly responsible for cross-linking of the cellulose chains [89].

Regarding the protecting group used for cellulose, most important examples are groups based on triphenylmethyl- and trialkylsilyl (with at least one bulky moiety). On the contrary, very bulky carboxylic acids are not appropriate for selective protection. The reason is that for esters the distance between the bulky moiety and the protected position is large (due to "insertion" of the –CO– group), allowing for esterification of the primary and the secondary hydroxyls. Cellulose esters prepared with bulky acyl groups including pivalate, adamantate, and 2,4,6-trimethylbenzoate are substituted not only at position 6 but also at position 2 and 3 at a DS below 1 [90].

### 4.4.1 Triphenylmethyl Ethers

The bulky trityl chloride reacts preferably with the primary OH group of cellulose due to its steric demand under heterogeneous [63] and homogeneous reaction conditions [91]. Typically, DMAc/LiCl as solvent and triethylamine as the base is employed. After addition of trityl chloride, the reaction is conducted for 48–72 h at 70 °C (Table 4.3). The polymer remains in solution and is precipitated and washed with methanol or ethanol. It can be further purified by reprecipitation from THF solution into methanol to remove traces of trityl carbinol. It has been found that methoxy groups attached to the benzene rings increase the rate of both formation and cleavage of the trityl ether. With respect to reaction rate, availability, and price, trityl- and monomethoxytrityl chloride are applied as blocking group reagents.

Due to its stability under alkaline conditions, 6-*O*-trityl cellulose is widely used for the preparation of 2,3-*O*-functionalized cellulose derivatives. Conversion of 6-*O*-trityl cellulose with acetic acid anhydride or propionic acid anhydride yields the corresponding 2,3-*O*-functionalized acetates or propionates. Treatment with HBr in acetic acid afforded the detritylated polymers [92]. Kadla et al. prepared 2,3-*O*-acetyl cellulose and studied the viscoelastic properties of gels in the ternary mixture cellulose acetate/DMAc/water in comparison with randomly functionalized derivatives. It is stated that the phase separation is caused by both hydrogen bonds and hydrophobic interactions. 2,3-*O*-Cellulose acetate with a OH group at position 6 possesses an increased elastic modulus compared with a randomly functionalized ester. In other words, the regioselective derivative shows phase separation, while the random derivative remains in solution at the same concentration of non-solvent [93]. In a comparable way, the preparation of cellulose sulfuric acid half esters (cellulose sulfate) with preferred functionalization of the secondary OH functions was realized [94]. Sulfur trioxide pyridine complex was used as reagent followed by detritylation. DS values up to 0.99 were obtained.

**Table 4.3** Tritylation of cellulose with different trityl chlorides (3 mol/mole AGU, in DMAc/LiCl at 70 °C) and detritylation (37% HCl aq. in THF, 1:25 v/v)

| Substituent | Protection | | | Deprotection rate |
|---|---|---|---|---|
| | Time (h) | DS | Rate | |
| Trityl | 4 | 0.41 | 1 | 1 |
| Trityl | 24 | 0.92 | | |
| Trityl | 48 | 1.05 | | |
| 4-Monomethoxytrityl | 4 | 0.96 | 2 | 18 |
| 4-Monomethoxytrityl | 24 | 0.92 | | |
| 4-Monomethoxytrityl | 48 | 0.89 | | |
| 4,4′-Dimethoxytrityl | 4 | 0.97 | $2 \times 10^5$ | 100 |
| 4,4′,4″-Trimethoxytrityl | 4 | 0.96 | $6 \times 10^6$ | 590 |

Adapted from [91]

Regioselectively functionalized 2,3-*O*-methyl- and 2,3-*O*-ethyl celluloses were prepared via 6-*O*-trityl cellulose as well [63]. Control of the $DS_{Me}$ by maintaining the regioselectivity is possible by choosing appropriate reaction conditions (Table 4.4) [95].

2,3-*O*-Allyl cellulose can be formed in an analogous fashion. Compared to other cellulose ethers described here, the allyl ether can be selectively cleaved and, hence, it may act as protecting group as well [96]. Further details are discussed in Sect. 4.4.5.

Ionic 2,3-*O*-CMC was synthesized via 6-*O*-trityl cellulose applying sodium monochloroacetate as etherifying reagent with solid NaOH as base in DMSO [97, 98]. After a reaction time of 29 h at 70 °C, the product was detritylated with

**Table 4.4** Partial values of the degree of substitution (DS) and the amount of the different repeating units depending on the conditions of the methylation of 6-*O*-trityl cellulose

| Sample | Procedure[a] | Partial DS at position | | DS | Amount of methylated repeating units (%)[b] | | |
|---|---|---|---|---|---|---|---|
| | | 2 | 3 | | None | 2- or 3-mono-*O*- | Di-*O*- |
| 4a | A | 0.10 | 0.24 | 0.40 | 62 | 36 | 2 |
| 4b | A | 0.25 | 0.25 | 0.50 | 45 | 42 | 4 |
| 4c | A | 0.39 | 0.28 | 0.67 | 63 | 47 | 10 |
| 4d | A | 0.69 | 0.22 | 0.91 | 31 | 47 | 22 |
| 4e | B | 0.56 | 0.31 | 0.87 | 34 | 45 | 21 |
| 4f | B | 0.49 | 0.23 | 0.72 | 43 | 42 | 15 |
| 4g | B | 0.56 | 0.37 | 0.93 | 33 | 41 | 23 |
| 4h | B | 0.78 | 0.34 | 1.12 | 22 | 44 | 34 |
| 4i | C | 0.51 | 0.26 | 0.77 | 41 | 41 | 18 |
| 4j | C | 0.36 | 0.18 | 0.54 | 56 | 34 | 10 |
| 4k | C | 0.54 | 0.37 | 0.91 | 28 | 53 | 19 |
| 4l | D | 0.46 | 0.35 | 0.81 | 34 | 51 | 15 |
| 4m | D | 0.45 | 0.38 | 0.83 | 32 | 53 | 15 |
| 4n | D | 0.20 | 0.19 | 0.39 | 64 | 33 | 3 |
| 4o | D | 0.38 | 0.32 | 0.70 | 42 | 46 | 12 |
| 4p | D | 0.30 | 0.24 | 0.54 | 55 | 36 | 9 |
| 4q | D | 0.39 | 0.08 | 0.47 | 61 | 31 | 8 |
| 4r | D | 0.26 | 0.22 | 0.48 | 60 | 32 | 8 |
| 4s | D | 0.31 | 0.33 | 0.64 | 45 | 46 | 9 |
| 4t | D | 0.35 | 0.16 | 0.51 | 61 | 27 | 12 |

Adapted from [95]

[a]A: Trityl cellulose dissolved in dimethyl sulfoxide (DMSO), NaOH powder
B: Trityl cellulose dissolved in DMSO containing 1.6% water, NaOH powder
C: Trityl cellulose dissolved in DMSO containing 1.6% water, KOH powder
D: Trityl cellulose suspended in 2-propanol, aqueous NaOH

[b]The calculation was carried out based on the $^1$H-NMR spectra of the perpropionylated samples in combination with line fitting analysis

gaseous HCl in dichloromethane for 45 min at 0 °C. Alternatively, the detritylation can be carried out in ethanol slurry with aqueous hydrochloric acid. The 2,3-*O*-CMC synthesized possess a DS of up to 1.91. The polymer is water soluble starting with DS 0.3 [99].

2,3-*O*-Hydroxyalkyl ethers of cellulose have been prepared starting from 6-*O*-monomethoxytrityl cellulose [100]. Homogeneous reaction conditions cannot be applied because the epoxides react with DMSO in the presence of NaOH. Other reaction media like aqueous alcohols, which are useful for carboxymethylation reactions are not appropriate because they do not efficiently wet the hydrophobic monomethoxytrityl cellulose. It has been shown that surfactants, in particular, mixtures of nonionic and anionic ones, are able to mediate the conversion. The reaction of monomethoxytrityl cellulose with ethylene- and propylene oxide in isopropanol/water mixtures containing sodium dodecyl sulfate and polyethyleneglycol $C_{11}$–$C_{15}$-ether (IMBENTIN AGS-35) afforded 2,3-*O*-hydroxyalkyl celluloses with MS of up to 2.0 after detritylation. Interestingly, the polymers become water-soluble starting with MS 0.25 (hydroxyethyl cellulose) and 0.5 (hydroxypropyl cellulose, HPC), while a conventional HPC is water soluble with MS > 4. $^{13}C$ NMR spectroscopy revealed the etherification of the secondary hydroxyl groups of the AGU. As shown in Fig. 4.11, only one signal can be observed for the $CH_2$ group of position 6. In addition, the peaks of the etherified positions 2 and 3 appear in the range from 80–83 ppm.

Conversion of cellulose derivatives with epoxides may lead to oxyalkylene side chains. NMR studies on these samples revealed different hydration behavior depending on its type. Thus, dimeric side chains of 2,3-*O*-HPC are more difficult to hydrate than the monomeric units [101].

6-*O*-Monomethoxytrityl cellulose has been converted to 2-isocyanatoethyl methacrylate followed by detritylation to obtain the corresponding 2,3-*O*-functionalized cellulose derivatives [102].

4-Alkoxytrityl ethers of cellulose bearing a $C_4$–$C_{18}$ alkyl chain were found to dissolve in solvents of different polarity, depending on the alkyl chain length. These derivatives and their acetates show interesting anisotropic optical properties above their melting temperature [103].

### *4.4.2 Trialkylsilyl Ethers*

Trimethylchlorosilane, the simplest trialkylchlorosilane, readily reacts with alcoholic hydroxyl groups but does not show regioselectivity. A sufficient regioselectivity is ensured by attaching one bulky alkyl moiety. Thus, trialkylsilyl chloride like tert.-butyl- and thexyldimethylsilyl (TDMS) chloride are valuable protecting groups. With respect to its performance, the TDMS ether is the most versatile protecting group. It can be used for the preparation of two different types of protected cellulose derivatives because the regioselectivity of the silylation depends on the state of dispersion of cellulose in the reaction mixture, i.e., the selectivity is

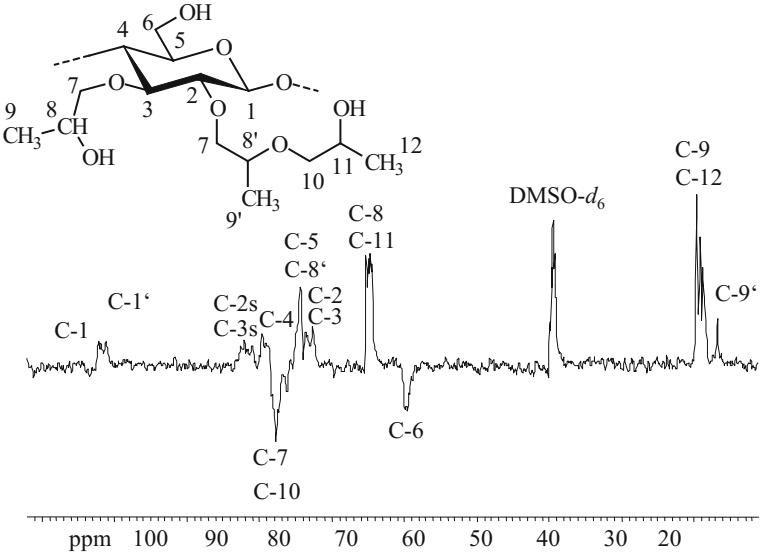


**Fig. 4.11** $^{13}$C DEPT $^{13}$C NMR spectrum of 2,3-*O*-hydroxypropyl cellulose (molar substitution 0.33) recorded in dimethyl sulfoxide (DMSO)-$d_6$ at 40 °C. Reproduced from [100] with permission from John Wiley and Sons

medium controlled (Fig. 4.12). Starting from cellulose that is swollen in a mixture of ammonia and aprotic-dipolar solvents, in particular, NMP at −15 to −25 °C, the conversion with TDMS-Cl leads to an exclusive silylation of the primary OH group [104, 105].

2,6-di-*O*-Silylation of cotton linters with DP 1433 in DMAc/LiCl was studied [106]. Mercerization of cotton linters prior to the dissolution process ensured the formation of optically clear cellulose solutions. It was found that the maximum DS was reached already after 4 h reaction time (Fig. 4.13, top). The molar ratio of AGU:TDMS-Cl may be reduced from 1:4 to 1:3 provided the reaction is conducted for 24 h (Fig. 4.13, bottom). NMR investigations of the polymer after methylation of position 3, desilylation and acetylation revealed the structural uniformity of the 2,6-di-*O*-TDMS cellulose.

Although the formation of TBDMS cellulose with DS 0.7 was already described in 1987 [107], this derivative did not receive much attention in regioselective cellulose chemistry during the past years. Later the synthesis of TBDMS cellulose with DS 0.97 was carried out [108]. Selective silylation of position 6 was described. TBDM silylation of cellulose of up to DS 2 could also be realized [109]. Detailed NMR investigations after methylation, desilylation, and acetylation revealed the structural uniformity of this polymer. Moreover, a conversion at a temperature of 100 °C was found to be inappropriate because side reactions occur,

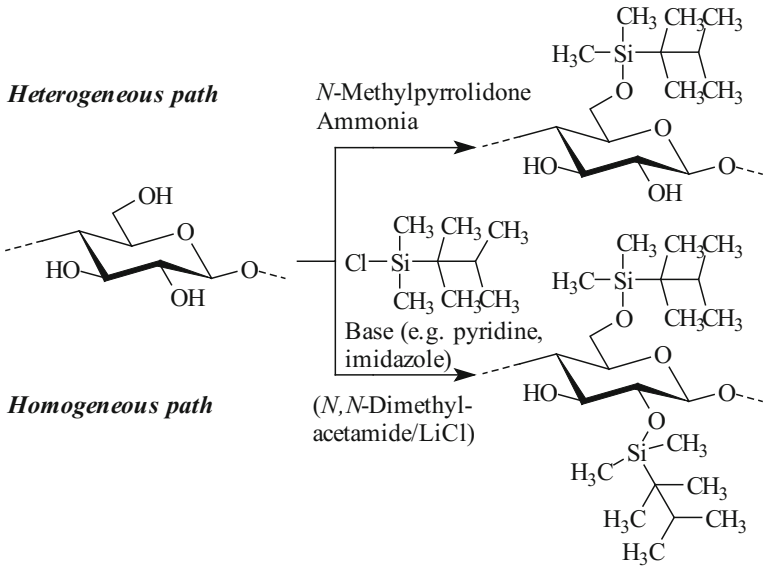


**Fig. 4.12** Heterogeneous and homogeneous path of silylation leading to cellulose selectively protected at position 6 and position 2 and 6

i.e., a change in selectivity; 6-mono-*O*-TBDMS-, 3,6-di-*O*-TBDMS- and 2,3,6-tri-*O*-TBDMS moieties were detected.

Following this approach, the synthesis of cellulose-2,6-*O*-diesters and subsequently cellulose-2,6-A-*O*-3-B-O-triesters with a high degree of regioselectivity could be prepared employing 3-*O*-allylcellulose as a key protected precursor while 3-*O*-benzyl cellulose is not appropriate. The synthesis of regioselectively functionalized cellulose esters is even more difficult as the etherification due to the difficulty of attaching and detaching many protecting groups in the presence of cellulose ester moieties without removing the ester groups [110].

### *4.4.3 3-O-Ethers of Cellulose*

The preparation of 3-mono-*O*-functionalized cellulose ethers follows the general scheme of 2,6-di-*O*-protection, 3-*O*-alkylation, and 2,6-di-*O*-deprotection. Alkylating agents are usually alkyl iodides, while alkyl bromides, chlorides, and sulfonic acid esters are scarcely applied. Usually, sodium hydride is used as a base under anhydrous conditions. Sodium hydroxide, which is much easier to handle, cannot be used because anhydrous conditions are difficult to achieve and traces of water induce partial desilylation and, hence, loss of structural uniformity. Finally, the silyl ethers are cleaved off by treatment with fluoride ions usually applying

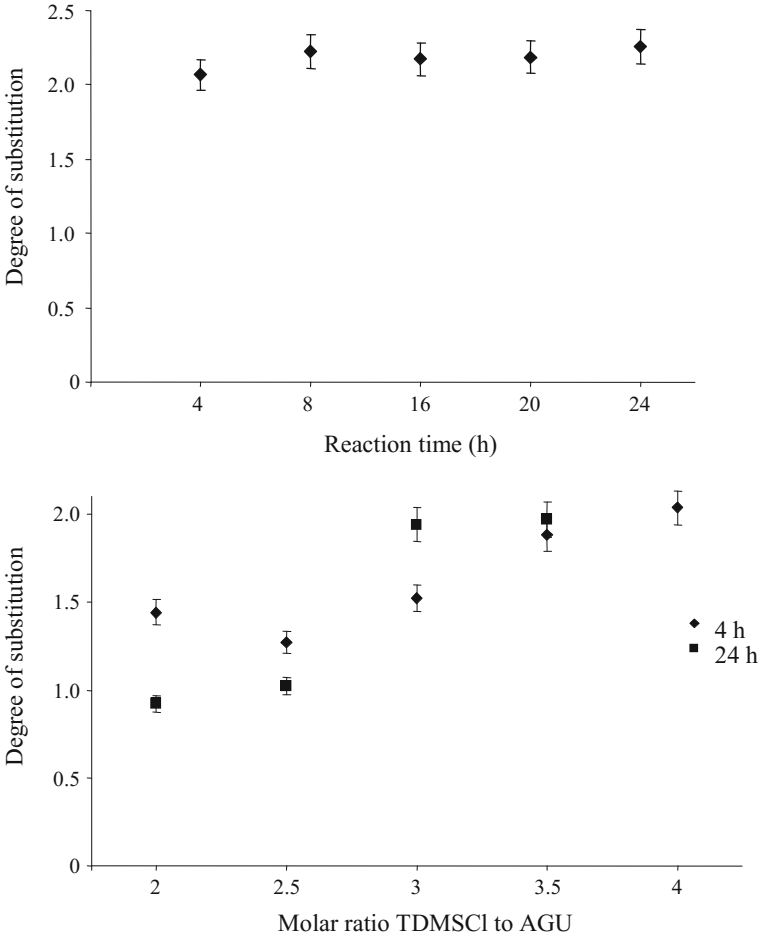


**Fig. 4.13** Degree of substitution (DS) obtained by the conversion of cellulose dissolved in DMAc/LiCl with thexyldimethylchlorosilane (TDMSCl) in the presence of imidazole. Dependency of the DS from the reaction time (top, molar ratio anhydroglucose unit, AGU: TDMSCl:imidazole 1:4:4.7) and from the molar ratio AGU:TDMSCl at 4 and 24 h reaction time (bottom). Reproduced from [106] by permission of Romanian Academy Publishing House, the owner of the publishing rights

TBAF $\times$ $3H_2O$ as a reagent. The 3-*O*-alkyl celluloses known up to now and their typical solubility are summarized in Table 4.5.

The synthesis of 3-mono-*O*-propargyl cellulose is a challenging task [117]. Although the proton of the triple bond is acidic, there is no hint of chain elongation by the formation of C–C-bonds, i.e., pure 3-mono-*O*-propargyl cellulose was obtained. However, hydrogen bonds are present that hinder a detailed structure characterization by means of 2D NMR techniques.

**Table 4.5** 3-*O*-alkyl celluloses known up to now and their solubility

| Alkyl | Solubility in[a] | | | | | References |
|---|---|---|---|---|---|---|
| | Ethanol | DMSO | DMA | $H_2O$ (<20 °C) | $H_2O$ (room temperature) | |
| Methyl | − | − | − | − | − | [111] |
| Ethyl | − | + | + | + | + | [112] |
| Hydroxyethyl | − | + | + | + | + | [113] |
| Methoxyethyl | − | + | + | + | + | [114] |
| 3′-Hydroxypropyl | − | + | + | + | + | [115] |
| Allyl | − | + | + | − | − | [111] |
| Propyl | + | + | + | + | − | [116] |
| Propargyl | − | + | − | − | − | [117] |
| Butyl | + | + | + | − | − | [118] |
| n-Pentyl | + | + | + | − | − | [119] |
| iso-Pentyl | + | + | + | − | − | [119] |
| Dodecyl | − | − | − | − | − | [9, 119] |
| Oligo (Ethylenglycol) | − | − | − | − | − | [10, 120] |

[a]Dimethyl sulfoxide (DMSO), *N,N*-dimethyl acetamide (DMA), soluble (+), insoluble (−)

Table 4.5 shows that not only short-chain ethers were prepared. Interestingly, 3-*O*-ethers bearing long-chain methoxypoly(ethylene glycol) ethers with 3–16 ethylene glycol moieties could be obtained by conversion of 2,6-di-*O*-TDMS cellulose with methoxypoly(ethylene glycol) tosylates in the presence of imidazole [121]. Applying methoxypoly(ethylene glycol) iodide as an alkylating agent in the presence of sodium hydride yielded products having a DS as high as 0.8 [120]. This synthesis concept had also been adopted to the synthesis of 3-*O*-azidopropoxypoly (ethylene glycol)-2,6-di-*O*-thexyldimethylsilyl cellulose, which forms honeycomb structures at surfaces. The azide group can then be used for click-reactions, e.g., with propargylated biotin derivative [122].

### *4.4.4 Thermal Properties in Aqueous Solution*

It had been demonstrated that the aggregation behavior of, e.g., ethyl cellulose, strongly depends on the functionalization pattern. Samples of 3-mono-*O*-ethyl cellulose and ethyl cellulose with random functionalization pattern with comparable DS dissolve in water. However, the LCST of the randomly functionalized polymer is at 30 °C, while the regioselective ether becomes insoluble at 60 °C. This behavior was examined by different techniques like observation with the naked eye, micro DSC, rheology in oscillatory shear mode, and NMR spectroscopy [123].

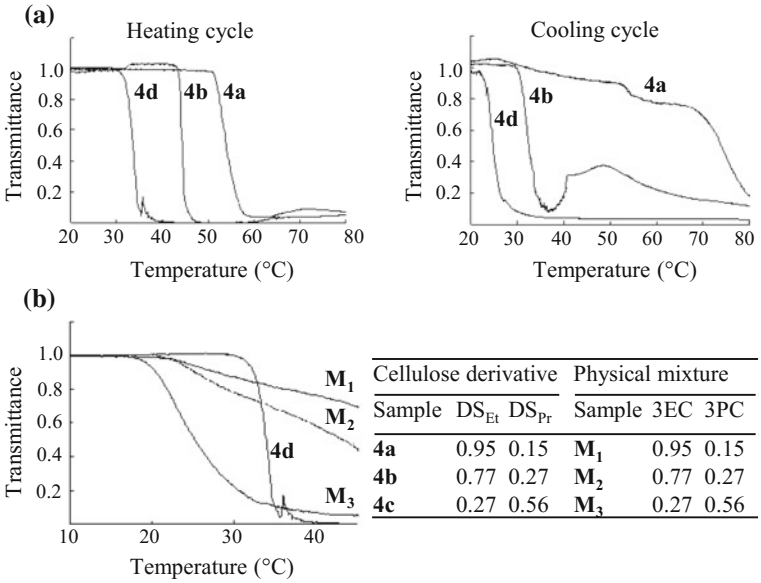


| Cellulose derivative | | | Physical mixture | | |
|---|---|---|---|---|---|
| Sample | $DS_{Et}$ | $DS_{Pr}$ | Sample | 3EC | 3PC |
| **4a** | 0.95 | 0.15 | $\mathbf{M_1}$ | 0.95 | 0.15 |
| **4b** | 0.77 | 0.27 | $\mathbf{M_2}$ | 0.77 | 0.27 |
| **4c** | 0.27 | 0.56 | $\mathbf{M_3}$ | 0.27 | 0.56 |

**Fig. 4.14** Temperature-dependent transmittance of 3-mono-*O*-alkyl cellulose derivatives in aqueous solution: **a** 3-mono-*O*-ethyl/propyl celluloses with different ratios of ethyl (Et) and propyl (Or) groups as well as **b** physical mixtures of 3-mono-*O*-ethyl cellulose (3EC) and 3-mono-*O*-propyl cellulose (3PC). Reprinted from [124], Copyright (©2012) with permission from Elsevier

Obviously, the LCST of 3-*O*-ethers discussed here depends on the alkyl chain length (see Table 4.5) and may also be below room temperature. Later works reported attempts on tuning the LCST by mixing two different 3-*O*-alkyl celluloses [124]. However, physical mixing of polymers with different LCST does not tune the LCST. In any case, the solubility behavior is governed by the compound with the lowest LCST (Fig. 4.14b). Nevertheless, attachment of different alkyl moieties at position 3 of the same polymer chain significantly influenced the LCST of the sample. This was achieved by applying the general scheme of 3-*O*-alkylation. Instead of a single alkylating agent, a mixture of two different alkyl iodides was used. Owing to the quite different reactivity of the alkylating agents, their ratio must be carefully selected to obtain derivatives with the desired ratio of substituents. However, a clear LCST can be observed, which is between the LCST of the single polymers (Fig. 4.14a).

Further investigations of these mixed cellulose ethers revealed network formation upon heating of the aqueous solutions. The strength of this network increases with increasing content of propyl groups of a 3-mono-*O*-ethyl/propyl cellulose derivative. This aggregation is coupled with phase separation, i.e., the mixture turns opaque [125].

### 4.4.5 Application of Orthogonal Protecting Groups

The use of orthogonal protecting group strategies enables the preparation of cellulose ethers, which are not directly accessible by using a single blocking group. As one of the first examples, Kondo described the synthesis of 6-*O*-alkyl celluloses [96] (Fig. 4.15). This procedure comprises the application of two different protecting groups. First, 6-*O*-trityl cellulose is converted with allyl chloride in the presence of NaOH yielding allylation of position 2 and 3. After detritylation, isomerization of the 2,3-*O*-allyl cellulose to 2,3-*O*-(1-propenyl) cellulose with potassium tert.-butoxide is carried out. Position 6 is alkylated and the 1-propenyl groups at the secondary positions are cleaved off with HCl in methanol.

Another important field is the preparation of selectively hydroxyalkylated cellulose ethers. Hydroxyalkyl celluloses are prepared in technical scale by conversion of cellulose with alkylene oxides, which may generate side chains to a certain extent. In case of hydroxyethyl cellulose, neither ethylene oxide nor 2-bromoethanol will yield a uniform product. This could be avoided using orthogonal protecting group approach for the synthesis of 2,3-*O*-HEC [126] and 3-*O*-HEC [113] (Fig. 4.16).

2-Bromoethanol was allowed to react with 3,4-dihydro-2*H*-pyran in the presence of *p*-toluenesulfonic acid as catalyst to yield 2-(2-bromethoxy)tetrahydropyran as the alkylating agent [127]. The order of deprotection of the alkylated 2,6-di-*O*-TDMS cellulose was found to be crucial, i.e., the TDMS groups have to be removed first before acid treatment cleaves off the tetrahydropyran moieties [113]. Obviously, the nonpolar TDMS groups prevent the proton-induced hydrolysis.

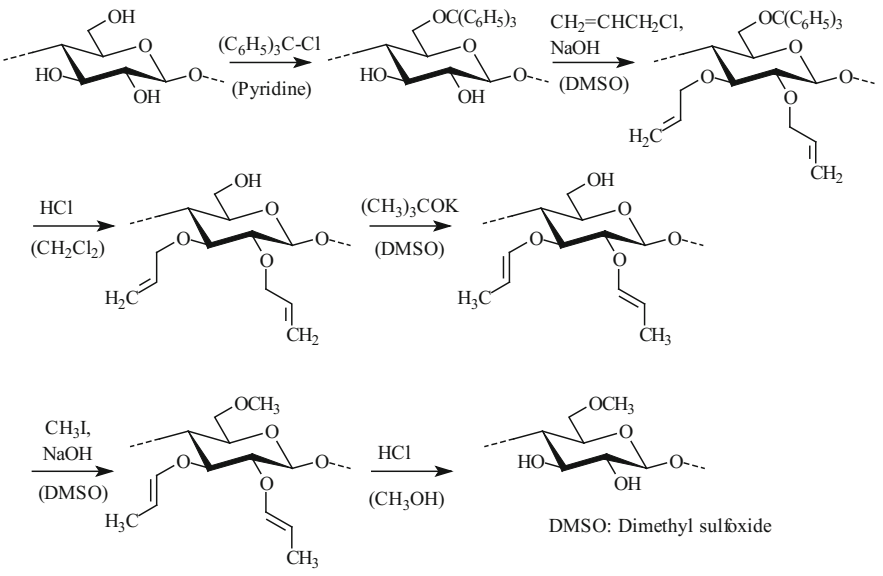


**Fig. 4.15** Preparation of 6-*O*-methyl cellulose [96]

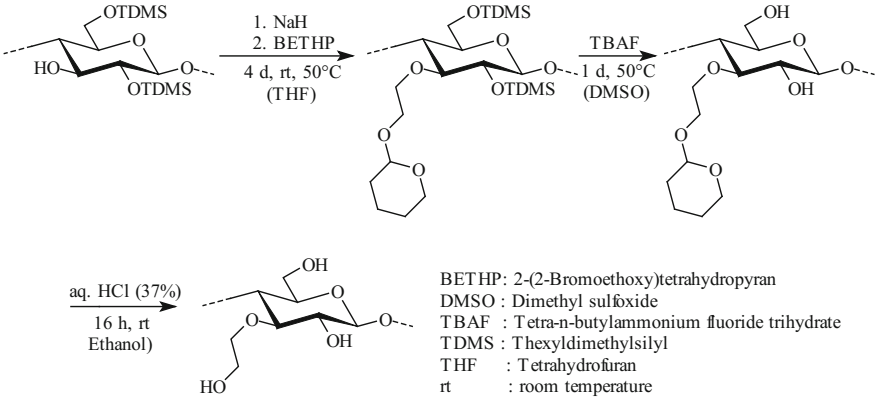


**Fig. 4.16** Preparation of 3-mono-*O*-hydroxyethyl cellulose from 2,6-di-*O*-thexyldimethylsilyl cellulose via orthogonal protecting groups. Adapted from [113]

The ether moiety regioselectively introduced at position 3 can be used as protecting group itself. Despite the stability of the alkyl ethers, allyl groups can be easily removed, e.g., by isomerization to the 1-propenyl ether followed by acidic cleavage [96] or by a palladium-catalyzed hydrogenolysis reaction [128]. This makes the allyl ether a valuable protection group. Methylation of 3-mono-*O*-allyl cellulose and subsequent deallylation affords the corresponding 2,6-di-*O*-methylcellulose, which is not accessible by other polymer-analogous reactions. This derivative was found to be insoluble in organic solvents and in water, probably due to its high crystallinity.

The synthesis of 2-mono-*O*- and 3,6-di-*O*-cellulose ethers requires a sophisticated synthesis strategy applying several protecting groups [4]. 3-mono-*O*-Allyl cellulose prepared via 2,6-di-*O*-TDMS cellulose is the key intermediate for the preparation of 2-mono-*O*-methylcellulose. The allyl ether is tritylated at position 6, and methylated at position 2, before trityl and allyl groups were cleaved off. The synthesis of 3,6-di-*O*-methyl cellulose starts from 3-mono-*O*-methylcellulose as a key intermediate, that was tritylated at position 6, allylated at position 2, detritylated at position 6. The resulting polymer was then methylated at position 6 and de-allylated.

Based on the easily accessible 3-mono-*O*-allyl cellulose, Edgar et al. applied this scheme for the preparation of regioselectively functionalized cellulose esters [110]. Consequently, the cellulose ether was peracylated and de-allylated by a palladium-catalyzed reaction. Nevertheless, a feasible synthesis route for the preparation of 3-*O*-esters of cellulose is not realized up to now. Obviously, the bottleneck of this reaction is the cleavage of the protecting group, which interferes with the acyl moiety located at position 3.

## References


1. Siegmund G, Klemm D (2002) Cellulose sulfonates: preparation, properties, subsequent reactions. Polym News 27:84–90
2. Heinze T (2009) Hot topics in polysaccharide chemistry—selected examples. Macromol Symp 280:15–27
3. Heinze T, Koschella A, Brackhagen M, Engelhardt J, Nachtkamp K (2006) Studies on non-natural deoxyammonium cellulose. Macromol Symp 244:74–82
4. Nakagawa A, Ishizu C, Sarbova V, Koschella A, Takano T, Heinze T, Kamitakahara H (2012) 2-*O*-methyl- and 3,6-di-*O*-methyl-celluloses from natural cellulose: synthesis and structure characterization. Biomacromol 13:2760–2768
5. Fox SC, Li B, Xu D, Edgar KJ (2011) Regioselective esterification and etherification of cellulose: a review. Biomacromol 12:1956–1972
6. Heinze T, Koschella A (2005) Carboxymethyl ethers of cellulose and starch–A review. Macromol Symp 223:13–39
7. Steinmeier H (2004) Chemistry of cellulose acetylation. Macromol Symp 208:49–60
8. Philipp B, Schempp W (2009) Progress in cellulose research in the reflection of the Zellcheming cellulose symposium. Macromol Symp 280:4–14
9. Petzold K, Koschella A, Klemm D, Heublein B (2003) Silylation of cellulose and starch-selectivity, structure analysis, and subsequent reactions. Cellulose 10:251–269
10. Gericke M, Liebert T, El Seoud OA, Heinze T (2011) Tailored media for homogeneous cellulose chemistry: ionic liquid/co-solvent mixtures. Macromol Mater Eng 296:483–493
11. Heinze T, Gericke M (2013) Ionic liquids as solvents for homogeneous derivatization of cellulose: challenges and opportunities. In: Fang Z, Smith RL, Qi X (eds) Production of biofuels and chemicals with ionic liquids. Springer, Berlin, pp 107–144
12. Heinze T, Liebert T (2004) Chemical characteristics of cellulose acetate. Macromol Symp 208:167–237
13. Law RC (2004) Cellulose acetate in textile application. Macromol Symp 208:255–265
14. Malm CJ, Tanghe LO, Laird BC, Smith GD (1953) Relative rates of acetylation of the hydroxyl groups in cellulose acetate. J Am Chem Soc 75:80–84
15. Jain RK, Agnish SL, Lal K, Bhatnagar HL (1985) Reactivity of hydroxyl groups in cellulose towards chloro(p-tolyl)methane. Makromol Chem 186:2501–2512
16. Kwatra HS, Caruthers JM, Tao BY (1992) Synthesis of long chain fatty acids esterified onto cellulose via the vacuum-acid chloride process. Ind Eng Chem Res 31:2647–2651
17. Edgar KJ (2009) Direct synthesis of partially substituted cellulose esters. In: Edgar KJ, Heinze T, Buchanan CM (eds) Polysaccharide materials: performance by design, ACS Symp Ser 1017:213–229
18. Yan L, Li W, Qi Z, Liu S (2006) Solvent-free synthesis of cellulose acetate by solid superacid catalysis. J Polym Res 13:375–378
19. Edgar KJ, Pecorini TJ, Glasser WG (1998) Long-chain cellulose esters: preparation, properties, and perspective. ACS Symp Ser 688:38–60
20. Heinze T, Liebert TF, Pfeiffer KS, Hussain MA (2003) Unconventional cellulose esters: synthesis, characterization and structure-property relations. Cellulose 10:283–296
21. Ratanakamnuan U, Atong D, Aht-Ong D (2012) Cellulose esters from waste cotton fabric via conventional and microwave heating. Carbohydr Polym 87:84–94
22. Ramos LA, Assaf JM, El Seoud OA, Frollini E (2005) Influence of the supra-molecular structure and physico-chemical properties of cellulose on its dissolution in the lithium chloride/*N*,*N*-dimethylacetamide solvent system. Biomacromol 6:2638–2647
23. El Seoud OA, Heinze T (2005) Organic esters of cellulose: new perspectives for old polymers. Adv Polym Sci 186:103–149
24. Trulove PC, Reichert WM, De Long HC, Kline SR, Rahatekar SS, Gilman JW, Muthukumar M (2009) The structure and dynamics of silk and cellulose dissolved in ionic liquids. ECS Trans 16:111–117

25. Kuzmina O, Sashina E, Troshenkowa S, Wawro D (2010) Dissolved state of cellulose in ionic liquids: the impact of water. Fibres Text East Eur 18:32–37
26. Ramos LA, Morgado DL, El Seoud AO, da Silva VC, Frollini E (2011) Acetylation of cellulose in LiCl-N, N-dimethylacetamide: first report on the correlation between the reaction efficiency and the aggregation number of dissolved cellulose. Cellulose 18:385–392
27. Sescousse R, Le KA, Ries ME, Budtova T (2010) Viscosity of cellulose imidazolium-based ionic liquid solutions. J Phys Chem B 114:7222–7228
28. Parviainen A, King AWT, Mutikainen I, Hummel M, Selg C, Hauru LKJ, Sixta H, Kilpeläinen I (2013) Predicting cellulose solvating capabilities of acid-base conjugate ionic liquids. Chemsuschem 6:2161–2169
29. Olsson C, Westman G (2013) Wet spinning of cellulose from ionic liquid solutions-viscometry and mechanical performance. J Appl Polym Sci 127:4542–4548
30. Gericke M, Schlufter K, Liebert T, Heinze T, Budtova T (2009) Rheological properties of cellulose/ionic liquid solutions: from dilute to concentrated states. Biomacromol 10:1188–1194
31. Xu A, Zhang Y, Zhao Y, Wang J (2013) Cellulose dissolution at ambient temperature: role of preferential solvation of cations of ionic liquids by a cosolvent. Carbohydr Polym 92:540–544
32. Nawaz H, Pires PAR, Bioni TA, Arêas EPG, El Seoud OA (2014) Mixed solvents for cellulose derivatization under homogeneous conditions: kinetic, spectroscopic, and theoretical studies on the acetylation of the biopolymer in binary mixtures of an ionic liquid and molecular solvents. Cellulose 21:1193–1204
33. Marson GA, El Seoud OA (1999) A Novel, efficient procedure for acylation of cellulose under homogeneous solution conditions. J Appl Polym Sci 74:1355–1360
34. Fidale LC, Possidonio S, El Seoud OA (2009) Application of 1-allyl-3-(1-butyl)imidazolium chloride in the synthesis of cellulose esters: properties of the ionic liquid, and comparison with other solvents. Macromol Biosci 9:813–821
35. Gericke M, Fardim P, Heinze T (2012) Ionic liquids—Promising but challenging solvents for homogeneous derivatization of cellulose. Molecules 17:7458–7502
36. Strlic M, Kolar J (2003) Size exclusion chromatography of cellulose in LiCl/*N*,*N*-dimethylacetamide. J Biochem Biophys Methods 56:265–279
37. Wang Z, Yokoyama T, Chang H-M, Matsumoto Y (2009) Dissolution of beech and spruce milled woods in LiCl/DMSO. J Agric Food Chem 57:6167–6170
38. Kostag M, Liebert T, El Seoud OA, Heinze T (2013) Efficient cellulose solvent: quaternary ammonium chlorides. Macromol Rapid Commun 34:1580–1584
39. Amigues E, Hardacre C, Keane G, Migaud M, O'Neill M (2006) Ionic liquids—media for unique phosphorus chemistry. Chem Commun 1:72–74
40. Regiani AM, Frollini E, Marson GA, Arantes GM, El Seoud OA (1999) Some aspects of acylation of cellulose under homogeneous solution conditions. J Polym Sci Part A 37:1357–1363
41. Possidonio S, Fidale LC, El Seoud AO (2010) Microwave-assisted derivatization of cellulose in an ionic liquid: an efficient, expedient synthesis of simple and mixed carboxylic esters. J Polym Sci Part A 48:134–143
42. Koehler S, Heinze T (2007) New solvents for cellulose: dimethyl sulfoxide/ammonium fluorides. Macromol Biosci 7:307–314
43. Duchemin BJ-CZ, Newman RH, Staiger MP (2007) Phase transformations in microcrystalline cellulose due to partial dissolution. Cellulose 14:311–320
44. Peres de Paula M, Lacerda TM, Frollini E (2008) Sisal cellulose acetates obtained from heterogeneous reactions. Express Polym Lett 2:423–428
45. Yang Z, Xu S, Ma X, Wang S (2008) Characterization and acetylation behavior of bamboo pulp. Wood Sci Technol 42:621–632
46. Diamantoglou M, Lemke HD, Vienken J (1994) Cellulose-ester as membrane materials for hemodialysis. Int J Artif Org 17:385–391

47. Heinze T, Liebert T, Koschella A (2006) Esterification of polysaccharides. Springer, Berlin, p 43
48. Klug ED, Tinsley JS (1950) Carboxyalkyl ethers of cellulose. US Patent 2,517,577, 08 Aug 1950
49. Broderick AE (1954) Hydroxyalkylation of polysaccharides. US Patent 2,682,535, 29 June 1954
50. Felcht UH, Perplies E (1983) Cellulose ethers with dimethoxyethane as a dispersing adjuvant. DE Patent 3,147,434 A1, 09 June 1983
51. Isogai A, Ishizu A, Nakano J (1984) Preparation of tri-*O*-benzylcellulose by the use of nonaqueous cellulose solvents. J Appl Polym Sci 29:2097–2109
52. Isogai A, Ishizu A, Nakano J (1984) Preparation of tri-*O*-substituted cellulose ethers by the use of a nonaqueous cellulose solvent. J Appl Polym Sci 29:3873–3882
53. Isogai A, Ishizu A, Nakano J (1986) Preparation of tri-*O*-alkylcelluloses by the use of a nonaqueous cellulose solvent and their physical characteristics. J Appl Polym Sci 31:341–352
54. Isogai A, Ishizu A, Nakano J (1987) Dissolution mechanism of cellulose in sulfur dioxide-amine-dimethyl sulfoxide. J Appl Polym Sci 33:1283–1290
55. Schaub M, Fakirov C, Schmidt A, Lieser G, Wenz G, Wegner G, Albouy PA, Wu H, Foster MD, Majrkzak C et al (1995) Ultrathin layers and supramolecular architecture of isopentylcellulose. Macromolecules 28:1221–1228
56. Fakirov C, Lieser G, Wegner G (1997) Chain conformation and packing of isopentyl cellulose in thin films. Macromol Chem Phys 198:3407–3424
57. D'Aprano G, Henry C, Godt A, Wegner G (1998) Design, characterization, and processing of cellulose-S-acetyl: a precursor to an electroactive cellulose. Macromol Chem Phys 199:2777–2783
58. Petrus L, Gray DG, BeMiller JN (1995) Homogeneous alkylation of cellulose in lithium chloride/dimethyl sulfoxide solvent with dimsyl sodium activation. A proposal for the mechanism of cellulose dissolution in lithium chloride/DMSO. Carbohydr Res 268:319–323
59. Takaragi A, Minoda M, Miyamoto T, Liu HQ, Zhang LN (1999) Reaction characteristics of cellulose in the lithium chloride/1,3-dimethyl-2-imidazolidinone solvent system. Cellulose 6:93–102
60. Takahashi S, Fujimoto T, Miyamoto T, Inagaki H (1987) Relationship between distribution of substituents and water solubility of O-methyl cellulose. J Polym Sci Part A Polym Chem 25:987–994
61. Nojiri M, Kondo T (1996) Application of regioselectively substituted methylcelluloses to characterize the reaction mechanism of cellulase. Macromolecules 29:2392–2395
62. Itagaki H, Takahashi I, Natsume M, Kondo T (1994) Gelation of cellulose whose hydroxyl groups are specifically substituted by the fluorescent groups. Polym Bull 32:77–81
63. Kondo T, Grey DG (1991) The preparation of O-methyl- and O-ethylcelluloses having controlled distribution of substituents. Carbohydr Res 220:173–183
64. Kern H, Choi S, Wenz G (1998) New functional derivatives from 2,3-di-O-alkyl-celluloses. Polym Prepr (Am Chem Soc Div Polym Chem) 39:80–81
65. Harkness BR, Gray DG (1990) Left- and right-handed chiral nematic mesophase of (trityl)(alkyl)cellulose derivatives. Can J Chem 68:1135–1139
66. Landoll LM (1982) Nonionic polymer surfactants. J Polym Sci Polym Chem Ed 20:443–455
67. Schulz DN, Block J, Valint PL Jr (1994) Synthesis and characterization of hydrophobically associating water-soluble polymers. In: Dubin P, Bock J, Davis R, Schulz DN, Thies C (eds) Macromolecular Complexes in Chemistry and Biology. Springer, Heidelberg, pp 3–13
68. Tanaka R, Meadows J, Williams PA, Philips GO (1992) Interaction of hydrophobically modified hydroxyethyl cellulose with various added surfactants. Macromolecules 25:1304–1310
69. Tanaka R, Meadows J, Phillips GO, Williams PA (1990) Viscometric and spectroscopic studies on the solution behavior of hydrophobically modified cellulosic polymers. Carbohydr Polym 12:443–459

70. Landoll LM (1979) Cellulose derivatives. US Patent 4,228,277 (Hercules)
71. Sau AC, Landoll LM (1989) Synthesis and solution properties of hydrophobically modified (hydroxyethyl) cellulose. In: Glass JE (ed) Polymers in Aqueous Media, vol 223. American Chemical Society, Washington, DC, pp 343–364
72. Höfer R, Schulte HG, Schmitz J (2007) In Kittel H, Ortelt M (eds) Rheologie in Farben und Lacken, 2nd ed. Lehrbuch der Lacke und Beschichtungen, Bd. 4. S. Hirzel Verlag, Stuttgart
73. Um S-U, Poptoshev E, Pugh RJ (1997) Aqueous solutions of ethyl (hydroxyethyl) cellulose and hydrophobic modified ethyl (hydroxyethyl) cellulose polymer: dynamic surface tension measurements. J Colloid Interface Sci 193:41–49
74. Schempp W, Krause T, Seifried U, Koura A (1984) Production of highly substituted trimethylsilyl celluloses in the system dimethylacetamide/lithium chloride. Papier (Darmstadt) 38:607–610
75. Weigel P, Gensrich J, Wagenknecht W (1996) Model investigations on the effect of an intermediate derivatization on structure and properties of regenerated cellulose filaments. Papier (Darmstadt) 50:483–490
76. Nicholson MD, Merritt FM (1985) Cellulose ethers. In: Nevell TP, Zeronian SH (eds) Cellulose Chemistry, its application. Horwood Publ., Chichester, pp 363–383
77. Nishio N, Takano T, Kamitakahara H, Nakatsubo F (2005) Preparation of high regioselectively mono-substituted carboxymethyl celluloses. Cellul Chem Technol 39:377–387
78. Karakawa M, Nakai S, Kamitakahara H, Takano T, Nakatsubo F (2007) Preparation of highly regioregular O-methylcelluloses and their water solubility. Cellul Chem Technol 41:569–573
79. Kamitakahara H, Funakoshi T, Nakai S, Takano T, Nakatsubo F (2009) Syntheses of 6-O-ethyl/methyl-celluloses via ring-opening copolymerization of 3-O-benzyl-6-O-ethyl/methyl-α-D-glucopyranose 1,2,4-orthopivalates and their structure-property relationships. Cellulose 16:1179–1185
80. Kamitakahara H, Funakoshi T, Takano T, Nakatsubo F (2009) Syntheses of 2,6-O-alkyl celluloses: influence of methyl and ethyl groups regioselectively introduced at O-2 and O-6 positions on their solubility. Cellulose 16:1167–1178
81. Kamitakahara H, Funakoshi T, Nakai S, Takano T, Nakatsubo F (2010) Synthesis and structure/property relationships of regioselective 2-O-, 3-O- and 6-O-ethyl celluloses. Macromol Biosci 10:638–647
82. Philipp B, Wagenknecht W, Wagenknecht M, Nehls I, Klemm D, Stein A, Heinze T, Heinze U, Helbig K (1995) Regioselective esterification and etherification of cellulose and cellulose derivatives. 1. Problems and description of the reaction systems. Papier (Bingen) 49:3–7
83. Koschella A, Fenn D, Illy N, Heinze T (2006) Regioselectively functionalized cellulose derivatives: a mini review. Macromol Symp 244:59–73
84. Deus C, Friebolin H, Siefert E (1991) Partially acetylated cellulose. Synthesis and determination of the substituent distribution via proton NMR spectroscopy. Makromol Chem 192:75–83
85. Wagenknecht W (1996) Regioselectively substituted cellulose derivatives by modification of commercial cellulose acetates. Papier (Darmstadt) 50:712–720
86. Altaner C, Saake B, Tenkanen M, Eyzaguirre J, Faulds CB, Biely P, Viikari L, Siika-aho M, Puls J (2003) Regioselective deacetylation of cellulose acetates by acetyl xylan esterases of different CE-families. J Biotechnol 105:95–104
87. Xu D, Edgar KJ (2012) TBAF and cellulose esters: unexpected deacylation with unexpected regioselectivity. Biomacromol 13:299–303
88. Zheng X, Gandour RD, Edgar KJ (2014) Remarkably regioselective deacylation of cellulose esters using tetraalkylammonium salts of the strongly basic hydroxide ion. Carbohydr Polym 111:25–32
89. Elschner T, Ganske K, Heinze T (2013) Synthesis and aminolysis of polysaccharide carbonates. Cellulose 20:339–353

90. Xu D, Li B, Tate C, Edgar KJ (2011) Studies on regioselective acylation of cellulose with bulky acid chlorides. Cellulose 18:405–419
91. Camacho Gomez JA, Erler UW, Klemm DO (1996) 4-methoxy substituted trityl groups in 6-O protection of cellulose: homogeneous synthesis, characterization, detritylation. Macromol Chem Phys 197:953–964
92. Iwata T, Azuma J, Okamura K, Muramoto M, Chun B (1992) Preparation and N.M.R. assignments of cellulose mixed esters regioselectively substituted by acetyl and propanoyl groups. Carbohydr Res 224:277–283
93. Hsieh C-WC, Kadla JF (2012) Effect of regiochemistry on the viscoelastic properties of cellulose acetate gels. Cellulose 19:1567–1581
94. Heinze T, Vieira M, Heinze U (2000) New polymers based on cellulose. Lenzinger Ber 79:39–44
95. Petzold-Welcke K, Kotteritzsch M, Heinze T (2010) 2,3-O-Methyl cellulose: studies on synthesis and structure characterization. Cellulose 17:449–457
96. Kondo T (1993) Preparation of 6-O-alkylcelluloses. Carbohydr Res 238:231–240
97. Heinze T, Röttig K, Nehls I (1994) Synthesis of 2,3-O-carboxymethylcellulose. Macromol Rapid Comm 15:311–317
98. Heinze U, Heinze T, Klemm D (1999) Synthesis and structure characterization of 2,3-O-carboxymethylcellulose. Macromol Chem Phys 200:896–902
99. Liu H-Q, Zhang L-N, Takaragi A, Miyamoto T (1997) Water solubility of regioselectively 2,3-O-substituted carboxymethylcellulose. Macromol Rapid Comm 18:921–925
100. Schaller J, Heinze T (2005) Studies on the synthesis of 2,3-O-hydroxyalkyl ethers of cellulose. Macromol Biosci 5:58–63
101. Larsen FH, Schobitz M, Schaller J (2012) Hydration properties of regioselectively etherified celluloses monitored by 2H and 13C solid-state MAS NMR spectroscopy. Carbohydr Polym 89:640–647
102. Halake KS, Choi S-Y, Hong SM, Seo SY, Lee J (2013) Regioselective substitution of 2-isocyanatoethyl methacrylate onto cellulose. J Appl Polym Sci 128:2056–2062
103. Ifuku S, Kamitakahara H, Takano T, Tanaka F, Nakatsubo F (2004) Preparation of 6-O-(4-alkoxytrityl)celluloses and their properties. Org Biomol Chem 2:402–407
104. Klemm D, Stein A (1995) Silylated cellulose materials in design of supramolecular structures of ultrathin cellulose films. J Macromol Sci Part A Pure Appl Chem A32:899–904
105. Koschella A, Klemm D (1997) Silylation of cellulose regiocontrolled by bulky reagents and dispersity in the reaction media. Macromol Symp 120:115–125
106. Fenn D, Pfeifer A, Heinze T (2007) Studies on the synthesis of 2,6-di-O-thexyldimethylsilyl cellulose. Cellul Chem Technol 41:87–91
107. Pawlowski WP, Sankar SS, Gilbert RD, Fornes RE (1987) Synthesis and solid state 13C-NMR studies of some cellulose derivatives. J Polym Sci Part A Polym Chem 25:3355–3362
108. Klemm D, Schnabelrauch M, Stein A, Philipp B, Wagenknecht W, Nehls I (1990) Recent results from homogeneous esterification of cellulose using soluble intermediate compounds. Papier (Bingen) 44:624–632
109. Heinze T, Pfeifer A, Petzold K (2008) Functionalization pattern of tert-butyldimethylsilyl cellulose evaluated by NMR spectroscopy. BioResources 3:79–90
110. Xu D, Voiges K, Elder T, Mischnick P, Edgar KJ (2012) Regioselective synthesis of cellulose ester homopolymers. Biomacromolecules 13:2195–2201
111. Koschella A, Heinze T, Klemm D (2001) First synthesis of 3-O-functionalized cellulose ethers via 2,6-di-O-protected silyl cellulose. Macromol Biosci 1:49–54
112. Koschella A, Fenn D, Heinze T (2006) Water soluble 3-mono-O-ethyl cellulose: synthesis and characterization. Polym Bull 57:33–41
113. Fenn D, Heinze T (2009) Novel 3-mono-O-hydroxyethyl cellulose: synthesis and structure characterization. Cellulose 16:853–861
114. Heinze T, Koschella A (2008) Water-soluble 3-O-methoxyethyl cellulose: synthesis and characterization. Carbohydr Res 343:668–673

115. Schumann K, Pfeifer A, Heinze T (2009) Novel cellulose ethers: synthesis and structure characterization of 3-mono-O-(3'-hydroxypropyl) cellulose. Macromol Symp 280:86–94
116. Heinze T, Pfeifer A, Sarbova V, Koschella A (2011) 3-O-Propyl cellulose: cellulose ether with exceptionally low flocculation temperature. Polym Bull 66:1219–1229
117. Fenn D, Pohl M, Heinze T (2009) Novel 3-O-propargyl cellulose as a precursor for regioselective functionalization of cellulose. React Funct Polym 69:347–352
118. Illy N (2006) Regioselective cellulose functionalization: characterization and properties of 3-O-cellulose ethers. Diploma Thesis, Friedrich Schiller University of Jena
119. Petzold K, Klemm D, Heublein B, Burchard W, Savin G (2004) Investigations on structure of regioselectively functionalized celluloses in solution exemplified by using 3-O-alkyl ethers and light scattering. Cellulose 11:177–193
120. Bar-Nir BB, Kadla JF (2009) Synthesis and structural characterization of 3-O-ethylene glycol functionalized cellulose derivatives. Carbohydr Polym 76:60–67
121. Kadla JF, Asfour FH, Bar-Nir B (2007) Micropatterned thin film honeycomb materials from regiospecifically modified cellulose. Biomacromol 8:161–165
122. Xu WZ, Zhang X, Kadla JF (2012) Design of functionalized cellulosic honeycomb films: site-specific biomolecule modification via "click chemistry". Biomacromol 13:350–357
123. Sun S, Foster TJ, MacNaughtan W, Mitchell JR, Fenn D, Koschella A, Heinze Th (2009) Self-association of cellulose ethers with random and regioselective distribution of substitution. J Polym Sci Part B Polym Phys 47:1743–1752
124. Heinze T, Wang Y, Koschella A, Sullo A, Foster TJ (2012) Mixed 3-mono-O-alkyl cellulose: synthesis, structure characterization and thermal properties. Carbohydr Polym 90:380–386
125. Sullo A, Wang Y, Mitchell JR, Koschella A, Heinze Z, Foster TJ (2012) New regioselective substituted cellulose ethers: thermo-rheological study. Special publication—Royal Society of Chemistry 335 (Gums Stab Food Ind 16:45–57)
126. Petzold-Welcke K, Koetteritzsch M, Fenn D, Koschella A, Heinze T (2010) Study on synthesis and NMR characterization of 2,3-O-hydroxyethyl cellulose depending on synthesis conditions. Macromol Symp 294:133–140
127. Arisawa M, Kato C, Kaneko H, Nishida A, Nakagawa M (2000) Concise synthesis of azacycloundecenes using ring-closing metathesis (RCM). J Chem Soc Perkin Trans 1:1873–1876
128. Kamitakahara H, Koschella A, Mikawa Y, Nakatsubo F, Heinze T, Klemm D (2008) Syntheses and comparison of 2,6-Di-O-methyl celluloses from natural and synthetic celluloses. Macromol Biosci 8:690–700

# Chapter 5
# Cellulose Esters

## 5.1 Esters of Carboxylic Acids

### *5.1.1 Industrial Preparation of Cellulose Esters*

The commercial process of cellulose esterification with acid anhydrides in the presence of catalysts (mineral acids) is exclusively carried out under heterogeneous reaction conditions. Cellulose acetate (CA) is industrially prepared by using either acetic acid or an organic solvent, e.g., dichloromethane as medium. In both processes, the biopolymer is dried to a moisture content of 4–7%. Lower values lead to decreased biopolymer reactivity; higher moisture content leads to increased consumption of acetic acid, and product degradation due to the fast, highly exothermic start of the reaction. After drying, the biopolymer is subjected to pretreatment usually by acetic acid or its mixture with small concentration of sulfuric acid. This pretreatment causes some swelling of cellulose, and hence increases its accessibility. Depending on process conditions, in particular the temperature, the reaction requires from one to several hours; the acetic acid/cellulose ratio employed range from 0.3 to 1.

In the "acetic acid process", cellulose is swollen with acetic acid/mineral acid catalyst (2–15% on cellulose) and then reacts with acetic anhydride (10–40% excess on cellulose). Esterification begins after the initial reaction of the water contained in cellulose with a fraction of the anhydride. The semi-liquid mass, uniformly saturated with the acetylation mixture, forms a fiber pulp (with temperature increase to about 50 °C), and ultimately a highly viscous system. One accepted mechanism involves the formation of mixed acetic–sulfuric acid anhydride (so-called "acetyl-sulfuric" acid, Fig. 5.1). Cellulose reacts with the later or with the acylium ion formed by its dissociation, to give the product. This mechanism explains the formation of some cellulose sulfate; this functional group is either largely substituted by acetate or is hydrolyzed during product workup [1–4].



T. Heinze et al., *Cellulose Derivatives*, Springer Series on Polymer and Composite Materials, https://doi.org/10.1007/978-3-319-73168-1_5

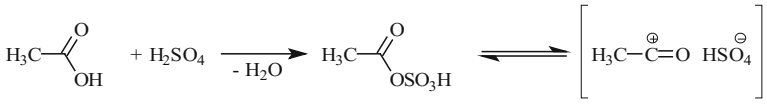


**Fig. 5.1** Formation and partial dissociation of the mixed acetic–sulfuric anhydride

The process variables are sulfuric acid concentration, reaction time, and temperature. In the medium (4–8%) and high (11–15%) catalyst processes, sulfuric acid acts as a solvating agent and confers enhanced solubility at the cellulose triacetate state. However, high catalyst concentration leads to cellulose degradation, so that these processes require lower temperatures (secured by cooling the reaction vessel) compared to low catalyst (<2%) counterpart. The reaction is topo-chemical wherein successive layers of the cellulose fibers react; the produced ester is "peeled off" due to its solubility in the medium. Perchloric acid is also employed as a catalyst for this reaction. It does not form mixed anhydrides with carboxylic acids; hence, the products are free of inorganic ester moieties.

At the end of the reaction, the solution is free of fibers. The degradation of the cellulose ester is left to proceed until the desired viscosity is reached (commercial CAs have DP in the range 100–360). Water is then added in order to terminate the reaction. Its content is adjusted to 5–10% (w/w) so that, aside from hydrolysis of the acetic anhydride present, no further decrease of the product molar mass occurs. At the same time, the bound sulfuric acid is almost completely hydrolyzed. The speed of hydrolysis depends on the temperature, which ranges from 40 to 80 °C, and on the concentrations of sulfuric acid and water in the medium.

In the methylene chloride (Dormagen) process, the chlorinated solvent substitutes acetic acid. Using DCM presents several advantages due to the fact that it is a solvent for cellulose triacetate. Thus, lower catalyst concentrations (ca. 1% sulfuric acid) are required. Furthermore, due to its low boiling point (41 °C), a part of the reaction heat is removed, leading to solvent reflux. The reaction of highly viscous solutions can thus be better controlled. Finally, only a half to a third as much dilute acetic acid must be recycled compared with the glacial acetic acid process.

Cellulose can be also esterified while maintaining its fibrous structure by adding sufficient amounts of a non-solvent to the triacetate during acetylation. The completely heterogeneous (non-solvent) process has been discontinued industrially.

Cellulose acetate with high DS (about 2.9) is partially hydrolyzed in one-pot procedure in order to obtain the acetone-soluble "diacetate" (acetate content ca. 40%, DS 2.4–2.6) that is employed for spinning or shaping processes in acetone. The reasons for not attempting the direct synthesis of CA by the heterogeneous process have been discussed in Chap. 4.

Mixed esters of different partial DS of each acyl moiety, in particular cellulose acetate/propionate and acetate/butyrate, have favorable properties, in particular thermal behavior and solubility that are not exhibited by their simple counterparts. They are prepared commercially by processes similar to that of the CA, i.e., by the reaction of the biopolymer with both anhydrides simultaneously. As shown

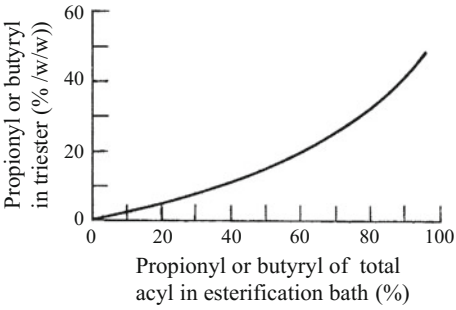


**Fig. 5.2** Composition of cellulose acetate butyrate (propionate) as a function of butyryl (propionyl) content of esterification bath

qualitatively [5, 6] and quantitatively, however, as studied under homogeneous reaction conditions [7], the order of reactivity of these anhydrides toward cellulose is acetic anhydride > propionic anhydride > butyric anhydride. This is in agreement with the effect of increasing the concentration of propionic or butyric anhydride on the composition of the corresponding mixed esters with acetate (Fig. 5.2).

## *5.1.2 Laboratory Synthesis of Cellulose Carboxylic Esters*

### 5.1.2.1 Heterogeneous Procedures

The simplest method is to react cellulose with the acylating agent without any solvent. Although direct esterification with carboxylic acids is inefficient, acyl chlorides have been employed, e.g., for the esterification of mercerized cotton under reduced pressure in order to remove the HCl produced. Thus, palmitates with DS of up to 2.5 were obtained [8]. Although simple, this method is limited by the tendency of the HCl formed to cause degradation of the biopolymer chain. Furthermore, the reaction does not proceed past DS 1.5 unless 10 equivalents of the acyl chloride are employed; the cellulose esters obtained are insoluble in organic solvents [9].

Esterification is carried out in the presence of a tertiary amine base, e.g., Py, DMAP, or TEA. These bases have several purposes: they enhance the reactivity of cellulose due to base-mediated swelling; they suppress biopolymer degradation by neutralizing the formed carboxylic acid (applying acid anhydrides) or HCl (acid chlorides). Moreover, they increase the reaction efficiency by transforming the acylating agent into more reactive species, namely the acylium ion, by a nucleophilic catalysis mechanism, as schematically shown in Fig. 5.3. The higher efficiency of DMAP relative to Py results from the extra resonance stabilization of the acylium ion [10]. The reaction conditions influence the results as shown by acylation of cellulose with propanoyl chloride in the presence of Py at 100 °C (Table 5.1).

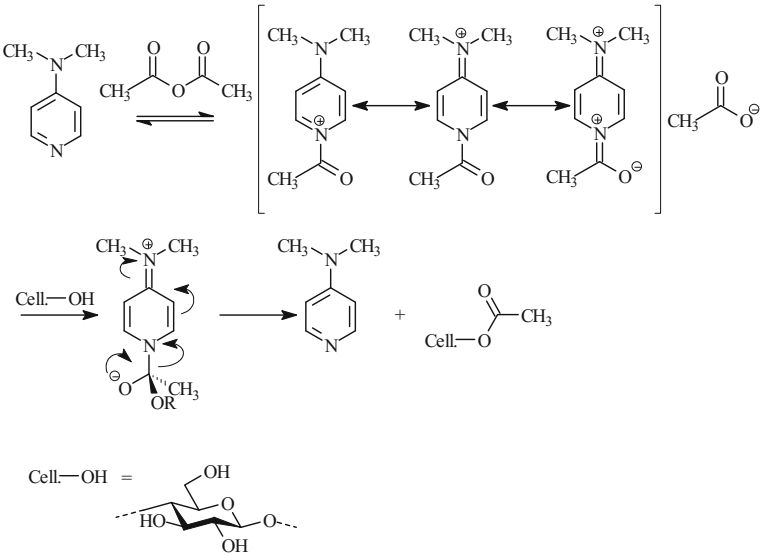

**Fig. 5.3** Formation and resonance stabilization of acetyl(4-*N*,*N*-dimethylamino)pyridinium acetate, and cellulose acetylation therefrom

Cellulose esterification with acyl chloride/pyridine mixture is industrially impracticable due to the high cost of the acylating agent, which is corrosive, as well as to the need to purify the product, e.g., to remove pyridinium chloride. Py represents the slurry medium (combined with swelling of the cellulose) and the acylation catalyst. The increase of the Py/RCOCl ratio above about 1 is not reflected in

**Table 5.1** DS and solubility of CA after acylation of cellulose in Py with propionyl chloride of different molar ratios at 100 °C for 4 h (adapted from [11], reprinted from esterification of polysaccharides, Chap. 4, with permission from Springer)

| Molar ratio | | | Product | |
|---|---|---|---|---|
| AGU | Py | Propionyl chloride | DS | Solubility in $Cl_2CHCHCl_2$ |
| 1 | 27.6 | 4.5 | 1.86 | − |
| 1 | 18.9 | 6.0 | 2.66 | + |
| 1 | 12.0 | 6.0 | 2.80 | + |
| 1 | 12.0 | 4.5 | 2.70 | + |
| 1 | 9.9 | 9.0 | 2.13 | + |
| 1 | 7.5 | 6.0 | 2.89 | + |
| 1 | 6.0 | 4.5 | 2.81 | + |
| 1 | 4.8 | 4.5 | 2.86 | + |
| 1 | 3.0 | 4.5 | 2.89 | + |
| 1 | 1.5 | 4.5 | 2.84 | + |

reaction efficiency, as determined by the value of DS. According to Fig. 5.3 acetyl (4-*N*,*N*-dimethylamino)pyridinium acetate acts as catalyst provided that the ratio Py/RCOCl is slightly above 1. However, the Py is consumed in neutralizing the acid formed (HCl). The presence of excess base can be problematic for several reasons. In the presence of adventitious water, deacylation of the ester formed may occur, e.g., by a general base-catalyzed mechanism of water attack on the ester acyl. Moreover, base-mediated enolization of the ester group may occur, and the enolate formed may add to the acylium ion, leading to the formation of β-ketoesters, as shown in Fig. 5.4.

The results summarized in Tables 5.2 and 5.3 indicate that the use of additional organic slurry media is efficient for the synthesis of short- and long-chain carboxylic esters in terms of DS.

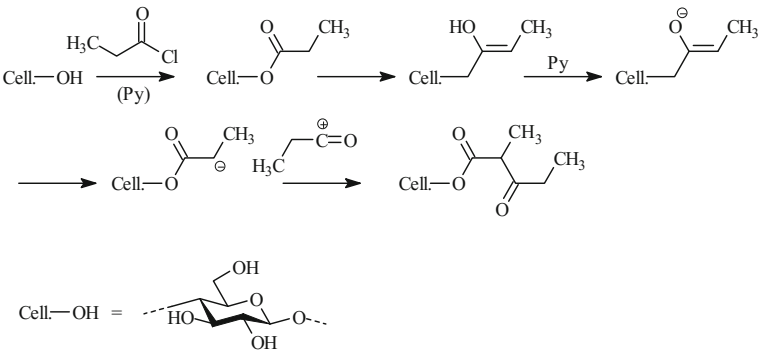


**Fig. 5.4** Base mediated formation of β-ketoesters

**Table 5.2** Cellulose propionylation with different diluents and tertiary amines using 1.5 mol propionyl chloride/mol AGU at 100 °C (reprinted from [12], with permission from Springer)

| Conditions | | | Product |
|---|---|---|---|
| Medium | Base | Time (h) | DS |
| Dioxane | Py | 4 | 2.81 |
| Dioxane | β-picoline | 4 | 2.70 |
| Dioxane | Quinoline | 4 | 2.18 |
| Dioxane | Dimethylaniline | 48 | 1.57 |
| Dioxane | γ-picoline | 24 | Negligible |
| Chlorobenzene | Py | 4 | 2.86 |
| Toluene | Py | 4 | 2.30 |
| Tetrachloroethane | Py | 24 | 2.23 |
| Ethyl propionate | Py | 5 | 2.16 |
| Isophorone | Py | 4 | 1.89 |
| Ethylene formal | Py | 22 | 0.34 |
| Propionic acid | Py | 5 | 0.20 |
| Dibutyl ether | Py | 22 | Negligible |

**Table 5.3** Polysaccharide esters synthesized in slurry containing an inert organic solvent and Py and using acid chlorides

| Polysaccharide | Fatty acid moiety | Molar ratio | | | Organic liquid | Time (h) | Temp. (° C) | DS | References |
|---|---|---|---|---|---|---|---|---|---|
| | | AGU | FACl | Py | | | | | |
| Cellulose | Pentanoate | 1 | 4.5 | 1.0 | Dioxane | 17 | 80 | 2.1 | [13] |
| Cellulose | Hexanoate | 1 | 4.5 | 1.0 | Dioxane | 17 | 80 | 2.5 | [13] |
| Cellulose | Octanoate | 1 | 4.5 | 1.0 | Dioxane | 17 | 80 | 2.4 | [13] |
| Cellulose | Nonanoate | 1 | 4.5 | 1.0 | Dioxane | 17 | 80 | 2.4 | [13] |
| Dextran | Palmitate | 1 | 3.0 | 8.0 | Toluene | 1.5 | 105 | 2.9 | [14] |

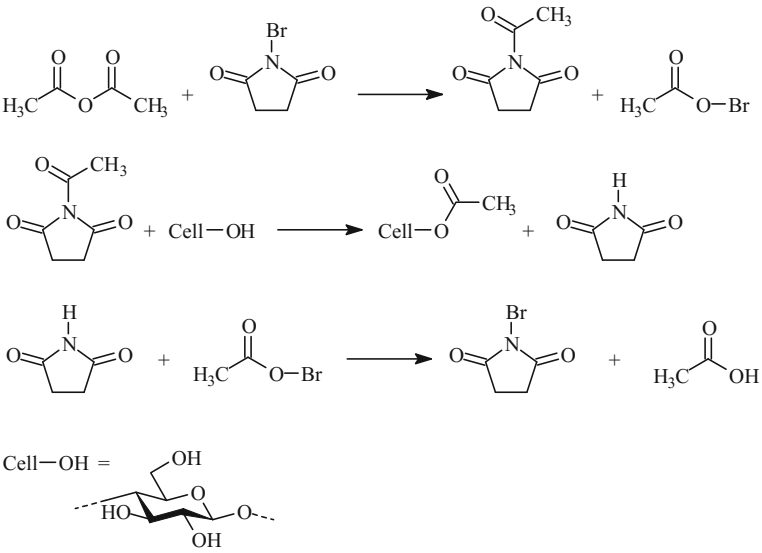


**Fig. 5.5** Proposed mechanism for the acetylation of polysaccharides with *N*-bromosuccinimide as catalyst

The esterification with carboxylic acid anhydrides has been employed, e.g., in the presence of toluene sulfonic acid and *N*-methylimidazole. Another transformation includes the reaction of an acid anhydride with *N*-bromosuccinimide, leading to the formation of *N*-acyl succinimide that reacts with cellulose with a two-step regeneration of the catalyst, as shown in Fig. 5.5.

There are several examples, where the leaving abilities of the two moieties of the mixed anhydride are distinctly different leading to efficient synthesis of a single cellulose carboxylic ester. The reaction of carboxylic acids with reactive anhydrides, e.g., chloroacetyl, methoxyacetyl, and, more importantly, trifluoroacetyl groups, produces asymmetric anhydrides, where the leaving ability of one of the groups is distinctly better than the other, leading to production of essentially one ester (impeller method). The following example shows the production of cellulose

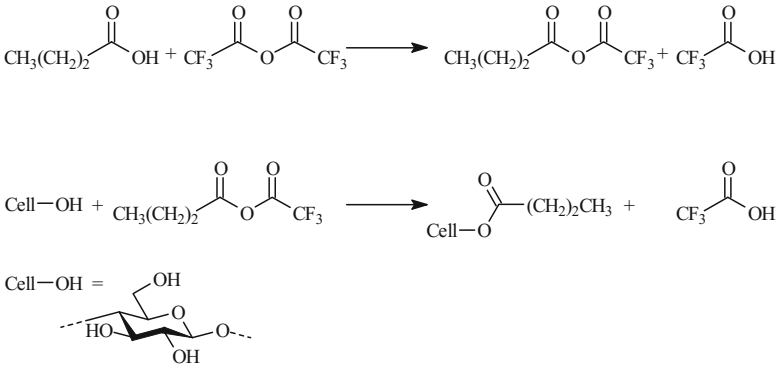


**Fig. 5.6** Acylation of polysaccharides via reactive mixed anhydrides (impeller method)

butyrate by the reaction of the biopolymer with the intermediate butyric-trifluoroacetic anhydride [5, 6] (Fig. 5.6). Although cellulose attack on both acyl groups of the asymmetric anhydride is possible; decomposition of the tetrahedral intermediate with leaving of TFA ($pK_a$ 0.23) is much more favorable than the alternative route, involving leaving of butyric acid ($pK_a$ 4.82).

Cellulose esters of high DS of both short- and long-chain carboxylic acids have been obtained by reacting dried cellulose with a solution of preformed RCO–O–$COCF_3$; the results obtained are summarized in Table 5.4 [15].

In the following chapter, efficient, however, up to now lab-scale, homogeneous paths of the introduction of ester moieties into cellulose are discussed. These paths are based on reactions starting with the dissolved biopolymer.

### 5.1.2.2 Synthesis of Cellulose Esters Applying Derivatizing Solvents

An approach to cellulose derivatization is to dissolve the biopolymer in a derivatizing solvent, introduce the desired functional group, and then remove the (solvent-based) functional group that is responsible for solubilization of the biopolymer. As discussed before (Chap. 3.2), certain solvents dissolve cellulose because the solvent-originated group disrupts hydrogen bonding within the biopolymer by a combination of steric interactions and decrease of the number of OH groups. Examples are (solvent system, cellulose derivative formed) $N_2O_4$/DMF, nitrite; $HCO_2H/H_2SO_4$, formate; $F_3CCOOH$, trifluoroacetate; paraformaldehyde/DMSO, hydroxymethyl; $ClSi(CH_3)_3$, trimethysilyl.

#### Cellulose Trifluoroacetate and -Formate

The importance of using cellulose dissolved in formic acid or trifluoroacetic acid is the fact that it can be employed to get products with an inverse pattern of

**Table 5.4** DS and $M_w$ values for long-chain aliphatic acid esters of cellulose obtained by the impeller method applying TFAA (adapted from [15])

| Acid moiety | Number of Carbons | DS | $M_w$ ($10^5$ g/mol) |
|---|---|---|---|
| Acetate | 2 | 2.8 | – |
| Propionate | 3 | 3.0 | 1.48 |
| Butyrate | 4 | 2.8 | 1.77 |
| Valerate | 5 | 2.8 | 2.15 |
| Hexanoate | 6 | 2.8 | 2.15 |
| Enanthate | 7 | 3.0 | 2.07 |
| Octanoate | 8 | 2.8 | 2.03 |
| Pelargonate | 9 | 2.9 | 3.54 |
| Decanoate | 10 | 2.9 | 2.32 |
| Laurate | 12 | 2.9 | 2.18 |
| Myristate | 14 | 2.9 | 2.87 |
| Palmitate | 16 | 2.9 | 3.98 |
| Stearate | 18 | 2.9 | 6.91 |

functionalization, provided that special reaction conditions are needed. Mostly, the secondary OH groups may be functionalized resulting from the fact that the primary, i.e., more reactive, hydroxyl group is transformed into ester during cellulose dissolution. For instance, cellulose has been dissolved by esterification of OH group at position 6 of the AGU with TFA/TFAA and the product formed in the surplus of TFA is allowed to react with 4-nitrobenzoyl chloride, which occurs at the remaining secondary hydroxyl moieties (Fig. 5.7). Hydrolysis of the mixed ester resulted in removal of the (more labile) trifluoroacetate group, leading to AGU esterified in the (less reactive) secondary positions. As can be concluded from the NMR spectrum, a slight modification of the C6–OH occurred as well.

During dissolution of cellulose in TFA, the biopolymer undergoes partial trifluoroacetylation to a DS of up to 1.5 with a completely derivatized primary position [17, 18]. Cellulose was treated with TFA and TFAA and allowed to react with carboxylic anhydrides, namely acetic, propionic, and 3-nitrophthalic anhydride. Alternatively, the solution of cellulose trifluoroacetate was treated with acyl chlorides, e.g., acetyl, acroyl, cinnamoyl, benzoyl, and 4-nitrobenzoyl chloride. IR spectra of the reaction products indicated that partial transesterification has occurred. That is, some of the $CF_3CO$ groups present have been substituted by the (more basic) RCO moiety. The DS values of the products are about 1.4 ($F_3CCO$–), and 0.5–1.6 for the other RCO groups [19].

Another derivatizing solvent is formic acid. The dissolution of cellulose is faster in the presence of a mineral acid as catalyst with some degradation of the biopolymer chain [20]. $^{13}C$ NMR studies of the formates showed a clear preference for esterification of the primary OH groups of cellulose [21–23].

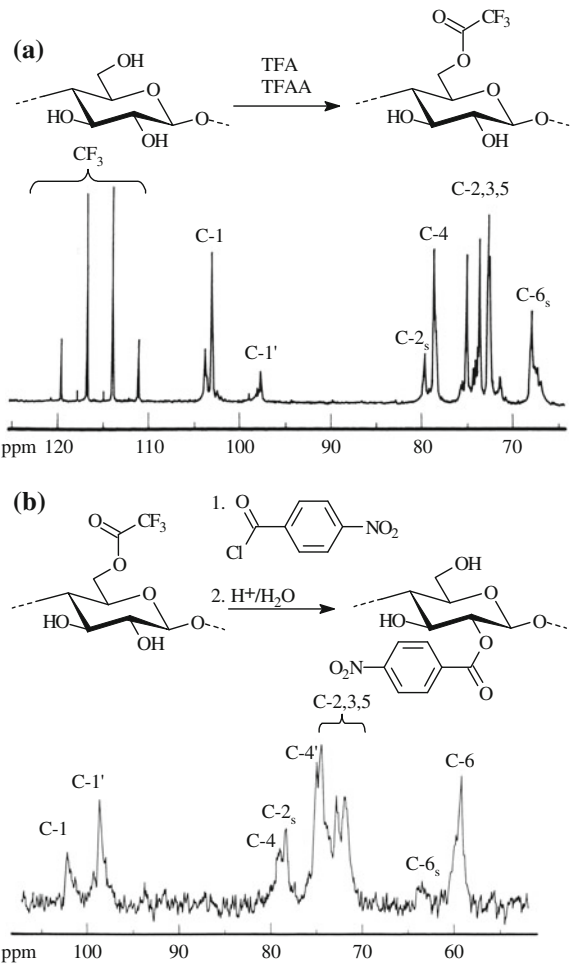


**Fig. 5.7** $^{13}C$ NMR spectrum of **a** cellulose trifluoroacetate (DS 1.50) and **b** cellulose nitrobenzoate (DS 0.76) obtained by subsequent esterification showing inverse patterns of functionalization (reprinted from [16], with permission from Springer)

## Methylol Cellulose

Cellulose dissolves in paraformaldehyde/dipolar aprotic solvent, including DMSO, DMAc, and DMF under formation of hydroxymethyl (methylol) moieties that may react further with formaldehyde resulting in cross-linking of cellulose chains [24–26] (Fig. 5.8). A similar hemiacetal is produced by the reaction of cellulose with chloral/DMF/Py. The product was allowed to react with $Ac_2O$ to give modified CA containing both acetate and $CH(OH)CCl_3$ that forms films from acetone. Different ratios of the groups were obtained by replacing DMF with DCM and Py with $HClO_4$ or $H_2SO_4$ [27].

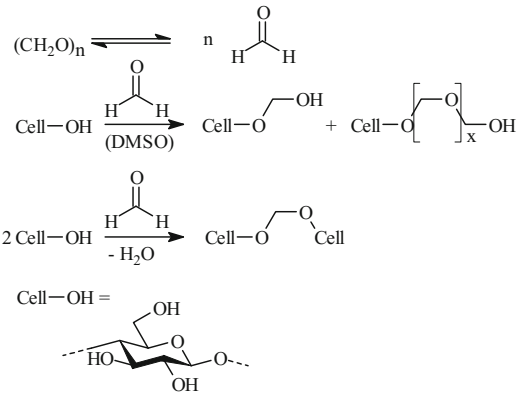


**Fig. 5.8** Dissolution and further reactions of cellulose in paraformaldehyde/DMSO

Methylol cellulose has been esterified, e.g., by acetic, butyric, and phthalic anhydride, as well as by unsaturated methacrylic and maleinic anhydride, in the presence of Py, or alkali metal acetates. DS values from 0.2 to 2.0 were obtained, being higher, 2.5 for CA. $^{1}$H– and $^{13}$C NMR spectroscopic data have indicated that the hydroxyl groups of the methylol chains are preferably esterified with the anhydrides. Dissolution of cellulose in this solvent system at 90 °C and treatment with methylene diacetate or ethylene diacetate in the presence of potassium acetate led to CA with DS of 1.5. DMAc or DMF can be substituted for DMSO [28–32].

Cellulose dissolved in paraformaldehyde/DMSO was allowed to react with trimethylacetic anhydride: 1,2,4-benzenetricarboxylic anhydride, trimellitic anhydride, and phthalic anhydride, in the presence of pyridine for 8 h at 80–100 °C, or 1 h at room temperature (trimellitic anhydride). The products are versatile compounds with interesting elastomeric and thermoplastic properties, and can be casted as films and membranes [33].

Acetic acid, acetyl chloride, and $Ac_2O$ were compared as acetylating agents for the reaction of cellulose dissolved in DMSO/paraformaldehyde. AcOH and acetyl chloride were ineffective; however, the mixture $Ac_2O$/Py reacts rapidly to give acetone-soluble CAs that were partially oxidized. The resulting thermoplastic resins exhibited thermal stabilities similar to those of native celluloses. As a function of the reaction time, the $DS_{Ac}$ ranged from 0.1 to 2.0 [31].

### Cellulose Nitrite

The derivatizing solvent $N_2O_4$/DMF has been employed for the preparation of organic esters (also of sulfates, see Sect. 5.3.3) that were obtained by the reaction of the cellulose nitrite formed during dissolution with acyl chlorides, or acid anhydrides in the presence of pyridine. Thus, successful transesterification has been achieved. The reaction with acetic anhydride/Py under pressure produced a CA with DS of 2.0. $^{13}$C NMR spectroscopy has indicated that esterification at *O*-2 occurs when the DS is kept low at about 0.5 [34–36].

The reactions discussed above are one-pot procedures, i.e., cellulose dissolution is followed by its (further) derivatization. Another approach, which leads to a better reaction control, is to isolate the intermediate, then submit it to further reaction in an inert (with regard to derivatization) organic solvent. This procedure suppresses the unavoidable side reactions (chain degradation and, e.g., methylol group condensation) that result from the long contact time of the polymer with the derivatizing solvent. Additionally, this approach allows a better control of the regioselectivity [37, 38]. For example, after isolation of cellulose formate under anhydrous conditions, esterification can be carried out in an organic solvent homogeneously. Cellulose formate with DS of ca. 1 is essentially modified at position 6 of the AGU. Thus, a modification at position 2 and 3 can be carried out and subsequently the formate moiety is easily removed by hydrolysis leading to a product with an inverse pattern of functionalization [37].

#### 5.1.2.3 Esterification of Cellulose in Nonderivatizing Solvents

Electrolytes/Dipolar Aprotic Solvents

The $pK_a$ of the hydroxyl groups of cellulose (13.3–13.5) [39] mean that direct acylation with carboxylic acid, if attempted, requires energetic conditions (170–200 °C) [40]. Therefore, cellulose acylation is usually carried out with reactive carboxylic acid derivatives, e.g., anhydrides and acyl halides. Alternatively, carboxylic acids can be employed after being activated prior, or simultaneously during the esterification reaction. Carboxylic acids may be activated by conversion into anhydrides, mixed (i.e., asymmetric) anhydrides, and *N*-acyl-diazoles or *N*-acyl-triazoles. Although the reagent employed is independent of the solvent, the latter may significantly influence the yield, DS, and the substituent distribution as well as may initiate side reactions. Table 5.5 summarizes representative examples of the syntheses of cellulose carboxylic esters by the routes that will be discussed below. Examples of derivatization of cellulose by homogeneous esterification in nonderivatizing solvents including ILs are available [49, 51].

**Table 5.5** Examples of solvents and reagents exploited for the homogeneous acetylation of cellulose

| Solvent | Acetylating reagent | $DS_{max}$ | References |
|---|---|---|---|
| *N*-Ethylpyridinium chloride | Acetic anhydride | 3 | [41] |
| 1-Allyl-3-methylimidazolium chloride | Acetic anhydride | 2.7 | [42] |
| *N*-methylmorpholine-*N*-oxide | Vinyl acetate | 0.3 | [43] |
| DMAc/LiCl | Acetic anhydride<br>Acetyl chloride | 3<br>3 | [44, 45] |
| LiCl/DMI | Acetic anhydride | 1.4 | [46] |
| TBAF × $3H_2O$/DMSO | Vinyl acetate<br>Acetic anhydride | 2.7<br>1.2 | [47, 48] |

DMAc/LiCl

The solvent system DMAc/LiCl is still the most extensively employed for homogeneous cellulose esterification because it is capable of dissolving different celluloses including samples of high DP and Ic, e.g., cotton linters and bacterial cellulose. The esterification of cellulose in DMAc/LiCl using carboxylic acid anhydrides and acyl chlorides was among the first attempts of chemical modification of the polysaccharide under homogeneous conditions [52, 53]. The advantages of acylation in homogeneous phase in DMAc/LiCl include the excellent control of DS and the uniform distribution of the functional groups along the polymer chains. Moreover, a selectivity of the functionalization reaction within the AGUs may be observed. Thus, the reaction of cellulose with acetyl chloride in the presence of Py gives a CA with complete functionalization of the primary hydroxyl groups at DS values starting from 1.6.

The (mineral acid-catalyzed) reaction of acetic anhydride with long-chain carboxylic acid (octanoic to octadecanoic; oleic) leads to the formation of mixed acetic/long-chain carboxylic anhydrides that react with cellulose (Fig. 5.9). The mixed anhydrides are not separated from the reaction medium, but react with cellulose to produce mixed esters. The two leaving groups of the mixed anhydride ($CH_3CO$– and RCO–) have comparable efficiencies; this leads to the formation of mixed acetate/long-chain carboxylate esters, with $DS_{Ac}/DS_{\text{long-chain caboxylate}}$ of about 3 [54–56].

It should be mentioned that side reactions may occur leading to decrease in the DS of ester applying DMAc/LiCl. For acetylation of mercerized sisal at 110 °C in

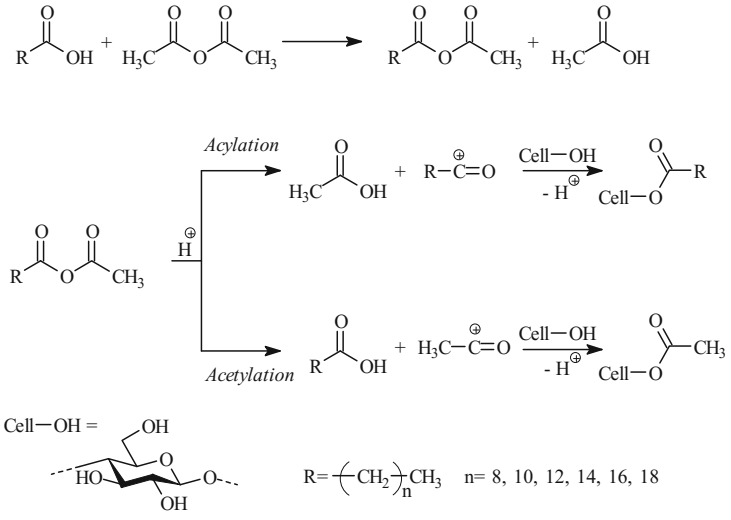


**Fig. 5.9** Synthesis of cellulose esters by reaction of the biopolymer with mixed carboxylic acid anhydrides formed in situ

DMAc/LiCl, the value of DS increases for 5 h then decreases. This has been attributed to a combination of LiCl-mediated deacetylation and product degradation, e.g., by the solvent-originated *N*,*N*-dimethylketeniminium ion ($CH_2$=C=$N^+(CH_3)_2$) [57].

### In Situ Activation of Carboxylic Acids

An important, experimentally simple approach is the reaction of cellulose with a mixture of carboxylic acid and TsCl applying DMAc/LiCl as reaction medium. This is a typical example for in situ activation of the carboxylic acid. As evaluated by $^1$H NMR spectroscopy, the carboxylic–sulfonic mixed anhydride is formed and further reacts to yield acetyl chloride and acetic acid anhydride (Fig. 5.10). These three reactive species are able to esterify cellulose [59]. The preferential attack of cellulose on the C=O group can be traced to the facts that nucleophilic attack on sulfur is slow, and the tosylate moiety is a much better leaving group ($pK_a$ of 4-toluene sulfonic acid = −2.8) than the carboxylate group.

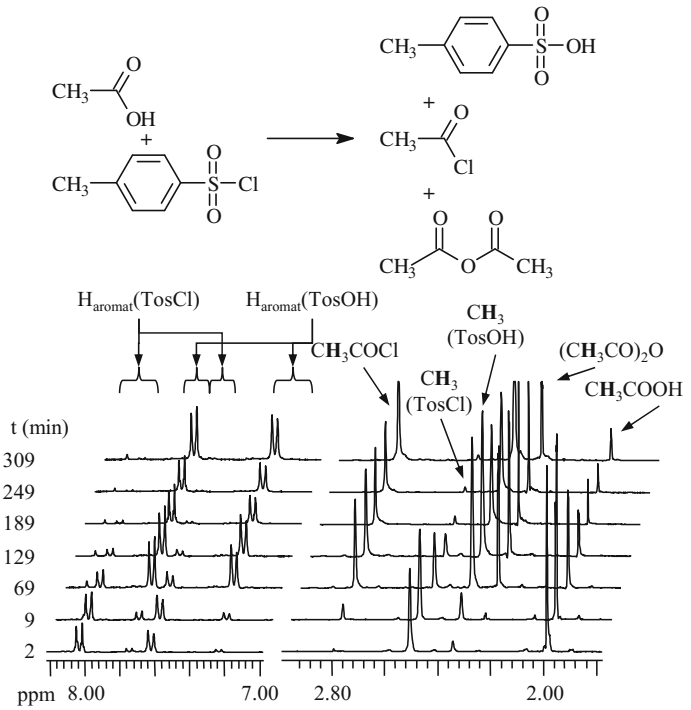


**Fig. 5.10** Evolution as a function of time of the $^1$H NMR spectra of mixture of acetic acid plus TsCl, showing the formation of mixture of $(CH_3CO)_2O$ plus $CH_3COCl$ (reprinted from [58], with permission from Springer)

Cellulose esters of several carboxylic acids, including fatty acids, dodecanoate to eicosanoate have been prepared applying TsCl to activate the corresponding carboxylic acids in DMAc/LiCl; DS values of up to 2.8–2.9 were obtained [60, 61]. The formation of the carboxylic–sulfonic mixed anhydride has also been suggested for the acylation of cellulose by a mixture of carboxylic acid anhydride and TsCl [62]. However, a recent study has shown that these intermediates are not formed [63].

Up to now, the most efficient in situ activation of carboxylic acids involves their transformation into the corresponding *N*-acyl derivatives (Fig. 5.11). *N*,*N*-carbonyldiimidazole (CDI) is a very promising substitute for DCC for acid activation. The acylating agent is *N*-acylimidazol that readily reacts with cellulose to give the ester and regenerates imidazole.

DCC may be used either alone or in combination with a powerful nucleophile, e.g., 4-pyrrolidinopyridine, leading to the formation of acid anhydride (Fig. 5.12). First, acid anhydride is produced by the reaction of the free acid with DCC. Nucleophilic attack by 4-pyrrolidinopyridine at the anhydride results in the corresponding, highly reactive, *N*-acylpyridinium carboxylate, leading to formation of cellulose ester and a carboxylate anion. The latter undergoes a DCC-mediated

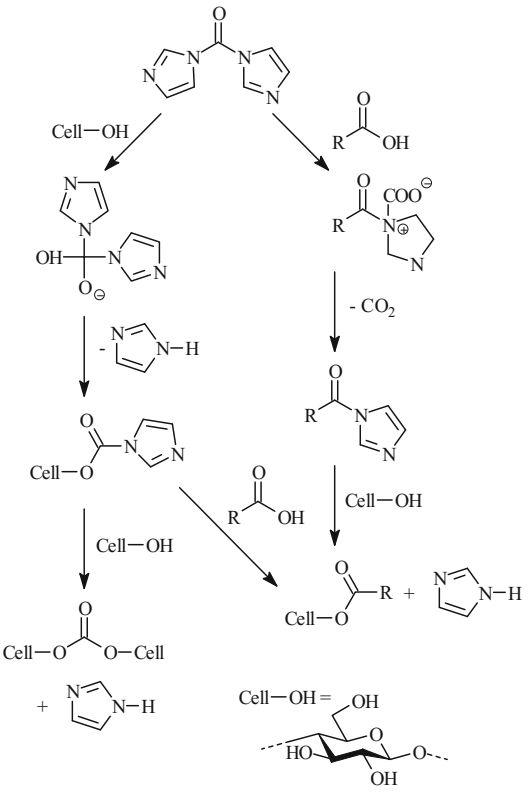


**Fig. 5.11** Activation of carboxylic acid via activation with CDI. The latter converts the acid into the corresponding anhydride

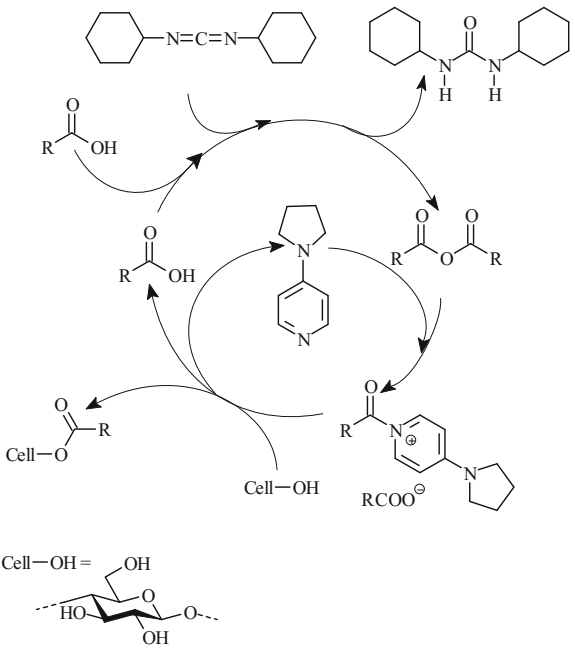


**Fig. 5.12** Scheme for the in situ activation of carboxylic acids via its transformation to the corresponding anhydride, by reaction with DCC plus 4-pyrrolinopyridine

condensation with a further molecule of acid to produce a second molecule of anhydride. Therefore, this conversion is more atom efficient than using DCC alone, where only half the anhydride is converted into cellulose ester.

Another variant of this approach is to use acyl-1*H*-1,2,3-benzotriazole, obtained by reacting the heterocyclic compound with $SOCl_2$, followed by reaction of the adduct formed with the carboxylic acid (Fig. 5.13). The reaction could be carried out under mild conditions. The *N*-acylbenzotriazole reacts with cellulose leading to CA, butyrate, caproate, benzoate, myristate, and stearate with DS values between 1.07 and 1.89. The reaction proceeds completely homogeneously in DMSO/TBAF using *N*-acylbenzotriazole as acylation agent [64].

Other coupling agents including 4-(4,6-dimethoxy-1,3,5-triazin-2-yl)-4-methyl-morpholinium chloride, *N*-methyl-2-bromopyridinium iodide, *N*-methyl-2-chloropyridinium iodide, and *N*-methyl-2-bromopyridinium tosylate have been investigated for homogeneous esterification of cellulose. Their effectiveness in terms of DS of resulting esters is far below those of the efficient in situ activation reagent *N*,*N*′-carbonyldiimidazole (Table 5.6) [65].

A similar approach has been employed by using *n*-propyl phosphonic acid anhydride (T3P®) for activation of the carboxylic acids (Fig. 5.14). In an one-pot homogeneous esterification reaction in LiCl/NMP, carboxylate (acetate, butyrate, caprinate, myrystate, stearate)-phosphonate mixed esters of cellulose ($DS_{carboxylate}$/$DS_{phosphonate}$ 1.8–2.8) were obtained within few hours [66]. Thus, *n*-propyl phosphonic acid anhydride acts during the reaction both as an activating agent for

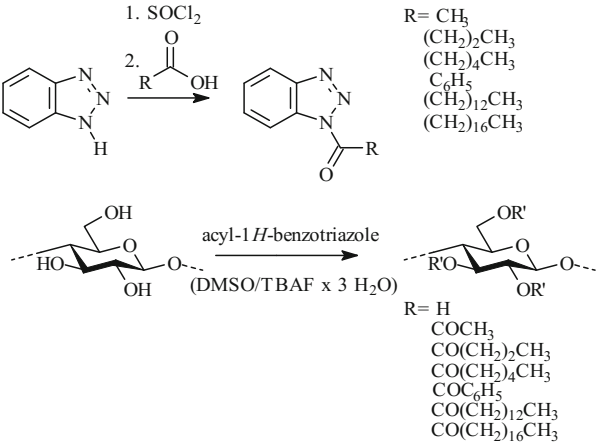


**Fig. 5.13** Reaction scheme for 1*H*-benzotriazole-mediated synthesis of cellulose esters

carboxylic acids and as esterification reagent, offering a rapid access to novel alkyl phosphonate containing cellulose mixed esters without any cross-linking. It may be concluded that it would be possible to get pure acylates by changing the reaction conditions [66].

### Quaternary Ammonium Fluorides/DMSO

A solution of TBAF × $3H_2O$ in DMSO dissolves cellulose very efficiently without any pretreatment due to the fact fluoride ion is a harder base than the chloride ion (of the solvent DMAc/LiCl). Furthermore, the voluminous cation acts as a "spacer" between individual cellulose chains, preventing their re-attachment [47, 67]. The commercially available, stable TBAF contains 3 mol of water. The water may influence the chemical modification of the dissolved cellulose due to hydrolysis of the reagent (acyl anhydride or chloride). However, the cellulose solution may be partially dehydrated by distilling off about 30% of the solvent, before addition of the reagent, e.g., acetic anhydride. The esterification yields products of higher DS (increases from 0.3 to 1.15) [48]. Even more efficient is the use of carboxylic acid vinyl esters that tolerate water and react with cellulose by transesterification. Vinyl esters of carboxylic acids can even applied in aqueous systems for effective esterification of alcohols [68].

A complete dehydration of TBAF × $3H_2O$ in the water-free electrolyte is impossible due to the fact that anhydrous TBAF is unstable, undergoing a rapid E2 elimination, resulting in the formation of hydrogen difluoride anions, on one hand [69]. On the other hand, it was described that anhydrous TBAF could be prepared in situ by reacting tetra-*n*-butylammonium cyanide with hexafluorobenzene in dry

**Table 5.6** Results for the homogeneous esterification of cellulose mediated with four different esterification agents (adapted from [65])

| Esterification agent | | Degree of substitution |
|---|---|---|
| 4-(4,6-Dimethoxy-1,3,5-triazin-2-yl)-4-methyl-morpholinium chloride | 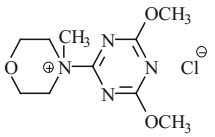 | 0.67 |
| *N*-Methyl-2-bromopyridinium iodide | 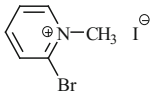 | 0.90 |
| *N*-Methyl-2-chloropyridinium iodide | 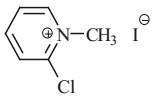 | 0.43 |
| *N*-Methyl-2-bromopyridinium tosylate | 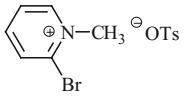 | 0.67 |
| *N*,*N'*-Carbonyldiimidazole | 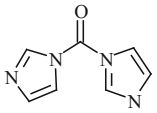 | 1.00 |

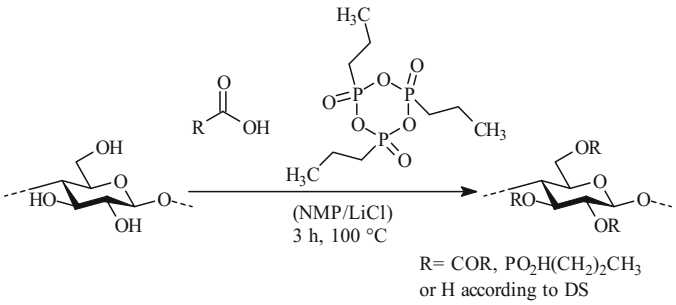


**Fig. 5.14** Reaction scheme for the cellulose acylation in LiCl/*N*-Methyl-2-pyrrolidone applying carboxylic acid and *n*-propyl phosphonic acid anhydride (T3P®)

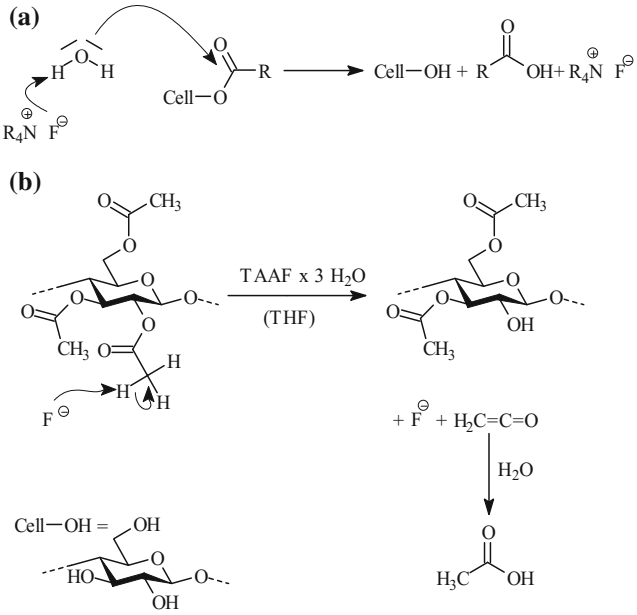


**Fig. 5.15** Suggested mechanisms for ester hydrolysis by TAAF in DMSO. In part (**a**), the fluoride ion acts as a general base for the attack of water on the ester acyl group. The fluoride ion acts via proton elimination (**b**)

DMSO [70]. The freshly prepared water-free DMSO/TBAF solution, even in the presence of the byproduct, hexacyanobenzene, dissolves cellulose easily.

For acylation in TBAF × $3H_2O$/DMSO, hydrolysis of the produced ester occurs either by a general base-catalyzed reaction [71] or via proton elimination followed by the formation of ketene (Fig. 5.15). Interestingly, the hydrolysis initiated by the electrolyte water of hydration has been employed for the synthesis of cellulose esters with special distribution of the substituents because it shows substantial selectivity for the removal of the acyl groups at C-2 and C-3, affording cellulose-6-*O*-esters by one-step reaction [72]. A problem of this electrolyte/DMSO as cellulose solvent may appear when acid chlorides are employed due to the known fact that DMSO may react with acid chlorides in Swern-like oxidation reactions. Other quaternary ammonium fluorides that have been successfully employed for cellulose derivatization are the tetraallylammonium and dibenzyldimethylammonium cations. These electrolytes are synthesized in the laboratory with lower water content, 1 and 0.1 water molecules, respectively [71, 73].

### Ionic Liquids

Today, homogeneous esterification in ILs is considered as a commercially attractive alternative for the preparation of the important CA, CAP, and CAB. Various patents

have been published, e.g., by Eastman Chemical Company, that describe the preparation of cellulose esters and mixed esters in imidazolium- and ammonium-based ILs [74, 75]. Conversion of cellulose with carboxylic acid chlorides and anhydrides proved to be efficient when performed homogeneously in an IL at elevated temperature ( $\geq 80$ °C). Consequently, the effect of high viscosity of cellulose/IL solution is less pronounced. The esterification of cellulose proceeds homogeneously even up to a complete derivatization (DS 3). The examples summarized in Table 5.7 indicate the efficiency of the reactions in ILs.

Cellulose esters of higher carboxylic acids, from propionates up to hexanoates, have been prepared in various ILs using the corresponding anhydrides [79–82]. The DS values of cellulose esters were found to decrease smoothly with increasing the number of carbon atoms in the acyl moiety from 2 to 4 but to increase again with further increase of the acyl chain length up to 6 carbon atoms [80]. The efficiency of cellulose esterification in ILs can be increased by adding pyridine (stoichiometric amounts) or DMAP (catalytic amounts) [77, 83]. Moreover, microwave-assisted esterification can yield products with an increased DS in comparison to products prepared under conventional heating [80, 84, 85].

Simultaneous conversion of cellulose, dissolved in an IL, with two different carboxylic acid anhydrides yields mixed cellulose esters (Table 5.8) [79, 80]. The product properties (e.g., hydrophobic/hydrophilic character) can be tailored by variation of ester moieties, their partial DS values, and the overall amount of substituents, attached to the cellulose backbone. As already pointed out, the reactivity of carboxylic acid anhydrides is dependent on the length of the alkyl chain [80]. In addition to reaction temperature, time, and amount of acylation reagent, the sequence of adding the two different anhydrides (simultaneous vs. stepwise) is consequently of huge importance.

Cellulose succinates and phthalates could be obtained by homogeneous derivatization in AlMeImCl or BuMeImCl using different acylation catalysts, e.g., DMAP, *N*-bromosuccinimide, or iodine [85–89]. DMSO has been utilized as molecular cosolvent to ensure homogeneous conditions. ILs, partly in combination with DMF as cosolvent, have been employed for the preparation of 2-bromo- and 2-chloro-carboxylic acid ester of cellulose, which could be used as macro-initiators for the grafting of polymethacrylate and polystyrene chains onto the polysaccharide backbone [90–93].

Cellulose dissolved in AlMeImCl could be converted to 4-tolyl, chlorobenzoyl, and 4-nitrobenzoyl cellulose with high DS values between 1.0 and 3.0 [94]. Also, mixed cellulose derivatives, carrying benzoate groups (preferentially at the primary hydroxyl group) and 4-nitrobenzoate moieties (preferentially at the secondary hydroxyl groups), have been prepared in ILs by stepwise conversion with the corresponding acid chlorides. In general, cellulose esters are well soluble in ILs even at high DS values meaning that completely homogeneous esterification is feasible. However, in case of fatty acid ester with long-chain alkyl groups, the cellulose derivatives become increasingly hydrophobic upon advancing substitution, which renders the products insoluble in the reaction mixture. Cellulose

**Table 5.7** Degrees of substitution (DS) and solubility of cellulose acetates prepared by homogeneous acetylation in various ionic liquids (IL) and under different reaction conditions

| Reaction conditions | | | | | | Product | | | |
|---|---|---|---|---|---|---|---|---|---|
| IL[a] | Cellulose type[b] | Temperature (°C) | Time [h] | Reagent | | DS | Solubility[c] | | References |
| | | | | Type[d] | Ratio[e] | | DMSO | $CHCl_3$ | |
| AlMeImCl | DIP | 100 | 3 | Anhydride | 3:1 | 1.99 | + | − | [42] |
| AlMeImCl | DIP | 100 | 3 | Anhydride | 4:1 | 2.09 | + | − | [42] |
| AlMeImCl | DIP | 100 | 3 | Anhydride | 5:1 | 2.30 | + | + | [42] |
| AlMeImCl | CH | 100 | 1 | Anhydride | 5:1 | 2.16 | + | − | [76] |
| AlMeImCl | CH | 100 | 4 | Anhydride | 5:1 | 2.49 | + | + | [76] |
| AlMeImCl | CH | 100 | 8 | Anhydride | 5:1 | 2.63 | + | + | [76] |
| BuMeImCl | MCC | 80 | 2 | Anhydride | 3:1 | 1.87 | + | − | [77] |
| BuMeImCl | MCC | 80 | 2 | Anhydride | 3:1[f] | 2.56 | + | − | [77] |
| BuMeImCl | MCC | 80 | 2 | Anhydride | 5:1 | 2.72 | + | − | [77] |
| BuMeImCl | MCC | 80 | 2 | Anhydride | 5:1[f] | 2.94 | + | + | [77] |
| BuMeImCl | MCC | 80 | 2 | Anhydride | 10:1[f] | 3.0 | + | + | [77] |
| BuMeImCl | MCC | 80 | 2 | Chloride | 3:1 | 2.81 | + | − | [77] |
| BuMeImCl | MCC | 80 | 0.25 | Chloride | 5:1 | 2.93 | + | + | [77] |
| BuMeImCl | MCC | 80 | 0.5 | Chloride | 5:1 | 3.0 | + | + | [77] |
| BuMeImCl | MCC | 80 | 2 | Chloride | 5:1 | 3.0 | + | + | [77] |
| BuMeImCl | MCC | 80 | 2 | Chloride | 5:1[f] | 2.93 | + | − | [77] |
| BuMeImCl | BC | 80 | 2 | Anhydride | 1:1 | 0.69 | + | n.a. | [78] |
| BuMeImCl | BC | 80 | 2 | Anhydride | 2:1 | 1.66 | + | n.a. | [78] |

(continued)

**Table 5.7** (continued)

| Reaction conditions | | | | | | Product | | | |
|---|---|---|---|---|---|---|---|---|---|
| IL[a] | Cellulose type[b] | Temperature (°C) | Time [h] | Reagent | | DS | Solubility[c] | | References |
| | | | | Type[d] | Ratio[e] | | DMSO | $CHCl_3$ | |
| BuMeImCl | BC | 80 | 2 | Anhydride | 3:1 | 2.25 | + | n.a. | [78] |
| BuMeImCl | BC | 80 | 2 | Anhydride | 5:1 | 2.50 | + | n.a. | [78] |
| BuMeImCl | BC | 80 | 2 | Anhydride | 10:1 | 3.0 | + | n.a. | [78] |

[a]AlMeImCl: 1-allyl-3-methylimidazolium chloride, BuMeImCl: 1-butyl-3-methylimidazolium chloride
[b]*BC* bacterial cellulose (DP 6,493), *CH* cellulose from corn husk (DP 530), *DIP* dissolving pulp (DP ≈ 650), MCC microcrystalline cellulose (DP 286)
[c]+ soluble, − insoluble, *n.a.* no information available
[d]Acetic acid derivative used
[e]Molar ratio of acetylation reagent to anhydroglucose units
[f]Additionally, 2.5 mol equivalent pyridine

**Table 5.8** Overview about mixed cellulose esters with different degrees of substitution (DS) prepared in the ionic liquid 1-allyl-3-(1-butyl)imidazolium chloride (AlBuImCl)

| Substituent 1 | | Substituent 2 | | Overall DS range | References |
|---|---|---|---|---|---|
| Type | DS range | Type | DS range | | |
| Acetate | 1.50 | Propionate | 1.30 | 2.80 | [80] |
| Acetate | 1.40–2.50 | Butyrate | 0.40–0.90 | 2.20–2.90 | [79, 80] |
| Acetate | 1.40 | Pentanoate | 1.10 | 2.50 | [80] |
| Acetate | 1.40 | Hexanoate | 1.10 | 2.50 | [80] |

laurates could be obtained in ILs but the derivatives rapidly precipitated upon derivatization of the polysaccharide [77].

#### 5.1.2.4 Factors Influencing the DS of the Produced Esters

The literature available on this particular subject is massive, and there are several recent review articles that address different aspects of cellulose esterification in electrolyte/dipolar aprotic solvent and ILs [49, 51, 95]. Therefore, here the most salient features of these publications are considered and specific examples are listed in Table 5.9. To summarize important factors that influence the esterification of cellulose, the emphasis has been on the DS obtained as a function of

(i) the physicochemical properties of cellulose,
(ii) the need for cellulose activation,
(iii) the nature of solvent,
(iv) the acylating reagent, and
(v) properties of the products obtained (solubility and distribution of the substituents).

With regard to (i), the DP and contents of α-cellulose, hemicellulose, and lignin are of interest. Thus, MCC is the starting material of preference when a new experimental procedure or reagent is tested because of its low DP, typically 150–250. The fact that MCC has a relatively high $I_c$ does not affect its reactivity noticeably because the importance of this experimental variable is essentially eliminated for homogeneous reactions after cellulose dissolution. Additionally, the decrystallization rate constants and activation parameters are only slightly dependent on the physicochemical properties of the starting celluloses. Fibrous celluloses react more slowly than MCC because of their higher molar mass. Thus, in order to obtain comparable DS for MCC and fibrous celluloses, it is common to employ longer reaction time, higher temperature, and larger ratio (acylating agent/OH of the AGU). The lower reactivity of fibrous cellulose may be traced to the fact that the persistent length of its (dissolved) chains is shorter than the length of the extended

**Table 5.9** Representative examples of the routes employed for the synthesis of cellulose derivatives

| Entry | Cellulose type | Derivatizing agent | Solvent | Product | DS range | References |
|---|---|---|---|---|---|---|
| 1 | MCC | Acid/DCC/tertiary amine catalyst | DMAc/LiCl | Esters of crotonic, vinyl acetic, methylmethacrylic, fumaric, and cinnamic acid | 0.84–1.65 | [96] |
| 2 | MCC | Fatty acid/$Ac_2O$ | DMAc/LiCl | Mixed esters acetic/long-chain carboxylic acid | Total DS 2.95–3.0 | [54] |
| 3 | MCC | Acid/TsCl | DMAc/LiCl | Cellulose esters of carpric, caprylic, decanoic, lauric, palmitic, and stearic | 0.36–2.56 | [45] |
| 4 | MCC, spruce, cotton | Acid/CDI | DMSO/TBAF | Cellulose esters of pyroglutamic, furane-2-carboxylic acid | 0.54–2.4 | [97] |
| 5 | MCC | Acid/$SOCl_2$/benzotriazole | DMSO/TBAF | Esters of acetic, benzoic, butyric, caproic, myristic, and stearic acid | 0.79–1.07 | [64] |
| 6 | Cotton, sugarcane, sisal | Carboxylic anhydride | DMAc/LiCl | Esters of acetic, propionic, and butyric acid | 1.5–3.0 | [98] |
| 7 | MCC, eucalyptus; cotton | Carboxylic anhydride | TAAF/DMSO | Esters and mixed esters of acetic, butyric, and hexanoic | 1.4–2.4 | [71] |
| 8 | Bacterial cellulose | Carboxylic anhydride | BuMeIMCl | CAs | 0.69–3.0 | [78] |
| 9 | MCC | Carboxylic anhydride | AlMeImCl | Cellulose esters and mixed esters of acetic, propionic, butyric, pentanoic, and hexanoic acid | 1.5–2.9 | [80] |
| 10 | Sugar cane bagasse | Carboxylic anhydride/base | BuMeImCl | Cellulose succinates | 0.24–2.34 | [85] |
| 11 | MCC | Carboxylic anhydride/Lewis acid | Choline chloride/$ZnCl_2$ | CAs | 0.45–1.41 | [99] |

(continued)

**Table 5.9** (continued)

| Entry | Cellulose type | Derivatizing agent | Solvent | Product | DS range | References |
|---|---|---|---|---|---|---|
| 12 | MCC | Acyl chloride/base | DMAc/LiCl | Esters of octanoic, lauric, and palmitic acid | 0.12-1.75 | [100] |
| 14 | Spruce pulp | Acyl chloride/base | BuMeIMCl; AlMeImCl | CAs | 2.40–2.70 | [101] |
| 15 | MCC | Acyl chloride/base | DMAc/LiCl; DMSO/TBAF; AlMeImCl | Cellulose esters of pivalic, adamantancarboxylic, 2,4,6-trimethylbenzoic acid | 0.34–2.72 | [102] |
| 16 | MCC | Vinyl ester | DMSO/TBAF | Esters of acetic, benzoic, butyric, and lauric acid | 0.3–2.72 | [45] |
| 17 | MCC | Lactone | DMAc/LiCl | L-lactide and ε-caprolactone-based cellulose esters | 0.5–0.7 | [103] |
| 18 | MCC, spruce sulphite pulp, and cotton | Lactam | LiCl/NMP; BuMeImCl | Amino cellulose esters | 0.12–1.15 | [104] |
| 19 | Hardwood pulp; MCC | Ketene dimer; tert-butylacetoacetate | DMAc/LiCl | Cellulose acetoacetate | 0.34–1.34 | [105] |
| 20 | MCC | $C_8^-$, $C_{10}$, $C_{12}$, $C_{14}$, $C_{16}$, $C_{18}$ alkyldiketene dimers<br>$C_8^-$, $C_{10}$, $C_{12}$, $C_{14}$, $C_{16}$, $C_{18}$ acid anhydrides/MeIm | LiCl/ 1,3-dimethyl-2-imidazolidinone | Cellulose esters | 2.5–2.9 | [106] |
| | | | | β-ketoesters of fatty acids | 1.9–2.9 | |

biopolymer chain, which leads to coiling (see Fig. 3.28), i.e., decreases the accessibility of the dissolved polymer due to steric crowding. At the same cellulose content, solutions of fibrous celluloses are more viscous, and the cellulose aggregates formed are larger than the corresponding ones of MCC. These factors slow down the reaction because of their adverse effect on the diffusion of cellulose chains and the acylating agent. An example of the effect of solution viscosity on reaction rate has been demonstrated for the Diels–Alder reaction of cyclopentadiene with methyl acrylate in a series of ILs derived from 1-*R*-3-MeImBF$_4$ ($R = C_2$ to $C_8$). The rate constants decrease almost linearly as a function of increasing IL viscosity [107].

Fibrous celluloses of high molar mass and $I_c$, in particular cotton linters may react sluggishly if the biopolymer is not mercerized. As shown before, this alkali treatment results, in most cases, in decreasing the $I_c$ and increasing its surface area by increasing the average diameter of the "pinholes" on the surface and joining these pinholes together. This speeds up cellulose dissolution and probably increases the accessibility within the formed aggregates. In principle, other fibrous celluloses, e.g., those from sisal, pine, and birch, react at a convenient rate without mercerization. Nevertheless, mercerization has a beneficial effect because of the accompanied decrease of $I_c$ and increase of biopolymer surface area (speeds up dissolution) and elimination of a part of the hemicellulose present; the latter affects cellulose aggregation, hence accessibility (see Fig. 3.27) [57, 108]. That is, cellulose mercerization speeds up derivatization reaction of fibrous cellulose due to speeding up of dissolution and possibly affects the size of aggregates formed.

With regard to (ii), as discussed before, biopolymer activation is required for cellulose dissolution in DMAc/LiCl, on one hand. On the other hand, MCC and fibrous cellulose dissolve readily in $R_4NF \times H_2O$/DMSO and ILs. In fact, heat activation does not affect DS of the product of acylation of cellulose in BuMeImCl. Of the above-discussed cellulose activation schemes, heat activation is the simplest, and the solvent displacement scheme is the more tedious and expensive. The relevant point is that cellulose activation, if required, adds to the cost and energy demand of the synthesis.

With regard to (iii), there are various nonderivatizing solvents for cellulose, either single component, e.g., NMMO and ILs, or multicomponent one, electrolyte/dipolar aprotic solvent. There are only very few studies aimed at comparing the efficiency of these solvents. Cellulose derivatization in DMAc/LiCl and TBAF $\times$ 3$H_2O$/DMSO by a variety of acylating agents has been compared. The reagents included carboxylic acid anhydrides, saturated, unsaturated, and aromatic carboxylic acids activated with CDI and with 1*H*-benzotriazole. The general conclusion is that acylations in DMAc/LiCl require more time and higher temperatures than the corresponding reaction in TBAF $\times$ 3$H_2O$/DMSO [109]. Under comparable reaction conditions, the rate constants of cellulose acetylation were found to be AlMeImCl-DMAc > LiCl-DMAc > AlMeImCl-acetonitrile [110].

There are few examples of cellulose esterification in NMP/LiCl leading to results comparable to DMAc/LiCl, whereas NMMO has been employed as well. However, NMMO does not tolerate reagents and turned to a heterogeneous system [43, 111, 112].

With regard to (iv), symmetric carboxylic acid anhydrides are reactive to transform cellulose into its esters heterogeneously (commercial production) and homogeneously. In the reaction of cellulose simultaneously with mixtures of acetic/propionic and acetic/butyric anhydride, the $DS_{Ac}$ is usually larger than $DS_{Propionate}$ or $DS_{Butyrate}$ because of the higher electrophilicity of the acyl group and smaller volume of the acetic anhydride [79]. The efficiency of acetylation of cellulose, expressed by the dependence of DS on the $(RCO)_2O$/AGU ratio, is described by an exponential decay equation:

$$DS = DS_0 + A \cdot e^{-\frac{\frac{(RCO)_2O}{AGU}}{B}}, \tag{5.1}$$

where A and B are the regression coefficients. Values of B were found to correlate linearly with the aggregation number, $N_{agg}$, of the dissolved cellulose chains [113]:

$$B = 1.709 + 0.034 \cdot N_{agg} \tag{5.2}$$

For different celluloses, under distinct reaction conditions, the dependence of DS on number of carbons of the acid anhydride (Nc) is not linear. It decreases from acetic to butyric anhydride and then increases from pentanoic to hexanoic anhydride (Fig. 5.16).

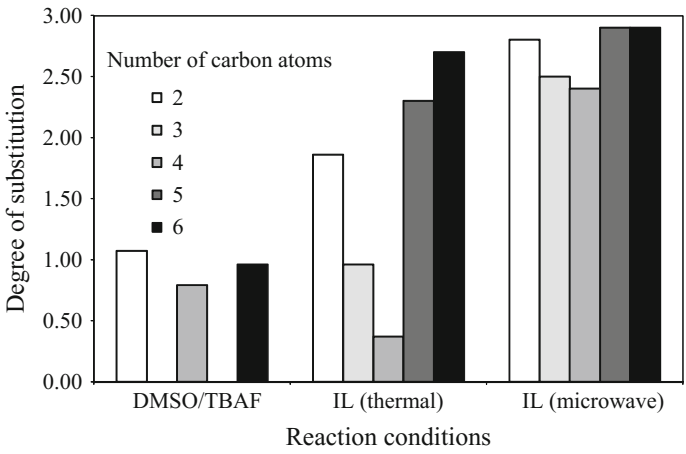


**Fig. 5.16** Dependence of DS on Nc under different experimental conditions, including the nonderivatizing solvent, and the method of heating, convection, and microwave (compiled from [7, 64, 80, 82])

This relationship is independent of the solvent (electrolyte/dipolar aprotic solvent or ionic liquid), cellulose type (MCC or fibrous), or the method of heating, conventional (i.e., by convection) or microwave. This is due to a complex dependence of the $\Delta H^{\neq}$ and $T\Delta S^{\neq}$ terms on Nc [7]. With regard to the nature of the side chains of the IL, those with heteroatoms, e.g., with ether links, are more efficient in cellulose solubilization and subsequent acylation, provided that hydrogen bonding and dipolar interactions are the dominant biopolymer–IL interactions. For longer side chains, hydrophobic interactions seem to predominate; and ILs with alkyl groups are more efficient than those with ether groups [84] in agreement with current opinion regarding the relevance to dissolution of (cellulose solvent) solvophobic interactions [114, 115].

### 5.1.3 *Some Properties and Applications of Cellulose Esters of Carboxylic Acids*

#### 5.1.3.1 Properties

Cellulose acetates, CAs are, by far, the most important cellulose esters. They are tasteless, odorless, nontoxic, and relatively stable to storage. Under hot, humid conditions, however, they may undergo autocatalytic hydrolysis, leading to the characteristic odor of the corresponding carboxylic acid. Therefore, before using commercial products in research, it is advisable to further purify the sample by repeated suspension in warm ethanol, followed by DS determination and storing in a refrigerator. The degree of acetylation is usually given as DS, % acetyl content, or % acetic acid content. The corresponding correlations between these scales are listed below:

$$\text{Acetyl content}\,(\%) = 3.771 + 19.270\,\text{DS} - 1.864\,(\text{DS})^2 \tag{5.3}$$

$$\text{Acetic acid content}\,(\%) = 4.513 + 27.690\,\text{DS} - 2.791\,(\text{DS})^2 \tag{5.4}$$

The so-called secondary CA has an average DS of ca. 2.5; the term cellulose triacetate (CTA) is used for esters with DS > 2.7. The latter exists as CTA-I and CTA-II allomorphs; a fact traced to parallel and antiparallel backbone conformation, respectively [116, 117]. The dependence of the thermal properties ($T_g$, $T_m$, $T_{Decomp}$) of CAs on DS has been discussed in Sect. 2.3.6.2; the results are listed in Table 2.25.

Cellulose secondary acetate ($T_g$ 160 °C, $T_m$ 225–250 °C with decomposition) [118] and CTA ($T_g$ 156 °C, $T_m$ 306 °C) [119] are high melting, high strength, nonconducting materials that exhibit excellent UV/vis stability, film transparency, and low inflammability. The values of $T_m$ decrease as a function of increasing chain length of the acyl moiety, being 234, 183, 122, 94, and 88 °C for the following

cellulose triesters: propionate, butyrate, pentanoate, hexanoate, and heptanoate, respectively. Therefore, cellulose mixed esters of acetate/higher carboxylate are expected to have lower $T_g$ and $T_m$, as shown by the following examples: CAP ($DS_{Propionate}$ 2.65, $DS_{Ac}$ 0.1) $T_g$ 136 °C and $T_m$ 178 °C [120]; and CAB ($DS_{Butyrate}$ 1.6 and $DS_{Ac}$ 1.0) $T_g$ 125 °C and $T_m$ 165 °C [121].

Water sorption of cellulose carboxylic triesters depends on the nature of substituent, the DS, and regularity of substitution, but not the MM of the ester. Water sorption increases as a function of the value of RH to which the material is submitted and, at constant RH, decreases as a function of increasing the hydrophobicity of the acyl moiety, e.g., from acetate to heptanoate [122, 123]. The relevant consequence of water uptake by CA fibers is that it causes increase both in fiber length and cross section, e.g., 1.5 and 4%, respectively, for CTA.

The formation of anisotropic solutions by cellulose esters has been investigated because fiber spinning from these lyotropic liquid crystalline solutions (cellulose derivative >30% (w/w)) is expected to produce strong fibers. In general, chiral nematic phases are formed, since the cellulose backbone is chiral. Thus, CTA forms liquid crystalline solutions in TFA and its mixtures with chlorinated solvents (DCM, DCE, and $CHCl_3$) and in dichloroacetic acid [124]. The effects of solvent composition, polymer concentration, temperature, and time on the onset of anisotropic phase formation have been investigated for CA with DS 2.45. It was concluded that the stronger the acid, the lower the onset of anisotropic solution formation, e.g., TFA-DCM > TFA-DCE > TFA > TFA-$CHCl_3$. Note that whereas TFA forms a dimer in DCE, which is a stronger acid than monomeric TFA, it does not interact appreciably with $CHCl_3$, in agreement with the above-shown chlorinated solvent effect [125]. Although the fibers obtained from these anisotropic dopes show high tenacity, this process has not generated commercial interest because of high cost, the corrosive, and environmental problems associated with the chemicals involved.

Solubilization of CAs in different solvents is a property of significant commercial and scientific importance. The following general solubility trend is observed (DS, solvent): 2.8–3, chloroform; 2.2–2.7, acetone; 1.2–1.8, 2-methoxyethanol; and 0.6–0.9, water. Higher esters of cellulose (from propionate to hexadecanoate) are also soluble in DCM, acetone, ethyl acetate, and toluene (starting from hexanoate for the last solvent). This solubility, however, depends not only on the total (average) DS, but also on the regioselective substitution within the AGU, and along the polymer chain [126, 127]. This dependence on the regularity of substitution explains the observed difference between the solubilities of commercialized samples from different manufactures. Thus, turbidity measurements have been employed in order to evaluate the solubility of seven commercial cellulose 2.5 acetate samples (1% (w/w)). Only one sample was soluble in ethyl acetate; solubility in DCM:methanol (4:1 (v/v)) and ethyl acetate:methanol (5.7:1 (v/v)) differed by factors of 7 and 11.2, respectively [128]. Partial DS at the position 6 of the AGU predominately determines the solubility in various solvents. For example, solubility

**Table 5.10** Solubility of cellulose CAs, obtained by partial deacetylation of CTA in some solvents [127, 129]

| Solvent | DS range of cellulose acetate partially deacetylated at position | |
|---|---|---|
| | *O*-2/*O*-3/*O*-6 | *O*-2/*O*-3 |
| Water | 08–1.0 | Insoluble |
| DMF | 1.8–2.7 | 1.3–2.8 |
| Acetone (<0.01% water) | Insoluble | Insoluble |
| Acetone (1% water) | 2.3–2.6 | 2.5–2.6 |
| Pyridine | 0.8–2.7 | 1.2–2.8 |
| Pyridine–water (1:1, V) | 0.6–2.0 | 1.2–2.6 |
| Ethyl acetate | 1.6–2.7 | 2.6–2.8 |

in water has been observed for CA of low DS (<0.8) only for samples with small partial DS at *O*-6. Regioselective deactetylation of CTA at *O*-2 and *O*-3 to the same (low) DS produced CA that was water insoluble. As summarized in Table 5.10, commercial cellulose 2.5 acetate is insoluble in dry acetone but dissolves in the same solvent in the presence of 1% water.

### 5.1.3.2 Applications

CTA is used in the textile industry because of its good processing performance; the ester fibers are used alone or in combination with other fibers, in woven fabrics, knits, and braids. The applications include medical gauze, ribbons, home furnishing, tricot knits, and lining of clothes.

A major field of application of CAs (DS 2.35–2.55) is to manufacture filter tow, intended for the selective removal of small particles, phenols, nitrosamines, quinolones, and other undesired components of cigarette smoke. The presence of dipolar and hydrophobic groups in the ester results in more efficient removal, e.g., of phenols, as compared with cellulose itself. The spinning process is carried out with (filtered) CA solution in acetone, in the presence of a small amount of titanium dioxide (added as a whitening agent) [130]. Cellulose diacetate is still the polymer of choice to manufacture many plastic products (by extrusion and blow molding) whose use implies direct and prolonged contact with humans, including fashion accessories, costume jewelry, combs, buttons, packing material, and toys [131].

A pharmaceutical application of cellulose esters is in enteric coating of solid drugs, granules, pellets, tablets, and capsules. An enteric coating is a polymer barrier applied on oral medication (Fig. 5.17) [132]. Most enteric coatings work by presenting a surface that is stable at the relatively low pH value found in the stomach ($\sim$3) but breaks down rapidly in the alkaline pH environment present in the small intestine (7–9). The most commonly used pH-sensitive enteric polymers include cellulose esters such as CA phthalate, CA trimellitate, and also modified

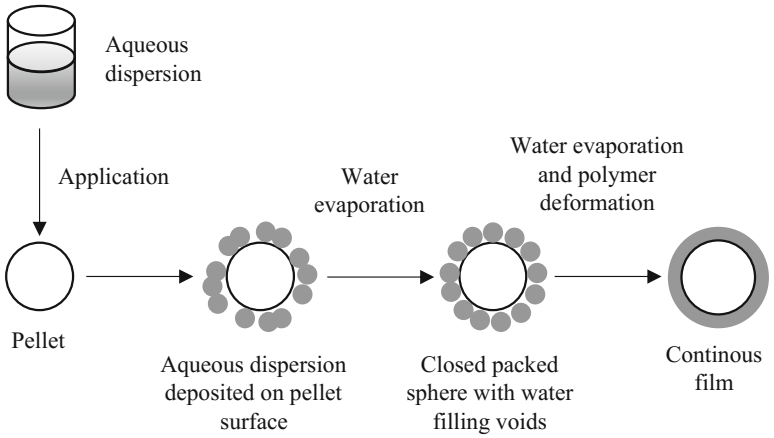


**Fig. 5.17** Schematic representation of enteric coating of a drug

cellulose ethers (e.g., hydroxypropyl methylcellulose phthalate). Typical examples of this application are those for drugs that have an irritant effect on the stomach, such as acetylsalicylic acid. Likewise, certain groups of azoles (esomeprazole, omeprazole, pan, and all grouped azoles) are acid-activated. For such types of drugs, enteric coating added to the formulation tends to avoid activation in the mouth and esophagus.

Another major field of application is in coating industry. Commercial mixed esters, e.g., CAP and CAB, have desirable properties not exhibited by the esters with a single acyl group, i.e., CA, CP, and CB, probably because of the juxtaposition of both acyl moieties in the same AGU. The applications include sheeting, molding plastics, film products, lacquer coatings, and melt dip coatings. The application intended depends on the partial DS of the substituents present. For example, products with $DS_{Ac}$ 1.4–2.1 and $DS_{Butyrate}$ 1.1–0.7 are used in lacquers, whereas a product with $DS_{Ac}$ 0.5 and $DS_{Butyrate}$ 2.3 is used in melt coating, due to its lower $T_m$. CAP and CAB are thermoplastics; they can be processed by injection molding and extrusion, and can be dissolved and cast as films. CAB is compatible with polyester-, acrylic-, vinyl-, and alkyd resins. The low viscosity of solutions of CAB with high butyryl content in inexpensive solvents makes it suitable for applications in lacquer coating, including wood furniture and in the car industry. The metallic appearance of many automobiles is achieved by using base coats that contain oriented metal flakes (Fig. 5.18). Cellulose mixed esters improve metal flake orientation in the base coats because they increase viscosity of the film during drying. This increase essentially freezes the orientation of the metal flakes, which are then aligned parallel to the surface by film shrinkage during drying [133].

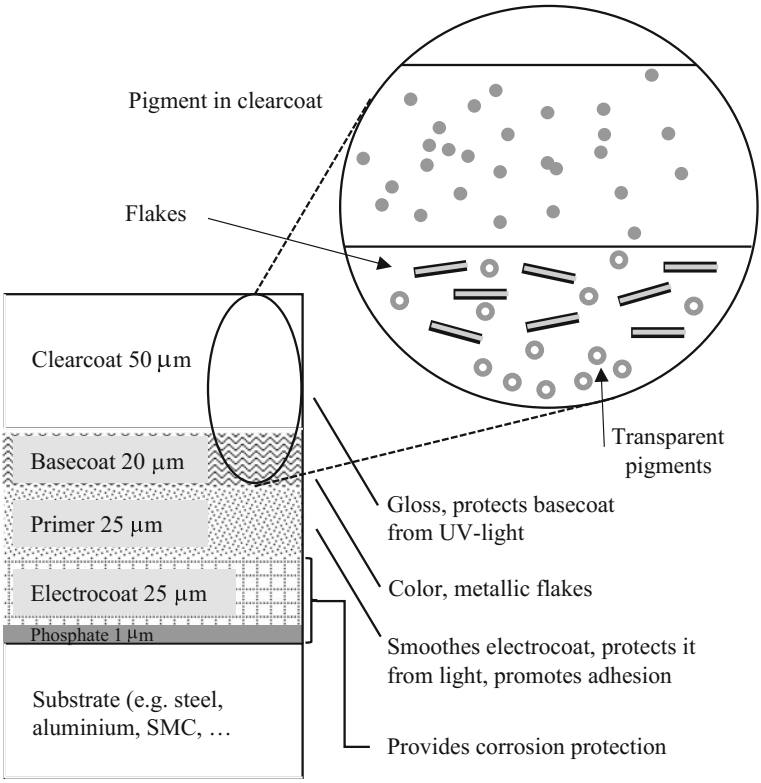


**Fig. 5.18** Schematic representation of the layers of car body coating. The coating outer layer is clear; metallic luster is produced by the metal flakes (usually aluminum) underneath the clear coating

## 5.2 Esters of Sulfonic Acids and Their Use for $S_N$ Reactions

### *5.2.1 Introduction*

Typical structures of sulfonic acid esters employed in cellulose chemistry are shown in Table 5.11. The most extensively studied derivative of this class is cellulose tosylate (CT) [134]. Although much less studied than cellulose carboxylic acid esters, cellulose sulfonates have found many applications in the preparation of cellulose derivatives by nucleophilic substitution ($S_N$) reactions yielding products with interesting structures and properties.

Thus, cellulose esters of sulfonic acids provide a straightforward and efficient route to the synthesis of deoxy cellulose derivatives including some exotic ones. By the introduction of the sulfonic acid ester, a subsequent nucleophilic substitution of the good leaving group, the sulfonate group by a myriad of nucleophiles, is

**Table 5.11** Examples of typical sulfonic acids employed in cellulose chemistry

| Ester derived from | Structure | Abbreviation |
|---|---|---|
| Benzenesulfonic acid | 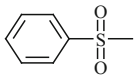 | |
| *p*-Toluenesulfonic acid | 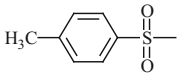 | Tosyl, Ts |
| *p*-Nitrobenzenesulfonic acid | 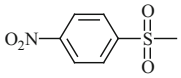 | |
| 2,4-Dinitrobenzenesulfonic acid | 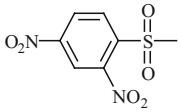 | |
| *p*-Bromobenzenesulfonic acid | 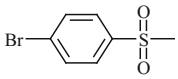 | Brosyl |
| *p*-Chlorobenzenesulfonic acid | 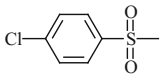 | |
| 2,4,6-Trimethylbenzenesulfonic acid | 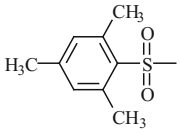 | |
| 5-*N*,*N*-Dimethylaminonaphthalenesulfonic acid | 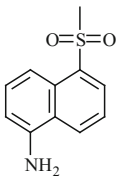 | |
| Methanesulfonic acid | 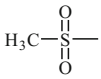 | Mesyl |

(continued)

**Table 5.11** (continued)

| Ester derived from | Structure | Abbreviation |
|---|---|---|
| Trifluoromethanesulfonic acid |  | Triflate |
| Trifluoroethanesulfonic acid | 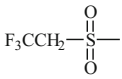 | Tresyl, tresylate |

possible. The synthesis of cellulose sulfonates is, therefore, intimately connected to their further chemical transformation. Most important in this context is CT as mentioned.

## 5.2.2 *Synthesis of Cellulose Sulfonates*

The synthesis of sulfonic acid esters can be carried out heterogeneously by the use of sulfonic acid chlorides in a tertiary organic base, e.g., pyridine. It can also be done in aqueous alkaline media via Schotten–Baumann reaction. A major drawback of the heterogeneous procedures is that long reaction time and high molar excess of the reagent must be applied. These reaction conditions may lead to the formation of cross-linked and hence insoluble products. As studied in detail for CTs, the tosyl groups may be partially substituted by chloride and pyridine to yield products that are unregularly functionalized. A typical example is the synthesis of CTs using large excess of TsCl in pyridine and reaction times of two to four days in order to obtain $DS_{Ts}$ 0.08–1.36 [135].

The synthesis of cellulose esters of sulfonic acids can be efficiently carried out homogeneously. The solvents employed being mostly strong electrolyte in combination with a dipolar aprotic solvent (e.g., DMAc/LiCl) and more recently ILs with chloride as anion.

In the pioneering work of McCormick, CTs were obtained in DMAc/LiCl with $\mathbf{DS_{Ts}}$ of up to 2.4 that was transformed almost completely into chlorodeoxy cellulose (DS 2.3) by further heating of the sulfonate in the reaction mixture [136]. It has been demonstrated that the formation of the chlorodeoxy cellulose can be suppressed by using tertiary base catalysts, e.g., TEA or 4-*N*,*N*-dimethyaminopyridine and low reaction temperature (10 °C) [137]. A series of CTs has been

prepared under homogenous conditions using TsCl/TEA in DMAc/LiCl. The values of $DS_{Ts}$ were found to be a function of molar ratio of TsCl to AGU. The solubility of the CTs depends on $DS_{Ts}$. For example, up to $DS_{Ts}$ of 0.46, CTs are soluble in DMAc and DMSO, 1.43 in dioxane or acetone and at 2.02 in THF [138].

Attempt to synthesize CTs in the IL EtMeImAc has resulted in the formation of pure CA (Fig. 5.19). The reaction of acetate ion of EtMeImAc with tosyl chloride has led to the formation of a mixed acetic–toluene sulfonic acid anhydride (demonstrated by NMR). Subsequent attack of cellulose on this intermediate occurs on the acetyl moiety because the tosyl counterpart is a better leaving group. However, it may also occur that the CT formed undergoes $S_N$ reaction with the acetate anion [139].

The synthesis of CTs is possible by using ILs with less basic/nucleophilic anions. For example, CTs with $DS_{CTs}$ from 0.71 to 1.08 have been obtained by the reaction of cellulose with TsCl/base in mixtures of ILs (AlMeImCl, EtMeIm $(EtO)_2PO_2^-$) and organic solvents including pyridine, DMF, and 1,3-dimethyl-2-imidazolidinone. Products with a $DS_{Ts} \leq 1.14$ and $DS_{Cl} \leq 0.16$ were obtained and, as expected for a homogeneous conversion, with predominant tosylation at the position 6 of the AGU. The tosylate group and the chloride of the chlorodeoxy product were further subjected to $S_N$ reaction by the azide group [140].

More recently, CTs have been prepared in aqueous media. A solution of cellulose in 5% aqueous NaOH has been obtained by agitation and cooling, followed by tosylation with TsCl/TEA (room temperature, 24 h) to give samples of $DS_{Ts}$ in the range 0.1–1.7 [141]. The resulting CT samples were characterized by FTIR and NMR spectroscopy. The $DS_{Ts}$ was determined by $^1$H NMR spectroscopy (in LiCl/DMSO-$d_6$) and compared to X-ray diffraction. Using LiCl/DMSO as solvent indicates that the products are not well soluble. For instance, CTs synthesized in DMAc/LiCl as reaction medium are very well soluble in organic solvents and no salt must be added as discussed above.

A transparent solution of cellulose was obtained in aqueous NaOH/urea after vigorous stirring and cooling. The tosylation of the dissolved cellulose in the

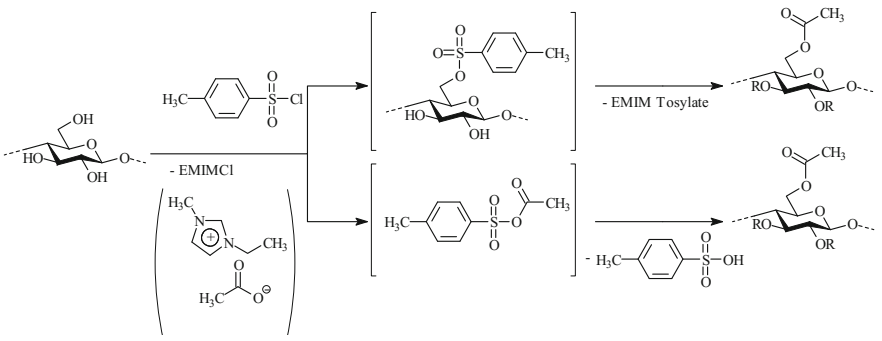


**Fig. 5.19** Explanation for the formation of cellulose acetate during the reaction of cellulose with TsCl in the IL EtMeImAc [139]

presence of a nonionic surfactant yields well-soluble samples with $DS_{Ts}$ from 0.43 to 0.95. These samples could be converted by typical $S_N$ reactions to various derivatives (6-deoxy-6-(ω-aminoethyl)amino cellulose (applying ethylenediamine, DMSO, 100 °C, 6 h), 6-deoxy-6-azido cellulose ($NaN_3$, DMF, 100 °C, 24 h), and 6-deoxy-6-thiosulfatecellulose (applying $Na_2S_2O_3$, DMSO, 80 °C, 20 h) [142]. The importance of 6-deoxy-6-(ω-aminoalkyl)amino cellulose will be discussed below.

### 5.2.3 *Modification of the Remaining Hydroxyl Groups of Cellulose Sulfonates*

Prior to the $S_N$ reaction, the remaining hydroxyl groups of cellulose sulfonates may be modified. The sulfonate group may be stable under ordinary conditions of esterification that is in particular true for the tosylate moieties (Fig. 5.20). Thus, CTs were converted into mixed esters (tosylate/carboxylates [143], tosylate/urethanes [144], and tosylate/sulfate [145]). Cellulose derivatives with interesting structures and properties, especially their solubility in organic solvents, were obtained by the homogeneous acylation of the remaining hydroxyl groups, starting from CTs of $DS_{Ts}$ from 0.5 to 2.0. The acylation reaction with various aliphatic, aromatic, and unsaturated carboxylic acid anhydrides as well as isocyanates has been carried out in pyridine, using sodium acetate as catalyst. The reactions proceeded homogeneously and products of a high $DS_{Acyl}$ were obtained. In the case of acetic and propionic acid anhydride, a complete functionalization of all remaining hydroxyl groups was achieved. The products are readily soluble in dipolar aprotic solvents such as acetone, DMSO, DMAc, and THF. They form films by casting from solution. In case of monoesters of CTs with carboxylic acids with more than one carboxylic group, the mixed esters are soluble in aqueous NaOH and even water depending on the values of $DS_{Ts}$ and $DS_{Acyl}$.

Values of $T_{Decomp}$ of CTs and the corresponding mixed esters with the same $DS_{Ts}$ were found to be comparable, i.e., these mixed esters can be processed, e.g., by extrusion from the melt [143]. CTs were even converted into the corresponding water-soluble cellulose tosylate sulfate by reaction with $SO_3$/pyridine, $DS_{Sulfate}$ 0.57, obtaining products that self-aggregate in water [146].

### 5.2.4 *Nucleophilic Displacement Reaction with Cellulose Tosylates*

The products of the reaction of cellulose with TsCl/TEA in DMAc/LiCl were allowed to react with methylamine, dimethylamine, and 2-cysteamine. In contrast to reactions of CTs with cysteamine, which resulted in completely insoluble,

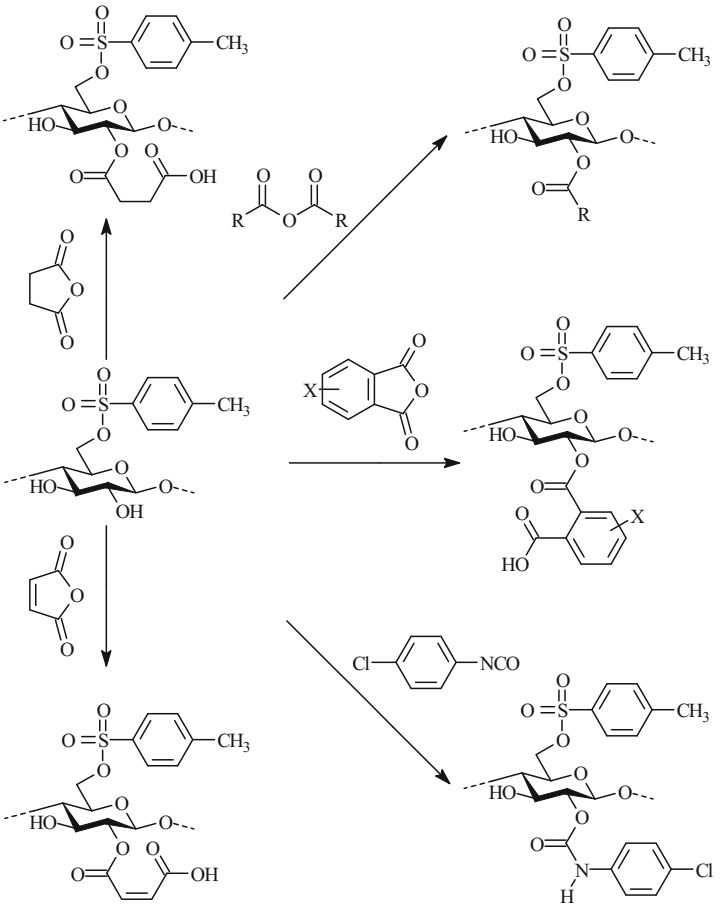

**Fig. 5.20** Examples of the modification of remaining hydroxyl groups of cellulose tosylate [143]

non-swelling products, reactions with methylamine and dimethylamine yielded products highly swellable in water [147].

A detailed study on the substitution of the tosylate group of CTs by the methylamino group has been carried out. The degree of group exchange was found to be a sensitive function of reaction temperature and time, as shown by the following (temperature, time, % group exchange): room temperature, 24 h, 50%; 40 °C, 24 h, 76%; 60 °C, 24 h, 100%; and 90 °C, 9 h, 98%. The results obtained indicated little hydrolysis of the tosylate group, in agreement with the known stability of tosylate esters in comparison with carboxylic acid esters [148]. All products showed poor solubility in ethanol, methanol, chloroform, pyridine, acetone, acetic acid, or aqueous sodium hydroxide. However, when substitution was complete, a high degree of swelling of the samples in water was observed [149].

The question of regioselectivity of the deoxy cellulose derivative has been, and still is, central to this line of research. Thus, a regioselective synthesis of 6-amino-6-deoxy cellulose with a DS of 1.0 at position 6, its 6-*N*-sulfonated and its 6-*N*-carboxymethylated derivatives, has been achieved by optimization of reaction conditions (Fig. 5.21) [150].

A sample with $DS_{Ts}$ of 2.02 was chosen because position 6 is fully tosylated. Reaction of this sample with $NaN_3$ in DMSO under controlled conditions (five mole excess of $NaN_3$, 50 °C, 38 h) leads to 100% azide/tosylate exchange at position 6 of the AGU. The azide group was reduced with $LiAlH_4$ in dioxane under conditions that led to complete reduction and removal of the tosyl groups at other positions of the AGU (molar excess of $LiAlH_4$ 5, 54 °C, 24 h). The 6-deoxyamino cellulose was further derivatized as shown in Fig. 5.21. These cellulose derivatives are candidates for the synthesis of mixed esters and studies on structure–function relations.

The azido group is interesting because it can be reduced to the amino group that can be further functionalized, e.g., quaternized to give a cellulose polyelectrolyte. Moreover, the azido moiety can be used in the click chemistry approach introduced by Sharpless et al. [151] (see Chap. 7).

Cellulose-based anionic polyelectrolytes can, in principle, be further quaternized to give zwitterionic products. Those have been prepared from CTs. As shown in Fig. 5.22, CTs were sulfated by reaction with $SO_3$/pyridine and subsequently, the sulfonate group was substituted ($S_N$) with ethylene diamine or tris-(2-aminoethyl) amine to give products that are water soluble, provided that the amino groups are not protonated. For example, these products are water soluble at pH = 11.5 and form colloidal solutions at pH ≈ 9.5. At pH < 9, they precipitate due to the

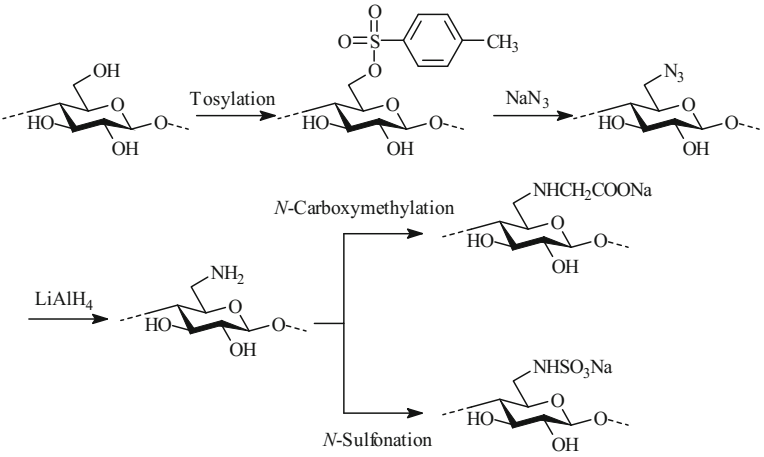


**Fig. 5.21** Scheme for the regioselective synthesis of 6-amino-6-deoxy cellulose and its *N*-sulfonated and *N*-carboxymethylated derivatives [150]

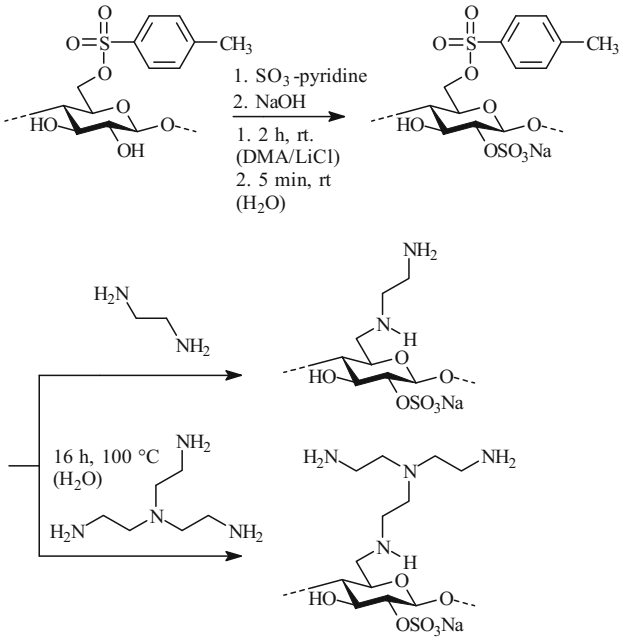


**Fig. 5.22** Scheme for the synthesis of 6-deoxy-(ω-aminoethyl)amino cellulose-2,3(6)-*O*-sulfate and 6-deoxy-6-(bis-*N*′,*N*′-aminoethyl)aminoethyl) amino cellulose-2,3(6)-*O*-sulfate, starting material is cellulose tosylate sulfate [152]

protonation of the amino groups and their strong association with the sulfate group [152].

Cross-linking of cellulose fibers leads to the formation of three-dimensional networks that is expected to enhance the strength of paper. This cross-linking has been achieved between azidodeoxy and propargyl cellulose. The first derivative was obtained from CTs (prepared in DMAc/LiCl) by MW-assisted $S_N$ reaction (DMF, 100 °C) with $NaN_3$, and the latter compound was obtained by MW-assisted reaction of alkali cellulose with propargyl bromide in DMAc/LiCl. The cross-linking was performed by the Huisgen 1,3-dipolar azide–alkyne cycloaddition catalyzed by Cu (CuAAC), a click chemistry reaction [153]. The copper-catalyzed Huisgen reaction has been employed to produce cellulose-based dendritic structures. Propargyl cellulose with regioselective functionalization pattern was synthesized by nucleophilic displacement reaction of CTs (DS 0.58) with propargylamine. The 6-deoxy-6-aminopropargyl cellulose obtained was employed as the starting material for the chemoselective dendronization of cellulose at position 6 of the AGU via the CuAAC reaction, yielding 6-deoxy-6-amino-(4-methyl-[1,2,3-triazolo]-1-propyl-polyamido amine) cellulose derivatives of first (DS 0.33; Fig. 5.23) and second (DS 0.25) generations. These products were found to be pure (no

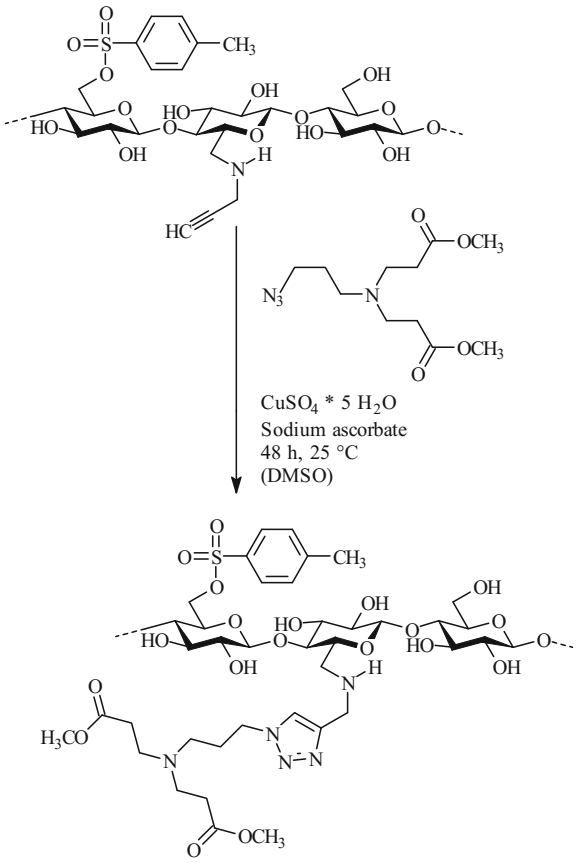


**Fig. 5.23** Homogeneous conversion of 6-deoxy-6-aminopropargyl cellulose (DS 0.48) with azidopropyl-polyamido amine dendron of the first generation [154]

cross-linking) and are soluble in polar aprotic solvents [154]. More information about click chemistry with cellulose can be found in Chap. 7.

In order to probe whether the chirality of the cellulose backbone affects the reactivity in the $S_N$ reaction of the tosylate at position 6, the derivative was synthesized in DMAc/LiCl (TEA, 24 h, 8 °C) with $DS_{Ts}$ of 0.74 and 1.29, and then reacted with *R*(+)-, *S*(−)- and racemic 1-phenylethylamine under homogeneous conditions in DMF and water (100 °C, 16 h). The line shapes of the CD spectra of the produced deoxyamino cellulose derivative showed pronounced positive and negative Cotton effects, similar to those of the starting amines. Therefore, the chirality of the cellulose backbone does not influence the $S_N$ reaction at the tosylated position 6 under the reaction conditions employed [155].

### 5.2.5 6-Deoxy-6-Amino Cellulose Derivatives—Synthesis and Properties

Soluble 6-deoxy-6-amino cellulose derivatives are a new class of cellulose derivatives with promising properties. As mentioned, the tosylation of cellulose in DMAc/LiCl occurs mainly at C-6 (at $DS_{Ts}$ below 1) and subsequently a reaction of the remaining hydroxyl groups with acid anhydrides (acetic, benzoic) or phenyl isocyanate may be carried out. The organo-soluble products possess $DS_{Ts}$ from 0.50 to 1.95 and DS of the second substituent from 0.8 to 2.4. The reaction ($S_N$ of the tosylate group) of these cellulose derivatives with phenylene diamine give amino cellulose derivatives that can be used for the immobilization of enzymes like glucose oxidase. The redox-chromogenic properties were demonstrated by oxidative coupling reaction of typical reagents, e.g., phenol and quinoline derivatives onto the phenylene diamine groups of the cellulose derivatives in the presence of $H_2O_2$ and the enzyme peroxidase (Fig. 5.24) [144].

Applying this approach, immobilization of various enzymes, e.g., glucose oxidase, lactate oxidase, and peroxidase on deoxyamino cellulose derivatives obtained from CTs carboxylates, has been carried out. The tosylate group has been substituted by not only phenylene diamine but also by bis(4-aminophenyl)methane and ethane and their *N*,*N*-dimethylamino analogues. The enzymes were immobilized by several coupling agents, e.g., glutaraldehyde and *L*-ascorbic acid, and their catalytic activity and stability were evaluated [156].

In general, this type of amino celluloses may be divided into four groups according to the spacer type (X, see Figs. 5.25, 5.26, 5.27 and 5.28) [157–159]:

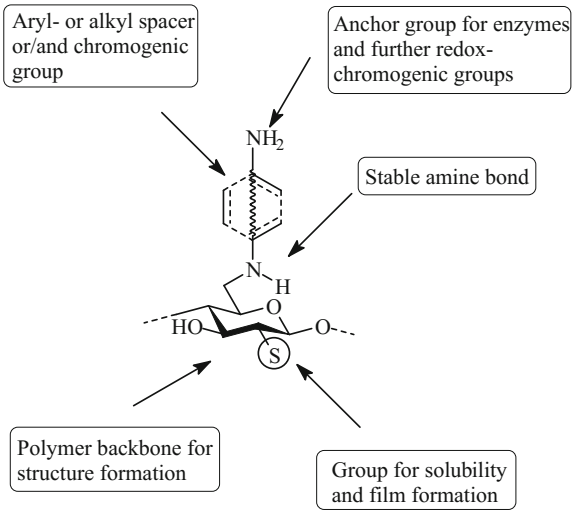


**Fig. 5.24** Schematic representation of the requirements of a support for enzyme immobilization for sensors [144]

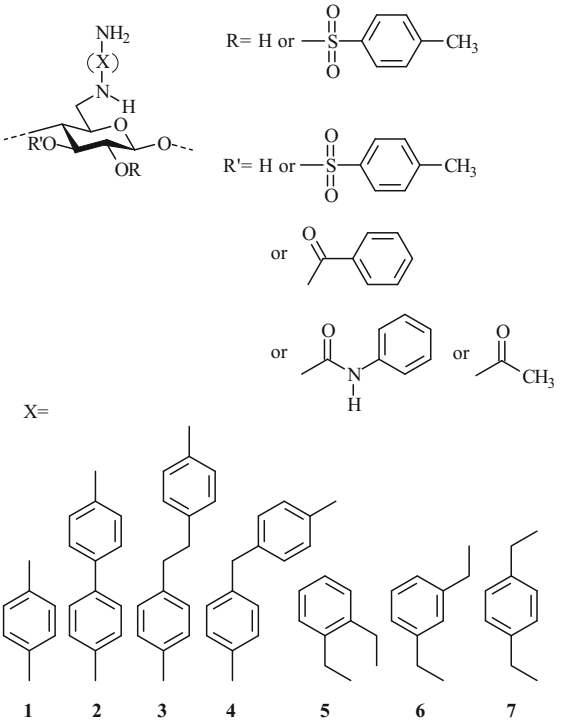


**Fig. 5.25** Examples of soluble amino cellulose derivatives with *p*-phenylene diamine (**1**), benzidine- (**2**), and aralkylene residues at position 6 (**3**–**7**)

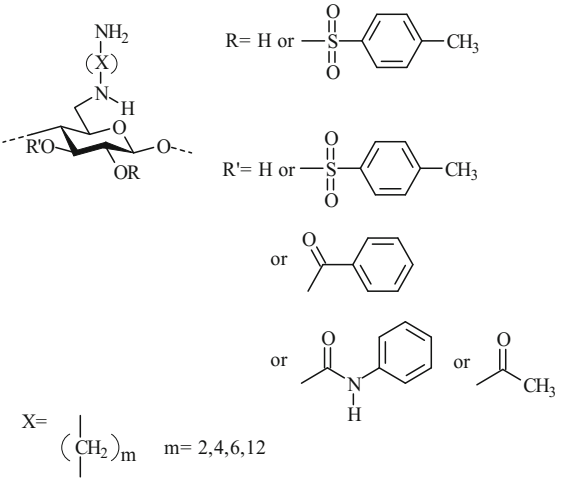


**Fig. 5.26** Examples of soluble alkylene diamine (ADA) cellulose derivatives at position 6

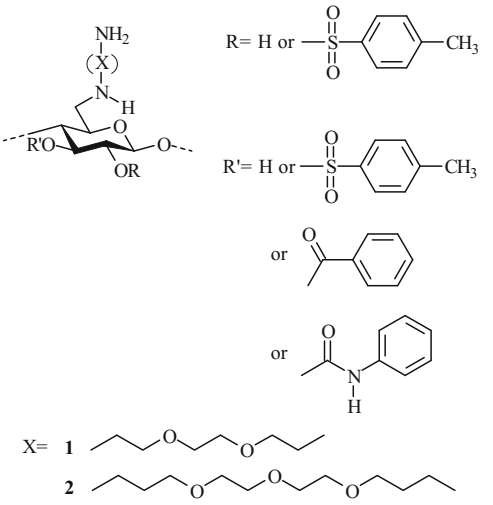


**Fig. 5.27** Examples of soluble amino cellulose derivatives with an *O*-alkylene diamine residue at position 6: (**1**) 1,8-diamino-3,6-dioxaoctan (DADO) cellulose derivative and (**2**) 4,7,10-trioxa-1,13-tridecanediamine (TODA) cellulose derivative

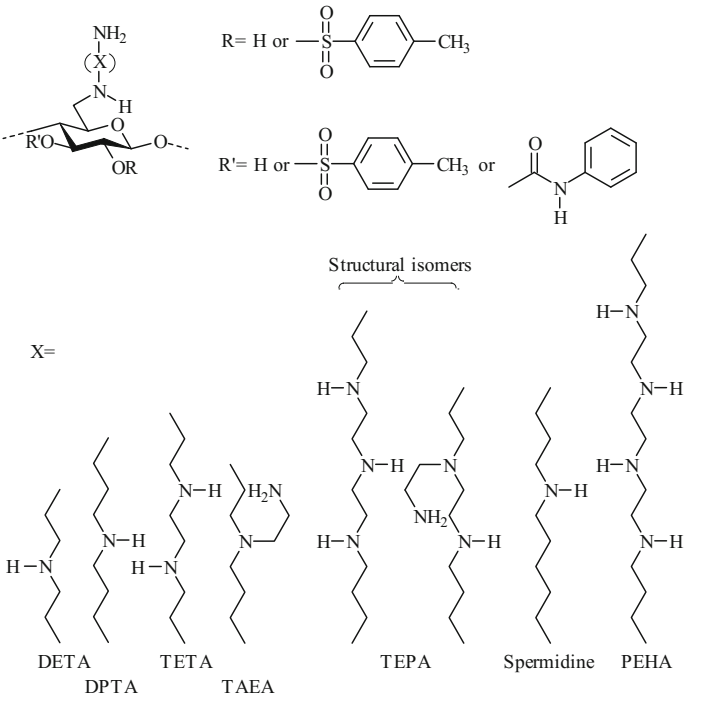


**Fig. 5.28** Examples of soluble amino cellulose esters with an oligoamine residue at position 6

(i) Amino celluloses with 1,4-*p*-phenylene diamine (PDA) or aralkylene diamine residue (Fig. 5.25)
(ii) Amino celluloses with alkylene diamine (ADA) residue (Fig. 5.26)
(iii) Amino celluloses with *O*-alkylene diamine residue (Fig. 5.27) and
(iv) Amino celluloses with oligoamine residue (Fig. 5.28).

#### 5.2.5.1 Alkylene Diamine (ADA) Cellulose Derivatives

The $DS_{ADA}$ values depend on the reaction temperature; at 100 °C (3 h), for example, EDA cellulose carbanilates with a maximum $DS_{EDA}$ are obtained that could not be achieved at lower reaction temperatures (70 °C) even after a reaction time of 24 h. In addition, tosylate moieties were cleaved without introduction of the amine moiety. Obviously, the tosylate and carbanilate moieties are cleaved by aminolysis with the ADAs (Fig. 5.26). Thus, tosylamide and phenylurea moieties are formed. Similar behavior is observed by conversions of tosyl cellulose carbamates with other ADAs ($m$ = 4, 6, 8, 12). However, the cleavage rates of the solubilizing ester groups decrease with increasing chain length of the ADA. The rate of cleavage of the carbanilate and benzoate groups is almost comparable [156, 160]. There is apparently no reactivity graduation as a function of the alkylene chain length of the diamine residue.

#### 5.2.5.2 Amino Cellulose Derivatives with Oligoamine Residues

Examples of amino cellulose esters containing oligoamine moieties at position 6, which even may be biogeneous, are of special interest for biofunctional applications including biochip and biofunctional nanoparticles with immunoaffine properties [161–163]. The conversion of tosyl cellulose ($DS_{Ts}$ 0.80) with oligoamines (Fig. 5.28) applying a reaction temperature of 100 °C for 6 h guarantees the maximal value of the $DS_{Amine}$ leading to water-soluble products [162].

The amino celluloses with the spacer structure are soluble in water already at low DS values (pH values of 10–11) provided the positions 2 and 3 possess hydroxyl groups. These amino celluloses are particularly suited as the support matrix for enzymes because optimal pH values could be adjusted by titration with aqueous acids like aqueous HCl. Another special characteristic of the amino cellulose is the formation of blue-stained chelate complexes with $Cu^{2+}$ ions (at $\lambda_{max}$ values between 560 and 630 nm)—similarly to the corresponding oligoamines [162]. They are therefore of particular significance for coupling with biological redox systems, especially with Cu proteins.

#### 5.2.5.3 Supramolecular Aggregation of Amino Cellulose

The cellulose derivative 6-deoxy-6-amino cellulose forms multiple oligomeric species that have been studied by the hydrodynamic technique of analytical ultracentrifugation. It was found that even a fully reversible self-association (tetramer formation) within this family of 6-deoxy-6-amino cellulose occurs (Fig. 5.29). Remarkably, these tetramers do associate further in a regular way into supramolecular complexes [164].

Based on the $s \sim M^{2/3}$ scaling relationship, the super-monomers associate into super-trimers, super-hexamers, and super-9-mers with evidence also for some super-dimers, although the latter were not evident at the highest loading concentration. The proportion of the super-monomers drops relative to the higher order species showing partial reversibility even with the higher order association.

This behavior was observed for the first time for carbohydrates while it is well known for polypeptides and proteins like hemoglobin and its sickle cell mutation [165]. The self-assembling renders them as mimicking the properties of histones and can be used as condensing or packing agents in DNA-based therapies [166].

Most importantly, however, our traditional perceptions as to what is "protein-like" and what is "carbohydrate-like" behavior may need to be reconsidered [167].

The amino celluloses may form ultrathin and transparent films as multi- or monolayers (SAMs) at various substrates like glass, gold, and Si wafer. Starting with a 5% solution of amino cellulose (in water or an organic solvent), by tipping, spraying, and spin coating nanoscale topography is formed [168–170].

Amino celluloses are biocompatible probably due to the fact that they display similarities to certain ECM structures (e.g., poly-L-lysine and polyornithine). A further major advantage is that amino celluloses could be firmly fixed to material surfaces of various chemical types via composite monolayers. The coupling of various oxidoreductases, e.g., indicates the usefulness of this approach. Products of high specific activity are obtained (Table 5.12).

Even spherical nanoparticles with a size in the range 80–200 nm could be obtained by self-assembly of highly functionalized, organo-soluble 6-deoxy-6-(ω-aminoalkyl) amino cellulose carbamates. The particles are very stable, nontoxic, and possess primary amino groups that are accessible to further modifications. The particles could be labeled with rhodamine B isothiocyanate without changing their size, stability, and shape (Fig. 5.30). The nanoparticles may be incorporated in cells like primary human foreskin fibroblasts and mamma carcinoma MCF-7 without any transfection reagent [171].

A strategy for the preparation of well-dispersed hybrid particles in organic media by a combination of the solution-based formation of magnetic nanoparticles (MNP) and subsequent coating with amino celluloses was developed. The hybrid

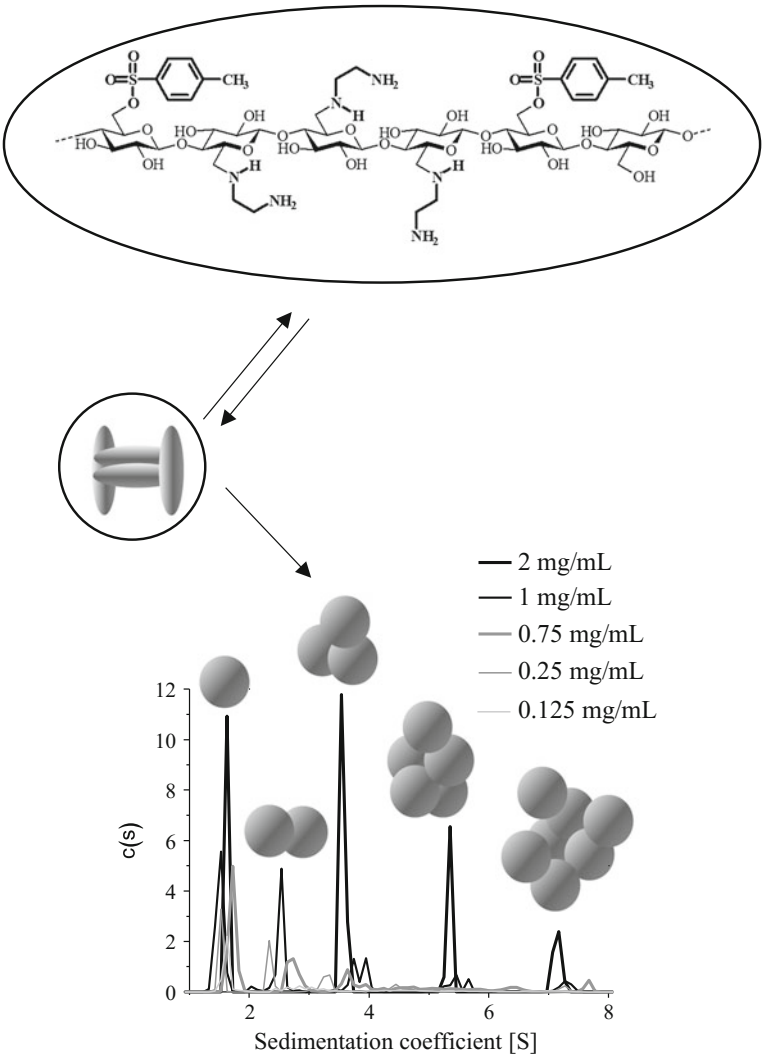


**Fig. 5.29** Reversible tetramer formation and further higher order association of the polysaccharide 6-deoxy-6-(ω-aminoethyl)amino cellulose (AEA cellulose). The structure shown at the top corresponds to a monomer unit of degree of polymerization ∼10, $DS_{Amine}$ at C-6 0.83 and $DS_{Ts}$ at C-2 0.2, corresponding to molar mass of ∼3250 g/mol and s ∼ 0.5 S. The aggregate shown in the middle corresponds to a tetramers with M ∼ 13,000 g/mol and s ∼ 1.7 S. The plot at the bottom shows the sedimentation coefficient distribution for AEA cellulose at different concentrations (from black to light gray) 2.0, 1.0, 0.75, 0.25, 0.125 mg/ml (reprinted with permission from [167] under the Creative Commons CC–BY license)

**Table 5.12** Covalent coupling of selected oxidoreductases (glucose oxidase, GOD, horseradish peroxidase, HRP, lactate oxidase, and LOD) to PDA cellulose films by different coupling agents

| Coupling agent | Activity (μ/cm$^2$) | | |
|---|---|---|---|
| | GOD | HRP | LOD |
| Diazo coupling | 194 | 135 | 220 |
| Glutaraldehyde | 187 | 206 | 100 |
| L-Ascorbic acid | 185 | 200 | 192 |
| Benzene-1,3-disulfonic acid chloride | 168 | 48 | – |
| 4,4′-Biphenyldisulfonic acid chloride | 27 | 35 | – |
| Benzene-1,3-dicarboxylic acid dichloride | 34 | 121 | 286 |
| Benzene-1,4-dicarboxylic acid chloride | 60 | 27 | 131 |
| Cyanuric chloride | 33 | 59 | 119 |
| Benzene-1,3-dialdehyde | 94 | 58 | 61 |
| Benzene-1,4-dialdehyde | 56 | 48 | 21 |
| 1,3-Diacetylbenzene | 51 | 76 | 123 |
| 1,4-Diacetylbenzene | 70 | 104 | 52 |

particles exhibit an average diameter of about 8 nm. The stability of the amino cellulose@MNP hybrid particles in polar organic solvents such as DMAc was exploited by using the materials as heterogeneous ligands in the atom transfer radical polymerization (ATRP) of styrene showing that PS with a near-narrow molecular weight distribution (PDIs < 1.3) and low Cu contents (5 ppm) can be prepared (Fig. 5.31). The amino cellulose@MNP hybrid particles could be separated from the reaction mixture by an external magnetic field and can be reused again in polymerization of styrene [172].

Typical examples of advanced cellulose derivatives that can be obtained from CTs are summarized in Table 5.13.

## 5.3 Esters of Inorganic Acids

Except for cellulose nitrate (sometimes erroneously called nitrocellulose), which is produced on a large scale and is currently employed in printing inks, wood lacquers, foil and film lacquers, auto refinish paints, nail lacquers, and leather finishes, cellulose esters of inorganic acid are commercially much less important compared to their organic acids counterparts. Of these, we discuss cellulose borate, carbonate, carbamate, nitrate, phosphate, and cellulose sulfate.

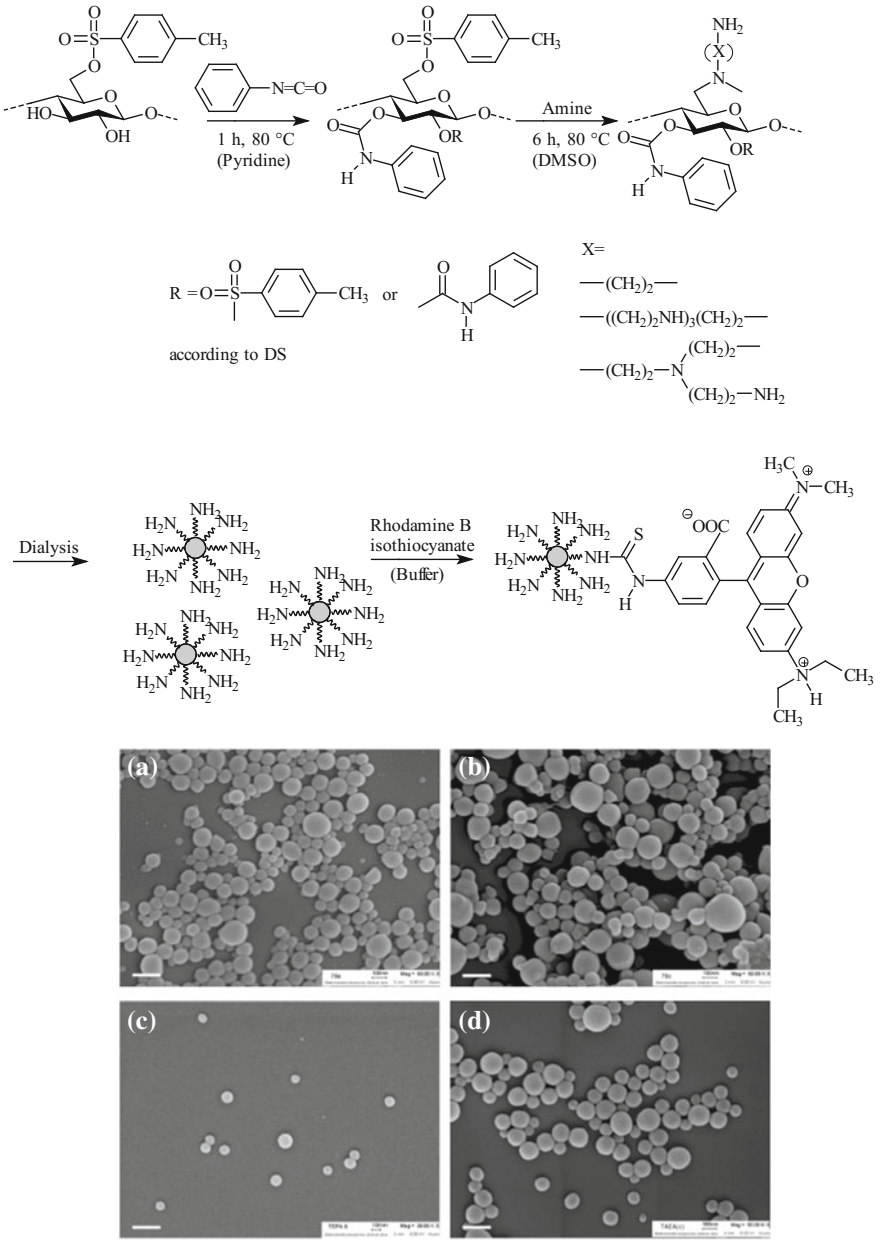


**Fig. 5.30** Schematic synthesis of different 6-deoxy-6-(ω-aminoethyl)amino cellulose carbamates followed by the modification of the particle systems obtained from dialysis by rhodamine B and selected SEM micrographs (reprinted from [171], with permission from John Wiley and Sons, copyright © 2012)

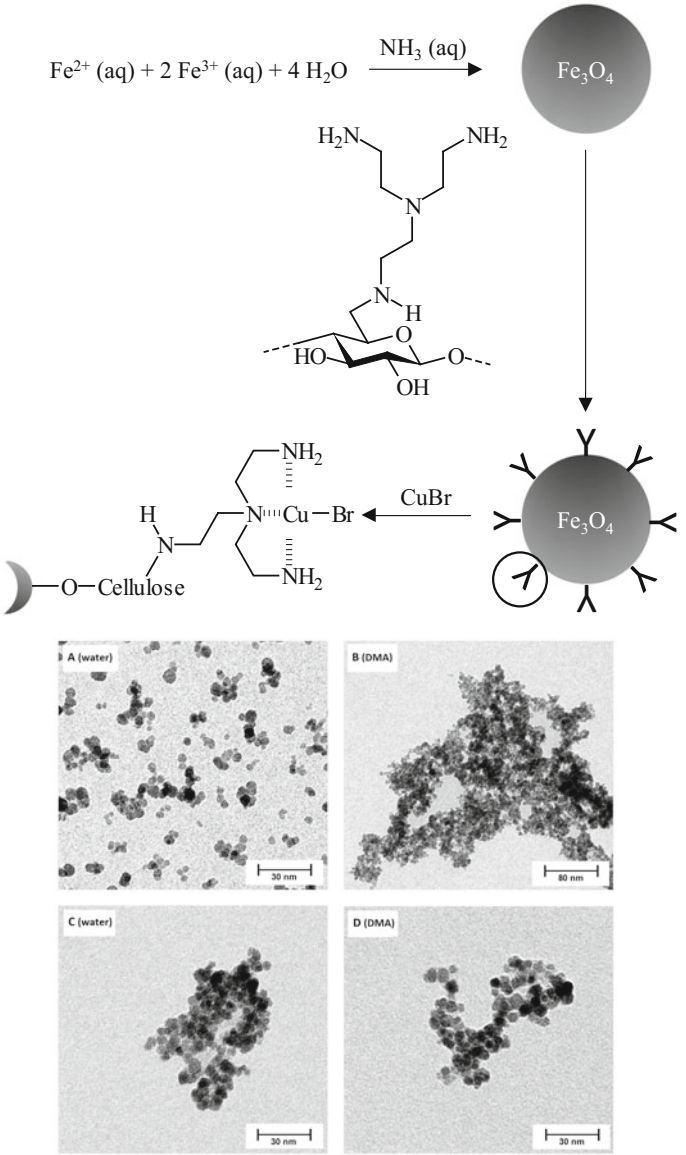


**Fig. 5.31** Synthesis of the $Fe_3O_4$ nanoparticles, coating with amino cellulose, and complexation of CuBr during heterogeneous ATRP procedures and TEM micrographs for MNP and amino cellulose@MNP; as-synthesized MNP from water (**a**) and DMAc (**b**); amino cellulose @MNP from water (**c**) and DMAc (**d**) (reprinted from [172] copyright © 2013 with permission from Elsevier)

**Table 5.13** Examples for the synthesis of cellulose tosylates and derivatives therefrom

| Cellulose type | Derivatizing agent | Solvent | Product | DS | References |
|---|---|---|---|---|---|
| MCC, cotton linters | TsCl and $SO_3$/pyridine | DMAc/LiCl | Cellulose tosylate sulfate | $DS_{Ts}$ 0.46–2.02 $DS_{Sulf}$ 0.34–0.85 | [146] |
| Cotton linters | TsCl, TEA, and acetic, propionic, caproic, stearic, phthalic, trimellitic, succinic, and maleic anhydride | DMAc/LiCl and pyridine | Cellulose tosylate acylate | $DS_{Ts}$ 0.93–2.02 $DS_{Ester}$ 1.61–2.07 | [145] |
| MCC | TsCl/TEA and then NaI, $NaN_3$ with $LiAlH_4$ | DMAc/LiCl, acetylacetone, DMSO, and dioxane | 6-Deoxycellulose | $DS_{Deoxy}$ up to 1 | [150] |
| MCC | TsCl/TEA, and then $NaN_3$; NaH and then propargyl bromide | DMAc/LiCl, DMF, aqueous NaOH | 6-Deoxycellulose | $DS_{Azido}$ 1.5 $DS_{Prop}$ 0.4 | [153] |
| MCC | TsCl/pyridine or TEA, and then $NaN_3$ | Mixtures of AlMeIMCl or EtMeIm $(EtO)_2PO_2^-$) and pyridine, DMF, DMI | 6-Deoxycellulose | $DS_{Cl}$ 0.16 $DS_{Ts}$ 0.02 $DS_{Azido}$ 0.90 $DS_{Cl}$ 0.02 | [140] |

## *5.3.1 Cellulose Nitrate*

### 5.3.1.1 Introduction

Cellulose nitrate, CN (often called nitrocellulose), was the first industrially prepared cellulose derivative, by Braconnot in 1832 [173] and later by Schönbein who developed the use of the nitrating mixture $HNO_3/H_2SO_4/H_2O$ [174]. Celluloid, a mixture of CN with camphor, was the first industrially produced thermoplastic material [175]; gun cotton is a highly nitrated cellulose derivative; its military use as explosive started on a large scale during the American Civil War (1861–1865) [176].

### 5.3.1.2 The Chemistry of Cellulose Nitration

This esterification reaction is equilibrium:

$$\text{Cell}-\text{OH} + \text{HNO}_3 \rightleftharpoons \text{Cell}-\text{O}-\text{NO}_2 + \text{H}_2\text{O} \tag{5.5}$$

It is carried out under heterogeneous conditions. The actual nitrating agent is the nitronium ion that is formed either by the auto-pyrolysis of nitric acid (that contains ca. 3% $NO_2^+$) or the acid protonated by sulfuric acid [177]:

$$2\ \text{HNO}_3 \rightleftharpoons \text{NO}_2^+ + + \text{H}_2\text{O} \tag{5.6}$$

$$\text{HNO}_3 + \text{H}_2\text{SO}_4 \rightleftharpoons \text{NO}_2^+ + \text{HSO}_4^- + \text{H}_2\text{O} \tag{5.7}$$

That $NO_2^+$ is the actual nitrating agent has been demonstrated by evidence similar to that employed in electrophilic aromatic substitution. For example, at constant nitric acid concentration (25%), increasing the concentration of sulfuric acid in the nitrating mixture from 55.8 to 66.5% increases $DS_{Nitrate}$ from 1.95 to 2.70, on one hand. On the other hand, increasing the water concentration from 8.5 to 18.4% decreases $DS_{Nitrate}$ from 2.70 to 2.05 because these composition variations shift equilibrium [178]. Additionally, cellulose can be nitrated by other reagents that contain/produce the $NO_2^+$ ion, e.g., ($NO_2^+BF_4^-$) in sulfolane; $KNO_3$ in 98% $H_2SO_4$ [178–180], and $N_2O_4$/DMF [181, 182], $HNO_3$/DCM, $HNO_3/H_3PO_4/P_2O_5$, and $HNO_3$/acetic acid/acetic anhydride [183]. $N_2O_4$ reacts with cellulose to form cellulose nitrite that interacts with the $HNO_3$ usually present in $N_2O_4$/DMF solutions, to form the Knecht addition compound [36]. The latter compound is also present in nitric acid solution whose concentration is <75%. The labile cellulose nitrite is converted in the presence of $HNO_3$ into the corresponding cellulose nitrate, Eq. (5.8) [184, 185]:

$$\text{Cell}-\text{ONO}\ +\ \text{HNO}_3 \rightleftharpoons \text{Cell}-\text{O}-\text{NO}_2 + \text{HNO}_2 \tag{5.8}$$

Despite its heterogeneous nature, cellulose nitration proceeds fast and the equilibrium nitrogen content is reached in ca. 10 min at room temperature with a thoroughly dispersed fibrous cellulose [186]. The course of the reaction depends on the degree and uniformity of cellulose swelling, hence on the macro- and micromorphology of the sample. Thus, cellulose dried at 105 °C (where some hornification may occur) reacts at half the rate of a sample dried under reduced pressure at 20 °C [187]. As the nitration reaction is accompanied by considerable change in the supramolecular structure of the biopolymer, its outcome depends both on the nitrating and cellulose swelling "power" of the reagent. WAXS has been employed to follow changes in the crystalline structure of the biopolymer as a function of extent of nitration. Up to $DS_{Nitrate}$ of 1.14, cellulose II diffraction pattern can be detected, but not that of cellulose nitrate. The amorphous diffraction pattern persists

up to $DS_{Nitrate}$ of 1.80. Cellulose nitrate diffraction pattern is fully developed at $DS_{Nitrate}$ of 2.50 [178].

Additionally, SEM micrographs taken after 5 and 30 s of nitration corroborate this fiber reorganization, Fig. 5.32, parts (A) and (B). Examination of these micrographs reveals that a "cracking" in the fiber surface has occurred between 5 and 30 s, i.e., destruction of the fiber surface is concomitant with nitration. It is envisaged that fiber cracking results from stresses, imposed by nitration, in the cellulose surface region [188].

Other relevant points regarding this reaction are as follows:

- The reaction shows regioselectivity up to rather high nitrogen content. The order of substitution is *O*-6 > *O*-2 > *O*-3. Thus, the equilibrium constants for nitration by $HNO_3/H_2SO_4/H_2O$ at these positions were calculated from integration of the areas of the corresponding $^{13}C$ NMR peaks, assuming that the nuclear Overhauser effect (NOE) is the same for all carbon atoms of the AGU. From peak areas of CN functionalized at *O*-2, *O*-3, *O*-6, and at *O*-3 and *O*-6 (after selective denitration at position 2 by hydroxylamine/pyridine), the equilibrium constants were calculated to be 5.8 (*O*-6), 1.8 (*O*-2), and 1 (*O*-3) [189]. Regioselectivity for esterification at *O*-6 was even larger when the less reactive (more selective) $HNO_3/H_2O$ was employed as nitration medium, 12.6 (*O*-6), 0.26 (*O*-2), and 0.12 (*O*-3) [186]. An increase in the water content favors nitration at position 2 in comparison with position 3.
- The distribution of substituents depends on the nitration system employed (Table 5.14).

Thus, the selective esterification at *O*-6 and the extent of the reaction are clearly favored by using $HNO_3$/DCM.

(i) Due to the presence of a large concentration of $H_2SO_4$ in the nitration mixture, cellulose sulfuric acid ester is formed along with the nitrate. The concentration of the sulfate decreases as a function of increasing the nitrogen

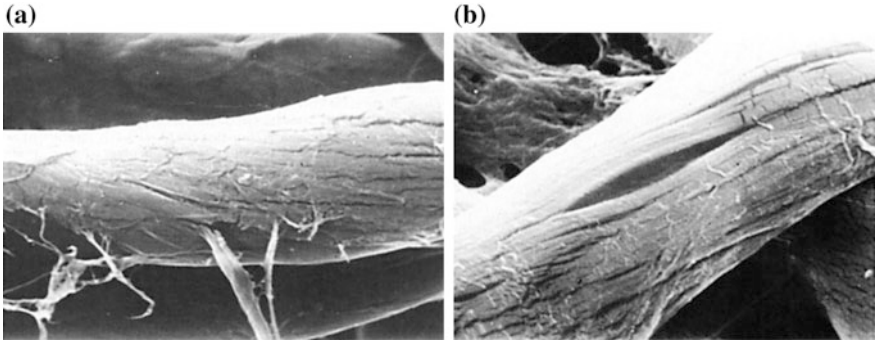


**Fig. 5.32** SEM micrographs of cellulose fiber after 5 s (**a**) and 30 s (**b**) nitration by $HNO_3/H_2SO_4/H_2O$ (22.5/75/2.5) (reproduced from [188], with permission of John Wiley and Sons)

**Table 5.14** $^{13}C$ NMR spectroscopy-based determination of the distribution of the nitrate group at the different positions of the AGU as a function of the nature of the nitration agent [179, 180]

| Nitration system | $DS_{Nitrate}$ | % Nitration at the different carbons of the AGU | | | |
|---|---|---|---|---|---|
| | | *O*-2,3,6 | *O*-2,6 | *O*-3,6 | *O*-6 |
| $HNO_3/H_2SO_4/H_2O$ | 1.80 | 36 | 22.5 | 15.5 | 9.5 |
| $HNO_3/H_2SO_4/H_2O$ | 2.10 | 49 | 18 | 10 | 6.0 |
| $HNO_3$/DCM | 1.95 | 23 | 38.5 | 19 | 15.5 |
| $HNO_3$/DCM | 2.19 | 32 | 39 | 16 | 13.0 |

content of the product, being ca. 3% for $DS_{Nitrate} < 2$ and between 0.2 and 0.5% for higher $DS_{Nitrate}$. This sulfate ester is eliminated by acid-catalyzed hydrolysis during the so-called "stabilization" step in the course of manufacturing of cellulose nitrate.

(ii) Highly functionalized cellulose nitrates are accessible by reaction of cellulose with mixture of $HNO_3$ (90%)/$H_3PO_4$/$P_4O_{10}$ [190] or with a nitric acid (90%)/acetic anhydride [191]. The reason for not using sulfuric acid as a catalyst is to avoid the formation of cellulose sulfate. Pure $HNO_3$ (100%) in chlorinated solvents (methylene chloride, chloroform) is used to prepare highly stable cellulose nitrates with DS of 2.87–2.94 [177].

(iii) Because of the strongly acidic conditions and presence of water, hydrolysis occurs, both of the starting material (glycosidic links) and the product via acid-catalyzed denitration. Nitration does not affect the DP of cellulose for derivatizing mixtures that do not contain water. The nitrate group is stable under mild, but not strongly acidic conditions. It can be removed by alkaline hydrolysis and, being a leaving group, can be efficiently eliminated by $Na_2S$/ethanol.

#### 5.3.1.3 Industrial Production of Cellulose Nitrate

Highly pure materials guarantee high-quality CNs. Thus, the raw materials for the industrial preparation of CN are cotton linters and refined hard- or softwood pulps with α-cellulose content between 92 and 96% with low hemicellulose and ash content, in particular $Ca^{2+}$ ions (in order to prevent $CaSO_4$ precipitation). Because of the short reaction time and the heterogeneous nature of the reaction, the morphology, porosity, $I_c$, and DP are of prime importance and determine not only the rate but also the uniformity of nitration [192]. The dependence of $DS_{Nitrate}$ on the composition of the nitrating solution is shown in Table 5.15.

Figure 5.33 shows a schematic representation of the industrial production of CN.

The nitration is carried out both as batch and continuous process, mostly with the nitrating mixture $HNO_3/H_2SO_4/H_2O$. Because water is present in the reaction medium, cellulose (as fluffs, shreds, or chips) is not dried before its use. In the batch

**Table 5.15** Dependence of the DS of cellulose nitrate on the composition of the $H_2SO_4/HNO_3$ mixture [adapted from [193] reprinted from Esterification of polysaccharides, Chap. 7, 2006, Heinze T, Liebert T, Koschella A, p. 141, with permission from Springer)]

| Composition of the nitrating acid | | | Cellulose nitrate | |
|---|---|---|---|---|
| $H_2O$ | $HNO_3$ | $H_2SO_4$ | Nitrogen content (%) | DS |
| 12.0 | 22.0 | 66.0 | 13.2 | 2.6 |
| 16.0 | 20.0 | 64.0 | 12.5 | 2.4 |
| 20.0 | 20.0 | 60.0 | 10.6 | 1.9 |

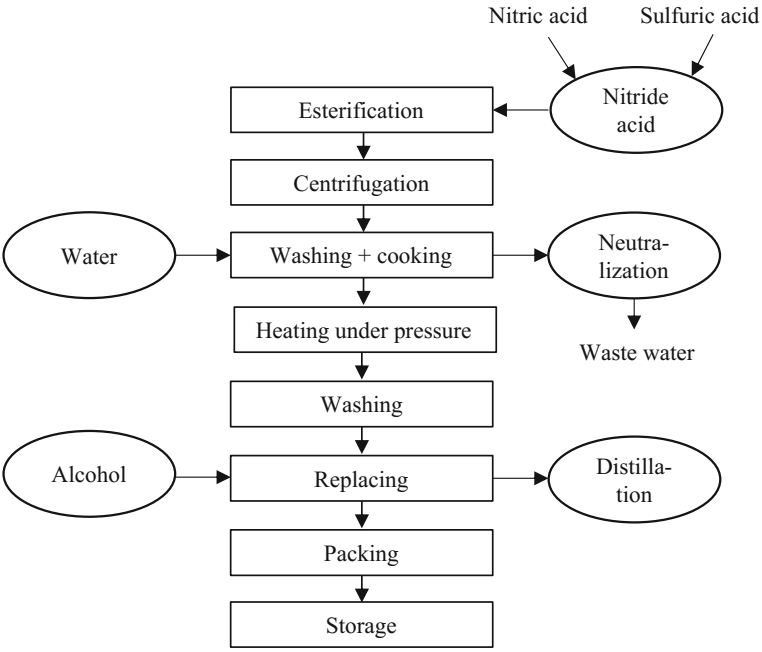


**Fig. 5.33** Schematic representation of the industrial production of CN

process, cellulose is reacted in a stainless steel tube reactor with the nitrating mixture at solid/liquid ratio of 1:20 to 1:50 at 10–35 °C. The lower temperature is employed for samples with high nitrogen content. The reaction mixture is then centrifuged to yield CN-embedded with the nitrating mixture [100–300% (w/w)] that is subjected to further treatment as discussed below.

The continuous process developed in the 1960s (Fig. 5.34) is advantageous in terms of process economy and uniformity of the product. The ingredients are fed simultaneously into the reactor with a dwell time of 30–55 min. A recent development consists of the use of a continuous-loop pressure reactor that reduces the dwell time to 6–12 min.

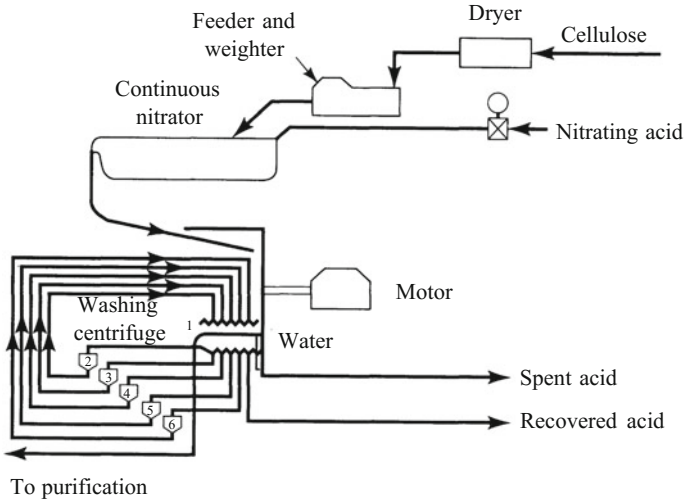


**Fig. 5.34** Flow diagram of nitration of cellulose by Hercules continuous process

As indicated above, the produced CN contains some sulfate moieties whose presence leads to instability of the crude CN. Elimination of CS occurs during the product "stabilization" step, which consists of a series of washings with water. First, the centrifuged mass is subjected to "cooking" with dilute nitric acid solution (0.1–1%) under pressure at 130–150 °C, followed by washing with water until the product is neutral. Stabilizers like citric, tartaric, stearic, or oxalic acid and diphenylamine are added to protect CN against thermal and photochemical degradation and discoloration. The lower end of the nitrogen content range, from 10.6 to 11.2%, is alcohol-soluble, whereas the higher end, i.e., 11.8 and 12.3% nitrogen, is soluble in ethyl acetate (so-called ester soluble cellulose nitrate, see also Table 5.16).

#### 5.3.1.4 Properties of Cellulose Nitrate

Cellulose nitrate is a white, odorless, and tasteless substance, whose properties and applications depend on its nitrogen content or $DS_{Nitrate}$. The nitrogen contents of cellulose mono-, di-, and trinitrate are 6.75, 11.11, and 14.14%, respectively. The relationship between both scales is given by

$$\%N = 1.060 + 6.355\,DS_{Nitrate} - 0.665(DS_{Nitrate})^2 \tag{5.9}$$

The dependence of CN solubility on its $DS_{Nitrate}$, along with some applications of these products, is summarized in Table 5.16. See Table 5.17 for further synthesis examples.

**Table 5.16** Solubility and application of commercially available cellulose nitrates

| Nitrogen content | DS | Solubility | Application |
|---|---|---|---|
| 10.9–11.2 | 1.94–2.02 | Ethanol, isopropanol | Plastic foils, flexographic inks |
| 11.8–12.2 | 2.20–2.32 | Esters, ketones, and ether–alcohol mixtures | Industrial coatings |
| 12.6–13.8 | 2.45–2.87 | Esters | Explosives |

**Table 5.17** Examples of the synthesis of cellulose nitrate

| Cellulose | | Derivatizing agent | Solvent | DS | References |
|---|---|---|---|---|---|
| Type | DP | | | | |
| Cotton linters | 1145–4580 | $HNO_3$/organic solvents | Dichloroethane, dichloromethane, and mixtures with diethyl ether | 1.25–2.94 | [177] |
| Wood cellulose | 855–1040 | $HNO_3/P_4O_{10}$ | Nitrating mixture | 3.0 | [190] |
| Filter paper, Whatman No. 1 | | $HNO_3/H_2SO_4/H_2O$ (22.5/75/2.5%) | Nitrating mixture | 2.30–2.40 | [188] |
| Filter paper, Whatman No. 1 | | $HNO_3/H_2SO_4$ | Methylene chloride | 1.80–2.67 | [199] |
| Filter paper, Whatman No. 1 | | $NO_2^+BF_4^-$ | Sulfolane | 1.10–2.70 | [179] |

**Table 5.18** Results of homogeneous phosphorylation of CA samples with tetrapolyphosphoric acid/(1-butyl)$_3$N/DMF (adapted from [218])

| $DS_{Ac}$ of CA | $DS_{Phosphate}$ (NMR) | Substitution pattern | | Solubility of CPhos after acetate group removal | |
|---|---|---|---|---|---|
| | | *O*-2,3 | *O*-6 | Water | NaOH |
| 2.40[a] | 0.25 | 0.05 | 0.20 | Swelling | Soluble |
| 1.90[a] | 0.75 | 0.50 | 0.25 | Soluble | Soluble |
| 2.60[b] | 0.1 | 0.1 | 0 | Swelling | Soluble |
| 1.74[b] | 0.65 | 0.55 | 0.1 | Insoluble | Swelling |

[a]Statistically substituted CA samples
[b]Regioselectively substituted

CN, as solid or in solution, is destroyed if brought into contact with strong acids (degradation), bases (denitration), or amines (decomposition). Of considerable practical importance is thermal decomposition of CN at $T > 130$ °C that leads to deflagration due to the formation of $NO_2$-free radicals

$$\text{Cell}-\text{O}-\text{NO}_2 \rightarrow \text{Cell}-\text{O}^{\cdot} + {}^{\cdot}\text{NO}_2 \tag{5.10}$$

This initiates a strongly exothermic radical chain reaction, resulting finally in $CO_2$, $NO_2$, $N_2$, and $CH_2O$. This thermal instability is the consequence of the weak bond energy of O–$NO_2$, in the range of 33.0–39.2 kcal/mol for a series of aliphatic nitrates [194]. The thermal stability of CNs is usually determined by the Bergmann-Junk test, which is based on the quantitative determination of nitrogen oxides evolved during thermal decomposition of a sample kept at 120 or 132 °C. The produced nitrogen oxides are absorbed in water and quantified by acidimetric analysis; the result is a measure of chemical stability of the sample. For safety reasons, the commercially available CNs are wetted with at least 25% water, or aliphatic alcohols, in particular ethanol, 2-propanol, and 1-butanol.

#### 5.3.1.5 Applications of Cellulose Nitrate

An everyday use of CN is in nitro lacquers where it is dissolved in organic solvents (alcohols or esters). These CN solutions are compatible with the essential substances in the lacquer formulation, e.g., alkyd-, maleic-, ketone-, and urea resins, and polyacrylates. A large list of softeners, e.g., adipates, phthalates, phosphates, and biobased materials, e.g., vegetable oils, are compatible with CNs. The most important uses for CN-based lacquers are those for wood, metals, paper, foil (also as hot sealing lacquers for cellophane, plastic, and metal foils), leather, adhesive cement, and printing inks (for gravure printing). CNs are also employed as explosives (guns, detonating, and igniting agents). In this use, the following distinction is made: monobasic powder, which is based solely on cellulose nitrate; dibasic powder, which contains further energy-rich substances, e.g., nitro glycerol or ethylene glycol dinitrate; tribasic powder that contains, in addition, the third component like nitro guanidine.

### *5.3.2 Cellulose Phosphate and Phosphite*

#### 5.3.2.1 Introduction

In principle, the reaction of cellulose with phosphorous compounds produces the following acid derivatives, or the corresponding salts after neutralization: phosphoric (Cell–O–$PO(OH)_2$), phosphorous (Cel–O–$P(OH)_2$), and phosphonic (Cell–$PO(OH)_2$). The most important of these derivatives is cellulose phosphate, CPhos,

due to its thermal stability (flame retarding properties), favorable biomedical properties, e.g., bio- and hemocompatibility, and capacity as green ion-exchange polymer.

Cellulose phosphorylation is usually carried out on cellulose under heterogeneous conditions. In contrast to cellulose sulfate, obtaining water-soluble CPhos is rather the exception than the rule due to polymer chain cross-linking. Phosphorylation of cellulose under homogenous condition has been carried out, e.g., in derivatizing solvents or in ILs as well as with cellulose derivatives, e.g., esters or ethers. These approaches usually lead to water-soluble products and permit control of regioselectivity.

#### 5.3.2.2 Synthesis of Cellulose Phosphate Under Heterogeneous Conditions

The most frequently employed reagents are those of pentavalent phosphorous, including $H_3PO_4$, alone or in the presence $P_4O_{10}$ or urea, and $POCl_3$ in an organic solvent. Compared with the corresponding hexavalent sulfur (e.g., $H_2SO_4$), these phosphorylation compounds are less reactive, the reaction leads to less biopolymer chain degradation, and there is a tendency to form cross-linked oligophosphates, leading to the above-mentioned water insolubility of the products obtained.

Because the first $pK_a$ of orthophosphoric acid is relatively small, 2.15, it is expected that CPhos can be synthesized by direct esterification of the biopolymer. Cellulose contact with the commercially available orthophosphoric acid (85% (w/w)) causes swelling, without formation of CPhos. In fact, treatment with this acid is employed for decrystallization of fibrous cellulose samples [196]. Water-free orthophosphoric acid has been employed for the preparation of CPhos, both water soluble and water insoluble, usually in the presence of a catalyst and an organic solvent. Thus, phosphorylation with a mixture of $H_3PO_4/P_4O_{10}$/2-PrOH resulted in products with $DS_{Phosphate}$ 0.1–1.0. These compounds were separated by centrifugation and neutralized [197]. The same procedure has been employed using $C_4$ to $C_8$ alcohols, or DMSO as solvents, and products with DS < 0.2 with appreciable biopolymer degradation were obtained [198]. See Table 5.19 for summary.

In addition to aliphatic alcohols, triethylphosphate has been employed as an organic solvent. Thus, MCC was first swollen in 1-hexanol, DMF, or 85% $H_3PO_4$, and then phosphorylated under optimized conditions (of swelling extent, and reaction time/temperature) with $H_3PO_4/P_4O_{10}/Et_3PO_4$/1-hexanol. The products obtained were water soluble, or showed strong swelling in water, with $DS_{Phosphate}$ 1.35–2.50; the latter value obtained for the first time [199]. A similar procedure has been applied, and the conditions (reaction time and temperature) optimized for the phosphorylation of cellulose samples from different sources, including MCC from oil palm empty fruit (30–50 °C; esterification mainly at *O*-2 and *O*-3; $DS_{Phosphate}$ 0.21–2.0). The use of wavelet neural model permitted predictions of the % P in the products (with 0.14–6.68% deviation), the reaction yield (with 0.47–4.07%

**Table 5.19** Summary of representative examples of the routes employed for the synthesis of cellulose phosphate and phosphite

| Cellulose/cellulose derivative | Derivatizing agent | Solvent | Product; DS range | References |
|---|---|---|---|---|
| MCC | $H_3PO_4/P_4O_{10}$ | Triethylphosphate/ 1-hexanol | CPhos, $DS_{Phosphate}$ 0.14–2.50 | [199] |
| MCC, spruce sulfite, CMC, 2-hydroxyethyl cellulose | $H_3PO_4$ | Urea/water | CPhos and mixed products containing phosphate/ carboxymethyl and 2-hydroxylethyl groups | [202] |
| Cotton yarn | $POCl_3$ | DMF, DMF-$CHCl_3$ | CPhos (0.49–4.73% P) and chlorodeoxy cellulose (0.07–0.78% Cl) | [207] |
| MCC | 1,3-Dimethylimidazolium methylphosphite | 1,3-Dimethylimidazolium methylphosphite | Cellulose dimethylimidazolium methylphosphite, $DS_{Methylphosphite}$ 0.4–1.3 | [216] |
| MCC | 1-Propyl phosphonic acid anhydride | LiCl/NMP | (1-Propyl)phosphonate and carboxylate (acetate, butyrate, octanoate, myristate, and stearate) | [66] |

deviation), and the water-swelling capacity of the products (with 0.03–6.07% deviation), see the resulting 3D plots in Fig. 5.35 [200].

Another catalyst is urea. Thus, spruce sulfite pulp, MCC, and cellulose beads have been phosphorylated with $H_3PO_4$/urea/water (0.1/0.3/1–2 molar ratio) yielding

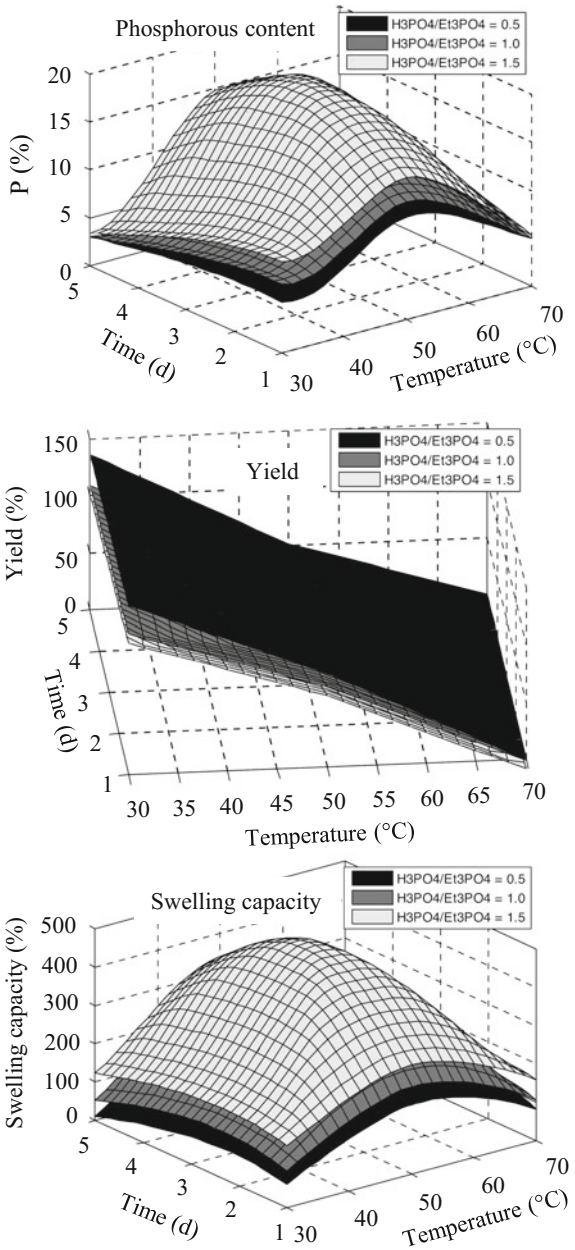


**Fig. 5.35** Surface plots of the wavelet neural model predicted P%, reaction temperature and time, and swelling capacity of CPhos obtained from oil palm empty fruit-based MCC (reprinted from [201] copyright © 2013)

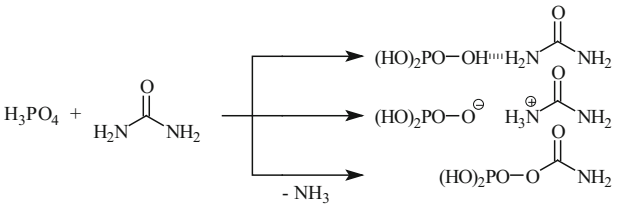


**Fig. 5.36** Interactions of orthophosphoric acid with urea

highly swollen, but still water-insoluble CPhos (due to cross-linking), with $DS_{Phosphate}$ 0.28–0.43, and 0.12–0.22% *N*. The catalytic role of urea has been explained on the basis of the interactions of $H_3PO_4$ with urea as shown in Fig. 5.36. Partial proton transfer leads to the formation of a six-membered hydrogen-bonded complex, Fig. 5.37 [202].

Complete protonation and loss of ammonia from urea lead to the formation of a mixed phosphoric–carbamic acid anhydride (bottom line of Fig. 5.36) leading to the formation of cellulose carbamate. Therefore, CPhos prepared by this route usually contains nitrogen (quantified by the Kjeldahl's method). The $H_3PO_4$/urea/water reaction mixture has been applied for the synthesis of CPhos, including MCC (7.54–7.71% P; 2.41–4.19% *N*) [203, 204] and viscose fibers ($DS_{Phosphate}$ 0.22–0.43; 0.1–1.1% *N*) [205]. Cellulose samples from rice straw and sugarcane bagasse were pretreated with NaOH, immersed in DMF, washed, dried and then phosphorylated using convection and microwave heating ($DS_{Phosphate}$ 0.12–0.51; water-insoluble products) [206].

$PCl_3$, $PCl_5$, and $POCl_3$ have been employed for the synthesis of cellulose phosphite and phosphate, in dipolar aprotic solvents, e.g., DMF and pyridine. Usually, these reactions result in degraded products that are partially soluble in water and contain deoxychlorocellulose. Thus, the reaction of cotton yarn with $PCl_3$/DMF and $PCl_3/CHCl_3$ produces cellulose phosphite and chlorodeoxycellulose according to the mechanism shown in Fig. 5.38 [207].

The reaction of cotton yarn with $POCl_3$/Py produced, after workup, cellulose phosphate (8.09–9.48% P) and chlorodeoxycellulose (2.08–7.37% Cl). Phosphorous and chlorine uptakes by the yarn were found to be sensitively dependent on the experimental conditions. Thus, during 24 h reaction time, the uptake of both elements was higher for never-dried, mercerized yarns (most efficient pretreatment); drying resulted in the least reactive sample [209]. Likewise, the

**Fig. 5.37** Catalytic role of urea as a proton transfer agent in the phosphorylation of cellulose by a mixture of $H_3PO_4$/urea/water [202]

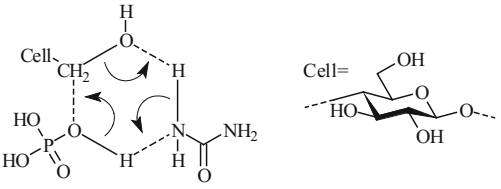

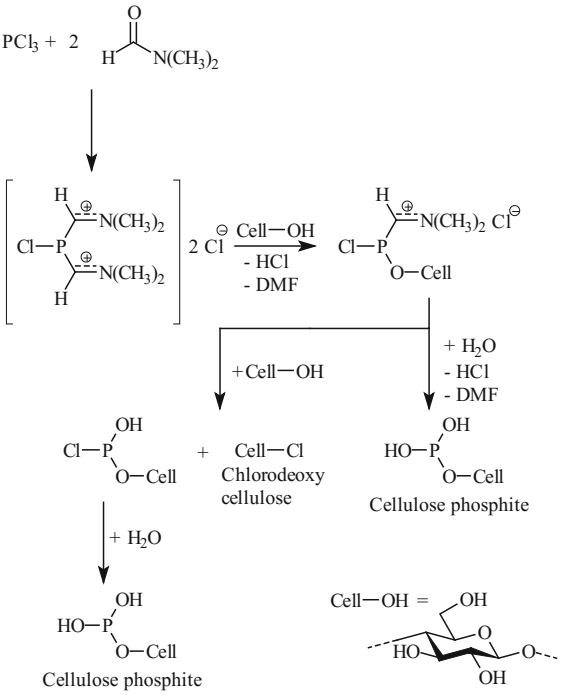


**Fig. 5.38** Suggested mechanism for the synthesis of cellulose phosphite via its reaction with $PCl_3$/DMF, with concomitant production of deoxychlorocellulose [208]

reaction of cotton yarn with $POCl_3$/DMF leads to products with $DS_{Phosphate}$ 0.02–0.13 and $DS_{Chlorine}$ 0.01–0.55 [210]. The following mechanism has been advanced for the phosphorylation with $POCl_3$/Py (Fig. 5.39 [211]).

Cellulose derivatives have been phosphorylated with $POCl_3$. Thus, a suspension of CMC in DMAc, with $DS_{CMC}$ 1.28 was activated with toluene sulfonic acid reacted with partially deactivated $POCl_3$ (by water) in order to decrease cross-linking. The products after neutralization have $DS_{Phosphate}$ 0.32–0.95 and were either soluble or swellable in water [212].

### 5.3.2.3 Synthesis of Cellulose Phosphate Under Homogeneous Conditions

The phosphorylation reaction can be carried out under homogenous conditions starting from cellulose or one of its derivatives, e.g., esters and ethers, giving mostly water-soluble products. Certain groups, including the carboxymethyl and acetyl, are stable in nonaqueous medium, permitting derivatization of the remaining OH groups. Homogeneous phosphorylation of cellulose is carried out in derivatizing or nonderivatizing solvents. Thus, cellulose is transformed into its nitrite ester by dissolution in $N_2O_4$/DMF; this is followed by transesterification by a pentavalent phosphorous compound, e.g., $POCl_3$, to produce the corresponding phosphate. In

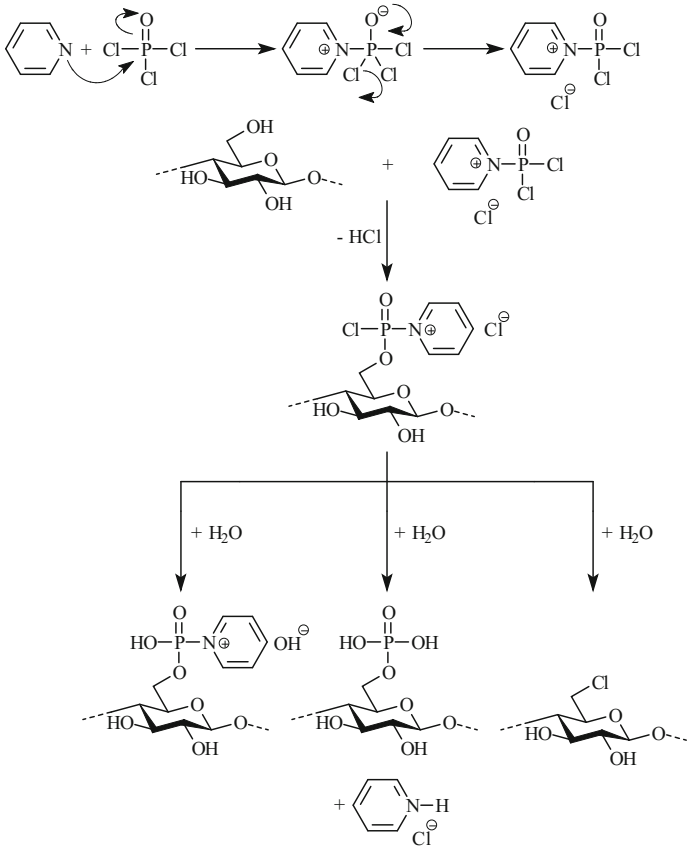

**Fig. 5.39** Suggested mechanism for the synthesis of cellulose phosphate via its reaction with $POCl_3$/Py, with concomitant production of chlorodeoxycellulose [211]

order to decrease the tendency to form cross-linked products, $POCl_3$ was partially "deactived", or transformed into a monochlorinated derivative, incapable of cross-linking. This has been achieved by addition of water, leading to the formation of $Cl_2PO(OH)$ and $ClPO(OH)_2$, or excess $N_2O_4$, leading to the formation of $ClPO(NO_2)_2$. Additionally, TEA was used as a base catalyst, and the product was treated with aqueous acetic acid in order to hydrolyze a part of the cross-linked products. The $DS_{Phosphate}$ of the products (0.05–1.24) was found to be sensitively dependent on the molar ratios of the reagent ($POCl_3$) and base (TEA) to AGU. The products were soluble in NaOH solution and soluble/swellable in water [213]. Controlling regioselectivity is possible by this route; treating cellulose nitrite with $P_2O_5$ leads to functionalization at position 6, whereas the reaction with $ClPO(OH)_2$/TEA leads to reaction at the positions 2 and 3 [214].

Cellulose phosphorylation has been carried out in ILs. Thus, MCC was transformed into diphenyl phosphate and acetate/diphenyl phosphate in AlMeImCl by

reaction of the solubilized biopolymer with diphenyl chlorophosphate and diphenyl chlorophosphate/acetyl chloride, respectively. Depending on the experimental conditions, the corresponding $DS_{Diphenylphosphate}$ were 0.21–1.23 and $DS_{Diphenylphosphate}/DS_{Ac}$ were from 0.08/2.77 to 1.23/1.49. Most of these products were soluble in DMSO, DMF, and Py [215]. A task-specific IL (1,3-dimethylimidazolium methylphosphite) was obtained by the reaction of 1-methylimidazole with dimethylphosphite. Dissolution followed by heating of MCC in this IL produced directly water-soluble cellulose dimethylimidazolium methylphosphite with $DS_{Methylphosphite}$ 0.4–1.3 [216].

Cellulose mixed esters containing (1-propyl)phosphonate and carboxylate (acetate, butyrate, octanoate, myristate, and stearate) groups were obtained homogeneously by one-pot synthesis using 1-propyl phosphonic acid anhydride in LiCl/NMP. The latter anhydride acts as both activating agent for carboxylic acid and phosphonation reagent (see Fig. 5.14). Cellulose mixed esters with $DS_{Acyl}$ ranging from 1.4 to 1.8, and $DS_{Phosphonate}$ up to 0.7 were obtained. The solubility of the obtained esters in $CHCl_3$, DMAc, DMF, NMP, and Py was tested [66].

Another approach is to start with cellulose derivatives like esters or ethers that are soluble in the medium. Thus, the $H_3PO_4$/urea/water system has been employed for the homogeneous phosphorylation of CMC and 2-hydroxyethylcellulose to give the mixed ether/phosphate products with $DS_{Phosphate}$ of 0.3 and 0.6, respectively. The higher phosphorous content of the 2-hydroxyethyl/phosphate derivative is due to esterification of the OH group of the 2-hydroxyethyl moiety. $^{13}C$ NMR spectroscopic results have indicated that esterification occurred mostly on the position 6 [202]. Trimethylsilyl cellulose fully substituted at position 6 and partially at position 2 was phosphorylated with $POCl_3$, $Cl_2PO(OH)$ in the presence of TEA to obtain water- and NaOH insoluble products with maximum $DS_{Phosphate}$ 0.6, with chlorodeoxycellulose formation ($DS_{Chlorine}$ 0.3); water-soluble products were obtained when the phosphorylation reagent and TEA were employed in excess. Water-soluble and water-insoluble products were also obtained by homogeneous reaction of CAs with $Cl_2PO(OH)$ or tetrapolyphosphoric acid ($H_6P_4O_{13}$) in DMF [214, 217].

The problem of phase separation during the reaction (mentioned in Chap. 4) also occurs with phosphorylation, e.g., with diphosphoryl tetrachloride where gelation occurs and the products obtained have poor water solubility in spite of their high $DS_{Phosphate}$ 0.5–1.0 [214]. The reaction of CA with different $DS_{Ac}$ with tetrapolyphosphoric acid/$(1\text{-butyl})_3N$/DMF stays homogeneous all through and gives phosphates, after removing the acetate moiety, that are mostly water- and alkali-soluble, as shown in Table 5.18 [218].

#### 5.3.2.4 Applications of Cellulose Phosphate

Interest in the transformation of cellulose into phosphorous-containing derivatives is because these products have enhanced thermal stability, are biodegradable and biocompatible and, due to the presence of ionizable groups, can be employed as

"green" cation exchangers. They are less crystalline than the parent cellulose, and the value of $I_c$ decreases as a function of $DS_{Phosphate}$ [199].

The generally accepted mechanism is that phosphorus flame retardancy occurs primarily in the condensed phase. The phosphoric acid, thermally generated in the first step of CPhos degradation, accelerates dehydroxylation of cellulose and formation of conjugated double bonds in the chains. Since the carbonized chains are thermally stable, the evolution of flammable gases is retarded and cellulose becomes self-extinguishing. On heating, phosphoric acid polymerizes to polyphosphoric acid that is a more effective catalyst for dehydroxylation reactions. Additionally, polyphosphoric acid shields the underneath fabric from contact with oxygen by forming a glassy film on the surface of the matrix, leading to flame extinguishing. CPhos prepared by chlorinated pentavalent phosphor compounds also contains chlorodeoxycellulose that enhances flame retardancy, because the liberated halogen atoms act as free-radical scavengers in the gas phase [211].

Some substituted cellulose phosphates can be shaped as films and fibers because of their solubility in organic solvents and relatively low $T_m$. Thus, many cellulose diphenyl phosphate and CA/diphenyl phosphate mixed esters are soluble in DMSO, DMF, Py, $CHCl_3$, THF, acetone, and ethyl acetate and were casted as films. Depending on their DS (phosphate or acetate/phosphate), their $T_m$ is 195 ± 15 °C and were processed by extrusion from the melt, as can be seen in Fig. 5.40 [215].

An important aspect in biomedical uses is that the material is stable to sterilization; CPhos was found to be stable under gamma radiation treatment [199]. Unmodified and phosphorylated cellulose hydrogels were implanted in rabbits, and bone regeneration was investigated. Histological observations showed no inflammatory response after implantation, with bone intra-spongious regeneration of cells and the integration of the unmodified as well as the phosphorylated cellulose

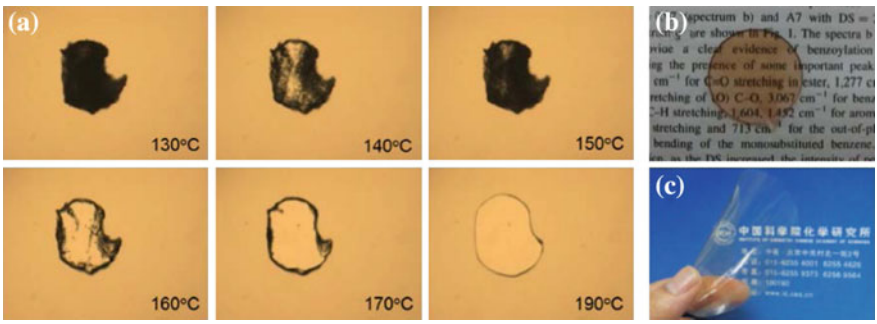


**Fig. 5.40** Optical micrographs of cellulose acetate/diphenyl phosphate at different temperatures (**a**); photographs of the disk produced by injection molding at 180 °C (**b**); film produced by thermal processing (**c**) (reproduced from [215], with permission of Springer)

implants. Histological observations and the measurement of the amount of $^{45}Ca$ incorporated in the surrounding tissue indicated a slightly better osseointegration of CPhos [219].

A successful implantation of an orthopedic material is closely associated with two major events at the interface biomaterial/bone tissue: formation of an apatite layer, and bone cells anchorage, attachment, spreading, and growth. Surface chemical structure exerts a significant influence over these two events. Regenerated cellulose hydrogels were surface modified by phosphorylation. The in vitro biocompatibility of unmodified as well as of phosphorylated cellulose, at varying degrees of phosphorylation, was evaluated in cultured human bone marrow stromal cells, in terms of cytotoxicity, cell attachment kinetics, proliferation rates, and immunohistochemistry. Calcium CPhos were not cytotoxic, independent of the phosphate content. Relatively hydrophilic, unmodified cellulose hydrogels showed good rates of attachment to the above-mentioned cells and proliferation, on one hand. On the other hand, strongly hydrophilic calcium CPhos surfaces showed poor attachment and proliferation, as well as poor alkaline phosphatase-specific activity. These results are in agreement with the known inverse relationship between surface hydrophilicity and cell adhesion [220].

An important application of CPhos is as relatively inexpensive ion-exchange polymer, especially because agriculture waste can be used as cellulose source. Thus, wastes of ground *Armeniaca vulgaris* Lam., *Amygdalus* L., *Populus* L., *Oryza* L., and *Gossypium* L. were phosphorylated by $H_3PO_4$, and their ion-exchange capacity was evaluated. The products showed the following order of ion-selectivity $Zn^{2+} > Ca^{2+} > Co^{2+}$, and exchange capacity of 4–12 mg-eq/g [221].

CPhos has been employed in the diffusive gradients in thin films techniques (DGT), where a polyacrylamide hydrogel (diffusive gel) covers a binding phase for retaining the analyte. Commercial CPhos thin membrane (Whatman P81) was used as a binding phase to efficiently retain $Cu^{2+}$, $Cd^{2+}$, $Zn^{2+}$, $Mn^{2+}$, $Ni^{2+}$, $Ca^{2+}$, $Mg^{2+}$, $K^+$, and $Na^+$. The corresponding capacity ratio was calculated based on the uptake value for $Cu^{2+}$; the following results were obtained: 1.00, 0.953, 1.31, 0.848, 0.801, 0.543, 0.599, 0.425, and 0.345, respectively, in agreement with the expectation that the affinity between ions and the membrane increases as a function of increasing the valence of the ion [222]. The monomer 1-vinyl-2-pyrrolidone was grafted (by gamma irradiation) onto CPhos, and the capacity of the grafted copolymer to adsorb iodine and retain metal ions was evaluated. Relative to CPhos proper, grafting with 1-vinyl-2-pyrrolidone increases the absorption of iodine by 50%, and the retention of $Fe^{2+}$ and $Cu^{2+}$ by 36 and 1090%, respectively [223]. A similar approach has been applied to CPhos synthesized from cellulose extracted from pine needles. Free-radical grafting with glycidyl methacrylate alone and with several comonomers (acrylic acid, acrylamide, and acrylonitrile) gave anionic products that swell appreciably in water and DMF, and retain $Cr^{6+}$, $Fe^{2+}$, and $Cu^{2+}$ [224].

## 5.3.3 *Esters of Sulfuric Acid*

### 5.3.3.1 Introduction

The sulfation of cellulose is akin to that of other hydroxyl-bearing compounds, as shown by Eqs. (5.11) and (5.12):

$$\text{Cell}-\text{OH} + \text{SO}_3 \rightarrow \text{Cell}-\text{OSO}_3\text{H} \tag{5.11}$$

$$\text{Cell}-\text{OH} + \text{XSO}_3\text{H} \rightarrow \text{Cell}-\text{OSO}_3\text{H} + \text{XH} \tag{5.12}$$

where X = $H_2N$, HO, Cl. Although the product is a half-ester of sulfuric acid (formation of the diester is consistently negligible), the common name cellulose sulfate, CS, will be employed here. Solubility in water is an important property of CSs. It depends on the regularity of substitution of the sulfate group within the AGU and along the biopolymer backbone, and is favored by substitution at the C6 position. Therefore, the question of distribution of sulfate moieties is central to this discussion.

The routes employed for the synthesis of CSs include

- direct sulfation of the hydroxyl groups of cellulose, usually under heterogeneous conditions;
- sulfation (mostly homogenous) of the hydroxyl groups present in partially substituted cellulose ethers or esters. The originally present group, in particular the acetate, is not removed during the sulfation reaction. It can be eliminated later, e.g., by alkaline hydrolysis;
- homogeneous sulfation either by partial/complete displacement of a labile group of a cellulose derivative, usually ester (e.g., nitrite) or ether (e.g., TMS) [225] and reactions carried out in molecular solvents.

The second and third strategies permit controlling regioselectivity of the products. These routes are depicted in Fig. 5.41 and representative examples are discussed below.

### 5.3.3.2 Direct Sulfation of Cellulose

The sulfation of cellulose has been carried out using, as in case of alcohols, $H_2SO_4$, $SO_3$/tertiary base complexes, and $ClSO_3H$. Other reagents include $SOCl_2$ (produces sulfite that is oxidized to sulfate), $SO_2Cl_2$, and $FSO_3H$. The reaction is carried out under heterogeneous condition either by a single sulfating agent, e.g., $H_2SO_4$, or in the presence of diluents of different polarities. In few cases, this route leads to regioselectively substituted products.

Two aspects are important for the applications of CSs, the DP of the product relative to that of the parent biopolymer, and the solubility in water. Attaining both

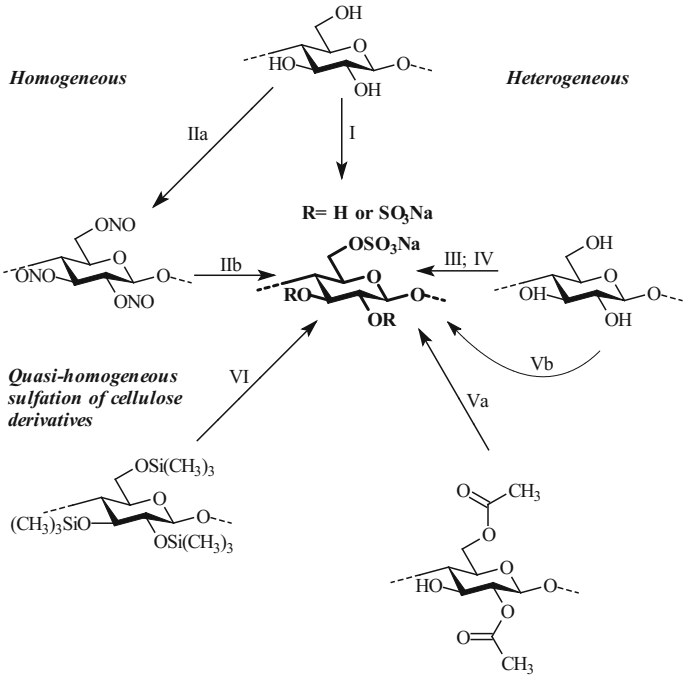


**Fig. 5.41** Schematic representation of the routes employed for the synthesis of cellulose sulfates, with indication of the reaction phase condition (heterogeneous, quasi-homogeneous or gel, and homogeneous) and the strategy employed: direct sulfation in an IL (I), transformation of cellulose in its trinitrite derivative (IIa) followed by substitution of this labile derivative, leading to sulfation (IIb); heterogeneous sulfation in propanol (III), DMF or pyridine (IV), sulfation of cellulose acetate (Va); competitive acetylation/sulfation (acetosulfation) of cellulose (Vb), and sulfation of a cellulose trimethylsilyl ether (VI) [226]

(little degradation and ready water solubility) is not simple by the heterogeneous route. For example, sulfation with $H_2SO_4$/ether has resulted in CS with $DS_{Sulfate}$ 0.3, although the product was found to be water-insoluble, probably because of the heterogeneous substitution pattern of the sulfate group [227]. An increase in $DS_{Sulfate}$ to 0.7 was achieved by increasing the polarity of the solvent, e.g., by using $H_2SO_4$/2-propanol/toluene. The reaction mixture was kept at −10 °C to reduce the extent of polymer degradation. The resulting CS are not uniformly substituted and can be separated into a water-soluble and a water-insoluble fraction, at least when no preactivation of cellulose is applied. Increasing reaction time, temperature, or the concentration of $H_2SO_4$ yields products with increasing overall DS with less insoluble fractions. This leads, however, to considerable polymer degradation as indicated by low aqueous solution viscosity [228]. Further increase of solvent polarity has a clear beneficial effect. Thus, reaction of the biopolymer with $SOCl_2$ or $SO_2Cl_2$ gave a much better yield in the presence of DMF due to better swelling by the amide solvent, coupled with the formation of Vilsmeier–Haack type adduct that

reacts with cellulose to produce, after hydrolysis, chlorodeoxycellulose, and cellulose sulfite ($SOCl_2$; oxidized to sulfate) or sulfate ($SO_2Cl_2$) [208].

In some cases, the heterogeneous reaction turns homogenous due to dissolution of the produced half-ester in the reaction medium. This is observed in the sulfation of cellulose in DMF using $SO_3$ complex at rather high DS $\geq$ 1.5. The sulfation is supposed to occur predominately at the surface of highly swollen amorphous parts of the cellulose fibers, whereas the crystalline regions remain almost unmodified. As a consequence, decreasing the amount of $SO_3$ complex only increases the amount of the insoluble fraction while the DS of the soluble one remains around 2. In addition, the conversion of microcrystalline cellulose (MCC), which possesses a rather high degree of crystallinity, proceeds rather slowly, even with an excess of sulfating reagent [229].

Still, it has been demonstrated that the direct sulfation can result in satisfactory $DS_{Sulfate}$ and aqueous solution viscosity. Thus, MCC was sulfated by $SO_3$/DMF to give products with $DS_{Sulfate}$ from 0.77 to 2.87; the order of reactivity was found to be *O*-6 > *O*-2, except for one sample; no substitution occurred at *O*-3 [230]. Cellulosic material isolated from *Agave lechuguilla* (lechuguilla) and *Agave fourcroydes* (henequen) (78 ± 1% cellulose; 5 ± 2% hemicellulose; 14.3 ± 1% lignin) has been sulfated as gels in pyridine by $ClSO_3H$ at 0 °C, for 16 h, to give partially, or completely water-soluble products with $DS_{Sulfate}$ from 0.68 to 1.15 [231]. Additionally, α-cellulose extracted from *Lantana camara*, a weed that is rich in lignocellulosic material, has been sulfated by the azeotrope of sulfuric acid and 1-butanol containing ammonium sulfate. The effects of reaction variables like sulfuric acid concentration and reaction temperature on the synthesis of CS have been studied and optimized (Fig. 5.42). $DS_{Sulfate}$ from 0.24 to 0.39 were obtained and the products showed excellent solubility in cold water at $DS_{Sulfate}$ 0.25. A 2% CS solution in water showed viscosity of 625 mPa s at 25 °C [232].

CS samples with different $DS_{Sulfate}$ (0.34–0.92) and regioselective distribution of the ester moieties ($DS_{Sulfate}$ at *O*-6 0.33–0.77, $DS_{Sulfate}$ at *O*-2 0.03–0.05, and $DS_{Sulfate}$ at *O*-3 trace) have been obtained by reacting a suspension of MCC in DMF with $ClSO_3H$ or with aceto-sulfuric acid anhydride. These CSs were converted into

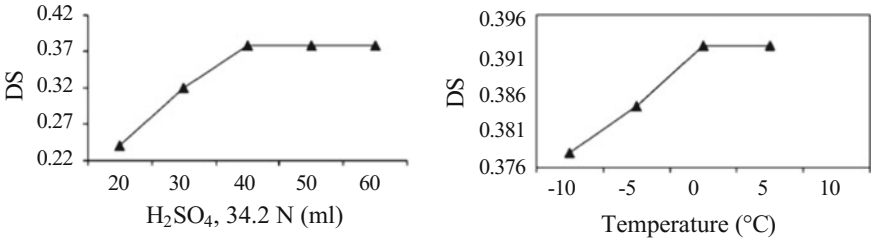


**Fig. 5.42** Effects of the experimental variables on $DS_{Sulfate}$ of α-cellulose extracted from *Lantana camara*. The plots refer to the effect of volume of sulfuric acid of constant concentration (34.2 N, left) and reaction temperature (right, reproduced from [232], with permission of John Wiley and Sons)

carboxylate/sulfate by oxidation with TEMPO/NaBr/NaClO, or through carboxymethylation with chloroacetic acid after alkali treatment with NaOH ($DS_{Sulfate}$ 0.33, $DS_{Carboxylate}$ 0.42 and 0.67); all CSs and CS/carboxylate were found to be water soluble [233].

In another approach of direct sulfation of cellulose, the reaction has been carried out under homogeneous conditions in a nonderivatizing solvent. Homogeneous reactions usually overcome the problem of irregular modification because the hydroxyl groups are more accessible for the derivatization reagent. Homogeneously prepared CSs may possess a more uniform distribution of sulfate groups along the polymer chain, especially at DS < 0.8, and are soluble in water at DS > 0.2–0.3 [234]. Several solvents have been tested for this purpose, including NMMO/DMF, DMAc/LiCl, and LiCl/HMPA, in the absence and presence of TEA. In all cases, higher $DS_{Sulfate}$ were obtained in the presence of TEA (0.14–0.70) than in its absence (0.06–0.64). Reaction media were homogeneous throughout (NMMO/DMF), showed coagulation then turned heterogeneous (LiCl/HMPA), or showed coagulation all through (DMAc/LiCl). Coagulation of the reaction mixture is problematic because it leads to uneven sulfate substitution, hence poor water solubility of the produced CSs [235]. Higher $DS_{Sulfate}$ was obtained by reacting cellulose with $ClSO_3H$ in the solvent system TEA/$SO_2$/formamide, e.g., 0.4 at 20 °C and 1.05 at 50 °C. Again the products were only partially soluble in water, probably because the reaction mixtures were gels [227]. Homogeneous sulfation by $ClSO_3H$ in NMMO has been tested but the products showed poor solubility in water [235]. Thus, direct sulfation in electrolyte/dipolar aprotic solvent is feasible, however, may lead to insoluble products.

Because ILs have been successfully employed as solvent for obtaining organic esters, they were also employed for direct sulfation of cellulose. Thus, biopolymer isolated from bagasse was sulfated by $ClSO_3H$/DMF in BuMeImCl to give CSs with $DS_{Sulfate}$ from 0.52 to 2.95 with a distribution of the sulfate moieties in the order *O*-6 > *O*-2 > *O*-3. No substitution at the latter position was obtained in the sample with $DS_{Sulfate}$ 0.61 [236]. Sulfation with $SO_3$/pyridine or $SO_3$/DMF complexes in EtMeImAc (an efficient IL for cellulose dissolution) has resulted in water-insoluble CS samples of low sulfur content (<1%). Both IR and $^{13}C$ NMR spectroscopic data indicated, however, the presence of an ester group in the product. This was attributed to substitution of the sulfate by the acetate group, akin to the result observed for the synthesis of cellulose tosylate in the same IL (see Sect. 5.2.2). The use of BuMeImCl containing an anion that is a much weaker nucleophile than the acetate did not solve the problem because the mixture solidified at room temperature. Attempts on sulfation at higher temperature by IL-dissolved $SO_3$/pyridine or $SO_3$/DMF at 60 °C resulted in biopolymer degradation or products insoluble in water or both. However, the problem was solved by using a dipolar aprotic solvent as a diluent for the IL. Thus, cellulose was sulfated at 25 °C by $SO_3$/pyridine, $SO_3$/DMF, and $ClSO_3H$ in a 4.5/7 (by volume) mixture of BuMeIMCl/DMF to give products with $DS_{Sulfate}$ 0.14–0.81. These were mostly water soluble; their aqueous solutions showed viscosities from 93.1 to 374.6 mPa s indicating little biopolymer degradation [237].

**Table 5.20** Degree of substitution (DS) and water solubility of cellulose sulfates obtained by sulfation of cellulose in BuMeImCl/DMF at 25 °C [238]

| Sulfating agent | | Product | |
|---|---|---|---|
| Type | Molar ratio | DS | Water solubility |
| $SO_3$-pyridine | 0.6 | 0.16 | − |
| $SO_3$-pyridine | 0.8 | 0.25 | + |
| $SO_3$-pyridine | 0.9 | 0.48 | + |
| $SO_3$-pyridine | 1.1 | 0.58 | + |
| $SO_3$-pyridine | 1.2 | 0.62 | + |
| $SO_3$-pyridine | 1.4 | 0.81 | + |
| $SO_3$-pyridine | 1.5 | 0.87 | + |
| $SO_3$-pyridine | 2.0 | 1.04 | + |
| $SO_3$-pyridine | 4.0 | 1.66 | + |
| $SO_3$-DMF | 1.0 | 0.34 | + |
| $SO_3$-DMF | 1.4 | 0.64 | + |
| $SO_3$-DMF | 1.5 | 0.78 | + |
| $ClSO_3H$ | 1.0 | 0.49 | + |

[a]Mol sulfating agent per mol anhydroglucose unit

Sulfation of cellulose in IL/cosolvent mixtures is of practical interest for possible commercial applications of CSs because there is little chain degradation, no additional chemicals, and waste production related to auxiliary substituents. However, it is necessary to implement recycling procedures for the ILs and cosolvents. Using this approach, the DS can be tuned easily by adjusting the amount of sulfating reagent per AGU (Table 5.20).

#### 5.3.3.3 Sulfation of Partially Substituted Cellulose Derivatives

The use of partially substituted biopolymer derivatives, e.g., cellulose esters and ethers as starting materials for sulfation, is advantageous because these derivatives

**Table 5.21** Sulfation of statistically (S) and regioselectively (R) deacetylated cellulose sulfate samples

| Entry | Type | $DS_{Ac}$ | Reagent | Molar ratio[a] | $DS_{Sulfate}$ | Partial $DS_{Sulfate}$ at | | |
|---|---|---|---|---|---|---|---|---|
| | | | | | | *O*-2 | *O*-3 | *O*-6 |
| 1 | S | 2.38 | $SO_3$ | 0.4 | 0.35 | 0.20 | 0 | 0.15 |
| 2 | S | 2.38 | $ClSO_3H$ | 0.5 | 0.22 | 0.04 | 0 | 0.18 |
| 3 | S | 2.38 | $H_2NSO_3H$ | 0.5 | 0.35 | 0.11 | 0.04 | 0.20 |
| 4 | S | 2.38 | $H_2NSO_3H$ | 1.0 | 0.52 | 0.17 | 0.15 | 0.20 |
| 5 | R | 2.64 | $H_2NSO_3H$ | 1 | 0.25 | 0.17 | 0.08 | 0 |
| 6 | R | 1.86 | $H_2NSO_3H$ | 2 | 0.95 | 0.55 | 0.20 | 0.20 |
| 7 | R | 1.48 | $H_2NSO_3H$ | 3 | 1.15 | 0.74 | 0.15 | 0.26 |

[a]Mol sulfating agent per mol anhydroglucose unit

are more easily soluble in reaction media compared to the parent cellulose; this eliminates the problem of gel formation. Equally important, however, this route can be employed for regioselective sulfation, provided that the originally present group is stable under the sulfation reaction conditions and can be later removed by a simple procedure that is specific, i.e., will not remove the sulfate group as well. The acetyl group proved to be convenient because it is stable under anhydrous acidic conditions (water content <0.05%) in contrast to the labile formyl or nitrite groups, vide infra [239]. Additionally, this ester group can be removed by alkaline hydrolysis (NaOH/ethanol) without affecting the sulfate group. An alternative, simple approach for obtaining a product with double functionality is to carry out acetylation/sulfation simultaneously and heterogeneously on the extensively solvent-swollen cellulose, and then to remove the acetate moiety. The disadvantages are the complex workup procedure, the use of extra chemicals, and production of more waste. This has been carried out by reacting $ClSO_3H$/acetic anhydride/$H_2SO_4$ or $ClSO_3H$/acetyl chloride with cotton linters that have been previously swollen by DMAc, DMF, NMP, and DMSO. In a subsequent step, the acetyl group was removed by hydrolysis in alcoholic NaOH solution. DMSO was not a convenient solvent. Most of the CSs obtained were water soluble with $DS_{Sulfate}$ 0.31–2.21 with regioselective substitution at *O*-6, no substitution at *O*-3, no or negligible substitution at *O*-2, except for one sample (results for samples with $DS_{Sulfate}$ 0.31–1.04); more product degradation occurred when sulfuric acid was the catalyst employed [240, 241]. $^{13}C$ NMR spectroscopic studies revealed differences in the distribution of sulfate groups within the AGU for CSs obtained by these techniques (Fig. 5.43). These different substitution patterns can, among others, result in different activities of the produced CSs, e.g., as anticoagulants.

Sulfation of CA with $DS_{Ac}$ of 0.80–2.5 has been carried out homogenously in DMF by different sulfating agents and the following reactivity order has been observed: $SO_3$ > oleum > $ClSO_3H$ > $SO_2Cl_2$ > acetic–sulfuric anhydride, $CH_3CO_2$–$SO_3H$ > $H_2NSO_3H$. There is a trade-off between reaction rate and even distribution of the sulfate group in the product. Thus, it is preferable to use the less reactive acetyl-sulfuric acid anhydride or amidosulfonic acid than the more reactive $ClSO_3H$. The stability of the acetate group has been demonstrated over a period of 4 h during sulfation of CA with $DS_{Ac}$ 0.5 and 2.5 by $ClSO_3H$ or amidosulfonic acid in DMF. Additionally, the stability of the sulfate group during the hydrolysis of the acetate group by alcoholic NaOH has been demonstrated [239].

Cellulose acetate (DS 2.5) and formate (DS 2.5) were prepared from MCC (DP 162), birch cellulose (DP 650), and cotton linters (DP 1400) and submitted to homogeneous sulfation by $SO_3$/DMF and $ClSO_3H$/DMF at or below room temperature. The partial DS of the products, e.g., $DS_{Sulfate}/DS_{Formate}$, was found to be a function of reaction time and the ratio of $SO_3$/AGU. The order of reactivity of the carboxylic esters was formate > acetate probably due to difference in the volume of these acyl groups. CS with maximum $DS_{Sulfate}$ of 0.88 and 0.29 were obtained for cellulose formate and acetate, respectively. Interestingly in case of cellulose formate, $DS_{Sulfate}$ was found to be higher than the amount of OH functions originally

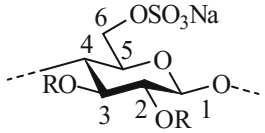


R= H or $SO_3Na$ according to degree of substitution

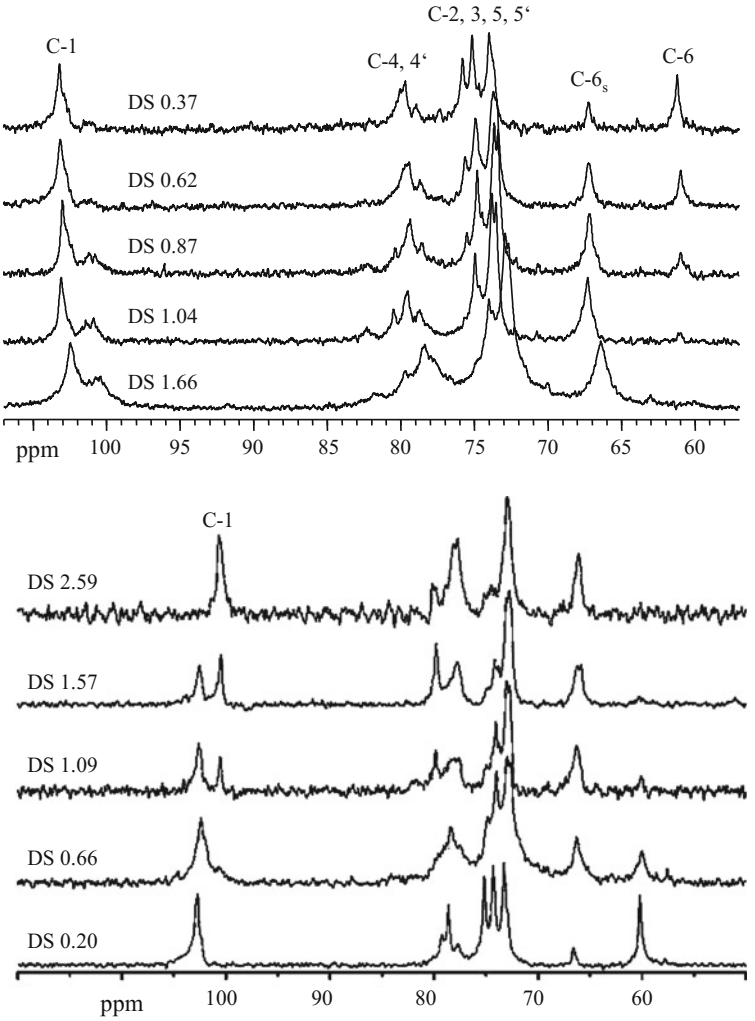


**Fig. 5.43** $^{13}C$ NMR spectra of cellulose sulfates with different degrees of substitution (DS), prepared by (top) sulfation of cellulose in ionic liquid/cosolvent mixtures [238] or (bottom) acetosulfation of cellulose, adapted from literature (reprinted from [242] copyright © 2011, with permission from Elsevier. Index s means substituted position. Dash (‘) means influenced by substituent at neighboring position

present indicating that the formate moiety was partially displaced by the sulfate group. In contrast, no transesterification occurred during sulfation of CA [21].

Sulfation of cellulose ethers has also been carried out with $CH_3CO_2SO_3H$, $SO_3$/pyridine complex or $ClSO_3H$ in DMAc, DMF, and DMSO. The reaction of $ClSO_3H$ with CMC was negligible ($DS_{Sulfate}$ 0.09) when the ether was not activated. Activation was carried out by swelling CMC by 4-toluene sulfonic acid, followed by cooling to room temperature and sulfation of the formed gel; yields 64–88%; $DS_{Sulfate}$ 0.25–1.48 [243].

#### 5.3.3.4 Sulfation of Cellulose Derivatives by Substitution of the Labile Group Present

In this approach, the solvent can be derivatizing or nonderivatizing. An example of the first is the dissolution of cellulose in $N_2O_4$/DMF that leads, as discussed in Sect. 3.2.2, to formation of the corresponding biopolymer nitrite. The resulting solution was treated with several sulfating agents for 2–4 h at 20–30 °C to produce CSs with $DS_{Sulfate}$ between 0.1 (sulfating agent: $H_2SO_4$) and 1.56 ($SO_2Cl_2$). Under comparable experimental conditions, the order of $DS_{Sulfate}$ was found to be $SO_2Cl_2$ > $SO_3$ > $ClSO_3H$ > $SO_2$ > $NOSO_3H$ ≫ $H_2SO_4$, with clear preference for sulfation at position 6 (Fig. 5.44). The solution of cellulose nitrite containing excess of $N_2O_4$ and nitric acid was employed [36].

Although this transesterification reaction proceeds with little degradation of the biopolymer and its regioselectivity can be controlled by reaction conditions, it has

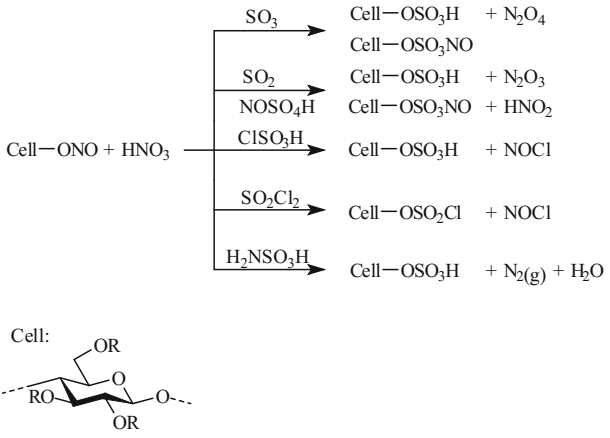


**Fig. 5.44** Scheme of the possible substitutions in the reaction of cellulose nitrite with different sulfating agents

not gained popularity because $N_2O_4$ is a very toxic and corrosive gas (b.p. 21.7 °C). Its use for making CS for biomedical applications is probably objectionable [36].

A typical example of other cellulose derivatives that undergo the transesterification reaction readily is TMS cellulose, whose use is advantageous because

- the synthesis with hexamethyldisilazane is relatively simple, e.g., in electrolyte/dipolar aprotic solvent or ILs;
- it is readily soluble in dipolar aprotic solvents, e.g., DMF and THF [244, 245];
- it reacts with $SO_3$/pyridine or $SO_3$/DMF; and
- the intermediate compound need not be isolated, i.e., the whole reaction sequence can be carried out "one-pot".

Thus, CSs samples with $DS_{Sulfate}$ between 0.2 and 2.5 have been prepared by reaction of TMS cellulose with $SO_3$ or $ClSO_3H$ in DMF or THF. The products showed little degradation of the biopolymer and good water solubility of the CS obtained. The distribution of the sulfate groups within the AGU was controlled by $DS_{Silylation}$, the type and concentration of the sulfating agent. The homogeneous sulfation of TMS cellulose indicated a reactivity of silyl ether groups in the order of *O*-6 > *O*-2 ≫ *O*-3 [246].

Similar to the sulfation of cellulose nitrite, the TMS moiety acts as leaving group. The first step consists of an insertion of $SO_3$ into the Si–O bond of the silyl ether (Fig. 5.45). The intermediate formed is unstable and usually not isolated. Subsequent workup with aqueous NaOH leads to a cleavage of the TMS group and the formation of CS [247]. More details about the regioselectivity of these reactions can be found elsewhere [226]. Further synthesis examples are summarized in Table 5.22 at the end of this chapter.

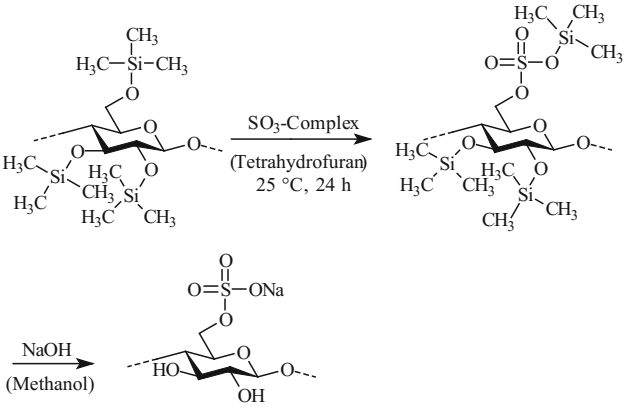


**Fig. 5.45** Schematic representation for the synthesis of cellulose sulfate via TMS cellulose [247]

**Table 5.22** Representative examples of the routes employed for the synthesis of cellulose sulfates

| Cellulose type DP | Derivatizing agent | Solvent | Product; DS range | References |
|---|---|---|---|---|
| Cotton linters 1090 | $ClSO_3H/Ac_2O$ | DMAc, DMF, NMP, DMSO | 0.31–2.21 | [241] |
| α-cellulose 430 | $H_2SO_4$ | 1-Butanol | 0.13–0.39 | [232] |
| MCC 160 | $N_2O_4$/DMF then $SO_2$, $SO_3$; $ClSO_3H$; $SO_2Cl_2$; $H_2NSO_3H$; $NOSO_4H$ | DMF | 0.35–1.91 | [36] |
| Cotton linters 800 | HMDS and then $SO_3$ in DMF, TEA | DMF | 1.01–1.88 | [247] |
| MCC 180 | $SO_3$/DMF; $SO_3$/pyridine; $ClSO_3H$ | BuMeImCl | 0.14–0.81 | [237] |

#### 5.3.3.5 Properties of Cellulose Sulfates

The acid form of CS (H–CS) can be isolated as a white hygroscopic product and is soluble in water and dipolar molecular solvents at $DS_{Sulfuric} > 0.2–0.3$. This product, however, is unstable in solution and undergoes autocatalytic hydrolysis, even in the solid state. Therefore, H–CSs are neutralized by bases, most commonly NaOH, to give a usually water-soluble Na–CS derivative at $DS_{Sulfate}$ of 0.2–0.3.

The properties of CS, such as water solubility, biological activity, and the ability to form superstructures, are strongly depending on the overall DS, the MM, and as the distribution of substituents within the AGU and along the polymer chain. These parameters are affected by the reaction conditions, e.g., type and amount of sulfating reagent, time, temperature, and the reaction course (heterogeneous, heterogeneous that turns homogeneous, or homogeneous). Experimental variables, e.g., rate of reagent addition, stirring of the reaction mixture, and phase transitions during the reaction, can have a significant impact on product composition. The sulfation of polysaccharides is very rapid, and significant fractions of the final DS values are already obtained within 0.5–2 h, while mass transfer in the reaction mixtures might be slow especially in case of high solution viscosities and temperatures $\leq 25$ °C. The distribution of sulfate moieties depends on the $DS_{Ac}$ and the sulfating agent employed (Table 5.21) [129, 214].

Except for entries **5** and **6** of Table 5.21, a preference for sulfation at the *O*-2 and *O*-6 of the AGU was found. A convenient route to preferential- or exclusive sulfation at *O*-6 is to use a mixture of acetic anhydride and $SO_3$ or $ClSO_3H$ in DMF with both reagents in equimolar concentration of the sulfating agent in excess (40%) [214].

The water solubility of CSs is intimately dependent on the regularity of substitution and the presence of other substituents (cellulose acetyl sulfate is less water soluble than CS). For Na–CS with $DS_{Sulfate}$ between 0.2 and 0.4, the Mark–Houwink equation is

$$[\eta] = (0.01356 \cdot M)^{0.94} \tag{5.13}$$

Very high viscosities (between 1000 and 5000 mPa s) have been reported for 1% aqueous solution of Na–CS synthesized via the cellulose nitrite (cellulose dissolved in DMF/$N_2O_4$), i.e., with negligible biopolymer degradation [248]. Aqueous solutions of Na–CS exhibit shear-thinning (thixotropic) behavior whose intensity increases with decreasing $DS_{Sulfate}$. They also exhibit remarkable stability against thermo-degradation and shear-degradation. Thus, heating aqueous solutions of Na–CS for 25 h at 100 °C has resulted in decrease of viscosity of 25% only [248]. As with other alkyl sulfates, e.g., sodium dodecylsulfate, Na–CS shows good tolerance for di- and trivalent cations and can be employed in aqueous alcohols.

#### 5.3.3.6 Applications of Cellulose Sulfates

Biomedical-Related Applications

CS has an anticoagulant activity, whose efficacy and its possible mechanism were investigated using in vitro and in vivo coagulation assays and amidolytic tests in comparison with heparin. The anticoagulant potential of Na–CS was assayed with standard clotting tests. Products with $DS_{Sulfate} > 1$ possess pronounced anticoagulant activity that reached a maximum at $DS_{Sulfate}$ of 1.5, then decreased at higher sulfation. Substitution at *O*-2 leads to pronounced activity (mainly due to antithrombin activity) [240]. This higher anticoagulation activity of Na–CS (including samples from bagasse-based cellulose) as compared with heparin has been corroborated by other studies based, e.g., on activated partial thromboplastin time assay. No effect was detected on the prothrombin time. Subcutaneous administration of Na–CS to mice increased the clotting time in a moderate dose-dependent manner. The anticoagulation activity occurs mainly by accelerating the inhibition of antithrombin III on coagulation factors FIIa and FXa [236, 249].

Polyetheylene terephthalate (PET) is used for synthetic vascular grafts after its surface has been modified by plasma treatment or adsorption of heparin. A more convenient approach for increasing the biocompatibility of PET is to adsorb a semi-synthetic cover, e.g., Na–CS. In order to enhance the adsorption of Na–CS on the PET surface, a layer-by-layer technique has been employed. First, PET was coated with a cationic polymer (protonated chitosan or several 6-deoxy-6-aminocelluloses), then a top layer of Na–CS was applied. The coated PET foils showed improved blood compatibility compared with the untreated material [250]. The biological activity of Na–CS and cellulose sulfate-carboxymethylate has been evaluated by a binding assay to fibroblast growth factor (b-FGF). It was found that Na–CS with maximum sulfation at position 6 and intermediate to high sulfation at position 2 was able to bind b-FGF comparable to natural heparin. Products that were sulfated and subsequently carboxymethylated at all three AGU positions were also able to bind substantial

quantities of b-FGF. Using HIV-infected MT-4 cells, it was possible to show that sulfated (synthetic) branched cellulose with high $DS_{Sulfate}$ exhibits high anti-HIV activity [230].

Another field of application is based on the use of complexes formed by CSs. Electrostatically self-assembled films are, in general, fuzzy materials because the assembly mechanism is largely entropy driven. The freshly adsorbed chains tend to penetrate into the underlying film and, thus, preventing real multilayers to form. These complexes are usually assembled via layer-by-layer deposition, e.g., on a solid surface for a polyelectrolyte complex (PEC, Fig. 5.46) [251].

It has been shown, however, that Na–CS/polyDADMAC form thin-walled PEC of excellent mechanical properties [252]. The strength of the PECs depends, *inter alia*, on the charge density as well as the distribution of the charged groups in the CS employed [253]. Thus, spherically shaped PEC capsules of enhanced mechanical properties (as demonstrated by their stability toward sonication for 24 h) were prepared from water-insoluble CS ($DS_{Sulfate}$ 0.16, dissolved in EtMeImAc) and polyDADMAC (dissolved in 0.9% NaCl solution), see Fig. 5.47 [254].

These PEC in different physical forms are potentially useful for the encapsulation of cells, proteins, and drugs [252, 255]. Cells imbedded within PEC are well protected against detection and attack by the immune system and, therefore, are expected to be suitable for xenotransplantation, for example in diabetes therapy [256]. Neither cell growth nor glucose-dependent insulin production is influenced

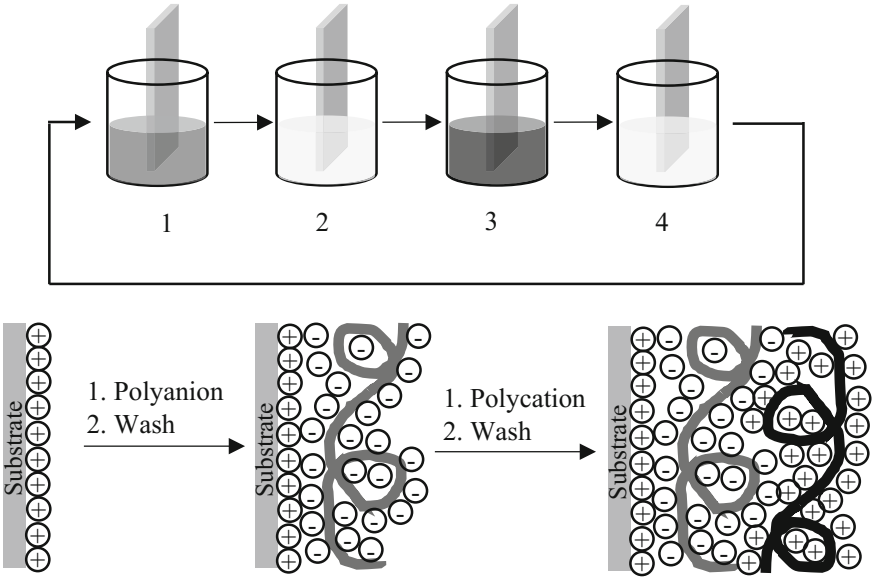


**Fig. 5.46** Schematic representation of layer-by-layer deposition of PEC on the surface of a slide using cellulose sulfate and polyDADMAC. Between the depositions of each polyelectrolye layer, the excess (previously deposited) electrolyte present is washed away (adapted from [251])

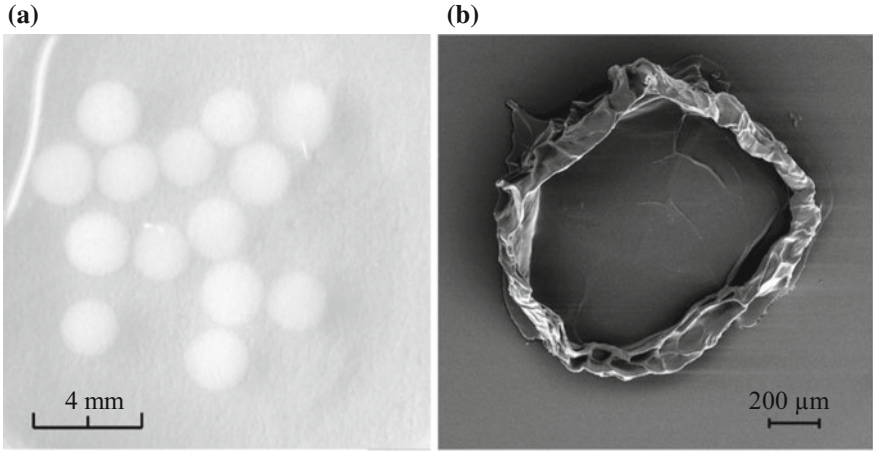


**Fig. 5.47** PEC capsules prepared from water-insoluble cellulose sulfate (**a**) and SEC image of a dried slice from the middle of one capsule (**b**) (reprinted with permission from [254] copyright © 2009 American Chemical Society)

by the encapsulation [257]. Enzymes entrapped into PEC capsules show higher stability and reusability in comparison to free enzymes and can easily be removed from solution and recycled after each reaction [258–260].

The following are selected examples to show the possibilities of biomedical applications of encapsulations by CS and/or its PEC: encapsulation of lactoferrin (an iron transporter glycoprotein) with antioxidant, anticarcinogenic, antiviral, and anti-inflammatory properties in PECs of chitosan and CS [261]; encapsulation of egg white albumin, bovine serum albumin, and yeast alcohol dehydrogenase in PECs of alginate and Na–CS with poly(methylene-*co*-guanidine) hydrochloride [262]; insulin encapsulation in microspheres of alginate/Na–CS/chitosan [263]; microencapsulation of bovine spermatozoa in PECs of Na–CS/polyDADMAC for the controlled release in cattle artificial insemination (Fig. 5.48) [264]; and microencapsulation of glucose oxidase in Na–CS/polyDADMAC and subsequent use for oxidation of glucose into δ-gluconolactone that is hydrolyzed to gluconic acid [237]. In summary, it is expected that the interest in CS will increase due to the fact that its regioselective synthesis is now established, in addition to its biocompatibility, biological activity, either alone or as PEC, and its chemical stability that renders recycling feasible and simple.

#### 5.3.3.7 Heterogeneous Catalysts in Organic Synthesis

Several novel applications have led to increased interest in CSs. H–CS is used as a catalyst, in particular for one-pot acid-catalyzed syntheses of heterocyclic

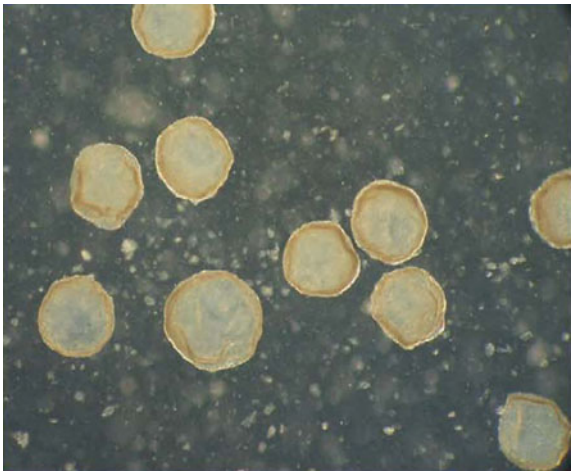

**Fig. 5.48** Na–CS/polyDADMAC microcapsules containing bovine sperm after cryopreservation and thawing (reprinted from [264] copyright © 2006 with permission from Elsevier)

compounds. The catalyst has been prepared heterogeneously by the reaction of cellulose with $ClSO_3H$ in solvents of low polarity, e.g., chloroform at low temperature (e.g., 0 °C). The acidity of H–CS was calculated by acid–base titration (0.5–0.68 meq/g). Examples of this use in Ugi reaction are shown in Fig. 5.49 [265], more examples are given elsewhere [265–274].

Using H–CS as a heterogeneous solid acid catalyst has proved advantageous because of its easy synthesis, low cost, biodegradability, and possibility of recycling by simple washing, e.g., with DCM. Compared with other solid acid catalysts, H–CS has proven very efficient as can be shown from the following data: compound generic name, yield % with H–CS as catalyst, yield range % for other acid catalysts, including liquid, solid, or liquid supported on solid, e.g., ion-exchange resins, $AlCl_3$, $H_2SO_4$, and $H_2SO_4/SiO_2$ [266]; 3,4-dihydropyrimidine-2(1*H*)-one, 96, 85–91 [269]; 2,4,5-triarylimidazoles [270, 271]; substituted pyrrols [274]; and products of the Ugi reaction [265].

### *5.3.4 Cellulose Borates and Boronates*

Boron-containing compounds, for example, borax, boric acid, and boronic acids, are frequently used as activating, protecting, and cross-linking agents for carbohydrates [275–278]. A broad variety of interactions was postulated for the reaction of boric acid with polyols like carbohydrates (including different cyclic esters). Examples are shown in Fig. 5.50 [275].

It is known that treatment of cellulose in an aqueous medium of boron compounds leads to a reactive form of the polymer, which can increase the reagent yield in modification reactions. During this activation step, a wide variety of structures are formed and consequently the interactions with hydroxyl moieties of saccharides

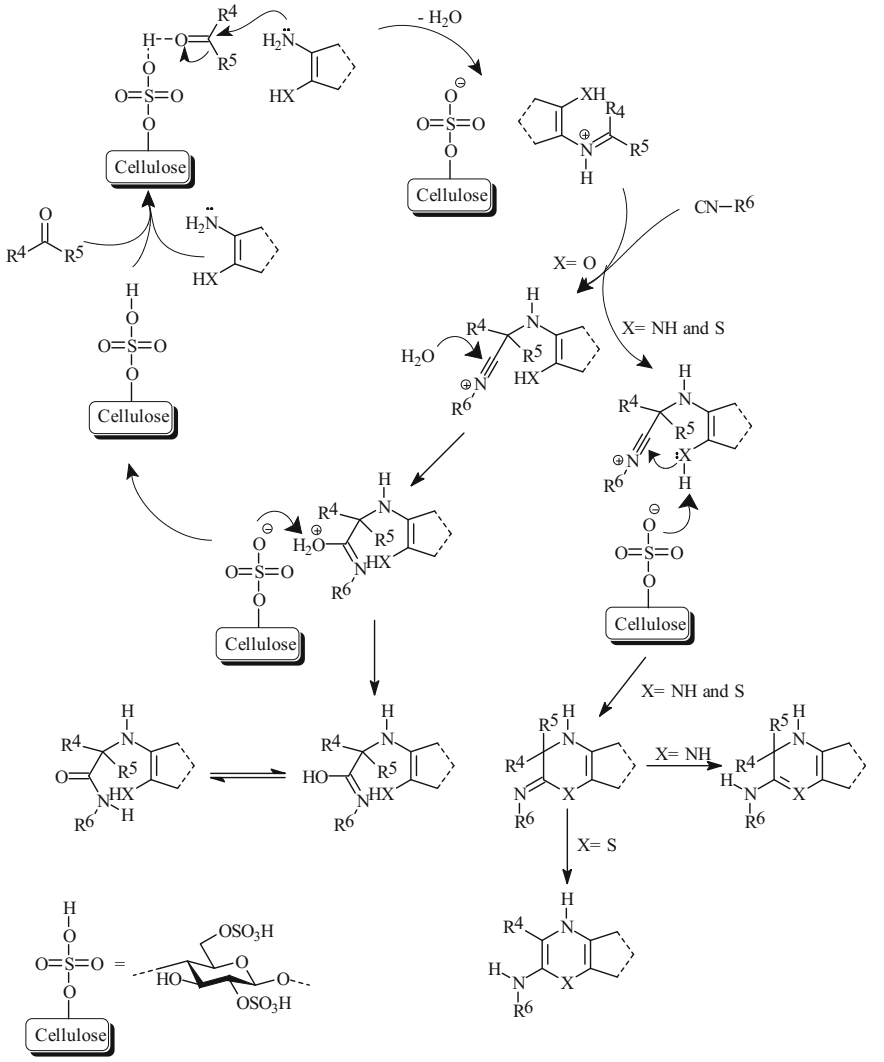


**Fig. 5.49** Suggested mechanisms for product formation of the Ugi reaction showing the catalytic effect of H–CS in the different steps of the reaction pathway [265]

are scarcely understood. Therefore, the exploitation of promising approaches in particular the development of new derivatizing solvents for cellulose on the basis of such interactions is still limited. A number of attempts have been made toward a basic understanding of the interactions between glucose-based polysaccharides and boron-containing compounds. It is known that glucose reacts preferably in its furanose form to give α-D-glucofuranose-1,2:3,5,6-bis(borate/boronate) complexes in alkaline aqueous media [279, 280]. However, this rearrangement to the furanose

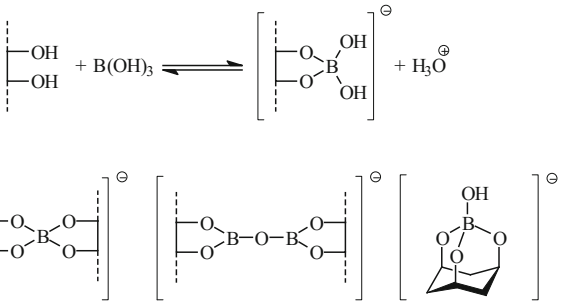

**Fig. 5.50** Cyclic ester structures postulated for the reaction of boric acid with polyols like carbohydrates

form, which gives the required diol coplanarity for the formation of cyclic complexes, is not conceivable for glucose-based oligomers and polymers. The interaction of cellulose with boric or boronic acid-type compounds is limited to the trans-1,2-diol system at *O*-2 and *O*-3 and conversion of the primary hydroxyl group at position 6. Therefore, studies attempted to understand such interactions were carried out with model systems, specifically the reaction of phenylboronic acid (PBA) with methyl-α-D-glucopyranoside (Me-α-D-Glc*p*) [281–283]. Fast formation of a six-membered ring at positions 4 and 6 and the existence of a seven-membered diboronate ring at the trans-1,2-diol moieties of positions 2 and 3 were concluded from NMR experiments (see Chap. 2). Furthermore, the transformation of Me-α-D-glc*p* with PBA was studied by MS. The expected fission processes are displayed in Fig. 2.66. An equimolar conversion yields a methyl-4,6-*O*-phenylboronate-α-D-glucopyranoside (Structure 1, Fig. 2.66), which was confirmed by a peak for the molecular ion at m/z 280 and one fragment ion I at m/z 160 for a 1,3,2-dioxaborinane structure. If an excess of PBA is employed, the methyl-2,3-*O*-(diphenylpyroboronate)-4,6-*O*-phenylboronate-α-D-glucopyranoside (2) should be formed.

The MS data show significant fragment ions at m/z 160 (I) and at m/z 250 (II) in addition to a peak for the molecular ion at m/z 470, confirming the existence of a seven- and a six-membered boronate ring. The formation of a seven-membered ring structure during the reaction of the carbohydrate with PBA has been verified by additional experiments with methyl-4,6-*O*-benzylidene-2,3-*O*-(diphenylpyroboronate)-α-D-glucopyranoside (see Fig. 2.66 structure 3). Again, a fragment ion at m/z 250 (II) is found, and the molecular ion at m/z 472 is detectable. A perfect fit of the predicted pattern with the fragment peaks for ion II of the 1,3,5,2,4-trioxadiborepane structure, and the signal for the molecular ion of 2 were found (Fig. 2.66). Additionally, the boron isotope pattern fits in the MS data (compare gray-calculated and black-found data set in Fig. 5.51).

An interesting technique, which supports the MS data, was $^{11}$B NMR spectroscopy giving the final evidence for the formation of the postulated ring system (see Sect. 2.3.3.2). On the basis of these data "coordination-induced shifts" (CIS) for $^{13}$C NMR spectra can be revealed, i.e., the trend of signal shift in $^{13}$C

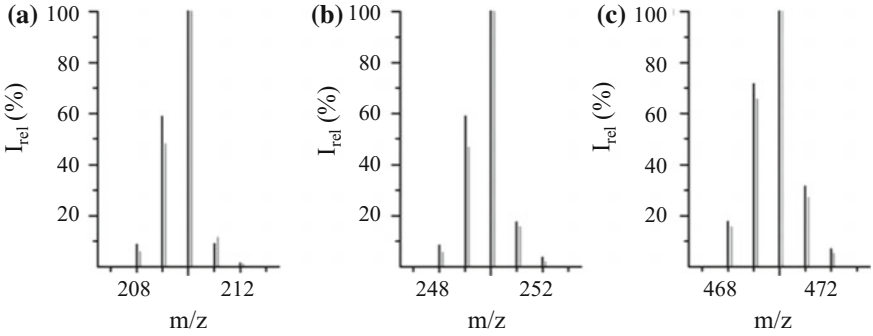


**Fig. 5.51** Comparison of calculated isotope pattern (gray) with fragment peaks for ion II of **a** methyl-2,3-*O*-(dibutylpyroboronate)-4,6-*O*-butylboronate-α-D-glucopyranoside (2a); **b** Me-2,3(PhB)2-4,6(PhB)-α-D-glc*p* (2) and molecular ion of (c) Me-2,3(PhB)2-4,6(PhB)-α-D-glc*p* (2) (reprinted from [283] copyright © 2009 with permission from Elsevier)

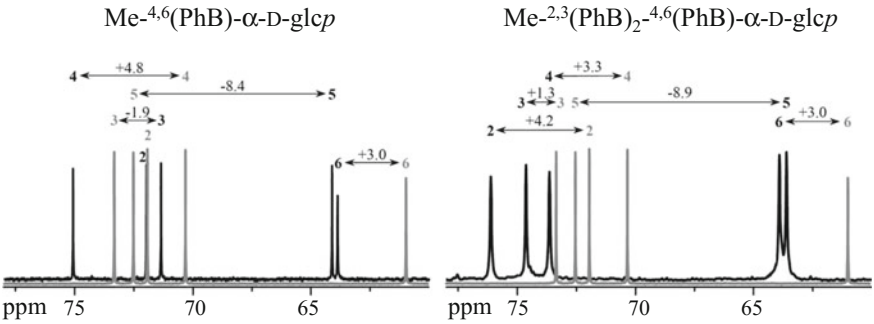


**Fig. 5.52** $^{13}$C NMR spectra with depicted "coordination-induced shifts" (arrows) of Me-4,6(PhB)-α-D-glcp (1) and Me-2,3(PhB)2-4,6(PhB)-α-D-glcp (2) in DMSO-$d_6$ (gray: Me-α-Dglcp, black: phenylboronate) (reprinted from [283] copyright © 2009 with permission from Elsevier)

NMR spectra as a result of esterification with PBA can be evaluated (Fig. 5.52, compare Chap. 2).

Comparison of the signal distribution of Me-α-D-glc*p* with phenylboronates 1–3 (Fig. 2.66) shows that binding-site carbons (e.g., C-2/3 in compound 3) are shifted downfield by 2–5 ppm, whereas the other ring carbons (C-5 or C-3 in compound 1) shift upfield by 1–9 ppm. Due to these identified "coordination-induced shifts", a transformation of all hydroxyl groups of phenylboronate 2 (Fig. 2.66) is observed. All carbon peaks are shifted downfield except the signals for C-5 and C-1. On the basis of these results, standard $^{13}$C NMR spectroscopy can be established as a fast and sensitive tool for the investigation of the interaction of cello-oligomers and finally cellulose with boric acid derivatives. In the latter case, quite a number of interactions have to be considered additionally as displayed in Fig. 2.32 (Chap. 2).

This increase of structural diversity already starts with the dimer methyl-β-D-cellobioside (Me-β-D-clb),

Nevertheless, NMR analyses show that in the first step PBA binds to *O*-4 and *O*-6 of the nonreducing glucose residue forming a six-membered ring [284], which is also observed during conversion of D-cellobiose in alkaline aqueous sodium tetraborate solutions [285]. A seven-membered pyroboronate ring at trans-1,2-diol group is generated if the PBA content in the reaction mixture is increased. In case of the boronation of Me-β-D-clb using a molar ratio 1:5.5, all secondary hydroxyl groups are esterified, one six- and two seven-membered rings are present (Fig. 2.34 ). The excess of reagent leads to the dimerization of Me-β-D-clb via a "PBA-bridge", confirmed by DOSY NMR studies.

Figure 2.67 shows a MALDI-TOF MS spectrum of the product obtained by a comparable interaction of Me-β-D-clb and triphenylboroxole (TPB). Remarkable are the recurring mass differences (Dm/z 86 and Dm/z 104), which originate from an additional PBA unit. Thus, the molecular ions $[M + Na]^+$ at m/z 465, m/z 569, m/z 655, and m/z 759 correlate with boronate structures with different numbers of boronic acid units. The detected molar masses confirm the transformation of secondary OH groups in positions 2 and 3 in addition to the expected six-membered ring at *O*-4 and *O*-6. Moreover, there is the molecular ion at m/z 759, which is consistent with an esterification product with two seven-membered pyroboronate rings at neighboring glucose units. This is a clear evidence for a multi-functionalization with diboronate moieties along an oligomer or polymer chain as shown in Table 2.23. Analysis of CIS in $^{13}C$ NMR spectra confirms functionalization at the trans-1,2-diol structure by occurrence of a sharp signal at 78.7 ppm (see Chap. 2).

The discussed model reactions lead to the conclusion that depending on the concentration of the boronic acid or its active derivatives, esterification or complexation occurs. In the first step, it is observed at the nonreducing end group that, in the following step (increased concentrations), seven-membered rings are formed at positions 2 and 3 and at higher concentrations cross-linking takes place preferably.

Rheological experiments on cello-oligomers dissolved in ILs show the same trend during conversion with boric acid. Up to 1% (w/w) boric acid in the system, the viscosity is not influenced meaning no cross-linking occurs. In the concentration range from 1 to 5% (w/w), the viscosity increases as a function of the amount of boronic acid. At about 8% (w/w), it drops drastically and precipitation is observed. Obviously, fast cross-linking is the reason.

Based on these results, an aqueous solvent system for cellulose containing NaOH and boric acid was developed. Thus, a homogeneous solution containing 2% cellulose, 7% NaOH, and 0.6% boric acid can be obtained by cooling for 3–5 h to −12 °C (see Fig. 5.53).

The dissolution process can also be visualized by means of light microscopy. In Fig. 5.54, a suspension of cellulose in the described mixture is shown before (A) and after cooling to 12 °C (B).

**Fig. 5.53** Cellulose (2%) dissolved in an aqueous mixture of 7% NaOH with 0.6% boric acid

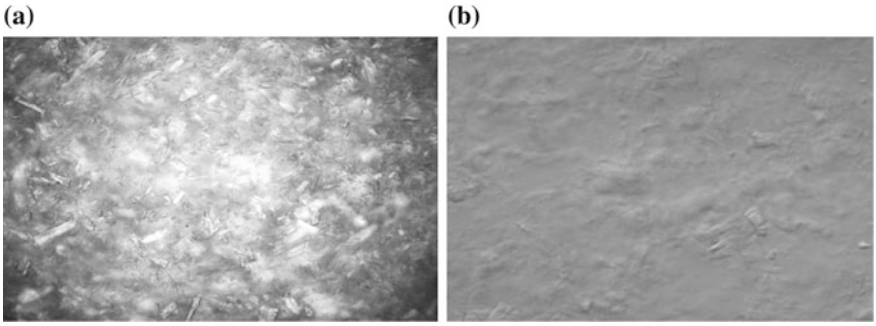


**Fig. 5.54** Microscopic images of cellulose (2%) dissolved in an aqueous mixture of 7% NaOH with 0.6% boric acid; **a** suspension without any treatment; **b** after cooling to −12 °C

The rather well-resolved $^{13}C$ NMR spectrum of cellulose dissolved in these solutions argue in favor of well-defined structures (Fig. 5.55). In the spectrum, two small signals are visible as shoulders on the peaks for the carbon atoms 1 and 4 with an upfield shift of 2 ppm. These signals are caused by an interaction at the OH groups at positions 2 and 3. In comparison to the model reaction described and the CIS measured, it can be concluded that this is a hint for the formation of a seven-membered boronate ring. This ring system is highly reactive and is unstable in the presence of a protic medium. Thus, a dynamic equilibrium between ring formation and ring opening can be assumed. This fast process is the reason for the

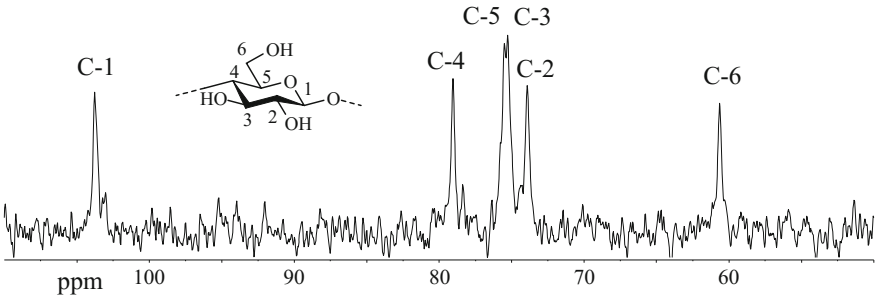


**Fig. 5.55** $^{13}C$ NMR spectrum of cellulose (2% (w/w)) dissolved in a mixture of 7% NaOH and 0.6% boric acid in $D_2O$

low intensity of the signals. Nevertheless, these results lead to the conclusion that this solvent system is a derivatizing medium.

In addition to this investigation toward the development and the basic understanding of an aqueous cellulose solvent containing boric acid, the formation of stable boron-containing cellulose derivatives was investigated. A serious problem is the strong tendency of boric acid and its derivatives toward cross-linking yielding insoluble products, which are hard to analyze. The direct conversion of cellulose with boric acid in a melt of urea at 150–200 °C leads to maximum DS values of 0.7 [286]. A more convenient approach is the transesterification of boric acid esters of aliphatic alcohols such as boron ethoxide and boron isopropoxide with cellulose, which can be carried out in the boron alkoxide or in solvents, e.g., the parent alcohol, benzene, pyridine, or ethylenediamine [287]. Complete conversion of all OH groups is concluded from elemental analyses [288]. The method is used to increase the reactivity of the polymer and to prepare flame-resistant products. Interestingly, trialkyl boranes may also be applied for the preparation of cellulose boronates. Accordingly, synthesis of per-*O*-diethylboranoylated cellulose was achieved [289]. Borax was reacted in an aqueous medium with cellulose and hydroxyethyl cellulose. In the latter case, formation of five-membered rings was postulated [290]. Again products with an increased thermal stability relative to native cellulose can be obtained [291]. Moreover, the boron-containing derivatives have a pronounced antibacterial activity [292]. Binding of boric acid ester moieties enhances the water sorption capacity of cellulose by the factor of 2.5–3, which is obviously due to an increased accessibility [293].

### 5.3.5 *Cellulose Esters of Carbonic Acid and Its Derivatives*

Carbonic acid $H_2CO_3$, some of its derivatives, and a number of the corresponding sulfur-containing compounds form esters with alcohols. In cellulose chemistry, the relevant esters are those of carbonic acid (Sect. 5.3.5.1), carbamic acid (the amide

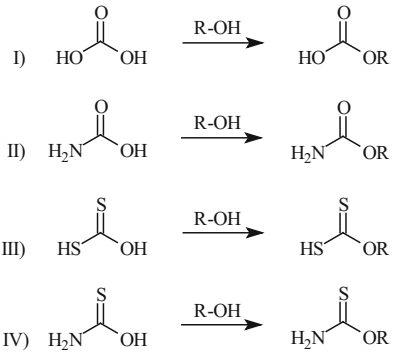


**Fig. 5.56** Molecular structures and reactions of carbonic acid and its derivatives with alcohols, showing carbonic acid (I), carbamic acid (II), thiolthiocarbonic acid (xanthogenic acid; III), and thiocarbonic acid amide (IV)

of the carbonic acid, Sect. 5.3.5.2), thiolthiocarbonic acid (xanthogenic acid, Sect. 5.3.5.3), and thiocarbonic acid amide (Sect. 5.3.5.4). These derivatives are shown in Fig. 5.56.

The acids themselves are generally regarded as elusive; attempts at their isolation in the free state at room temperature lead to decomposition products only [294]. The protonated counterparts of these acids are, however, remarkably stable and have been detected in superacid media at low temperatures [295].

The following cellulose derivatives are of importance: unsymmetric diesters of carbonic acid; unsubstituted and *N*-substituted esters of carbamic acid and thiocarbamic acid; and unsubstituted esters of xanthogenic acid. The general structures of these derivatives are depicted in Fig. 5.57 where, for simplicity, we show a single substitution at position C6 of the AGU.

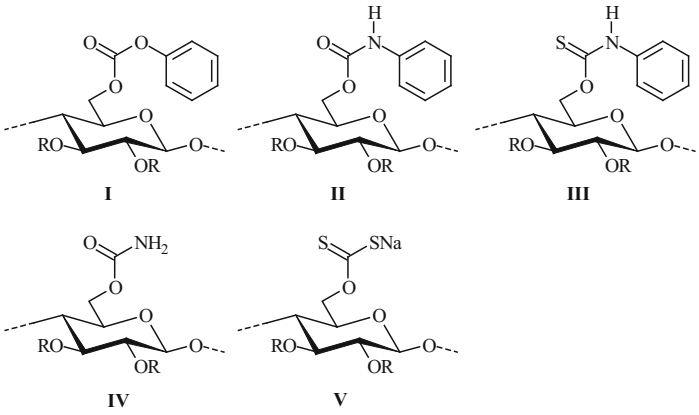


**Fig. 5.57** Molecular structures of relevant cellulose-based compounds of carbonic acid and its derivatives. For simplicity, we show structures that are limited to a single substitution at position C6 of the AGU. These are carbonates (I), carbamates (II), and thioncarbamates (III). Included also are unsubstituted carbamate (IV) and xanthate (V)

Cellulose carbonates are usually prepared using alkyl or aryl chloroformats. These compounds are applied in a variety of subsequent reactions as discussed in Sect. 5.3.5.1. The reaction of cellulose with urea produces the corresponding unsubstituted (at the nitrogen atom) carbamate, from which cellulose can be regenerated by acid hydrolysis (Sect. 5.3.5.2). This is a potential alternative to the viscose process for obtaining cellulose fibers. An important subclass of cellulose carbamates is the *N*-substituted derivatives. Aliphatic and aromatic esters can be prepared by the reaction of cellulose with the isocyanate. These derivatives are employed in different analytical and biochemical applications. Thus, *N*-phenyl carbamates of cellulose can be used as stationary phase in chromatography. Carbanilation is also a proper tool for structure determination of cellulose derivatives by NMR spectroscopy or chromatography. Additionally, the formation of carbamates is a state-of-the-art technique for labeling of cellulose, e.g., with fluorescent dyes. A valuable method in this regard is the reaction of cellulose with isothiocyanates resulting in the formation of isothiocarbamates, as the *N*-substituted esters of thiocarbonic acid amide are called. The sodium salt of cellulose xanthate is formed during the well-known viscose process (Sect. 5.3.5.3). It is obtained as an intermediate during the conversion of cellulose, in the presence of NaOH, with $CS_2$, which can be considered as the anhydride of the xanthogenic acid.

### 5.3.5.1 Cellulose Esters of Carbonic Acid

Simple Esters of Carbonic Acid

Although carbonic acid is unstable at room temperature, it has been isolated at low temperature and detected by FTIR [296] and $^{13}C$ NMR spectroscopy [297]. Equations 5.14 and 5.15 show the pH-independent, i.e., water-catalyzed, hydrolysis of a carbonate diester, where R is an aliphatic or aromatic group:

$$(RO)_2C = O + H_2O \rightarrow ROH + ROCOOH \tag{5.14}$$

$$ROCOOH \rightarrow ROH + CO_2 \tag{5.15}$$

The monoesters of carbonic acid shown in Eq. (5.15) are also unstable and decompose into $CO_2$ and the corresponding alcohols or phenols [298]. The diesters of carbonic acid, aliphatic, aromatic, acrylic, or cyclic are stable. Among organic carbonates, the simplest one is dimethyl carbonate, a "green" reactive solvent that can be used as a methylating agent (a convenient substitute for methyl halides or dimethyl sulfate) or for the preparation of derivatives of carbonic acid by nucleophilic substitution, according to Fig. 5.58, where Nu is a nucleophile [299].

The reaction of ethyl chloroformate, in the presence of triethylamine, with pyranoid compounds containing vicinal di-equatorial hydroxyl groups is known to give *trans*-five-membered cyclic derivatives. Thus, methyl 4,6-*O*-benzylidene-α-D-glucopyranoside gives methyl 4,6-*O*-benzylidene-α-D-glucopyranoside

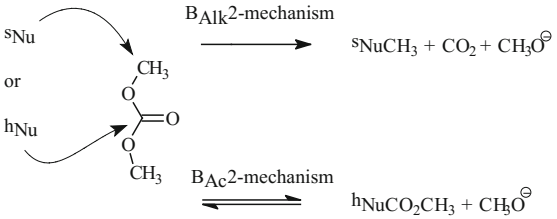


**Fig. 5.58** Use of dimethylcarbonate as a methylating agent (top) and in the synthesis of carbonic acid derivatives by nucleophilic substitution (bottom) [299]

2,3-carbonate, and methyl 2,6-di-*O*-(methylsulphonyl)-α-D-glucopyranoside gives the 3,4-cyclic ester. According to the reaction conditions, methyl 4,6-*O*-benzylidene-α-D-glucopyranoside can also give the 2,3-di-*O*-ethoxycarbonyl or the 2- and 3-monoesters [300, 301].

Figure 5.59 shows some applications of these carbonate cyclic esters in the synthesis of further sugar derivatives [302].

## Cellulose Esters of Carbonic Acid

Similar to sugar carbonates, the cellulose derivative was prepared under anhydrous conditions by the reaction of the biopolymer in DAS/base with reactive esters, in particular chloroformate and carbonate esters. This reaction should be carefully controlled in order to avoid cross-linked products, along with cyclic and linear carbonates [303, 304]. Additionally, one or more of the side reactions shown in Fig. 5.60 may occur. In this figure, reaction (a) is of interest, while the others (b–e) are side reactions.

(b) whereas the chloroformate ester may be consumed by reactions,
(c) hydrolysis,
(d) side reactions with the solvent, or
(e) $Cl^-$-mediated decomposition [305].

The molecular structure of cellulose carbonates can be evaluated by NMR, UV, and FTIR spectroscopy, titration, and elemental analysis. $^1$H-NMR spectroscopy of the peracetylated aliphatic or aromatic cellulose carbonate yields the corresponding $DS_{Carbonate}$ [305, 306]. For esters carrying an aromatic moiety, e.g., cellulose 4-nitrophenylcarbonate, the $DS_{Carbonate}$ can be also calculated from the UV–Vis spectrum after alkaline hydrolysis and measurement of the liberated phenol [307].

Different types of carbonate moieties can be detected by FTIR spectroscopy. At 1810–1835 $cm^{-1}$ ($\nu_{C=O}$), the adsorption of the cyclic carbonate appears. The signals arising from acyclic aromatic or aliphatic cellulose carbonates are at 1770 and 1750 $cm^{-1}$, respectively [308]. IR spectroscopy can be applied to determine the cyclic versus acyclic cellulose carbonate with the use of dextran carbonate as reference compound. Therefore, the carbonate content of soluble dextran carbonate was determined by titration after alkaline hydrolysis with barium hydroxide solution. Moreover, the aminolysis of cyclic carbonate moieties applying aqueous ammonia

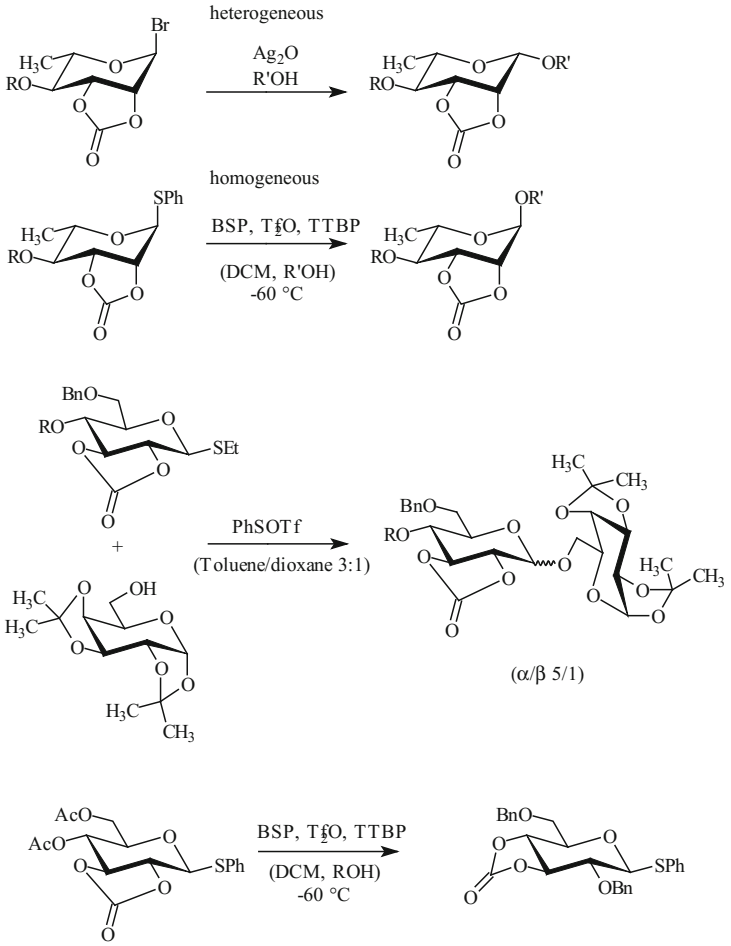


**Fig. 5.59** Some application of cyclic carbonate esters of monosaccharides in the synthesis of sugar derivatives [302]

or benzylamine and subsequent elemental analysis (nitrogen content) yield the $DS_{Carbonate}$ value, which is smaller due to the non-specific ring opening by water [308].

## Synthesis Under Heterogeneous Conditions

Cellulose carbonate was synthesized by reaction of its suspension in DMSO or DMF with ethyl chloroformate in the presence of trimethylamine as catalyst. The products showed IR bands at 1835 and 1810 $cm^{-1}$ due to trans-cyclic carbonate and 1750 $cm^{-1}$, due to the *O*-ethoxycarbonyl cellulose [308]. In an approach similar to

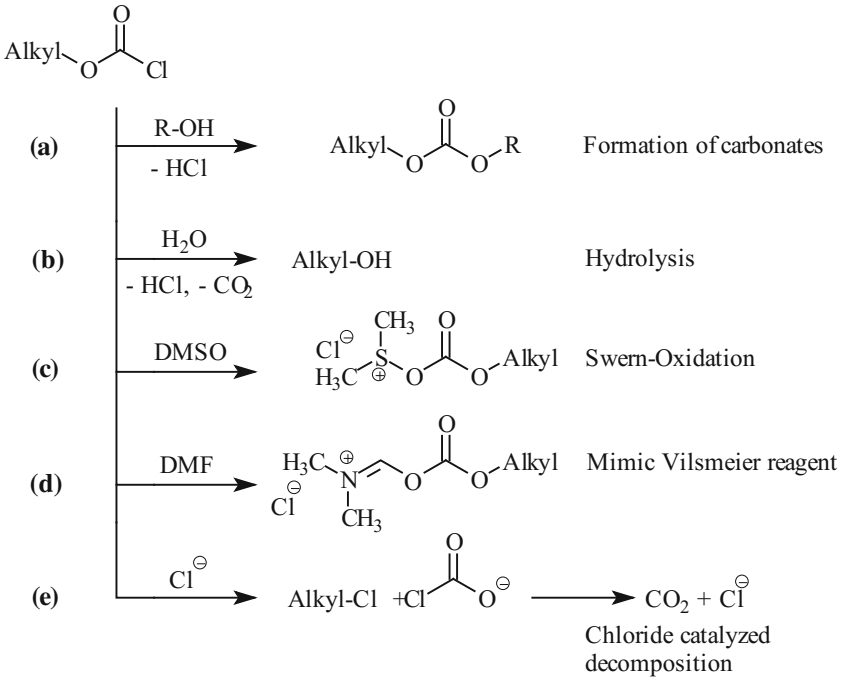


**Fig. 5.60** Possible side reactions that may occur during the carbonation of carbohydrates with chloroformate esters [305]

that employed for cellulose xanthation, see Fig. 5.61, cellulose carbonate was prepared by the reaction of soda–cellulose with $CO_2$ under pressure (30–50 bar) in the presence of $ZnCl_2$ and acetone or ethyl acetate (the organic solvent increases the solubility of $CO_2$). This treatment has resulted in negligible degradation of the biopolymer; the produced carbonate is soluble, completely or partially in ZnO/NaOH or ZnO/urea/NaOH solutions, from which cellulose II was regenerated by acidification [309, 310].

### Synthesis Under Homogeneous Conditions

Cellulose cyclic carbonates and monoesters of carbonic acid have been synthesized under homogeneous conditions by the conversion of the biopolymer with reactive esters, in particular alkyl and/or phenyl chloroformates, fluoroformates, and carbonates, in the presence of diverse catalysts. Thus, the biopolymer was dissolved in DMAc/LiCl and reacted with diphenylcarbonate at 100 °C for 4 days, in the presence of dibutyltin dilaurate as catalyst. The product showed IR bands due to the formation of cyclic carbonate (1810 and 1835 $cm^{-1}$) as well as cellulose phenylcarbonate (1767 $cm^{-1}$) [311]. Likewise, transesterification of cellulose triacetate in

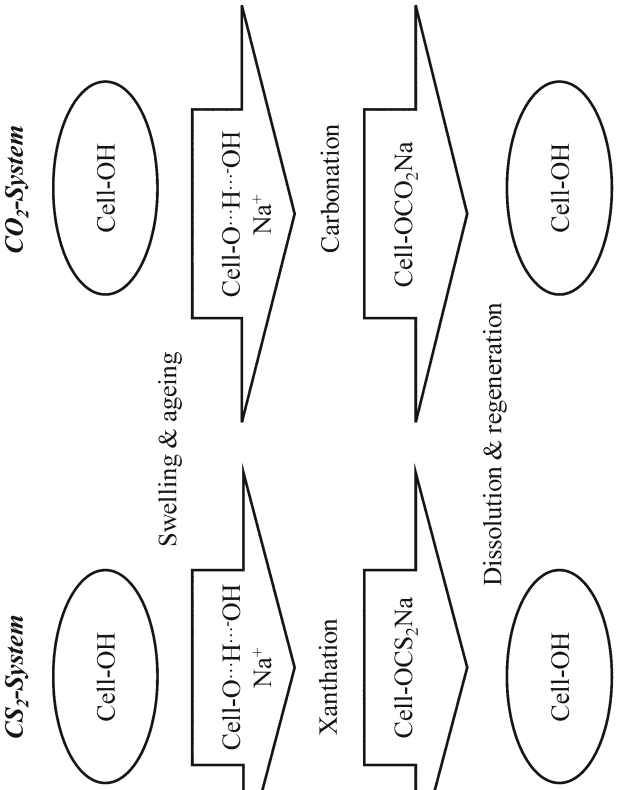


**Fig. 5.61** Comparison between the steps of xanthation and carbonation of soda–cellulose [309]

molten diphenyl carbonate and the esterification of cellulose dissolved in DMAc/LiCl with $(PhO)_2CO$ yield cellulose phenyl carbonates [312]. In these reactions, however, toxic dibutyltin laurate was used as catalyst, which is objectionable for biological applications of the products.

Different polysaccharides, including water-soluble dextran, cellulose, starch, and pullulan, have been transformed into their monocarbonate esters by reaction with diverse reactive esters including phenyl- and 4-nitrophenyl chloroformate, and phenyl fluoroformate [313]. The reaction of cellulose with 4-nitrophenyl chloroformate (molar ratio of 1:3) leads to a product with a $DS_{Carbonate}$ of 1.34 that jellifies in organic solvents, due to intermolecular cross-linking by the carbonate groups. A similar phenomenon was observed in case of cellulose phenyl carbonate of low $DS_{Carbonate}$. Although the reason for this cross-linking is not known in detail, it is plausible that the 4-nitrophenyl group is reactive enough for further transesterification, e.g., by the hydroxyl group of the AGU of another cellulose chain. Cross-linking of cellulose phenyl carbonates with low DS may be explained by the high number of nonderivatized hydroxy groups that are accessible for intra- and intermolecular carbonate formation. Figure 5.62 shows the $^{13}C$ NMR spectrum of a cellulose phenyl carbonate (DS 0.84) synthesized with phenyl chloroformate in DMAc/LiCl. The relevant information is that the spectrum shows only one C=O signal at 153 ppm, indicating regioselective substitution at position 6, in agreement with the fact that the resonances of positions 2 and 3 carbons of the AGU indicated no substitution [314].

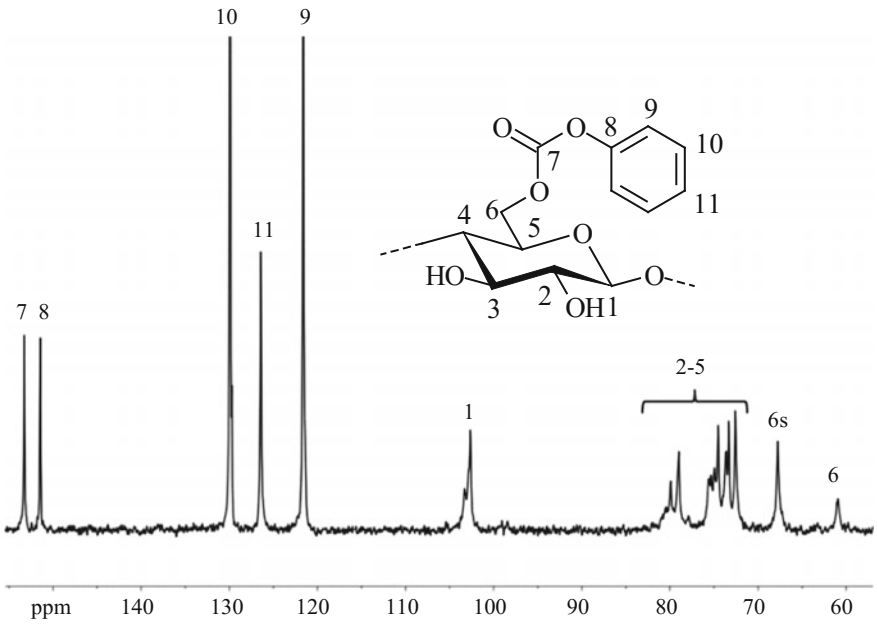


**Fig. 5.62** $^{13}C$ NMR spectrum of cellulose phenyl carbonate (DS 0.84) recorded in DMSO-$d_6$

Regioselective reaction of cellulose and further transformations at position 2 was achieved by using the 6-*O*-trityl ether, as depicted in Fig. 5.63 [314].

This synthetic route, namely reaction of cellulose with alkyl chloroformate in DMF/LiCl or DMSO/LiCl in the presence of a base (pyridine or NaH), has been applied to the synthesis of dextran ethyl, 1-butyl-, and tert-butyl carbonates from the corresponding alkyl chloroformates and fluoroformates. The products were investigated by elemental analysis and $^{13}C$ NMR spectroscopy (1D and HETCOR) and possessed $DS_{Carbonate}$ in the range 0.20–2.85 [315].

The reaction with diphenyl carbonate in pyridine/1-(1-butyl)-3-methylimidazolium chloride for 1–24 h at room temperature gave cellulose phenyl carbonates with $DS_{Carbonate}$ 0.44–3.0, and the products were investigated by $^{1}H$-, $^{13}C$ NMR spectroscopy, and by COSY and HETCOR experiments [316].

### Properties and Applications of Cellulose Carbonate

Physicochemical properties of cellulose carbonates were investigated. It was found that the tensile strength of cellulose alkyl carbonates decreases with increasing alkyl chain length, while the tensile elongation is increased. Moreover, the melting point becomes lower with increasing alkyl chain length (Table 5.23) [312].

Carbonic acid esters of cellulose provide interesting features compared to widely used carboxylic acid esters. The cyclic cellulose carbonates are of interest for the immobilization of biomacromolecules, including enzymes [306, 317–319], antibiotics [320], as well as amino- and mercapto compounds [321]. Cellulose carbonate was also used in the field of isolation and purification of antibodies [322–326]. Beyond the conjugation of cyclic cellulose carbonate with amines, alcohols, or thiols, the homogeneous aminolysis of acrylic cellulose phenyl carbonates has been developed [314, 327]. The corresponding cellulose carbamates formed were used in the field of catalysis and are promising compounds for gene complexation and delivery.

The most promising potential application for cellulose carbonate is that for fiber regeneration. As indicated in Table 5.24, there is a strong demand for using $CO_2$ as a starting material for the production of chemicals due to the accumulation of this gas in the atmosphere at an alarming rate. For example, its concentration has increased from 315–330 ppm in the period 1958–1975 to 370–388 ppm in the period 2002–2010, corresponding to increase of 0.9–2.25 ppm/year, respectively [328]. The production of cellulose carbonate by the reaction of alkali cellulose with ethyl chloroformate/DAS has been described [329] as well as the synthesis by reacting alkali cellulose with $CO_2$ in the presence of $ZnCl_2$/alcohol. In the latter case, the obtained carbonate was dissolved in ZnO/NaOH bath and cellulose II was regenerated by extrusion in an acid bath [330].

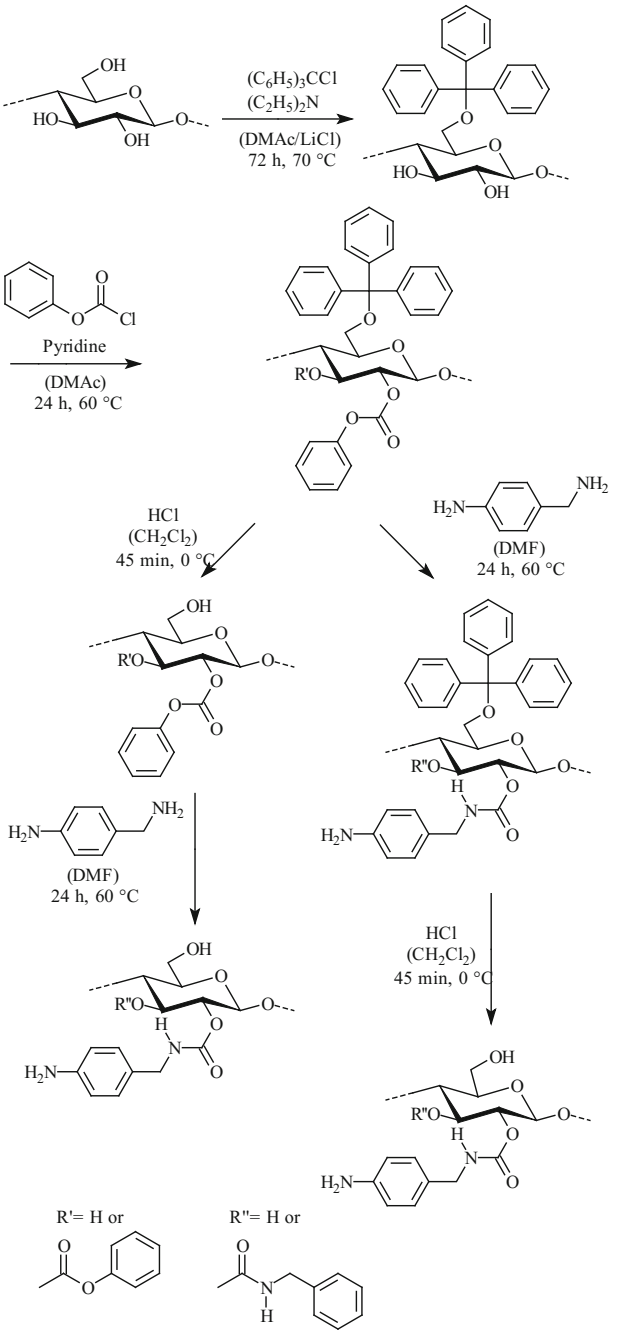


**Fig. 5.63** Regioselective synthesis of carbonic acid esters of cellulose (via trityl cellulose) and ester aminolysis at position 2 yielding cellulose carbamate [314]

**Table 5.23** Physicochemical properties of cellulose carbonates [312]

| Moiety R | Tensile strength ($kg/m^2$) | Tensile elongation (%) | Melting point (°C) | Decomposition temperature (°C) |
|---|---|---|---|---|
| Propyl | 780 | 66 | 245–255 | 332 |
| Butyl | 490 | 85 | 200–216 | 332 |
| 2-Ethylhexyl | 250 | 110 | 177–184 | 332 |
| Phenyl | 470 | 42 | 200–210 | 339 |

**Table 5.24** Representative examples of the strategies employed for the synthesis of cellulose carbonates

| Cellulose/ DP | Derivatizing agent | Reaction conditions medium/catalyst | Product $DS_{Cabonate}$ | References |
|---|---|---|---|---|
| MCC | RCOX (R = $C_1$–$C_4$, Ph), X = Cl, F | DMSO/dioxane/TEA/0 °C/10–240 min | 0.03–3.0 | [308] |
| Rayon cellulose/ 850 | $CO_2$ | Ethyl acetate/$ZnCl_2$/30–40 bar/−5–0 °C/2 h | – | [309] |
| MCC | Diphenyl carbonate | DMAc/LiCl/dibutyltin dilaurate/100 °C/4 d | – | [311] |
| MCC/330 | Phenyl chloro, fluoroformate | DMAc/LiCl/Py/0 °C/4 h | 1.69 | [314] |
| MCC/330 | Phenyl chloroformate | IL (BuMeImCl)/Py/RT/ 1–24 h | 0.44–3.0 | [316] |

### 5.3.5.2 Cellulose Esters of Thiocarbonic Acids

Sulfur-containing derivatives of carbonic acid include monothiocarbonic acid (HS–CO–OH ⇄ HO–CS–OH), dithiocarbonic (HOCS–SH), and trithiocarbonic acid $H_2CS_3$. The acids themselves have not been isolated at room temperature [331–333] but their monoesters are known. For example, carbonyl sulfide (COS), the anhydride of monothiocarbonic acid, is moderately stable [334, 335] and reacts with alkali cellulose to give the alkyl monoesters of monothiocarbonic acid [336]. This cellulose monoester is only stable at low temperature (0 °C). At higher temperature, it decomposes into sodium sulfide and carbonate under regeneration of cellulose. As will be shown below, COS is one of the byproducts formed in the viscose process; cellulose monothiocarbonate plays a role as an intermediate in cellulose xanthation during the viscose process.

The reaction of alkali cellulose with $CS_2$ (the anhydride of dithiocarbonic acid) produces sodium cellulose dithiocarbonate, during the xanthation step of cellulose fiber preparation by the viscose process [337, 338].

$$\text{Cell-O---H---}^{-}\text{OH Na}^{+} + \text{CS}_2 \rightarrow \text{Cell}-\text{O}-\text{C(S)}-\text{S Na} \tag{5.16}$$

The main side reaction in this process is the multistep base-catalyzed hydrolysis of $CS_2$, according to Eqs. (5.17)–(5.20).

$$\text{CS}_2 + \text{NaOH} \rightarrow \text{NaCS}_2\text{OH} \tag{5.17}$$

$$\text{NaCS}_2\text{OH} \rightleftarrows \text{COS} + \text{NaSH} \tag{5.18}$$

$$\text{COS} + 4\ \text{NaOH} \rightarrow \text{Na}_2\text{S} + \text{Na}_2\text{CO}_3 + 2\ \text{H}_2\text{O} \tag{5.19}$$

$$\text{NaSH} + \text{NaOH} \rightarrow \text{Na}_2\text{S} + \text{H}_2\text{O} \tag{5.20}$$

The sodium sulfide produced reacts irreversibly with $CS_2$ to form sodium perthiocarbonate [339].

$$\text{Na}_2\text{SH} + \text{CS}_2 \rightarrow \text{Na}_2\text{CS}_4 \tag{5.21}$$

Relevant to this discussion is that at 10 °C the rate constant for the reaction of Cell-O---H---$^{-}$OH $Na^{+}$ with $CS_2$ (Eq. 5.16) is about 522 times faster than the rate-limiting step of the reaction of $HO^{-}$ with $CS_2$, due to favorable enthalpy and entropy of activation [340]. Therefore, $CS_2$ consumption by hydrolysis is not a serious problem in the viscose process.

In acidic solution, cellulose xanthate decomposes fast to regenerate the biopolymer. That is, the viscose process amounts to alkali cellulose dissolution in a derivatizing solvent, $CS_2$, followed by biopolymer regeneration as fiber by decomposition of the formed xanthate (ester of a weak acid).

### Applications of Esters of Thiocarbonic Acids: The Viscose Process and the Rayon Fiber

The discovery in 1893 that cellulose when treated with sodium hydroxide and $CS_2$ is transformed into a soluble compound (viscose) has developed into a commercial method for cellulose fiber regeneration (the rayon fiber) [341]. By 1908, the fiber spun from viscose dope has become a key component in textile industry. Thanks to innovations in process engineering and diversity of the pulps that can be employed, the viscose process still enjoys the unique position of being the most versatile of all man-made fibers. Thus, the production of rayon fibers has continued to increase, totaling in 2012, 6.2% of all fibers, versus 31.6, 1.3, 60.9% for cotton, wool, and synthetic fibers, respectively [342].

A schematic representation of the viscose industrial process is shown in Fig. 5.64 (from Acordis), followed by a brief discussion of each step.

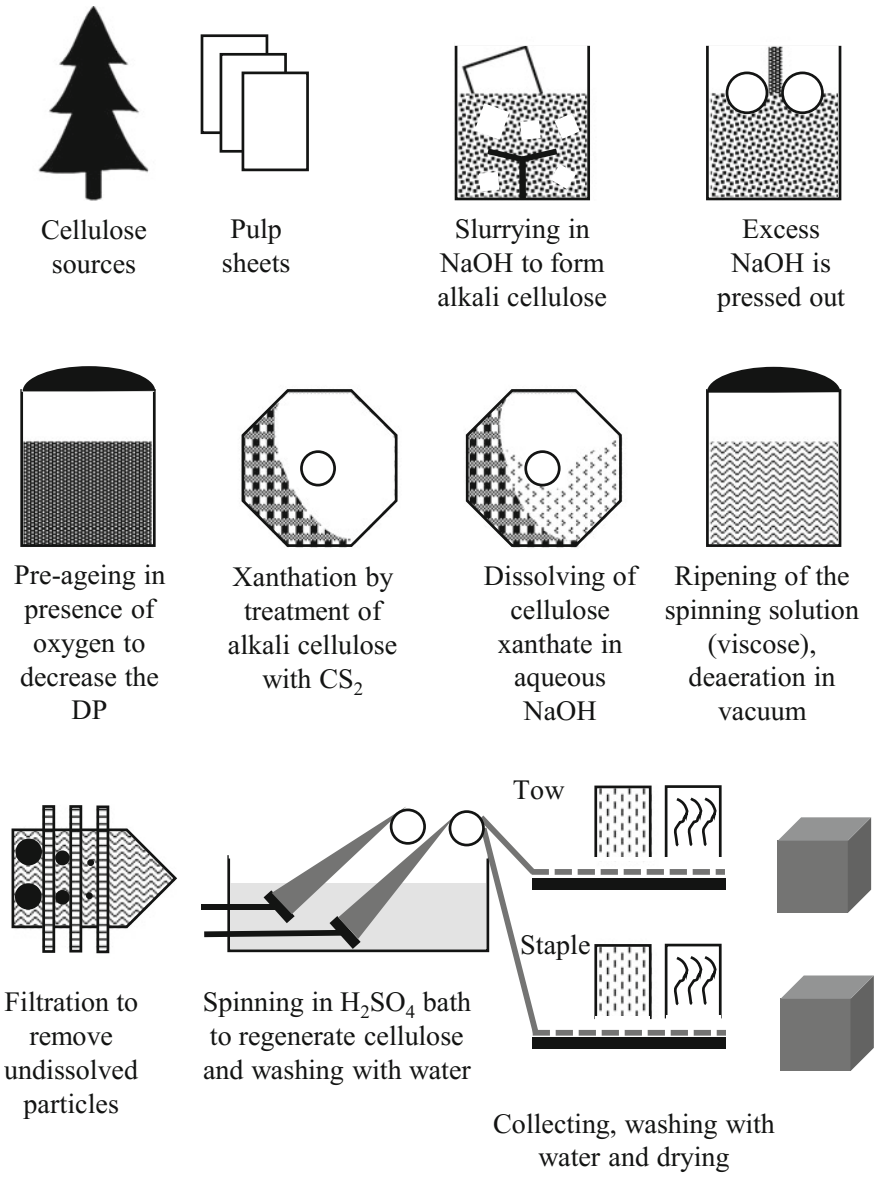


**Fig. 5.64** Schematic representation of the steps of the industrial viscose process [338]

### The Pulp

The wood pulps (Kraft or sulfite) employed are those from eucalyptus, acacia, spruce, birch, beech, and other wood species. The pulp properties that are relevant to the process are DP, $I_c$, and the contents of hemicellulose and non-cellulosic material, lignin, and inorganics. The pulps used are usually denoted as dissolving-grade pulp (dissolving pulp) that possess a high cellulose content and purity.

### The Steeping Step

The term steeping means to soak something in a liquid in order to clean or soften it, by making it thoroughly wet. In the viscose process, the objectives of this step are to convert the biopolymer (typically 6% (w/w) cellulose in aqueous NaOH solution) into alkali cellulose and to extract hemi- and γ-cellulose of low molecular mass. Extraction of these components is important because their xanthation potentially deteriorate fiber quality, in addition to increasing the consumption of $CS_2$. The process variables include temperature (45–55 °C), lye concentration (17–19% (w/w) NaOH), and time (15–30 min). A variant of this treatment is double-steeping, where the biopolymer is steeped in 17–19% (w/w) NaOH solution in order to convert it into soda–cellulose; steeping at lower lye concentration, 11–13% (w/w) NaOH solution causes further swelling, extra removal of hemicellulose, and results in pulp with lower NaOH content. The slurry is then pressed to typically 30–36% (w/w) cellulose and 13–17% (w/w) soda, and then shredded.

### DP Reduction: Pre-aging or Mercerization

For regular staple production, the DP of the alkali cellulose should be reduced from its original value to ca. 270–350. This is usually done by storing alkali cellulose for some time (0.5–5 h) under controlled temperature (40–60 °C) and humidity. Thus, the DP is reduced by oxidative degradation. This reaction occurs either at the chain ends (nibbling), which gives very little overall reduction in DP, or at reactive sites such as carbonyl groups on the chain backbone. The latter sites are present naturally in cellulose, or form during bleaching of the pulp. Hence, the DP of pulps with high copper numbers (a measure of the number of carbonyl groups in cellulose) will decrease faster than those with lower copper numbers. Increasing cellulose reactivity and quantification of this property is crucial to the viscose process. One method is due to Fock, where calculation of cellulose reactivity is based on the determination of the amount of cellulose that is converted into xanthate. Thus, cellulose xanthate is prepared under standardized conditions, filtered, and the cellulose regenerated by precipitation in sulfuric acid solution. The biopolymer obtained is then oxidized with $K_2Cr_2O_7$ solution, and the unreacted $Cr^{6+}$ is back titrated [343].

### Xanthation

The alkali cellulose reacts with $CS_2$ to produce alkali-soluble sodium cellulose xanthate. Pure $CS_2$ has a b.p. of 46.2 °C, and smells like chloroform. The commercial product often possesses a strong disagreeable and fetid odor due to the presence of very small concentrations of strong-smelling organic sulfur compounds. Carbon disulfide is highly toxic and flammable, having an explosive range in air, from 1.25 to 50% (v/v). Its flash point is −30 °C and its autoignition occurs at 100 °C, or even lower under certain conditions. Industrial ignition accidents have been reported [344].

The low b.p. of $CS_2$ is exploited industrially in the so-called "fiber-xanthation", where the alkali cellulose mass reacts under reduced pressure with $CS_2$ vapor, a procedure that results in efficient mass transfer. This heterogeneous (solid/gas) reaction is carried out either in batch or continuous mode with a reaction time from 30 to 90 min. For both homogeneous and heterogeneous xanthation of alkali cellulose, the position 2 is favored (kinetic product) over the positions 6 and 3, essentially for steric reasons [345]. Xanthation at the primary *O*-6 of the AGU is, however, thermodynamically favorable, compared to the secondary positions [346]. The maximum $DS_{Xanthate}$ is 0.9–1.0.

Based on the above-mentioned large difference in the rate constants of reaction of $CS_2$ with alkali cellulose and the hydroxide ion, the xanthation reaction has also been carried out in the laboratory in the liquid phase by the so-called "emulsion xanthation". In this procedure, liquid $CS_2$ is stirred with an aqueous suspension of the biopolymer in alkali at low temperature, e.g., 20 °C until complete formation of the viscose dope [347–349]. According to the IUPAC definition of the terms emulsion, suspension, and colloidal dispersion [350], the designation of the xanthation reaction as "emulsion" is a misnomer; the appropriate term is suspension xanthation, even when surface active agent is present, e.g., abietic or nonionic surfactant [351–353].

Cellulose xanthate of $DS_{Xanthate}$ 0.5–1.0 is a yellowish fibrous mass that dissolves easily in dilute aqueous alkali solutions (Fig. 5.65). It can be precipitated by addition of water-miscible organic solvents or, being charged, by salting-out with electrolytes. In aqueous media, it is unstable over the whole pH range. It decomposes by acids at room temperature, or by heat in water at ca. 100 °C, in both cases with evolution of $CS_2$.

Examples for xanthation reactions can be found in Table 5.25 at the end of this chapter.

### Viscose Aging

The viscose dope obtained is "aged" to permit distribution of the ester moieties evenly within cellulose chains, a vital step for achieving good spinning and quality of the fibers. During this step, "trans-xanthation" occurs, resulting in an increase in the concentration of the thermodynamically more stable xanthate at position 6, at

**Fig. 5.65** Cellulose xanthate solution in sodium hydroxide

**Table 5.25** Representative examples of the strategies employed for the synthesis of cellulose xanthate by conversion with $CS_2$ and heating by convection

| Entry | Cellulose/DP | Reaction phase/type and conditions of xanthation step | Product $DS_{Xanthate}$ | References |
|---|---|---|---|---|
| 1 | Cotton linters/1950; Bagasse/764 | Liquid; suspension xanthation/5 h, 20 °C | 0.43–0.54 | [349] |
| 2 | Eucalyptus, Spruce, and pine pulp/244–656 | Solid/gas; 150 min, RT | 0.31–0.42 | [361] |
| 3 | Kraft and sulfite pulp | Solid/gas; 150 min, 28–32 °C | 0.44–0.53 | [362] |
| 4 | Birch sulfite cellulose/480 | Liquid; suspension xanthation/3 h, 8–28 °C | 0.10–0.95 | [363] |
| 5 | Cotton linters/1135 | Liquid; suspension xanthation/6 h, 20 °C | 0.4–1.0 | [364] |

the expense of the moieties located at *O*-2 and *O*-3. This reaction can be followed by several methods, e.g., by $^1$H NMR spectroscopy after allylation of the remaining hydroxyl groups [354] or from the γ-number, whose value can be easily calculated from the solution UV/Vis absorbance at 303 nm [355]. The γ-number is defined as the amount of xanthate groups per 100 AGU, i.e., it is a measure of $DS_{Xanthate}$; the maximum γ-number being 300. As a function of time, value of the γ-number was found to decrease at *O*-2 and *O*-3, increase at position 6 and passes through a maximum [356].

Spinning

The viscose dope is filtered to remove particulates, usually through sintered metal screens with 10–20 μm orifices. It is degassed under reduced pressure in order to remove any dispersed gases that might otherwise cause small bubbles as the viscose is extruded into filaments through the jet. Additives are added, if required, before spinning the yarns. These include surface active agents, e.g., ethoxylated fatty acid or fatty amines, and $TiO_2$.

The conventional viscose spinning process consists of pressing the dope through corrosion-resistant spinnerets, into an acid bath containing $H_2SO_4$ and $Na_2SO_4$ at ca. 40 °C, and conveying the thread of the cellulose II formed onto a bobbin. Moreover, stretching is carried out to increase alignment and strength of the fibers. The number of holes in the spinnerets lies between 100 (rayon filaments) and several thousands (rayon staple), with hole diameter of 50–100 μm. Figure 5.66 shows one spinneret and the viscose jet as it is pressed out.

The main reaction in the acid bath is

$$2\ \text{Cell}-\text{OCS}_2\text{Na} + \text{H}_2\text{SO}_4 \rightarrow 2\ \text{Cell}-\text{OH} + \text{N}_2\text{SO}_4 + 2\ \text{CS}_2 \qquad (5.22)$$

The cellulose regeneration bath may also contain zinc sulfate and surface active agents, in particular ethoxylated fatty alcohols and fatty amines, for the production of the so-called “skin-core” filaments with outstanding properties for some applications, due to different fibrillary architectures in the outer skin and the inner core [357, 358]. The formation of these filaments is based on slower regeneration of

**Fig. 5.66** Enlarged photo of a spinneret (left, https://www.tradeindia.com/fp1246480/Spinneret-For-Staple-Fibre-Yarn.html, accessed on September 29, 2017) and the dope filaments as they are pressured out of the orifices (right, courtesy of Thuringian Institute for Textiles and Plastics Research, TITK, Rudolstadt, Germany)

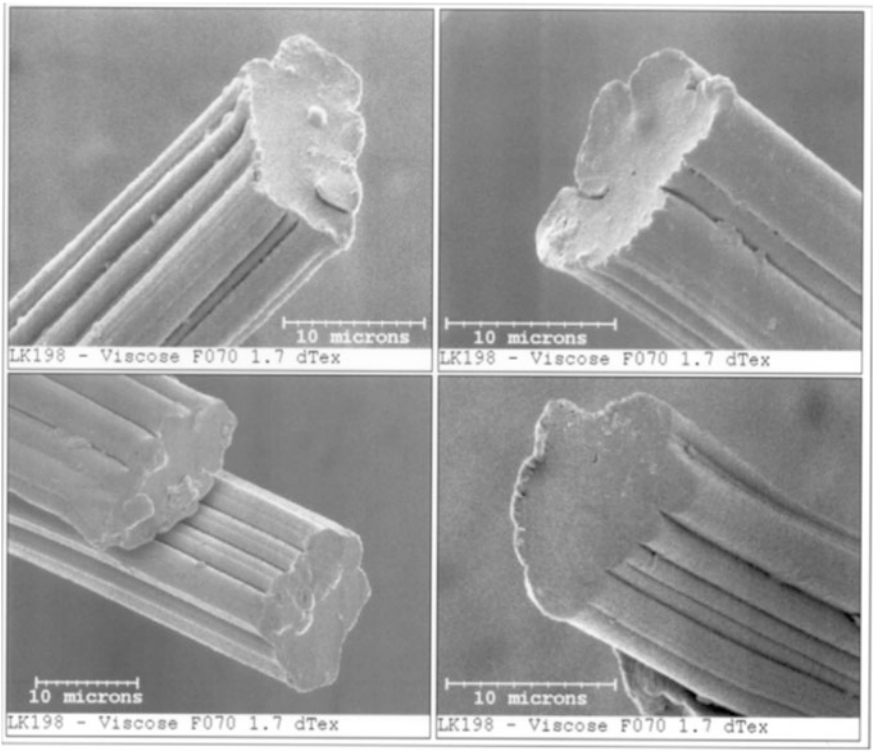


**Fig. 5.67** SEM micrographs of rayon fibers (reprinted from [338] copyright © 2001 with permission from Elsevier)

cellulose fiber, due to hampered diffusion of $H_3O^+$ into its structure. For example, after the initial formation of zinc cellulose xanthate (followed rapidly by regeneration to cellulose) in the outer regions of the filaments, further acid penetration is believed to be slowed down by the formation of other zinc species such as $Zn(OH)_2$ and ZnS, leading to slower regeneration of cellulose II. Note that mass transfer in wet spinning is a slow process (which accounts for the skin-core effect) as compared to the heat transfer in melt spinning. The skin contains numerous small crystallites and the core has fewer, but larger ones.

As with all fibers, finishing is the last step in production. Surface lubrication is required because friction is high when virgin fibers move at high speed on surfaces, e.g., metal cylinders. This will abrade the fiber and ultimately break the filaments. The most commonly used lubricants for rayon fibers are mixtures of fatty acids, their salts, and ethoxylated fatty acids and fatty alcohols. The antistatic agents of choice are either quaternary salts of fatty acids or phosphates. Figure 5.67 shows SEM micrographs of rayon fibers.

Properties and Application of Rayon Fibers [359, 360]

Process variations in manufacturing rayon provide fibers with a wide variety of properties including thickness, 1.7–5.0 dtex (dtex is a unit of measure for the linear mass density of fibers, yarns, and threads. It is given in grams per 10,000 m fiber), tenacity, 2.0–2.6 g/den when dry and 1.0–1.5 g/den when wet (den is the linear mass density of fibers, defined as the mass in grams per 9000 m), percentage elongation-at-break, 10–30% dry and 15–40% wet. Fiber elongation decreases with an increase in the degree of crystallinity and orientation of rayon. The rayon fiber absorbs more water than cotton; is soft, comfortable; drapes well; and is easy to dye. The fiber loses strength above 150 °C; chars and decomposes without melting at 177–204 °C.

With regard to chemical properties, hot dilute acids attack rayon, whereas it is not significantly attacked by bases. The fiber is degraded by concentrated bleaching agents, and prolonged exposure to sunlight. Rayon has both poor crease recovery and crease retention.

Among its major applications are apparel: Accessories, blouses, dresses, jackets, lingerie, linings, millinery, slacks, sport shirts, sportswear, suits, ties, and work clothes. Home furnishings include Bedspreads, blankets, curtains, draperies, sheets, slipcovers, tablecloths, upholstery. Industrial uses include industrial products, medical surgical products, nonwoven products, and tire cord.

#### 5.3.5.3 Esters of Carbamic Acid and Its *N*-Substituted Derivatives

Carbamic acids have been detected at low temperatures in SC–$CO_2$ [365] and in organic solvents rich in $CO_2$ [366]. The aliphatic and aromatic esters of carbamic acid, and the corresponding *N*-substituted, and *N*,*N*-disubstituted compounds are stable.

Carbamate esters can be generated from amines, e.g., by the reaction with chloroformates or dialkylcarbonates [367], and from alcohols and alkoxides, cellulose and alkali cellulose included, with aliphatic or aromatic isocyanates (Eq. 5.23), or isocyanic acid itself, generated by decomposition of urea above its m.p. (132.7 °C), e.g., at 140 °C (Eqs. 5.24 and 5.25).

$$\text{Cell}-\text{OH} + \text{R}-\text{N}=\text{C}=\text{O} \rightarrow \text{Cell}-\text{O}-\text{CO}-\text{N}-\text{HR} \tag{5.23}$$

$$(\text{H}_2\text{N})_2\text{C}=\text{O}/\Delta \rightarrow \text{HN}=\text{C}=\text{O} + \text{NH}_3 \tag{5.24}$$

$$\text{Cell}-\text{OH} + \text{HN}=\text{C}=\text{O} \rightarrow \text{Cell}-\text{O}-\text{CO}-\text{NH}_2 + \text{NH}_3 \tag{5.25}$$

Various methods for cellulose carbanilation have been carried out, e.g., solventless or under heterogeneous and homogeneous conditions by using conventional or MW heating.

## Synthesis of Cellulose Carbamates

### *Heterogeneous Reaction Without Solvent*

Solventless carbanilation has been carried out by heating (in oven or oil bath) urea with MCC or alkali-swollen cotton linters in the temperature range 110–185 °C, for 3–9 h, with urea/cellulose weight ratio of 1.5–4.0; the produced cellulose carbamates, CC, were then purified. The IR band intensity ratio at 1710 $cm^{-1}$ ($\nu_{C=O}$, carbamate)/1620 $cm^{-1}$ (native cellulose), $I_c$, and $T_m$ of the products were found to be a function of their nitrogen content. The correlation between the above-mentioned IR intensity ratio and N content is linear up to N% = 3.6 [368–370].

Carbamate formation has also been carried out heterogeneously under solvent- and catalyst-free conditions, by using pulsed MW heating for short times, as shown in Fig. 5.68 [371].

In a typical example, cotton linters, wood, bagasse, and reed cellulose samples (DP 392–1158) were suspended in 30% urea solution for 24 h, the urea-embedded biopolymers were filtered, dried under reduced pressure, and the reaction induced by pulsed MW heating, using 225 W power for 5 min. The dependence of the N% on reaction variables was studied. The yield increased as a function of increasing urea uptake by cellulose [10–50% (w/w)], reaction scale (10–50 g), and the number of applied MW pulses (1–5 pulses/3 min). The CC samples obtained were characterized by FTIR, $^{13}$C-CP/MAS NMR, X-ray diffraction, SEM, and TGA [372].

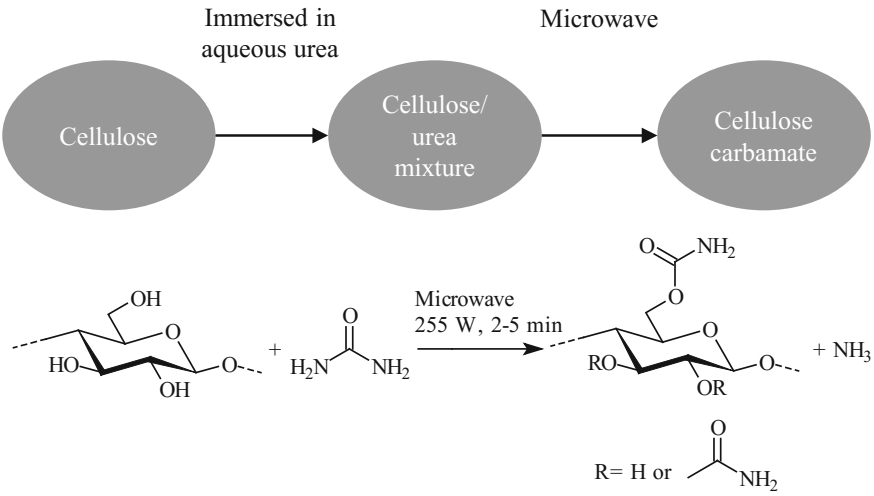


**Fig. 5.68** General scheme for the solventless, MW-assisted synthesis of CC. Cellulose is imbedded by urea, the sample dried, and the reaction induced by pulsed MW heating [371]

*Heterogeneous Carbanilation in the Presence of Solvent*

The carbanilation has been carried out with native cellulose or its base-activated counterpart. Many of these reactions start heterogeneously (suspension) and turn homogeneously. Thus, a suspension of cotton linters in refluxing pyridine was reacted with phenyl isocyanate or α-naphthyl isocyanate to give the corresponding tricarbanilates; the reaction mixture became homogeneously after 36 and 40 h, respectively [373]. Cellulose tricarbanilate was obtained by the reaction of a suspension of the biopolymer in DMF, with phenyl isocyanate in the presence of triethylenediamine as catalyst at 95–100 °C. The suspension turned homogeneously within 30–60 min; CC films were casted directly from the reaction mixture [374]. The reaction of cellulose with phenyl isocyanate in pyridine, at 80 °C for 2 d, produced a clear solution (MCC) or was incomplete (α-pulp). The effect of the medium employed for product precipitation on the MM distributions of CC was investigated by SEC. Precipitation of CC in methanol resulted in the loss (5–26% (w/w)) of a low MM fraction, whereas precipitation in water/methanol mixture (volume ratio 30/70) resulted in less [375] or no product fractionation [376]. Incomplete carbanilation of fibrous cellulose (bisulfite pulp; 86.3–97.1% α-cellulose; decrystallized cotton linters) was later avoided by pretreatment (activation) of the biopolymer with liquid ammonia. The reaction was carried out for 2 d at 80 °C in pyridine, DMF or DMSO. Clear solutions of cellulose tricarbanilate were obtained in all cases; the distribution of molar masses was studied with SEC and LALLS [377]. Kenaf core cellulose was suspended in urea solutions [0.9–4.5% (w/w)] and the mixture was stirred under normal and then reduced pressure; the latter to enhance urea penetration within the biopolymer fibers. The reaction was induced by MW heating (380 W power) for 10–30 min; the CC separated, purified, and examined by FTIR, X-ray diffraction, and SEM. The N% in CC increased as a function of increasing the urea concentration in the solution and the reaction time [378].

Cellulose derivatization can be better controlled, and the reaction temperature reduced, e.g., to 100–130 °C if an activated biopolymer is employed, and the carbanilation is carried out in the presence of a solvent [379, 380]. A usual approach is to activate the biopolymer in a separate step, and then react the resulting alkali cellulose with urea solution. Alternatively, the activation and derivatization steps can be carried out simultaneously; this approach is advantageous because of the observed synergism. Thus, $^{13}$C-CP/MAS NMR spectroscopy indicated the formation of a cellulose/NaOH/urea complex, comparable to the structure of alkali cellulose, except that it is formed at a much lower base concentration (7% aqueous NaOH plus 30% urea). The consequence of formation of this less structured, i.e., more reactive complex, has been demonstrated by the fact that $DS_{Carbamate}$ was higher (0.35) than that obtained when alkali cellulose was formed separately in 18% aqueous NaOH, washed with water or methanol, and then reacted with 30% urea aqueous solution ($DS_{Carbamete}$ 0.16 and 0.15, respectively) [381].

Another approach to obtain CC under heterogeneous conditions is to use SC–$CO_2$ as solvent to introduce urea into the biopolymer fiber, as depicted

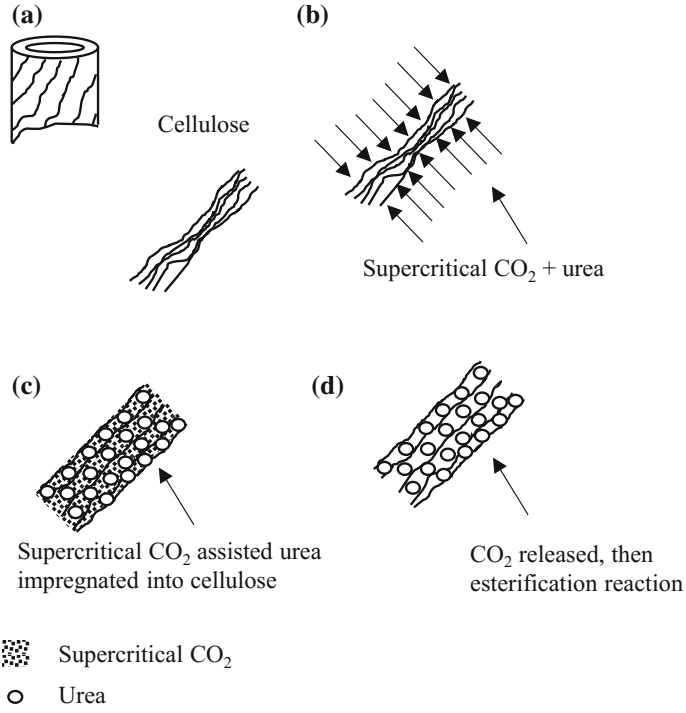


**Fig. 5.69** Scheme for the SC–$CO_2$ impregnation of cellulose fibers with urea. Both components are introduced in an autoclave, in the presence of alcohol, and left for impregnation. Cellulose carbamate is obtained by heating the urea-embedded fiber [382]

schematically in Fig. 5.69. Usually, ethanol is placed at the bottom of the pressure reactor in order to enhance solubility of urea in SC–$CO_2$. The alcohol, however, does not touch the solids (cellulose and urea) that are introduced in a stainless steel cage. A mixture of cotton cellulose and urea was introduced in a pressure reactor, which was later charged with $CO_2$. Cellulose impregnation with urea was done at 50 °C during 6 h, under 18 MPa gas pressure. After releasing $CO_2$, the urea-embedded biopolymer was heated at 140 °C in order to induce the carbanilation reaction. The dependence of product N% on the impregnation pressure and reaction time (after impregnation with urea, at 140 °C) was studied. The CC produced was characterized by TGA, $^{13}C$ NMR spectroscopy, X-ray diffraction, FTIR, and SEM. The products showed good solubility in aqueous NaOH and the rheology of these alkaline solutions showed either Newtonian behavior or shear-thinning depending on CC concentration [382, 383].

Later, this strategy was modified so that SC–$CO_2$ acted as solvent for both urea impregnation of cellulose and the carbanilation reaction. Softwood pulp was placed outside a stainless steel cage, and urea was placed inside the cage; both reactants were not in direct contact. The cage was introduced into the pressure reactor,

charged with $CO_2$, and heated for 2–10 h, at 150–170 °C and 17.9–22.1 MPa pressure. The highest N% (4.41) was reached after 8 h at 150 °C and 20.7 MPa; the products were characterized by FTIR spectroscopy, X-ray diffraction, TGA, and SEM [384].

*Carbanilation Under Homogeneous Reaction Conditions*

The simplest approach to prepare CC under homogeneous conditions is to derivatize the remaining hydroxyl groups of the AGU of a cellulose derivative, e.g., CA that is soluble in the medium. Thus, CA with $DS_{Ac}$ 0.75–2.33 was reacted with methyl, ethyl, and phenyl isocyanate in pyridine to give products with $DS_{Carbamate}$ 0.67–2.25. All products were soluble in pyridine and most of them dissolve in 1,4-dioxane too. Pure cellulose phenyl carbamate was obtained from the mixed acetate/carbamate esters by (sulfuric) acid hydrolysis [373, 385]. High yield of cellulose phenyl carbamate (89–92%) was obtained under homogeneous conditions by the reaction of MCC dissolved in DMAc/LiCl with phenyl isocyanate or 4-ethylphenyl isocyanate in the presence of pyridine as catalyst (12 h, RT). The products (DS 2.6 and 1.0, respectively) showed the expected FTIR- ($\nu_{C=O}$, 1730–1740 $cm^{-1}$) and $^{13}C$ NMR ($\delta_{C=O}$, 162.4–165 ppm) peaks [386].

Cellulose tricarbanilate from MCC, cotton linters, sulfate pulp, and cellulose obtained from wheat straw and hardwood by steam explosion was obtained by the reaction of phenyl isocyanate with the biopolymer dissolved in DMAc/LiCl, for 2–3 h, at 60–80 °C, in the presence or absence of pyridine catalyst. The produced tricarbanilated samples were characterized by viscometric and light scattering measurements in THF. The data of the products obtained, as well as literature data on CC synthesized under heterogeneous conditions (a total of 40 samples), indicated that the viscosity in THF increases linearly as a function of the MM of sample (from 110,000 to 1,300,000 g/mol, corresponding to $DP_{Tricarbanilate}$ of 212–2505). LS measurements indicated that precipitation of CC with methanol instead of water–methanol gives much more homogeneous samples, with lower polydispersity [376].

Cellulose carbamates having α-amino acid moieties were synthesized under homogeneous conditions by the reaction of cellulose dissolved in DMAc/LiCl with *N*-carbonyl α-amino acid esters (100 °C, 3 h), including *N*-carbonyl L-leucine ethyl- and 2-propyl ester, *N*-carbonyl L-phenylalanine ethyl ester and *N*-carbonyl L-aspartic acid ethyl ester. High reaction yields were obtained (>90%) and the $DS_{Carbamate}$ was from 1.0 to 3.0. All products were characterized by elemental analysis, FTIR, and NMR spectroscopy; they were soluble in DMSO, most of them showed solubility in $CHCl_3$ and THF [387].

The conditions employed for carbamate formation under homogenous conditions may also lead to the formation of side products, as shown in Fig. 5.70. Side products include alkyl carbanilate (compound 4, produced by reaction quenching with an alcohol), phenyl isocyanate dimer (compound 3) and trimer (compound 2), and 1,3-diphenylurea (5, formed by hydrolysis) [388, 389].

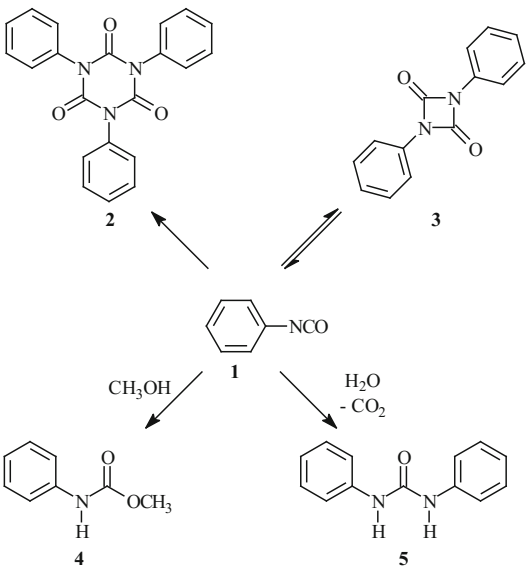


**Fig. 5.70** Molecular structures of the side products that may be formed under typical conditions of homogeneous cellulose carbanilation [388]

Formation of these side products was avoided by using anhydrous reaction conditions, low reaction temperature 60–70 °C, and long time 24–48 h as well as di(1-butyl)tin dilaurate as catalyst, controlled amount of isocyanate (phenyl- and 1-butyl), and product workup that did not include quenching with an alcohol. The reaction of MCC, cotton linters, or partially silylated cellulose in DMAc started heterogeneously and then turned homogeneously. Good to high yields (65–94%) of products with $DS_{Carbanilate}$ from 1.74 to 3.0 were obtained that were characterized by IR and NMR ($^{1}H$ and $^{13}C$) [390].

Di(1-butyl)tin dilaurate proved to be an efficient catalyst for the synthesis of highly substituted aliphatic carbamates. The reaction of cellulose with aromatic isocyanates, e.g., phenyl-, 4-methoxyphenyl-, and 2,4-dimethylphenylisocyanate in hot pyridine (90 °C), starts heterogeneously and then turns homogeneously after some time to yield CC with $DS_{Carbamate}$ of ca. 3.0 (reaction time 3–24 h), on one hand. On the other hand, the reaction of cellulose under the same conditions with 1-hexyl-, cyclohexyl-, 1-octyl-, and undecylisocyanates failed because it did not turn homogeneously. Therefore, it was carried out in hot DMAc (90 °C) in the presence of di(1-butyl)tin dilaurate catalyst to yield CC with DS 3 after 24 h reaction time. The CCs obtained were characterized by FTIR, $^{1}H$- and $^{13}C$ NMR spectroscopy, DSC, TGA, GPC, and SEM [391].

### *Applications of Cellulose Carbamates*

Cellulose carbamates have been employed for decades because product characteristics, in particular its crystallinity and swelling/solubility in different solvents, can be controlled relatively easily. Carbamates with high DS do not aggregate in solution, and hence have been used for the determination of the MM and MM

distribution of cellulose, if no complications occur during this derivatization. These may include biopolymer oxidative degradation by the dimethylsulfonium ion and its derived ylide, when the carbanilation reaction is carried out in DMSO [392]. Another potential problem is solvent-induced loss of low MM fraction during CC precipitation [375]. Nevertheless, it is now established that carbanilation, followed by MM determination, e.g., by viscosity, light scattering, or SEC is a reliable approach for this application. Thus, the biopolymer is completely functionalized under mild conditions by phenyl isocyanate/pyridine. It is then dissolved in an appropriate solvent (e.g., acetone or THF) and employed for determination of the MM of the parent polymer by viscosity, light scattering [376, 393], and SEC [394, 395].

Another application is the carbamoylation of cellulose esters and use of NMR spectroscopy ($^{1}H$ and $^{13}C$) of the resulted mixed ester for the determination of the partial DS values; this application is comparable to the perpropionylation method. An example of this method is shown in Fig. 5.71, where CA is transformed into the mixed ester, followed by analysis by two-dimensional $^{1}H$ NMR spectroscopy. The same derivatives can be deacylated and depolymerized by perchloric acid hydrolysis. HPLC of the produced simple sugars carbamates can be employed to calculate the mole fractions of the basic building units (un-, mono-, di-, and tri-substituted glucoses) of the polymer [396].

Cellulose derivatives have been employed as chiral stationary phases, CSPs for separation of enantiomeric mixtures; cellulose tribenzoates [397, 398] and tricarbamates [399, 400] are already employed commercially as CSPs. Research has been continued on this subject in order to introduce new derivatives with improved properties, hence widen their applicability, as shown by the following representative examples. The 3,5-dimethylphenylcarbamate derivatives of amylose and cellulose, chemically bonded to 3-aminopropylsilica gel were prepared with 4,4′-diphenylmethane diisocyanate as a spacer and their efficiency was evaluated as CSPs in HPLC. The AGU of the carbohydrate was linked either at position 6 or 2/3, as shown in Fig. 5.72. These CSPs have been tested for the separation of the racemates shown in Fig. 5.73.

The amylose derivative bonded to silica gel at position 6 showed higher optical resolving power than that bonded at position 2 or 3. The cellulose CSPs did not show this dependence on the position of link to the derivatized AGU. These CSPs can be used with solvents that dissolve or swell CC, e.g., $CHCl_3$. In fact, better separation of some racemates was achieved when the mobile phase contained some chloroform [401]. Later, several strategies have been employed for the immobilization of cellulose 3,5-dimethylphenylcarbamate derivatives on silica: the carbamate moiety contained a vinyl group at position 6, via reaction of partially functionalized cellulose (3,5-dimethylphenyl carbamate at positions 2 and 3) with 4-vinylphenylcarbamate or 2-methacryloyloxyethylcarbamate; a vinyl group was introduced attached to the surface of silica gel by reaction with 2-methacryloyloxyethyl isocyanate. The CSPs were then immobilized by free-radical copolymerization in the presence of a small amount of styrene. The vinyl monomer content on the surface of silica gel or cellulose derivative was varied. For comparison, a silica gel sample was

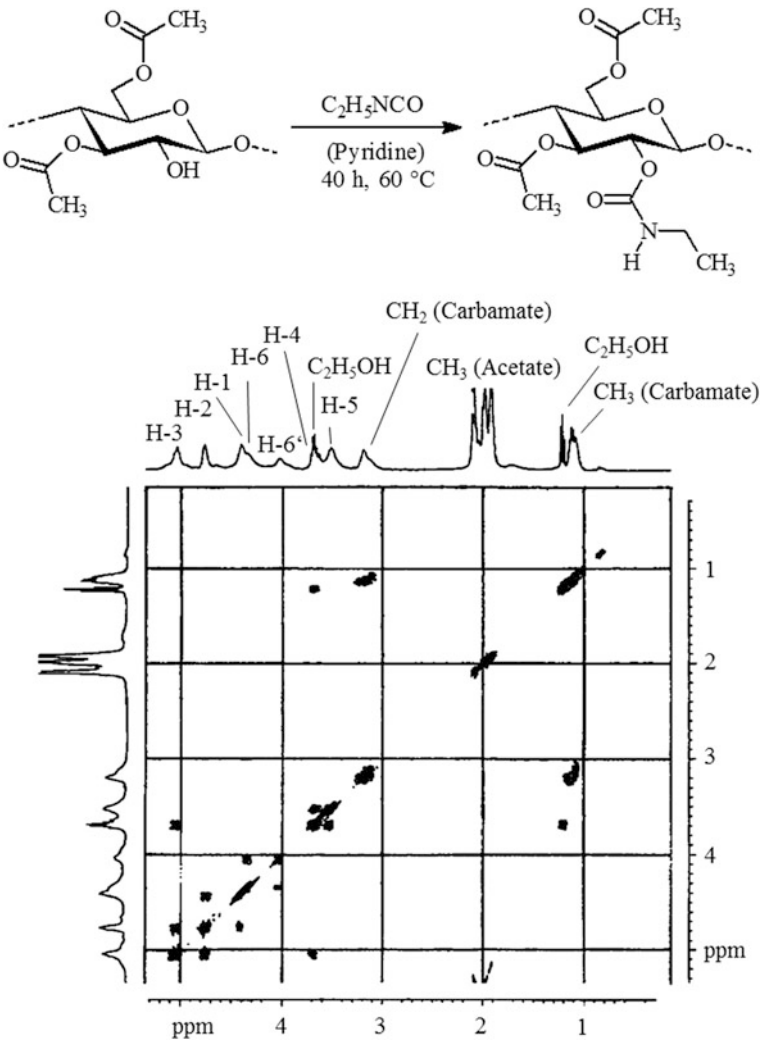


**Fig. 5.71** Reaction scheme for ethylcarbamoylation of CA, and the corresponding COSY $^{1}$H NMR spectrum of the mixed ester [396]

simply coated with 3,5-dimethylphenylcarbamate. These CSPs were tested for the separation of the same racemates shown in Fig. 5.73. The introduction of a vinyl group onto the surface of silica resulted in a more efficient immobilization of the cellulose phenylcarbamate derivatives. These immobilized CSPs can be used with an eluent containing 10% chloroform, a solvent that cannot be used with the CSP prepared by simple adsorption of 3,5-dimethylphenylcarbamate onto the surface of silica gel [402]. CSPs that carry α-amino acid moieties were immobilized on the surface of macroporous silica gel via 3-aminopropyl-triethoxysilane linking agent. The chiral

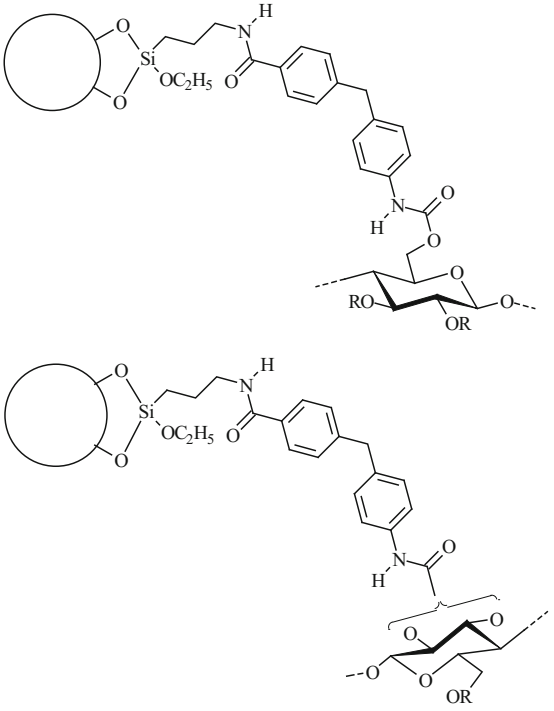


**Fig. 5.72** Regioselective bonding of the amylose carbamate to the silica surface through position 6 (top) or position 2/3 (bottom) of the AGU

discrimination ability of the CSP containing L-Leucine was found to be higher than those of cellulose carbamates having L-phenylalanine and L-aspartic acid moieties [387]. As stated above, cellulose tribenzoates and tricarbamates are already used as CSPs. Therefore, cellulose derivatives containing both groups have been synthesized in order to assess the effect of combination of both functional groups, if it is present, on the efficiency of separation the racemates shown in Fig. 5.74. Among these derivatives, 2,3-bis-*O*-(3,5-dimethylphenylcarbamate)-6-*O*-benzoate-cellulose and 2,3-bis-*O*-(benzoate)-6-*O*-(3,5-dichlorophenylcarbamate) cellulose showed the best separation of the tested racemates.

*The Carbamate Process for Cellulose Fiber Spinning*

The viscose process for cellulose fiber production is well over 100 years old and is still the dominant industrial method. It has some drawbacks: the preparation of the spinning solution is laborious; $CS_2$ used for alkali cellulose xanthation is toxic and inflammable. Additionally, some $CS_2$ is transformed into $H_2S$, which is toxic and explosive [404]. The presence of residual sulfates (8 mg/100 g multifilament) in viscose rayon limits its application in some fields [405]. Therefore, there is a

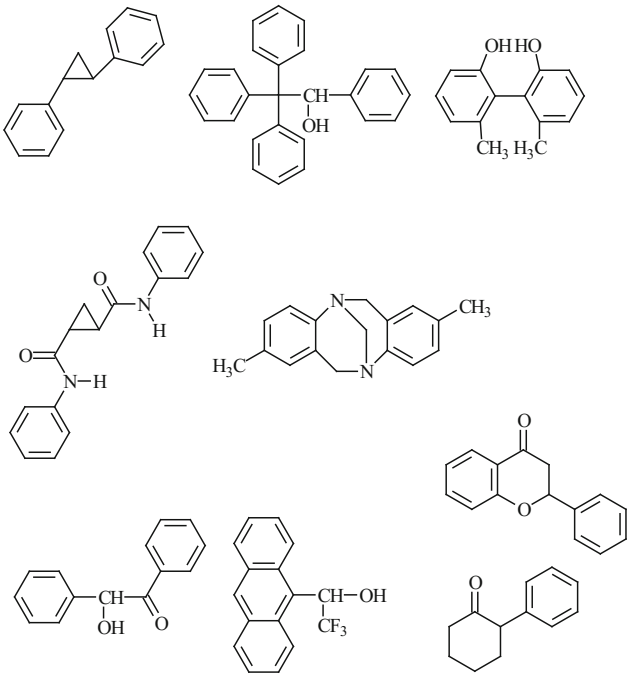


**Fig. 5.73** Molecular structures of racemates whose separation was tested on amylose and cellulose CSPs derivatives [401]

continuous effort to substitute the viscose process by more environmental-friendly alternatives; the Lyocell process that uses NMMO for physical dissolution of cellulose has been in commercial operation for about 25 years [406]. The general schemes for the processes that are employed for cellulose fiber regeneration without or with derivatization are shown in Fig. 5.75 [407].

Of these, the so-called CarbaCell process is gaining importance, in which cellulose is regenerated from CC by hydrolysis. The patented CarbaCell technology starts by swelling highly reactive dissolving pulp (DP ca. 300) in aqueous urea solution [ca. 40% (w/w)] for several hours at RT. The urea-embedded mass is filtered, dried, and heated for 1–2 h at 140–150 °C, either in air or in xylene as heat/mass transfer liquid. The produced yellowish CC with $DS_{Carbamate}$ of 0.25–0.3 is extracted with water and dissolved in 10–11% (w/w) NaOH–ZnO solution. The spinning solution is filtered and degassed prior to wet spinning in an acidic bath, for the hydrolysis of the carbamate groups, i.e., for cellulose fiber regeneration [408–410]. The cellulose structural changes that occur during the above-mentioned processing are clearly seen in the $^{13}C$–CP/MAS solid-state NMR spectra (Fig. 5.76).

Figure 5.77 shows a flow sheet of a process developed on a pilot-scale, where the carbanilation reaction of the urea-embedded cellulose is done quickly by MW

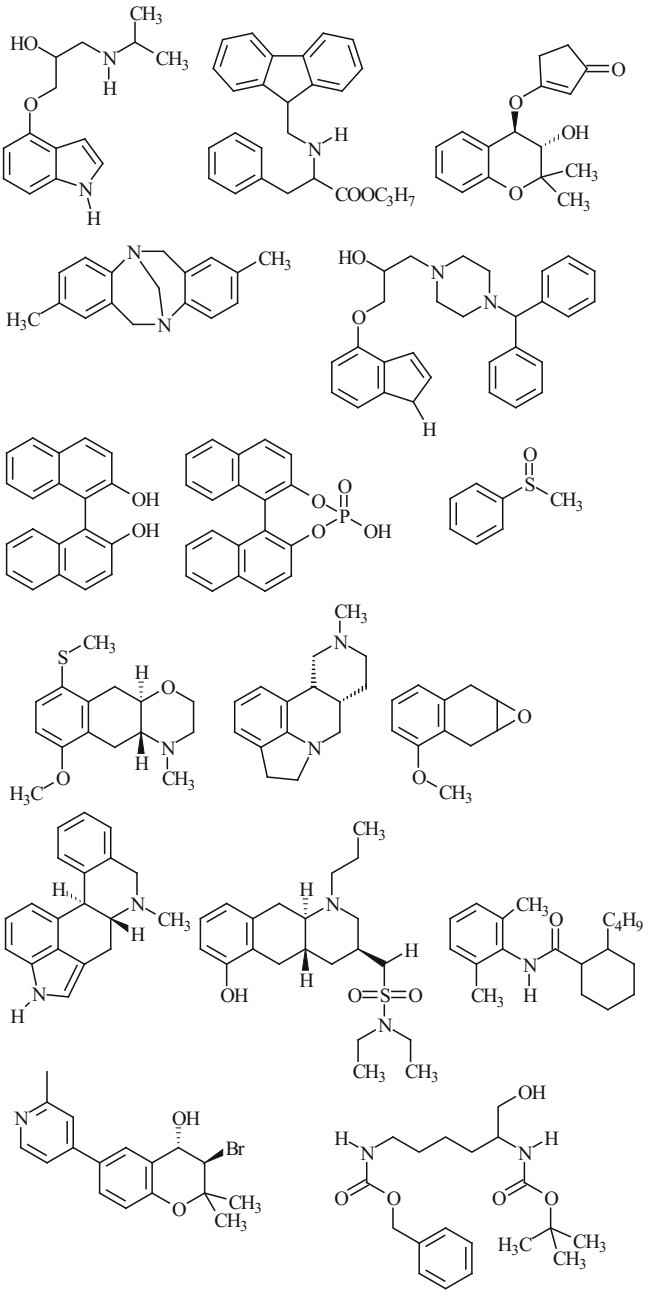

**Fig. 5.74** Racemates separated by regioselectively substituted cellulose ester/carbamates [403]

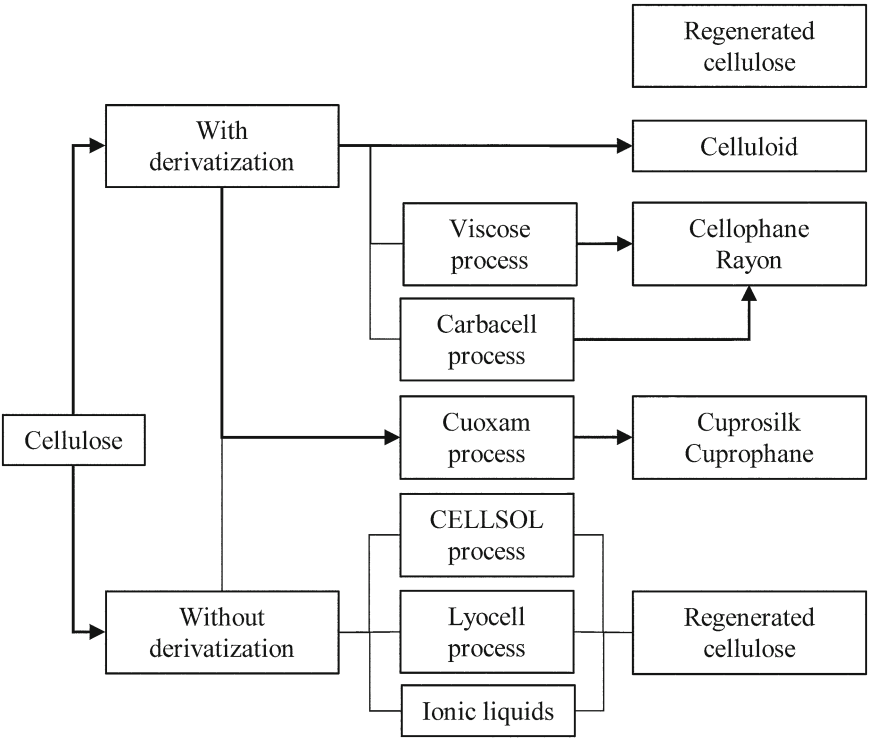


**Fig. 5.75** Flow diagrams for processes that are employed for cellulose shaping with or without derivatization

heating (e.g., 12 min at 450 W heating power) and the CC is dissolved in NaOH/ZnO [411]. Addition of the latter improved the solubility and stability of CC in the alkaline solution. Figure 5.78 shows a photograph of cellulose fibers obtained on a pilot machine from cellulose carbamate [412].

As shown in Fig. 5.75, the steps of the CarbaCell process are similar to those of the viscose method. Apart from using environmental-friendly urea (as compared with $CS_2$), the advantage of the CarbaCell process is that the cellulose derivative is relatively stable at RT, which permits storage times of more than a year without loss of quality. Thus, the synthesis of cellulose carbamate can be carried out on a large scale in a central facility, whereas fiber spinning can be decentralized in different smaller factories. Industrial tests have shown that cellulose carbamate can be conveniently processed on viscose spinning machines [404]. These advantages may move the CarbaCell process from pilot to full industrial scale production in the not distant future (Table 5.26).

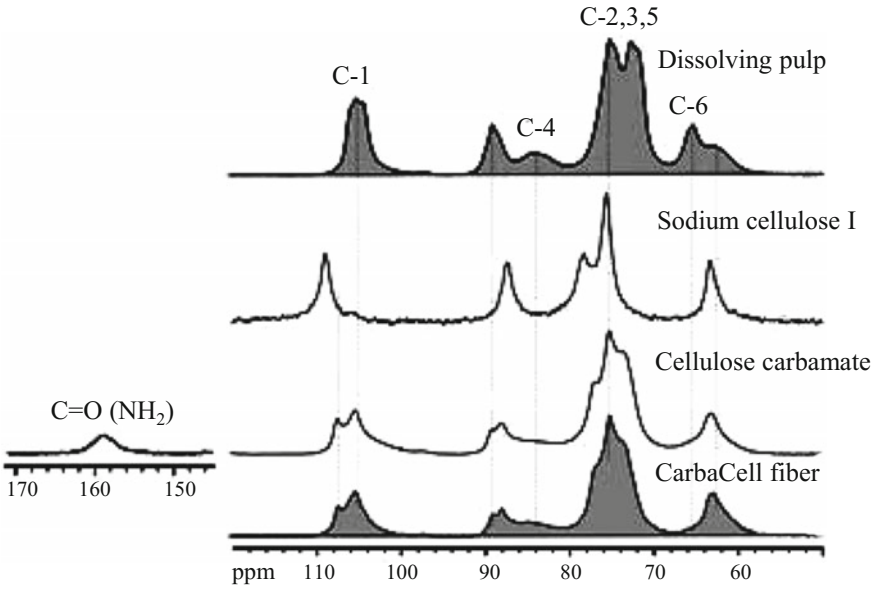


**Fig. 5.76** Structural changes of cellulose in the carbamate process as shown by $^{13}$C-CP/MAS NMR spectroscopy (adapted from [404])

**Table 5.26** Representative examples of the strategies employed for the synthesis of cellulose carbamates

| Entry | Cellulose | Derivatizing agent | Reaction phase/solvent/heating (convection or MW) | Product N% or $DS_{Carbamte}$ | References |
|---|---|---|---|---|---|
| 1 | Cotton linters; DP 900 | Urea | Solid/convection/140 °C | N% = 1.3–1.8 | [369] |
| 2 | Cotton linters; DP 550 | Urea | Solid/MW/255 W, 5 min | N% = 0.65–2.43 | [371] |
| 3 | Kenaf core cellulose, DP 3416 | Urea | Liquid/MW/380 W, 10–30 min | N% = 0.3–5.7 | [378] |
| 4 | MCC | Phenyl isocyanate | Liquid/LiCl-DMAc-pyridine/RT, 12 h | DS = 2.6 | [386] |
| 5 | Cotton linters; DP 565 | Phenyl isocyanate; 1-butyl isocyanate | Liquid; DMAc/di (1-butyl)tin diluarate | DS = 1.3–3.0 | [390] |

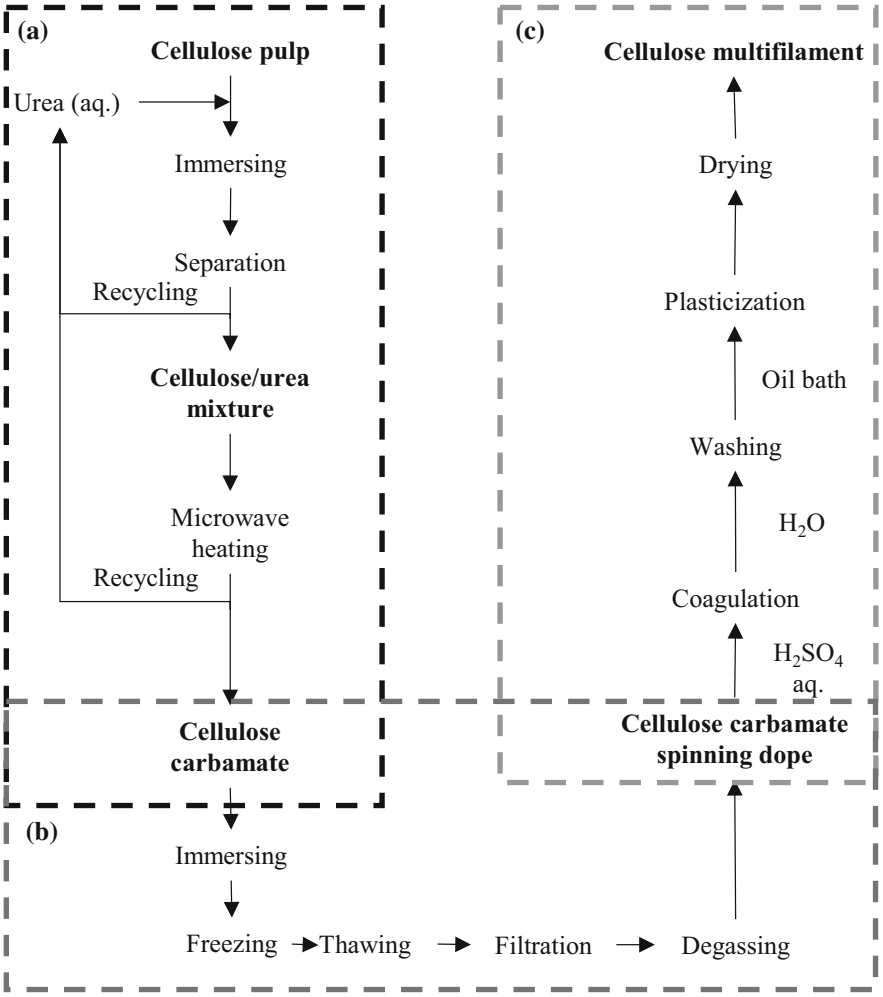


**Fig. 5.77** Flow sheet of the CarbaCell cellulose fiber process, using MW heating and NaOH/ZnO for cellulose solubilization

**Fig. 5.78** Cellulose fibers produced on pilot plant scale from cellulose carbamate (reprinted with permission from [412] copyright © 2014 American Chemical Society)

## References


1. Malm CJ, Tanghe LJ (1955) Chemical reactions in the making of cellulose acetate. Ind Eng Chem 47:995–999
2. Bogan RT, Brewer RJ (1985) Cellulose esters, organic. In: Kroschwitz JI, Bickford M, Klingsberg A, Muldoon J, Salvatore A (eds) Encyclopedia of polymer science and engineering. Wiley, NY, pp 158–181
3. Treece LC, Johnson GI (1993) Cellulose acetate. Chem Ind 49:241–256
4. Heinze T, Liebert T (2012) Cellulose and polyoses/hemicelluloses. In: Matyjaszewski K, Moeller M (eds) Polymer science: a comprehensive reference, vol 10. Elsevier, Amsterdam, pp 83–152
5. Iwata T, Fukushima A, Okamura K, Azuma JI (1997) DSC study on regioselectively substituted cellulose heteroesters. J Appl Polym Sci 65:1511–1515
6. Mueller F (1985) Organic cellulose esters. Papier (Bingen, Germany) 39:591–600
7. Nawaz H, Casarano R, El Seoud OA (2012) First report on the kinetics of the uncatalyzed esterification of cellulose under homogeneous reaction conditions: a rationale for the effect of carboxylic acid anhydride chain-length on the degree of biopolymer substitution. Cellulose 19:199–207
8. Kwatra HS, Caruthers JM, Tao BY (1992) Synthesis of long chain fatty acids esterified onto cellulose via the vacuum-acid chloride process. Ind Eng Chem Res 31:2647–2651
9. Edgar KJ, Pecorini TJ, Glasser WG (1998) Long-chain cellulose esters: preparation, properties, and perspective. In: Heinze TJ, Glasser WG (eds) Cellulose derivatives: modification, characterization, and nanostructures. ACS, Washington, pp 38–60
10. Hoefle G, Steglich W, Vorbrueggen H (1978) New synthetic methods. 25. 4-dialkylaminopyridines as acylation catalysts. 4. Puridine syntheses. 1. 4-dialkylaminopuridines as highly active acylation catalysts. Angew Chem 90:602–615
11. Malm CJ, Mench JW, Kendall DL, Hiatt GD (1951) Aliphatic acid esters of cellulose. Preparation by acid chloride-pyridine procedure. Ind Eng Chem (Seoul) 43:684–688
12. Heinze T, Liebert T, Koschella A (2006) Esterification of polysaccharides. Springer, Table 4.6, p 50
13. Riemschneider R, Sickfeld J (1964) Cellulose esters. Monatsh Chem 95:194–202
14. Novac LJ, Tyree JT (1956) Water-resistant textiles. US 2734005, CAN 50:46838
15. Morooka T, Norimoto M, Yamada T, Shiraishi N (1984) Dielectric properties of cellulose acylates. J Appl Polym Sci 29:3981–3990
16. Heinze T, Liebert T, Koschella A (2006) Esterification of polysaccharides. Springer, Fig. 5.12, p 73
17. Nehls I, Wagenknecht W, Philipp B, Stscherbina D (1994) Characterization of cellulose and cellulose derivatives in solution by high resolution carbon-13 NMR spectrometry. Prog Polym Sci 19:29–78
18. Hasegawa M, Isogai A, Onabe F, Usuda M (1992) Dissolving states of cellulose and chitosan in trifluoroacetic acid. J Appl Polym Sci 45:1857–1863
19. Emel'yanov YG, Grinshpan DD, Kaputskii FN (1988) Homogeneous synthesis of cellulose esters in nonaqueous cellulose solutions. 3. Low-substituted cellulose trifluoroacetate acylation in trifluoroacetic acid and dimethylformamide. Koksnes Kim 1:23–28
20. Fujimoto T, Takahashi S, Tsuji M, Miyamoto T, Inagaki H (1986) Reaction of cellulose with formic acid and stability of cellulose formate. J Polym Sci C: Polym Lett 24:495–501
21. Philipp B, Wagenknecht W, Nehls I, Ludwig J, Schnabelrauch M, Kim HR, Klemm D (1990) Comparison of cellulose formate and cellulose acetate under homogeneous reaction conditions. Cellul Chem Technol 24:667–678
22. Schnabelrauch M, Vogt S, Klemm D, Nehls I, Philipp B (1992) Readily hydrolyzable cellulose esters as intermediates for the regioselective derivatization of cellulose. 1. Synthesis and characterization of soluble, low-substituted cellulose formats. Angew Makromol Chem 198:155–164

23. Liebert T, Klemm D, Heinze T (1996) Synthesis and carboxymethylation of organo-soluble trifluoroacetates and formates of cellulose. J Macromol Sci, Pure Appl Chem A33:613–626
24. Shigemasa Y, Kishimoto Y, Sashiwa H, Saimoto H (1990) Dissolution of cellulose in dimethyl sulfoxide. Effect of thiamine hydrochloride. Polym J 22:1101–1103
25. Masson JF, Manley RSJ (1991) Cellulose/poly(4-vinylpyridine) blends. Macromolecules 24:5914–5921
26. Masson JF, Manley RSJ (1991) Miscible blends of cellulose and poly(vinylpyrrolidone). Macromolecules 24:6670–6679
27. Clermont LP, Manery N (1974) Modified cellulose acetate prepared from acetic anhydride reacted with cellulose dissolved in a chloral-dimethylformamide mixture. J Appl Polym Sci 18:2773–2784
28. Arai K, Ogiwara Y (1980) Homogeneous butyration of cellulose dissolved in dimethyl sulfoxide-formaldehyde system. Sen'i Gakkaishi 36:T82–T84
29. Morooka T, Norimoto M, Yamada T, Shiraishi N (1982) Viscoelastic properties of (cellulose oligo-oxymethylene ether) acrylates. J Appl Polym Sci 27:4409–4419
30. Miyagi Y, Shiraishi N, Yokota T, Yamashita S, Hayashi Y (1983) Preparation and thermal properties of acetates derived from cellulose dissolved in DMSO-PF. J Wood Chem Technol 3:59–78
31. Seymour RB, Johnson EL (1978) Acetylation of DMSO:PF solutions of cellulose. J Polym Sci Polym Chem Ed 16:1–11
32. Leoni R, Baldini A (1982) The acetylation of cellulose in the dimethylacetamide-paraformaldehyde system. Carbohydr Polym 2:298–301
33. Saikia CN, Dutta NN, Borah M (1993) Thermal behavior of some homogeneously esterified products of high α-cellulose pulps of fast growing plant species. Thermochim Acta 219:191–203
34. Mansson P, Westfelt L (1980) Homogeneous acetylation of cellulose via the nitrite ester. Cellul Chem Technol 14:13–17
35. Shimizu Y, Nakayama A, Hayashi J (1993) Preparation of cellulose esters with aromatic carboxylic acids. Sen'i Gakkaishi 49:352–356
36. Wagenknecht W, Nehls I, Philipp B (1993) Studies on the regioselectivity of cellulose sulfation in a nitrogen oxide ($N_2O_4$)-N, N-dimethylformamide-cellulose system. Carbohydr Res 240:245–252
37. Liebert T (1995) Cellulose esters as hydrolytically instable intermediates and pH-sensitive carriers. PhD Thesis, University of Jena, Germany
38. Stein A, Klemm D (1988) Syntheses of cellulose derivatives via O-triorganosilyl celluloses. 1. Effective synthesis of organic cellulose esters by acylation of trimethylsilyl celluloses. Makromol Chem, Rapid Commun 9:569–573
39. Saric SP, Schofield RK (1946) The dissociation constants of the carboxyl and hydroxyl groups in some insoluble and sol-forming polysaccharides. Proc R Soc London Ser A 185:431–447
40. Thomas R (1970) New process for the partial esterification of cellulose with carboxylic acids under practice conditions. Textilveredlung 5:361–368
41. Husemann E, Siefert E (1969) N-Ethylpyridinium chloride as solvent and reaction medium for cellulose. Makromol Chem 128:288–291
42. Wu J, Zhang J, Zhang H, He J, Ren Q, Guo M (2004) Homogeneous acetylation of cellulose in a new ionic liquid. Biomacromol 5:266–268
43. Klohr EA, Koch W, Klemm D, Dicke R (2000) Manufacture of regioselectively substituted esters of oligo- and polysaccharides. DE 19951734, CAN 133:224521
44. Ibrahim AA, Nada AMA, Hagemann U, El Seoud OA (1996) Preparation of dissolving pulp from sugarcane bagasse, and its acetylation under homogeneous solution condition. Holzforschung 50:221–225
45. Heinze T, Liebert T, Pfeiffer KS, Hussain MA (2003) Unconventional cellulose esters: synthesis, characterization and structure-property relations. Cellulose 10:283–296

46. Takaragi A, Minoda M, Miyamoto T, Liu HQ, Zhang LN (1999) Reaction characteristics of cellulose in the lithium chloride/1,3-dimethyl-2-imidazolidinone solvent system. Cellulose 6:93–102
47. Heinze T, Dicke R, Koschella A, Kull AH, Klohr E-A, Koch W (2000) Effective Preparation of cellulose derivatives in a new simple cellulose solvent. Macromol Chem Phys 201:627–631
48. Ciacco GT, Liebert TF, Frollini E, Heinze TJ (2003) Application of the solvent dimethyl sulfoxide/tetrabutylammonium fluoride trihydrate as reaction medium for the homogeneous acylation of Sisal cellulose. Cellulose 10:125–132
49. El Seoud OA, Nawaz H, Arêas EPG (2013) Chemistry and applications of polysaccharide solutions in strong electrolytes/dipolar aprotic solvents: An overview. Molecules 18:1270–1313
50. Heinze T, Petzold K (2008) Cellulose Chemistry: Novel products and synthesis paths. In Belgacem MN, Gandini A (eds) Monomers, polymers and composites from renewable resources, Elsevier, pp 343–367
51. Gericke M, Fardim P, Heinze T (2012) Ionic liquids-promising but challenging solvents for homogeneous derivatization of cellulose. Molecules 17:7458–7502
52. McCormick CL, Dawsey TR (1990) Preparation of cellulose derivatives via ring-opening reactions with cyclic reagents in lithium chloride/N, N-dimethylacetamide. Macromolecules 23:3606–3610
53. McCormick CL, Lichatowich DK (1979) Homogeneous solution reactions of cellulose, chitin, and other polysaccharides to produce controlled-activity pesticide systems. J Polym Sci Polym Lett Ed 17:479–484
54. Vaca-Garcia C, Thiebaud S, Borredon ME, Gozzelino G (1998) Cellulose esterification with fatty acids in lithium chloride/N, N-dimethylacetamide medium. J Am Oil Chem Soc 75:315–319
55. Vaca-Garcia C, Borredon ME (1999) Solvent-free fatty acylation of cellulose and lignocellulosic wastes. Part 2: reactions with fatty acids. Bioresour Technol 70:135–142
56. Peydecastaing J, Vaca-Garcia C, Borredon E (2009) Consecutive reactions in an oleic acid and acetic anhydride reaction medium. Eur J Lipid Sci Technol 111:723–729
57. Ciacco GT, Morgado DL, Frollini E, Possidonio S, El Seoud OA (2010) Some aspects of acetylation of untreated and mercerized sisal cellulose. J Braz Chem Soc 21:71–77
58. Heinze T, Liebert T, Koschella A (2006) Esterification of polysaccharides. Springer, Figure 5.14, p 77
59. Heinze T, Liebert T (2001) Unconventional methods in cellulose functionalization. Prog Polym Sci 26:1689–1762
60. Sealey JE, Samaranayake G, Todd JG, Glasser WG (1996) Novel cellulose derivatives. IV. Preparation and thermal analysis of waxy esters of cellulose. J Polym Sci, Part B: Polym Phys 34:1613–1620
61. Gräbner D, Liebert T, Heinze T (2002) Synthesis of novel adamantoyl cellulose using differently activated carboxylic acid derivatives. Cellulose 9:193–201
62. Tosh B, Saikia CN, Dass NN (2000) Homogeneous esterification of cellulose in the lithium chloride-N, N-dimethylacetamide solvent system: effect of temperature and catalyst. Carbohydr Res 327:345–352
63. Nawaz H, Pires PAR, El Seoud OA (2012) Kinetics and mechanism of imidazole-catalyzed acylation of cellulose in LiCl/N, N-dimethylacetamide. Carbohydr Polym 92:997–1005
64. Nagel MCV, Heinze T (2010) Esterification of cellulose with acyl-1H-benzotriazole. Polym Bull 65:873–881
65. Hasani MM, Westman G (2007) New coupling reagents for homogeneous esterification of cellulose. Cellulose 14:347–356
66. Heinze T, Sarbova V, Nagel MCV (2012) Simple synthesis of mixed cellulose acylate phosphonates applying n-propyl phosphonic acid anhydride. Cellulose 19:523–531
67. Berger W, Keck M, Philipp B (1988) On the mechanism of cellulose dissolution in nonaqueous solvents, especially in O-basic systems. Cellul Chem Technol 22:387–397

68. Yang K, Wang Y-J (2003) Lipase-catalyzed cellulose acetylation in aqueous and organic media. Biotechnol Prog 19:1664–1671
69. Sharma RK, Fry JL (1983) Instability of anhydrous tetra-n-alkylammonium fluorides. J Org Chem 48:2112–2114
70. Sun H, DiMagno SG (2005) Anhydrous tetrabutylammonium fluoride. J Am Chem Soc 127:2050–2051
71. Casarano R, Nawaz H, Possidonio S, da Silva VC, El Seoud OA (2011) A convenient solvent system for cellulose dissolution and derivatization: mechanistic aspects of the acylation of the biopolymer in tetraallylammonium fluoride/dimethyl sulfoxide. Carbohydr Polym 86:1395–1402
72. Xu D, Edgar KJ (2012) TBAF and cellulose esters: unexpected deacylation with unexpected regioselectivity. Biomacromol 13:299–303
73. Casarano R, Pires PAR, El Seoud OA (2014) Acylation of cellulose in a novel solvent system: solution of dibenzyldimethylammonium fluoride in DMSO. Carbohydr Polym 101:444–450
74. Buchanan CM, Buchanan NL (2008) Reformation of ionic liquids in cellulose esterification. WO 2008100569 A1 20080821, CAN149:269762
75. Buchanan CM, Buchanan NL (2008) Process and apparatus for production of ionic liquids in cellulose esterification. WO 2008100577 A1 20080821, CAN149:269760
76. Cao Y, Wu J, Meng T, Zhang J, He J, Li H, Zhang Y (2007) Acetone-soluble cellulose acetates prepared by one-step homogeneous acetylation of cornhusk cellulose in an ionic liquid 1-allyl-3-methylimidazolium chloride (AmimCl). Carbohydr Polym 69:665–672
77. Barthel S, Heinze T (2006) Acylation and carbanilation of cellulose in ionic liquids. Green Chem 8:301–306
78. Schlufter K, Schmauder H-P, Dorn S, Heinze T (2006) Efficient homogeneous chemical modification of bacterial cellulose in the ionic liquid 1-N-butyl-3-methylimidazolium chloride. Macromol Rapid Commun 27:1670–1676
79. Fidale LC, Possidonio S, El Seoud OA (2009) 1-butyl)imidazolium chloride in the synthesis of cellulose esters: properties of the ionic liquid, and comparison with other solvents. Macromol Biosci 9:813–821
80. Possidonio S, Fidale LC, El Seoud OA (2010) Microwave-assisted derivatization of cellulose in an ionic liquid: an efficient, expedient synthesis of simple and mixed carboxylic esters. J Polym Sci, Part A: Polym Chem 48:134–143
81. Dorn S, Schöbitz M, Schlufter K, Heinze Z (2010) Novel cellulose products prepared by homogeneous functionalization of cellulose in ionic liquids. ACS Symp Ser 1033:275–285
82. Heinze T, Dorn S, Schöbitz M, Liebert T, Köhler S, Meister F (2008) Interactions of Ionic Liquids with Polysaccharides—2: cellulose. Macromol Symp 262:8–22
83. Luan Y, Zhang J, Zhan M, Wu J, Zhang J, He J (2013) Highly efficient propionylation and butyralation of cellulose in an ionic liquid catalyzed by 4-dimethylminopyridine. Carbohydr Polym 2:307–311
84. El Seoud OA, da Silva VC, Possidonio S, Casarano R, Arêas EPG, Gimenes P (2011) Microwave-assisted derivatization of cellulose: 2—the surprising effect of the structure of ionic liquids on the dissolution and acylation of the biopolymer. Macromol Chem Phys 212:2541–2550
85. Li WY, Jin AX, Liu CF, Sun RC, Zhang AP, Kennedy JF (2009) Homogeneous modification of cellulose with succinic anhydride in ionic liquid using 4-dimethylaminopyridine as a catalyst. Carbohydr Polym 78:389–395
86. Liu CF, Zhang AP, Li WY, Yue FX, Sun RC (2009) Homogeneous modification of cellulose in ionic liquid with succinic anhydride using N-bromosuccinimide as a catalyst. J Agric Food Chem 57:1814–1820
87. Liu CF, Zhang AP, Li WY, Yue FX, Sun RC (2010) Succinoylation of cellulose catalyzed with iodine in ionic liquid. Ind Crops Prod 31:363–369
88. Liu CF, Sun RC, Zhang AP, Ren JL (2007) Preparation of sugarcane bagasse cellulosic phthalate using an ionic liquid as reaction medium. Carbohydr Polym 68:17–25

89. Granström M, Kavakka J, King A, Majoinen J, Mäkelä V, Helaja J, Hietala S, Virtanen T, Maunu S-L, Argyropoulos D, Kilpeläinen I (2008) Tosylation and acylation of cellulose in 1-allyl-3-methylimidazolium chloride. Cellulose 15:481–488
90. Sui X, Yuan J, Zhou M, Zhang J, Yang H, Yuan W, Wei Y, Pan C (2008) Synthesis of cellulose-graft-poly (N, N-dimethylamino-2-ethyl methacrylate) copolymers via homogeneous ATRP and their aggregates in aqueous media. Biomacromol 9:2615–2620
91. Meng T, Gao X, Zhang J, Yuan J, Zhang Y, He J (2009) Graft copolymers prepared by atom transfer radical polymerization (ATRP) from cellulose. Polymer 50:447–454
92. Xin T-T, Yuan T, Xiao S, He J (2011) Synthesis of cellulose-graft-poly(methyl methacrylate) via homogeneous ATRP. BioResources 6:2941–2953
93. Lin C-X, Zhan H-Y, Liu M-H, Fu S-Y, Zhang J-J (2009) Preparation of cellulose graft poly (methyl methacrylate) copolymers by atom transfer radical polymerization in an ionic liquid. Carbohydr Polym 78:432–438
94. Zhang J, Wu J, Cao Y, Sang S, Zhang J, He J (2009) Synthesis of cellulose benzoates under homogeneous conditions in an ionic liquid. Cellulose 16:299–308
95. Mäki-Arvela P, Anugwom I, Virtanen P, Sjöholm R, Mikkola JP (2010) Dissolution of lignocellulosic materials and its constituents using ionic liquids—a review. Ind Crops Prod 32:175–201
96. Zhang ZB, McCormick CL (1997) Structopendant unsaturated cellulose esters via acylation in homogeneous lithium chloride/N, N-dimethylacetamide solutions. J Appl Polym Sci 66:293–305
97. Köhler S, Heinze T (2007) New solvents for cellulose: dimethyl sulfoxide/ammonium fluorides. Macromol Biosci 7:307–314
98. El Seoud OA, Marson GA, Ciacco GT, Frollini E (2000) An efficient, one-pot acylation of cellulose under homogeneous reaction conditions. Macromol Chem Phys 201:882–889
99. Abbott AP, Bell TJ, Handa S, Stoddart B (2005) O-Acetylation of cellulose and monosaccharides using a zinc based ionic liquid. Green Chem 7:705–707
100. Guo Y, Wang X, Li D, Du H, Wang X, Sun R (2012) Synthesis and characterization of hydrophobic long-chain fatty acylated cellulose and its self-assembled nanoparticles. Polym Bull 69:389–403
101. Xie H, King A, Kilpelainen I, Granstrom M, Argyropoulos DS (2007) Thorough chemical modification of wood-based lignocellulosic materials in ionic liquids. Biomacromol 8:3740–3748
102. Xu D, Li B, Tate C, Edgar KJ (2011) Studies on regioselective acylation of cellulose with bulky acid chlorides. Cellulose 18:405–419
103. Mayumi A, Kitaoka T, Wariishi H (2006) Partial substitution of cellulose by ring-opening esterification of cyclic esters in a homogeneous system. J Appl Polym Sci 102:4358–4364
104. Zarth CSP, Koschella A, Pfeifer A, Dorn S, Heinze T (2011) Synthesis and characterization of novel amino cellulose esters. Cellulose 18:1315–1325
105. Edgar KJ, Arnold KM, Blount WW, Lawniczak JE, Lowman DW (1995) Synthesis and properties of cellulose acetoacetates. Macromolecules 28:4122–4128
106. Yoshida Y, Isogai A (2005) Preparation and characterization of cellulose β-ketoesters prepared by homogeneous reaction with alkylketene dimers: comparison with cellulose/fatty acid esters. Cellulose 14:481–488
107. Singh G, Kumar A (2008) Ionic liquids: physicochemical, solvent properties and their applications in chemical processes. Indian J Chem Sect A Inorg Bioinorg Phys Theor Anal Chem 47A:495–503
108. Henniges U, Schiehser S, Rosenau T, Potthast A (2010) Cellulose solubility: dissolution and analysis of "problematic" cellulose pulps in the solvent system DMAc/LiCl. ACS Symp Ser 1033:165–177
109. Nagel MCV, Heinze T (2012) Study about the efficiency of esterification of cellulose under homogeneous condition: dependence on the chain length and solvent. Lenzinger Ber 90:85–92

110. Nawaz H, Pires PAR, Bioni TA, Arêas EPG, El Seoud OA (2014) Mixed solvents for cellulose derivatization under homogeneous conditions: kinetic, spectroscopic, and theoretical studies on the acetylation of the biopolymer in binary mixtures of an ionic liquid and molecular solvents. Cellulose 21:1193–1204
111. Johnson DL (1969) Cyclic amine oxide as solvents for natural and synthetic polymers. GB 1144048 19690305, CAN70:106537
112. Uschanov P, Johansson L-S, Maunu SL, Laine J (2011) Heterogeneous modification of various celluloses with fatty acids. Cellulose 18:393–404
113. Ramos LA, Morgado DL, El Seoud OA, da Silva VC, Frollini E (2011) Acetylation of cellulose in LiCl-N, N-dimethylacetamide: first report on the correlation between the reaction efficiency and the aggregation number of dissolved cellulose. Cellulose 18:385–392
114. Liu H, Sale KL, Holmes BM, Simmons BA, Singh S (2010) Understanding the interactions of cellulose with ionic liquids: a molecular dynamics study. J Phys Chem B 114:4293–4301
115. Medronho B, Romano A, Miguel MG, Stigsson L, Lindman B (2012) Rationalizing cellulose (in)solubility: reviewing basic physicochemical aspects and role of hydrophobic interactions. Cellulose 19:581–587
116. Hess K, Trogus C (1928) X-ray investigations on cellulose derivatives. III. Reversible and irreversible lattice changes of cellulose triacetate. Z physik Chem B5:161–176
117. Hess K, Trogus C (1930) Higher orientations of cellulose materials. Naturwissenschaften 18:437–441
118. Yin J, Xue C, Alfonso GC, Turturro A, Pedemonte E (1997) Study of the miscibility and thermodynamics of cellulose diacetate-poly(vinyl pyrrolidone) blends. Polymer 38:2127–2133
119. Buchanan CM, Hyatt JA, Kelley SS, Little JL (1990) α-D-cellooligosaccharide acetates: physical and spectroscopic characterization and evaluation as models for cellulose triacetate. Macromolecules 23:3747–3755
120. Buchanan CM, Gedon SC, White AW, Wood MD (1993) Cellulose acetate propionate and poly(tetramethylene glutarate) blends. Macromolecules 26:2963–2967
121. Buchanan CM, Gedon SC, White AW, Wood MD (1992) Cellulose acetate butyrate and poly(hydroxybutyrate-co-valerate) copolymer blends. Macromolecules 25:7373–7381
122. Serad GA (1990) Cellulose esters, organic fibers. In: Kroschwitz JI (ed) Polymers: fibers and textiles. A compendium, Wiley, pp 55–81
123. Sheppard SE, Newsome PT (1935) Some properties of cellulose esters of homologous fatty acids. J Phys Chem 39:143–152
124. Patel DL, Gilbert RD (1983) Mesomorphic solutions of cellulose triacetate in trifluoroacetic acid halogenated solvent mixtures: phase separations and factors affecting the cholesteric pitch. J Polm Sci Polym Phys Ed 21:1079–1090
125. Aharoni SM (1980) Rigid backbone polymers. XIII. Effects of the nature of the solvent on the lyotropic mesomorphicity of cellulose acetate. Mol Cryst Liq Cryst 56:237–241
126. Miyamoto T, Sato Y, Shibata T, Tanahashi M, Inagaki H (1985) Carbon-13 NMR spectral studies on the distribution of substituents in water-soluble cellulose acetate. J Polym Sci Polym Chem Ed 23:1373–1381
127. Deus C, Friebolin H, Siefert E (1991) Partially acetylated cellulose. Synthesis and determination of the substituent distribution via proton NMR spectroscopy. Makromol Chem 192:75–83
128. Fischer S, Thuemmler K, Volkert B, Hettrich K, Schmidt I, Fischer K (2008) Properties and applications of cellulose acetate. Macromol Symp 262:89–96
129. Philipp B, Klemm D, Wagenknecht W, Wagenknecht M, Nehls I, Stein A, Heinze T, Heinze U, Helbig K, Camacho J (1995) Regioselective esterification and etherification of cellulose and cellulose derivatives. Part 1. Problems and description of the reaction systems. Papier (Darmstadt) 49:3–7
130. Rustemeyer P (2004) CA filter Tow for cigarette filters. Macromol Symp 208:267–291
131. Carollo P, Grospietro B (2004) Plastic materials. Macromol Symp 208:335–351

132. Ahuja N, Bhandari A (2012) Review on development of HPMCP based aqueous enteric coating polymer. Int J Res Pharm Chem 2:570–574
133. Edgar KJ, Buchanan CM, Debenham JS, Rundquist PA, Seiler BD, Shelton MC, Tindall D (2001) Advances in cellulose ester performance and application. Prog Polym Sci 26:1605–1688
134. Petzold-Welcke K, Michaelis N, Heinze T (2009) Unconventional cellulose products through nucleophilic displacement reactions. Macromol Symp 280:72–85
135. Honeyman J (1947) Reactions of cellulose I. J Chem Soc 168–173
136. McCormick CL, Callais PA (1987) Derivatization of cellulose in lithium chloride and N, N-dimethylacetamide solutions. Polymer 28:2317–2323
137. McCormick CL, Dawsey TR, Newman JK (1990) Competitive formation of cellulose *p*-toluenesulfonate and chlorodeoxycellulose during homogeneous reation of *p*-toluenesulfonyl chloride with cellulose in *N*, *N*-dimethylacetamide–lithium chloride. Carbohydr Res 208:183–191
138. Rahn K, Diamantoglou M, Klemm D, Berghmans H, Heinze T (1996) Homogeneous synthesis of cellulose *p*-toluenesulfonates in *N*, *N*-dimethylacetamide/LiCl solvent system. Angew Makromol Chem 238:143–163
139. Köhler S, Liebert T, Schöbitz M, Schaller J, Meister F, Günther W, Heinze T (2007) Interactions -of ionic liquids with polysaccharides 1. unexpected acetylation of cellulose with 1-ethyl-3-methylimidazolium acetate. Macromol Rapid Commun 28:2311–2317
140. Gericke M, Schaller J, Liebert T, Fardim P, Meister F, Heinze T (2012) Studies on the tosylation of cellulose in mixtures of ionic liquids and a co-solvent. Carbohydr Polym 89:526–536
141. Elchinger P-H, Faugeras P-A, Zerrouki C, Montplaisir D, Brouillette F, Zerrouki R (2012) Tosylcellulose synthesis in aqueous medium. Green Chem 14:3126–3131
142. Schmidt S, Liebert T, Heinze T (2014) Synthesis of soluble cellulose tosylates in an eco-friendly medium. Green Chem 16:1941–1946
143. Heinze T, Rahn K, Jaspers M, Berghmans H (1996) p-Toluenesulfonyl esters in cellulose modifications: acylation of remaining hydroxyl groups. Macromol Chem Phys 197:4207–4224
144. Tiller J, Berlin P, Klemm D (2000) Novel matrices for biosensor applications by structural design of redox-chromogenic aminocellulose esters. J Appl Polym Sci 75:904–915
145. Heinze T, Rahn K (1997) Cellulose p-toluenesulfonates: a valuable intermediate in cellulose chemistry. Macromol Symp 120:103–113
146. Heinze T, Rahn K (1996) The first report on a convenient synthesis of novel reactive amphiphilic polysaccharides. Macromol Rapid Commun 17:675–681
147. Mais U, Knaus S, Binder WH, Gruber H (2000) Functionalization of cellulose. Lenzinger Ber 79:71–76
148. Gordon IM, Maskill H, Ruasse MF (1989) Sulfonyl transfer reactions. Chem Soc Rev 18:123–151
149. Knaus S, Mais U, Binder WH (2003) Synthesis, characterization and properties of methylaminocellulose. Cellulose 10:139–150
150. Liu C, Baumann H (2002) Exclusive and complete introduction of amino groups and their N-sulfo and N-carboxymethyl groups into the 6-position of cellulose without the use of protecting groups. Carbohydr Res 337:1297–1307
151. Lewis WG, Green LG, Grynszpan F, Radic Z, Carlier PR, Taylor P, Finn MG, Sharpless KB (2002) Click chemistry In situ: Acetylcholinesterase as a reaction vessel for the selective assembly of a femtomolar inhibitor from an array of building blocks. Angew Chem Int Ed 41:1053–1057
152. Heinze T, Genco T, Petzold-Welcke K, Wondraczek H (2012) Synthesis and characterization of aminocellulose sulfates as novel ampholytic polymers. Cellulose 19:1305–1313
153. Faugers P-A, Brouilette F, Zerrouki R (2012) Crosslinked cellulose developed by CuAAC, a route to new materials. Carbohydr Res 356:247–251

154. Pohl M, Heinze T (2008) Novel biopolymer structures synthesized by dendronization of 6-deoxy-6-aminopropargyl Cellulose. Macromol Rapid Commun 29:1739–1745
155. Heinze T, Koschella A, Magdaleno-Maiza L, Ulrich AS (2001) Nucleophilic displacement reactions on tosyl cellulose by chiral amines. Polym Bull 46:7–13
156. Berlin P, Klemm D, Tiller J, Rieseler R (2000) A novel soluble aminocellulose derivative type: its transparent film-forming properties and its efficient coupling with enzyme proteins for biosensors. Macromol Chem Phys 201:2070–2082
157. Heinze T, Siebert M, Berlin P, Koschella A (2016) Biofunctional materials based on amino cellulose derivatives - a nanobiotechnological concept. Macromol Biosci 16:10–42
158. Tiller J, Berlin P, Klemm D (1999) Soluble and film-forming cellulose derivatives with redox-chromogenic and enzyme-immobilizing 1,4-phenylenediamine groups. Macromol Chem Phys 200:1–9
159. Berlin P, Rieseler R, Tiller J, Klemm D (1998) Cellulose-based supramolecular recognition structures. Papier (Heidelberg) 52:737–742
160. Tiller J, Klemm D, Berlin P (2001) Designed aliphatic aminocellulose derivatives as transparent and functionalized coatings for enzyme immobilization. Des Monomers Polym 4:315–328
161. Nikolajski M (2014) Multifunktionale Nanopartikel aus 6-Desoxy-6-ω-aminoalkyl-aminocellulosen. PhD Thesis, Friedrich Schiller University Jena
162. Jung A, Berlin P (2005) New water-soluble and film-forming aminocellulose tosylates as enzyme support matrices with $Cu^{2+}$-chelating properties. Cellulose 12:67–84
163. Miethe P, Scholz F, Heinze T, Berlin P, Pietraszczyk M (2011) Immunofiltration assays based on aminocellulose modified sintered polyethylene. Abstr Pap Am Chem Soc CELL-4
164. Heinze T, Nikolajski M, Daus S, Besong TMD, Michaelis N, Berlin P, Morris GA, Rowe AJ, Harding SE (2011) Protein-like oligomerisation of carbohydrates. Angew Chem Int Ed 50:8602–8604
165. Ferrone FA, Hofrichter J, Eaton WA (1985) Kinetics of sickle hemoglobin polymerization. II. A double nucleation mechanism. J Mol Biol 183:611–631
166. Teif VB, Bohinc K (2011) Condensed DNA: condensing the concepts. Prog Biophys Mol Biol 105:208–222
167. Nikolajski M, Adams GG, Gillis RB, Besong DTabot Rowe AJ, Heinze T, Harding SE (2014) Protein-like fully reversible tetramerisation and super-association of an aminocellulose. Sci Rep 4:3861/1-3861/5
168. Berlin P, Klemm D, Jung A, Liebegott H, Rieseler R, Tiller J (2003) Film-forming aminocellulose derivatives as enzyme-compatible support matrices for biosensor developments. Cellulose 10:343–367
169. Jung A, Berlin P, Wolters B (2004) Biomolecule-compatible support structures for biomolecule coupling to physical measuring principle surfaces. IEE Proc Nanobiotechnol 151:87–94
170. Jung A, Wolters B, Berlin P (2007) (Bio)functional surface structural design of substrate materials based on self-assembled monolayers from aminocellulose derivatives and amino (organo)polysiloxanes. Thin Solid Films 515:6867–6877
171. Nikolajski M, Wotschadlo J, Clement JH, Heinze T (2012) Amino-functionalized cellulose nanoparticles: preparation, characterization, and interactions with living cells. Macromol Biosci 12:920–925
172. Fidale LC, Nikolajski M, Rudolph T, Dutz S, Schacher FH, Heinze T (2013) Hybrid Fe3O4@amino cellulose nanoparticles in organic media—heterogeneous ligands for atom transfer radical polymerizations. J Colloid Interface Sci 390:25–33
173. Braconnot H (1833) Ueber einige Eigenschaften der Salpetersäure. Ann Pharm (Lemgo, Ger.) 1:242–245
174. Schönbein CF (1847) Philos Mag 31:7
175. Hyatt JW, Hyatt IS (1870) Improvement in treating and molding pyroxyline. US 105388 A CAN0:127772

176. Fengl R (1993) Cellulose esters (inorganic). In: Kroschwitz JI, Howe-Grant M (eds) Kirk-Othmer encyclopedia of chemical technology, vol 5. Wiley, New York, Chichester, Brisbane, Toronto, Singapore
177. Thinius K, Thuemmler W (1966) Analytical chemistry of plastics. XXX. Polymer-like conversion of cellulose to cellulose nitrate. Makromol Chem 99:117–125
178. Miles FD (1955) Cellulose nitrate, the physical chemistry of nitrocellulose, its formation and use. Oliver and Boyd, London
179. Short RD, Munro HS (1989) Nitration of cellulose by nitronium ion salt. Polym Commun 30:366–368
180. Short RD, Munro HS (1990) Some conclusions drawn from a study of cellulose nitration in technical mixed acids by x-ray photoelectron spectroscopy [XPS] and carbon-13 nuclear magnetic resonance [NMR]. In Kennedy JF, Phillips GO, Williams PA (eds) Cellul Sour Exploit 263–268
181. Clermont LP, Bender F (1972) Water-soluble cellulose derivatives prepared by the action of solutions of nitrogen dioxide in dimethylformamide. J Polym Sci Part A-1 Polym Chem 10:1669–1677
182. Schweiger RG (1974) Anhydrous solvent systems for cellulose processing. Tappi 57:86–90
183. Balser K, Hoppe L, Eichler T, Wandel M, Astheimer H-J (1986) Cellulose esters. In Gerhartz W, Yamamoto YS, Campbell FT, Pfefferkorn R, Rounsaville JF (eds) Ulmann's encyclopedia of industrial chemistry, VCH Weinheim, A5, pp 419–459
184. Urbanski T, Zyszczynski S (1965) Structure of cellulose-Nitric acid Knecht compounds. I. Spectroscopic examination. Bull Acad Pol Sci Ser Sci Chim 13:377–382
185. Gert EV (1997) Labile products of interaction of cellulose with nitrogen oxide compounds. Russ Chem Rev 66:73–92
186. Klemm D, Philipp P, Heinze T, Heinze U, Wagenknecht W (1998) Comprehensive cellulose chemistry. Wiley, pp 101–114
187. Philipp B (1958) Effect of cellulosic materials on the rate of cellulose nitrate formation. Faserforsch Textiltech 9:520–526
188. Munro HS, Short RD (1990) A study of the low temperature nitration of cellulose in mixed acids. J Appl Polym Sci 39:539–551
189. Wu TK (1980) Carbon-13 and proton magnetic resonance studies of cellulose nitrates. Macromolecules 13:74–79
190. Alexander WJ, Mitchell RL (1949) Rapid measurement of cellulose viscosity by the nitration methods. Anal Chem 21:1497–1500
191. Bennett CF, Timell TE (1955) Preparation of cellulose trinitrate. Sven Papperstidn 58:281–286
192. Kassenbeck P (1983) Faktoren, die das Nitrierverhalten von Baumwoll-Linters und Holzzellstoffen beschreiben. Report 3/83, ICT-Fraunhofer-Institut für Treib- und Explosivstoffe, Pfinztal-Berghausen
193. Green JW (1963) Nitration with mixtures of nitric and sulfuric acids. In: Whistler RL (ed) Methods in carbohydrate chemistry, vol III. Academic Press, New York, p 213
194. Khrapkovskii GM, Shamsutdinov TF, Chachkov DV, Shamov AG (2004) Energy of the O–$NO_2$ bond dissociation and the mechanism of the gas-phase monomolecular decomposition of aliphatic alcohol nitroesters. J Mol Struct Theochem 686:185–192
195. Short RD, Munro HS, Matthews R, Pritchard T (1989) Carbon-13 NMR study of cellulose nitrates: a comparison between nitration in nitric acid-dichloromethane mixes and technical mixed acids. Polym Comm 30:217–220
196. Bansal P, Hall M, Realff MJ, Lee JH, Bommarius AS (2010) Multivariate statistical analysis of X-ray data from cellulose: A new method to determine degree of crystallinity and predict hydrolysis rates. Bio-resour Technol 101:4461–4471
197. Touey GP (1956) Cellulose phosphates. US 2759924 19560821, CAN51:3440
198. Nuessle AC, Ford FM, Hall WP, Lippert AL (1956) Some aspects of the cellulose phosphate-urea reaction. Text Res J 26:32–39

199. Granja PL, Pouysegu L, Petraud M, De Jeso B, Baquey C, Barbosa MA (2001) Cellulose phosphates as biomaterials. I. Synthesis and characterization of highly phosphorylated cellulose gels. J Appl Polym Sci 82:3341–3353
200. Wanrosli WD, Rohaizu R, Ghazali A (2011) Synthesis and characterization of cellulose phosphate from oil palm empty fruit bunches microcrystalline cellulose. Carbohydr Polym 84:262–267
201. Wanrosli WD, Zainuddin Z, Ong P, Rohaizu R (2013) Optimization of cellulose phosphate synthesis from oil palm lignocellulosics using wavelet neural networks. Ind Crops Prod 50:611–617
202. Nehls I, Loth F (1991) Carbon-13 NMR spectroscopic investigations on phosphorylation of cellulose products in the system orthophosphoric acid/urea. Acta Polym 42:233–235
203. Pan Z-W, Shang Y-L, Li J-R, Gao S, Shang Y-L, Huang R-L, Wang J, Zhang S-H, Zhang Y-J (2006) A new class of electrorheological material: synthesis and electrorheological performance of rare earth complexes of phosphate cellulose. J Mater Sci 41:355–362
204. Kaputskii FN, Yurkshtovich NK, Yurkshtovich TL, Golub NV, Kosterova RI (2007) Preparation and physicochemical and mechanical properties of low-substituted cellulose phosphate fibers. Russ J Appl Chem 80:1135–1139
205. Yurkshtovich NK, Yurkshtovich TL, Kaputskii FN, Golub NV, Kosterova RI (2007) Esterification of viscose fibers with orthophosphoric acid and study of their physicochemical properties. Fibre Chem 39:31–36
206. Rungrodnimitchai S (2014) Rapid preparation of biosorbents with high ion exchange capacity from rice straw and bagasse for removal of heavy metals. Sci World J 634837/1-634837/10
207. Vigo TL, Collins AM, Welch CM (1973) Flame-retardant cotton fabrics by reaction of cellulose with phosphorus trichloride-DMF [N, N-dimethylformamide] adduct. J Appl Polym Sci 17:571–584
208. Wagenknecht W, Philipp B, Schleicher H (1979) The esterification and dissolution of cellulose with sulfur and phospho-rous acid anhydrides and chlorides. Acta Polym 30:108–112
209. Zeronian SH, Adams S, Alger K, Lipska AE (1980) Phosphorylation of cellulose: effect of the reactivity of the starting polymer on the properties of the phosphorylated product. J Appl Polym Sci 25:519–528
210. Vigo TL, Welch CM (1974) Chlorination and phosphorylation of cotton cellulose by reaction with phosphoryl chloride in N, N-dimethylformamide. Carbohydr Polym 32:331–338
211. Kaur B, Gur IS, Bhatnagar HL (1987) Thermal degradation studies of cellulose phosphates and cellulose thiophosphates. Angew Makromolekul Chem 147:157–183
212. Vogt S, Klemm D, Heinze T (1996) Effective esterification of carboxymethyl cellulose (CMC) in a new nonaqueous swelling system. Polym Bull 36:549–555
213. Philipp B, Wagenknecht W, Nehls I, Schnabelrauch M, Klemm D (1989) Synthesis of soluble cellulose phosphate and sulfate esters by homogeneous reaction in nonaqueous system. Papier (Bingen) 43:700–706
214. Philipp B, Klemm D, Wagenknecht W (1995) Regioselective esterification and etherification of cellulose and cellulose derivatives Part 2. Synthesis of regioselective cellulose esters. Papier (Bingen) 49:58–64
215. Xiao P, Zhang J, Feng Y, Wu J, He J, Zhang J (2014) Synthesis, characterization and properties of novel cellulose derivatives containing phosphorus: cellulose diphenyl phosphate and its mixed esters. Cellulose 21:2369–2378
216. Vo HT, Kim YJ, Jeon EH, Kim CS, Kim HS, Lee H (2012) Ionic-liquid-derived, water-soluble ionic cellulose. Chem Eur J 18:9019–9023
217. Whistler RL, Towle GA (1969) Preparation and characterization of polysaccharide phosphates. Arch Biochem Biophys 135:396–401
218. Wagenknecht W (1996) Regioselectively substituted cellulose derivatives by modification of commercial cellulose acetates. Papier (Darmstadt) 50:712–720

219. Fricain JC, Granja PL, Barbosa MA, De Jéso B, Barthe N, Baquey C (2002) Cellulose phosphates as biomaterials. In vivo biocompatibility studies. Biomaterials 23:971–980
220. Granja PL, De Jéso Bernard, Bareille R, Rouais F, Baquey C, Barbosa MA (2006) Cellulose phosphates as biomaterials. In vitro biocompatibility studies. React Funct Polym 66:728–739
221. Ubaidullaev BKh, Kudratov AM, Salimov ZS (2004) Preparation and ion-exchange properties of P-containing cellulose derivatives from certain plant species. Chem Nat Compd 40:410–411
222. Li W, Zhao H, Teasdale PR, John R, Zhang S (2002) Application of a cellulose phosphate ion exchange membrane as a binding phase in the diffusive gradients in thin films technique for measurement of trace metals. Anal Chim Acta 464:331–339
223. Chauhan GS, Singh B, Kumar S (2005) Synthesis and characterization of N-vinyl pyrrolidone and cellulosics based functional graft copolymers for use as metal ions and iodine sorbents. J Appl Polym Sci 98:373–382
224. Chauhan GS, Guleria L, Sharma R (2005) Synthesis, characterization and metal ion sorption studies of graft copolymers of cellulose with glycidyl methacrylate and some comonomers. Cellulose 12:97–110
225. Klemm D, Phillip B, Heinze T, Heinze U, Wagenknecht W (1998) Comprehensive cellulose chemistry, vol 2. Wiley-VCH, Weinheim, pp 115–133
226. Heinze T, Daus S, Gericke M, Liebert T (2010) Semi-synthetic sulfated polysaccharides—promising materials for biomedical applications and supramolecular architecture. In: Tiwari A (ed) Polysaccharides: deveoplment, properties and applications. Nova Science, NY, pp 213–259
227. Philipp B, Wagenknecht W (1983) Cellulose sulfate half-ester. synthesis, structure, and properties. Cellul Chem Technol 17:443–459
228. Lukanoff B, Dautzenberg H (1994) Sodium cellulose sulfate as a component in the creation of microcapsules through forming polyelectrolyte. Part 1. Heterogeneous sulfation of cellulose by the use of sulfuric acid/propanol as reaction medium and sulfating agent. Papier (Darmstadt) 48:287–298
229. Schweiger RG (1972) Polysaccharide Sulfates. 1. Cellulose sulfate with a high degree of substitution. Carbohydr Res 21:219–228
230. Yamamoto I, Takayama K, Honma K, Gonda T, Matsuzaki K, Hatanaka K, Uryu T, Yoshida O, Nakashima H, Yamamoto N, Kaneko Y, Mimura T (1991) Synthesis, structure and antiviral activity of sulfates of cellulose and its branched derivatives. Carbohydr Polym 14:53–63
231. Vieira MC, Heinze T, Antonio-Cruz R, Mendoza-Martinez AM (2002) Cellulose derivatives from cellulosic material isolated from Agave lechuguilla and fourcroydes. Cellulose 9:203–212
232. Bhatt N, Gupta PK, Naithan S (2008) Preparation of cellulose sulfate from α-cellulose isolated from Lantana camara by the direct esterification method. J Appl Polym Sci 108:2895–2901
233. Zhang K, Peschel D, Brendler E, Groth T, Fischer S (2009) Synthesis and bioactivity of cellulose derivatives. Macromol Symp 280:28–35
234. Saake B, Puls J, Wagenknecht W (2002) Endoglucanase fragmentation of cellulose sulfates derived from different synthesis concepts. Carbohydr Polym 48:7–14
235. Wagenknecht W, Philipp B, Keck M (1985) Acylation of cellulose dissolved in O-base solvent systems. Acta Polym 36:697–698
236. Wang Z-M, Li L, Xiao K-J, Wu J-Y (2009) Homogeneous sulfation of bagasse cellulose in an ionic liquid and anticoagulation activity. Bioresour Technol 100:1687–1690
237. Liebert T, Wotschadlo J, Gericke M, Köhler S, Laudeley P, Heinze T (2009) Modification of cellulose in ionic liquids towards biomedical applications. ACS Symp Ser 1017:115–132
238. Gericke M (2011) Cellulose sulfates prepared in ionic liquids—from challenging synthesis to promising biomedical applications. Der Andere Verlag, Uelvesbüll, pp 22–29

239. Wagenknecht W, Nehls I, Koetz J, Philipp B, Ludwig J (1991) Sulfonation of partially substituted cellulose acetate under homogeneous reaction conditions. Cellul Chem Technol 25:343–354
240. Groth T, Wagenknecht W (2001) Anticoagulant potential of regioselective derivatized cellulose. Biomaterials 22:2719–2729
241. Hettrich K, Wagenknecht W, Volkert B, Fischer S (2008) New possibilities of the acetosulfation of cellulose. Macromol Symp 262:162–169
242. Zhang K, Brendler E, Geissler A, Fischer S (2011) Synthesis and spectroscopic analysis of cellulose sulfates with regulable total degrees of substitution and sulfation patterns via 13C NMR and FT Raman spectroscopy. Polymer 52:26–32
243. Vogt S, Heinze T, Roettig K, Klemm D (1995) Preparation of carboxymethylcellulose sulfate of high degree of substitution. Carbohydr Res 266:315–320
244. Heinze T (1998) New ionic polymers by cellulose functionalization. Macromol Chem Phys 199:2341–2364
245. Koehler S, Liebert T, Heinze T (2008) Interactions of ionic liquids with polysaccharides. VI. Pure cellulose nanoparticles from trimethylsilyl cellulose synthesized in ionic liquids. J Polym Sci, Part A: Polym Chem 46:4070–4080
246. Wagenknecht W, Nehls I, Stein A, Klemm D, Philipp B (1992) Synthesis and substituent distribution of sodium cellulose sulfates via trimethylsilyl cellulose as intermediate. Acta Polym 43:266–269
247. Richter A, Klemm D (2003) Regioselective sulfation of trimethylsilyl cellulose using different $SO_3$-complexes. Cellulose 10:133–138
248. Schweiger RG (1979) New cellulose sulfate derivatives and applications. Carbohydr Res 70:185–198
249. Wang Z-M, Li L, Zheng BS, Normakhamatov N, Guo SY (2007) Preparation and anticoagulation activity of sodium cellulose sulfate. Int J Biol Macromol 41:376–382
250. Gericke M, Ales Doliska, Stana J, Liebert T, Heinze T, Stana-Kleinschek K (2011) Semi-synthetic polysaccharide sulfates as anticoagulant coating for PET, 1-cellulose sulfate. Macromol Biosci 11:549–556
251. Decher G (1997) Fuzzy nanoassemblies: toward layered polymeric multicomposites. Science 277:1232–1237
252. Dautzenberg H, Schuldt U, Grasnick G, Karle P, Mueller P, Löhr M, Pelegrin M, Piechaczyk M, Rombs KV, Günzburg WH, Salmons B, Saller RM (1999) Development of cellulose sulfate-based polyelectrolyte complex microcapsules for medical applications. Ann N Y Acad Sci 875:46–63
253. Koetse M, Laschewsky A, Jonas AM, Wagenknecht W (2002) Influence of charge density and distribution on the internal structure of electrostatically self-assembled polyelectrolyte films. Langmuir 18:1655–1660
254. Gericke M, Liebert T, Heinze T (2009) Polyelectrolyte synthesis and in situ complex formation in ionic liquids. J Am Chem Soc 131:13220–13221
255. de Vos P, Lazarjani HA, Poncelet D, Faas MM (2014) Polymers in cell encapsulation from an enveloped cell perspective. Adv Drug Delivery Rev 67–68:15–34
256. Löhr M, Müller P, Karle P, Stange J, Mitzner S, Jesnowski R, Nizze H, Nebe B, Liebe S, Salmons B, Günzburg WH (1998) Targeted chemotherapy by intratumor injection of encapsulated cells engineered to produce CYP2B1, an ifosfamide activating cytochrome P450. Gene Ther 5:1070–1078
257. Schaffellner S, Stadlbauer V, Stiegler P, Hauser O, Halwachs G, Lackner C, Iberer F, Tscheliessnigg KH (2005) Porcine islet cells microencapsulated in sodium cellulose sulfate. Transplant Proc 37:248–252
258. Mansfeld J, Förster M, Schellenberger A, Dautzenberg H (1991) Immobilization of invertase by encapsulation in polyelectrolyte complexes. Enzyme Microb Technol 13:240–244
259. Gemeiner P, Stefuca V, Bales V (1993) Biochemical engineering of biocatalysts immobilized on cellulosic materials. Enzyme Microb Technol 15:551–566

260. Vikartovska A, Bucko M, Mislovicova D, Paetoprsty V, Lacik I, Gemeiner P (2007) Improvement of the stability of glucose oxidase via encapsulation in sodium alginate-cellulose sulfate-poly(methylene-co-guanidine) capsules. Enzyme Microb Technol 41:748–755
261. Wu QX, Zhang QL, Lin DQ, Yao SJ (2013) Characterization of novel lactoferrin loaded capsules prepared with polyelectrolyte complexes. Int J Pharm 455:124–131
262. Nurdin N, Canaple L, Bartkowiak A, Desvergne B, Hunkeler D (2000) Capsule permeability via polymer and protein ingress/egress. J Appl Polym Sci 75:1165–1175
263. Silva CM, Ribeiro AJ, Ferreira D, Veiga F (2006) Insulin encapsulation in reinforced alginate microspheres prepared by internal gelation. Eur J Pharm Sci 29:148–159
264. Weber W, Rimann M, Schafroth T, Witschi U, Fussenegger M (2006) Design of high-throughput-compatible protocols for microencapsulation, cryopreservation and release of bovine spermatozoa. J Biotechnol 123:155–163
265. Mofakham H, Hezarkhani Z, Shaabani A (2012) Cellulose-$SO_3H$ as a biodegradable solid acid catalyzed one-pot three-component Ugi reaction: Synthesis of α-amino amide, 3,4-dihydroquinoxalin-2-amine, 4H-benzo[b][1, 4]thiazin-2-amine and 1,6-dihydropyrazine-2,3-dicarbonitrile derivatives. J Mol Cat A: Chem 360:26–34
266. Shaabani A, Maleki A, Rad JM, Soleimani E (2007) Cellulose sulfuric acid catalyzed one-pot three-component synthesis of imidazoazines. Chem Pharm Bull 55:957–958
267. Shaabani A, Maleki A (2007) Cellulose sulfuric acid as a bio-supported and recyclable solid acid catalyst for the one-pot three-component synthesis of α-aminonitriles. Appl Catal A 331:149–151
268. Shaabani A, Rezayan AH, Behnam M, Heidary M (2009) Green chemistry approaches for the synthesis of quinoxaline derivatives: comparison of ethano and water in the presence of the reusable catalyst cellulose sulfuric acid. C R Chim 12:1249–1252
269. Reddy PN, Reddy YT, Reddy MN, Rajitha B, Crooks PA (2009) Cellulose sulfuric acid: an efficient biodegradable and recyclable solid acid catalyst for the one-pot synthesis of 3,4-dihydropyrimidine-2(1H)-ones. Synth Commun 39:1257–1263
270. Shelke KF, Sapkal SB, Kakade GK, Shingate BB, Shingare MS (2010) Cellulose sulfuric acid as a bio-supported and recyclable solid acid catalyst for the one-pot synthesis of 2,4,5-triarylimidazoles under microwave irradiation. Green Chem Lett Rev 3:27–32
271. Subba Reddy BV, Venkateswarlu A, Madan Ch, Vinu A (2011) Cellulose-$SO_3H$: an efficient and biodegradable solid acid catalyst for the synthesis of quinazolin-4(1H)-ones. Tetrahedron Lett 52:1891–1894
272. Shaterian HR, Rigi F, Arman M (2012) Cellulose sulfuric acid: an efficient and recyclable solid acid catalyst for the protection of hydroxyl groups using HMDS under mild conditions. Chem Sci Trans 1:155–161
273. Alinezhad H, Haghighi AH, Salehian F (2010) A green method for the synthesis of bis-indolylmethanes and 3,3′-indolyloxindole derivatives using cellulose sulfuric acid under solvent-free conditions. Chin Chem Lett 21:183–186
274. Rahmatpour A (2011) Cellulose sulfuric acid as a bioderadable and recoverable solid acid catalyst for one pot synthesis of substituted pyrroles under solvent-free conditions at room temperature. React Funct Polym 71:80–83
275. Lehmann J, Redlich HG (1996) Kohlenhydrate: chemie und biologie, 2nd edn. Stuttgart and New York, Thieme
276. Majewicz TG (1981) Carboxymethyl cellulose with improved substituent uniformity using borax. US 4306061 A, CAN96:54146
277. Huybrechts S, Detemmerman A, De Pooter J, Blyweertt RE (1988) WO 8807059 A1, CAN110:2927
278. Bishop M, Shahid N, Yang J, Barron AR (2004) Determination of the mode and efficacy of the crosslinking of guar by borate using MAS 11B NMR of borate crosslinked guar in combination with solution 11B NMR of model systems. Dalton Trans 17:2621–2634

279. Norrild JC, Eggert H (1995) Evidence for mono- and bisdentate boronate complexes of glucose in the furanose form. Application of 1JC–C coupling constants as a structural probe. J Am Chem Soc 117:1479–1484
280. Bielecki M, Eggert H, Norrild JC (1999) A fluorescent glucose sensor binding covalently to all five hydroxy groups of α-D-glucofuranose. A reinvestigation. J Chem Soc Perkin Trans 3:449–456
281. Ferrier RJ (1961) Interaction of phenylboronic acid with hexosides. J Chem Soc 2325–2330
282. Ferrier RJ (1978) Carbohydrate boronates. Adv Carbohydr Chem Biochem 35:31–80
283. Meiland M, Heinze T, Guenther W, Liebert T (2009) Seven-membered ring boronates at trans-diol moieties of carbohydrates. Tetrahedron Lett 50:469–472
284. Meiland M, Heinze T, Guenther W, Liebert T (2010) Studies on the boronation of methyl-β-D-cellobioside -a cellulose model. Carbohydr Res 345:257–263
285. Nicholls MP, Paul PKC (2004) Structures of carbohydrate-boronic acid complexes determined by NMR and molecular modeling in aqueous alkaline media. Org Biomol Chem 2:1434–1441
286. Ermolenko IN, Vorob'eva NK, Kofman AE, Zonov YuG (1071) Reaction of cellulose acetate with boric acid. Vestsi Akademii Navuk BSSR, Seryya Khimichnykh Navuk 6:59–62
287. Arthur JC, Bains MS (1974) Methyl cellulose-boron alkoxide compounds. US 3790562 A, CAN81:39285
288. Gertsev VV, Nesterenko LYa, Romanov YaA (1990) Boric cellulose, a modified polymer having antiseptic, antifungal, and hemostatic properties. Khim-Farm Zh 24:36–38
289. Dahlhoff WV, Imre J, Köster R (1988) Poly(1,4-anhydro-D-glucitols) by regioselective reductions of amylose or cellulose. Macromolecules 21:3342–3343
290. Sato T, Tsujii Y, Fukuda T, Miyamoto T (1992) Reversible gelation of short-chain O-(2,3-dihydroxypropyl)cellulose/borax solutions. 1. A 11B-NMR study on polymer-ion interactions. Macromolecules 25:3890–3895
291. Arthur JC, Bains MS (1975) Carbohydrate-boron alkoxide compounds. US 3891621 (CAN83):114817
292. Ermolenko IN, Luneva NK (1977) New group of cellulose derivatives produced by the interaction of cellulose with inorganic poly acids. Cellul Chem Technol 11:647–653
293. Ermolenko IN, Luneva NK, Shukurov T, Abbosov B (1990) Spectroscopic control of boration of cotton fibers from wilted plants. Zh Prikl Spektrosk 53:812–815
294. Bailar JC, Emelius HJ, Nyholm R, Trotman-Dickenson AF (eds) (1973) Comprehensive Inorganic chemistry. Pergamon Press, Oxford
295. Olah GA, Heiner T, Rasul G, Prakash GKS (1998) 1H, 13C, 15N NMR and theoretical study of protonated carbamic acids and related compounds. J Org Chem 63:7993–7998
296. Hage W, Hallbrucker A, Mayer E (1993) Carbonic acid: synthesis by protonation of bicarbonate and FTIR spectroscopic characterization via a new cryogenic technique. J Am Chem Soc 115:8427–8431
297. Rasul G, Reddy VP, Zdunek LZ, Prakash GKS, Olah GA (1993) Carbonic acid and Its mono- and diprotonation: 12. NMR, ab Initio, and IGLO investigation. J Am Chem Soc 115:2236–2238
298. Possidonio S, Siviero F, El Seoud OA (1999) Kinetics of the pH-independent hydrolysis of 4-nitrophenyl chloroformate in aqueous micellar solutions: Effects of the charge and structure of the surfactant. J Phys Org Chem 12:325–332
299. Aricò F, Tundo P (2010) Dimethyl carbonate as a modern green reagent and solvent. Russ Chem Rev 79:479–489
300. Doane WM, Shasha BS, Stout EI, Russell CR, Rist CE (1967) A facile route to trans cyclic carbonates of sugars. CarbohydrRes 4:445–451
301. Shasha BS, Doane WM, Russell CR, Rist CE (1967) Novel method for preparation os some sugar carbonates. Carbohydr Res 5:346–348

302. Litjens REJN, van den Bos LJ, Codée JDC, Overkleeft HS, van der Marel GA (2007) The use of cyclic bifunctional protecting groups in oligosaccharide synthesis—an overview. Carbohydr Res 342:419–429
303. Sanches Chaves M, Arranz F (1985) Water-insoluble dextrans by grafting 2: reaction of dextrans with n-alkyl chloroformates—chemical and enzymatic hydrolysis. Macromol Chem 186:17–29
304. Rudel M, Gabert A, Möbius G (1978) Carbonate group-containing crosslinked dextran as a support material for covalent immobilization of trypsin. Z Chem 18:178–179
305. Wondraczek H, Elschner T, Heinze T (2011) Synthesis of highly functionalized dextran alkyl carbonates showing nanosphere formation. Carbohydr Polym 83:1112–1118
306. Kennedy JF, Rosevear A (1974) Improvement of enzyme immobilisation characteristics of macroporous cellulose *trans*-2,3-carbonate by preswelling in dimethyl-sulfoxide. J Chem Soc, Perkin Trans 1(1972–1999):757–762
307. Vandoorne F, Vercauteren R, Permentier D, Schacht E (1985) Reinvestigation of the 4-nitrophenyl chloroformate activation of dextran—evidence for the formation of different types of carbonate moieties. Makromol Chem 186:2455–2460
308. Barker SA, Tun HC, Doss SH, Gray CJ, Kennedy JF (1971) Preparation of cellulose carbonate. Carbohydr Res 17:471–474
309. Oh SY, Yoo DI, Shin Y, Lee WS, Jo SM (2002) Preparation of regenerated cellulose fiber via carbonation. I. Carbonation and dissolution in an aqueous NaOH solution. Fibers Polym 3:1–7
310. Oh SY, Yoo DI, Shin Y, Kim HY, Kim HC, Chung YS, Park WH, Youk JH (2005) Preparation of regenerated cellulose fiber via carbonation (II)—spinning and characterization. Fibers Polym 6:95–102
311. Fleischer M, Blattmann H, Mülhaupt R (2013) Glycerol-, pentaerythritol- and trimethylolpropane-based polyurethanes and their cellulose carbonate composites prepared via the non-isocyanate route with catalytic carbon dioxide fixation. Green Chem 15:934–942
312. Hayashi S (2002) Synthesis and properties of cellulose carbonate derivatives. Kobunshi Ronbunshu 59:1–7
313. Dang VA, Olofson RA (1990) Advantages of fluoroformates as carboalkoxylating reagents for polar reactants. J Org Chem 55:1851–1854
314. Elschner T, Ganske K, Heinze T (2013) Synthesis and aminolysis of polysaccharide carbonates. Cellulose 20:339–353
315. Elschner T, Wondraczek H, Heinze T (2013) Synthesis and detailed structure characterization of dextran carbonate. Carbohydr Polym 93:216–223
316. Elschner T, Koetteritzsch M, Heinze T (2014) Synthesis of cellulose tricarbonate in 1-butyl-3-methylimidazolium chloride/pyridine. Macromol Biosci 14:161–165
317. Barker SA, Doss JH, Gray CJ, Kennedy JF, Stacey M, Yeo TH (1971) Beta-D-Glucosidase chemically bound to microcrystalline cellulose. Carbohydr Res 20:1–7
318. Kennedy JF, Zamir A (1973) Use of cellulose carbonate for insolubilization of enzymes. Carbohydr Res 29:497–501
319. Kennedy JF, Barker SA, Rosevear A (1973) Preparation of a water-insoluble trans-2,3-cyclic carbonate derivative of macroporous cellulose and its use as a matrix for enzyme immobilisation. J Chem Soc Perkin Trans 1(1972–1999):2293–2299
320. Kennedy JF, Tun HC (1973) Active insolubilized antibiotics based on cellulose and cellulose carbonate. Antimicrob Agents Chemother 3:575–579
321. Kennedy JF, Tun HC (1973) Reaction of cellulose carbonate with amino and mercapto compounds. Carbohydr Res 29:246–251
322. Kennedy JF, Tun HC (1973) Use of cellulose carbonate for preparation of immunosorbents. Radioimmunoassay of follicle-stimulating hormone. Carbohydr Res 30:11–19
323. Kennedy JF, Keep PA, Catty D (1982) The use of cellulose carbonate-based immunoadsorbents in the isolation of minor allotypic components of rabbit immunoglobulin populations. J Immunol Methods 50:57–75

324. Kennedy JF, Keep PA, Catty D (1976) Separation of rabbit allotypic B4 immunoglobulin from B4-negativ immunoglobulin by affinity chromatogaphy on immunoadsorbents prepared from cellulose trans-2,3-carbonate. Biochem Soc Trans 4:135–137
325. Kennedy JF, Catty D, Keep PA (1980) Production of immunoadsorbents based on cellulose carbonates and their application to the isolation of specific immunoglobulin light chains. Int J Biol Macromol 2:137–142
326. Catty D, Kennedy JF, Drew RL, Tun HC (1973) Application of cellulose carbonate to preparation of water-insoluble immunoadsorbents used in purification of antibodies to immunoglobulins. J Immunol Methods 2:353–369
327. Pourjavadi A, Seidi F, Afjeh SS, Nikoseresht N, Salimi H, Nemati N (2011) Synthesis of soluble N-functionalized polysaccharide derivatives using phenyl carbonate precursor and their application as catalysts. Starch/Staerke 63:820–820
328. Omae I (2012) Recent developments in carbon dioxide utilization for the production of organic chemicals. Coord Chem Rev 256:1384–1405
329. Barker SA, Kennedy JF, Gray CJ (1972) Cellulose carbonates. US 3705890 A 19721212, CAN78:59964
330. Yoo DI, Oh SY, Park KH, Oh YS, Park WH, Choi CN, Yang KS (2000) Regenerated cellulose fibers from cellulose carbonate derivatives and manufacture thereof WO 2000012790 A1 20000309, CAN132:181986
331. Bhasu VCJ, Sathyanarayana DN (1980) A PPP and CNDO study of dithiocarbonic anionic derivatives. Phosphorus Sulfur Relat Elem 8:171–175
332. Krebs B, Henkel G, Dinglinger HJ, Stehmeier G (1980) New determination of the crystal structure of trithiocarbonic acid $\alpha$-$H_2CS_3$ at 140 K. Z Kristallogr 153:285–296
333. Krebs B, Henkel G (1987) Sulfur-hydrogen-sulfur hydrogen bridges: the crystal structure of a new modification of trithiocarbonic acid. Z Kristallogr 179:373–382
334. Neels J, Meisel M, Moll R (1984) Synthesis of carbonyl sulfide from phosphorous sulfide and urea. Z Chem 24:389–390
335. Erben MF, Boese R, Della Védova CO, Oberhammer H, Willner H (2006) Toward an intimate understanding of the structural properties and conformational preference of oxoesters and thioesters: Gas and crystal structure and conformational analysis of dimethyl monothiocarbonate, $CH_3OC(O)SCH_3$. J Org Chem 71:616–622
336. Kalashnikov SM, Imashev UB (1996) Synthesis, reactions and characteristics of organic thiocarbonates. Bashk Khim Zh 3:50–59
337. Klemm D, Philipp B, Heinze T, Heinze U, Wagenknecht W (1998) Comprehensive cellulose chemistry, vol 2. Wiley, pp 145–161
338. Wilkes AG (2001) The viscose process. In: Woodings C (ed) Regenerated cellulose fibers. Woodhead Publishing Series in Textiles, Elsevier, New York, pp 37–61
339. Kipershlak EZ, Pakshver AB (1976) New trends in the study of viscose. (Review). Khim Volokna 5:42–48
340. Dautzenberg H, Philipp B (1971) Interaction of alkaline cellulose with carbon disulfide. Khim Volokna 5:23–29
341. Kauffman GB (1993) Rayon: the first semi-synthetic fiber product. J Chem Educ 70:887–893
342. https://www.google.com.br/?gfe_rd=cr&ei=o6auVJ3IKoOX8QfTh4GwDw&gws_rd=ssl#q=LENZING+INVESTOR+PRESENTATION+%E2%80%93+INVESTOR+CONFERENCE+STEGERSBACH. Accessed 8 Jan 2015
343. Fock W (1959) A modified method for determining the reactivity of viscose-grade dissolving pulps. Papier (Bingen, Germany) 13:92–95
344. Hall DS, Losee LA (1997) Carbon disulfide incidents during viscose rayon processing. Process Saf Prog 16:251–254
345. Nevell TP (1985) Oxidation of cellulose. In Nevell TP, Zeronian SH (eds) Cellulose chemistry and its applications, Ellis Horwood Ltd., Chichester, UK, pp 243–265
346. Dunbrant S, Samuelson O (1965) Determination of primary and secondary xanthate groups in cellulose xanthate. J Appl Polym Sci 9:2489–2499

347. Fahmy YA, Fadl MH (1964) Emulsion xanthation of cellulose. I. Xanthation in the presence of sodium hydroxide and potassium hydroxide solutions. Sven Papperstidn 67:101–109
348. Fahmy YA, Fadl MH (1964) Emulsion xanthation of cellulose. II. Aspects of the reaction mechanism and acceleration of cellulose emulsion xanthation by inclusion or occlusion with CS2 in fibers. Sven Papperstidn 67:279–285
349. Abou-State MA, Abd El-Megeid FF, Michael MG (1984) Emulsion xanthation of cotton and bagasse celluloses in presence of sodium and potassium hydroxides. Angew Makromol Chem 127:59–66
350. Everett DH (1972) Manual of symbols for physicochemical quantities and units. Appendix II, definitions, terminology and symbols in colloid and surface chemistry. Pure Appl Chem 31:577–638
351. Jayme G, Rosenstock KH (1957) Determination of the degree of polymerization (D.P.) of cellulose by the Jayme-Wellm emulsion xanthation technique. Papier (Bingen, Germany) 11:77–82
352. Lindström M, Ödberg L, Stenius P (1988) Resin and fatty acids in kraft pulp washing. Physical state, colloid stability and washability. Nord Pulp Pap Res J 3:100–106
353. Claus W, Schmiedeknecht H (1966) Heterogeneous reaction between aqueous sodium hydroxide, carbon disulfide, and cellulose. V. Influence of wetting agents on the xanthation in emulsion. Faserforsch Textiltech 17:571–576
354. Schwaighofer A, Zuckerstätter G, Schlagnitweit J, Sixta H, Müller N (2011) De-termination of the xanthate group distribution on viscose by liquid-state 1H NMR spectroscopy. Anal Bioanal Chem 400:2449–2456
355. Lanieri DB, Olmos GV, Alberini IC, Maximino MG (2014) Rapid estimation of gamma number of viscose by UV spectroscopy. Papel 75:60–65
356. Koutu BB, Bhagwat VW (1999) Study of xanthate group distribution during ripening of viscose. Indian J Chem Technol 6:172–175
357. Bockno GC (1980) Viscose rayon and method of making same. US 4242405 A, CAN94:85590
358. Bockno GC (1981) Method of making viscose rayon. US 4388260 A
359. http://www.engr.utk.edu/mse/Textiles/Rayon%20fibers.htm. Accessed 10 Jan 2015
360. http://www.fibersource.com/f-tutor/rayon.htm.accessed. Accessed 10 Jan 2015
361. Strunk P, Lindberg Å, Eliasson B, Agnemo R (2012) Chemical changes of cellulose pulps in the processing of viscose dope. Cellul Chem Technol 46:559–569
362. Östberg L, Haakansson H, Germgaard U (2012) Some aspects of the reactivity of pulp intended for high-viscosity viscose. BioResources 7:743–755
363. Philipp B, Liu K-T (1959) On the group distribution in fibrous cellulose xanthate and viscoses. Faserforsch Textiltech 10:555–562
364. Cornell RH (1961) Uniformity of substitution during the emulsion xanthation of cellulose. J Appl Polym Sci 5:364–369
365. Khanna RK, Moore MH (1999) Carbamic acid: molecular structure and IR spectra. Spectrochim Acta, Part A 55A:961–967
366. Dijkstra ZJ, Doornbos AR, Weyten H, Ernsting JM, Elsevier CJ, Keurentjes JTF (2007) Formation of carbamic acid in organic solvents and in supercritical carbon dioxide. J Supercrit Fluids 41:109–114
367. Sima T, Guo S, Shi F, Deng Y (2002) The syntheses of carbamates from reactions of primary and secondary aliphatic amines with dimethyl carbonate in ionic liquids. Tetrahedron Lett 43:8145–8147
368. Nozawa Y, Higashide F (1981) Partially carbamate reaction of cellulose with urea. J Appl Polym Sci 26:2103–2107
369. Nada AMA, Kamel S, El-Sakhawy M (2000) Thermal behavior and infrared spectroscopy of cellulose carbamates. Polym Degrad Stab 70:347–355
370. Chen G-M (2001) Study on nitrogen content of cellulose carbamates by Fourier transform infrared spectroscopy. Asian J Chem 13:93–98

371. Guo Y, Zhou J, Song Y, Zhang L (2009) An efficient and environmentally friendly method for the synthesis of cellulose carbamate by microwave heating. Macromol Rapid Commun 30:1504–1508
372. Guo Y, Zhou J, Wang Y, Zhang L, Lin X (2010) An efficient transformation of cellulose into cellulose carbamates assisted by microwave irradiation. Cellulose 17:1115–1125
373. Hearon WM, Hiatt GD, Fordyce CR (1943) Carbamates of cellulose and cellulose acetate. I. Preparation. J Am Chem Soc 65:829–833
374. Hall DM, Horne JR (1973) Preparation of cellulose triacetate and cellulose tricarbanilate by nondegradative methods. J Appl Polym Sci 17:3729–3734
375. Wood BF, Conner AH, Hill CG (1986) The effect of precipitation on the molecular weight distribution of cellulose tricarbanilate. J Appl Polym Sci 32:3703–3712
376. Terbojevich M, Cosani A, Camilot M, Focher B (1995) Solution studies of cellulose tricarbanilates obtained in homogeneous phase. J Appl Polym Sci 55:1663–1671
377. Evans R, Wearne RH, Wallis AFA (1989) Molecular weight distribution of cellulose as its tricarbanilate by high performance size exclusion chromatography. J Appl Polym Sci 37:3291–3303
378. Gan S, Zakaria S, Chia CH, Kaco H, Padzil FNM (2014) Synthesis of Kenaf cellulose carbamate using microwave irradiation for preparation of cellulose membrane. Carbohydr Polym 106:160–165
379. Valta K, Sivonen E (2005) Method for manufacturing cellulose carbamate. US 2005/0054848 A1
380. Valta K, Sivonen E (2010) Method for manufacturing cellulose carbamate, US 7,662,953 B2
381. Kunze J, Fink H-P (2005) Structural changes and activation by caustic soda with urea. Macromol Symp 223:175–187
382. Yin C, Li J, Xu Q, Peng Q, Liu Y, Shen X (2007) Chemical modification of cotton cellulose in supercritical carbon dioxide: synthesis and characterization of cellulose carbamate. Carbohydr Polym 67:147–154
383. Yin C, Shen X (2007) Synthesis of cellulose carbamate by supercritical CO2-assisted impregnation: structure and rheological properties. Eur Polym J 43:2111–2116
384. Zhang Y, Yin C, Zhang Y, Wu H (2013) Synthesis and characterization of cellulose carbamate from wood pulp, assisted by supercritical carbon dioxide. BioResources 8:1398–1408
385. Hearon WM, Hiatt GD, Fordyce CR (1943) Carbamates of cellulose and cellulose acetates. II Stability towards hydrolysis. J Am Chem Soc 65:833–836
386. Williamson SL, McCormick CL (1998) Cellulose derivatives synthesized via isocyanate and activated ester pathways in homogeneous solutions of lithium chloride/N, N-dimethylacetamide. J Macromol Sci Part A Pure Appl Chem A35:1915–1927
387. Shen X, Sugie N, Duan Q, Kitajyo Y, Satoh T, Kakuchi T (2005) Synthesis and characterization of cellulose carbamates having α-amino acid moieties. Polym Bull 55:317–322
388. Wallis AFA, Wearne RH (1990) Side reactions of phenylisocyanate during amine-catalyzed carabanilation of cellulose. Eur Polym J 26:1217–1220
389. Evans R, Wearne RH, Wallis AFA (1991) Effect of amines on the carbanilation of cellulose with phenyl isocyanate. J Appl Polym Sci 42:813–820
390. Mormann W, Michel U (2002) Improved synthesis of cellulose carbamates without by-products. Carbohydr Polym 50:201–208
391. Labafzadeh SR, Kavakka JS, Vyavaharkar K, Sievänen K, Kilpeläinen I (2014) Preparation of cellulose and pulp carbamates through a reactive dissolution approach. RSC Adv 4:22434–22441
392. Henniges U, Kloser E, Patel A, Potthast A, Kosma P, Fischer M, Fischer K, Rosenau T (2007) Studies on DMSO-containing carbanilation mixtures: chemistry, oxidations and cellulose integrity. Cellulose 14:497–511
393. Burchard W, Husemann E (1961) A comparative structure analysis of cellulose and amylose tricarbanilates in solution. Makromol Chem 44–46:358–387

394. Saake B, Patt R, Puls J, Philipp B (1991) Molecular weight distribution of cellulose. Papier (Bingen, Germany) 45:727–735
395. Stol R, Pedersoli JL Jr, Poppe H, Kok WT (2002) Application of size exclusion electrochromatography to the microanalytical determination of the molecular mass distribution of celluloses from objects of cultural and historical value. Anal Chem 74:2314–2320
396. Liebert T, Pfeiffer K, Heinze T (2005) Carbamoylation applied for structure determination of cellulose derivatives. Macromol Symp 223:93–108
397. Okamoto Y, Aburatani R, Hatada K (1987) Chromatographic chiral resolution. XIV. Cellulose tribenzoate derivatives as chiral stationary phases for high-performance liquid chromatography. J Chromatogr 389:95–102
398. Francotte E, Wolf RM (1992) Chromatographic resolution on methylbenzoylcellulose beads. Modulation of the chiral recognition by variation of the position of the methyl group on the aromatic ring. J Chromatogr 595:63–75
399. Okamoto Y, Kawashima M, Hatada K (1986) Controlled chiral recognition of cellulose triphenylcarbamate derivatives supported on silica gel. Controlled chiral recognition of cellulose triphenylcarbamate derivatives supported on silica gel. J Chromatogr 363:173–186
400. Okamoto Y, Kaida Y (1990) Polysaccharide derivatives as chiral stationary phases in HPLC. J High Resolut Chromatogr 13:708–712
401. Yashima E, Fukaya H, Okamoto Y (1994) (3,5-Dimethylphenyl)carbamates of cellulose and amylose regioselectively bonded to silica gel as chiral stationary phases for high-performance liquid chromatography. J Chromatogr A 677:11–19
402. Kubota T, Yamamoto C, Okamoto Y (2003) Preparation of chiral stationary phase for HPLC based on immobilization of cellulose 3,5-dimethylphenylcarbamate derivatives on silica gel. Chirality 15:77–82
403. Acemoglu M, Küsters E, Baumann J, Hernandez I, Mak CP (1998) Synthesis of regioselectively substituted cellulose derivatives and applications in chiral chromatography. Chirality 10:294–306
404. Klemm D, Heublein B, Fink H-P, Bohn A (2005) Cellulose: Fascinating biopolymer and sustainable raw material. Angew Chem Int Ed 44:3358–3393
405. Cai J, Zhang L, Zhou J, Qi H, Chen H, Kondo T, Chen X, Chu B (2007) Multifilament fibers based on dissolution of cellulose in NaOH/urea aqueous solution: structure and properties. Adv Mater 19:821–825
406. Borbély É (2008) Lyocell, the new generation of regenerated cellulose. Acta Polytech Hung 5:11–18
407. Rose M, Palkovits R (2011) Cellulose-based sustainable polymers: state of the art and future trends. Macromol Rapid Commun 32:1299–1311
408. Huttunen JI, Turunen O, Mandel L, Eklund V, Ekman K (1982) Alkali-soluble cellulose derivative. EP 57105 A2 19820804, CAN97:146443
409. Voges M, Brück M, Fink H-P, Gensrich J (2000) The CarbaCell process—an environmentally friendly alternative for cellulose man-made fiber production. In: Proceedings of the Akzo-Nobel Cellulosic Man-made Fibre Seminar, Stenungsund, pp 13–15
410. Fink H-P, Gensrich J, Rihm R, Voges M, Brück M (2001) Structure and properties of CarbaCell-type cellulosic fibres. In: Proceedings of the 6th Asian Textile Conference, Hong Kong, 1–7
411. Fu F, Xu M, Wang H, Wang Y, Ge H, Zhou J (2015) Improved synthesis of cellulose carbamates with minimum urea based on an easy scale-up method. ACS Sustainable Chem Eng 3:1510–1517
412. Fu F, Yang Q, Zhou J, Hu H, Jia B, Zhang L (2014) Structure and properties of regenerated cellulose filaments prepared from cellulose carbamate-NaOH/ZnO aqueous solution. ACS Sustainable Chem Eng 2:2604–2612

# Chapter 6
# Etherification of Cellulose

Cellulose ethers are of huge importance and produced commercially in large scales; the worldwide consumption of cellulosic ethers in 2006 was estimated to be 637,000 t. A non-exhaustive list of the industrially most important cellulose ethers together with their commonly used abbreviations is provided below (Table 6.1). Most technical cellulose ethers are nontoxic, odor- and tasteless, nonflammable, and most importantly well soluble in water. These features predestine them for the use, e.g., as solution thickeners, protective colloids, flow-control agents, water binders, film formers, liquid crystals, or thermoplastics. They are employed in many industrial fields, including paints, building materials, oil recovery, ceramics, and textiles, and they are also approved for the applications in food, cosmetics, and pharmaceutics (see E-numbers in Table 6.1 as well as Tables 6.2 and 6.3).

The following chapter discusses cellulose ethers based on their chemical structure, namely, ionic alkyl ethers (6.1), nonionic alkyl ethers (6.2), and silyl ethers of cellulose (6.3). These derivatives are basically obtained by reaction of cellulose with an etherifying agent (e.g., alkyl/silyl chlorides or bromides, oxiranes, vinyl compounds; Fig. 6.1), either in a heterogeneous or homogeneous reaction.

Homogeneous procedures, in which cellulose or a cellulose derivative (e.g., regioselectively substituted with a protection group; see Sect. 4.4) is dissolved in an organic solvent, have been employed in lab-scale processes for obtaining cellulose ethers with well-defined molecular structures in terms of overall DS and distribution of functional groups within the AGU (regioselective vs. random) and/or along the polymer chain (nonuniform vs. statistical substitution).

In large-scale production, cellulose ethers are prepared exclusively under heterogeneous conditions by a slurry process (Sect. 4.3). Therein, cellulose is swollen in a mixture of aqueous NaOH of different concentrations in the range from about 15–50% and an organic solvent (usually an alcohol, e.g., isopropanol). The alkali acts as activator by weakening the hydrogen bonds within the cellulose crystallites, thus making the individual polymer chains accessible for a uniform



T. Heinze et al., *Cellulose Derivatives*, Springer Series on Polymer and Composite Materials, https://doi.org/10.1007/978-3-319-73168-1_6

**Table 6.1** Overview of important commercial cellulose ethers

| Cellulose ether | Abbreviation | E-Number[a] |
|---|---|---|
| *Ionic ethers* | | |
| Carboxymethyl cellulose | CMC | 466 |
| *Alkyl ethers* | | |
| Methyl cellulose | MC | 461 |
| Ethyl cellulose | EC | 462 |
| Ethylmethyl cellulose | EMC | 465 |
| *Hydroxyalkyl ethers* | | |
| Hydroxyethyl cellulose | HEC | – |
| Hydroxypropyl cellulose | HPC | 463 |
| *Mixed ethers* | | |
| Hydroxyethylmethyl cellulose | HEMC | – |
| Hydroxypropylmethyl cellulose | HPMC | 464 |
| Hydroxypropyl hydroxyethyl cellulose | HPHEC | – |
| Ethylhydroxyethyl cellulose | EHEC | 467 |
| Hydroxybutylmethyl cellulose | HBMC | – |
| Hydrophobically modified hydroxyethyl cellulose | HMHEC | – |
| Carboxymethyl hydroxyethyl cellulose | CMHEC | – |

[a]E-numbers are codes used by the European Food Safety Authority to designate substances that are permitted to be used as food additives

chemical modification (Fig. 6.2). Moreover, the alkali increases the nucleophilicity of the hydroxyl groups of cellulose. The organic solvent acts as a diluent to

(i) effectively disperse the polymer,
(ii) promote distribution of the alkylation reagent,
(iii) transfer heat during the reaction, and
(iv) facilitate recovery of the reaction product.

A general concern in the slurry process is the hydrolysis of the alkylation agent, resulting in reagent loss and formation of by-products. However, the side reactions can be controlled to a certain extent by alteration of the reaction conditions, reactivity of the alkylating reagent, the amount of water, and addition of catalysts. The differences and similarities of heterogeneous and homogeneous etherification processes will be exemplified in the following (Sect. 6.1.1) for carboxymethyl cellulose (CMC) as one of the most important commercial ethers. In addition, it will be demonstrated how the molecular structure of cellulose ether can be characterized, in particular the distribution of substituents within the AGU as well as along the individual repeating units along the polymer chain.

**Table 6.2** Typical application fields of cellulose ethers

| Application | Cellulose ether[a] | | | | | | |
|---|---|---|---|---|---|---|---|
| | MC | MHEC | MHPC | EHEC | HEC | HPC | CMC |
| Glue | | + | + | + | | | + |
| Paints, coatings | | + | + | + | + | | + |
| Building materials | | + | + | + | + | | + |
| Ceramics | | | + | | | | + |
| Petroleum production, mining | | | | | | | + |
| Films | + | | | | + | + | |
| Textiles | + | | + | | | | + |
| Paper | | + | + | | + | | + |
| Suspension polymerization | | | + | | + | + | |
| Cable production | | | | | | | + |
| Agriculture | + | | | | + | | + |
| Grocery | + | | + | | | | + |
| Tobacco industry | + | | + | + | + | | + |
| Pharmaceutical industry | + | | + | + | | + | + |
| Laundry products | | + | + | | + | | + |
| Cosmetics | + | | + | | + | | + |

[a]*MC* Methyl cellulose, *MHEC* Methylhydroxyethyl cellulose, *MHPC* Methylhydroxypropyl cellulose, *EHEC* Ethylhydroxyethyl cellulose, *HEC* Hydroxyethyl cellulose, *HPC* Hydroxypropyl cellulose, *CMC* Carboxymethyl cellulose

## 6.1 Ionic Cellulose Ethers

### *6.1.1 Anionic Cellulose Ethers*

CMC, in the form of its sodium salt, is the most important commercialized ionic cellulose ether, with an estimated worldwide consumption of 355,000 t in 2006. It finds use, among others, as additive (e.g., solution thickener, stabilizer, dispersion agent, and emulsifier) in food, beverages, cosmetics, and drug formulations, as viscosity modifier and water retention agent in drilling fluids, as well as for paper and textile processing. Owing to its anionic nature, CMC readily dissolves in water and aqueous alkali starting at DS values around 0.4. Moreover, no complete carboxymethylation can be achieved due to electrostatic repulsion of the reagent and the increasingly charged cellulose chains. The maximum DS, which has been obtained for CMC in a one-step reaction, is ca. 1.3–1.4. By subsequent conversion of CMC, it may be increased up to 2.9. Carboxymethylation of cellulose is achieved by conversion of the polysaccharide with chloroacetatic acid or the corresponding sodium salt in the presence of a base. The molecular structure of CMC, in particular the overall DS, the distribution of carboxymethyl moieties within the AGU (regioselectivity), and the substitution pattern along the polymer chain are determined

**Table 6.3** Comparison of properties, action, and application of cellulose ethers

| | Property | Hydrophile | Solubility | Amphiphile | Association | Ion |
|---|---|---|---|---|---|---|
| | Action | Swelling, water retention | Viscosity, flow behavior | Surface activity, solubility behavior | Film formation, binding ability | Complex formation, salt instability |
| Application | | | | | | |
| Glue | | + | + | + | + | + |
| Paints, coatings | | + | + | | + | |
| Building materials | | + | + | + | + | |
| Ceramics | | + | + | + | + | |
| Petroleum production, mining | | + | + | + | + | + |
| Films | | | + | | + | |
| Textiles | | | + | + | + | |
| Paper | | | + | + | + | |
| Suspension polymerization | | | | + | | |
| Cable production | | + | | | | |
| Agriculture | | + | + | + | + | + |
| Grocery | | + | + | + | | + |
| Tobacco industry | | | | + | + | |
| Pharmaceutical industry | | + | + | + | + | |
| Laundry products | | | | + | | + |
| Cosmetics | | + | + | + | | + |

not only by the reaction conditions (time, temperature, and amount of reagent) but also on the derivatization process (Fig. 6.3).

The heterogeneous slurry process for the preparation of CMC, in which cellulose is activated and swollen in a mixture of aqueous NaOH and isopropanol (Fig. 6.3), results in a uniform derivatization along the polymer chains and yields products with DS values in the range of 0.5–1.3 [1–3]. Due to the heterogeneous nature of this procedure, different process parameters (e.g., stirring speed, heating/cooling rates, and reactor dimension) can greatly affect the outcome of the derivatization. Nevertheless, the slurry process is well established on an industrial scale and yields products with controllable batch properties. The carboxymethyl group can be introduced at three different hydroxyl groups within the AGU (*O*-2, *O*-3, and *O*-6). This means that the produced CMC may contain, in principle, up to eight components, including the unsubstituted, partially, or fully functionalized repeating

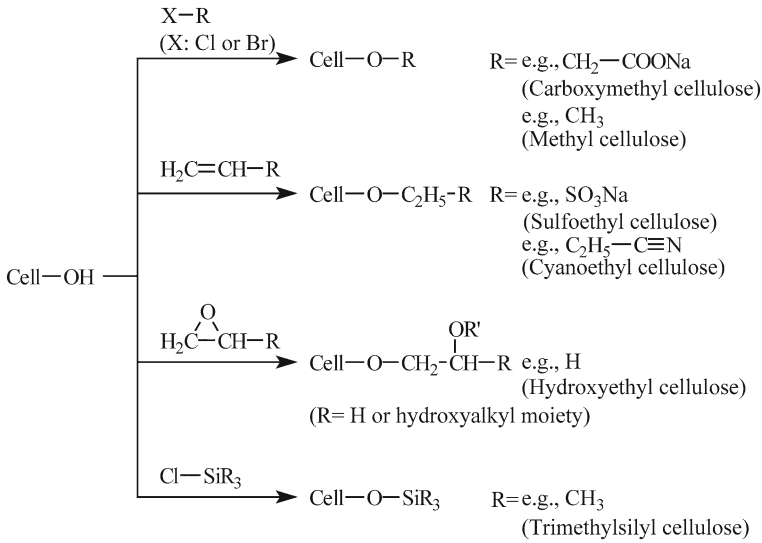


**Fig. 6.1** General routes for the etherification of cellulose and typical examples of the cellulose ethers obtained

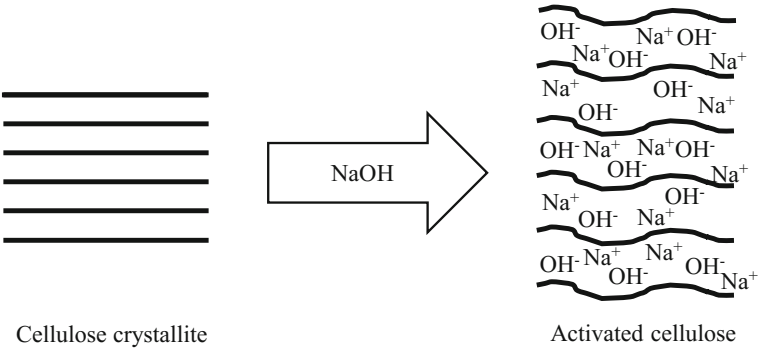


**Fig. 6.2** Schematic illustration for the conversion of a cellulose crystallite into activated cellulose by aqueous NaOH

units (unmodified AGU; 2-, 3-, and 6-mono-*O*-carboxymethyl unit; 2,3-, 2,6-, and 3,6-di-*O*-carboxymethyl unit; 2,3,6-tri-*O*-carboxymethyl unit; Fig. 6.4). For heterogeneously prepared CMC samples, it was revealed by means of $^{1}$H- and $^{13}$C NMR spectroscopy [4–6] as well as high-pH anion exchange chromatography with pulsed amperometric detection of hydrolytically degraded samples [7] that the carboxymethyl moieties are distributed within the AGU according to the reactivity order: $O\text{-}2 \geq O\text{-}6 > O\text{-}3$. The relative proportion of the individual repeating units as function of the overall DS can be obtained by mathematical processing of the $^{13}$C NMR spectra [5] (Fig. 6.4b). This technique is somewhat laborious and limited in

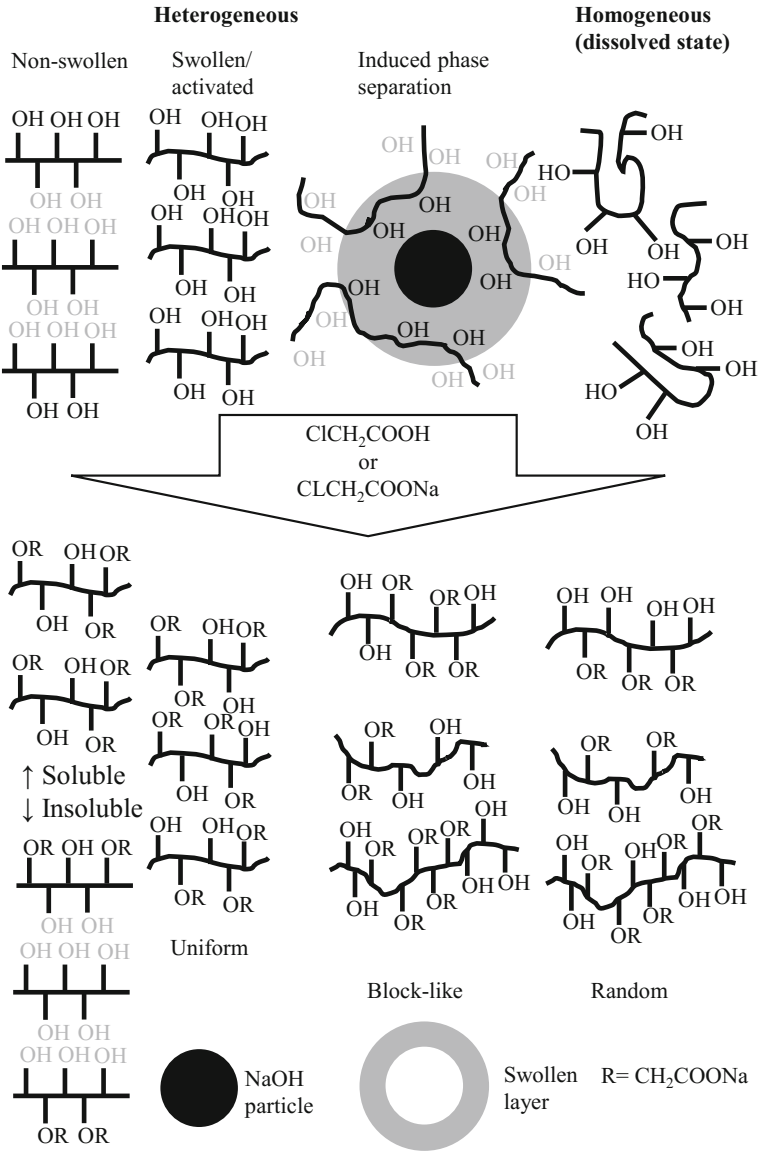


**Fig. 6.3** Schematic representation of the different processes for carboxymethylation of cellulose and their effect on the molecular structure of the products obtained

terms of resolution. Similar quantitative information can be obtained by complete hydrolysis of the cellulose ether, e.g., in perchloric acid, and HPLC analysis of the sugars released [8, 9]. Thereby, the mole fractions of un-, mono-, di-, and tri-carboxymethylated units as well as of glucose are quantified. The different

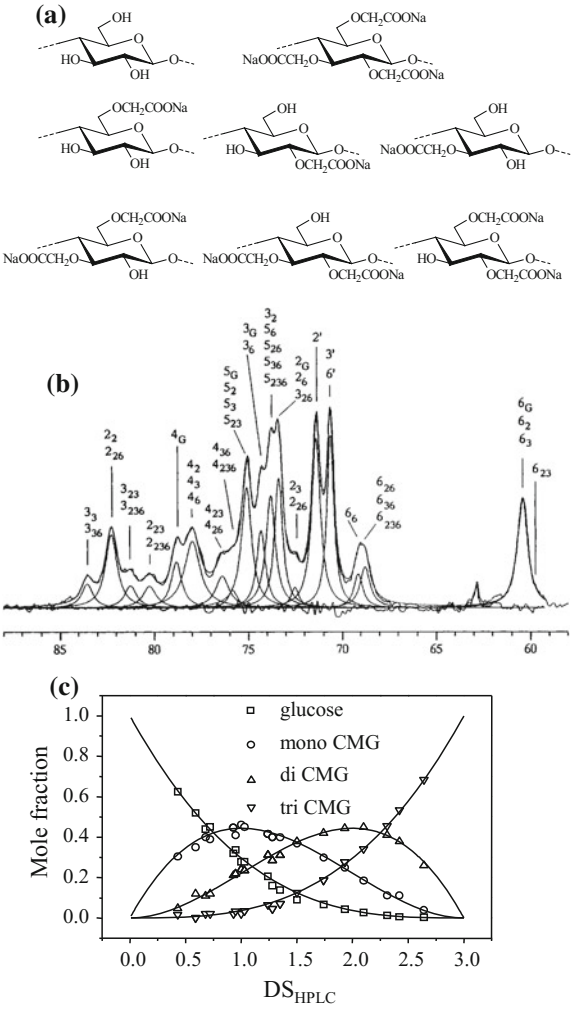


**Fig. 6.4** **a** Different repeating units present in carboxymethyl cellulose (CMC) at degree of substitution (DS) <3. **b** Deconvolution of a quantitative $^{1}$H-decoupled $^{13}$C NMR spectra of a heterogeneously prepared CMC with a DS of 1.19 with the carbon atoms of the eight different monomer units assigned, adapted from [4]. **c** Mole fractions of glucose, mono-*O*-carboxymethyl glucoses (CMG), di-*O*-CMG, and tri-*O*-CMG in hydrolyzed carboxymethyl cellulose samples (heterogeneous synthesis) plotted as function of DS$_{HPLC}$ determined by means of HPLC

positions of both the mono- and dicarboxymethylated units are not discriminated in this method. Under the assumptions that reactivity of the carboxymethylation is not affected by (i) the position of the repeating units along the polymer chains and (ii) the amount of carboxymethyl moieties already attached to the repeating unit, the statistical functionalization pattern can be predicted as a function of the overall DS by a binomial distribution (Eq. 6.1).

$$c_i = \binom{3}{k}\left(\frac{DS}{3}\right)^{k}\left(1-\frac{DS}{3}\right)^{3-k} \tag{6.1}$$

($c_i$) represents the mole fractions of unsubstituted, mono-, di-, and trisubstituted glucose units, respectively, ($k$) is the number of substituents per AGU ($k$ = 0, 1, 2, 3), and DS is the average degree of substitution.

For a broad variety of CMC samples prepared by the conventional slurry process, no significant deviation from the predicted theoretical pattern could be detected [8, 10]. Representative results are depicted in Fig. 6.4c for CMC samples within a wide DS range prepared under heterogeneous conditions using aqueous NaOH of mercerization concentration.

Activation with aqueous NaOH is a crucial step for the etherification of cellulose. Using alkali concentration in the range of 5–30% (w/v), an optimum is reached at 15% (w/v) (Table 6.4). Surprisingly, the mole fractions of the non-, partially-, and fully carboxymethylated sugar units, which were determined by means of HPLC after hydrolysis, are in good agreement with the statistical model independent of the concentration of the aqueous NaOH used [9]. This means that heterogeneous carboxymethylation in the slurry medium is determined by statistics even at low degree of activation.

Aqueous cellulose solvents, such as $Ni(tren)(OH)_2$ [11], offer the possibility for a completely homogeneous carboxymethylation of the biopolymer (Fig. 6.3d). In case of a careful addition of an aqueous NaOH up to concentrations of 31% (w/v), neither gelation nor precipitation of the cellulose occurs. No regeneration was observed during the subsequent addition of 36% (w/v) aqueous sodium monochloroacetate. This totally homogeneous procedure gives a maximum DS of 0.54 at a molar ratio AGU:NaOH:sodium monochloroacetate of 1:20:10 (Table 6.5). The stepwise addition of reagents leads to a slight increase of the DS to 0.71 due to a diminished hydrolysis of the sodium monochloroacetate, which is an important side reaction during the etherification. Nevertheless, with respect to the reaction efficiency, i.e., relation of total DS versus the molar excess of etherifying agent, the carboxymethylation in the aqueous solvent is less effective compared to the heterogeneous conversion in a slurry medium [12].

CMC samples, which were prepared homogeneously in $Ni(tren)(OH)_2$, show a similar structure compared to samples obtained by heterogeneous carboxymethylation in a slurry medium, with respect to the distribution of substituents within the AGU as well as the relative mole fractions of non-, mono-, di-, and tri-functionalized

**Table 6.4** Dependence of the degree of substitution (DS) of carboxymethyl cellulose on the concentration of aqueous NaOH (reaction of spruce sulfite pulp, DP 650, in isopropanol and aqueous NaOH with monochloroacetic acid (2 mol per Mol AGU) for 5 h at 55 °C)

| NaOH concentration (%, w/v) | $DS_{CM}$ |
|---|---|
| 5 | 0.59 |
| 8 | 0.93 |
| 10 | 1.00 |
| 15 | 1.24 |
| 20 | 1.03 |
| 30 | 0.95 |

**Table 6.5** Conditions for and results of the homogeneous carboxymethylation of cellulose in $Ni(tren)(OH)_2$ including HPLC analyses after hydrolysis, values in brackets represent calculated values according to Eq. 6.1 [12]

| Reaction conditions | | | | Carboxymethyl cellulose | | | | | |
|---|---|---|---|---|---|---|---|---|---|
| | | | | HPLC mole fraction after hydrolysis[a] | | | | | |
| Solvent | Molar ratio[b] | Time (h) | Temperature (°C) | DS | Soluble in water | Glc | Mono-CMG | Di-CMG | Tri-CMG |
| $Ni(tren)(OH)_2$ | 1:5:2.5 | 3 | 80 | 0.11 | No | 0.789 (0.796) | 0.199 (0.189) | 0.012 (0.015) | 0.00 (0.000) |
| $Ni(tren)(OH)_2$ | 1:10:5 | 3 | 80 | 0.25 | No | 0.890 (0.894) | 0.107 (0.102) | 0.00 (0.003) | 0.00 (0.000) |
| $Ni(tren)(OH)_2$ | 1:20:10 | 3 | 80 | 0.54 | Yes | 0.765 (0.770) | 0.216 (0.210) | 0.020 (0.019) | 0.000 (0.001) |
| $Ni(tren)(OH)_2$ | 1:40:20 | 3 | 80 | 0.50 | Yes | 0.574 (0.551) | 0.333 (0.363) | 0.072 (0.080) | 0.020 (0.006) |
| $Ni(tren)(OH)_2$ | 1:20:10 | 24 | 80 | 0.44 | Yes | 0.564 (0.579) | 0.367 (0.347) | 0.070 (0.069) | 0.00 (0.005) |
| $Ni(tren)(OH)_2$ | 1:40:20[c] | 4 | 80 | 0.71 | Yes | 0.634 (0.621) | 0.310 (0.320) | 0.082 (0.055) | 0.047 (0.003) |
| NaOH/urea[d] | 1:28.4:1.7 | 5 | 55 | 0.05 | No | 0.900 (0.951) | 0.055 (0.048) | 0.000 (0.001) | 0.000 (0.000) |
| NaOH/urea[d] | 1:28.4:3.4 | 5 | 55 | 0.10 | No | 0.869 (0.903) | 0.103 (0.094) | 0.000 (0.003) | 0.000 (0.000) |
| NaOH/urea[d] | 1:28.4:6.8 | 5 | 55 | 0.25 | Yes | 0.770 (0.770) | 0.212 (0.210) | 0.018 (0.019) | 0.000 (0.001) |
| NaOH/urea[d] | 1:28.4:10.2 | 5 | 55 | 0.29 | Yes | 0.692 (0.737) | 0.249 (0.237) | 0.022 (0.025) | 0.000 (0.001) |
| NaOH/urea[d] | 1:28.4:13.6 | 5 | 55 | 0.32 | Yes | 0.692 (0.737) | 0.249 (0.237) | 0.022 (0.025) | 0.000 (0.001) |

(continued)

**Table 6.5** (continued)

| Reaction conditions | | | | Carboxymethyl cellulose | | | | | |
|---|---|---|---|---|---|---|---|---|---|
| | | | | HPLC mole fraction after hydrolysis[a] | | | | | |
| Solvent | Molar ratio[b] | Time (h) | Temperature (°C) | DS | Soluble in water | Glc | Mono-CMG | Di-CMG | Tri-CMG |
| NaOH/urea[d] | 1:28.4:6.8 | 5 | 25 | 0.05 | No | 0.906 (0.951) | 0.055 (0.048) | 0.000 (0.001) | 0.000 (0.000) |
| NaOH/urea[d] | 1:28.4:6.8 | 5 | 75 | 0.20 | Yes | 0.722 (0.813) | 0.188 (0.174) | 0.008 0.013 | 0.000 (0.000) |
| NaOH/urea[d] | 1:14.2:6.8 | 5 | 55 | 0.36 | Yes | 0.621 (0.681) | 0.290 (0.279) | 0.035 (0.038) | 0.000 (0.002) |
| NaOH/urea[d] | 1:7.1:6.8 | 5 | 55 | 0.50 | Yes | 0.562 (0.579) | 0.322 (0.347) | 0.084 (0.069) | 0.002 (0.005) |
| NaOH/urea[d] | 1:5.5:6.8 | 5 | 55 | 0.62 | Yes | 0.514 (0.499) | 0.331 (0.390) | 0.123 (0.102) | 0.015 (0.009) |
| NaOH/urea[d] | 1:3.6:3.4 | 5 | 55 | 0.36 | Yes | 0.669 (0.681) | 0.255 (0.279) | 0.054 (0.038) | 0.000 (0.002) |
| LiOH/urea[e] | 1:7.5:1 | 5 | 55 | 0.10 | No | | | | |
| LiOH/urea[e] | 1:7.5:3 | 5 | 55 | 0.26 | No | | | | |
| LiOH/urea[e] | 1:7.5:6 | 5 | 55 | 0.50 | Yes | | | | |
| LiOH/urea[e] | 1:7.5:9 | 5 | 55 | 0.65 | Yes | | | | |
| LiOH/urea[e] | 1:7.5:6 | 3 | 55 | 0.42 | Yes | | | | |
| LiOH/urea[e] | 1:7.5:6 | 7 | 55 | 0.60 | Yes | | | | |
| LiOH/urea[e] | 1:7.5:6 | 17 | 55 | 0.61 | Yes | | | | |

[a]*Glc* Glucose, *CMG* carboxymethyl glucose
[b]Mole anhydroglucose unit:NaOH (20% in water):sodium monochloroacetate
[c]Addition in four steps
[d]7% (w/w) NaOH, 12% (w/w) urea
[e]4.6% (w/w) LiOH, 12% (w/w) urea

repeating units. Structure analysis of the homogeneously prepared CMC samples, carried out by means of $^1$H NMR spectroscopy and HPLC (both after complete hydrolytic depolymerization), indicated a distinct distribution of substituent within the AGU following a reactivity order of *O*-2 > *O*-6 > *O*-3 (e.g., for a sample with DS 0.44: $DS_{O\text{-}2}$ = 0.17; $DS_{O\text{-}6}$ = 0.19; $DS_{O\text{-}2}$ = 0.08). An analogous substitution pattern within the AGU was observed for CMC prepared in totally heterogeneous reactions (slurry process) [4, 13]. The amounts of sugars that are released upon acid hydrolysis of homogeneously prepared CMC show a good correlation with the theoretically predicted values for a statistical substitution (Table 6.5) [5]. Despite their differences in terms of the state of dissolution of cellulose and the inter-/intramolecular hydrogen bond network, completely homogeneous carboxymethylation on one hand and heterogeneous conversions, after previous activation with aqueous NaOH, on the other hand, yields CMC with an even distribution of substituents (see e.g., [3, 9]). Thus, it can be concluded that carboxymethylation of cellulose under these conditions is not diffusion controlled.

In the quest for environmentally friendly polysaccharide solvents, aqueous systems composed of an alkali (NaOH, LiOH) in combination with gelation preventing additives (urea, ZnO) have been considered for etherification of cellulose. Cellulose dissolves in these solvents at low temperatures, i.e., homogeneous carboxymethylation is feasible. The reaction efficiency of these reactions is higher compared to the likewise homogeneous conversion in Ni(tren)$(OH)_2$ (Table 6.5). A crucial factor is the ratio of NaOH to sodium monochloroacetate. The higher the alkali concentration, the more pronounced the hydrolysis, i.e., inactivation, of the carboxymethylation reagent. The ratio NaOH to sodium monochloroacetate can be shifted indirectly toward the later by increasing the cellulose concentration in the aqueous solution, which yields higher DS values. HPLC analysis revealed a statistical distribution of non-, mono-, di-, and tri-carboxymethylated repeating units, which is in accordance with results described before for the slurry process and homogeneous conversion in Ni(tren)$(OH)_2$. However, the distribution of CM moieties is different with a preferred conversion of the primary hydroxyl group according to *O*-6 > *O*-2 > *O*-3.

Nonaqueous cellulose solvents have been tested for the carboxymethylation as well but these approaches suffer from the incompatibility of NaOH and aprotic solvents. The first report on chemical modification of cellulose in IL, which was followed by many more, was a patent describing the carboxymethylation in the presence of solid NaOH catalyst [14]. DMSO can be added as a beneficial cosolvent; however, the maximum DS that can be achieved in this systems is limited to about 0.5 due to gelation of the reaction mixture [15]. This gelation process has been exploited for preparing CMC with high DS values and unique properties by using DMAc/LiCl to dissolved cellulose instead of an IL. As has been demonstrated by means of FTIR and polarizing light microscopy at solid–liquid interface, gelation in water-free DMAc/LiCl is due to the regeneration of cellulose II at the surface of the NaOH particles [6, 8, 10]. FTIR experiments with low molecular weight alcohols in the gas phase indicate that this “induced phase separation” termed process generates free OH groups (i.e., not or less involved in hydrogen bonds) in

direct vicinity of the inorganic particles. The conversion of cellulose, dissolved in DMAc/LiCl containing solid NaOH, with sodium monochloroacetate yields CMC with DS values as high as 2.2 in a one-step procedure. This value is significantly higher compared to the heterogeneous reaction and the carboxymethylation in $Ni(tren)(OH)_2$ or ILs.

Using $^{1}H$- and $^{13}C$ NMR spectroscopy, it was demonstrated that the CMC prepared via induced phase separation possess a much higher degree of etherification at positions 6 and 3 compared with conventionally prepared samples of similar total DS. A comparison of the mole fractions of the different repeating units, determined by HPLC after chain degradation, with values calculated by statistics [5], revealed that the amount of unmodified and fully converted tri-*O*-carboxymethylated AGU is significantly higher compared to the predicted value (Fig. 6.5). These results indicate that carboxymethylation via induced phase separation yields CMC with a gradient-like distribution of ether functions along the backbone, which is in contrast to the statistical distribution pattern of CMC prepared homogeneously or in the slurry process. It is assumed that carboxymethylation is limited to areas of the cellulose chain that are located in direct vicinity of the polymer–solid interface at the NaOH particles (Fig. 6.3c).

The synthesis concept of induced phase separation is not limited to cellulose dissolved in DMAc/LiCl. The reaction of cellulose dissolved in DMSO/TBAF trihydrate via activation with NaOH powder gives CMC of high DS of up to 2 possessing a nonstatistical content of the different repeating units (Table 6.6) [16, 17]. In contrast, utilization of aqueous NaOH yields a statistical substitution pattern. Carboxymethylation of cellulose dissolved in NMMO in combination with solid NaOH yields nonstatistical CMC with high DS that are comparable to the derivatives obtained in DMSO/TBAF [12].

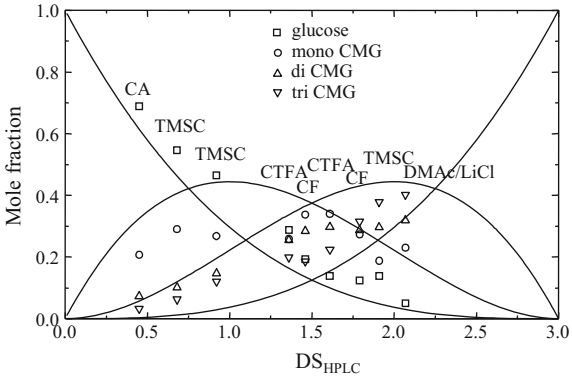


**Fig. 6.5** The mol fractions of glucose, mono-*O*-carboxymethyl glucoses, di-*O*-carboxymethyl glucoses, and 2,3,6-tri-*O*-carboxymethyl glucose in hydrolyzed carboxymethyl cellulose samples (polymers were synthesized via induced phase separation starting from cellulose acetate, CA, trimethylsilyl cellulose, TMSC, cellulose trifluoroacetate, CTFA, cellulose formate, CF dissolved in DMSO, and cellulose dissolved in DMAc/LiCl) plotted as function of degree of substitution ($DS_{HPLC}$) determined by means of HPLC

**Table 6.6** Conditions for and results of the carboxymethylation of cellulose in NMMO/DMSO and DMSO/TBAF × $3H_2O$ and the results of the HPLC analysis (after complete depolymerization) in comparison with statistic calculations (CMG, carboxymethyl glucose)

| Reaction conditions | | | | Mole fractions[a] | | | | $DS_{CMC}$ |
|---|---|---|---|---|---|---|---|---|
| Medium | Molar ratio[b] | Time (h) | Temperature (°C) | Glc | Mono- | Di- | Tri- | |
| DMSO/TBAF | 1:5:10 | 0.5 | 70 | 0.106 (0.061) | 0.267 (0.282) | 0.327 (0.434) | 0.299 (0.223) | 1.82 |
| DMSO/TBAF | 1:5:10 | 2 | 70 | 0.081 (0.035) | 0.215 (0.198) | 0.444 (0.305) | 0.30 (0.428)5 | 2.02 |
| DMSO/TBAF | 1:5:10 | 4 | 70 | 0.068 (0.028) | 0.198 (0.192) | 0.305 (0.442) | 0.428 (0.338) | 2.09 |
| DMSO/TBAF | 1:5:10 | 16 | 70 | 0.084 (0.048) | 0.253 (0.252) | 0.331 (0.442) | 0.332 (0.258) | 1.91 |
| DMSO/TBAF | 1:10:20 | 48 | 70 | – | – | – | – | 1.89 |
| NMMO | 1:10:20 | 2 | 80 | 0.772 (0.6815) | 0.130 (0.2788) | 0.066 (0.0380) | 0.031 (0.0017) | 0.36 |
| NMMO + 2 ml DMSO per g cellulose | 1:20:10 | 2 | 80 | 0.307 (0.1951) | 0.282 (0.4238) | 0.227 (0.3069) | 0.183 (0.0741) | 1.26 |
| NMMO + 2.5 ml DMSO per g cellulose | 1:20:10 | 2 | 80 | 0.419 (0.3191) | 0.295 (0.4436) | 0.198 (0.2056) | 0.087 (0.0317) | 0.95 |
| NMMO + 3 ml DMSO per g cellulose | 1:20:10 | 2 | 80 | 0.627 (0.4625) | 0.159 (0.4067) | 0.120 (0.1192) | 0.093 (0.0116) | 0.68 |

[a]Molar fractions of glucose (Glc), mono-, di-, and tri-*O*-carboxymethyl glucose; values in brackets represent theoretical values calculated according to the Spurlin statistic

[b]Molar ratio of anhydroglucose unit:NaOH:sodium monochloroacetate

Various cellulose intermediates (formed upon dissolution of cellulose in derivatizing solvents) and even cellulose derivatives of different hydrolytic stabilities react under water-free conditions to give products with a nonstatistic content of the repeating units. Solutions of cellulose trifluoroacetate ($DS_{CTFA}$ 1.5, DP 460), cellulose formate ($DS_{CF}$ 2.2, DP 260), commercial cellulose acetate ($DS_{CA}$ 1.8, DP 220), and trimethylsilyl cellulose ($DS_{TMS}$ 1.1, DP 220) in DMSO (5.7%, w/v, polymer) treated with solid NaOH particles suspended in DMSO show phase separation and formation of a reactive microstructure (see Fig. 6.3). Examples of the conditions and results of the described synthesis method are given in Table 6.7. Overall DS values of up to 2.2 can be obtained [18]. The addition of solid NaOH to the dissolved derivatives of cellulose results in a cleavage of the primary substituents, e.g., trifluoroacetate, and the formation of cellulose II that is regenerated on the solid particles. The particle size of the NaOH powder affects the overall DS but does not influence the distribution of the functional groups. The decrease in the size of NaOH particles from 1.00 mm to <0.25 mm increases the DS from 0.64 to 1.12 if the reaction is performed with cellulose trifluoroacetate (Table 6.7).

The analytical characterization of CMC, and cellulosic ethers in general, can be supplemented by subjecting the polysaccharide derivatives to endoglucanase treatment. The fragments obtained by selective cleavage of non-modified cellulose

**Table 6.7** Conditions for and results of the carboxymethylation of cellulose via induced phase separation starting from dissolved cellulose and cellulose derivatives (reaction temperature: 70 °C)

| Reaction conditions | | | Carboxymethyl cellulose | |
|---|---|---|---|---|
| Starting material | Molar ratio[a] | Time (h) | DS | Soluble in water |
| Cellulose in DMAc/LiCl | 1:2:4 | 48 | 1.13 | No |
| Cellulose in DMAc/LiCl | 1:4:8 | 48 | 1.88 | Yes |
| Cellulose in DMAc/LiCl | 1:5:10 | 48 | 2.07 | Yes |
| Cellulose trifluoroacetate/DMSO | 1:5:10 | 2 | 0.11 | No |
| Cellulose trifluoroacetate/DMSO | 1:10:20 | 4 | 1.86 | Yes |
| Cellulose trifluoroacetate/DMSO | 1:10:20 | 16 | 1.54 | Yes |
| Cellulose trifluoroacetate/DMSO | 1:10:20[b] | 4 | 0.62 | No |
| Cellulose trifluoroacetate/DMSO | 1:10:20[c] | 16 | 0.97 | No |
| Cellulose formate/DMSO | 1:10:20 | 2 | 1.46 | Yes |
| Cellulose formate/DMSO | 1:10:20 | 4 | 1.91 | Yes |
| Cellulose formate/DMSO | 1:20:40 | 2 | 2.21 | Yes |
| Trimethylsilyl cellulose/DMSO | 1:10:20 | 0.5 | 2.04 | Yes |
| Trimethylsilyl cellulose/DMSO | 1:10:20 | 1 | 1.91 | Yes |
| Trimethylsilyl cellulose/DMSO | 1:10:20 | 2 | 1.97 | Yes |
| Cellulose acetate/DMSO | 1:10:20 | 2 | 0.36 | No |
| Cellulose acetate/DMSO | 1:10:20 | 4 | 0.45 | No |

[a]Molar ratio anhydroglucose unit:NaOH:sodium monochloroacetate
[b]NaOH particle size: 0.63–1.00 mm
[c]NaOH particle size: 0.25–0.63 mm

units are separated by preparative SEC and hydrolyzed separately into the corresponding sugars that can be analyzed by means of anion exchange chromatography with pulsed amperometric detection. From the combined results, quantitative information on the substitution pattern along the polymer chain can be obtained. Samples with a DS of up to 1.9, prepared by the phase separation approach, were intensively degraded by the enzyme, which indicates a highly block-like functionalization pattern. Moreover, the highly carboxymethylated fragments were dominated by 2,3,6-tri-*O*-carboxymethyl glc units [19].

Cellulose ethers bearing sulfonate groups are strongly negative charged polyelectrolytes that are well soluble in water with a higher salt and pH tolerance compared to CMC. Nevertheless, these compounds are far less important on a commercial scale. Sulfoethyl cellulose (as sodium salt) is water soluble above DS > 0.3 and received certain interest due to its polyanionic nature. In combination with cationic polymers [e.g., chitosan, poly(dimethyldiallylammonium chloride)] or surfactants (e.g., benzyldodecyldimethylammonium chloride), the strong polyanion forms polyelectrolyte complexes in the form of flat membranes [20–22] or spherical hollow capsules [23] (Fig. 6.6). In addition, sulfoethyl cellulose has been studied as a strong cation exchanger [24] and superabsorbing material [25]. Mixed alkyl and hydroxyalkyl cellulose ethers with a small content of sulfoethyl moieties (DS 0.01–0.50) have been described in this context as well, e.g., as solution thickeners for dispersion paints [26], coatings [27], and construction materials such as cement and gypsum [28].

The synthesis of sulfoalkyl ethers of cellulose can be achieved by alkali activation of biopolymer and subsequent conversion with (Fig. 6.7)

(i) chloro/bromoalkane sulfonates, analogue to the carboxymethylation,
(ii) vinyl sulfonates, according to a Michael-type addition (compare cyanoethylation, Sect. 6.2.2), or
(iii) cyclic sulfonic acid esters (e.g., propane sultone).

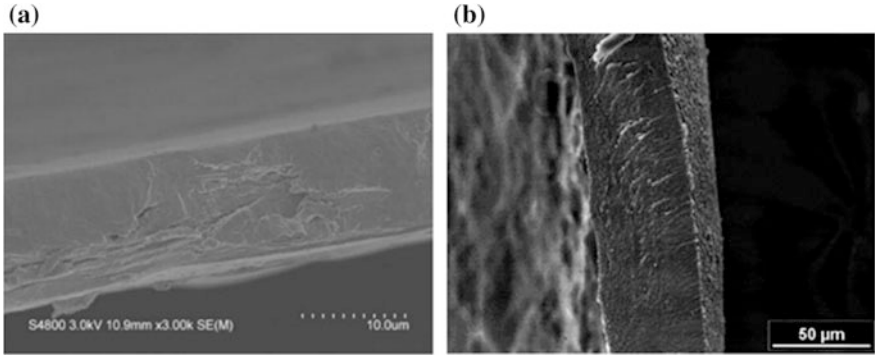


**Fig. 6.6** Scanning electron microscopy images of **a** chitosan–sulfoethyl cellulose symplex membrane (Reprinted (adapted) with permission from [20]. Copyright (2006) American Chemical Society) and **b** sulfoethyl cellulose-poly(dimethyldiallylammonium chloride) symplex capsule

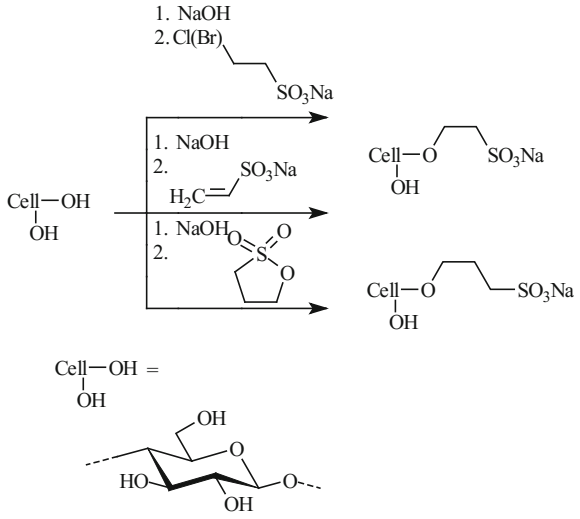


**Fig. 6.7** Synthesis of sulfoalkyl cellulose derivatives by conversion of cellulose with chloro-/bromoalkane sulfonates (top), vinyl sulfonates (middle), and cyclic sulfonic acid esters (bottom)

As has been described for CMC, sulfoethylation is usually performed heterogeneously in a slurry medium [29]. Activation with aqueous or solid NaOH is a key step and strongly affects the DS values reached (Table 6.8). The reaction medium influences the outcome of the derivatization reaction. The highest DS values were obtained in isopropanol, whereas solvents of low polarity such as cyclohexane and toluene were less efficient. The most reactive reagent for the preparation of sulfoethyl cellulose was found to be vinyl sulfonate followed by 2-bromoethanesulfonic acid. The corresponding chloro-compound yielded the lowest DS values. A water-soluble sulfoethyl ether with DS 0.5 was also prepared by homogeneous derivatization of cellulose in the solvent DMSO/$SO_2$/diethylamine [30].

### *6.1.2 Cationic Cellulose Ethers*

Two types of cationic cellulose ethers can be distinguished:

(i) Aminoalkyl ethers are "weak polycations" with functional groups that carry amino groups (mostly primary or tertiary), which can be protonated/deprotonated, i.e., the charge density is pH-dependent.
(ii) Quaternary tetraalkyl ammonium ethers of cellulose bear a permanent positive charge and can be classified as "strong polycations" (Fig. 6.8).

Compared to the anionic (in particular CMC, Sect. 6.1.1) and nonionic counterparts (Sect. 6.2), cationic cellulose ethers are far less common in scientific literature. In particular, early attempts (1960s–1980s) to synthesize cationic cellulose

**Table 6.8** Conditions for and results of the sulfoethylation of cellulose [29]

| Reaction medium | Reagent[a] | State of NaOH | Temperature (°C) | Time (h) | DS |
|---|---|---|---|---|---|
| Isopropanol | NaVS | Solution | 80 | 5 | 0.00 |
| Isopropanol | NaVS | Powder | 65 | 5 | 0.58 |
| Isopropanol | NaVS | Powder | 80 | 5 | 0.65 |
| Isopropanol | NaVS | Pellet | 65 | 5 | 0.47 |
| Isopropanol | NaVS | Pellet | 65 | 24 | 0.50 |
| Isopropanol | NaVS | Pellet | 80 | 3 | 0.46 |
| Isopropanol | NaVS | Pellet | 80 | 5 | 0.60 |
| Isopropanol | NaVS | Pellet | 80 | 24 | 0.33 |
| Cyclohexane | NaVS | Pellet | 80 | 5 | 0.31 |
| Toluene | NaVS | Pellet | 80 | 5 | 0.35 |
| n-Octanol | NaVS | Pellet | 80 | 5 | 0.33 |
| n-Butanol | NaVS | Pellet | 80 | 5 | 0.39 |
| Dioxane | NaVS | Pellet | 80 | 5 | 0.39 |
| Isopropanol | NaCES | Pellet | 80 | 3 | 0.12 |
| Isopropanol | NaCES | Pellet | 80 | 5 | 0.19 |
| Isopropanol | NaBES | Pellet | 65 | 5 | 0.17 |
| Isopropanol | NaBES | Pellet | 65 | 24 | 0.34 |
| Isopropanol | NaBES | Pellet | 80 | 5 | 0.31 |
| Isopropanol | NaBES | Pellet | 80 | 24 | 0.56 |

[a]*NaVS* Sodium vinylsulfonate, *NaCES* Sodium 2-chloroethane sulfonic acid monohydrate, *NaBES* Sodium 2-bromoethane sulfonic acid

ethers usually produced water-insoluble materials (fabrics, beads, or fibers) with a maximum DS $\approx$ 0.2. The main objective was to modify the surface properties of cellulosic fabrics and paper pulps or to obtain anion exchange materials for chromatography applications. In commercial applications, however, other cationic polysaccharide derivatives, in particular cationic starch ethers that are produced and employed in papermaking, textile processing, and cosmetics, play a much bigger role nowadays [31].

Aminoethyl (AE) cellulose is an ether with a primary aminoalkyl substituent. It has been obtained by reacting cellulose, dispersed in toluene, with aziridine and a small amount of benzyl chloride in an autoclave at 70 °C [32]. The reaction proceeds similar to the hydroxyalkylation of cellulose with oxiranes (see Sect. 6.2.3) but is of little interest nowadays due to the toxicity of aziridine. Alternatively, conversion of cellulose with 2-aminoethyl sulfuric acid in aqueous alkaline media yielded AE cellulose with a DS $\leq$ 0.17 [33]. These derivatives were studied as ion exchange material for chromatographic protein purification but found little use in this regard.

Tertiary aminoalkyl ethers of cellulose are much more common in scientific literature than their primary and secondary counterparts. Latter have not been reported up to now. Diethylaminoethyl (DEAE) cellulose, the most frequently

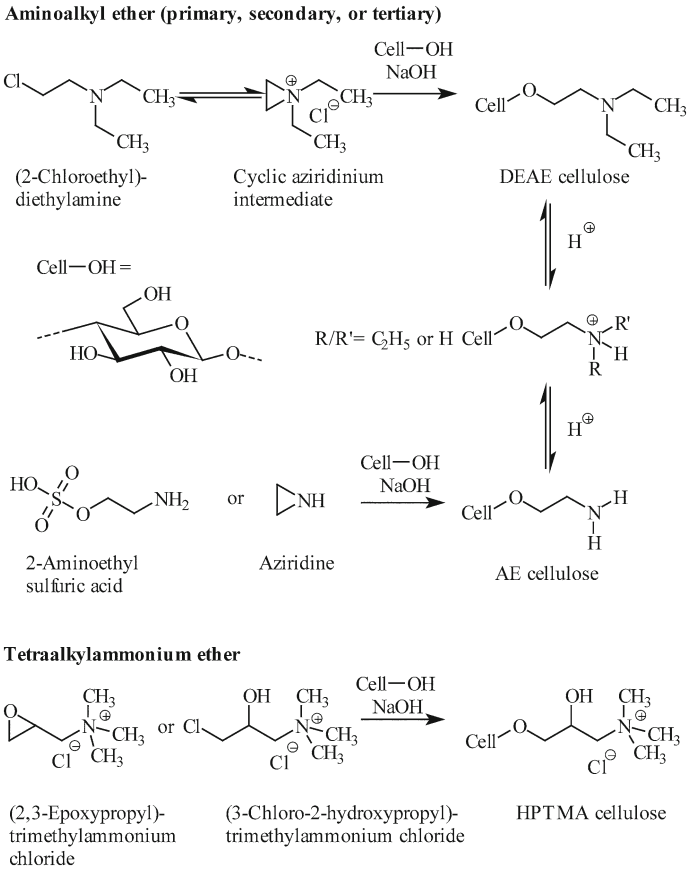


**Fig. 6.8** Reaction scheme for and molecular structure of diethylaminoethyl (DEAE), aminoethyl (AE), and hydroxypropyltrimethylammonium (HPTMA) cellulose

employed representative of this class, was prepared by alkali activation of cellulose and conversion with (2-chloroethyl) diethylamine hydrochloride [34, 35] (Table 6.9). The reaction is supposed to proceed via a cyclic aziridinium intermediate that is formed by intramolecular alkylation [36]. The DS values obtained depended on the alkali concentration and were rather low ($\leq 0.2$). *N*,*N*-Diethylepoxypropyl amine (DEEPA) was employed for the etherification of cellulose as well, activated by different procedures [37]. DEAE cellulose is frequently used as anion exchanger for the purification and immobilization of biomolecules such as proteins, DNA, and polysaccharides [38]. It is commercially available in the form of pre-swollen cellulosic beads ($\approx$0.1 $mmol_{DEAE}$/ml medium) or as dried fibrous material ($\approx$1 $mmol_{DEAE}$/g) [39].

An indirect approach for a homogeneous synthesis of tertiary aminoalkyl ethers is the conversion of CA, which is soluble in DMF, with an alkylation reagent,

**Table 6.9** Conditions for and results of the treatment of cotton fabrics with (2-chloroethyl) diethylamine hydrochloride [34, 35]

| NaOH concentration [% (w/w)] | Amine·HCl concentration [% (w/w)] | Time (min) | DS |
|---|---|---|---|
| 2 | 20 | 10 | 0.03 |
| 4 | 20 | 10 | 0.04 |
| 8 | 10 | 50 | 0.02 |
| 8 | 20 | 10 | 0.06 |
| 8 | 20 | 50 | 0.06 |
| 15 | 20 | 10 | 0.10 |
| 20 | 20 | 10 | 0.10 |
| 24 | 20 | 10 | 0.12 |

e.g., DEEPA, in the presence of water traces [40] (Fig. 6.9). Thereby, two simultaneous reactions occur. DEEPA acts as etherification reagent and likewise as basic catalyst for the hydrolysis of acetyl moieties. Depending on the reaction conditions, completely deacetylated products could be obtained within up to 4 h. In the same time, the hydroxyl groups were alkylated, which lead to an increase in the nitrogen content up to about 5%, corresponding to a $DS_{amine} \approx 1.0$. Solubility of the alkylated products strongly depends on the amount of acetyl groups as well as hydroxyalkyl amine moieties. Only products with a sufficiently low degree of acetylation (<15%) and a nitrogen content of 1–4% readily dissolved in water. Higher acetylated derivatives were found to be water insoluble, whereas a high $DS_{amine}$ induced gelation.

The primary and tertiary aminoalkyl ethers described above are partly/fully protonated or deprotonated, depending on the pH value of the system. On the contrary, quaternary cellulose ethers carry permanently charged cationic moieties. Two approaches can be utilized for the synthesis of the latter compounds.

(i) Cellulose ethers with tertiary amine moieties, e.g., prepared by etherification of cellulose with DEEPA, are quaternized with an alkylation reagent, e.g., ethyl iodide, to yield derivatives with permanently charged ammonium moieties [41]. However, alkylation of the hydroxyl groups of the cellulose backbone and the introduced hydroxyalkyl chains occurs as a side reaction and nonuniform derivatives are obtained.

(ii) A more convenient method for obtaining quaternary derivatives with a well-defined molecular structure is the conversion of cellulose with etherification reagents that already contain ammonium moieties.

Hydroxypropyltrimethylammonium (HPTMA) cellulose, the most common quaternary cationic cellulose ether with a permanent cationic charge, is prepared by treating cellulose with (3-chloro-2-hydroxypropyl) trimethylammonium chloride (CHPTMA Cl) or (2,3-epoxypropyl) trimethylammonium chloride (EPTMA Cl) in the presence of a base [42]. Both reagents and several others, which contain longer alkyl chains are commercially available as highly concentrated aqueous solutions

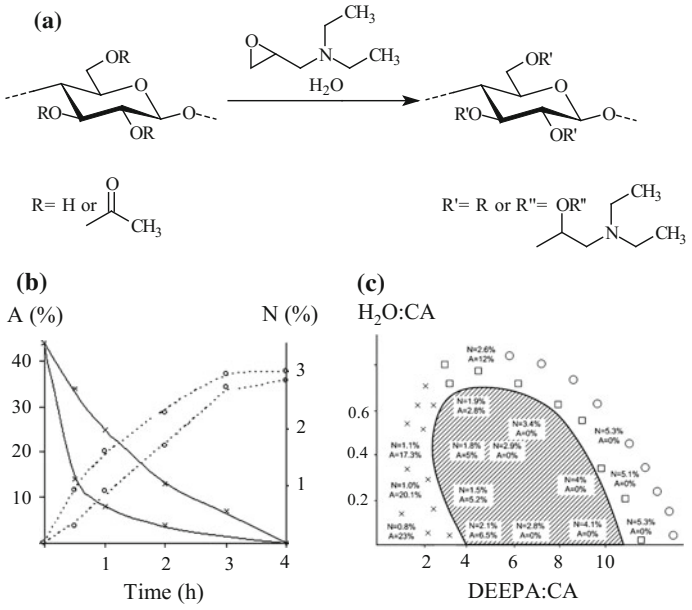


**Fig. 6.9** **a** Reaction scheme for the conversion of cellulose acetate (CA, degree of acetylation 1.73) with *N*,*N*-diethylepoxypropyl amine (DEEPA) into tertiary amino group containing ethers. **b** Changes of percentage of acetylation (A, %) and nitrogen (N, %) as a function of reaction time; 1 and 4: ratio CA:DMF:DEEPA:$H_2O$ of 1:20:8:1, 2 and 3: ratio CA:DMF:DEEPA:$H_2O$ of 1:20:8:0. **c** Dependence of the chemical composition and water solubility on the reaction conditions; shaded area represents water-soluble samples, *x* insoluble products, *Square* gelation in water, *Circle* gelation of the reaction mixture (compiled from [40], © Springer Science + Business Media B.V. 2009. With permission of Springer)

(≈70%) [43]. CHPTMA Cl generates the corresponding epoxide in situ but consumes a stoichiometric amount of NaOH in the process. It has been reported for the quaternization of starch that the epoxy reagent is more reactive in terms of reaction efficiency and maximum DS [41]. However, it is also more toxic and unstable toward hydrolysis. Another possibility to obtain quaternary ammonium ethers is the conversion of cellulose with epichlorohydrin in the presence of tertiary amines [44]. However, cross-linking occurs as one side reaction.

The heterogeneous quaternization techniques described have in common that only low DS values (<0.2) were targeted, i.e., no water-soluble derivatives were obtained. The procedures have mostly been studied on paper pulp, to improve papermaking [42] or cotton fabrics to improve the bleaching and dying process [45, 46]. Water-soluble cellulose ethers with a much higher content of cationic groups have been prepared by homogeneous derivatization of the polysaccharide (Table 6.10). Using DMAc/LiCl as reaction medium, quaternary cellulose ethers

**Table 6.10** Conditions for and results of the homogeneous quaternization of cellulose with (3-chloro-2-hydroxypropyl) trimethylammonium chloride (CHPTMA Cl) and (2,3-epoxypropyl) trimethylammonium chloride (EPTMA Cl) [47–50]

| Solvent[a] | Reagent | Cellulose content (%) | Temperature (°C) | Time (h) | Molar ratio[b] | DS |
|---|---|---|---|---|---|---|
| DMA/LiCl | EPTMA Cl | 1.4 | 70 | 0.5 | 3:1 | 0.35 |
| DMA/LiCl | EPTMA Cl | 1.4 | 70 | 1 | 3:1 | 0.44 |
| DMA/LiCl | EPTMA Cl | 1.4 | 70 | 2 | 3:1 | 0.57 |
| DMA/LiCl | EPTMA Cl | 1.4 | 70 | 4 | 3:1 | 0.70 |
| DMA/LiCl | EPTMA Cl | 1.4 | 70 | 5 | 3:1 | 0.75 |
| DMA/LiCl | EPTMA Cl | 1.4 | 70 | 8 | 3:1 | 0.82 |
| DMA/LiCl | EPTMA Cl | 1.4 | 70 | 18 | 3:1 | 0.81 |
| DMA/LiCl | EPTMA Cl | 1.4 | 70 | 32 | 3:1 | 0.80 |
| DMA/LiCl | EPTMA Cl | 1.5 | 70 | 8 | 5:1 | 1.50 |
| DMA/LiCl | EPTMA Cl | 1.5 | 70 | 8 | 10:1 | 1.88 |
| DMA/LiCl | EPTMA Cl | 1.5 | 70 | 8 | 20:1 | 2.05 |
| BTEA-OH | CHPTMA Cl | 3 | 25 | 1 | 2:1 | 0.12 |
| BTEA-OH[c] | CHPTMA Cl | 3 | 25 | 1 | 2:1 | 0.15 |
| BTEA-OH | CHPTMA Cl | 3 | 25 | 1 | 1.4:1 + 0.6:1[d] | 0.15 |
| BTEA-OH | CHPTMA Cl | 3 | 25 | 1 | 2.5:1 | 0.19 |
| BTEA-OH | CHPTMA Cl | 3 | 25 | 1 | 2:1 + 2:1[d] | 0.25 |
| BTEA-OH | CHPTMA Cl | 4 | 25 | 1 | 2:1 | 0.14 |
| BTEA-OH | CHPTMA Cl | 5 | 25 | 1 | 2:1 | 0.17 |
| BTEA-OH | CHPTMA Cl | 6 | 25 | 1 | 2:1 | 0.19 |
| BTEA-OH[c] | CHPTMA Cl | 6 | 25 | 1 | 2:1 | 0.22 |
| BTEA-OH | CHPTMA Cl | 6 | 25 | 1 | 2.5:1 | 0.18[e] |
| BTEA-OH | CHPTMA Cl | 6 | 25 | 1 | 3:1 | 0.15[e] |
| NaOH/urea | CHPTMA Cl | 2 | 25 | 8 | 3:1 | 0.20 |
| NaOH/urea | CHPTMA Cl | 2 | 25 | 8 | 4.5:1 | 0.29 |
| NaOH/urea | CHPTMA Cl | 2 | 25 | 8 | 6:1 | 0.31 |
| NaOH/urea | CHPTMA Cl | 2 | 25 | 4 | 9:1 | 0.35 |
| NaOH/urea | CHPTMA Cl | 2 | 25 | 8 | 9:1 | 0.46 |
| NaOH/urea | CHPTMA Cl | 2 | 25 | 16 | 9:1 | 0.46 |
| NaOH/urea | CHPTMA Cl | 2 | 25 | 8 | 12:1 | 0.47 |
| NaOH/urea | CHPTMA Cl | 2 | 25 | 16 | 12:1 | 0.63 |
| NaOH/urea | CHPTMA Cl | 2 | 45 | 8 | 9:1 | 0.42 |
| NaOH/urea | CHPTMA Cl | 2 | 60 | 8 | 9:1 | 0.44 |
| NaOH/urea | EPTMA Cl | 2 | 25 | 6 | 5:1 | 0.17 |

(continued)

**Table 6.10** (continued)

| Solvent[a] | Reagent | Cellulose content (%) | Temperature (°C) | Time (h) | Molar ratio[b] | DS |
|---|---|---|---|---|---|---|
| NaOH/urea | EPTMA Cl | 2 | 25 | 24 | 5:1 | 0.26 |
| NaOH/urea | EPTMA Cl | 2 | 25 | 6 | 10:1 | 0.32 |
| NaOH/urea | EPTMA Cl | 2 | 25 | 9 | 10:1 | 0.47 |
| NaOH/urea | EPTMA Cl | 2 | 25 | 24 | 10:1 | 0.50 |

[a]BTEA-OH: 1.6 M benzyltrimethylammonium hydroxide solution in water, NaOH/urea: 7.5% (w/w) NaOH and 11% (w/w) urea in water for CHPTMA and 6% (w/w) NaOH and 4% (w/w) urea in water for EPTMA, DMA: *N,N*-dimethyl acetamide
[b]molar ratio etherification reagent:anhydroglucose units
[c]addition of 0.1 g benzyltrimethylammonium chloride per g cellulose
[d]stepwise addition of CHPTMAC at 0 and 40 min
[e]gelation of reaction mixture

with a DS up to around 2 have been obtained by homogeneous conversion of cellulose with EPTMA Cl. Homogeneous quaternization has also been achieved using aqueous cellulose solvents (Table 6.10). Conversion of cellulose, dissolved in benzyltrimethylammonium hydroxide, with CHPTMA Cl yielded HPTMA cellulose with rather low maximum DS $\approx$ 0.3 [48]. Attempts to increase the DS by increasing the amount of etherification reagent resulted in gelation of the reaction medium. Moreover, the etherification reagent is slowly hydrolyzed in the aqueous system, which results in decreased reactivity. This can be slightly attenuated by stepwise addition of the reagent or adding benzyltrimethylammonium chloride, which is hygroscopic and thus removes water from the equilibrium of the hydrolysis reaction. Using aqueous NaOH/urea as reaction medium, water-soluble products with higher DS values of up to about 0.6 could be achieved by significantly increasing the amount of etherification reagent (up to 12 mol per mol AGU) [49]. Likewise, etherification in NaOH/urea has been achieved with EPTMA Cl [50]. The reactivity of both reagents was found to be very similar and $^{13}$C NMR spectroscopy indicated an etherification on the primary and secondary hydroxyl groups in similar proportions for these derivatives. The quaternized HPTMA derivatives obtained by homogeneous synthesis in NaOH/urea were studied as gene delivery agents that are slightly less efficient than poly(ethylene imine) in terms of transfection efficiency but at the same time far less cytotoxic (Fig. 6.10) [49, 51]. Moreover, they can be employed as flocculation aids for the sedimentation of kaolin and montmorillonite suspensions [50, 52].

Cationic mixed ethers of cellulose are of commercial interest in cosmetic formulations, in particular for hair and skin care products. The most prominent examples are “quaternized hydroxyethyl celluloses” that are commercialized under the INCI (International Nomenclature of Cosmetic Ingredients) names “Polyquaternium-10” and “Polyquaternium-67” [53] (Fig. 6.11). These derivatives are obtained by quaternization of hydroxyethyl cellulose (HEC, see Sect. 6.2.3) and should not be confused with HPTMA cellulose described above [54].

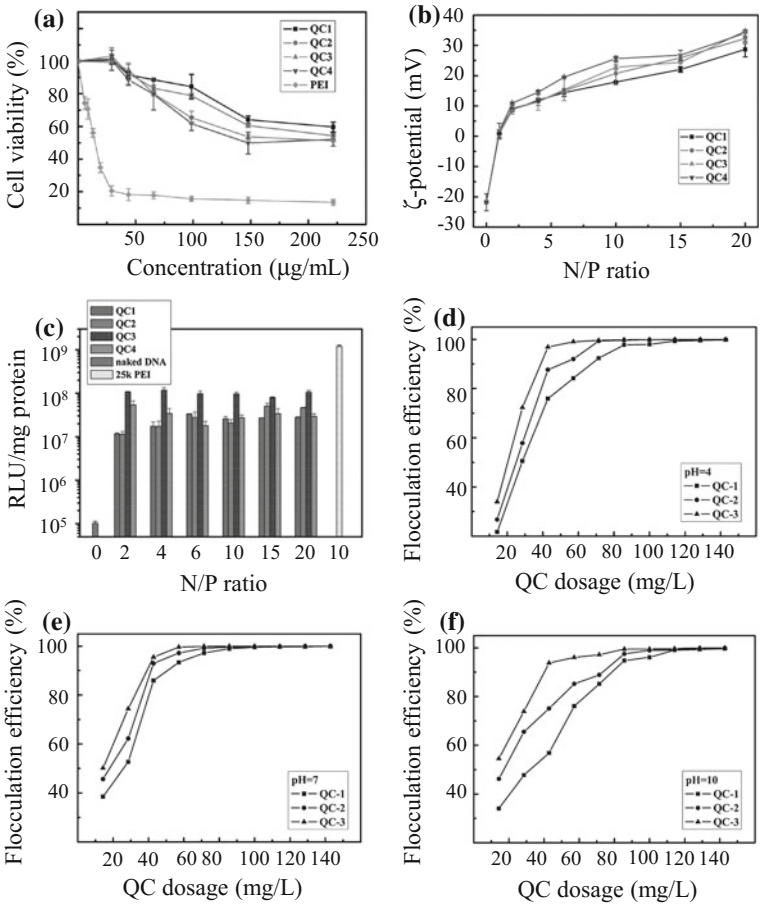


**Fig. 6.10** **a** Viabilities of 293T cells in the presence of quaternary cellulose ethers (QC) and polyethyleneimine (PEI). **b** Zeta potential of QC/DNA complexes at different nitrogen to phosphorous (N/P) ratios. **c** Transfection efficiency, represented by luciferase expression in 293T cells, of QC/DNA and PEI/DNA complexes. **d–f** Flocculation efficiency of QC in montmorillonite suspension at different pH values (part **a–c**: Reprinted (adapted) with permission from [51]. Copyright (2010) American Chemical Society; part **d–f**: Reprinted (adapted) with permission from [52]. Copyright (2010) American Chemical Society)

## 6.2 Nonionic Cellulose Ethers

The class of nonionic cellulose ethers can be subdivided according to the general structure of their substituents into alkyl ethers (Sect. 6.2.1), ethers carrying aromatic or unsaturated moieties (Sect. 6.2.2), and hydroxyalkyl ethers (Sect. 6.2.3). The latter derivatives are often found as mixed alkyl hydroxyalkyl ethers, in particular in commercial products. The following chapter will provide an overview on these

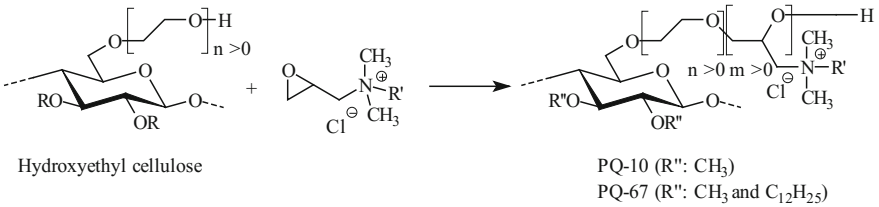


**Fig. 6.11** Reaction scheme for the preparation of the quaternized hydroxyethyl ethers (HEC) Polyquaternium (PQ) 10 and 67

classes of nonionic cellulose ethers. For general principles of the preparation and characterization of cellulose ethers, the reader is referred to Sect. 6.1.1.

### *6.2.1 Alkyl Ethers*

Methylcellulose (MC) and ethyl cellulose (EC), the two most important nonionic alkyl ethers of cellulose, are produced on industrial scale for the use as adhesives and solution thickeners in different applications including food and pharmaceutical products (Table 6.11) [55–58]. Higher ethers such as propyl and butyl cellulose have been prepared as well but mostly for academic purposes. Of particular interest for commercial applications are cold water-soluble MC with a DS ≈ 1.8, which is the optimum for solubility in aqueous media. EC is water soluble at DS ≈ 0.8–1.7 (Fig. 6.11). However, the commercial products are mainly derivatives with DS ≈ 2.2–2.8 because they are thermoplastic and can be dissolved in and processed from organic solvents, in particular alcohols, hydrocarbons, and mixtures

**Table 6.11** Overview on applications of nonionic cellulose ethers

| Use in | For/as |
|---|---|
| Ceramics | Water retention, lubricity, green strength |
| Construction products | Water retention, workability |
| Cosmetics | Rheology control, emulsification, stabilization, foam stabilization |
| Food | Thickener, binder, emulsification |
| Paint | Protective colloid, thickener, suspending aid |
| Paper | Film formation, adhesive |
| Pharmaceuticals | Binder, granulating agent, film former, stabilizer |
| (HEC) Polymerization | Protective colloid for polymerization of vinyl acetate and vinyl chloride |
| Printing inks | Thickener, suspending agent |
| Textile | Binder, sizing agents, coating |
| Tobacco | Thickener, film former, adhesive |

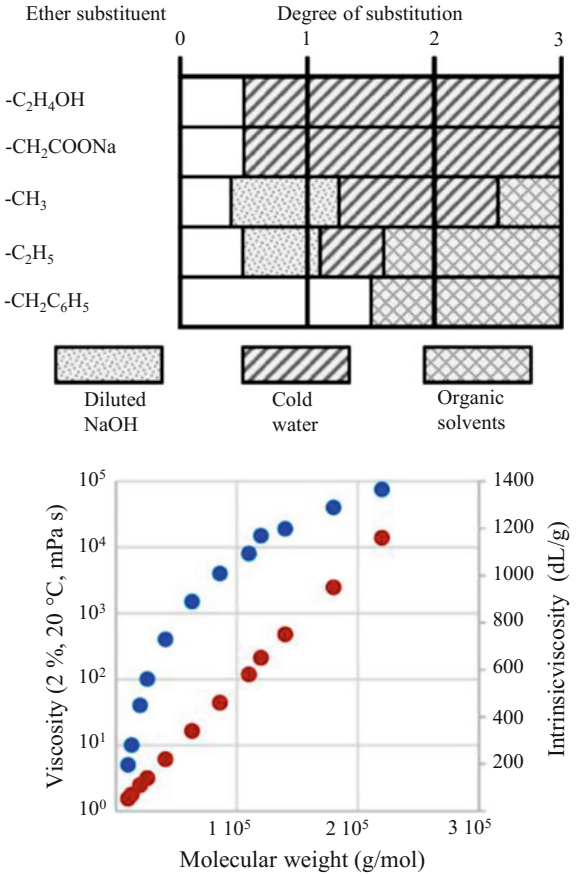


**Fig. 6.12** (Top) Solubility of typical cellulose ethers as a function of degree of substitution (DS), adapted from [59]. (Bottom) Apparent and intrinsic viscosity of commercial methyl celluloses (DS 1.8) with different molecular weights, dissolved in water, adapted from [55]

therefrom. In addition to the solubility, solution viscosity is an important property that determines the suitability and performance in the particular areas of applications. Commercialized cellulose ethers are produced with different viscosity grades, i.e., with different average molar masses, which are expressed as values of the intrinsic viscosity or the apparent viscosity of polymer solutions with a defined concentration within a particular solvent or solvent mixture (Fig. 6.12).

Commercially, cellulose alkyl ethers are exclusively prepared heterogeneously. The basics of this process that involves swelling and activation of cellulose in aqueous alkali were described in Sect. 6 as well as in Sects. 6.1.1. Alkylation is achieved by conversion of alkali-activated cellulose with an alkyl halide, in most cases the chloride (Fig. 6.1). Considerable amounts of NaCl are produced that need to be removed in the workup. Due to the necessary presences of large quantities of water, roughly 20–30% of the alkylation agent is consumed either by hydrolysis into the corresponding alcohol or by the subsequent reaction with the alcohol to yield the corresponding ether.

In particular for methylation of cellulose, other reagents such as methyl iodide, dimethyl sulfate, diazomethane, or methyl triflate were employed as well. These derivatizations, however, are mainly of interest for academic purposes such as the synthesis of cellulose ethers with well-defined DS and distribution pattern (within the AGU and along the polymer chain) as well as for the analysis of polysaccharide molecular structures by methylation analysis (permethylation of polysaccharides followed by hydrolysis and quantitative identification of the monosaccharide units by GC–MS) [60].

Several homogeneous reactions were established mainly for academic purposes. MC and EC have been prepared homogeneously in DMAc/LiCl and DMSO/LiCl by using NaH/DMSO (sodium dimsyl) as a base instead of NaOH [61, 62]. Thereby, a strong deviation in the composition of un-, mono-, di-, and tri-functionalized sugar units has been observed between commercial MC and homogeneously prepared derivatives (Table 6.12).

Aqueous cellulose solvents, NaOH/urea/water and LiOH/urea/water, were utilized for the homogeneous methylation of cellulose by conversion with dimethyl sulfate [63, 64]. Upon dissolution, which is usually achieved around −20 °C, the polysaccharide is activated by the alkali for the subsequent etherification, which is usually performed at 20–50 °C for 24 h (Table 6.13). The regioselectively of the homogeneous methylation is in the order *O*-2 > *O*-6 > *O*-3, which is similar to that found for commercialized synthesis in the heterogeneous state. The distribution of alkyl substituents within the AGU influences the properties of the cellulose ethers.

Cellulose ethers (alkyl and hydroxyalkyl) within a specific DS range readily dissolve in cold water (≈25 °C) but flocculate and form gels upon heating to a specific temperature (Fig. 6.13a). This phenomenon is exploited in the commercial synthesis of MC in which the reaction mixture is poured into and washed with hot water in order to isolate and purify the reaction product. Moreover, the gel formation of cellulose ethers has extensive use in pharmaceutical and food areas, e.g., for the stabilization of foam structures [65]. The process is reversible with a hysteresis loop and thus often termed “thermoreversible gelation” or “thermoreversible flocculation” (Fig. 6.13b). It is suggested that the flocculation at higher temperature is due to an increased interaction of hydrophobic regions of the modified backbone combined with the expulsion of water molecules [66, 67]. The gel temperature is invariant with molecular weight and polymer concentration but is influenced by the

**Table 6.12** Comparison of individual mol fractions of commercial methyl cellulose (MC 1) and methyl celluloses prepared by homogeneous derivatization in DMAc/LiCl (MC 2–4), adapted from [62]

| Sample | Mole fraction (%)[a] | | | | |
|---|---|---|---|---|---|
| | Glc | Mono | Di | Tri | $DS_{Me}$[b] |
| MC 1 | 10 | 29 | 39 | 22 | 1.7 |
| MC 2 | 5 | 51 | 29 | 15 | 1.5 |
| MC 3 | 9 | 12 | 36 | 43 | 2.2 |
| MC 4 | 9 | 6 | 19 | 4 | 1.0 |

[a]Mole fractions of glucose (Glc), mono-, di-, and tri-*O*-carboxymethylated glucose
[b]Degree of substitution of methyl groups

**Table 6.13** Conditions for and results of the methylation of cellulose in aqueous media with dimethyl sulfate, adapted from [63, 64]

| Reaction conditions | | | | | Results | | | |
|---|---|---|---|---|---|---|---|---|
| Solvent | Cellulose type[a] | Molar ratio[b] | Temperature (°C) | Time (h) | $DS_{overall}$ | $DS_2$ | $DS_3$ | $DS_6$ |
| NaOH/urea | MC | 7.5 | 25 | 20 | 1.08 | 0.52 | 0.26 | 0.30 |
| NaOH/urea | MC | 9 | 25 | 20 | 1.43 | 0.66 | 0.38 | 0.39 |
| NaOH/urea | MC | 12 | 25 | 20 | 1.51 | 0.69 | 0.41 | 0.41 |
| LiOH/urea | SSP | 9 | 22 | 24 | 1.19 | 0.56 | 0.24 | 0.39 |
| LiOH/urea | SSP | 12 | 22 | 24 | 1.33 | 0.63 | 0.27 | 0.43 |
| LiOH/urea | SSP | 12 | 30 | 24 | 1.59 | 0.72 | 0.36 | 0.52 |
| LiOH/urea | SSP | 12 | 40 | 24 | 1.62 | 0.73 | 0.37 | 0.53 |
| LiOH/urea | SSP | 12 | 50 | 24 | 1.50 | 0.69 | 0.32 | 0.49 |
| LiOH/urea | SSP | 15 | 30 | 4 | 1.27 | 0.59 | 0.28 | 0.41 |
| LiOH/urea | SSP | 15 | 30 | 8 | 1.65 | 0.75 | 0.37 | 0.53 |
| LiOH/urea | SSP | 15 | 30 | 12 | 1.66 | 0.76 | 0.37 | 0.53 |
| LiOH/urea | SSP | 15 | 30 | 24 | 1.64 | 0.75 | 0.36 | 0.53 |

[a]*MC* Microcrystalline cellulose, *SSP* Spruce sulfite pulp
[b]Molar ratio anhydroglucose unit:dimethyl sulfate

rate of heating, shear rate, and the presence of additives, especially salts [68]. Moreover, the molecular structure of the cellulose ethers, not only overall DS but also especially the substitution pattern, has a huge impact on the gelation behavior. It was demonstrated that many commercial ethers with random distribution of substituents within the AGU behave differently from regioselective 2-*O*, 3-*O*, and 6-*O*-analogues with a same DS (see Sect. 4.4). For example, aqueous solutions of randomly functionalized EC become turbid around 30 °C, while those of regioselective 3-mono-*O*-ethyl cellulose are optically clear up to around 60 °C on one hand [69]. On the other, 3-*O*-propyl cellulose has a much lower flocculation temperature (≈15–20 °C), while 3-*O*-butyl cellulose is completely insoluble in water.

### 6.2.2 *Aromatic and Unsaturated Alkyl Ethers*

Cellulose aryl ethers have received little attention in academia and industry. More common, but still of less importance than alkyl and hydroxyalkyl esters, are alkyl ethers with aromatic substituents. In past decades, benzyl cellulose with DS > 2 had a certain commercial importance for the production of lacquers and as thermoplastics. The derivatives are insoluble in water but dissolve in many organic solvents. They are thermoplastic with melting points in the range of 90–155 °C and electrically insulating [70, 71]. Benzylated cellulosic materials with a low DS ≪ 0.1 were employed in hemodialysis membranes.

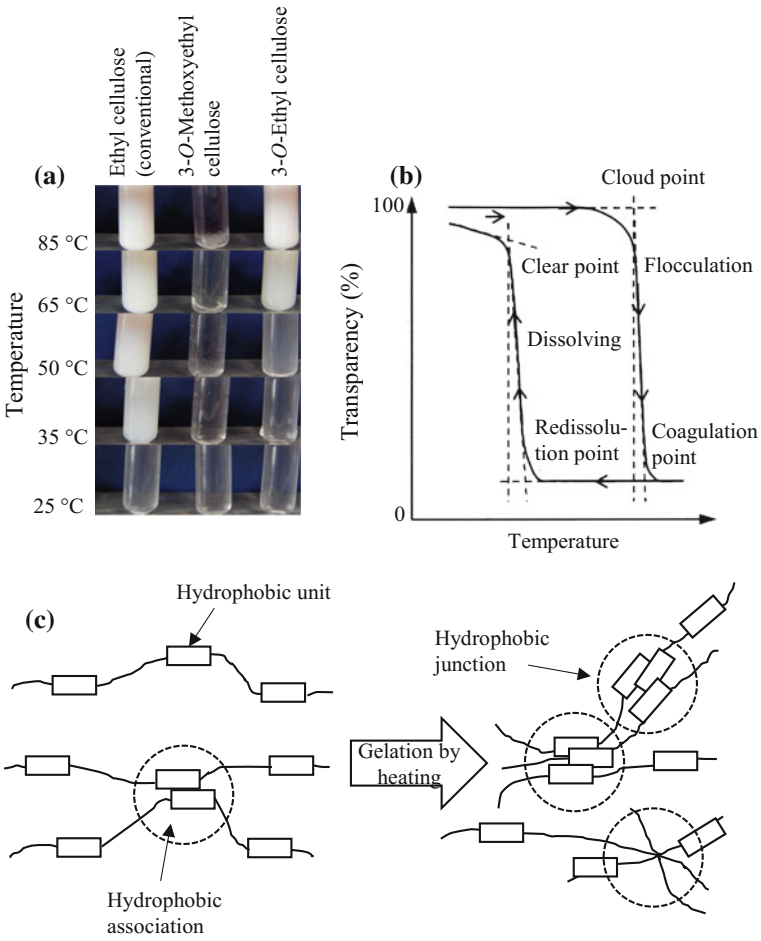


**Fig. 6.13** **a** Thermoreversible gelation of conventional (DS 1.3) and regioselectively modified cellulose alkyl ethers (DS 1.0) upon heating, adapted from [65]. **b** Scheme of the flocculation and redissolution cycle [59]. **c** Proposed mechanism of the thermoreversible gelation of cellulose alkyl ethers, adapted from [66]

The benzylation of cellulose proceeds analogous to the synthesis of alkyl ethers by reaction of alkali treated cellulose with benzyl chloride. Conventionally, the reaction is performed heterogeneously in aqueous NaOH. A high excess of etherifying reagent is required to compensate the loss by hydrolysis. The alkali-activated cellulose is hydrophilic, while benzyl chloride forms a hydrophobic phase. As a result, heterogeneous benzylation is strongly controlled by mixing and diffusion processes and results in a more block-like distribution of benzyl groups; benzylated regions of the polysaccharide are becoming increasingly hydrophobic. Consequently, they concentrated in vicinity of the etherification reagent and are

more prone toward further etherification than unmodified regions [72, 73]. This effect can be compensated by adding phase transfer catalysts to a certain extent.

Homogeneous benzylation has been reported using aqueous NaOH/urea as cellulose solvent [74]. Despite the fact that the cellulose chains are more accessible in the dissolved state, rather low DS values (≈0.5) are obtained in this system due to the hydrolysis of the etherification reagent (Table 6.14). Using an excess of benzyl chloride is not feasible due to its immiscibility with water. Benzyl cellulose with a much higher DS of up to 2.9 can be obtained by dissolving cellulose in DMSO/TBAF and using either solid or aqueous NaOH as a base [71, 73].

The benzyl substituent has received some interest in advanced cellulose chemistry as a non-regioselective, protection group. It can be cleaved under mild conditions by reduction, e.g., with molecular hydrogen in the presence of palladium catalysts. Di- and triarylmethyl moieties are more bulky than the mono-aryl analogues and thus were studied as regioselective protecting group for the primary hydroxyl group in cellulose (Fig. 6.14). The most notable substituent in this regard is triphenylmethyl (trityl) that is introduced up to a maximum DS around 1.0 by homogeneous conversion in DMAc/LiCl, DMSO/$N_2O_4$, or DMSO/$SO_2$/DEA using the corresponding trityl chloride [76]. The bulky di-/triarylmethyl substituents are predominately introduced at the sterically least hindered primary hydroxyl group in position 6 leaving the majority of secondary hydroxyl groups free for further conversion. This leads to regioselectively modified 2,3-*O*-cellulose derivatives after deprotection. Removal of the 6-*O*-arylmethyl ether substituents, which is achieved by HCl treatment, is a crucial step because it is combined with acid catalyzed polymer degradation. Thus, alternatives to the trityl protecting group have been investigated [75, 77]. As a general trend, diphenylmethyl chlorides reacted much

**Table 6.14** Conditions of and results for the benzylation of cellulose in different reaction media at 70 °C, adapted from [71, 73, 74]

| Medium | Reaction course | Base | Molar ratio[a] | Time (h) | DS |
|---|---|---|---|---|---|
| NaOH/urea | Homogeneous | Solution | 1.0:1.5 | 4 | 0.29 |
| NaOH/urea | Homogeneous | Solution | 1.0:2.0 | 4 | 0.41 |
| NaOH/urea | Homogeneous | Solution | 1.0:3.0 | 4 | 0.51 |
| NaOH/urea | Homogeneous | Solution | 1.0:4.0 | 4 | 0.54 |
| $NaOH_{aq}$ | Heterogeneous | Solution | 1.0:0.5 | 6 | 0.02 |
| $NaOH_{aq}$ | Heterogeneous | Solution | 1.0:0.5 | 8 | 0.05 |
| $NaOH_{aq}$ | Heterogeneous | Solution | 1.0:0.5 | 10 | 0.07 |
| $NaOH_{aq}$ | Heterogeneous | Solution | 1.0:0.5 | 15 | 0.25 |
| DMSO/TBAF[b] | Phase transition | Solid | 1.0:3.0:3.0 | 4 | 1.22 |
| DMSO/TBAF[b] | Phase transition | Solid | 1.0:6.0:6.0 | 4 | 2.30 |
| DMSO/TBAF[b] | Phase transition | Solid | 1.0:6.0:12.0 | 4 | 2.85 |
| DMSO/TBAF[b] | Phase transition | Solid | 1.0:9.0:18.0 | 4 | 2.69 |

[a]Molar ratio of anhydroglucose unit:benzyl chloride:NaOH, 9% tetra-*n*-butylammonium fluoride trihydrate in DMSO

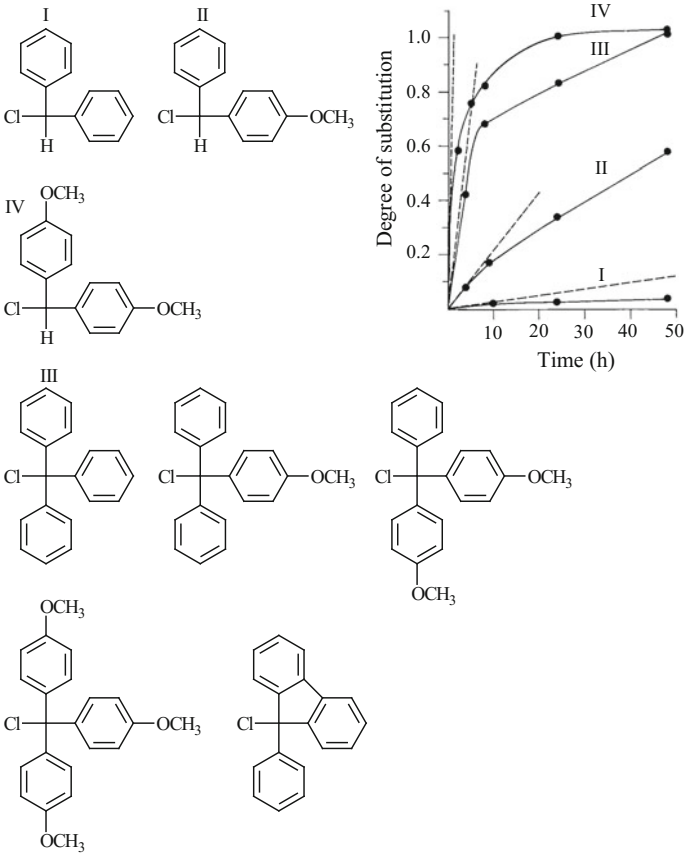


**Fig. 6.14** (Left) Overview of di- and triphenylmethyl chlorides used for homogeneous derivatization of cellulose. (Right) Time dependence of the degree of substitution obtained by homogeneous etherification of cellulose with different arylmethyl chlorides (3 mol per anhydroglucose unit) in DMAc/LiCl with pyridine as a base, adapted from literature [75]

slower and yielded lower $DS_{max}$ compared to triphenylmethyl chlorides, while modification of the aryl moieties with electron-donating methoxy substituents significantly increased the velocity of alkylation as well as deprotection (Fig. 6.14). For further information on the synthesis and unique properties of regioselective cellulose derivatives with the aid of protecting groups, the reader is referred to Sect. 4.4.

Cellulose alkyl ethers with unsaturated alkyl substituents were studied as intermediates for "click-chemistry" approaches. Propargyl cellulose selectively reacts with azides via copper-catalyzed 1,3-dipolar cycloaddition, which can be exploited to introduce highly functional substituents in a very controlled manner [78, 79]. Even very bulky moieties such as highly branched dendrons could be attached to the cellulose backbone (Fig. 6.15). Thiol-ene reaction was employed for

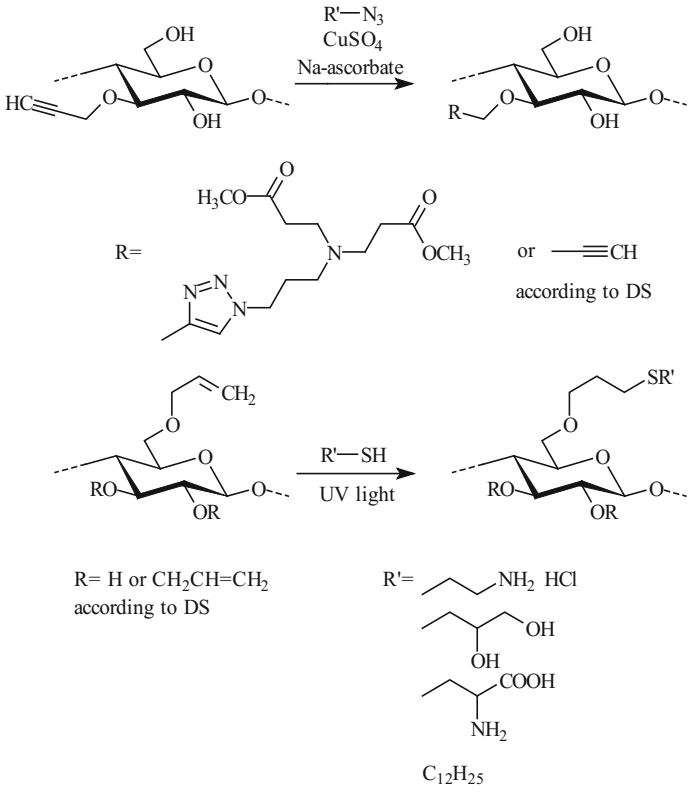


**Fig. 6.15** (Top) Reaction scheme for conversion of 3-*O*-propargyl cellulose with azido-propyl-polyamidoamine dedrons of the first generation [78]. (Bottom) Scheme for thiol-ene reaction of cellulose allyl ethers [80]

selective modification of cellulose allyl ether with functional substituents. The reaction proceeds under UV irradiation by a radical mechanism [80]. Allyl ethers are also of interest as non-regioselective protecting groups (see Sect. 4.4).

Cellulose reacts with α,β-unsaturated compounds according to the Michael addition mechanism to form ethers. Cyanoethylation of cellulose is the most prominent example of this reaction. It can be performed heterogeneously in aqueous NaOH with a large excess of acrylonitrile or homogeneously in NMMO/water/cosolvent mixtures or aqueous alkali/urea-based solvents [81–83]. Depending on the DS, cyanoethyl cellulose exhibits interesting properties such as improved thermostability, high dielectric constants, and resistance toward degradation by acid hydrolysis or microorganisms compared to cellulosic materials. Moreover, the derivatives can be further functionalized, e.g., by conversion with hydroxylamine into amidoximes or act as precursor for the grafting of copolymer side chains [84, 85].

### 6.2.3 Hydroxy Alkyl and Mixed Alkyl/Hydroxy Alkyl Ethers

Cellulose hydroxyalkyl ethers feature similar properties as alkyl ethers. Depending on the content of ether moieties, they dissolve in water or dipolar organic solvents. The most important representatives of this class of derivatives are hydroxyethyl cellulose (HEC) and hydroxypropyl cellulose (HPC) that are produced industrially in large quantities with different product specifications (Table 6.15). Both derivatives are employed in similar areas as cellulose alkyl ethers, e.g., as solution thickeners, stabilizers, and coatings in food, pharmaceuticals, paints, construction materials, etc. [86–88]. Despite their similar molecular structure, HPC shows thermoreversible gelation while HEC does not. This is of certain relevance for specific application where gelation should be hindered (e.g., oil drilling aids) because the latter can also be employed at elevated temperatures.

**Table 6.15** Overview of industrially relevant cellulose hydroxyalkyl and mixed alkyl hydroxyalkyl ethers. For better understanding, the formation of oxyalkylene side-chains is not considered here

| Abbreviation | Name | Substituents | | |
|---|---|---|---|---|
| | | Hydroxy alkyl | Alkyl-1 | Alkyl-2 |
| HEC | Hydroxyethyl cellulose | 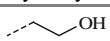 | | |
| EHEC | Ethyl hydroxyethyl cellulose | 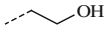 |  | |
| MEHEC | Methyl ethyl hydroxyethyl cellulose | 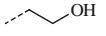 |  | 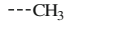 |
| hmHEC | Hydroxyethyl cellulose, hydrophobically modified | 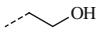 | 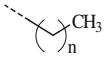 n= 13, 15 | |
| hmEHEC | Ethyl hydroxyethyl cellulose, hydrophobically modified | 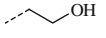 |  | 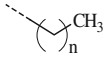 n= 13, 15 |
| HPC | Hydroxypropyl cellulose | 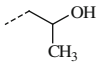 | | |
| MHPC | Hydroxypropyl methyl cellulose, "hypromellose" | 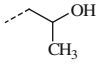 |  | |

By mixing alkyl and hydroxyalkyl substituents of different types and DS, the physical properties (e.g., solubility in water and organic media, solution viscosity) and application, relevant characteristics (e.g., workability and water retention of mortar and paint formulation, swelling, and dissolution properties of tablet films) of cellulose ethers can be fine-tuned. Thus, mixed alkyl hydroxyalkyl ethers of cellulose, such as ethyl HEC and methyl ethyl HEC (Table 6.15), find comparable technical applications as their non-mixed analogues. Hydroxypropyl methyl cellulose (HPMC, "hypromellose") is of great importance as food additive (E number 464) and in particular as excipient in pharmaceutics. Due to the unique dissolution properties of this cellulose ether, HPMC-based drug matrices disintegrate in a timely controlled manner (Fig. 6.16) [89]. An initially rapid water uptake results in hydration of the polymer and formation of a protective outer gel layer that slows further water penetration. With time, the size of the gel layer increases at expense of the solid core. Incorporated drugs are gradually released by diffusion through and erosion of the gel layer until the whole matrix disintegrates.

In addition to mixed cellulose ethers with short-chain alkyl substituents, in particular methyl and ethyl moieties, "hydrophobically modified" hydroxyalkyl cellulose ethers that carry rather long alkyl chains, e.g., $C_{14}$ and $C_{16}$ are commercially available. Due to secondary hydrophobic interactions of the side chains, these compounds show increased solution viscosity at similar molecular weight compared to the original cellulose ethers (Fig. 6.16c) [90]. Moreover, the hydrophobic modification can have beneficial effects on the stabilization of emulsions and colloid dispersion [91, 92].

Hydroxyalkyl ethers of cellulose are prepared by conversion of alkali-activated cellulose with epoxides that react with ring opening. The main difference to alkyl ethers is that a hydroxyl group is generated within the side chain of the substitution that is accessible for further chemical derivatization as well. Excess of etherification reagent can react either with the cellulose backbone, which would increase the overall DS, or with the hydroxyalkyl group of the substituents, which will result in prolongation of the substituent but not in an increase in DS (Fig. 6.17a). Thus, another descriptor, termed "molecular degree of substitution" (MS), was introduced. It describes the overall number of substituents attached to the repeating unit and is always $\geq$ DS, which only quantifies the number of substituents directly attached to the cellulosic hydroxyl moieties. The overall reaction rate as well as the individual reaction rates at positions 2, 3, and 6 and the newly introduced hydroxyl group strongly depend on the alkali concentration (Fig. 6.17b). As a general trend for the heterogeneous conversion of cellulose with ethylene oxide (hydroxyethylation) in aqueous alkali, an increasing NaOH content increases reactivity and strongly favors etherification of the side chain as well as the primary hydroxyl group within the cellulose backbone [59]. The secondary hydroxyl group at position 3 is the least reactive one. The average chain length of the hydroxyalkyl moieties increases upon increasing derivatization; however, only till an MS/DS ratio of about 1.5 is reached (Fig. 6.17c) [93]. Thus, chain propagation is strongly

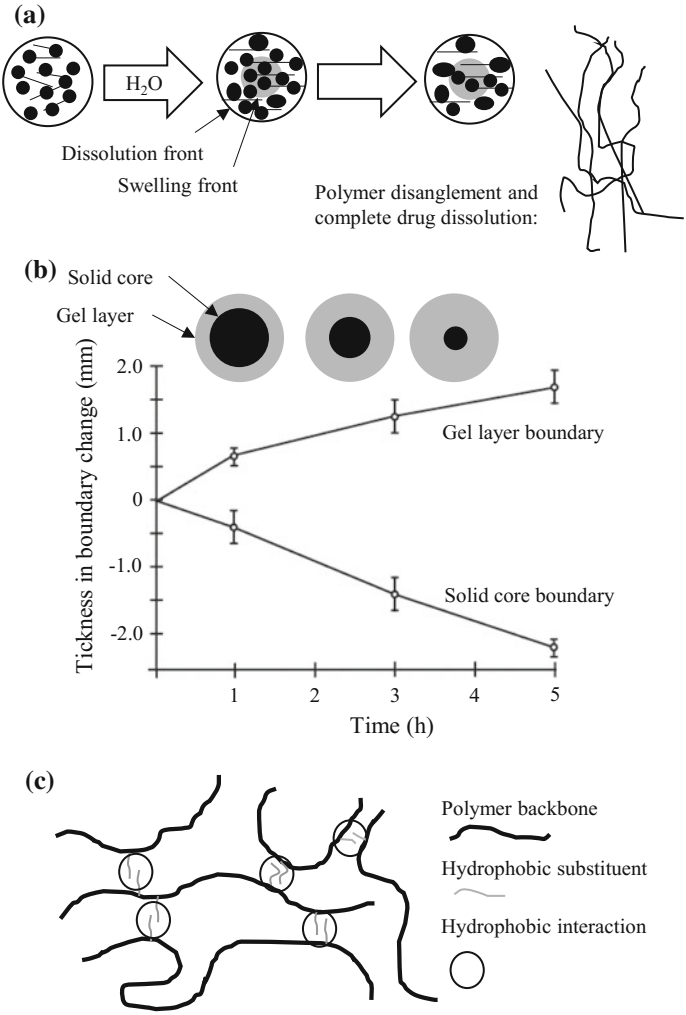


**Fig. 6.16** **a** Schematic representation of drug distribution and matrix swelling during dissolution of a hypromellose-based matrix and **b** schematics and actual changes in boundary regions of a hypromellose–pectin matrix (6:3) in water, adapted from [89]. **c** Schematic illustration of the interaction of chains of hydrophobic alkyl hydroxyalkyl cellulose ethers in solution

favored at the beginning of the reaction, while the formation of new substituents is the dominating reaction at later stages of the reaction. Heterogeneous hydroxypropylation of cellulose follows a similar trend with a reactivity order of *O*-6 > *O*-2 > *O*-3 [94].

Heterogeneous conversion of alkali-activated cellulose is by far the most important procedure for the preparation of hydroxyalkyl ethers. In academic research, homogeneous hydroxyalkylation was studied as well. HEC and HPC have

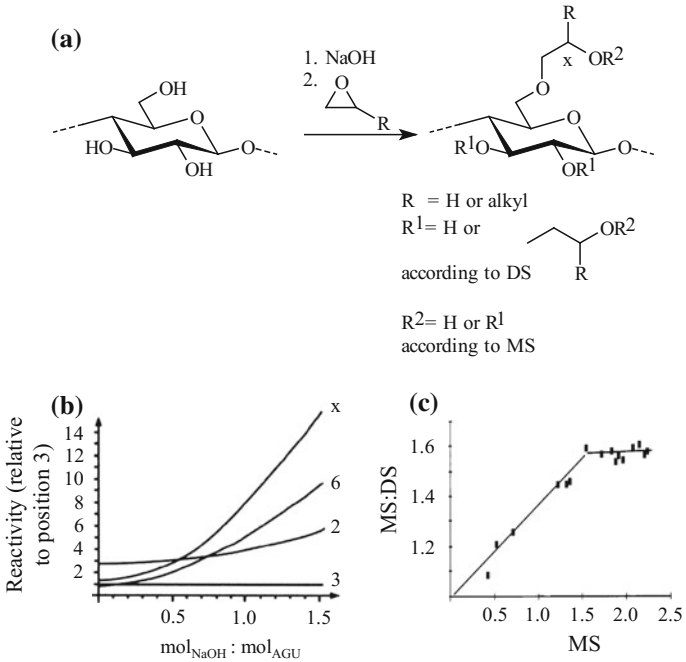


**Fig. 6.17** **a** Reaction scheme for the preparation of cellulose hydroxyalkyl ethers. **b** Qualitative scheme for the evolution of partial reaction rates (relative to the reaction at position 3) for the heterogeneous hydroxyethylation of cellulose, adapted from [59]. **c** Ratio of molar degree of substitution (MS) to degree of substitution (DS) as a function of MS for hydroxyethyl celluloses prepared heterogeneously in an aqueous alkali/alcohol slurry ([93], (© 1996) "With permission of Springer")

been prepared by homogeneous etherification in different ILs with ethylene and propylene oxide (Table 6.14) [95]. It was found that acetate ions, either present as anionic part of the IL or added as catalyst, catalyze the ring-opening reaction and result in increased MS. The viscosity of the reaction mixture strongly effects the course of the reaction. Addition of dipolar aprotic cosolvents strongly favors the dissolution of the gaseous reagents and yields highly substituted derivatives. Direct comparison with a commercial reference HEC that was prepared conventionally in a heterogeneous process demonstrated that the hydroxyalkylation in ILs results in a lower MS: DS ratio, i.e., alkylation at the ether substituent is less favorable. Moreover, the order of reactivity is *O*-2 > *O*-6 ≈ *O*-3 instead of *O*-6 > *O*-2 > *O*-3 that was reported for conventional HEC.

Aqueous NaOH/urea was employed as homogeneous reaction medium for the synthesis of HEC (Table 6.16) [96]. Chlorohydrin was used, which reacted faster and with greater reactivity compared to the conversion with epoxides in IL solutions. Only at higher MS > 1, a noticeable difference in the partial DS values was observed (*O*-2 ≥ *O*-6 > *O*-3).

**Table 6.16** Conditions for and results of the homogeneous hydroxyalkylation of cellulose, adapted from [95, 96]

| Solvent[a] | Additive[b] | Temperature (°C) | Reagent[c] | Ratio[d] | Time (h) | MS | $DS_{O\text{-}2}$ | $DS_{O\text{-}3}$ | $DS_{O\text{-}6}$ |
|---|---|---|---|---|---|---|---|---|---|
| Conventional reference | | | | | | 1.37 | 0.32 | 0.17 | 0.40 |
| EMIMAc (4%, SSP) | – | 80 | EtO | 1:10 | 19 | 0.39 | | | |
| EMIMAc (4%, SSP) | – | 80 | PrO | 1:20 | 19 | 0.22 | | | |
| EMIMAc (4%, SSP) | – | 80 | PrO | 1:40 | 19 | 1.34 | 0.42 | 0.32 | 0.32 |
| EMIMAc (4%, SSP) | – | 80 | PrO | 1:50 | 19 | 1.27 | | | |
| EMIMAc (4%, SSP) | DMSO | 80 | PrO | 1:50 | 19 | 1.25 | 0.46 | 0.36 | 0.35 |
| EMIMAc (8%, SSP) | DMSO | 80 | PrO | 1:50 | 19 | 2.24 | 0.86 | 0.78 | 0.75 |
| EMIMAc (8%, SSP) | DMF | 80 | PrO | 1:50 | 19 | 2.41 | | | |
| BMIMCl (4%, SSP) | – | 80 | PrO | 1:50 | 19 | 0.09 | | | |
| BMIMCl (4%, SSP) | $CH_3COOK$ | 80 | PrO | 1:50 | 19 | 0.45 | 0.14 | 0.12 | 0.08 |
| NaOH/urea (2% cotton) | – | 50 | ClH | 1:7.5 | 5 | 0.86 | 0.28 | 0.21 | 0.23 |
| NaOH/urea (2% cotton) | – | 50 | ClH | 1:9 | 3 | 0.90 | 0.29 | 0.19 | 0.25 |
| NaOH/urea (2% cotton) | – | 50 | ClH | 1:9 | 4 | 0.98 | 0.30 | 0.25 | 0.26 |
| NaOH/urea (2% cotton) | – | 50 | ClH | 1:9 | 5 | 1.04 | 0.29 | 0.26 | 0.29 |
| NaOH/urea (2% cotton) | – | 50 | ClH | 1:9 | 6 | 1.06 | 0.31 | 0.26 | 0.29 |
| NaOH/urea (2% cotton) | – | 50 | ClH | 1:12 | 5 | 1.44 | 0.44 | 0.30 | 0.40 |

[a]Cellulose concentration given in parenthesis, *EMIMAc* 1-ethyl-3-methylimidazolium acetate, *BMIMCl* 1-butyl-3-methylimidazolium chloride, *SSP* spruce sulfite pulp

[b]DMSO and DMF added as cosolvent [29% (w/w)], $CH_3COOK$ added as catalyst (0.2 mol/mol AGU)

[c]*EtO* ethylene oxide, *PrO* propylene oxide, *ClH* chlorohydrin

[d]Molar ratio AGU:reagent

Hydroxybutyl and higher hydroxyalkyl ethers are scarcely reported in scientific and patent literature. Hydroxymethyl cellulose ("methylol cellulose"), which can be regarded as the first member in the series of hydroxyalkyl ethers, was of certain academic interest. It can be regarded as a half-acetal of formaldehyde and was identified as a compound formed during the dissolution of cellulose in the systems of a dipolar aprotic solvent (e.g., DMSO, DMF, DMA, and NMP) with paraformaldehyde or formaldehyde (see Sect. 3.2.2 and Fig. 5.8) [97]. The methylolation occurs for instance at elevated temperatures (≈130 °C) in DMSO containing paraformaldehyde. The reagent, which is in an equilibrium with the monomeric formaldehyde, can react with the cellulose backbone and/or the newly introduced hydroxyl moiety to yield hydroxymethyl substituents of various chain lengths. A high MS of 15–25 is required to achieve dissolution. In addition, acetal formation with two equivalents of cellulose can occur. The hydroxymethyl group is easily cleaved by reaction with water or methanol, which can be exploited for shaping and regeneration of cellulose.

## 6.3 Silyl Ethers

Compared to alkyl ethers that are rather chemically inert, the Si–O bond in silyl ethers is much more prone to be cleaved in the presence of acids, e.g., gaseous HCl and aqueous acid or aqueous alkali solutions. Thus, cellulose silyl ethers are not employed in a similar way as their alkyl analogous that are commercially produced as additives in aqueous dispersions. Silylated cellulose derivatives are very lipophilic and capable of self-assembling into well-defined two- and three-dimensional structures that can easily be converted into cellulosic materials by hydrolysis of the Si–O bonds under mild conditions. Moreover, silyl ether substituents found use as protection groups for the synthesis of regioselective cellulose derivatives.

The following chapter is mostly dedicated to trimethylsilyl cellulose (TMSC) as the first and most representative silyl ether of cellulose. For further information on the synthesis of silyl ethers with higher alkyl moieties, in particular branched ones, and their use as protection groups, the reader is forwarded to Sect. 4.4. TMSC is obtained by conversion of cellulose with silylation reagents typically trimethylsilyl chloride (TMSCl) or 1,1,1,3,3,3-hexamethyldisilazane (HMDS, Fig. 6.18). The reaction can be performed homogeneously (either completely or partly if phase separation occurs), heterogeneously (cellulose is not dissolved but dispersed in the reaction medium), or in a liquid two-phase system (cellulose is dissolved in a hydrophilic solvent and the silylation reagent is dissolved in an immiscible hydrophobic solvent), depending on the solubility of cellulose and the silylated products in the chosen reaction medium. TMSC is soluble in different organic solvents only in distinct and rather narrow windows of DS values (Fig. 6.19) [98]. Consequently, transition from homogeneous to heterogeneous reaction or vice versa is likely to occur, in particular if high DS > 1.5 are targeted.

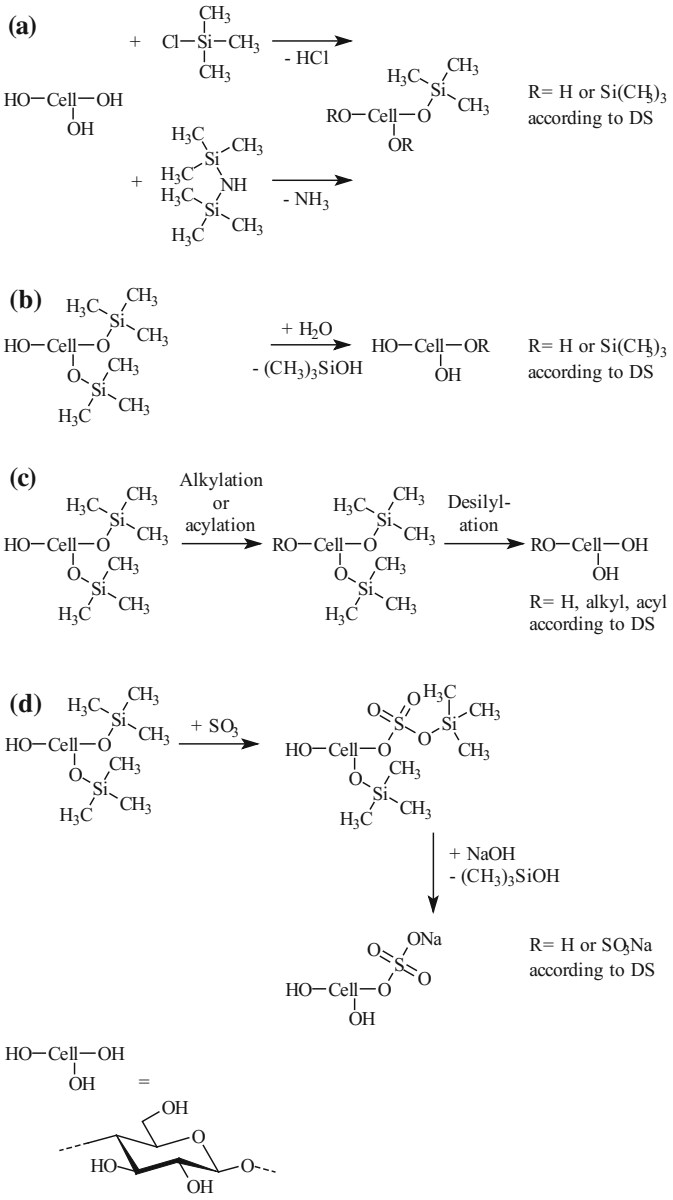


**Fig. 6.18** Reaction scheme for **a** the synthesis, **b** hydrolysis, **c** esterification and etherification, and **d** sulfation of cellulose silyl ethers

Completely homogeneous silylation of cellulose is only feasible if all components (starting cellulose, the silylation reagent, and the TMSC that becomes increasingly hydrophobic with increasing DS) are soluble over the whole course of

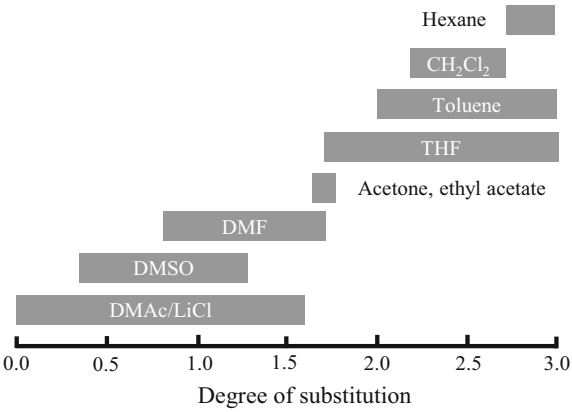


**Fig. 6.19** Dependence of the solubility of trimethylsilyl cellulose in different solvents on the degree of substitution, adapted from [98]

the reaction. The silylation of cellulose in DMAc/LiCl with HMDS and catalytic amounts of TMSCl starts homogeneous until a DS ≈ 1.5 is reached; then, TMSC becomes insoluble and the mixture becomes heterogeneous. The further conversion continues and TMSC with a high DS of up to 2.9 was achieved in this system (Table 6.17) [99]. ILs have also been evaluated as reaction media for the synthesis of TMSC. However, the derivatization reagents, e.g., HMDS, are only partly soluble in those IL that are capable of dissolving cellulose (Table 6.18) [100]. Moreover, TMSC with DS > 1 is no longer soluble in the IL reaction media tested. Completely homogeneous synthesis of TMSC with DS of up to 3 could be achieved in mixtures of IL with chloroform as a cosolvent and HMDS as reagent (Table 6.17) [99, 101]. At low concentrations, 1-methylimidazole, which is found as an impurity in IL of minor grade, can catalyze the silylation reaction yielding high DS values. Imidazolium acetate based IL proved to be the most efficient reaction media.

The silylation of cellulose in IL can also be performed in a liquid two-phase system [100]. HMDS forms a separate layer and conversion occurs at the interphase with the hydrophilic cellulose/IL solution. Toluene, which is also immiscible with the ILs employed, can be added to solubilize the hydrophobic HMDS as well as TMSC of high DS. Upon derivatization in a two-phase reaction mixture, TMSC that is formed at the liquid–liquid interphase becomes increasingly hydrophobic and will partly diffuse from the IL phase into the hydrophobic phase where the reaction velocity for further silylation is much faster. Thus, this approach is suited for the synthesis of TMSC with high DS > 2. If a lower overall DS is targeted, inhomogeneous product mixtures can be expected.

The "classical" heterogeneous etherification in aqueous alkali slurry media is not feasible, due to the sensitivity of the reagents and silylated products toward hydrolysis and because of the limited solubility of silylated compounds (reagent and cellulose derivative) in protic solvents. Pyridine was employed as heterogeneous reaction medium for the activation of cellulose and subsequent conversion with TMSCl [102, 103]. Impurities of pyridinium hydrochloride, which is formed as a side product, can induce desilylation in the presence of water traces, e.g., from

**Table 6.17** Conditions for and results of the silylation of cellulose, dissolved in different reaction media using hexamethyldisilazane (HMDS), adapted from [99–101]

| Reaction course[a] | Solvent[b] | Cosolvent | Additive[c] | Molar ratio[d] | Temperature (°C) | Time (h) | DS[e] |
|---|---|---|---|---|---|---|---|
| hom → het | DMAc/LiCl | – | TMSCl | 1:1:0.1 | 80 | 1 | 0.5 |
| hom → het | DMAc/LiCl | – | TMSCl | 1:1.5:0.1 | 80 | 1 | 1.4 |
| hom → het | DMAc/LiCl | – | TMSCl | 1:2:0.1 | 80 | 1 | 2.2 |
| hom → het | DMAc/LiCl | – | TMSCl | 1:3:0.1 | 80 | 1 | 2.2 |
| hom → het | DMAc/LiCl | – | TMSCl | 1:8:0.1 | 80 | 1 | 2.9 |
| hom → het | EMIMAc | – | – | 1:3 | 80 | 1 | 2.7 |
| hom → het | EMIMAc | – | – | 1:8 | 80 | 1 | 2.9 |
| hom → het | BMIMCl | – | – | 1:5 | 80 | 1 | – |
| hom → het | BMIMCl | – | – | 1:8 | 80 | 1 | 1.9 |
| hom → het | BMIMAc | – | – | 1:9.2 | 100 | 16 | 2.9 |
| hom → het | BMIMBz | – | – | 1:9.2 | 100 | 16 | 2.9 |
| hom → het | BMIMPr | – | – | 1:9.2 | 100 | 16 | 2.9 |
| Two liquid phases | BMIMCl | Toluene | Saccharin | 1:2:0.01 | 80 | 16 h | 0.0 |
| Two liquid phases | BMIMCl | Toluene | Saccharin | 1:3.2:0.01 | 80 | 16 h | 2.2 |
| Two liquid phases | BMIMCl | Toluene | Saccharin | 1:4.3:0.01 | 80 | 16 h | 2.1 |
| Two liquid phases | BMIMCl | Toluene | Saccharin | 1:4.3:0.01 | 100 | 16 h | 2.2 |
| Two liquid phases | BMIMCl | Toluene | Saccharin | 1:4.3:0.01 | 120 | 16 h | 2.2 |
| Two liquid phases | BMIMCl | Toluene | Saccharin | 1:9.2:0.01 | 120 | 16 h | 2.3 |
| hom | EMIMAc | Chloroform | – | 1:3 | 80 | 1 h | 2.2 |
| hom | EMIMAc | Chloroform | – | 1:5 | 80 | 1 h | 2.3 |
| hom | EMIMAc | Chloroform | – | 1:8 | 80 | 1 h | 2. 9 |
| hom | EMIMAc | Chloroform | MI | 1:3:0.01 | 80 | 1 h | 2.7 |
| hom | EMIMAc | Chloroform | MI | 1:3:3 | 80 | 1 h | 2.1 |
| hom | BMIMCl | Chloroform | – | 1:3 | 80 | 1 h | 1.9 |
| hom | BMIMCl | Chloroform | – | 1:5 | 80 | 1 h | 1.7 |

(continued)

**Table 6.17** (continued)

| Reaction course[a] | Solvent[b] | Cosolvent | Additive[c] | Molar ratio[d] | Temperature (°C) | Time (h) | DS[e] |
|---|---|---|---|---|---|---|---|
| hom | BMIMCl | Chloroform | – | 1:8 | 80 | 1 h | 0.4 |
| hom | BMIMCl[f] | Chloroform | MI | 1:8:0 | 80 | 1 h | 0.0 |
| hom | BMIMCl[f] | Chloroform | MI | 1:8:0.07 | 80 | 1 h | 1.9 |
| hom | BMIMCl[f] | Chloroform | MI | 1:8:0.2 | 80 | 1 h | 0.8 |

[a]*hom* Homogeneous, *het* Heterogeneous, *hom* → *het* Transition from homogeneous to heterogeneous
[b]*BMIM* 1-butyl-3-methyl imidazolium, *EMIM* 1-ethyl-3-methyl imidazolium, *Ac* Acetate, *Bz* Benzoate, *Cl* Chloride, *Pr* Propionate
[c]*TMSCl* Trimethylsilyl chloride, *MI* 1-methyl imidazole
[d]molar ratio anhydroglucose unit:HMDS:additive
[e]degree of substitution
[f]high purity ionic liquid (>99%)

**Table 6.18** Solubility of hexamethyldisilazane (HMDS) in different ionic liquids [100]

| Ionic liquid[a] | Solubility of HMDS (mol%) |
|---|---|
| BMIMCl | 1 |
| BMIMAc | 3 |
| BMIMPr | 4 |
| BMIMBz | 3 |
| EMIMDEP | 8 |

[a]*DMA* *N,N*-dimethylacetamide, *BMIM* 1-butyl-3-methyl imidazolium, *EMIM* 1-ethyl-3-methyl imidazolium, *Ac* Acetate, *Bz* Benzoate, *Cl* Chloride, *DEP* Diethylphosphate, *Pr* Propionate

humid air. Liquid ammonia was employed successfully as reaction medium for the synthesis of TMSC with defined DS > 1.5. Moreover, the regioselective synthesis of 6-mono-*O*-thexyldimethylsilyl cellulose in this system was described (see also Sect. 4.4.2) [104].

Initial trials were performed at −70 °C using TMSCl, which generates ammonium chloride as an acidic side product that can catalyze desilylation [103]. It is convenient to perform the reaction in an autoclave at elevated temperatures of 80 °C to avoid technologically challenging cooling operations [105]. More importantly, HMDS can be employed in this case because it is completely soluble in liquid ammonia above 25 °C. Silylation with HMDS only generates more ammonia as side product, which can easily be recovered from the reaction mixture. Cellulose and TMSC with DS < 2.2 and DS > 2.7 are not soluble in the reaction mixture meaning that the conversion is mostly heterogeneous. For an optimum reaction, a ratio HMDS:$NH_{3(l)}$ of 0.9–1.3 and saccharin as a catalyst were employed to achieve high $DS_{TMS}$ up to 3.0. TMSC prepared in liquid ammonia show a higher content of unmodified repeating units and a lower content of 2,6-disilylated repeating units when compared to derivatives with a similar DS that was prepared by two-phasic silylation in IL (Table 6.19) [100].

**Table 6.19** Substitution pattern of trimethylsilyl celluloses prepared in ionic liquids and liquid ammonia as determined by methylation analysis, adapted from [100]

| Medium[a] | DS[b] | Partial DS[c] | | | Mole fractions[d] | | | | | | | |
|---|---|---|---|---|---|---|---|---|---|---|---|---|
| | | 2 | 3 | 6 | 0 | 2 | 3 | 6 | 2-3 | 2-6 | 3-6 | 2-3-6 |
| BMIMCl | 0.9 | 0.30 | 0.17 | 0.43 | 33.7 | 12.8 | 6.5 | 26.6 | 4.5 | 9.5 | 3.6 | 2.8 |
| Ammonia | 0.8 | 0.19 | 0.12 | 0.47 | 38.3 | 9.3 | 4.7 | 35.2 | 1.3 | 5.4 | 3.0 | 2.8 |
| BMIMCl | 1.9 | 0.81 | 0.26 | 0.83 | 2.2 | 8.4 | 2.2 | 6.8 | 5.3 | 56.9 | 8.4 | 10.5 |
| Ammonia | 1.9 | 0.80 | 0.40 | 0.70 | 3.1 | 14.0 | 3.2 | 8.1 | 9.4 | 31.5 | 7.6 | 23.1 |

[a]*BMIMCl* 1-butyl-3-methyl imidazolium chloride
[b]degree of substitution (DS)
[c]partial DS at the individual hydroxyl groups
[d]unmodified: 0; mono-silylated: 2,3,6; di-silylated: 2-3,2-6, 3-6; tri-silylated: 2-3-6

As stated above, the silyl ether linkage in TMSC is susceptible to hydrolysis either under acidic or basic conditions. Partial desilylation in THF/ammonia with saccharine as a catalyst was employed for obtaining TMSC with defined DS starting from highly substituted products [106]. Analogue to the technical synthesis of acetone-soluble cellulose acetate (see Sect. 5.1.1), this approach can circumvent the limitation of heterogeneous silylation procedures regarding product uniformity at low overall DS. The desilylation is limited to the amount of water added; the DS values predicted and obtained correlate well down to a DS $\approx$ 1. At lower DS, TMSC becomes insoluble in THF and the rate of hydrolysis becomes slower.

Completely desilylation, which can be achieved by hydrolysis with 1 N HCl (aq) or gaseous HCl, has been employed to convert organosoluble TMSC that was processed into a specific shape into defined cellulosic materials. For the preparation of cellulose fibers, analogue to the viscose process, this approach found little interest due to limitations regarding costs and applicability of the silylation in larger scales [103]. However, TMSC is widely employed for the fabrication of cellulose films and model surfaces that can be used, e.g., to study adsorption processes and enzymatic or chemical conversion of cellulose at the surfaces, and the assembling/disassembling of bio-composites [107, 108]. TMSC can be dissolved in organic solvents, spin coated, and regenerated by solvent evaporation to generate films with a thickness of 10–50 nm after conversion to cellulose by exposure to gaseous HCl [109]. TMSC with DS > 2 are strongly hydrophobic and self-assemble on water into Langmuir monolayers surfaces after applying a TMSC solution in chloroform and evaporation of the solvent [110, 111]. Thin TMSC films on different supports can be prepared by Langmuir–Blodgett or Langmuir–Schaeffer deposition (Fig. 6.20a, b).

The tendency of TMSC for supramolecular self-assembling in aqueous systems was exploited for the preparation of cellulosic nanoparticles [99]. Upon the dialysis of TMSC solutions in a suitable solvent (e.g., DMA or THF) against water, the hydrophobic silyl ethers form spherical particles. The particles sizes and polydispersity strongly depend on the content of silyl moieties; at DS 1.4–1.9 rather uniform particles with a polydispersity index (PDI) of 0.1–0.3 and sizes in the range

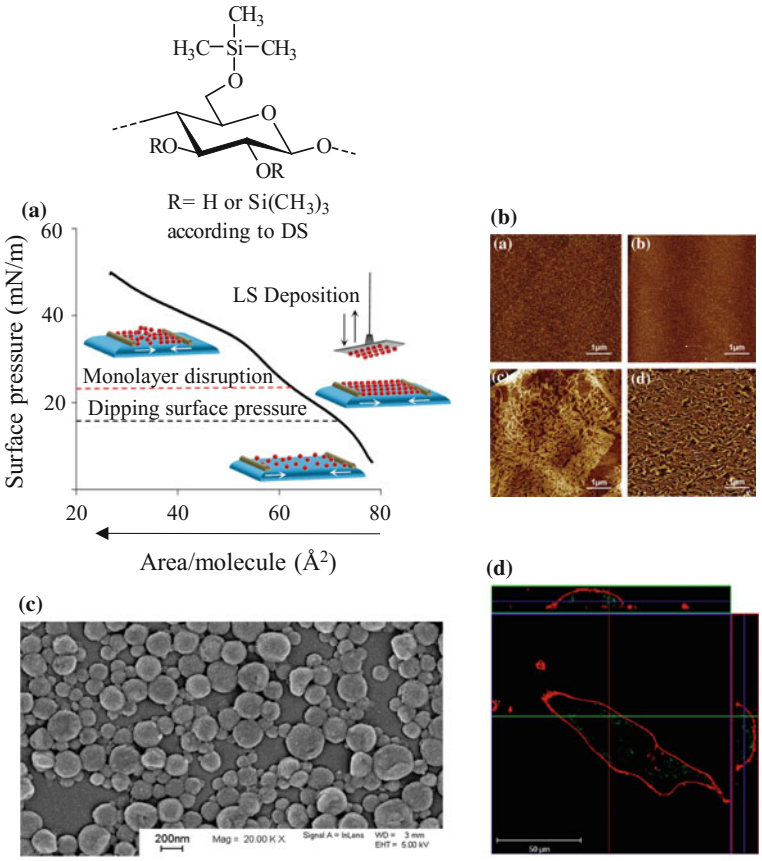


**Fig. 6.20** **a** Schematic and surface pressure-area isotherm for the deposition of trimethylsilyl cellulose (TMSC) as Langmuir Schaefer films and **b** atom force microscopy images of TMSC films on different surfaces (Reproduced (adapted) from Ref. [111] with permission of The Royal Society of Chemistry), **c** Scanning electron microscopy image of cellulose particles obtained by dialysis of TMSC and **d** confocal micrograph of human fibroblasts (red: cell membrane) after incubation with dye labeled cellulose nanoparticles (green) obtained from TMSC, Reproduced (adapted) from Ref. [112] with permission of John Wiley and Sons

of 180–270 nm are obtained (Fig. 6.20c). At higher DS, the particles become much larger (>1 μm) while at lower DS no particles are formed. The particle formation process is similar to the self-assembling of hydrophobic cellulose esters into nanoparticles [113]. However, the silyl moieties are completely cleaved during the dialysis leading to the formation of cellulose nanoparticles. In comparison, the ester groups are stable under the same conditions, i.e., cellulose ester particles are obtained. TMSC-based cellulose nanoparticles bear OH groups that are available for further chemical modification, e.g., with dyes or drugs. They are also taken up by cells without showing cytotoxicity (Fig. 6.20d).

In the absence of water, silyl moieties are stable under the conditions of common esterification and etherification reactions. The remaining hydroxyl groups in partially silylated cellulose derivatives can be further modified to yield derivatives with a molecular structure that is predefined by the DS and substitution pattern of the original silyl ether (see Fig. 6.18c). This approach was employed extensively for the synthesis of regioselectively modified cellulose derivatives with the aid of bulky silyl ether protecting groups such as thexyldimethylsilyl (see Sect. 4.4.2). TMSC was also used as intermediate for the synthesis of cellulose ester [98]. The TMS group imparts solubility in organic media, i.e., enables homogeneous reaction conditions and limits the maximum DS achievable. Conversion of TMSC with acyl chlorides in the presence of a tertiary amine as a base yields silylated and esterified mixed derivatives. The silyl group can be cleaved under mild acidic conditions, e.g., treatment with 1 M HCl for 1 h at room temperature, without removal of the acyl groups. At elevated temperatures (80–160 °C) and in the absence of a base, TMS groups are partially removed during the esterification with acyl chlorides. The $DS_{ester}$ exceeds the initial $DS_{TMS}$.

In contrast to the synthesis of organic cellulose esters from TMSC, which occurs at the remaining hydroxyl groups, sulfation of TMSC proceeds via an insertion of $SO_3$ into the Si–O bond (see Fig. 6.18d) [114]. The maximum $DS_{sulfate}$ that can be achieved is limited to the starting $DS_{TMS}$ and the residual silyl moieties are removed during the workup with aqueous alkali. Depending on the type of sulfation reagent, different substitution patterns can be achieved [115]. $SO_3$–DMF complex results in predominant sulfation of position 6, whereas $SO_3$–triethylamine complex favors sulfation of position 2 over positions 3 and 6.

## References

1. Dahlgren L (1987) Cellulose ethers—properties and applications. In: Kennedy JF, Phillips GO, Williams PA (eds) Wood Cellulose. Horwood Publishing, Chichester, pp 427–439
2. Nicholson MD, Merritt FM (1989) Cellulose ethers. In: Nevell TP, Zeronian SH (eds) Cellulose chemistry. Its application. Horwood Publishing, Chichester, UK, pp 363–383
3. Feddersen RL, Thorp SN (1993) In: Whistler RL, BeMiller JN (eds) Industrial gums, polysaccharides and their derivatives, 3rd edn. Academic Press, Inc., San Diego, Boston, New York, USA, p 537
4. Baar A, Kulicke W-M, Szablikowski K, Kiesewetter R (1994) Nuclear magnetic resonance spectroscopic characterization of carboxymethyl cellulose. Macromol Chem Phys 195:1483–1492
5. Reuben J, Conner HT (1983) Analysis of the carbon-13 NMR spectrum of hydrolyzed O-(carboxymethyl)cellulose: monomer composition and substitution patterns. Carbohydr Res 115:1–13
6. Tezuka Y, Tsuchiya Y, Shiomi T (1996) Proton and carbon-13 NMR structural study on cellulose and polysaccharide derivatives with carbonyl groups as a sensitive probe. Part II. Carbon-13 NMR determination of substituent distribution in carboxymethyl cellulose by use of its peresterified derivatives. Carbohydr Res 291:99–108

7. Kragten EA, Kamerling JP, Vliegenthart JFG (1992) Composition analysis of carboxymethylcellulose by high-pH anion-exchange chromatography with pulsed amperometric detection. J Chromatogr 623:49–53
8. Heinze T, Erler U, Nehls I, Klemm D (1994) Determination of the substituent pattern of heterogeneously and homogeneously synthesized carboxymethyl cellulose by using high-performance liquid chromatography. Angew Makromol Chem 215:93–106
9. Liebert T, Heinze T (1998) Induced phase separation: a new synthesis concept in cellulose chemistry. ACS Symp Ser 688:61–72
10. Heinze T (1997) Ionische Funktionspolymere aus Cellulose: Neue Synthesekonzepte, Strukturaufklärung und Eigenschaften. Habilitation Thesis, Friedrich Schiller University of Jena
11. Burger J, Kettenbach G, Klüfers P (1995) Polyol metal complexes. Part 14. Coordination equilibria in transition metal based cellulose solvents. Macromol Symp 99:113–126
12. Heinze T, Liebert T, Klüfers P, Meister F (1999) Carboxymethylation of cellulose in unconventional media. Cellulose 6:153–165
13. Käuper P, Kulicke W-M, Horner S, Saake B, Puls J, Kunze J, Fink H-P, Heinze U, Heinze T, Klohr EA, Thielking H, Koch W (1998) Development and evaluation of methods for determining the pattern of functionalization in sodium carboxymethylcelluloses. Angew Makromol Chem 260:53–63
14. Myllymaeki V, Aksela R (2005) Etherification of cellulose in ionic liquid solutions. WO2005054298A1. CAN 143:28326
15. Heinze T, Schwikal K, Barthel S (2005) Ionic liquids as reaction medium in cellulose functionalization. Macromol Biosci 5:520–525
16. Ramos LA, Frollini E, Heinze T (2005) Carboxymethylation of cellulose in the new solvent dimethyl sulfoxide/tetrabutylammonium fluoride. Carbohydr Polym 60:259–267
17. Heinze T, Köhler S (2010) Dimethyl sulfoxide and ammonium fluorides—a novel cellulose solvent. ACS Symp Ser 1033:108–118
18. Liebert T, Klemm D, Heinze T (1996) Synthesis and carboxymethylation of organo-soluble trifluoroacetates and formates of cellulose. J Macromol Sci Part A Pure Appl Chem A33:613–626
19. Saake B, Horner S, Kruse T, Puls J, Liebert T, Heinze T (2000) Detailed investigation on the molecular structure of carboxymethyl cellulose with unusual substitution pattern by means of an enzyme-supported analysis. Macromol Chem Phys 201:1996–2002
20. Clasen C, Wilhelms T, Kulicke W-M (2006) Formation and characterization of chitosan membranes. Biomacromol 7:3210–3222
21. Baklagina YG, Kononova SV, Petrova VA, Kruchinina EV, Nud'ga LA, Romanov DP, Klechkovskaya VV, Orekhov AS, Bogomazov AV, Arkhipov SN (2013) Study of polyelectrolyte complexes of chitosan and sulfoethyl cellulose. Crystallogr Rep 58:287–294
22. Schwarz H-H, Lukáš J, Richau K (2003) Surface and permeability properties of membranes from polyelectrolyte complexes and polyelectrolyte surfactant complexes. J Membr Sci 218:1–9
23. Rose T, Neumann B, Thielking H, Koch W, Vorlop K-D (2000) Hollow beads of Sulfoethyl Cellulose (SEC) on the basis of polyelectrolyte complexes. Chem Eng Technol 23:769–772
24. Shimizu T, Tadokoro K, Suganuma A, Hirose M (1984) Chromatography of inorganic ions on sulfoethyl cellulose layer in mixed sulfuric acid-organic solvent media. Chromatographia 18:692–694
25. Glasser WG, Michalek A (2006) Sulfoalkylated cellulose having superabsorbent properties and method for its manufacture. US 20060142560 A1 20060629, CAN 145:105442
26. Donges R, Kirchner J (2000) Water-soluble hydrophobically modified sulfoalkyl cellulose ethers, process for making the same and their use in dispersion paints. EP 997478 A1 20000503, CAN 132:323031
27. Höhl F, Schlesiger H, Kiesewetter R (2001) Manufacture of (methyl- and hydroxyalkyl-substituted) sulfoalkyl-modified cellulose ethers as nonassociative thickeners for aqueous coating systems. DE 19935323 A1 20010201 CAN134:133138

28. Kiesewetter R, Szablikowski K, Lange W (1993) Water-soluble sulfoalkyl-hydroxyalkyl cellulose derivatives, and their use in cement and/or gypsum compositions. EP 554749 A2 19930811, CAN120:306034
29. Zhang K, Brendler E, Gebauer K, Gruner M, Fischer S (2011) Synthesis and characterization of low sulfoethylated cellulose. Carbohydr Polym 83:616–622
30. Talába P, Sroková I, Ebringerová A, Hodul P, Marcinčin A (1997) Cellulose-based biodegradable polymeric surfactants. J Carbohydr Chem 16:573–582
31. Heinze T, Haack V, Rensing S (2004) Starch derivatives of high degree of functionalization. 7. Preparation of cationic 2-hydroxypropyltrimethylammonium chloride starches. Starch/Staerke 56:288–296
32. Podgornyi VF, Gur'ev VP (1981) Simple method for the synthesis of AE-cellulose—matrix for profenzym production. Immobilizovannye Proteoliticheskie Fermnty Lech Gnoino-Nekroticheskikh Protsessov 124–131
33. Bischoff KH, Dautzenberg H (1977) Aminoethylated cellulose powder. DD 124419 A1 19770223, CAN88:24439
34. Soignet DM, Benerito RR (1967) Improved preparation of diethylaminoethyl-cotton-fabrics. Text Res J 37:1001–1003
35. Rousseau RW, Ferrell JK, Reardon RF (1984) Synthesis of diethylaminoethyl cellulose on cotton fabric. Ind Eng Chem Prod Res Dev 23:250–252
36. Yang H, Thyrion FC (1996) Kinetic studies of the reaction of 2-diethylaminoethylchloride with nucleophilic reagents in N, N-dimethylformamide. Bull Soc Chim Belg 105:23–31
37. Noreika R, Zdanavicius J (1971) Reaction of cellulose with diethylepoxypropylamine. Cellul Chem Technol 5:117–129
38. Acikara ÖB (2013) Ion-exchange chromatography and its applications. In: Martin D (ed) Chapter 2 in column chromatography, InTech
39. www.gelifesciences.co.jp/tech_support/manual/pdf/71710000.pdf. Accessed May 2015; www.himedialabs.com/TD/MB110.pdf. Accessed May 2015
40. Liesiene J (2010) Synthesis of water-soluble cationic cellulose derivatives with tertiary amino groups. Cellulose 17:167–172
41. Prado HJ, Matulewicz MC (2014) Cationization of polysaccharides: a path to greener derivatives with many industrial applications. Eur Polym J 52:53–75
42. Käufer K, Krause T, Schempp W (1980) Production of cationic pulps. Effect of different variables on the degree of substitution and on yield. Papier (Bingen, Germany) 34:575–579
43. www.quab.com. Accessed May 2015; www.dow.com/quat. Accessed May 2015
44. Gruber E, Granzow C, Ott T (1996) New ways to cationic cellulose. Papier (Darmstadt) 50:729–734
45. Hashem M, El-Bisi M, Sharaf S, Refaie R (2010) Pre-cationization of cotton fabrics: an effective alternative tool for activation of hydrogen peroxide bleaching process. Carbohydr Polym 79:533–540
46. Acharya S, Abidi N, Rajbhandari R, Meulewaeter F (2014) Chemical cationization of cotton fabric for improved dye uptake. Cellulose 21:4693–4706
47. Ott G, Schempp W, Krause T (1989) Preparation of cationic cellulose with high degree of substitution in lithium chloride/dimethylacetamide. Papier (Bingen, Germany) 43:694–699
48. Pašteka M (1988) Quaternization of regenerated cellulose under homogeneous reaction conditions. Acta Polym 39:130–132
49. Song Y, Sun Y, Zhang X, Zhou J, Zhang L (2008) Homogeneous quaternization of cellulose in NaOH/urea aqueous solutions as gene carriers. Biomacromolecules 9:2259–2264
50. Yan L, Tao H, Bangal PR (2009) Synthesis and flocculation behavior of cationic cellulose prepared in a NaOH/urea aqueous solution. Clean Soil Air Water 37:39–44
51. Song Y, Wang H, Zeng X, Sun Y, Zhang X, Zhou J, Zhang L (2010) Effect of molecular weight and degree of substitution of quaternized cellulose on the efficiency of gene transfection. Bioconjug Chem 21:1271–1279

52. Song Y, Zhang J, Gan W, Zhou J, Zhang L (2010) Flocculation properties and antimicrobial activities of quaternized celluloses synthesized in NaOH/urea aqueous solution. Ind Eng Chem Res 49:1242–1246
53. Hossel P, Dieing R, Norenberg R, Pfau A, Sander R (2000) Conditioning polymers in today's shampoo formulations—efficacy, mechanism and test methods. Int J Cosmet Sci 22:1–10
54. Liesiene J, Kazlauske J (2013) Functionalization of cellulose: synthesis of water-soluble cationic cellulose derivatives. Cellul Chem Technol 47:515–525
55. Methocell cellulose ethers technical handbook, 2002. The Dow Chemical Company, USA
56. Ethocell ethylcellulose polymers technical handbook, 2005. The Dow Chemical Company, USA
57. Benecel high purity methylcellulose, methylhydroxypropylcellulose, hypromellose physical and chemical properties. Ashland Inc., USA
58. Aqualon ethylcellulose physical and chemical properties, 2002. Ashland Inc., USA
59. Dönges R (1990) Nonionic cellulose ethers. Brit Polym J 23:315–326
60. Jay A (1996) The methylation reaction in carbohydrate analysis. J Carbohydr Chem 15:897–923
61. Hirrien M, Desbrières J, Rinaudo M (1997) Physical properties of methyl celluloses in relation with the conditions for cellulose modification. Carbohydr Polym 31:243–252
62. Petruš L, Gray DG, BeMiller JN (1995) Homogeneous alkylation of cellulose in lithium chloride/dimethyl sulfoxide solvent with dimsyl sodium activation. A proposal for the mechanism of cellulose dissolution in LiCl/$Me_2S$. Carbohydr Res 268:319–323
63. Zhou J, Xu Y, Wang X, Qin Y, Zhang L (2008) Microstructure and aggregation behavior of methylcelluloses prepared in NaOH/urea aqueous solutions. Carbohydr Polym 74:901–906
64. Nagel MCV, Koschella A, Voiges K, Mischnick P, Heinze T (2010) Homogeneous methylation of wood pulp cellulose dissolved in LiOH/urea/$H_2O$. Eur Polym J 46:1726–1735
65. Sun S, Foster TJ, MacNaughtan W, Mitchell JR, Fenn D, Koschella A, Heinze T (2009) Self-association of cellulose ethers with random and regioselective distribution of substitution. J Polym Sci Part B Polym Phys 47:1743–1752
66. Li L, Thangamathesvaran PM, Yue CY, Tam KC, Hu X, Lam YC (2001) Gel network structure of methylcellulose in water. Langmuir 17:8062–8068
67. McAllister JW, Schmidt PW, Dorfman KD, Lodge TP, Bates FS (2015) Thermodynamics of aqueous methylcellulose solutions. Macromolecules 48:7205–7215
68. Wang Q, Li L (2005) Effects of molecular weight on the thermoreversible gelation and gel elasticity of methylcellulose in aqueous solution. Carbohydr Polym 62:232–238
69. Heinze T, Pfeifer A, Sarbova V, Koschella A (2011) 3-O-Propyl cellulose: cellulose ether with exceptionally low flocculation temperature. Polym Bull 66:1219–1229
70. Braun D, Meuret B (1989) Benzyl cellulose as thermoplastic resin. I. Preparation and characterization. Papier (Bingen, Germany) 43:688–694
71. Ramos LA, Frollini E, Koschella A, Heinze T (2005) Benzylation of cellulose in the solvent dimethylsulfoxide/tetrabutylammonium fluoride trihydrate. Cellulose 12:607–619
72. Daly WH, Caldwell JD (1979) Influence of quaternary ammonium salts on cellulose benzylation. J Polym Sci Polym Lett Ed 17:55–63
73. Rohleder E, Heinze T (2010) Comparison of benzyl cellulose synthesized in aqueous NaOH and dimethyl sulfoxide/tetrabutylammonium fluoride. Macromol Symp 294:107–116
74. Li MF, Sun SN, Xu F, Sun RC (2011) Cold NaOH/urea aqueous dissolved cellulose for benzylation: synthesis and characterization. Eur Polym J 47:1817–1826
75. Erler U, Klemm D, Nehls I (1992) Homogeneous synthesis of diphenylmethyl ethers of cellulose in N, N-dimethylacetamide/lithium chloride solvent system. Makromol Chem Rapid Commun 13:195–201
76. Hagiwara I, Shiraishi N, Yokota T, Norimoto M, Hayashi Y (1981) Homogeneous tritylation of cellulose in a sulfur dioxide—diethylamine—dimethyl sulfoxide medium. J Wood Chem Technol 1:93–109

77. Camacho Gómez JA, Erler UW, Klemm DO (1996) 4-Methoxy substituted trityl groups in 6-O protection of cellulose: homogeneous synthesis, characterization, detritylation. Macromol Chem Phys 197:953–964
78. Fenn D, Pohl M, Heinze T (2009) Novel 3-O-propargyl cellulose as a precursor for regioselective functionalization of cellulose. React Funct Polym 69:347–352
79. Faugeras PA, Elchinger PH, Brouillette F, Montplaisir D, Zerrouki R (2012) Advances in cellulose chemistry—microwave-assisted synthesis of propargylcellulose in aqueous medium. Green Chem 14:598–600
80. Hu H, You J, Gan W, Zhou J, Zhang L (2015) Synthesis of allyl cellulose in NaOH/urea aqueous solutions and its thiol—ene click reactions. Polym Chem 6:3543–3548
81. Volkert B, Wagenknecht W, Mai M (2010) Structure-property relationship of cellulose ethers—influence of the synthetic pathway on cyanoethylation. ACS Symp Ser 1033:319–341
82. Zhou J, Li Q, Song Y, Zhang L, Lin X (2010) A facile method for the homogeneous synthesis of cyanoethyl cellulose in NaOH/urea aqueous solutions. Polym Chem 1:1662–1668
83. Li Q, Wu P, Zhou J, Zhang L (2012) Structure and solution properties of cyanoethyl celluloses synthesized in LiOH/urea aqueous solution. Cellulose 19:161–169
84. Li W, Liu R, Kang H, Sun Y, Dong F, Huang Y (2013) Synthesis of amidoxime functionalized cellulose derivatives as a reducing agent and stabilizer for preparing gold nanoparticles. Polym Chem 4:2556–2563
85. Kamel S, Hassan EM, El-Sakhawy M (2006) Preparation and application of acrylonitrile-grafted cyanoethyl cellulose for the removal of copper (II) ions. J Appl Polym Sci 100:329–334
86. Natrosol® Hydroxyethylcellulose A nonionic water-soluble polymer, 1999. Ashland Inc., USA
87. Cellosize hydroxyethyl cellulose, 2005. The Dow Chemical Company, USA
88. Klucel hydroxypropylcellulose physical and chemical properties, 2012. Ashland Inc., USA
89. Li CL, Martini LG, Ford JL, Roberts M (2005) The use of hypromellose in oral drug delivery. J Pharm Pharmacol 57:533–546
90. Sharma V, Haward SJ, Serdy J, Keshavarz B, Soderlund A, Threlfall-Holmes P, McKinley GH (2015) The rheology of aqueous solutions of ethyl hydroxy-ethyl cellulose (EHEC) and its hydrophobically modified analogue (hmEHEC): extensional flow response in capillary break-up, jetting (ROJER) and in a cross-slot extensional rheometer. Soft Matter 11:3251–3270
91. Wang J, Somasundaran P (2006) Mechanisms of ethyl(hydroxyethyl) cellulose–solid interaction: influence of hydrophobic modification. J Colloid Interface Sci 293:322–332
92. Karlberg M, Thuresson K, Lindman B (2005) Hydrophobically modified ethyl(hydroxyethyl) cellulose as stabilizer and emulsifying agent in macroemulsions. Colloids Surf A 262:158–167
93. Arisz PW, Thai HTT, Boon JJ, Salomons WG (1996) Changes in substituent distribution patterns during the conversion of cellulose to O-(2-hydroxyethyl) celluloses. Cellulose 3:45–61
94. Asandei N, Perju N, Nicolescu R, Ciovica S (1995) Some aspects concerning the synthesis and properties of hydroxypropyl cellulose. Cellul Chem Technol 29:261–271
95. Köhler S, Liebert T, Heinze T, Vollmer A, Mischnick P, Möllmann E, Becker W (2010) Interaction of ionic liquids with polysaccharides 9. Hydroxyalkylation of cellulose without additional inorganic bases. Cellulose 17:437–448
96. Zhou J, Qin Y, Liu S, Zhang L (2006) Homogeneous synthesis of hydroxyethylcellulose in NaOH/urea aqueous solution. Macromol Biosci 6:84–89
97. Baker TJ, Schroeder LR, Johnson DC (1981) Formation of methylol cellulose and its dissolution in polar aprotic solvents. Cellul Chem Technol 15:311–320

98. Klemm D, Schnabelrauch M, Stein A, Philipp B, Wagenknecht W, Nehls I (1990) New results for homogeneous esterification of cellulose by soluble intermediates. Papier (Bingen, Germany) 44:624–632
99. Kostag M, Köhler S, Liebert T, Heinze T (2010) Pure cellulose nanoparticles from trimethylsilyl cellulose. Macromol Symp 294(II):96–106
100. Mormann W, Wezstein M (2009) Trimethylsilylation of cellulose in ionic liquids. Macromol Biosci 9:369–375
101. Köhler S, Liebert T, Heinze T (2008) Interactions of ionic liquids with polysaccharides. VI. Pure cellulose nanoparticles from trimethylsilyl cellulose synthesized in ionic liquids. J Polym Sci Part A Polym Chem 46:4070–4080
102. Klebe JF, Finkbeiner HL (1969) Silyl celluloses: a new class of soluble cellulose derivatives. J Polym Sci Part A-1 Polym Chem 7:1947–1958
103. Greber G, Paschinger O (1981) Silyl derivates of cellulose. Papier (Bingen, Germany) 35:547–554
104. Petzold K, Koschella A, Klemm D, Heublein B (2003) Silylation of cellulose and starch—selectivity, structure analysis, and subsequent reactions. Cellulose 10:251–269
105. Mormann W (2003) Silylation of cellulose with hexamethyldisilazane in ammonia—activation, catalysis, mechanism, properties. Cellulose 10:271–281
106. Mormann W, Demeter J (2000) Controlled desilylation of cellulose with stoichiometric amounts of water in the presence of ammonia. Macromol Chem Phys 201:1963–1968
107. Tammelin T, Saarinen T, Österberg M, Laine J (2006) Preparation of Langmuir/Blodgett-cellulose surfaces by using horizontal dipping procedure. Application for polyelectrolyte adsorption studies performed with QCM-D. Cellulose 13:519–535
108. Mohan T, Kargl R, Doliška A, Ehmann HMA, Ribitsch V, Stana-Kleinschek K (2013) Enzymatic digestion of partially and fully regenerated cellulose model films from trimethylsilyl cellulose. Carbohydr Polym 93:191–198
109. Kontturi E, Thüne PC, Niemantsverdriet JW (2003) Cellulose model surfaces—simplified preparation by spin coating and characterization by x-ray photoelectron spectroscopy, infrared spectroscopy, and atomic force microscopy. Langmuir 19:5735–5741
110. Schaub M, Wenz G, Wegner G, Stein A, Klemm D (1993) Ultrathin films of cellulose on silicon wafers. Adv Mater 5:919–922
111. Niinivaara E, Kontturi E (2014) 2D dendritic fractal patterns from an amphiphilic polysaccharide. SoftMatter 10:1801–1805
112. Liebert T, Kostag M, Wotschadlo J, Heinze T (2011) Stable cellulose nanospheres for cellular uptake. Macromol Biosci 11:1387–1392
113. Wondraczek H, Petzold-Welcke K, Fardim P, Heinze (2013) Nanoparticles from conventional cellulose esters: evaluation of preparation methods. Cellulose 20:751–760
114. Wagenknecht W, Nehls I, Stein A, Klemm D, Philipp B (1992) Synthesis and substituent distribution of Na-cellulose sulphates via trimethylsilyl cellulose as intermediate. Acta Polym 43:266–269
115. Richter A, Klemm D (2003) Regioselective sulfation of trimethylsilyl cellulose using different $SO_3$-complexes. Cellulose 10:133–138
116. Liebert T, Heinze T (1998) Synthesis path versus distribution of functional groups in cellulose ethers. Macromol Symp 130:271–283

# Chapter 7
# Miscellaneous Cellulose Derivatives and Reactions

## 7.1 Oxidation of Cellulose

### *7.1.1 Introduction*

Oxidation of cellulose is another important synthesis path to modify the properties of the biopolymer to get value-added products. Various macroscopic properties and the chemical behavior may be changed (Fig. 7.1). Moreover, oxidation may lead to bioactive materials that find applications in the medical field. For instance, oxidized cellulose is used as absorbable hemostatic scaffold material because it is restorable and degradable under physiological conditions [1, 2]. The oxidized cellulose may also be applied for postsurgical adhesion prevention layer [3, 4] and show pronounced blood-clotting activity [5].

### *7.1.2 Reagents for and Products of the Oxidation of Cellulose*

In principal, cellulose may be oxidized by introduction of carboxy-, aldehyde-, and keto groups (see Fig. 7.1); the products obtained are denoted as carboxy cellulose, (di)aldehyde cellulose, and ketocellulose, respectively. In various cases, different groups are formed by the same reaction and, thus, oxidation products of cellulose are often denoted "oxycellulose". Regarding product properties, a selective oxidation is desired with regard to the functional group and the regioselectivity of oxidation. There are various reagents to oxide cellulose, however, compared to low molecular organic chemistry, many reagents cannot be used because strong acidic or basic media must be applied leading to biopolymer degradation. Oxidizing reagents for cellulose can be divided into nonselective (nitrogen oxides [6], alkali



T. Heinze et al., *Cellulose Derivatives*, Springer Series on Polymer and Composite Materials, https://doi.org/10.1007/978-3-319-73168-1_7

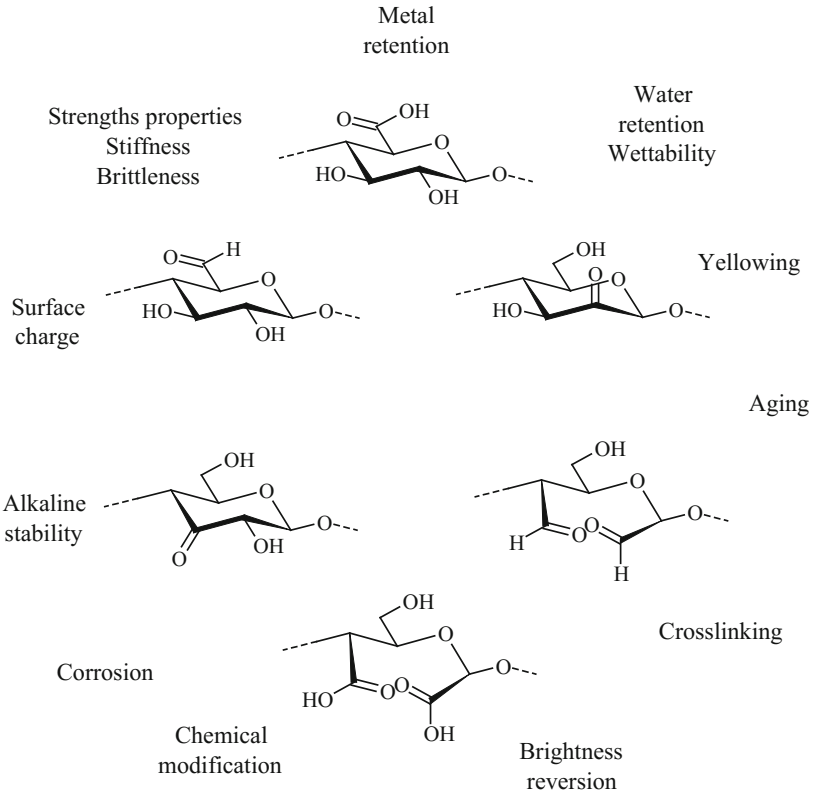


**Fig. 7.1** Effects of carbonyl- and carboxyl groups on macroscopic properties of cellulose

metal nitrites and nitrates [7], ozone [8], permanganates [9], peroxides [10]), and selective ones (most popular periodates, [11–13], and nitroxyl radicals [14–22]).

### *7.1.3 Oxidation of the Primary Hydroxyl Groups at Position 6 of the AGU*

Cellulose can be oxidized at position 6 of the AGU to yield 6-aldehyde- and 6-carboxycellulose. 6-Carboxycellulose may be obtained by reaction with nitrogen dioxide ($NO_2$ respectively $N_2O_4$) applying a nonpolar solvent like tetrachloromethane as reaction medium [23] at least with certain selectivity. The reaction of cellulose with $NO_2$ ($N_2O_4$) was studied in detail and it turned out that some carbonyl groups are formed. Moreover, the products contain nitrogen and a severe degradation occurred [24].

An improved method of the oxidation of cellulose with nitrogen oxides is based on a reaction of the biopolymer in a highly swollen system. Cellulose in phosphoric acid is treated with $NaNO_2$ that formed $N_2O_3$ as oxidation agent [7, 25]. The liberated oxidation agent $N_2O_3$ generated a foam, which guarantees the contact between the gas and the cellulose and prevents the loss of the gaseous oxidation agent. As an interesting consequence, the degree of oxidation reached is increased with increasing MM of the starting cellulose [25]. The chemical shift of the signals in the $^{13}C$ NMR spectra clearly indicate the selective oxidation. Figure 7.2 shows spectra of a sample (in $D_2O$) with a degree of oxidation of 0.62 and of an almost completely oxidized sample (degree of oxidation of 0.82). In addition to signals found in spectra of cellulose, a new signal occurs at 175.5 ppm, which can be assigned to the carboxyl moiety at position 6 of the AGU. At relatively low degree

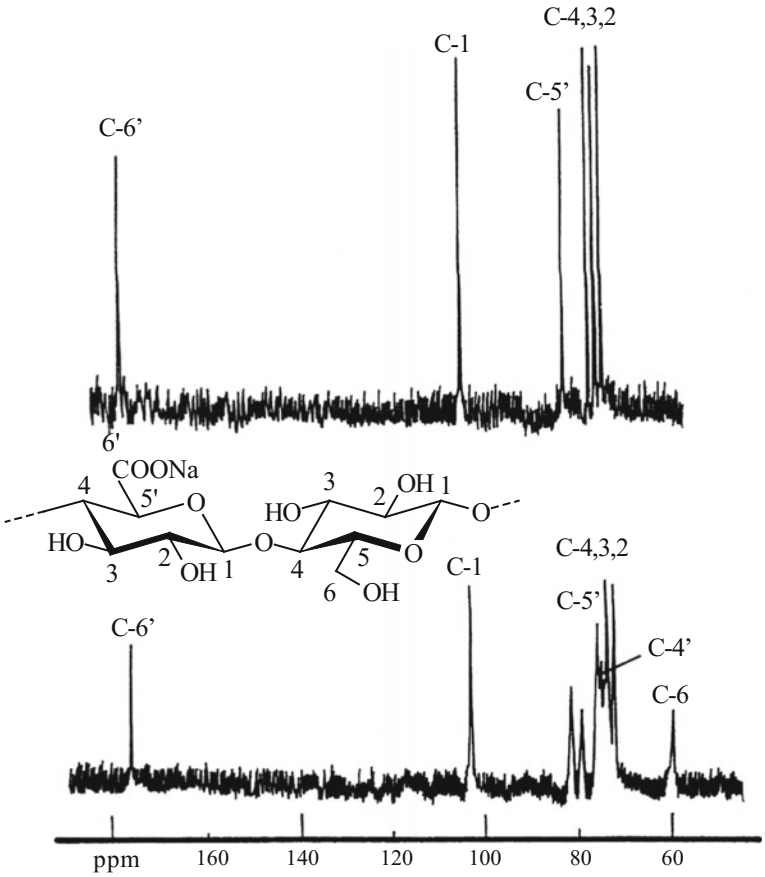


**Fig. 7.2** $^{13}C$ NMR spectra of 6-carboxy cellulose with degree of oxidation of 62% (bottom) and 82% (top, adapted from [26])

of oxidation, the signal of the primary hydroxyl groups is still visible (as expected) while the samples of higher degree of oxidation does not show this signals anymore.

The carboxylic acid formed is usually transferred into the salt mostly with aqueous sodium hydroxide.

Surprisingly, the samples show an additional signal in the carbonyl range of the $^{13}C$ NMR spectra at about 165 ppm, which could be assigned to formic acid ester groups. Formic acid is used to destroy the remaining oxidation agent and, thus, under the acidic conditions a formic acid ester may be formed. If sodium borohydride is used to transfer the carboxylic acid group into the sodium salt, the 6-carboxy cellulose is free of any ester moiety. Thus, a pure product can be obtained. The existence of keto groups as discussed by Painter et al. [27] could not be confirmed because of the absence of NMR signals typical for C=O groups [28].

The cellulose oxidation by nitrogen dioxide dissolved in pressurized carbon dioxide was reported [29]. Although supercritical $CO_2$ is of growing interest as reaction medium for various chemical modifications, for oxidation of cellulose, it appears that its role is not as neutral as expected and the degree of oxidation of cellulose depends on the amount of $CO_2$ introduced [29]. It is assumed that $CO_2$ interacts with $NO_2$, thus, inhibiting the reactivity of $NO_2$ towards cellulose.

Starting with the pioneering work of de Nooy et al. in 1994 [30], the oxidation system 2,2,6,6-tetramethylpiperidine-*N*-oxyl (TEMPO)/KBr/NaClO has gained importance for the transformation of primary hydroxyl groups in polysaccharides into the corresponding polyuronic analogues. This reaction is mostly studied in the field of selective oxidation of various polysaccharides including cellulose. TEMPO-oxidation ensures high reaction rate and yields. The selectivity is very high with a modest degradation of polysaccharide throughout process [18].

The actual oxidizing species is the nitrosonium ion (**C**, Fig. 7.3) that is formed from TEMPO (**B**, Fig. 7.3). The generation of nitrosonium ion takes place in situ by the reaction of TEMPO with oxidants, mainly hypobromite ions, which in turn are being generated from bromide salts and sodium hypochlorite (Fig. 7.3). In the oxidation process, **C** is converted into *N*-hydroxy-2,2,6,6-tetramethylpiperidine (**A**, Fig. 7.3), the reduced form of TEMPO.

The oxidation of cellulose under the action of NaOCl is usually carried out in alkaline aqueous media in the presence of 0.5–4 mol% TEMPO and 5–30 mol% NaBr as catalyst (with respect the substrate) at low temperature [31]. The lowest depolymerization of amorphous cellulose was found for conversions at pH 10 and 4 °C [16]. The oxidation at room temperature using TEMPO/NaBr/NaClO has been used to increase the content of carboxyl groups of several different cellulosic samples [19]. In this work, it was stated that the key factors controlling the depolymerization of cellulose (regenerated or mercerized) are the charge of TEMPO, reaction time, and temperature. The treatment of native celluloses with TEMPO/NaBr/NaClO in water at pH value of 10 results in efficient cellulose surface oxidation yielding sodium carboxylate groups, maintaining the original fibrous morphologies, crystallinities, and crystal sizes [32].

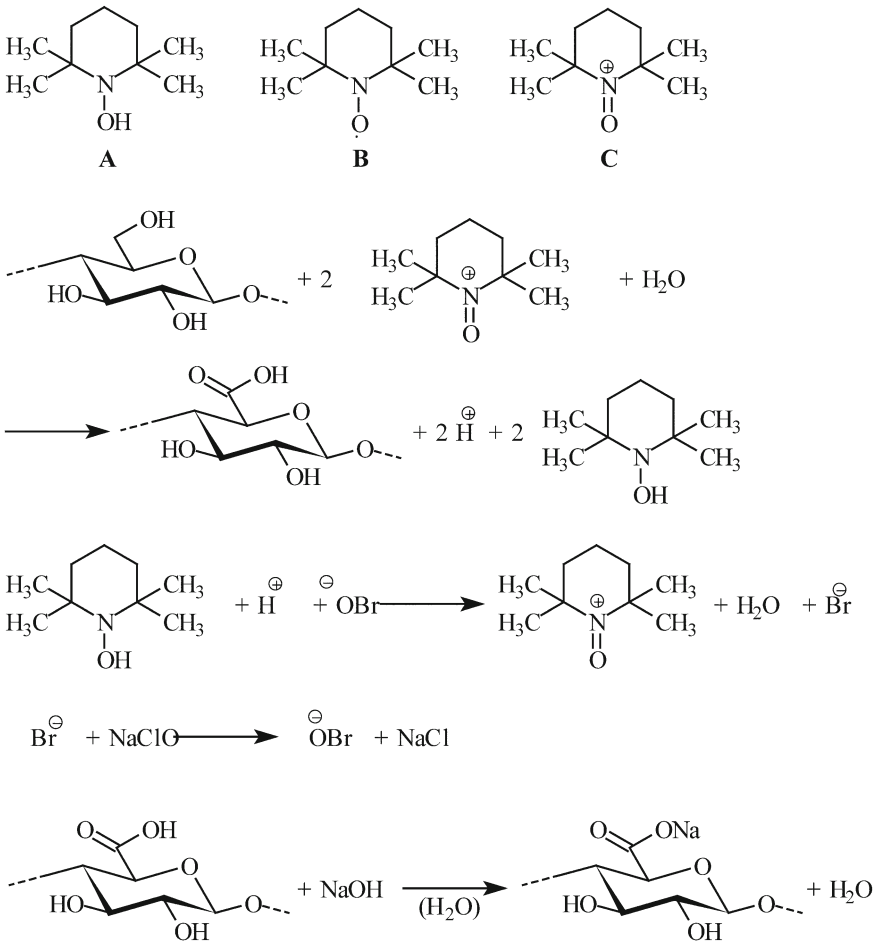


**Fig. 7.3** Oxidation of primary hydroxyl groups of cellulose to carboxyl groups by the 2,2,6,6-tetramethylpiperidine-*N*-oxyl (TEMPO)-mediated oxidation

The depolymerization of cellulose during TEMPO-mediated oxidation was attibuted to sodium hypochlorite, which causes cleavage of the C2–C3 bond of the AGU forming dialdehyde and dicarboxylic moieties [30]. The formation of carbonyl groups at position 2 and position 3 of the AGU facilitates depolymerization of celluloses via β-alkoxy fragmentation in alkaline medium [11]. Depolymerization during TEMPO-oxidation can occur also via β-elimination reaction (Fig. 7.4).

Different modifications of TEMPO/KBr/NaClO oxidation were studied to overcome the depolymerization. Thus, working with the TEMPO-derivative 4-acetamide-TEMPO at 60 °C and pH values of 4.8–6.8 for 1–5 *d* [33, 34] leads to high yields of water-soluble 6-carboxy cellulose with high degree of

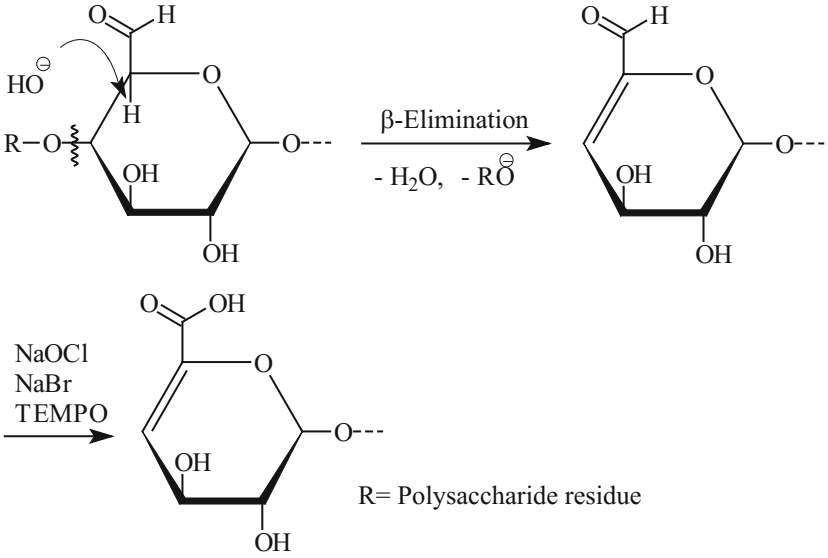


**Fig. 7.4** Polymer degradation during the 2,2,6,6-tetramethylpiperidine-*N*-oxyl (TEMPO) mediated oxidation via β-elimination

polymerization. Here $NaClO_2$ was added as primary oxidant, whereas NaClO present in catalytic amounts starts the oxidation cycle. However, side reactions caused by NaClO or $NaClO_2$ cannot be avoided.

The TEMPO oxidation is appropriate for surface oxidation as documented in many papers about the introduction of carboxy group into cellulose nanoparticles, nanofibrilated cellulose, and whiskers, e.g. [35].

The development of electrochemical methods for oxidation of organic compounds (i.e. electro-organic oxidation) has attracted attention as a "green" chemistry approach [36, 37]. The main future of the electro-organic oxidation of cellulose in the presence of TEMPO is the decrease of depolymerization. TEMPO-electromediated oxidation of some polysaccharides including regenerated cellulose fiber takes place in a 0.1 M phosphate buffer at pH 6.8 and at room temperature for 45 h [38]. 4-Acetamide-TEMPO catalyst was found to be quite specific, differing from other TEMPO-mediated oxidations. Significant amounts of 6-carboxylate- and 6-aldehyde groups (1.1 and 0.6 mmol/g, respectively) were formed.

The high selectivity of the TEMPO oxidation is substantiated by theoretical calculations [39]. The oxidation of cellulose in alkaline medium starts with a nucleophilic attack of an alkoxide on the nitrogen or oxygen atom of the strongly polarized N=O bond of nitrosonium cation, which results in the formation of either complex I or II (Fig. 7.5). The oxidation via peroxide complex is less probable according to calculations, hence the reaction path via complex I is more likely (Fig. 7.5).

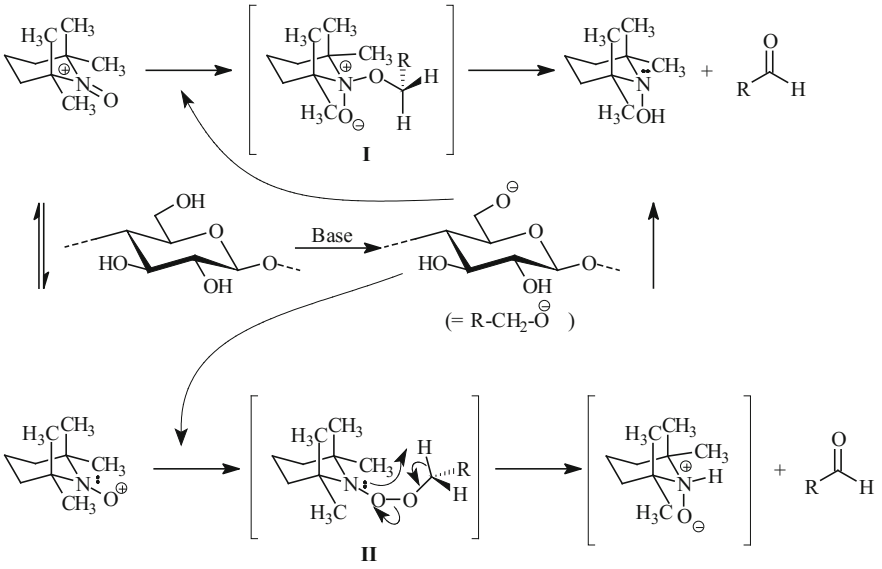


**Fig. 7.5** Mechanism of the 2,2,6,6-tetramethylpiperidine-*N*-oxyl-mediated oxidation of cellulose under alkaline conditions

The 6-carboxycellulose could be further modified by introducing another functional group. Further manipulation of ionic cellulose derivatives is difficult because of lack of solubility in organic solvents employed for chemical modifications of cellulose and its derivatives. Thus, after a pretreatment consisting of the precipitation of the aqueous solution of carboxy cellulose in DMF and water elimination, a highly swollen and reactive system was obtained. The biopolymer derivative could be transferred to the corresponding carboxycellulose sulfate with $SO_3$ or $HSO_3Cl$ and subsequent neutralization of the sulfuric acid half ester formed with aqueous NaOH [40]. These polyelectrolytes may be used for the formation of special supramolecular aggregates by interacting with low molecular- or polymeric cations. Using the same activation procedure for carboxy cellulose, the corresponding acyl chloride was generated by reaction with $SOCl_2$ and transformed into amides by reaction with amines [41].

### *7.1.4 Oxidation of the Secondary Hydroxyl Groups*

The oxidation of the secondary hydroxyl groups may yield 2-keto-, 3-keto- and/or 2,3-diketo cellulose (Fig. 7.1). Moreover, a bond cleavage between position 2 and position 3 may occur, as well akin for vicinal diols, yielding 2,3-dialdehyde cellulose. The latter is an important intermediate for subsequent modification in particular by reductive amination for, e.g., enzyme immobilization.

Cellulose dissolved in DMSO/paraformaldehyde can be oxidized to 3-keto cellulose with the mild oxidant acetic anhydride/DMSO [42]. On the contrary, 6-protected cellulose derivatives (6-*O*-triyl- and 6-*O*-acetyl cellulose) are oxidized at positon 2 under comparable conditions. Detailed studies show a content of both keto groups of 54% at position 2 and 36% at positon 3 [43]. It is assumed that the unmodified cellulose reacts via the *O*-2 and *O*-6 hemiacetal that protects these positons and hence position 3 is oxidized. An appropriate oxidation agent is also DCC/DMSO/pyridine/trifluoroacetic acid (Pfitzer-Moffatt reagent, [44]).

A selective process of oxidation is the treatment of cellulose with periodic acid and its salts under aqueous conditions forming 2,3-DAC (Fig. 7.6, [45]). In order to avoid free radical-induced depolymerization reactions, it is recommended to carry out the synthesis in the dark and to use radical scavengers such as propane-1-ol, on one hand [46]. On the other hand, to minimize the polymer degradation, a homogeneous periodate oxidation should be considered. An illustrative example in this regard is the oxidation of cellulose performed by methylol cellulose produced by dissolution of the polymer in paraformaldehyde/DMSO [47]. The oxidation level reaches almost 100% within 10 h, while the DP remains unchanged.

The effects of periodate oxidation on cellulose were studied by means of gel permeation chromatography (GPC) using multiple detection and carbonyl-selective fluorescence labeling according to the CCOA methodology profiling of carbonyl groups. At low degree of oxidation, the average molecular mass distribution was maintained. Surprisingly, the molecular weight was found to be increased at higher degree of oxidation that is due to cross-linking effects [48].

2,3-Dialdehyde cellulose has found considerable interest for various subsequent reaction of the aldehyde groups. By oxidation of 2,3-DAC with sodium chlorite/hydrogen peroxide, an acyclic stereoregular polycarboxylic acid derivative, 2,3-DCC (Fig. 7.6), is obtained. The Na-2,3-DCC shows typical properties of a polyelectrolyte such as continuous increase in reduced viscosity with decreasing

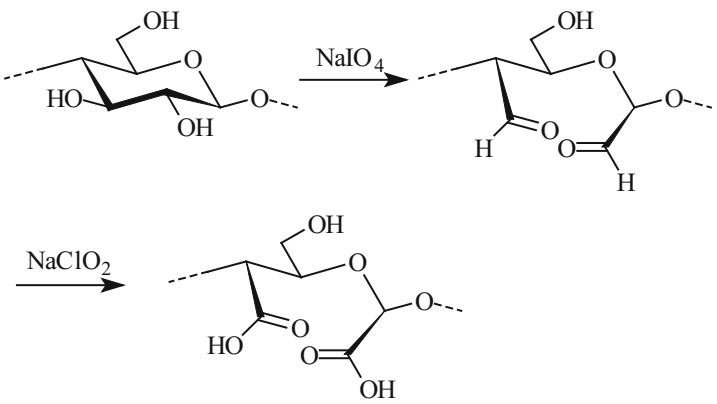


**Fig. 7.6** Oxidation of cellulose in a two-step process yielding 2,3-dialdehyde cellulose and 2,3-dicarboxy cellulose

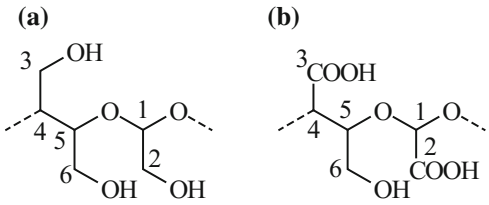


**Fig. 7.7** Structures of poly(2R,4S,5R)-2,4,5-tris(hydroxymethyl)-1,3-dioxopentamethylene (**a**) and the corresponding product after oxidation (**b**)

concentration below 2 mg/l in aqueous solution and flocculation of multivalent metal cations. Moreover, 2,3-DCC displays high calcium-binding capacity and is biodegradable [49–51].

Reductive amination was used to prepare ion-exchange materials, including spherical cellulose beads [52], for the immobilization of enzymes [53, 54], and reduction of the aldehyde with reducing agents like sodium tetrahydrido boranate [55, 56]. In the latter case, the water-soluble stereoregular 2,4,5-tris(hydroxymethyl)-1,3-dioxopentamethylene (simply denoted 2,3-dialkohol cellulose) is obtained (Fig. 7.7).

Cellulose and nanocellulosic materials were modified by periodate oxidation followed by treatment with sodium bisulfite to yield the corresponding sulfonates. The impact of this chemical modification path on physical properties of the biopolymer was evaluated by determining in particular the water absorbency properties. It was found that the water absorbency of cellulosic material can be significantly enhanced [56, 57].

The periodate oxidation is applied to cellulose nanostructures to obtain products of rather low degree of oxidation. However, the amount of functional groups introduced is sufficient to change the properties of the cellulose nanomaterials significantly [58].

A fully oxidized 2,3,6-tricarboxy cellulose could be obtained by combining the two most selective oxidation approaches, namely TEMPO- and periodate oxidation simultaneously [59].

Not only cellulose but also cellulose derivatives were subject of oxidation. Thus, due to the water-solubility of HEC, the partial oxidation of primary OH-groups by TEMPO/hypochlorite was an alternative approach to new ionic cellulosics. A selective oxidation of the OH-groups of hydroxyethyl moieties is possible [60]. Figure 7.8 shows a $^{13}C$ NMR spectrum of a completely oxidized sample in comparison with the starting HEC (tylose), both acquired in $D_2O$.

The carbonyl groups in oxidized cellulose is indicated by the copper number. However, this method is not very accurate since the copper number is not directly linked with the quantity of a specific oxidized function. Group-selective fluorescence labeling in combination with multi-detector gel permeation chromatography

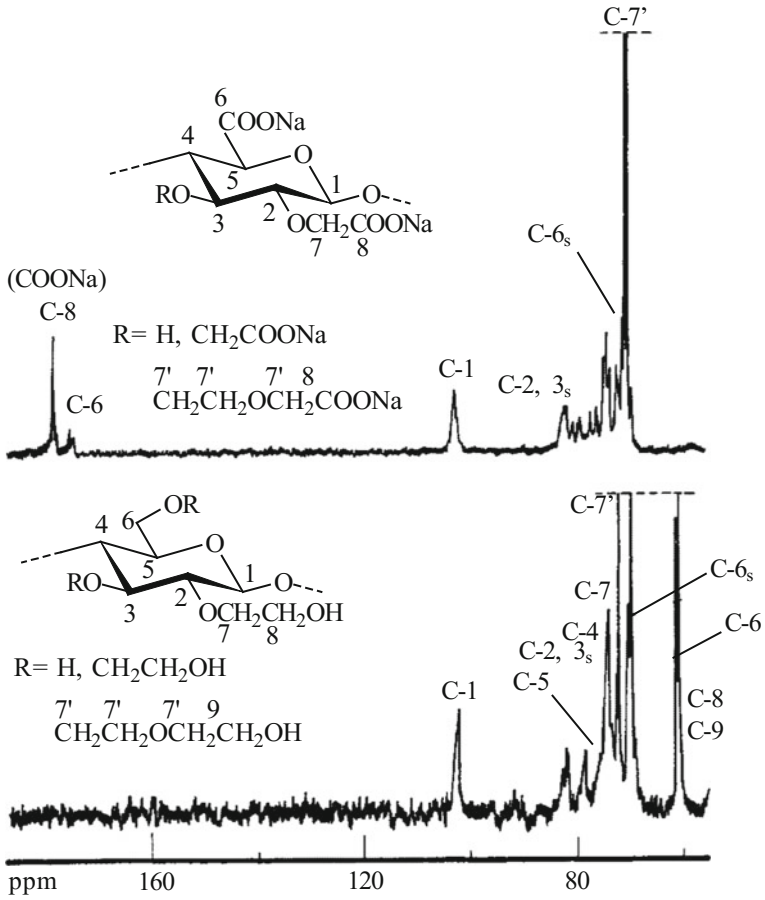


**Fig. 7.8** $^{13}C$ NMR spectra of hydroxyethyl cellulose (bottom) and its 2,2,6,6-tetramethylpiperidine-*N*-oxyl-mediated oxidation product (top), recorded at 50 °C in $D_2O$ (adapted from [61])

(multi-angle laser light scattering, refractive index, fluorescence) are valuable and powerful techniques developed in the last years for cellulose analytics [62, 63]. A comprehensive review about the determination of functional groups obtained by oxidation of cellulose was published. This lucid overview focuses on oxidized functionalities in celluloses, i.e., carbonyl and carboxyl groups, with regard to their chemical structure, the different synthesis strategies, and their analytical methods [64].

## 7.2 Click Chemistry with Cellulose

### *7.2.1 Introduction*

In recent years, interesting and efficient new paths for cellulose modification were established, which significantly broadened the number of sophisticated cellulose derivatives. On one hand, the development of new reaction media (Sect. 3.2) in particular ionic liquids in combination with molecular solvents and polar liquids with electrolytes, which facilitate derivatization under homogeneous conditions, have broadened the reagents that may react with the biopolymer. On the other hand, it is the exploitation of new paths of organic chemistry for the design of chemical structures of polysaccharide derivatives. Most of these efficient processes are based on click chemistry, a term coined by K. B. Sharpless [65]. Click chemistry summarizes reactions consisting of a modular approach that uses only the most practical and reliable transformation, which are experimentally simple, needing no protection from oxygen, requiring only stoichiometric amounts of starting materials, and either generate no byproducts, or byproducts that can be removed easily. These reactions show bioorthogonality [66] meaning they proceed selectively without protection even in the presence of numerous other functional groups, which may be very important in case of polysaccharides. Reactions fulfilling these prerequisites are, for example:

- 1,3-dipolar cycloaddition of an azide moiety and a triple bond, the Huisgen cycloaddition reaction
- [4 + 2] cycloaddition reaction of an electron rich diene with an electron poor double bond, the well-known Diels–Alder reaction; and hetero- and inverse electron demand Diels–Alder reactions
- thiol-Michael addition that features a reaction of a thiol anion with an α,β-unsaturated carbonyl-type compound and
- photoinitiated thiol-ene reactions (see Fig. 7.9).

### *7.2.2 Click Chemistry with Cellulose*

#### 7.2.2.1 Huisgen Reaction

Among the first examples of click reactions widely studied in cellulose chemistry was the 1,3-dipolar cycloaddition of an azide moiety and a triple bond (Huisgen reaction), which is still the most popular click reaction to date [67–69]. The reaction can be carried out with or without the aid of a catalyst, usually Cu(I). The disadvantage of a simple thermally induced reaction without catalyst is the long reaction time, side reactions due to the high temperature, and lack of stereoselectivity. Cu-catalysis guarantees fast reaction and selective conversion but may cause

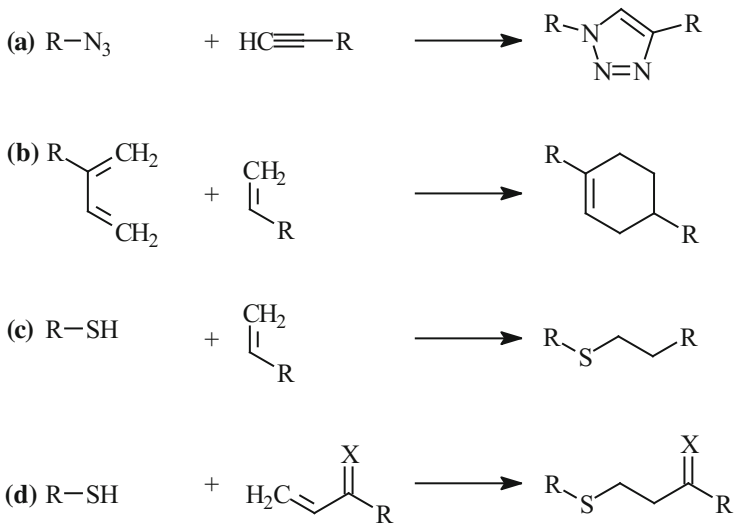


**Fig. 7.9** Typical examples of click reactions suitable for cellulose chemistry: 1,3-dipolar cycloaddition of an azide moiety and a triple bond (Huisgen reaction, **a**), [4 + 2] cycloaddition reaction of an electron rich diene with an electron poor double bond (Diels–Alder reaction, **b**), thiol ene reaction (**c**), and addition of a thiol anion to an unsaturated carbonyl (thiol-Michael addition, **d**)

problems concerning product purification. An alternative to Cu-catalysis that yields Cu-contaminated products is the metal-free strain-promoted azide-alkyne cycloaddition [70]. This concept, first developed by Bertozzi et al., takes advantage of the ring strain of cyclooctyne formed during the conversion. Until now, this route was applied for a number of polysaccharides but not for cellulose.

Various approaches were developed to introduce the azide moiety or the triple bond into the cellulose backbone to obtain a "clickable" starting material. For the introduction of triple bond containing moieties, esterification and etherification reactions were applied. Thus, the etherification of cellulose with a propargyl halide [71–73] or esterification with 5-hexynoic- or undec-10-ynoic acid [74] was realized by conventional conversions (see Fig. 7.10).

Another path to introduce a triple bond consists in the tosylation of the biopolymer followed by nucleophilic displacement with a triple bond containing amine such as propargyl amine as a typical example of a nucleophile (Fig. 7.11, [75]). Thus, a very stable bond of the substituent to the backbone in the final product is introduced contrary to the ester links mentioned above.

Alternatively, esterification and etherification was used to decorate cellulose with $N_3$-functions, e.g., with 4-azidomethylene benzoic acid groups (Fig. 7.12, [76]). Etherification was carried out with epoxides like 1-azido-2,3-epoxypropane (Fig. 7.12, [77]). The reactive function can also be linked to a cellulose derivative as shown for carboxymethyl cellulose, both azide or triple bond were bound as amide

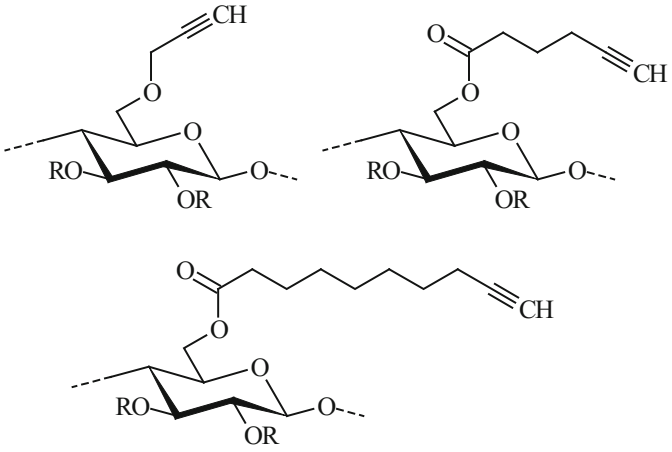


**Fig. 7.10** Triple bond containing precursors for the [2 + 3] cycloaddition

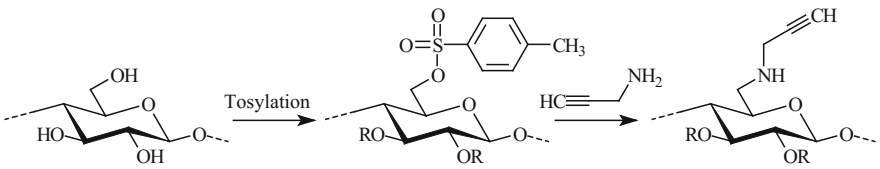


**Fig. 7.11** Introduction of a triple bond by tosylation and nucleophilic substitution with propargyl amine

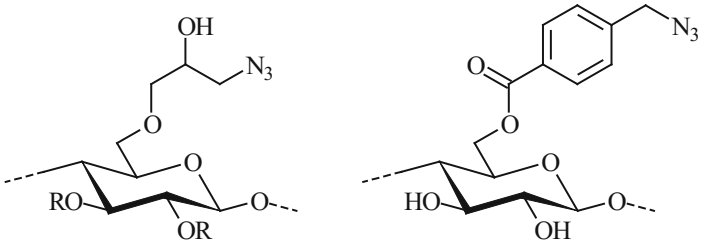


**Fig. 7.12** Cellulose derivatives carrying azido moieties introduced by etherification and esterification

[78, 79] by coupling the corresponding amine to the carboxy function with 1-ethyl-3-(3-dimethylaminopropyl)carbodiimide (EDC)/*N*-hydroxysuccinimide (NHS).

An unconventional path leading in principle to a clickable cellulose product is the conversion of chitosan into the deoxyazido compound [80]. For this purpose,

chitosan has to be treated with trifluoromethanesulfonyl azide (TFMSA) yielding a clickable product with a preferred substitution in position 2. About 95% of the amino functions at the chitosan backbone can be converted but the reaction condition is harsh, leading to strong polymer degradation.

The introduction of a desoxyazido-function in cellulose is probably the most suitable and straightforward path to obtain a biopolymer-based precursor for the Huisgen reaction, as shown in Fig. 7.13. Cellulose is converted with tosyl chloride into the corresponding cellulose tosylate. Subsequently, 6-deoxy-6-azido cellulose is obtained with high selectivity by a nucleophilic substitution reaction with azide anion. An alternative path to introduce the azide moiety is the reaction of cellulose deoxybromo derivative, obtained by reacting the biopolymer in DMAc/LiCl (or LiBr) with triphenylphosphine and tetrabromomethane or *N*-bromosuccinimide with aide anion [81, 82]. It is claimed that the bromation is more selective than the tosylation concerning position 6. However, from the author's point of view the chemistry starting with the toslyate is more convenient and easy to handle.

Using the reactive cellulose precursors shown above, thermal or Cu-catalyzed Huisgen reactions can be carried out. Copper(I)-catalyzed Huisgen reaction was mostly performed starting with azide-decorated cellulose with molecules containing terminal triple bond. The copper(I)-catalyst is usually prepared in situ from copper (II) sulfate pentahydrate and sodium ascorbate. The substituent formed is fixed directly to the polymer backbone via a fairly stable 1,4-disubstituted 1,2,3-triazol as linker. Thus, the derivatives obtained constitute a new class of cellulose derivatives. The reactions were carried out both in homogeneous phase or heterogeneously on a cellulose surface. Homogeneous conversion was used for the modification of cellulose with methylcarboxylate, 2-aniline and 3-thiophene moieties, e.g., (Fig. 7.13). The cellulose modification occurs without side reactions yielding pure and well-soluble products with reagent efficiency of the azido moiety of 75–98% depending on the reaction temperature and the molar ratio. Even at elevated temperatures (70 °C), no hints for structural impurities due to undesired side reactions are observed. The structure characterization of the products was carried out by FTIR and NMR spectroscopy. Due to the completeness of the reaction, the stepwise conversion into the final product can be conveniently confirmed by FTIR spectroscopy (Fig. 7.14, [83]).

The cellulose derivatives obtained by this path show properties of polyelectrolytes or can selectively bind to surfaces. In a comparable manner, cellulose derivatives were prepared having oligosaccharide side chains such as *O*- or *N*-linked β-maltoside and *O*- or *N*-linked β-lactoside moieties [84]. The synthesis was carried out by bromination of cellulose and subsequent reaction with azide anion and finally by coupling with oligosaccharides having terminal alkyne moieties (Fig. 7.15).

The structure of the polymers could be verified with NMR spectroscopy and MS experiments. In $^{13}C$ NMR spectra, all structural elements of the cellulose-based polymer were identified (Fig. 7.16).

The most stable conformations for these new cellulose-based glycopolymers were calculated by molecular dynamics simulations (Fig. 7.17). They have

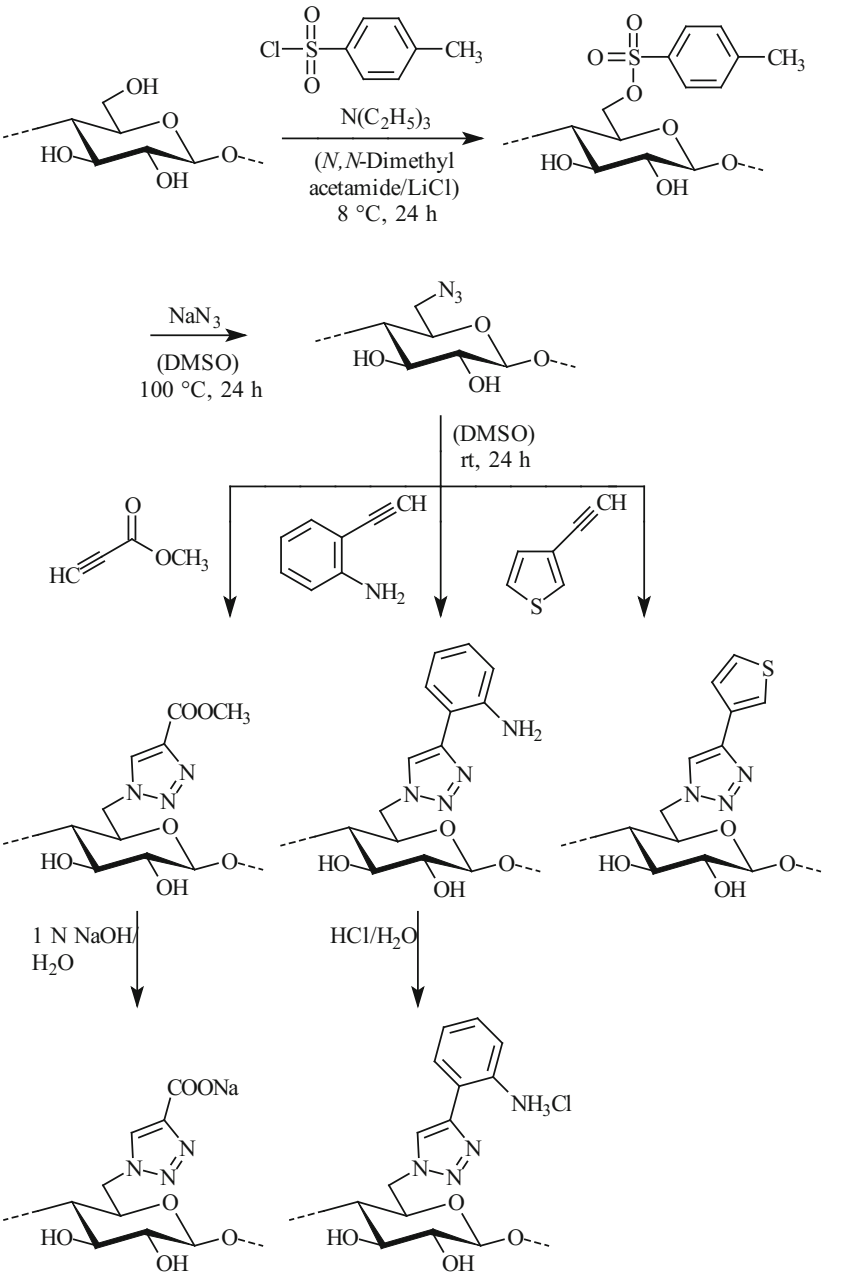


**Fig. 7.13** Reaction path for the preparation of 6-deoxy-6-azido cellulose and subsequent copper (I)-catalyzed Huisgen reaction resulting in 1,4-disubstituted 1,2,3-triazols as linker for cellulose with methylcarboxylate, 2-aniline, and 3-thiophene moieties

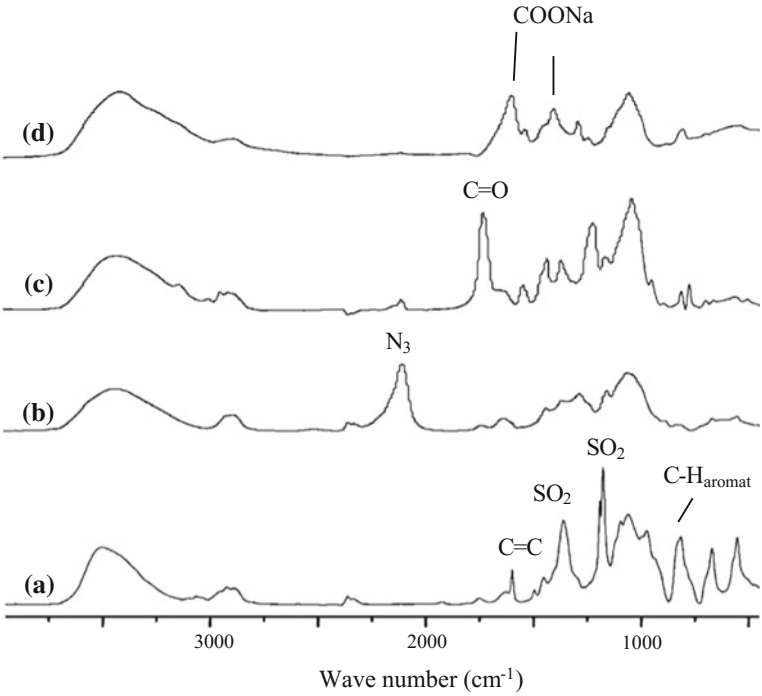


**Fig. 7.14** FTIR spectra of 6-tosyl cellulose (**a**), 6-azido-6-deoxy cellulose (**b**) methylcarboxylate bound onto cellulose with a 1,4-disustituted 1,2,3-triazole linker (**c**) and the corresponding free acid obtained by saponification (**d**, adapted from [83])

sheet-like structures with their hydrophobic phenyl/triazole spacers exposed to the solvent. These sheet-like structures should result in enhanced intermolecular networks composed of hydrophobic interactions and hydrogen bonding and, hence, reduced water solubility of the polymer.

Huisgen reaction of desoxy-azido cellulose was frequently used for the surface modification of the biopolymer. An illustrative example for the use of clickable precursors for the surface modification of cellulose was shown [74]. The click reaction was performed between hexynoic acid modified cellulose and 3-azidocoumarin. The non-fluorescent azidocoumarin forms an intensely fluorescent 1,2,3-triazole product upon 1,3-dipolar cycloaddition reactions with terminal alkynes. Consequently, the corresponding cellulose product is highly fluorescent, which might be further derivatized, and a successful derivatization can be clearly demonstrated (see Fig. 7.18). Interestingly, saponification of the triazole-modified filter paper with aqueous NaOH gives a highly fluorescent solution, which is a result of the release of the triazole coumarin acid (Fig. 7.18d, left vial).

It is possible to modify cellulose with both reactive sites necessary for a Huisgen process and react the two cellulose derivatives. Thus, cellulose derivatives bearing azide- and alkyne moieties were prepared by conversion of cellulose tosylate with

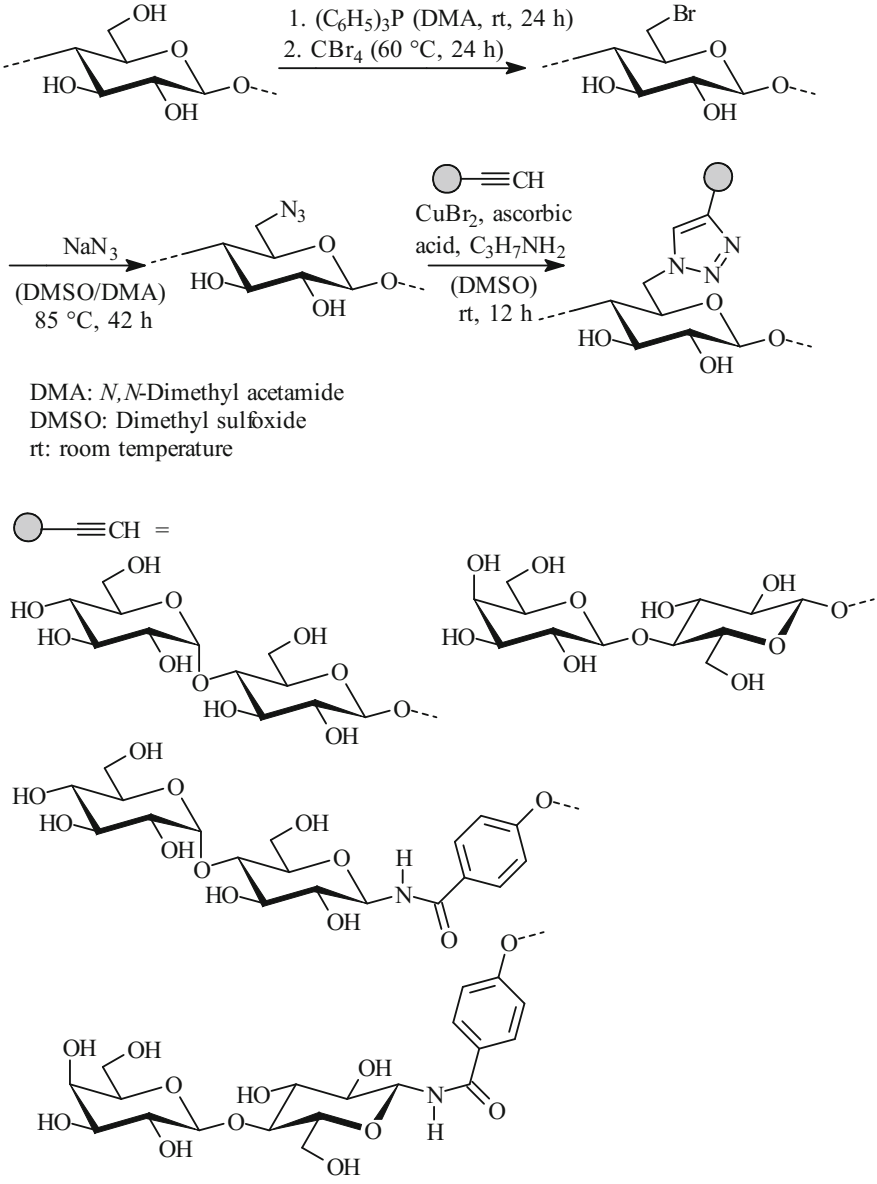


**Fig. 7.15** Cellulose derivatives with oligosaccharide side chains such as *O*- or *N*-linked β-maltoside and *O*- or *N*-linked β-lactoside moieties prepared via Huisgen reaction (adapted from [84])

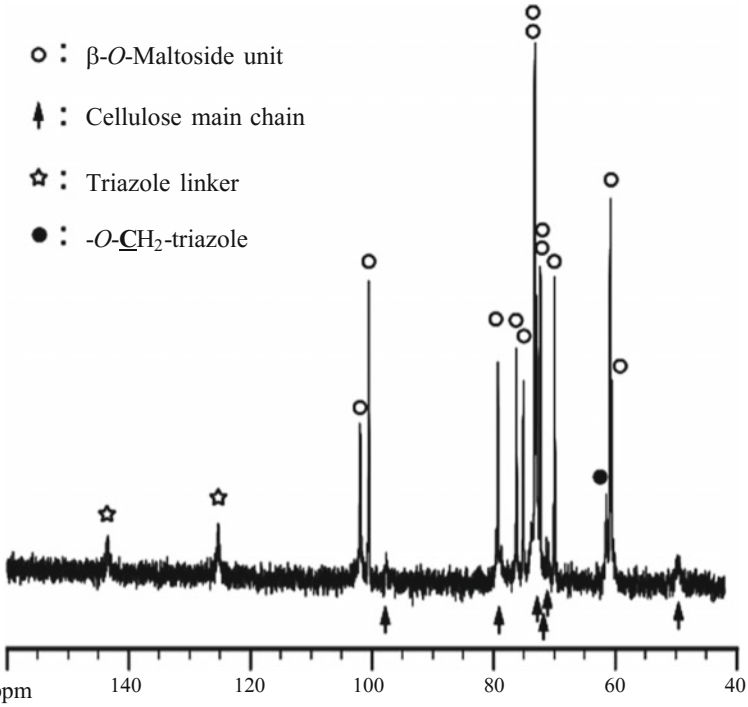


**Fig. 7.16** $^{13}$C NMR spectrum of a cellulose molecules bearing a *O*- linked β-maltoside side group (adapted from [84] published under the Creative Commons Attribution License)

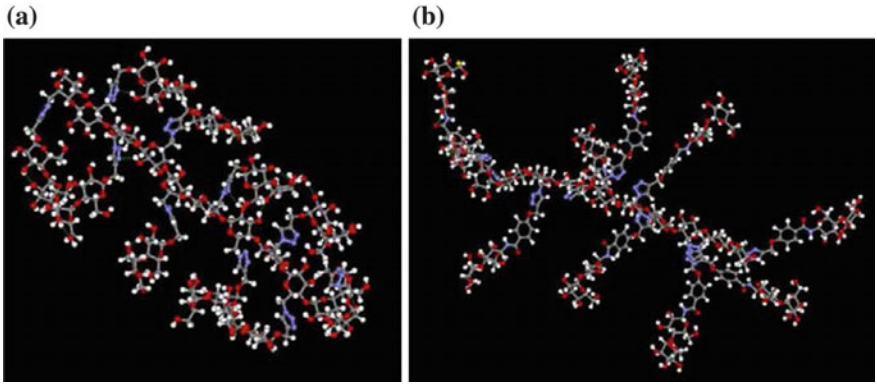


**Fig. 7.17** The most stable conformation of **a** Cel-*O*-Mal and **b** Cel-*N*-Mal (10-mer) during the dynamics simulation (adapted from [84] published under the Creative Commons Attribution License)

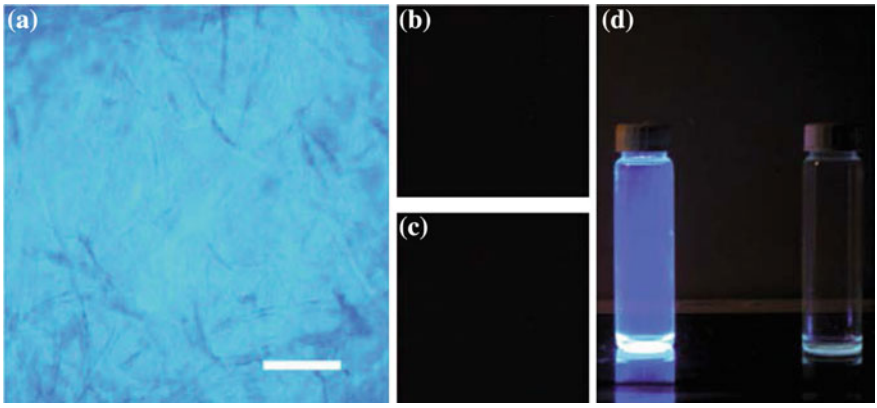


**Fig. 7.18** **a** Fluorescence photomicrograph of filter paper modified with hexynoic acid and subsequent click reaction with 3-azidocoumarin (scale bar: 150 mm). **b** and **c** Blank experiments with filter paper and hexynoic acid modified material. **d** The left vial contains the aqueous phase after treatment of modified filter paper with aqueous NaOH under UV light (right vial negative control) (Reproduced from [74] with permission of John Wiley and Sons)

sodium azide, on one hand, and propargyl amine, on the other hand (see Fig. 7.19). The products obtained were carboxymethylated to yield water-soluble cellulose derivatives. Huisgen reaction of the two cellulose products led to cross-linking. Gel formation occurred within 55 and 1600 s after mixing of the aqueous solutions of both components and copper-(I) catalyst. The gelation time was found to depend on both the degree of functionalization and the amount of copper-(I) catalyst. The gels contain up to 98.4% water. Freeze-drying led to spongy materials with different porous structure as visualized by SEM (Fig. 7.20). Consequently, this conversion leads to new hydrogel materials with tuneable properties [75].

For further details, the reader is referred to comprehensive review giving a broad variety of examples of click chemistry with polysaccharide [85].

#### 7.2.2.2 Dendronization of Cellulose

A promising approach for the synthesis of new cellulose derivatives with unconventional properties is the modification of the cellulose backbone with dendrons, which are easily accessible through the convergent synthesis of dendrimers [86]. Beside amino-triester-based dendrons (Behera's amine) with an isocyanate moiety [87, 88] and carboxylic acid-containing dendrons [89, 90], regioselective introduction of dendrons in cellulose was realized via the $S_N$ reaction starting from cellulose tosylate by sodium azide. For the synthesis of the first generation of dendronized polyamidoamino (PAMAM) cellulose bound by 1,4-disubstituted 1,2,3-triazole linker, 6-deoxy-6-azido cellulose were allowed to react with propargyl-PAMAM-dendron in DMSO homogeneously or in methanol

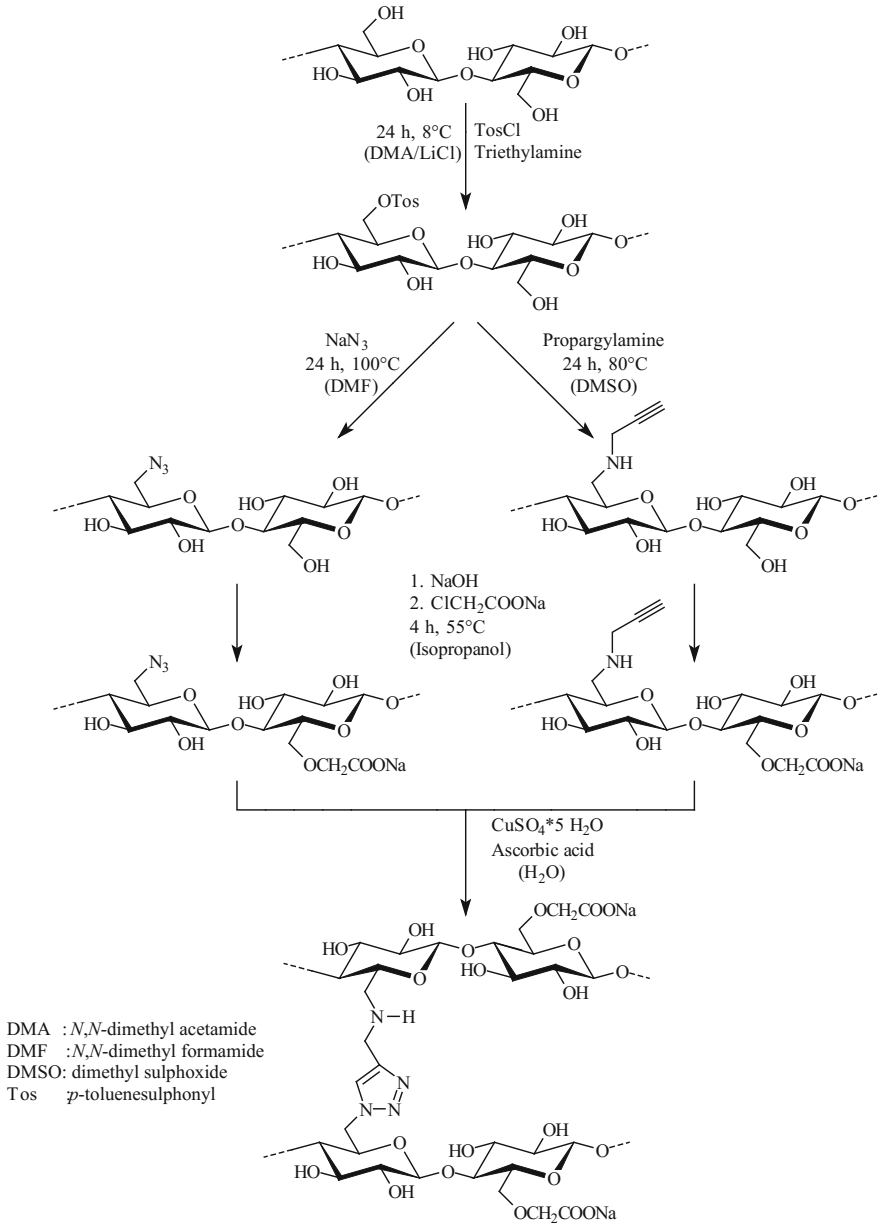


**Fig. 7.19** Synthesis path for the preparation of hydrogels by copper-catalyzed 1,3-dipolar cycloaddition reaction of carboxymethyl-6-azido-6-deoxy cellulose and carboxymethyl-6-deoxy-6-aminopropargyl cellulose (adapted from [75])

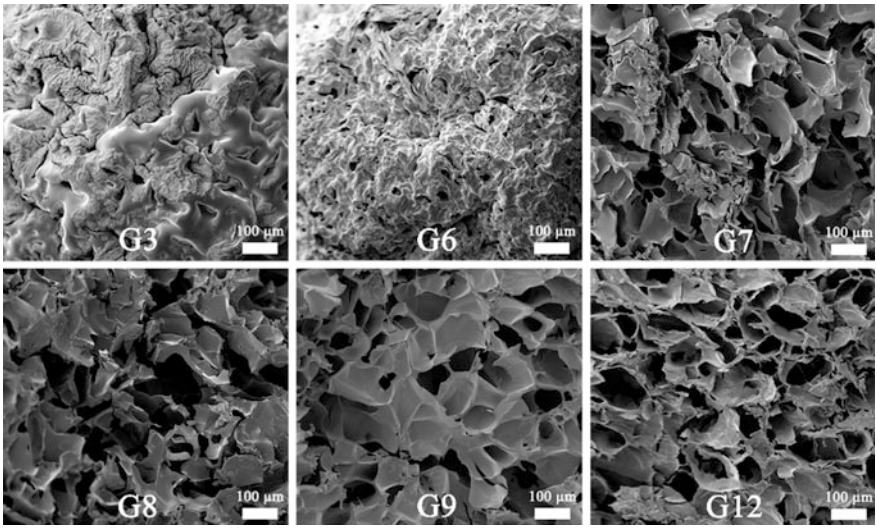


**Fig. 7.20** SEM images of freeze dried gels obtained by copper-catalyzed 1,3-dipolar cycloaddition reaction of carboxymethyl-6-azido-6-deoxy cellulose and carboxymethyl-6-deoxy-6-aminopropargyl cellulose (Reprinted from [75], Copyright (2011), with permission from Elsevier)

heterogeneously in the presence of $CuSO_4 \cdot 5H_2O$/sodium ascorbate. The homogeneous introduction of the propargyl-PAMAM-dendron into cellulose could be realized applying ILs like 1-ethyl-3-methylimidazolium acetate (EtMeImAc) as reaction medium because of the solubility of 6-deoxy-6-azidocellulose in this solvent (Fig. 7.21, [91]).

Under homogeneous conditions, 6-deoxy-6-azido cellulose reacts also with propargyl-PAMAM dendrone of second and third generation. The structure characterization of the dendric PAMAM-triazolo celluloses was achieved by FTIR- and NMR spectroscopy including two-dimendsional techniques. Figure 7.22 shows the HSQC-DEPT NMR spectrum of second generation PAMAM-triazolo cellulose, which allows the complete assignment of the proton signals of this complex molecule. $^{13}C$ NMR spectra of first, second, and third generation PAMAM-triazolo cellulose synthesized in the ionic liquid EtMeImAc demonstrate the possibility to assign the signals of the dendrons and the AGU. However, the intensity of the peaks of the carbon atoms of the AGU decreases due to the large number of branches and corresponding carbon atoms.

Cellulose-type block copolymers can be synthesized in a comparable way, e.g., by linking fully acetylated cellooligomer to fully methylated oligomers via a triazol unit [92, 93] or binding cellooligomers to synthetic blocks like polymethacrylate [94]. More detailed information on grafting of cellulose via click chemistry can be found in [95].

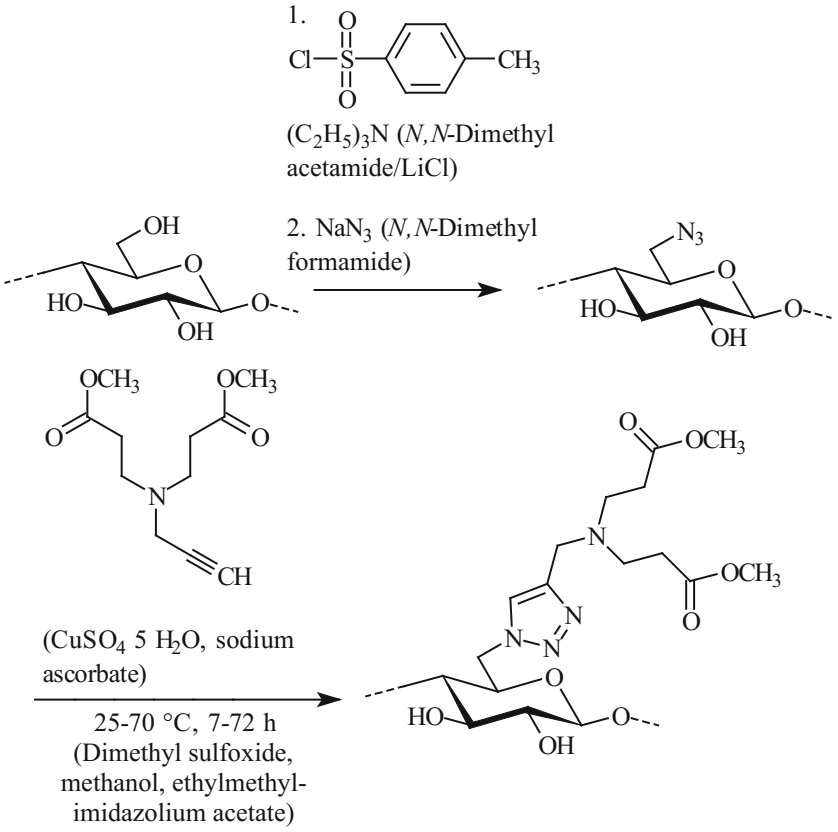


**Fig. 7.21** Reaction path for conversion of cellulose with propargyl-PAMAM dendron of first generation via tosylation and nucleophilic displacement by sodium azide

Although wide in scope, it should be mentioned that the Huisgen reaction has a number of shortcomings. First of all, azido compound especially low molecular weight azids are explosive and need to be handled with care. Most of them are toxic. The same is true for the Cu(I), this is especially challenging because during the reaction the triazole ring is formed which might form a complex with the Cu. Thus, proper work up is needed. The Cu can also initiate pronounced chain degradation because it may form reactive oxygen species with oxygen.

### 7.2.2.3 Diels–Alder Reaction

A reaction that is classified today as click chemistry is the Diels–Alder reaction discovered in 1928. The [4 + 2] cycloaddition reaction of an electron-rich diene with an electron poor double bond usually called dienophile is used frequently in

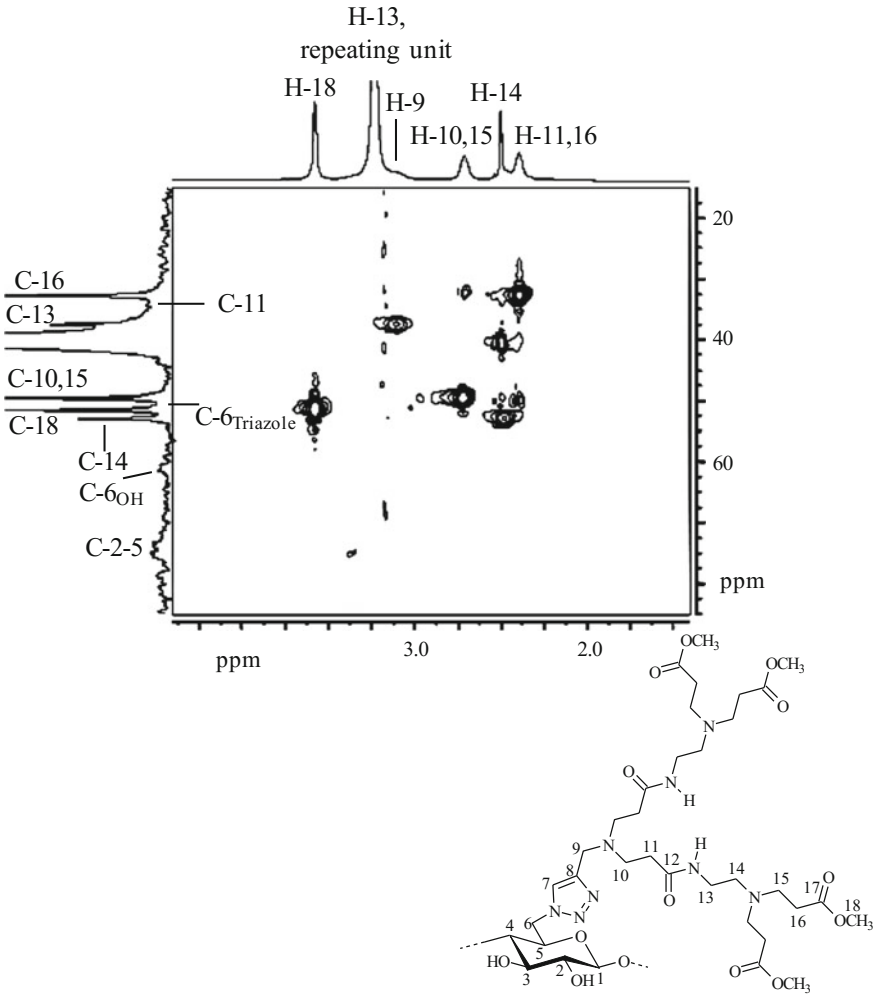


**Fig. 7.22** HSQC-DEPT NMR spectrum of second generation PAMAM-triazolo cellulose (DS 0.59)

polymer analogous chemistry. It was applied for conjugation of functional moieties and for the formation of hydrogels, cross-linking and surface modification on cellulose and cellulose derivatives. Especially for the functionalization of polysaccharide films, this robust and highly effective reaction is able to achieve high surface load and allows for a controlled and uniform modification. In addition, the reaction sequence requires no catalysis by toxic metals, and is carried out under mild reaction conditions. In case of biopolymer surface functionalization, Diels–Alder reactions are used for so-called "grafting-to" approaches where pre-defined macromolecules are grafted onto the cellulose surface. Moreover,

Diels–Alder reactions can be combined with light-induced effects such as isomerization and can therefore be a tool for spatially controlled functionalization of cellulose. This technique was exploited for the modification of cellulose with tailor-made peptide and polymer strands under spatial and/or temporal control of the reaction. Thus, filter paper was decorated by *N,N′*-carbodiimide mediated esterification with a photoenol moiety like *o*-quinodimethane. On irradiation, a 2-formyl-3-methylphenoxy derivative isomerizes to a highly reactive *o*-quinodimethane species, which can be trapped in a Diels–Alder reaction employing maleimides in particular poly(trifluoroethylmethylacrylate) or a maleimidine-functionaized model protein as dienophile (Fig. 7.23, [96]).

Successful grafting of the model peptide onto cellulose films can be illustrated by means of ToF-SIMS imaging. If a meander-type shadow mask is employed during UV irradiation grafting occurs only in the predefined areas. If the molecule conjugated to the cellulose backbone is a peptide, nitrogen-containing species can be detected. Figure 7.24 shows time-of-flight secondary ion mass spectrometry (ToF-SIMS) images of peptide labeled cellulose. Both the assignment of the CNO- and the CN-fragments shows the expected meander-type grafting regions. The results can be confirmed with XPS measurements. The product of the Diels–Alder reaction is again detectable only in the irradiated parts of the cellulose material (Fig. 7.25).

In case of cellulose derivatives, a number of examples for Diels–Alder reactions are known for the functionalization of hydroxyalkyl celluloses with furoyl moieties and conversion with maleimides (Fig. 7.26). For this system, the retro process can be achieved easily at elevated temperature. Such retro Diels–Alder reactions of Diels–Alder products can be used for the fabrication of self-healing materials.

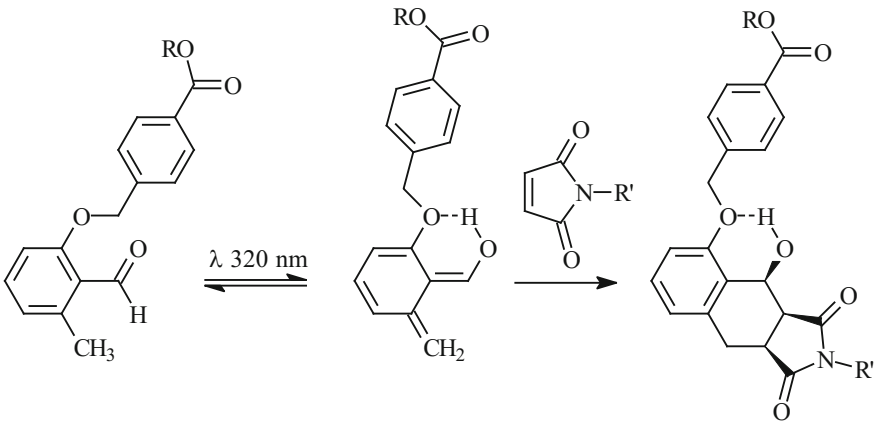


**Fig. 7.23** General reaction scheme for the photo-isomerization of a 2-formyl-3-methylphenoxy derivative and Diels–Alder trapping of the reactive o-quinodimethane intermediate with a maleimide as dienophile (R = polymer backbone or other organic moiety, adapted from [96])

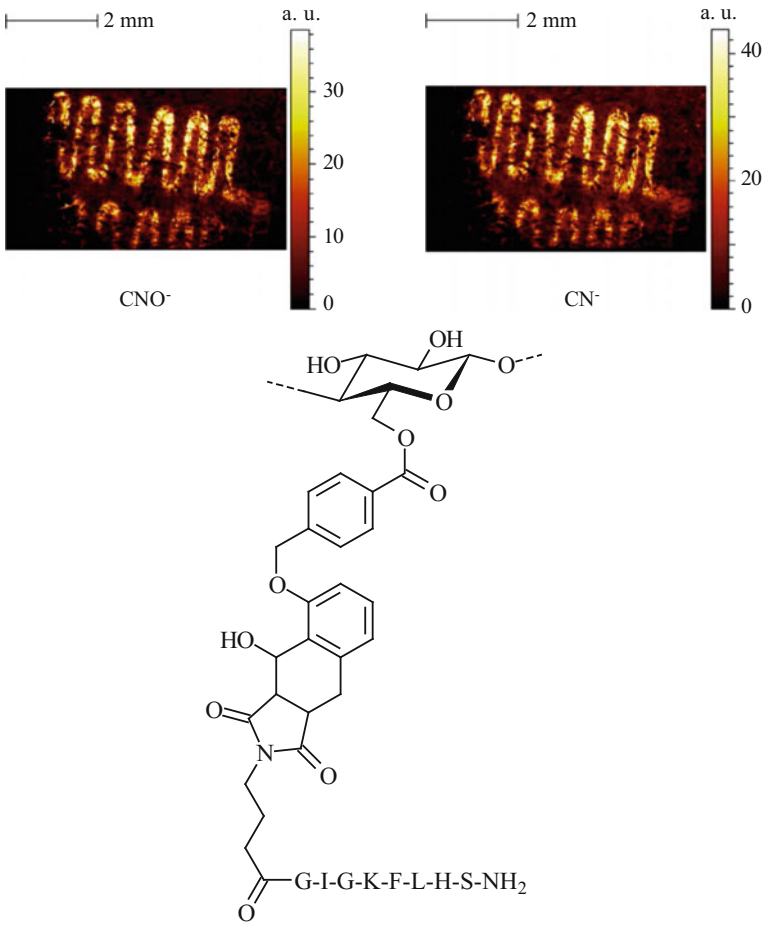


**Fig. 7.24** ToF-SIMS images of peptide modified cellulose as a result of a photochemically triggered selective Diels–Alder reaction. Left: $CNO^-$; right: $CN^-$ fragment. Both fragments originate from the tethered model peptide (Reprinted (adapted) with permission from [96]. Copyright 2013 American Chemical Society)

On the basis of a Diels–Alder conversion, remendable materials were obtained by thermoreversible cross-linking of the corresponding cellulosic diene with a flexible bis(dienophile). Hydroxyethyl cellulose was esterified with furoyl chloride and cross-linking was carried out with 1,6-bis(*N*-maleimido) hexane under moderate heating. Because at higher temperature, the retro Diels–Alder reaction occurs, temperature-cycling may trigger subsequent Diels–Alder processes that can lead to self-healing materials [97].

In the same way, the Diels–Alder reaction was used to fabricate hydroxypropyl methylcellulose (HPMC)-based hydrogels. First, HPMC was modified with a diene

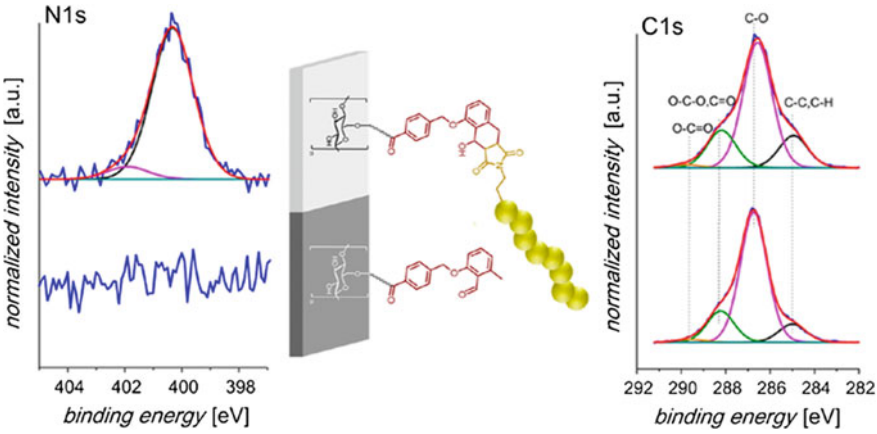


**Fig. 7.25** N1s (left) and C1s (right) XPS spectra of cellulose modified with a peptide strand top: irradiated area, bottom: dark control area (Reprinted (adapted) with permission from [96]. Copyright 2013 American Chemical Society)

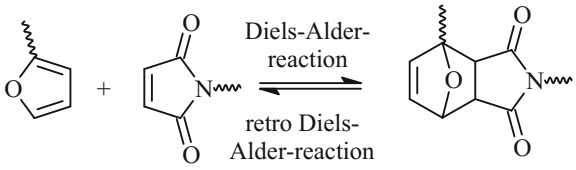


**Fig. 7.26** General formula for the Diels–Alder/retro Diels–Alder process based on furoyl moieties and conversion with maleimides

moiety synthesized from furfurylamine and succinic anhydride. Concomitantly, HPMC was decorated with a dienophile by coupling *N*-maleoyl alanine to the polymer using *N,N′*-dicyclohexylcarbodiimide/4-*N,N*-dimethylaminopyridine. Both the furan- and maleimide-modified HPMC were dissolved in water, and the mixture heated to start Diels–Alder reaction-based gelation. The Diels–Alder reaction and in turn the swelling behavior of the hydrogels can be tailored by the temperature applied [98].

Beside conventional Diels–Alder reactions, modification of cellulose is also possible by hetero- or inverse electron demand Diels–Alder reactions. The hetero Diels–Alder reaction is initiated between a diene and a highly electron deficient heteroatom-containing double bond. An example of such conversion at cellulose surface is the reaction of cyclopentadienyl-functionalized cellulose with thiocarbonylthio compounds such as thiocarbonylthio-capped poly(isoborenyl acrylate) or a thioamide-functionalzed peptide [99, 100]. The furan containing precursor was prepared by tosylation of cellulose surface and subsequent nucleophilic substitution by a highly reactive cyclopentadienyl functionality (Cp). Thiocarbonyl thio-capped poly(isobornyl acrylate) prepared by reversible addition-fragmentation chain

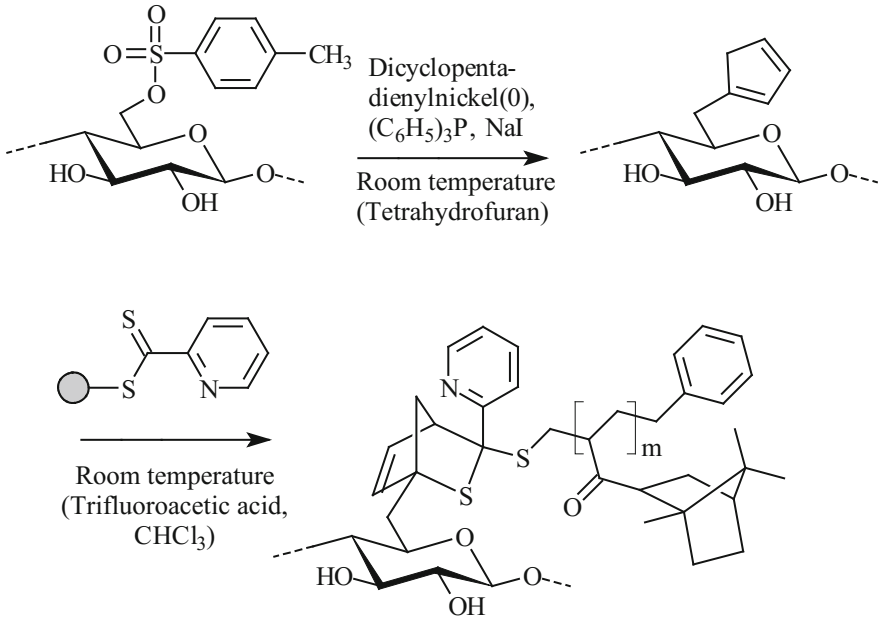


**Fig. 7.27** Hetero Diels–Alder of cyclopentadienyl-functionalized cellulose (prepared starting from tosyl cellulose) with thiocarbonylthio-capped poly(isoborneyl acrylate)

transfer (RAFT) was used for the hetero Diels–Alder cycloaddition onto a solid cellulose substrate (Fig. 7.27). The dimerization reaction of the cyclopentadienyl-moieties is avoided because the reaction is conducted at room temperature.

In addition to the Diels–Alder reactions discussed, other pericyclic processes are used for cellulose surface modification with high efficiency, yield, and selectivity. Thus, photoactive derivatives of cellulose were prepared by a mild esterification of the biopolymer with 2-[(4-methyl-2-oxo-2*H*-chromen-7-yl)oxy]acetic acid via the activation of the carboxylic acid with *N,N′*-carbonyldiimidazole [101]. Subsequently, modification with the cationic carboxylic acid (3-carboxypropyl) trimethylammonium chloride was carried out. Thus, water-soluble polyelectrolytes decorated with high amounts of photochemically active chromene moieties were obtained. The light triggered photodimerization of the chromene moieties of the dissolved biopolymer derivative (in water) can be confirmed by means of UV/Vis spectroscopy. The process is useable for control of material properties. On this basis, photoresponsive pulp fibers can be fabricated by self-assembly of photoactive cationic cellulose derivatives with pulp fibers in aqueous environment. The photoactive groups of the derivatives undergo [2π + 2π] cycloaddition reaction under UV-light irradiation [102]. Fast photo cross-linking leads to the formation of covalent bonds between the photoactive groups on the fiber surfaces (Fig. 7.28).

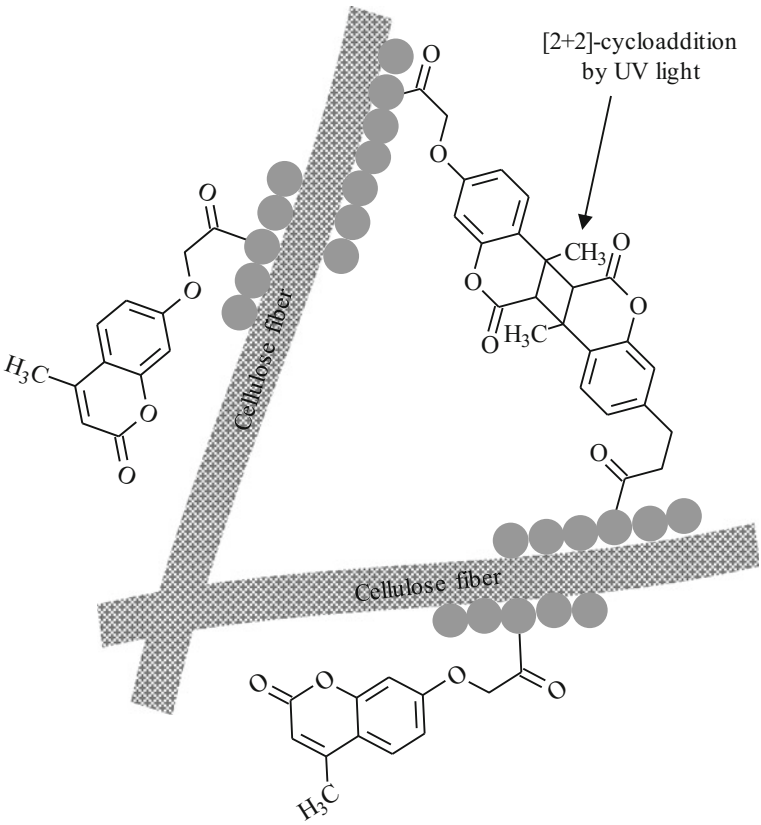


**Fig. 7.28** Schematic visualization of the [2π + 2π] cycloaddition reaction creating covalent bonds between pulp fibers and along the fibrils of the fiber (adapted from [102])

The cross-linking results in drastic enhancement of the mechanical properties of the fiber network. Tensile strength and Z-directional tensile strength increase by 81 and 84% compared to the original fiber network. Stiffness of the individual fibers increases by 60%.

#### 7.2.2.4 Thiol-Michael Reaction/Thiol-Ene Reaction

Although Michael reactions are used frequently in cellulose modification (see chapter Etherification), only the thiol-Michael addition (that uses an electron deficient thiol moiety) is considered as click process because it is selective, and may lead to quantitative yield under mild reactions conditions [103]. An overview of reactions for polymer functionalization is given in Fig. 7.29. In cellulose chemistry, it is frequently used for the surface modification especially of cellulose

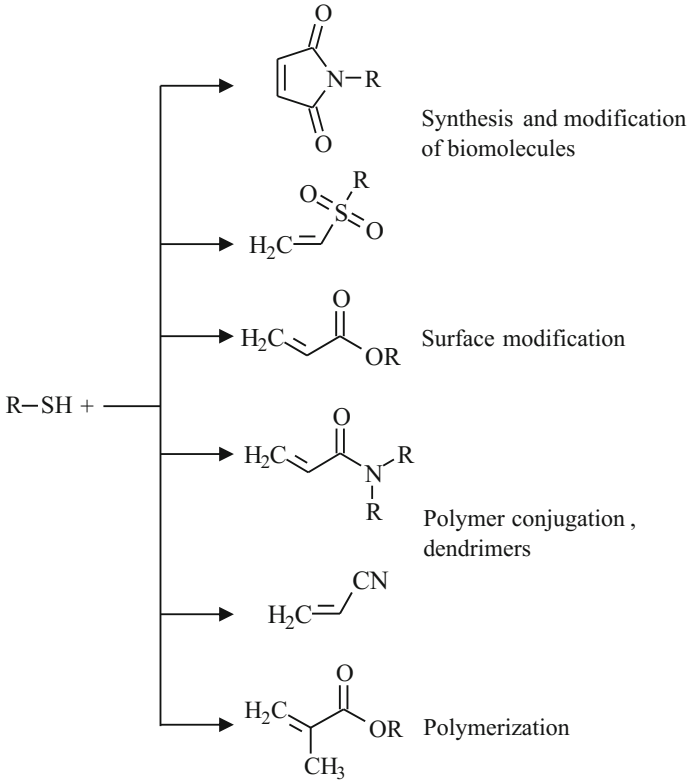


**Fig. 7.29** Overview of reactions for polymer functionalization via thiol-Michael addition (adapted from [103])

nanocrystals. An example is the attachment of a disulfide moiety to cellulose nanocrystals, reduction, and a thiol-Michael addition to graft cellulose nanocrystals with pentabromobenzyl acrylate [104].

A related approach is the thiol-ene reaction that is unlike the thiol-Michael addition, a radical based reaction. The radicals are formed by UV irradiation or by free-radical initiators. The thiol radical attacks a carbon-carbon double bond forming the C–S bond (Fig. 7.30).

This path was also used widely for the surface modification of cellulose nanocrystals. To obtain a suitable precursor, the nanocrystals were esterified with methacrylic acid, e.g., using *N,N′*-diisopropylcarbodiimide/4-*N,N*-dimethylaminopyridine as catalysts. The methacrylate cellulose nanocrystals were reacted by thiol-ene reaction with cysteamine to introduce a primary amine, which can in turn be converted with an activated fluorophore, e.g., 5-(and-6)-carboxytetramethylrhodaminesuccinimidyl ester (see Fig. 7.31). In this way, cellulose nanocrystals are converted into ratiometric (the ratio output voltage/supply voltage) pH-sensing nanoparticles by dual fluorescent labelling employing ene-thiol reactions [105].

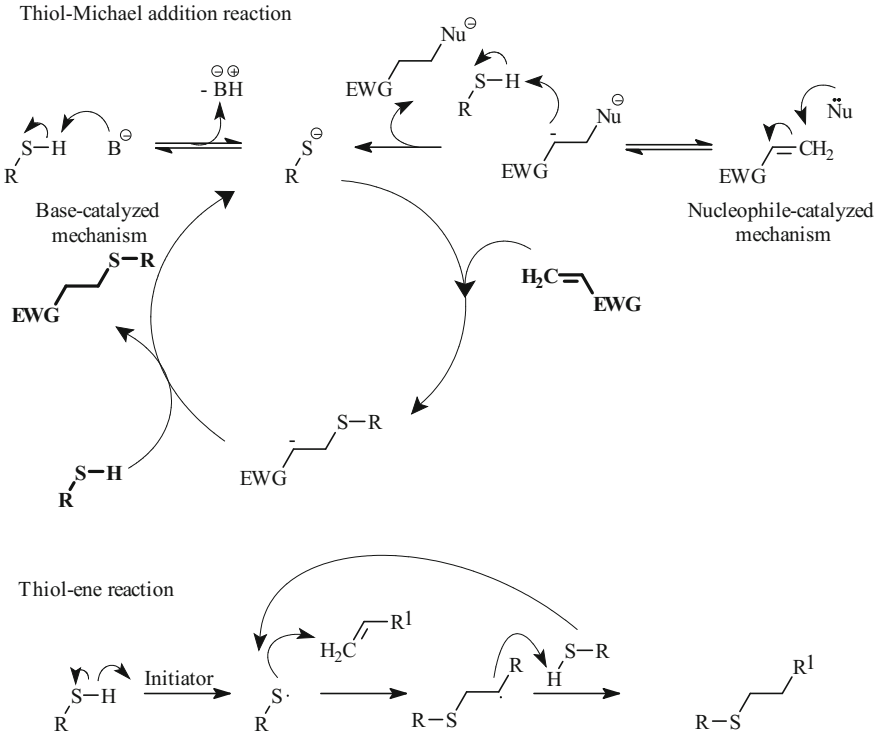


**Fig. 7.30** Different mechanisms for the thiol-Michael and the thiol-ene reactions (EWG: electron-withdrawing group)

Furthermore, acrylate functions with a spacer were introduced into the cellulose backbone (porous cellulose nanocrystal–poly(vinyl alcohol) scaffolds) by conversion with an acrylated isocyanate. The acrylated nanocrystal surface can be decorated with thiolated dyes or biomolecules [106]. Moreover, cellulose surfaces may be decorated with long chain esters carrying terminal olefins. Thus, 9-decenoic acid, undec-10-enoyl chloride, or 2-(oct-7-enyl)oxirane were reacted with cellulose surfaces (Fig. 7.32, [107]). The subsequent thiol-ene modification was initiated by UV irradiation. Thus, a simple surface functionalization was possible, e.g., by treatment of the 9-decenoic acid modified cellulose with benzyl mercaptan in the presence of 1% (w/w) DMPA and irradiated with UV light. Successful conjugation was confirmed by fluorescence—the precursor cellulose did not fluoresce while the benzyl mercaptan treated substrate did.

The same chemistry was applied to prepare covalently linked composites of rigid cellulose nanocrystals in a polybutadiene matrix. Composite films were obtained by UV-light initiated thiol-ene click reactions with bifunctional dithiol like nonanedithiol as cross-linkers leading to a material with intercalated domains [108]. The ene moiety may also be introduced by silylation of the cellulose [109].

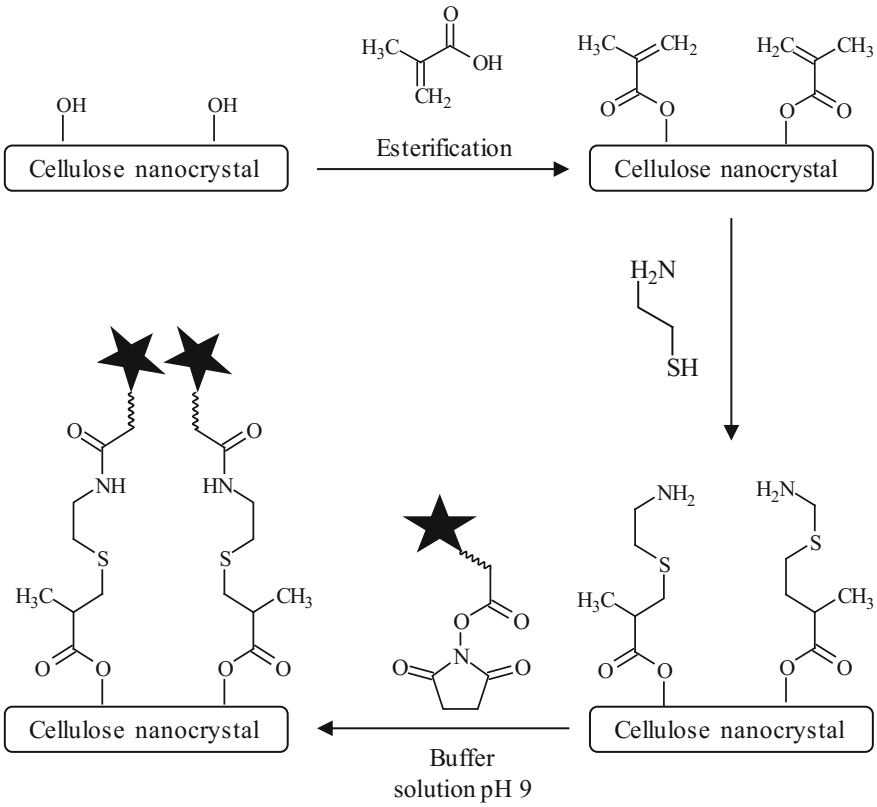


**Fig. 7.31** Fluorescent labelling of cellulose nanocrystals with succinimidyl ester dyes (adapted from [105])

In this example, ene-functionalized cellulose films were synthesized using vinyltrimethoxysilane as coupling agent, and this intermediate was photochemically coupled with methylthioglycolate (Fig. 7.33).

Besides the functionalization of the cellulose surfaces with unsaturated groups, it is possible to introduce the thiol moiety and react it with an unsaturated reagent. Thus, functionalization of cellulose nanocrystal was achieved by introduction of thiol groups by silylation of hydroxyl groups on cellulose with 3-mercaptopropyltrimethoxysilane (Fig. 7.34, [109]).

This functionalization step is followed by thiol-ene click chemistry using acetophenone as photoinitiator. Proper (ene) components were allylbutyrate [109], *N*-phenylmaleimide, and *N*-(1-pyrenyl)maleimide (ene–dye), see Fig. 7.35, [110]. The efficiency of the conversion can be confirmed by solid state $^{13}C$ NMR spectroscopy (Fig. 7.36).

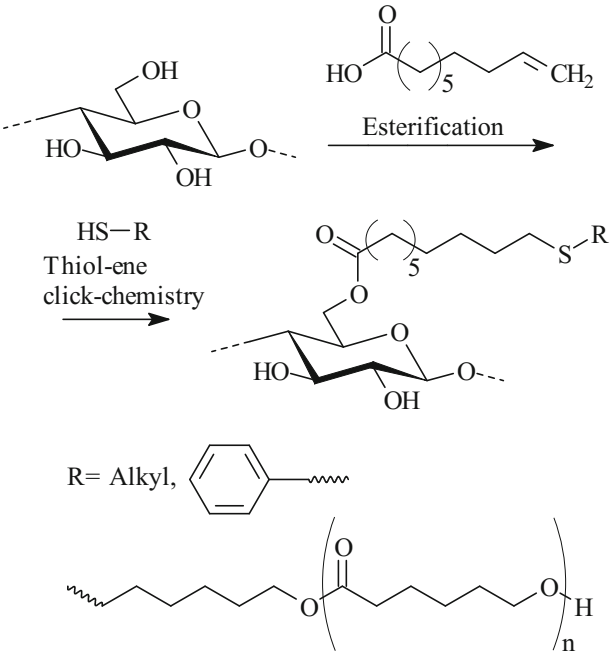


**Fig. 7.32** Chemical modification of cellulose to introduce pendent "(ene) functionality susceptible to radical thiol-ene addition" (adapted from [107])

## 7.3 Grafting of Cellulose

### *7.3.1 Introduction*

Because of its abundance and biodegradability, cellulose fibers are natural candidates for the fabrication of composites. A composite is defined as the combination of two or more different components, one plays the role of filler or reinforcement (such as biofibers), while the other polymer is the matrix material. Composites based on biopolymers have low density and high mechanical strength and, most importantly, low environmental impact due to their improved biodegradability. The hydrophilicity of cellulose fiber can result, however, in poor interfacial bonding/adhesion between fibers and the generally hydrophobic polymer matrix. Poor adhesion adversely affects the composite durability (e.g., due to weathering, water absorption, and bio-deterioration) and mechanical properties. To decrease the hydrophilicty of cellulose fibers and increase their compatibility with the matrix material, their surface properties have been changed whether through physical adsorption or chemical modification including grafting. These approaches are also employed in the textile industry in order to increase the crease-resistance and dimensional stability of the fiber as well as to introduce antimicrobial activity [111].

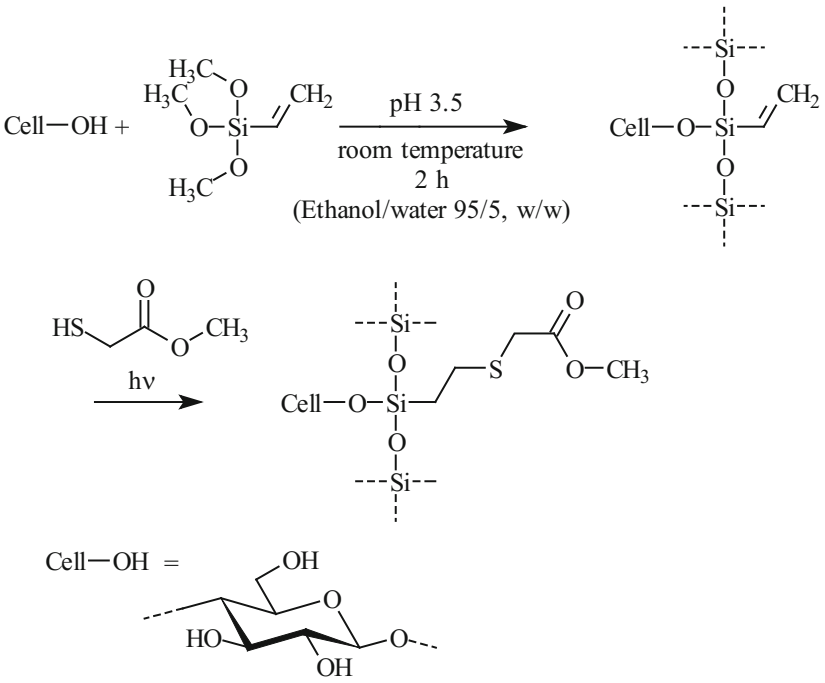


**Fig. 7.33** Chemical modification of cellulose by surface modification with vinyltrimethoxysilane and photochemical coupling with methylthioglycolate (adapted from [109])

Controlled derivatization and grafting of cellulose with selected monomers leads to desirable changes in the properties of the obtained materials, relative to those of the starting biopolymer, inter alia, changes in the mechanical and thermal properties; large increase or decrease in hydrophilicity.

An example of fiber surface modification is the physical adsorption of copolymer micelles and their subsequent spreading on the surface of cellulose, as shown in Fig. 7.37. This technique is used, e.g., in the paper industry to improve properties such as wet/dry strength, creep, and sizing. A cationic polyelectrolyte is employed because the presence of carboxylate and sulfonate groups on the surface (generated mostly during paper making) makes it weakly anionic [112]. Filler-matrix compatibility can be also improved by chemical derivatization of cellulose, e.g., into esters (carboxylates and mixed carboxylates), nonionic ethers (methyl and 2-hydroxypropyl) and ionic ones, in particular CMC. The reaction of cellulose with bi- or poly-functional compounds, e.g., dicarboxylic acids, glyoxal and its analogues leads to stable cross-linked products and can impart crease-resistance, or "durable press" properties to cellulose [113]. As indicated in Chaps. 5 and 6 of this book, the applications of these cellulose derivatives include coatings, laminates, optical films, sorption, pharmaceuticals, foodstuffs, and cosmetics [114].

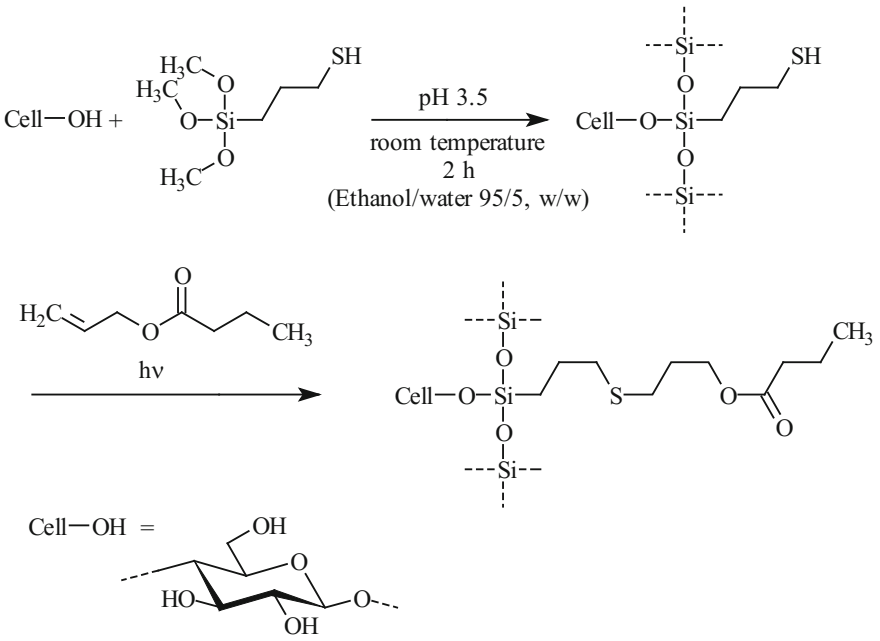


**Fig. 7.34** Thiolation of cellulose followed by thiol-ene reaction with unsaturated moieties (adapted from [109])

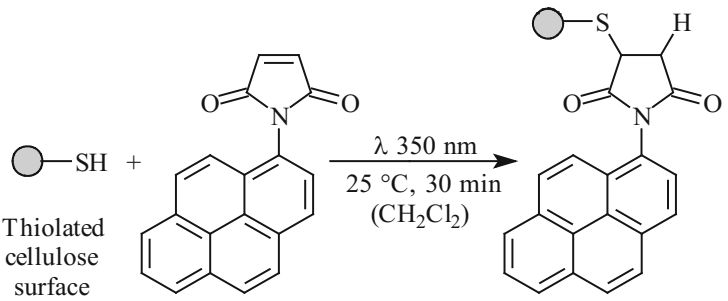


**Fig. 7.35** Thiol-ene conversion of a thiolated cellulose surface with *N*-(1-pyrenyl)maleimide

Graft copolymerization of cellulose and cellulose derivatives is a more sophisticated approach that is used to modify their properties. The reaction is carried out under heterogeneous- (usually on cellulose) as well as homogeneous conditions using an organic- or a water-soluble cellulose derivative, e.g., cellulose acetate and cellulose 2-hydroxyethyl ether, respectively [115–121]. A graft copolymer consists of a long sequence of one monomer that forms the main chain (or backbone) of the polymer, with one or more attached branches or "grafts" of a sequences of a different monomer [122]. The three main methods of graft polymerization are

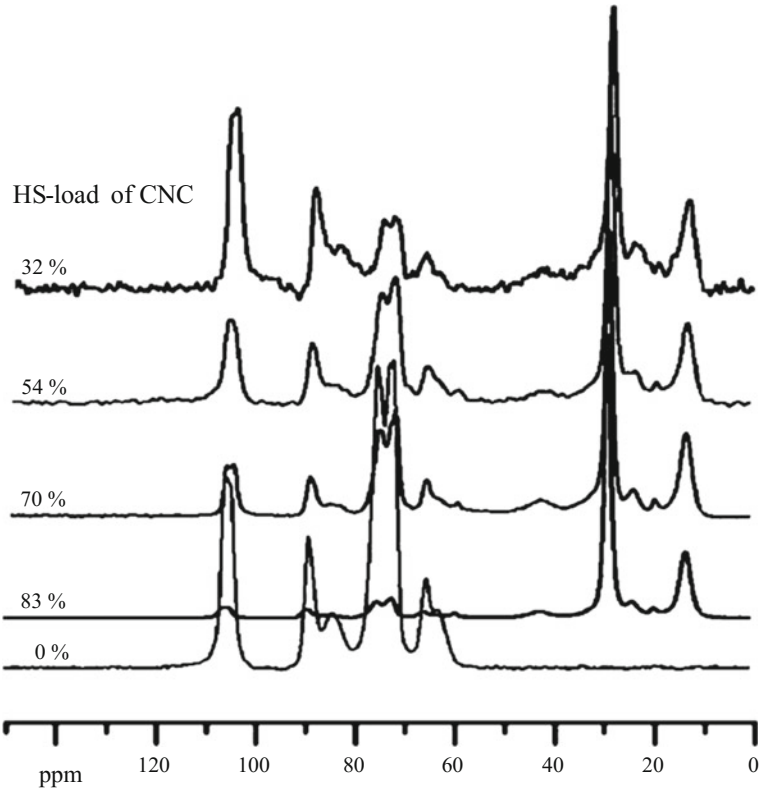


**Fig. 7.36** Solid state $^{13}C$ NMR spectra of the pure cellulose nanocrystals (CNC) and the different HS load modified cellulose nanocrystals (adapted from Ref. [110] with permission of The Royal Society of Chemistry)

shown in Fig. 7.38, namely "grafting from", "grafting to" and "grafting through" [122].

In the "grafting-from" technique, the growth of polymer chains occurs from initiating sites on the cellulose backbone. This technique is most commonly employed because a high graft density can be achieved due to the relatively easy access of the monomer that is being added to the chain ends of the growing grafts. This grafting can be carried out with a single monomer, or a mixture of monomers (usually binary). When a single monomer is employed, the grafting usually occurs in stepwise steps. In grafting with binary monomer mixtures, the reaction is carried out in sequence, i.e., with a single monomer at a time, or with both monomers simultaneously [123].

In the "grafting-to" approach, a preformed polymer with a reactive end functional group is covalently bound to the functional groups, e.g., the hydroxyl moieties, of the cellulose backbone. The polymer load that is grafted onto cellulose (graft density) is limited by steric crowding of the grafts at cellulose surface.

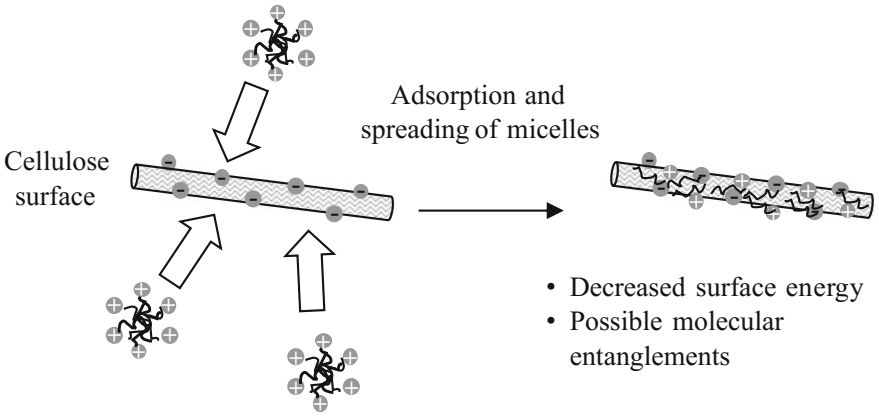


**Fig. 7.37** Adsorption of micelles of a block copolymer, and their subsequent spreading on the surface of cellulose. This leads to decreased surface energy and better compatibility with a matrix polymer (adapted from [112])

Therefore, for grafting of cellulose with the same monomers, the graft density obtained by "grafting-to" is less than that observed for "grafting-from".

The "grafting-through" approach involves the copolymerization of cellulose that carries a polymerizable chain, e.g., a vinyl macro-monomer or macromer with a low molecular weight co-monomer. This technique is less employed because it requires previous synthesis of the cellulose derivative.

Because cellulose is insoluble in water or common organic solvents, grafting has been carried out on the biopolymer proper under heterogeneous conditions. Consequently, the supramolecular and morphological structure of the cellulose employed strongly affect the outcome of the grafting reaction, including the structure and properties of the grafted material. By a proper choice of the reaction conditions it is possible to induce preferential surface grafting of cellulose, or rather a uniform grafting in the biopolymer, a point that is relevant to the application envisaged. For example, predominant surface grafting is enough if the goal is to increase compatibility of the filler (grafted cellulose) with the matrix. An example of this control is provided by $Mn^{3+}$-initiated grafting with acrylic acid esters, where uniform grafting was observed with methyl acrylate and predominantly surface grafting was observed with butyl acrylate. The diffusion of the voluminous butyl acrylate into the cellulose matrix is limited, leading to more surface grafting [115]. The state of cellulose swelling (the reaction proceeds most readily in the amorphous region) greatly affect the properties of the grafted products. Thus, radiation-induced grafting of dried cellulose did not start until the temperature of the thermal polymerization of the monomer was reached. This temperature decreased, however, as a function of increasing the water content of cellulose from 5 to 20% (w/w) [124]. Alternatively, the usual reagents that cause cellulose swelling were employed in the pretreatment step before grafting, e.g., $ZnCl_2$ solution alone, or followed with

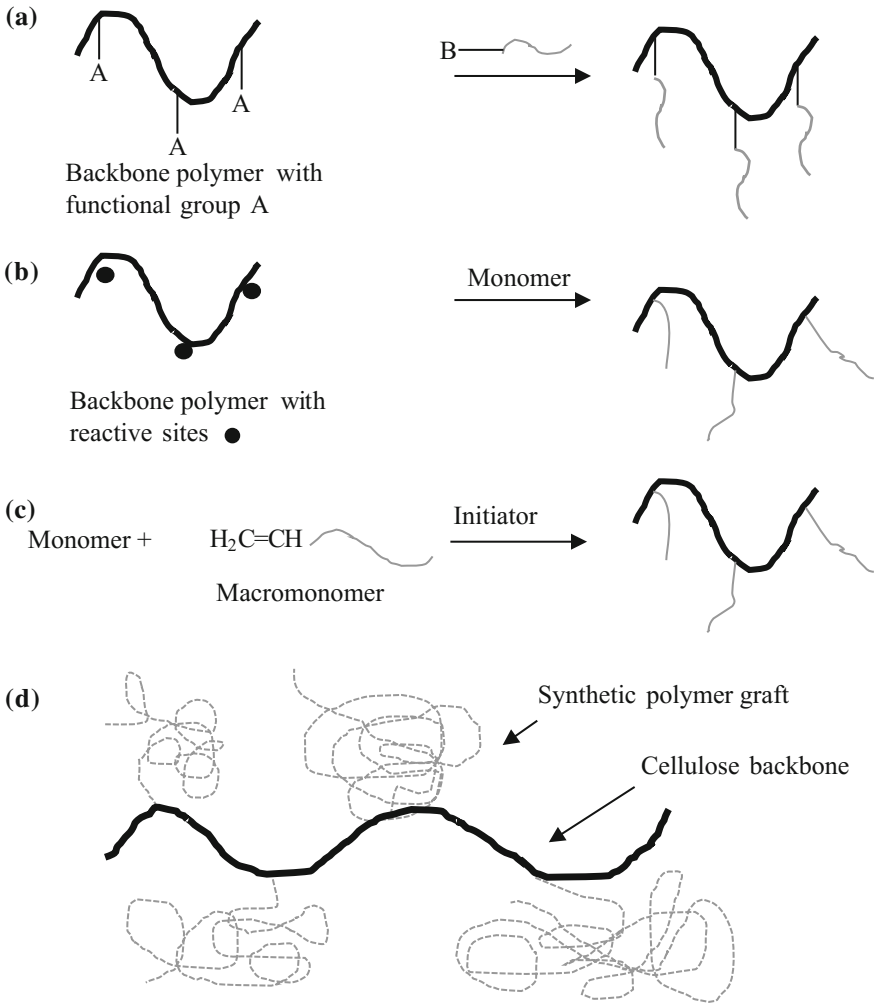


**Fig. 7.38** Schematic representation of the three methods of polymer grafting. These are "grafting to" (**a**), "grafting from" (**b**), "grafting through" (**c**), as well as a schematic representation of final grafted cellulose (**d**)

NaOH solution treatment [125], different concentrations of alkali solutions [126], and dilute nitric acid solution [127].

Under homogeneous conditions, e.g., using soluble cellulose derivatives, the extent and frequency of grafting as well as the molar masses of the products are much better controlled than in the heterogeneous reaction [128]. Organic solvent-soluble esters, e.g., CA's and cellulose cinnamate in DMAc/LiCl and paraformaldehyde/DMSO [129–131], and water soluble nonionic ethers, e.g., methyl-, ethyl- and hydroxyethyl cellulose and CMC have been used [132–134].

Typical routes employed for grafting cellulose and some representative examples of the monomers are: free radical, styrene after redox initiation and acrylonitrile after high-energy irradiation; anionic, acrylonitrile onto "alkali cellulose"; cationic, cardanol after initiation with a Lewis acid ($BF_3$-etherate); ring opening, ε-caprolactam; polyaddition, ethylene oxide/NaOH aq; "grafting to", polyamide and polyester.

## *7.3.2 Mechanisms of Grafting*

### 7.3.2.1 Free Radical Grafting

In addition to the above-mentioned grafting techniques, there is the question of the nature of polymerization, radical or ionic, in particular with ring opening. Free-radical grafting is the most employed method because of its versatility and applicability to the polymerization of important monomers, e.g., methyl acrylates, styrene, butadiene, vinyl acetate, as well as water-soluble monomers, e.g., acrylic acid and acrylamide. In the free-radical "grafting-from", the radicals can be generated on the cellulose backbone by several methods, including free radicals formed by decomposition of an initiator [135], irradiation either by UV light [136], or γ-radiation from radioactive isotopes, e.g., $^{60}Co$ source, or electron-beams [137] or by exposure to a plasma ion beam [138]. The monomers present react with the free radicals on the backbone, forming a new radical site that adds more monomers. The propagation step leads to extension of the branch until termination occurs by one of the usual reactions in free radical polymerization. These include combination of two growing chains; hydrogen atom abstraction from another chain (disproportionation), and reaction with (an added) chain terminator. As initiators for cellulose grafting with acrylic acid and acrylamide, potassium persulfate [139–141], Fenton's reagent ($Fe^{2+}/H_2O_2$ system) [142, 143], Ce(IV) ion oxidation [144], and azobisisobutyronitrile [126] were employed. Figures 7.39, 7.40 and 7.41 show the mechanism of initiation by persulfate, Fenton's reagent, and Ce(IV) ions respectively of the "graft from" cellulose. Any of the above-mentioned initiation methods can be employed with cellulose derivatives that carry a double bond, e.g., allyl ethers; the free radical is generated by oxidation of this functionality [145].

Alternatively, cellulose can be partially converted into its hydroperoxide, e.g., by ozonization or by irradiation in hydrogen peroxide solution. Decomposition of this reactive intermediate into the corresponding radical (Cell-$O^{\bullet}$) initiates the "grafting-from" reaction, i.e., cellulose itself is the initiator. In this case, homopolymer formation can be suppressed by the use of a reducing agent [146].

Generation of free radicals in cellulose by irradiation (γ-radiation; UV; plasma) has received considerable attention because of the simplicity of the experimental setup. The drawbacks of this approach are associated with the energy of the radiation employed; they include radiation-induced biopolymer chain splitting; relatively few and high molar mass side-chains; potential extensive formation of homopolymers [147–150].

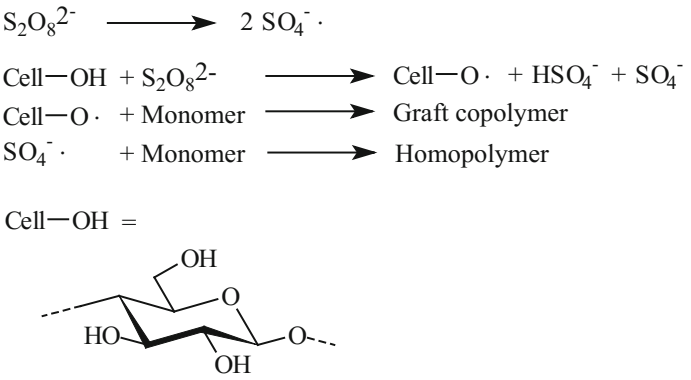


**Fig. 7.39** Simplified mechanism of perfsulfate initiated graft polymerization of cellulose (adapted from [139])

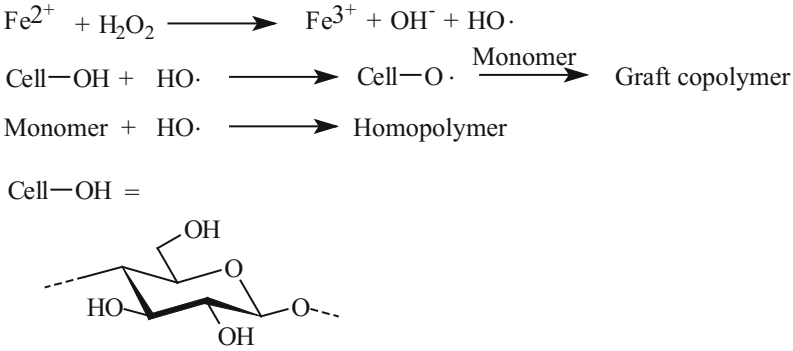


**Fig. 7.40** Suggested mechanism of Fenton's reagent initiated graft polymerization of cellulose (adapted from [143])

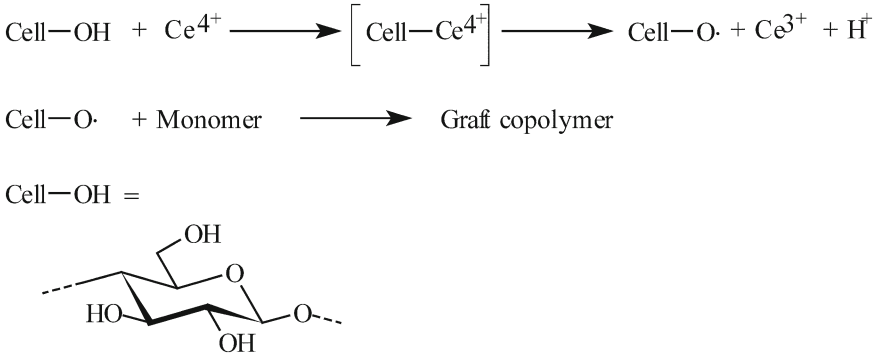


**Fig. 7.41** Simplified mechanism Ce(IV)-induced cellulsoe radical formation and subsequent grafting (adapted from [144])

There are two techniques for radiation-induced grafting. In the pre-irradiation method, cellulose substrate is irradiated first to generate radicals that are trapped within the solid biopolymer matrix. This is followed by the introduction of a cellulose swelling agent (e.g., aqueous alkali solution) and the monomers. Alternatively, cellulose is irradiated in the presence of the swelling agent and the monomers; this is the mutual irradiation method. The former approach leads to much less homopolymerization as compared with the latter one [151], although the degradation of the cellulose backbone is usually more extensive, especially if the irradiation is not done under an inert atmosphere [144]. The use of low-energy UV irradiation for grafting of vinyl and acrylic monomers to cellulose causes less biopolymer degradation, and offers a better control of grafting as compared with γ-irradiation. In order to enhance the formation of cellulose free radical, UV-irradiation relies on the use of photo-initiators whose decomposition generates radicals that reacts with cellulose [152, 153]. Plasma treatment has also been successively employed to graft acrylamide and 2-hydroxyethyl methacrylate onto cellulose fibers [154, 155].

#### 7.3.2.2 Ionic Grafting by Ring Opening Polymerization (ROP)

ROP, developed in the 1930s by Carothers et al. [156], leads to macromolecules with defined end-groups and high molar masses. Numerous cyclic monomers such as lactones, lactides, cyclic carbonates, siloxanes can be easily polymerized by ring opening [157]. The ease of polymerization of cyclic monomers is due to both kinetic and thermodynamic factors; the presence of a heteroatom (oxygen, nitrogen, sulfur, etc.) in the ring facilitates the ring opening via a nucleophilic or electrophilic attack of the initiator. The catalyst system employed determines whether an anionic, a cationic, monomer-activated or coordination-insertion mechanism occurs [158]. Several different catalytic systems have been explored: metal-based, organic, or enzymatic. Examples of metal-based catalysts are stannous 2-ethylhexanoate ($Sn(Oct)_2$), titanium *n*-butoxide ($Ti(O\text{-}n\text{-}Bu)_4$), and the organic super-base 1,5,7-triazabicyclo[4.4.0]dec-5-ene (TBD).

As the ring-opening step of the ROP mechanism can be initiated with an alcohol, cellulose can be employed as initiator; no pretreatment is required. Part a of Fig. 7.42 shows the mechanism of an alcohol initiated polymerization of ε-caprolactam; part b exemplifies the case cellulose with ε-caprolactam, using organic or amino-acid catalysts [159].

A hyper-branched graft copolymer was obtained by ROP by reacting cellulose with 3-methyl-3-oxetanemethanol with ring opening (Fig. 7.43). This grafting largely increased the number of hydroxyl groups present on the fiber surface, hence the material obtained is water super-absorbent [160].

Interest in investigation the "grafting-from" approach by the ROP mechanism under homogeneous conditions is motivated by the better control of the reaction that often results in amphiphilic block copolymers, with a comb-like architecture, giving rise to interesting three-dimensional structures. The resulting materials are

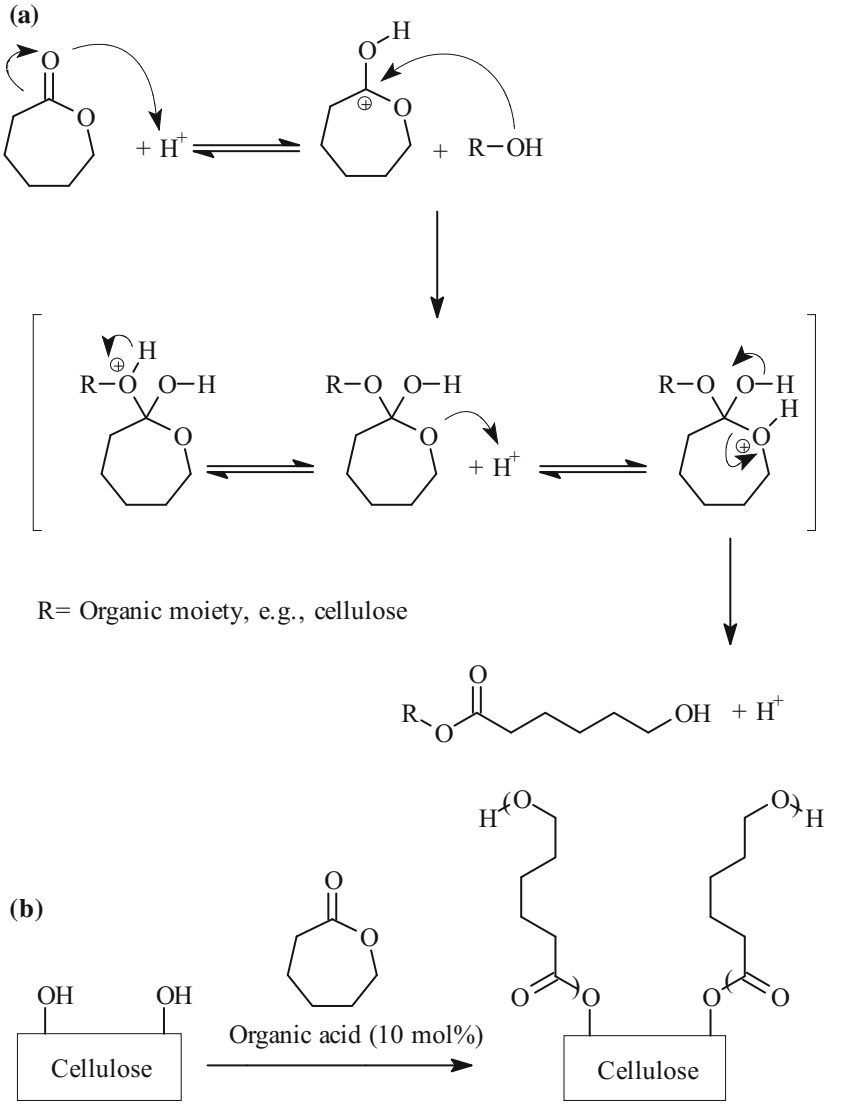


**Fig. 7.42** The mechanism of an alcohol initiated polymerization of ε-caprolactam (**a**, adapted from [158]) and grafting of cellulose with ε-caprolactam, using tartaric acid catalyst (**b**, adapted from [159])

often biodegradable and may be employed in drug delivery. Figure 7.44 shows the grafting of soluble CTs with 2-methyloxazoline [161].

Other approaches for ionic grafting of polymers are known, but their use with cellulose is rather limited due to the stringent reaction conditions required

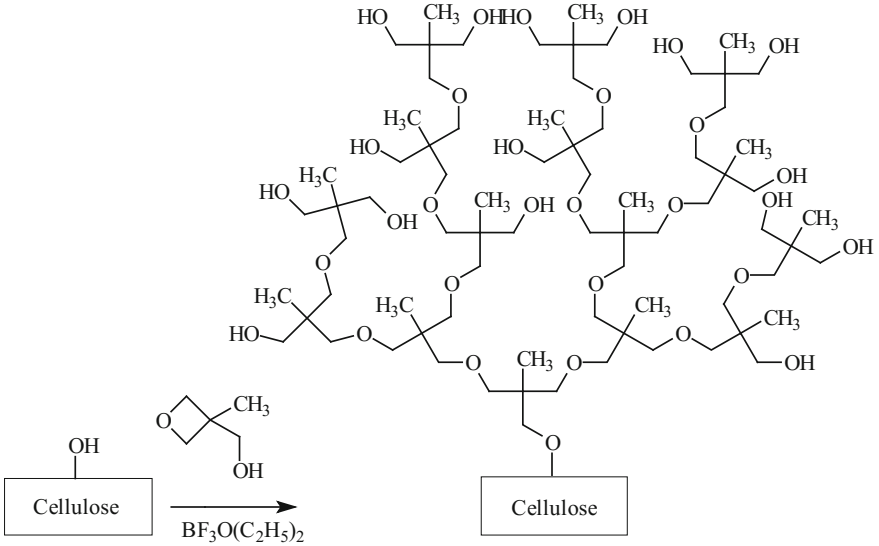


**Fig. 7.43** Grafting of hyper-branched polyether from a cellulose fiber surface (adapted from [160])

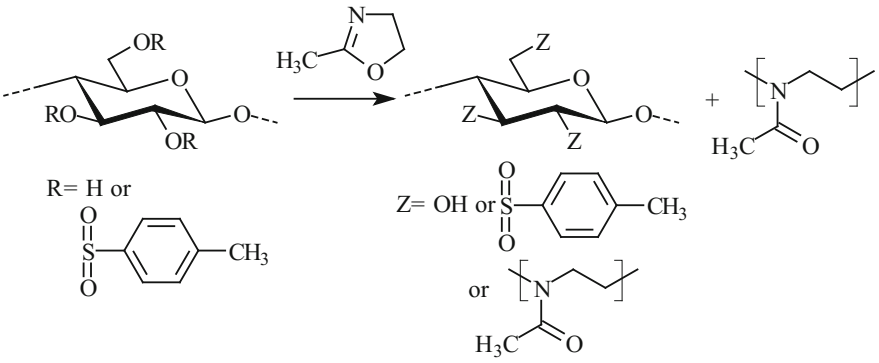


**Fig. 7.44** Scheme for the grafting of cellulose tosylate with 2-methyloxazoline (adapted from [161])

[162, 163]. Of increasing interest are methods for cellulose grafting by living radical polymerization. Possible techniques are nitroxide-mediated polymerization (NMP) [164, 165], atom transfer radical polymerization (ATRP) [166, 167], and reversible addition–fragmentation chain transfer (RAFT) polymerization [168, 169].

### 7.3.3 Characterization of Cellulose Graft Copolymers

After grafting cellulose under heterogeneous conditions, the resulting graft copolymer is purified by removing the homopolymer, generally by solvent extraction. In case of the homogeneous reaction, the graft copolymer is purified by precipitation. The occurrence of grafting can be demonstrated by various techniques, e.g., swelling, thermal analysis (DTA/TGA), and spectroscopy (FTIR and NMR). In addition, morphological analysis, e.g., SEM, are useful tools to get information about the structure.

FTIR is a simple and informative technique that grafting has occurred because of the appearance of characteristic peaks of new bonds, e.g., –C=O, –C≡N [170] and the disappearance of others, e.g., double bonds [171]. When the IR peaks in questions are intense and symmetric, or when they can be unambiguously defined by peak deconvolution, this technique is excellent for quantitative analysis [172]. NMR spectroscopy (both $^{1}H$ and $^{13}C$) can be employed to show the presence of grafting and also permits quantitative analysis (using the inverse-gated decoupling technique for $^{13}C$ NMR spectroscopy).

Grafting also leads to changes in the thermal properties. Whereas it is not possible to determine ($T_g$) and ($T_m$) for the starting cellulose (due to very strong hydrogen-bonding and biopolymer decomposition, respectively), these temperatures can be determined (depending on grafting percentage, vide infra) for the grafted sample by thermogravimetric analytical methods [173].

After demonstrating that grafting has occurred, the product is then characterized by parameters such as grafting percentage (GP%, Eq. 7.1); grafting efficiency (GE%, Eq. 7.2); and the number of grafts per cellulose chain (Ng).

$$GP = \frac{W_1 - W_0}{W_0} \cdot 100\% \tag{7.1}$$

$W_1$ Mass of the biopolymer after grafting
$W_0$ Initial mass of the biopolymer

GE shows the fraction of monomer grafted onto cellulose relative to the total monomer mass consumed.

$$GE = \frac{W_1 - W_0}{W_1 - W_0 - W_2} \cdot 100\% \tag{7.2}$$

$W_1$ Mass of the biopolymer after grafting
$W_0$ Initial mass of the biopolymer
$W_2$ Mass of the homopolymer formed

The average molar mass of the product is determined by one of the techniques discussed in Chap. 2, including viscosimetry and GPC. The grafting frequency (GF, Eq. 7.3) is defined as the number of grafted polymer chains [174, 175].

$$GF = \frac{M_{\text{Cellulose}}}{M_{\text{GraftedPolymer}} \cdot \frac{GP}{100\%}} \tag{7.3}$$

When grafting is done in order to change the hydrophilicity of the biopolymer, the water absorption capacity is calculated from the masses of the water-swollen material and the dry, starting biopolymer, respectively.

### 7.3.4 Applications of Cellulose Graft Copolymers

Most of the information available on the changes of properties due to grafting concerns fibers, filaments, fabrics, and cellulose-based membranes. The properties of fibers that are affected by grafting include: tensile strength; elongation at break; elastic modulus; water vapor uptake; thermoplasticity; dimensional stability, wrinkle resistance; water- and oil repellency; microbial resistance, and flame retardancy.

The applications of cellulose graft copolymers depend on the nature of polymer grafted on cellulose. For example, cellulose samples grafted with hydrophilic polymers, e.g., poly(acrylic acid), poly-*N*-vinyl-2-pyrrolidone, or polyacrylamide have high or very high water absorption capacity (e.g., from 60 to 2700 g/g) [176]. They have medical applications as body fluid absorbing material [145] and fabrics for manufacturing underwear and athlete wear [177]. Cellulose graft copolymers synthesized in DMSO–paraformaldehyde solvent system have been used as permeability selective membranes [178, 179]. The cellulose copolymers obtained by grafting with functional groups such as acrylamide [180], acrylic acid [181], acrylonitrile, and 2-acrylamidomethylpropane sulfonic acid [182] have been used in the adsorption of hazardous contaminants such as heavy metal ions or dyes from aqueous solutions [183, 184]. The product of poly(4-vinyl pyridine)-grafted cellulose with sodium borohydride has been used as reducing agents for some carbonyl compounds, e.g., benzaldehyde, cyclohexanone, crotonaldehyde, acetone, and furfural [171] whereas cellulose grafted with poly(2-diethylamino) ethyl methacrylate is pH-responsive [185]. Finally, cellulose graft copolymers with thermosensitive graft chains such as poly(*N*-isopropylacrylamide) or poly(*N,N*-diethylacrylamide) have been used in the removal of heavy metal ions from aqueous solutions by temperature swing adsorption, i.e., thermally triggered contraction and aggregation, which is different from the removal of metal ions by complexation or ion-exchange [186, 187].

# References


1. Dias GJ, Peplow PV, Teixeira F (2003) Osseous regeneration in the presence of oxidized cellulose and collagen. J Mater Sci Mater Med 14:739–745
2. Galgut PN (1990) Oxidized cellulose mesh: I. Biodegradable membrane in periodontal surgery. Biomaterials 11:561–564
3. Dimitrijevich SD, Tatarko M, Gracy RW, Linsky CB, Olsen C (1990) Biodegradation of oxidized regenerated cellulose. Carbohydr Res 195:247–255
4. Wiseman DM, Saferstein L, Wolf S (2002) Bioresorbable oxidized cellulose composite material for prevention of postsurgical adhesions. US 6,500,777 B1
5. Pameijer CH, Jensen S (2007) Agents and devices comprising oxidized cellulose fibers for providing blood clotting for wound healing promotion. US 20,070,190,110 A1 20070816 CAN 147:243491
6. Butrim SM, Bil'dyukevich TD, Butrim NS, Yurkshtovich TL (2007) Structural modification of potato starch by solutions of nitrogen (IV) oxide in $CCl_4$. Chem Nat Compd 43:302–305
7. Painter TJ (1977) Preparation and periodate oxidation of C-6-oxycellulose: conformational interpretation of hemiacetal stability. Carbohydr Res 55:95–103
8. Johansson E, Lind J (2005) Free radical mediated cellulose degradation during high consistency ozonation. J Wood Chem Technol 25:171–186
9. Manhas MS, Mohammed F, Khan Z (2007) A kinetic study of oxidation of β-cyclodextrin by permanganate in aqueous media. Colloids Surf A 295:165–171
10. Borisov IM, Shirokova EN, Mudarisova RKh, Muslukhov RR, Zimin YuS, Medvedeva SA, Tolstikov GA, Monakov YB (2004) Kinetics of oxidation of an arabinogalactan from larch (Larix sibirica L.) in an aqueous medium in the presence of hydrogen peroxide. Russ Chem Bull 53:318–324
11. Calvini P, Conio G, Lorenzoni M, Pedemonte E (2004) Viscometric determination of dialdehyde content in periodate oxycellulose. Part I. Methodology. Cellulose 11:99–107
12. Zimnitsky DS, Yurkshtovich TL, Bychkovsky PM (2004) Synthesis and characterization of oxidized cellulose. J Polym Sci, Part A: Polym Chem 42:4785–4791
13. Fras L, Johansson LS, Stenius P, Laine J, Stana-Kleinschek K, Ribitsch V (2005) Analysis of the oxidation of cellulose fibres by titration and XPS. Colloids Surface A 260:101–108
14. de Nooy AEJ, Besemer AC, van Bekkum H (1995) Highly selective nitroxyl radical-mediated oxidation of primary alcohol groups in water-soluble glucans. Carbohydr Res 269:89–98
15. Chang PS, Robyt JF (1996) Oxidation of primary alcohol groups of naturally occurring polysaccharides with 2,2,6,6-tetramethyl-1-piperidine oxoammonium ion. J Carbohydr Chem 15:819–830
16. Tahiri C, Vignon MR (2000) TEMPO-oxidation of cellulose: synthesis and characterisation of polyglucuronans. Cellulose 7:177–188
17. Davis NJ, Flitsch SL (1993) Selective oxidation of monosaccharide derivatives to uronic acids. Tetrahedron Lett 34:1181–1184
18. Gomez-Bujedo S, Fleury E, Vignon MR (2004) Preparation of cellouronic acids and partially acetylated cellouronic acids by TEMPO/NaClO oxidation of water-soluble cellulose acetate. Biomacromol 5:565–571
19. Isogai A, Kato Y (1998) Preparation of polyuronic acid from cellulose by TEMPO-mediated oxidation. Cellulose 5:153–164
20. Kato Y, Kaminaga J, Matsuo R, Isogai A (2004) TEMPO-mediated oxidation of chitin, regenerated chitin and N-acetylated chitosan. Carbohydr Polym 58:421–426
21. Coseri S, Nistor G, Fras L, Strnad S, Harabagiu V, Simionescu BC (2009) Mild and selective oxidation of cellulose fibers in the presence of N-hydroxyphthalimide. Biomacromol 10:2294–2299

22. Biliuta G, Fras L, Strnad S, Harabagiu V, Coseri S (2010) Oxidation of cellulose fibers mediated by nonpersistent nitroxyl radicals. J Polym Sci, Part A: Polym Chem 48:4790–4799
23. Yackel EC, Kenyon WO (1942) Oxidation of cellulose by nitrogen dioxide. J Am Chem Soc 64:121–127
24. Nevell TP (1963) Oxidation. In: Whistler RL, BeMiller JN (eds) Methods in carbohydrate chemistry, vol 3. Academic Press, New York, pp 164–185
25. Heinze T, Klemm D, Schnabelrauch M, Nehls I (1993) Properties and following reactions of homogeneously oxidized celluloses. In: Kennedy JF, Phillips GO, Williams PA (eds) Cellulosics: chemical, biochemical and material aspects. Ellis Horwood, New York, pp 349–354
26. Heinze T (1998) Ionische Funktionspolymere aus Cellulose: Neue Synthesekonzepte, Strukturaufklärung und Eigenschaften. Habilitation thesis, Friedrich Schiller University of Jena, Jena
27. Painter TJ, Cesaro A, Delben F, Paoletti S (1985) New glucuronoglucans obtained by oxidation of amylose at position 6. Carbohydr Res 140:61–68
28. Nehls I, Heinze T, Philipp B, Klemm D, Ebringerova A (1991) Carbon-13 NMR studies of oxidation of cellulose in phosphoric acid-sodium nitrite systems. Acta Polym 42:339–340
29. Camy S, Montanari S, Rattaz A, Vignon M, Condoret J-S (2009) Oxidation of cellulose in pressurized carbon dioxide. J Supercrit Fluids 51:188–196
30. de Nooy AEJ, Besemer AC, van Bekkum H (1994) Highly selective TEMPO mediated oxidation of primary alcohol groups in polysaccharides. Recl Trav Chim Pays-Bas 113:165–166
31. Bragd PL, van Bekkum H, Besemer AC (2004) TEMPO-mediated oxidation of polysaccharides: survey of methods and applications. Top Catal 27:49–66
32. Saito T, Isogai A (2004) TEMPO-mediated oxidation of native cellulose. The effect of oxidation conditions on chemical and crystal structures of the water-insoluble fractions. Biomacromol 5:1983–1989
33. Hirota M, Tamura N, Saito T, Isogai A (2009) Oxidation of regenerated cellulose with $NaClO_2$ catalyzed by TEMPO and NaClO under acid-neutral conditions. Carbohydr Polym 78:330–335
34. Hirota M, Tamura N, Saito T, Isogai A (2009) Surface carboxylation of porous regenerated cellulose beads by 4-acetamide-TEMPO/NaClO/$NaClO_2$ system. Cellulose 16:841–851
35. Li B, Xu W, Kronlund D, Määttänen A, Liu J, Smått J-H, Peltonen J, Willför S, Mu X, Xu C (2015) Cellulose nanocrystals prepared via formic acid hydrolysis followed by TEMPO-mediated oxidation. Carbohydr Polym 133:605–612
36. Zhang Y, Zhang L, Shuang S, Feng F, Qiao J, Guo Y, Choi MMF, Dong C (2010) Electro-oxidation of methane on roughened palladium electrode in acidic electrolytes at ambient temperatures. Anal Lett 43:1055–1065
37. Danaee I, Jafarian M, Mirzapoor A, Gobal F, Mahjani MG (2010) Electrooxidation of methanol on NiMn alloy modified graphite electrode. Electrochim Acta 55:2093–2100
38. Isogai T, Saito T, Isogai A (2010) TEMPO electromediated oxidation ofs polysaccharides including regenerated cellulose fiber. Biomacromol 11:1593–1599
39. Bailey WF, Bobbitt JM, Wiberg KB (2007) Mechanism of the oxidation of alcohols by oxoammonium cations. J Org Chem 72:4504–4509
40. Schnabelrauch M, Heinze T, Klemm D, Nehls I, Koetz J (1991) Investigations on synthesis and characterization of carboxy group-containing cellulose sulfates. Polym Bull 27:147–153
41. Rahn K, Heinze T, Klemm D (1995) Investigations of amidation of C-6 car-boxy cellulose. In: Kennedy HF, Phillips GO, Williams PA, Piculell L (eds) Cellulose and cellulose derivatives, physico-chemical aspects and industrial applications. Ellis Horwood, New York, pp 213–218

42. Bosso C, Defaye J, Gadelle A, Wong CC, Pedersen C (1982) Homopolysaccharides interaction with the dimethyl sulfoxide-paraformaldehyde cellulose solvent system. Selective oxidation of amylose and cellulose at secondary alcohol groups. J Chem Soc, Perkin Trans 1 (1972–1999):1579–1585
43. Defaye J, Gadelle A (1977) Selective oxidation of secondary vicinal diols. Part III. Selective oxidation of vicinal hydroxyl groups of methyl-4,6-O-benzylidene-β-d-glucopyranoside by dimethyl sulfoxide and acetic anhydride. Carbohydr Res 56:411–414
44. Bredereck K (1967) Synthesis of ketocellulose. Tetrahedron Lett 8:695–698
45. Maekawa E, Koshijima T (1984) Properties of 2,3-dicarboxy cellulose combined with various metallic ions. J Appl Polym Sci 29:2289–2297
46. Painter TJ (1988) Control of depolymerization during the preparation of reduced dialdehyde cellulose. Carbohydr Res 179:259–268
47. Morooka T, Norimoto N, Yamada T (1989) Periodate oxidation of cellulose by homogeneous reaction. J Appl Polym Sci 38:849–858
48. Potthast A, Kostic M, Schiehser S, Kosma P, Rosenau T (2007) Studies on oxidative modifications of cellulose in the periodate system: molecular weight distribution and carbonyl group profiles. Holzforschung 61:662–667
49. Floor M, Hofsteede LPM, Groenland WPT, Verhaar LAT, Kieboom APG, van Bekkum H (1989) Preparation and calcium complexation of oxidized polysaccharides. II. Hydrogen peroxide as coreactant in the chlorite oxidation of dialde-hyde glucans. Recl Trav Chim Pays-Bas 108:384–392
50. Matsumura S, Nishioka M, Shigeno H, Tanaka T, Yoshikawa S (1993) Builder performance in detergent formulations and biodegradability of partially dicarboxylated cellulose and amylose containing sugar residues in the backbone. Angew Makromol Chem 205:117–129
51. Varma AJ, Chavan VB (1995) Some preliminary studies on polyelectrolyte and rheological properties of sodium 2,3-dicarboxycellulose. Carbohydr Polym 27:63–67
52. Csanady G, Narayanan P, Mueller K, Wegscheider W, Knapp G (1989) Synthesis of various oxine celluloses for enriching processes for trace analysis. Angew Makromol Chem 170:159–172
53. Valentova O, Marek M, Svec F, Stamberg J, Vodrazka Z (1981) Comparison of different methods of glucose oxidase immobilization. Biotechnol Bioeng 23:2093–2104
54. Turkova J, Vajcner J, Vancurova D, Stamberg J (1979) Immobilization on cellulose in bead form after periodate oxidation and reductive alkylation. Collect Czech Chem Commun 44:3411–3417
55. Maekawa E (1991) Analysis of oxidized moiety of partially periodate-oxidized cellulose by NMR spectroscopy. J Appl Polym Sci 43:417–422
56. Rahn K, Heinze T (1998) New cellulosic polymers by subsequent modification of 2,3-dialdehyde cellulose. Cellul Chem Technol 32:173–183
57. Zhang J, Jiang N, Dang Z, Elder TJ, Ragauskas AJ (2008) Oxidation and sulfonation of cellulosics. Cellulose 15:489–496
58. Sun B, Hou Q, Liu Z, Ni Y (2015) Sodium periodate oxidation of cellulose nanocrystal and its application as a paper wet strength additive. Cellulose 22:1135–1146
59. Coseri S, Biliuta G, Zemljic LF, Srndovic JS, Larsson PT, Strnad S, Kreze T, Naderi A, Lindstrom T (2015) One-shot carboxylation of microcrystalline cellulose in the presence of nitroxyl radicals and sodium periodate. RSC Adv 5:85889–85897
60. Calado Vieira M (2000) Studien zur regioselektiven Oxidation von Celluloseethern sowie Celluloseestern und Funktionalisierung cellulosereicher Fasern. Ph.D. thesis, Friedrich Schiller University of Jena, Jena
61. Heinze T (1998) New ionic polymers by cellulose functionalization. Macromol Chem Phys 199:2341–2364
62. Potthast A, Roherling J, Rosenau T, Borgards A, Sixta H, Kosma P (2003) A novel method for the determination of carbonyl groups in cellulosics by fluorescence labeling. 3. Monitoring oxidative processes. Biomacromolecules 4:743–749

63. Kostic M, Potthast A, Rosenau T, Kosma P, Sixta H (2006) A novel approach to determination of carbonyl groups in DMAc/LiCl-insoluble pulps by flu-orescence labeling. Cellulose 13:429–435
64. Potthast A, Rosenau T, Kosma P (2006) Analysis of oxidized functionalities in cellulose. Adv Polym Sci 205:1–48
65. Kolb HC, Finn MG, Sharpless KB (2001) Click chemistry: diverse chemical function from a few good reactions. Angew Chem Int Ed 40:2004–2021
66. Sletten EM, Bertozzi CR (2009) Bioorthogonal chemistry: fishing for selectivity in a sea of functionality. Angew Chem Int Ed 48:6974–6998
67. Huisgen R (1963) 1,3-Dipolar cycloadditions. Past and future. Angew Chem Int Ed 2:565–598
68. Rostovtsev VV, Green LG, Fokin VV, Sharpless KB (2002) A stepwise Huisgen cycloaddition process: copper(I)-catalyzed regioselective "ligation" of azides and terminal alkynes. Angew Chem Int Ed 114:2596–2599
69. Lewis WG, Green LG, Grynszpan F, Radic Z, Carlier PR, Taylor P, Finn MG, Sharpless KB (2002) Click chemistry in situ: Acetylcholinesterase as a reaction vessel for the selective assembly of a femtomolar inhibitor from an array of building blocks. Angew Chem Int Ed 41:1053–1057
70. Agard NJ, Prescher JA, Bertozzi CR (2004) A strain-promoted [3 + 2] azide-alkyne cycloaddition for covalent modification of biomolecules in living systems. J Am Chem Soc 126:15046–15047
71. Fenn D, Pohl M, Heinze T (2009) Novel 3-O-propargyl cellulose as a precursor for regioselective functionalization of cellulose. React Funct Polym 69:347–352
72. Peng P, Cao X, Peng F, Bian J, Xu F, Sun R (2012) Binding cellulose and chitosan via click chemistry: synthesis, characterization, and formation of some hollow tubes. J Polym Sci, Part A: Polym Chem 50:5201–5210
73. Pierre-Antoine F, Francois B, Rachida Z (2012) Crosslinked cellulose developed by CuAAC, a route to new materials. Carbohydr Res 356:247–251
74. Hafren J, Zou W, Cordova A (2006) Heterogeneous 'organoclick' derivatization of polysaccharides. Macromol Rapid Commun 27:1362–1366
75. Koschella A, Hartlieb M, Heinze T (2011) A "click-chemistry" approach to cellulose-based hydrogels. Carbohydr Polym 86:154–161
76. Montanez MI, Hed Y, Utsel S, Ropponen J, Malmstroem E, Wagberg L, Hult A, Malkoch M (2011) Bifunctional dendronized cellulose surfaces as biosensors. Biomacromol 12:2114–2125
77. Pahimanolis N, Hippi U, Johansson L-S, Saarinen T, Houbenov N, Ruokolainen J, Seppaelae J (2011) Surface functionalization of nanofibrillated cellulose using click-chemistry approach in aqueous media. Cellulose 18:1201–1212
78. Crescenzi V, Cornelio L, Di Meo C, Nardecchia S, Lamanna R (2007) Novel hydrogels via click chemistry: synthesis and potential biomedical applications. Biomacromol 8:1844–1850
79. Gattás-Asfura KM, Stabler CL (2013) Bioorthogonal layer-by-layer encapsulation of pancreatic islets via hyperbranched polymers. ACS Appl Mater Interfaces 5:9964–9974
80. Zhang F, Bernet B, Bonnet V, Dangles O, Sarabia F, Vasella A (2008) 2-Azido-2-deoxycellulose: synthesis and 1,3-dipolar cycloaddition. Helv Chim Acta 91:608–618
81. Fox SC, Edgar KJ (2012) Staudinger reduction chemistry of cellulose: synthesis of selectively O-acylated-6-amino-6-deoxy-cellulose. Biomacromol 13:992–1001
82. Furuhata K, Koganei K, Chang HS, Aoki N, Sakamoto M (1992) Dissolution of cellulose in lithium bromide-organic solvent systems and homogeneous bromination of cellulose with N-bromosuccinimide-triphenylphosphine in lithium bromide-N,N-dimethylacetamide. Carbohydr Res 230:165–177
83. Liebert T, Hänsch C, Heinze T (2006) Click chemistry with polysaccharides. Macromol Rapid Commun 27:208–213

84. Negishi K, Mashiko Y, Yamashita E, Otsuka A, Hasegawa T (2011) Cellulose chemistry meets click chemistry: syntheses and properties of cellulose-based glycoclusters with high structural homogeneity. Polymers 3:489–508
85. Meng X, Edgar KJ (2016) "Click" reactions in polysaccharide modification. Prog Polym Sci 53:52–85
86. Vögtle F, Richardt G, Werner N (2007) Dendritische Moleküle, Konzepte, Synthesen, Eigenschaften und Anwendungen. Teubner Studienbücher Chemie, Wiesbaden
87. Hassan ML, Moorefield CN, Newkome GR (2004) Regioselective dendritic functionalization of cellulose. Macromol Rapid Commun 25:1999–2002
88. Hassan ML, Moorefield CN, Kotta K, Newkome GR (2005) Regioselective combinatorial-type synthesis, characterization, and physical properties of dendronized cellulose. Polymer 46:8947–8955
89. Heinze T, Pohl M, Schaller J, Meister F (2007) Novel bulky esters of cellulose. Macromol Biosci 7:1225–1231
90. Pohl M, Schaller J, Meister F, Heinze T (2008) Selectively dendronized cellulose: synthesis and characterization. Macromol Rapid Commun 29:142–148
91. Heinze T, Schöbitz M, Pohl M, Meister F (2008) Interactions of ionic liquids with polysaccharides. IV. Dendronization of 6-azido-6-deoxy cellulose. J Polym Sci, Part A: Polym Chem 46:3853–3859
92. Kamitakahara H, Nakatsubo F (2005) Synthesis of diblock copolymers with cellulose derivatives. 1. Model study with azidoalkyl carboxylic acid and cellobiosylamine derivative. Cellulose 12:209–219
93. Nakagawa A, Kamitakahara H, Takano T (2012) Synthesis and thermoreversible gelation of diblock methylcellulose analogues via Huisgen 1,3-dipolar cycloaddition. Cellulose 19:1315–1326
94. Enomoto-Rogers Y, Kamitakahara H, Yoshinaga A, Takano T (2012) Comb-shaped graft copolymers with cellulose side-chains prepared via click chemistry. Carbohydr Polym 87:2237–2245
95. Thakur VK (2015) Cellulose-based graft copolymers: structure and chemistry. CRC Press, Boca Raton, Fla
96. Tischer T, Claus TK, Bruns M, Trouillet V, Linkert K, Rodriguez-Emmenegger C, Goldmann AS, Perrier S, Boerner HG, Barner-Kowollik C (2013) Spatially controlled photochemical peptide and polymer conjugation on biosurfaces. Biomacromol 14:4340–4350
97. Ax J, Wenz G (2012) Thermoreversible networks by Diels-Alder reaction of cellulose furoates with bismaleimides. Macromol Chem Phys 213:182–186
98. Wang G-F, Chu H-J, Wei H-L, Liu X-Q, Zhao Z-X, Zhu J (2014) Click synthesis by Diels-Alder reaction and characterisation of hydroxypropyl methylcellulose-based hydrogels. Chem Pap 68:1390–1399
99. Goldmann AS, Tischer T, Barner L, Bruns M, Barner-Kowollik C (2011) Mild and modular surface modification of cellulose via hetero Diels-Alder (HDA) cycloaddition. Biomacromol 12:1137–1145
100. Tischer T, Goldmann AS, Linkert K, Trouillet V, Boerner HG, Barner-Kowollik C (2012) Modular ligation of thioamide functional peptides onto solid cellulose substrates. Adv Funct Mater 22:3853–3864
101. Wondraczek H, Pfeifer A, Heinze T (2012) Water soluble photoactive cellulose derivatives: synthesis and characterization of mixed 2-[(4-methyl-2-oxo-2H-chromen-7-yl)oxy]acetic acid-(3-carboxypropyl)trimethylammonium chloride esters of cellulose. Cellulose 19:1327–1335
102. Grigoray O, Wondraczek H, Daus S, Kuehnoel K, Latifi SK, Saketi P, Fardim P, Kallio P, Heinze T (2015) Photocontrol of mechanical properties of pulp fibers and fiber-to-fiber bonds via self-assembled polysaccharide Derivatives. Macromol Mater Eng 300:277–282

103. Nair DP, Podgorski M, Chatani S, Gong T, Xi W, Fenoli CR, Bowman CN (2014) The thiol-Michael addition click reaction: a powerful and widely used tool in materials chemistry. Chem Mater 26:724–744
104. Eyley S (2013) Surface modification of cellulose nanocrystals. Ph.D. thesis, University of Nottingham, Nottingham
105. Nielsen LJ, Eyley S, Thielemans W, Aylott JW (2010) Dual fluorescent labelling of cellulose nanocrystals for pH sensing. Chem Commun 46:8929–8931
106. Schyrr B, Pasche S, Voirin G, Weder C, Simon YC, Foster EJ (2014) Biosensors based on porous cellulose nanocrystal–poly(vinyl alcohol) scaffolds. ACS Appl Mater Interfaces 6:12674–12683
107. Zhao GL, Hafren J, Deiana L, Cordova A (2010) Heterogeneous "organo-click" derivatization of polysaccharides: photochemical thiol-ene click modification of solid cellulose. Macromol Rapid Commun 31:740–744
108. Rosilo H, Kontturi E, Seitsonen J, Kolehmainen E, Ikkala O (2013) Transition to reinforced state by percolating domains of intercalated brush-modified cellulose nanocrystals and poly (butadiene) in cross-linked composites based on thiol-ene click chemistry. Biomacromol 14:1547–1554
109. Tingaut P, Hauert R, Zimmermann T (2011) Highly efficient and straight-forward functionalization of cellulose films with thiol-ene click chemistry. J Mater Chem 21:16066–16076
110. Huang JL, Li CJ, Gray DG (2014) Functionalization of cellulose nanocrystal films via "thiol-ene" click reaction. RSC Adv 4:6965–6969
111. Hebeish A, Guthrie JT (1981) The chemistry and technology of cellulosic copolymers. Springer, Berlin
112. Wågberg L (2000) Polyelectrolyte adsorption onto cellulose fibers—a review. Nord Pulp Pap Res J 15:586–597
113. Stevens MP (1999) Polymer chemistry, 3rd ed. Oxford University Press, New York
114. Klemm D, Heublein B, Fink HP, Bohn A (2005) Cellulose: fascinating biopolymer and sustainable raw material. Angew Chem Int Ed 44:3358–3393
115. Klemm D, Philipp B, Heinze T, Heinze U, Wagenknecht W (1998) Comprehensive cellulose chemistry, vol 2. Wiley-VCH, Weinheim, pp 17–27
116. Roy D, Semsarilar M, Guthrie JT, Perrier S (2009) Cellulose modification by polymer grafting: a review. Chem Soc Rev 38:2046–2064
117. Carlmark A, Larsson E, Malmstrom E (2012) Grafting of cellulose by ring-opening polymerization—a review. Eur Polym J 48:1646–1659
118. Heinze T, Liebert T (2012) Celluloses and polyoses/hemicelluloses. In: Matyjaszewski K, Möller M (eds) Polymer science: a comprehensive reference, vol 10, pp. 83–152
119. Gürdag G, Sarmad S (2013) Cellulose graft copolymers: synthesis, properties, and applications. In: Kalia S, Sabaa MW (eds) Polysaccharide based graft copolymers. Springer, Berlin
120. Tosh B, Routray CR (2014) Grafting of cellulose based materials: a review. Chem Sci Rev Lett 3:74–92
121. Wei L, McDonald AG (2016) A review on grafting of biofibers for biocomposites. Materials 9:303. https://doi.org/10.3390/ma9040303
122. Odian G (2004) Principles of polymerization, 4th ed. Wiley, New York
123. Bhattacharya A, Misra BN (2004) Grafting: a versatile means to modify polymers techniques, factors and applications. Prog Polym Sci 29:767–814
124. Bahattacharyya SN, Maldas D (1984) Graft copolymerization onto cellulosics. Prog Polym Sci 10:171–270
125. Okieimen EF (1987) Studies on the graft copolymerization of cellulosic materials. Eur Polym J 23:319–322
126. Ouajai S, Hodzic A, Shanks RA (2004) Morphological and grafting modification of natural cellulose fibers. J Appl Polym Sci 94:2456–2465

127. Gurdag G, Guclu G, Ozgumus S (2001) Graft copolymerization of acrylic acid onto cellulose: effects of pretreatments and crosslinking agent. J Appl Polym Sci 80:2267–2272
128. Diamantoglou M, Kundinger EF (1995) Derivatisation of cellulose in homogeneous reaction. In: Kennedy JF, Phillips GO (eds) Cellulose and cellulose derivatives: physico-chemical aspects and industrial applications. Woodhead Publishers, Cambridge
129. Zhang ZB, McCormick CL (1997) Graft copolymerization of cellulose with structopendant unsaturated ester moieties in homogeneous solution. J Appl Polym Sci 66:307–317
130. Bhattacharyya SN, Maldas D (1982) Radiation-Induced graft copolymerization of mixtures of styrene and acrylamide onto cellulose acetate. I. Effect of solvents. J Polym Sci: Polym Chem Ed 20:939–950
131. Nishioka N, Matsumoto Y, Yumen T, Monmae K, Kosai K (1986) Homogeneous graft copolymerization of vinyl monomers onto cellulose in a dimethyl sulfoxide-paraformaldehyde solvent system IV. 2-hydroxyethyl methacrylate. Polym J 18:323–330
132. Abdel-Razik EA (1990) Homogeneous graft copolymerization of acrylamide onto ethyl cellulose. Polymer 31:1739–1744
133. Ibrahim MM, Flefel EM, El-Zawawy WK (2002) Cellulose membranes grafted with vinyl monomers in a homogeneous system. Polym Adv Technol 13:548–557
134. Ibrahim MM, Flefel EM, El-Zawawy WK (2002) Cellulose membranes grafted with vinyl monomers in homogeneous system. J Appl Polym Sci 84:2629–2638
135. Kunze J, Fink HP (2005) Structural changes and activation of cellulose by caustic soda solution with urea. Macromol Symp 223:175–187
136. Shukla SR, Rao GVG, Athalye AR (1992) Ultraviolet-radiation-induced graft copolymerization of styrene and acrylonitrile onto cotton cellulose. J Appl Polym Sci 45:1341–1354
137. Takacs E, Wojnarovits L, Borsa J, Papp J, Hargittai P, Korecz L (2005) Modification of cotton-cellulose by preirradiation grafting. Nucl Instrum Methods Phys Res, Sect B 236:259–265
138. Andreozzi L, Castelvetro V, Ciardelli G, Corsi L, Faetti M, Fatarella E, Zulli F (2005) Free radical generation upon plasma treatment of cotton fibers and their initiation efficiency in surface-graft polymerization. J Colloid Interface Sci 289:455–465
139. Ghosh P, Das D (2000) Modification of cotton by acrylic acid (AA) in the presence of $NaH_2PO_4$ and $K_2S_2O_8$ as catalysts under thermal treatment. Eur Polym J 36:2505–2511
140. Suo A, Qian J, Yao Y, Zhang W (2007) Synthesis and properties of carboxymethyl cellulose-graft-poly(acrylic acid-co-acrylamide) as a novel cellulose-based superabsorbent. J Appl Polym Sci 103:1382–1388
141. Aliouche D, Sid B, Ait-Amar (2006) Graft-copolymerization of acrylic monomers onto cellulose. Influence on fiber swelling and absorbency. Ann Chim (Cachan, Fr.) 31:527–540
142. Ogiwara Y, Kubota H (1970) Graft copolymerization to cellulose by the metallic ion-hydrogen peroxide initiator system. J Polym Sci, Part A-1, Polym Chem 8:1069–1076
143. Misra BN, Dogra R, Kaur I, Jassal JK (1979) Grafting onto cellulose. IV. Effect of complexing agents on Fenton's reagent (iron(2+)-hydrogen peroxide)-initiated grafting of poly(vinyl acetate). J Polym Sci Polym Chem Ed 17:1861–1863
144. Stannett VT, Hopfenberg HB (1971) Graft copolymers. In: Bikales NM, Segal L (eds) Cellulose and cellulose derivatives, vol 5. Wiley, New York, pp 907–936
145. Toledano-Thompson T, Loria-Bastarrachea MI, Aguilar-Vega MJ (2005) Characterization of henequen cellulose microfibers treated with an epoxide and grafted with poly(acrylic acid). Carbohydr Polym 62:67–73
146. Kubota H, Kuwabara S (1997) Cellulosic absorbents for water synthesized by grafting of hydrophilic vinyl monomers on carboxymethyl cellulose. J Appl Polym Sci 64:2259–2263
147. Jianqin L, Maolin Z, Hongfei H (1999) Pre-irradiation grafting of temperature sensitive hydrogel on cotton cellulose fabric. Radiat Phys Chem 55:55–59

148. Lu J, Yi M, Li J, Ha H (2001) Preirradiation grafting polymerization of DMAEMA onto cotton cellulose fabrics. J Appl Polym Sci 81:3578–3581
149. Carlmark A, Malmstrom EE (2003) ATRP grafting from cellulose fibers to create block-copolymer grafts. Biomacromol 4:1740–1745
150. Kumar V, Bhardwaj YK, Jamdar SN, Goel NK, Sabharwal S (2006) Preparation of an anion-exchange adsorbent by the radiation-induced grafting of vinylbenzyltrimethylammonium chloride onto cotton cellulose and its application for protein adsorption. J Appl Polym Sci 102:5512–5521
151. Lawrence KDN, Verdin D (1973) Graft polymerization of acrylamide onto paper preirradiated with high energy electrons. J Appl Polym Sci 17:2653–2666
152. Shukla SR, Rao GVG, Athalye AR (1993) Improving graft level during photoinduced graft copolymerization of styrene onto cotton cellulose. J Appl Polym Sci 49:1423–1430
153. Shukla SR, Athalye AR (1992) Bifunctional monomers in photoinduced vinyl grafting on cotton cellulose: use of divinylbenzene in grafting of styrene. Polymer 33:3729–3733
154. Vander Wielen LC, Ragauskas AJ (2004) Grafting of acrylamide onto cellulosic fibers via dielectric-barrier discharge. Eur Polym J 40:477–482
155. Zubaidi Hirotsu TH (1996) Graft polymerization of hydrophilic monomers onto textile fibers treated by glow discharge plasma. J Appl Polym Sci 61:1579–1584
156. Carothers WH, Dorough GL, Van Natta FJ (1932) Polymerization and ring formation. X. Reversible polymerization of six-membered cyclic esters. J Am Chem Soc 54:761–772
157. Dubois P, Coulembier O, Raquez J-M (2009) Handbook of ring-opening polymerization. Wiley-VCH, Germany, pp 1–408
158. Labet M, Thielemans W (2009) Synthesis of polycaprolactone: a review. Chem Soc Rev 38:3484–3504
159. Cordova A, Hafren J (2005) Direct organic acid-catalyzed polyester derivatization of lignocellulosic material. Nord Pulp Pap Res J 20:477–480
160. Yang Q, Pan X, Huang F, Li K (2011) Synthesis and characterization of cellulose fibers grafted with hyperbranched poly(3-methyl-3-oxetanemethanol). Cellulose 18:1611–1621
161. Kahovec J, Jelinkova M, Janout V (1986) Polymer-supported oligo (N-acetyliminoethylenes). New phase-transfer catalysts Polym Bull 15:485–490
162. Cohen E, Avny Y, Zilkha A (1971) Anionic graft polymerization of propylene sulfide on cellulose. I. J Polym Sci, Part A-1 9:1469–1479
163. Ikeda I, Kurushima Y, Takashima H, Suzuki K (1988) Cationic graft polymerization of 2-oxazolines on cellulose derivatives. Polym J 20:243–250
164. Hawker CJ (2002) Nitroxide-mediated living radical polymerizations. In: Matyjaszewski K, Davis TP (eds) Handbook of radical polymerization. Wiley, Hoboken, pp 463–521
165. Daly WH, Evenson TS, Iacono ST, Jones RW (2001) Recent developments in cellulose grafting chemistry utilizing Barton ester intermediates and nitroxide mediation. Macromol Symp 174:155–163
166. Wang JS, Matyjaszewski K (1995) Controlled/"living" radical polymerization. Atom transfer radical polymerization in the presence of transition-metal complexes. J Am Chem Soc 117:5614–5615
167. Carlmark A, Malmstroem E (2002) Atom transfer radical polymerization from cellulose fibers at ambient temperature. J Am Chem Soc 124:900–901
168. Rizzardo E, Chiefari J, Mayadunne RTA, Moad G, Thang SH (2000) Synthesis of defined polymers by reversible addition-fragmentation chain transfer: the RAFT process. ACS Symp Ser 768:278–296
169. Perrier S, Takolpuckdee P, Westwood J, Lewis DM (2004) Versatile chain transfer agents for reversible addition fragmentation chain transfer (RAFT) polymerization to synthesize functional polymeric architectures. Macromolecules 37:2709–2717
170. Dahou W, Ghemati D, Oudia A, Aliouche D (2010) Preparation and biological characterization of cellulose graft copolymers. Biochem Eng J 48:187–194

171. Dhiman PK, Kaur I, Mahajan RK (2008) Synthesis of a cellulose-grafted polymeric support and its application in the reductions of some carbonyl compounds. J Appl Polym Sci 108:99–111
172. Mao C, Qiu Y, Sang H, Mei H, Zhu A, Shen J, Lin S (2004) Various approaches to modify biomaterial surfaces for improving hemocompatibility. Adv Colloid Interface Sci 110:5–17
173. Hatakeyama T, Nakamura K, Hatakeyama H (1982) Studies on heat capacity of cellulose and lignin by differential scanning calorimetry. Polymer 23:1801–1804
174. Gupta KC, Khandekar K (2006) Ceric(IV) ion-induced graft copolymerization of acrylamide and ethyl acrylate onto cellulose. Polym Int 55:139–150
175. Gupta KC, Khandekar K (2002) Graft copolymerization of acrylamide-methylacrylate comonomers onto cellulose using ceric ammonium nitrate. J Appl Polym Sci 86:2631–2642
176. Kim BS, Mun SP (2009) Effect of $Ce^{4+}$ pretreatment on swelling properties of cellulosic superabsorbents. Polym Adv Technol 20:899–906
177. Mondal MIH, Uraki Y, Ubukata M, Itoyama K (2008) Graft polymerization of vinyl monomers onto cotton fibres pretreated with amines. Cellulose 15:581–592
178. Nishioka N, Watase K, Arimura K, Kosai K, Uno M (1984) Permeability through cellulose membranes grafted with vinyl monomers in a homogeneous system. 1. Diffusive permeability through acrylonitrile grafted cellulose membranes. Polym J 16:867–875
179. Nishioka N, Yoshimi S, Iwaguchi T, Kosai K (1984) Permeability through cellulose membranes grafted with vinyl monomers in homogeneous system. 2. States of water in acrylonitrile grafted cellulose membranes. Polym J 16:877–885
180. Bicak N, Sherrington DC, Senkal BF (1999) Graft copolymer of acrylamide onto cellulose as mercury selective sorbent. React Funct Polym 41:69–76
181. Wen OH, Kuroda SI, Kubota H (2001) Temperature-responsive character of acrylic acid and N-isopropylacrylamide binary monomers-grafted celluloses. Eur Polym J 37:807–813
182. Gueclue G, Guerdag G, Oezguemues S (2003) Competitive removal of heavy metal ions by cellulose graft copolymers. J Appl Polym Sci 90:2034–2039
183. O'Connell DW, Birkinshaw C, O'Dwyer TF (2006) A modified cellulose adsorbent for the removal of nickel(II) from aqueous solutions. J Chem Technol Biotechnol 81:1820–1828
184. Liu S, Sun G (2008) Radical graft functional modification of cellulose with allyl monomers: chemistry and structure characterization. Carbohydr Polym 71:614–625
185. Wang D, Tan J, Kang H, Ma L, Jin X, Liu R, Huang Y (2011) Synthesis, self-assembly and drug release behaviors of pH-responsive copolymers ethyl cellulose-graft-PDEAEMA through ATRP. Carbohydr Polym 84:195–202
186. Bokias G, Mylonas Y, Staikos G, Bumbu GG, Vasile C (2001) Synthesis and aqueous solution properties of novel thermo-responsive graft copolymers based on a carboxymethyl-cellulose backbone. Macromolecules 34:4958–4964
187. Li Y, Liu R, Liu W, Kang H, Wu M, Huang Y (2008) Synthesis, self-assembly, and thermosensitive properties of ethyl cellulose-g-p(PEGMA) amphiphilic copolymers. J Polym Sci, Part A: Polym Chem 46:6907–6915